

**Synthesis and Functionalization of Highly Biologically Active Terpene
Natural Products**

-

**Total Synthesis of (+)-Darwinolide
and
Semisynthesis of (-)-Englerin A and
Structure-Activity Relationship Studies of Analogs**

Inaugural-Dissertation
to obtain the academic degree
Doctor rerum naturalium (Dr. rer. nat.)

submitted to the Department of Biology, Chemistry and Pharmacy
Freie Universität Berlin

by
Thomas Siemon
from Berlin

November 2019

Hereby, I declare that the submitted thesis is my own work and was prepared autonomously without the aid of other sources than the ones cited and acknowledged. The work was not submitted to any other prior doctoral procedure.

Thomas Siemon

19.11.2019

The following doctoral work has been carried out within the research group of Prof. Dr. MATHIAS CHRISTMANN from June 2015 until August 2019 at the Institute of Chemistry and Biochemistry of the Freie Universität Berlin.

1st Reviewer: Prof. Dr. MATHIAS CHRISTMANN

(Institute of Chemistry and Biochemistry, Freie Universität Berlin)

2nd Reviewer: Prof. Dr. MARKUS KALESSE

(Institute for Organic Chemistry, Leibniz Universität Hannover)

Date of disputation: 07.02.2020

Part of this dissertation has been published in:

T. Siemon, S. Steinhauer, M. Christmann, *Angew. Chem. Int. Ed.* **2019**, *58*, 1120 – 1122; *Angew. Chem.* **2019**, *131*, 1132 – 1134.

I. Burkhardt, **T. Siemon**, M. Henrot, L. Studt, S. Rösler, B. Tudzynski, M. Christmann, J. S. Dickschat, *Angew. Chem. Int. Ed.* **2016**, *55*, 8748 – 8751; *Angew. Chem.* **2016**, *128*, 8890 – 8893.

Part of this dissertation has been submitted:

T. Siemon, Z. Wang, G. Bian, T. Seitz, Z. Ye, Y. Lu, S. Cheng, Y. Ding, Z. Deng, T. Liu, M. Christmann, *J. Am. Chem. Soc.* **2020**.

Content

Danksagung.....	V
Abbreviations.....	VII
Zusammenfassung.....	XI
Abstract.....	XV
1 Motivation.....	1
1.1 Natural Products as Lead Structures in Drug Discovery.....	1
1.2 Natural Product Synthesis in Drug Development.....	3
2 (+)-Darwinolide – A Biofilm-Penetrating Anti-MRSA Agent.....	7
2.1 Introduction.....	7
2.1.1 Methicillin-resistant <i>Staphylococcus Aureus</i> – A Global Health Risk.....	7
2.1.2 Microbial Biofilms.....	10
2.1.3 Darwinolide – Isolation and Biological Profile.....	13
2.2 Scientific Goal.....	15
2.3 Publication.....	17
2.3.1 Synthesis of (+)-Darwinolide, a Biofilm-Penetrating Anti-MRSA Agent.....	17
2.4 Summary and Outlook.....	21
3 (–)-Englerin A – A Highly Active and Selective Inhibitor of Renal Cancer Cell Growth.....	23
3.1 Introduction.....	23
3.1.1 Renal Cancer.....	23
3.1.2 Isolation and Biological Evaluation of (–)-Englerin A.....	24
3.1.3 Biosynthesis of (–)-Englerin A.....	27
3.1.4 Syntheses of Englerin A.....	30
3.1.5 Structure-Activity-Relationship Studies of (–)-Englerin A.....	42
3.2 Scientific Goal.....	47
3.3 Publications.....	49
3.3.1 Mechanistic Characterisation of Two Sesquiterpene Cyclases from the Plant Pathogenic Fungus <i>Fusarium fujikuroi</i>	49

3.3.2	Microbe Engineering of Guaia-6,10(14)-diene as a Building Block for the Semisynthetic Production of Plant-Derived (-)-Englerin A.....	55
3.4	Unpublished Results	65
3.4.1	Synthesis of aza-Englerin A Analogs.....	65
3.4.2	Synthesis of C10 Methyl Analogs of (-)-Englerin A.....	67
3.5	Summary and Outlook	69
4	List of References and Illustration Credits	73
4.1	References	73
4.2	Illustration Credits.....	79
	Appendix.....	81
	Supporting Information – Synthesis of (+)-Darwinolide	81
	Supporting Information – Terpene Cyclase Characterization	135
	Supporting Information – Semisynthesis of (-)-Englerin A.....	165
	Unpublished Results	213

Danksagung

An erster Stelle möchte ich mich bei meinem Doktorvater Prof. Dr. Mathias Christmann für die freundliche Aufnahme in die Arbeitsgruppe, die sehr interessanten Themenstellungen und die wissenschaftliche Unterstützung bei deren Bearbeitung bedanken.

Prof. Dr. Markus Kalesse danke ich für die Übernahme des Zweitgutachtens.

Der gesamten Arbeitsgruppe gilt mein besonderer Dank für die wunderbare Zeit im Labor und auch darüber hinaus. Bei meinem Laborkollegen Matthias Henrot möchte ich mich für die gute Zusammenarbeit während des ersten Jahres meiner Promotion im Exil (24.01) bedanken. Dem gesamten Labor 24.02 gilt mein besonderer Dank, namentlich Sven Hahn, Tobias Seitz, Tobias Olbrisch und den „Gastarbeitern“ Bence Hartmayer und Florian Bartels für die angenehme Arbeitsatmosphäre, die vielen hervorragenden Diskussionen und die besonderen Labortraditionen (Scooter-Friday, Rammstein-Montag, Asiamannday etc.).

Meinen Studenten Malte Brie und Jonas Genz danke ich für die gute Zusammenarbeit und die Unterstützung bei meiner Forschung.

Christiane Groneberg danke ich für die Durchführung der HPLC-, GC- und IR-Messungen und die Trennung meiner Verbindungen. Luise Schefzig danke ich für die Unterstützung beim Nachziehen meiner Verbindungen.

Der NMR-Abteilung danke ich für das Messen meiner NMR-Spektren und der MS-Abteilung für die Messung der EI-MS-Spektren und die Möglichkeit, meine ESI-Proben selbst messen zu dürfen. Dr. Simon Steinhauer danke ich für die Durchführung der Einkristall-Röntgenstrukturanalysen.

Für das Korrekturlesen meiner Doktorarbeit und weiterer Arbeiten danke ich Caroline Apel, Merlin Kleoff, Bence Hartmayer und Stefan Leisering.

Den Arbeitsgruppen um Prof. Dr. Jeroen S. Dickschat, Prof. Dr. Tiangang Liu, Prof. Dr. Marc Stadler und Dr. Robin Bon danke ich für die sehr fruchtbaren Kooperationen. Der Lead Discovery Center GmbH danke ich für die finanzielle Unterstützung und die biologischen Tests meiner Englerin-Derivate.

Meinen Kommilitonen Axel Haupt, Karsten Sonneberg und Kai Töpfer danke ich für die gute Zusammenarbeit seit dem ersten Semester meines Studiums.

Der Kochgruppe danke ich für viele Gourmet-Abende und der Xletix-Truppe für die gemeinsame Zeit im Matsch. Bei der „Schlag den Champ“-Gruppe bedanke ich mich für viele unvergessliche Momente, auch wenn am Ende fast immer Max gewonnen hat. Besonders bei Till möchte ich mich bedanken für die lange gemeinsame Zeit, aber auch insbesondere seit Beginn der Promotion in der Hage.

Abschließend gilt natürlich der größte und herzlichste Dank meiner Familie, insbesondere meinen Eltern, die mich seit 29 Jahren stets unterstützt haben, immer an meiner Seite standen und mir den Rücken freigehalten haben, sodass ich zunächst mein Studium und nun die Promotion erfolgreich abschließen konnte.

Abbreviations

Å	Angström	ABNO	9-azabicyclo[3.3.1]nonane <i>N</i> -oxyl
Ac	acetyl	acac	acetylacetonate
ATPase	adenosine triphosphatase	ATR	attenuated total reflection
aq.	aqueous	Bn	benzyl
bpy	bipyridine	br.	broad
Bu	butyl	Bz	benzoyl
c	concentration/ cyclo-/ centi-	CAS	CRISPR associated
CoA	Coenzyme A	COSY	correlation spectroscopy
CRISPR	Clustered Regularly Interspaced Short Palindromic Repeats	δ	chemical shift
d	doublet/ day	Da	Dalton
DABCO	1,4-diazabicyclo[2.2.2]octane	DABAL-Me ₃	Bis(trimethylaluminum)-1,4-diazabicyclo[2.2.2]octane adduct
DBA	dibenzylideneacetone	DBU	1,8-diazabicyclo[5.4.0]undecane
DCC	<i>N,N'</i> -dicyclohexylcarbodiimide	(DHQD) ₂ PHAL	hydroquinidine 1,4-phthalazinediyl diether
DIAD	diisopropyl azodicarboxylate	DIPEA	<i>N,N</i> -diisopropylethylamine
DMAPP	dimethylallyl pyrophosphate	DMAP	<i>N,N</i> -dimethylaminopyridine
DMDO	dimethyldioxirane	DMF	dimethylformamide
DMSO	dimethyl sulfoxide	2,2-DMP	2,2-dimethoxypropane
DNA	deoxyribonucleic acid	d.r.	diastereomeric ratio
ee	enantiomeric excess	EI	electron ionization
<i>ent</i>	enantiomer	<i>epi</i>	epimer
ESI	electrospray ionization	et al.	and others
equiv.	equivalents	FDA	Food and Drug Administration
FID	flame ionization detector	FTICR	Fourier-transform ion cyclotron resonance
FTIR	Fourier-transform infrared spectroscopy	FPP	farnesyl pyrophosphate
g	gram	GC	gas chromatography
GI ₅₀	half maximal growth inhibition	h	hour
hept	heptet	HMBC	heteronuclear multiple bond correlation
HMDS	hexamethyldisilazane	HMG	3-hydroxy-3-methyl-glutaryl
HMQC	heteronuclear multiple quantum correlation	HMPA	hexamethylphosphoric triamide
HPLC	high performance liquid chromatography	HRMS	high resolution mass spectrometry
HSF1	heat shock factor 1	Hz	Hertz

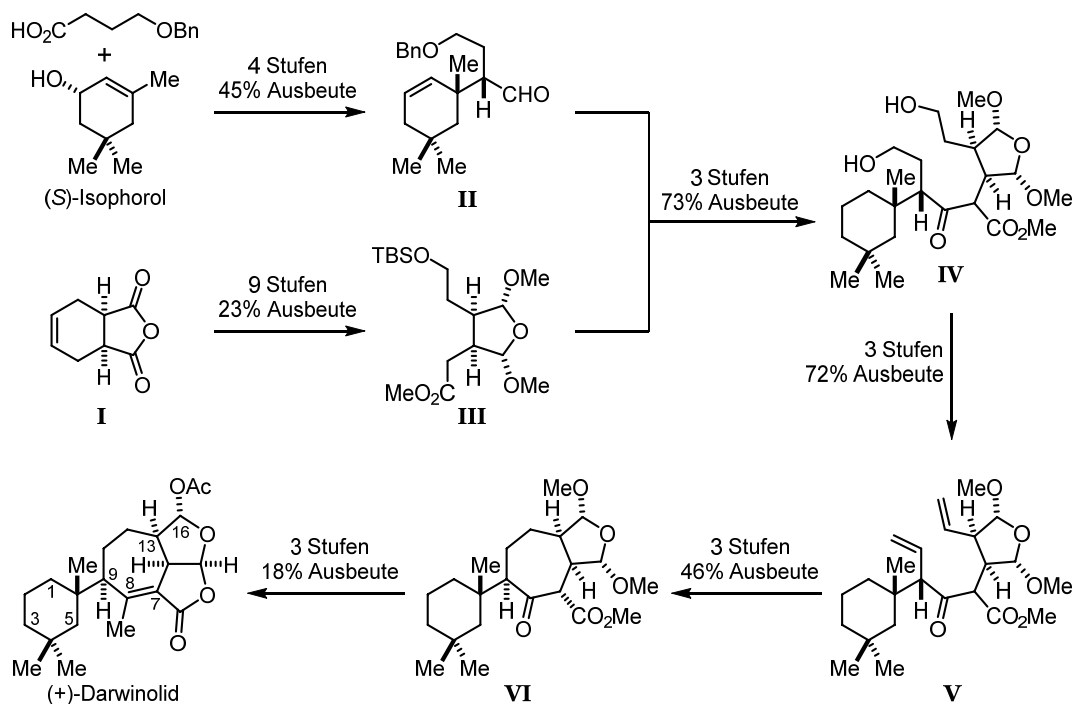
IBX	2-iodoxybenzoic acid	<i>i</i>	<i>iso-</i>
IC ₅₀	half maximal inhibitory concentration	imid	imidazolyl
IPP	isopentenyl pyrophosphate	IR	infrared spectroscopy
<i>J</i>	coupling constant	L	liter
λ	wavelength	LDA	lithium diisopropylamide
m	multiplet/ <i>meta-</i> / milli-/ meter	M	molar (mol/L)/ mega-
μ	micro-	<i>m</i> -CPBA	<i>meta</i> -chloroperoxybenzoic acid
Me	methyl	MEP	2- <i>C</i> -methyl-D-erythritol 4-phosphate
MIC	minimum inhibitory concentration	min	minute
MS	mass spectrometry/ molecular sieves	Ms	methanesulfonyl
m.p.	melting point	MRSA	methicillin-resistant <i>Staphylococcus Aureus</i>
MVA	mevalonate	n	<i>nano-</i>
$\bar{\nu}$	wave numbers	NADPH	nicotinamide adenine dinucleotide phosphate
NCI	National Cancer Institute	NMI	<i>N</i> -methylimidazole
NME	new molecular entity	NMR	nuclear magnetic resonance
NMO	<i>N</i> -methylmorpholine <i>N</i> -oxide	nor-AZADO	9-azanoradamantane <i>N</i> -oxyl
NOESY	nuclear Overhauser effect spectroscopy	NP	natural product
o	<i>ortho-</i>	oct	octanoate
p	<i>para-</i>	PCR	polymerase chain reaction
Ph	phenyl	PP	diphosphate
ppm	parts per million	Pr	propyl
q	quartet	quint	quintet
R	rest	rac	racemic
RCC	renal cell carcinoma	RCM	ring-closing metathesis
RNA	ribonucleic acid	rpm	revolutions per minute
s	singlet/ second/ <i>sec-</i>	SAR	structure-activity relationship
t	triplet/ <i>tert-</i>	T	temperature
TBAF	tetrabutylammonium fluoride	TBDPS	<i>tert</i> -butyl diphenylsilyl
TBHP	<i>tert</i> -butyl hydroperoxide	TBTU	1- [bis(dimethylamino)methylene]- 1 <i>H</i> -benzotriazolium 3-oxide tetrafluoroborate
TBS	<i>tert</i> -butyl dimethylsilyl	TCBC	trichlorobenzoyl chloride
TES	triethylsilyl	Tf	trifluoromethanesulfonyl
TFA	trifluoroacetic acid	TFAA	trifluoroacetic anhydride

THF	tetrahydrofuran	TMS	trimethylsilyl
TRPC	transient receptor potential canonical	Ts	toluenesulfonyl
UHP	urea hydrogen peroxide	XPhos	2-dicyclohexylphosphino-2',4',6'- triisopropylbiphenyl

Zusammenfassung

Im Rahmen dieser Doktorarbeit wurden zwei Naturstoffsynthese-Projekte bearbeitet. Das erste Thema war die erstmalige Totalsynthese des umgelagerten Diterpenoids (+)-Darwinolid (**1**). Dieser Naturstoff wurde 2016 von BAKER et al. aus dem antarktischen Schwamm *Dendrilla Membranosa* isoliert und weist eine inhibitorische Aktivität gegen die Biofilm-Phase von Methicillin-resistenten *Staphylococcus aureus*-Bakterien auf, die viermal höher ist, als die Aktivität gegenüber deren planktonischen Zellen.^[1] Auf Grund dieser einzigartigen biologischen Aktivität sollte ein synthetischer Zugang zu (+)-Darwinolid geschaffen werden.

Die erstmalige Synthese von (+)-Darwinolid konnte in 21 Stufen in der längsten linearen Sequenz und mit 1% Gesamtausbeute erfolgreich abgeschlossen werden (Schema 1).^[2] Über eine konvergente Strategie konnte die C7–C8-Bindung im zentralen siebengliedrigen Ring mittels einer Aldol-Addition des Esters **III** an den Aldehyd **II** installiert werden. Das Ester-Fragment **III** wurde in neun Stufen und 23% Ausbeute ausgehend vom kommerziell erhältlichen *meso*-Anhydrid **I** erhalten. Der Schlüsselschritt in dieser Synthesesequenz war eine enantioselektive, organokatalytische Desymmetrisierung eines *meso*-Diols.



Schema 1. Zusammenfassung der Totalsynthese von (+)-Darwinolid.

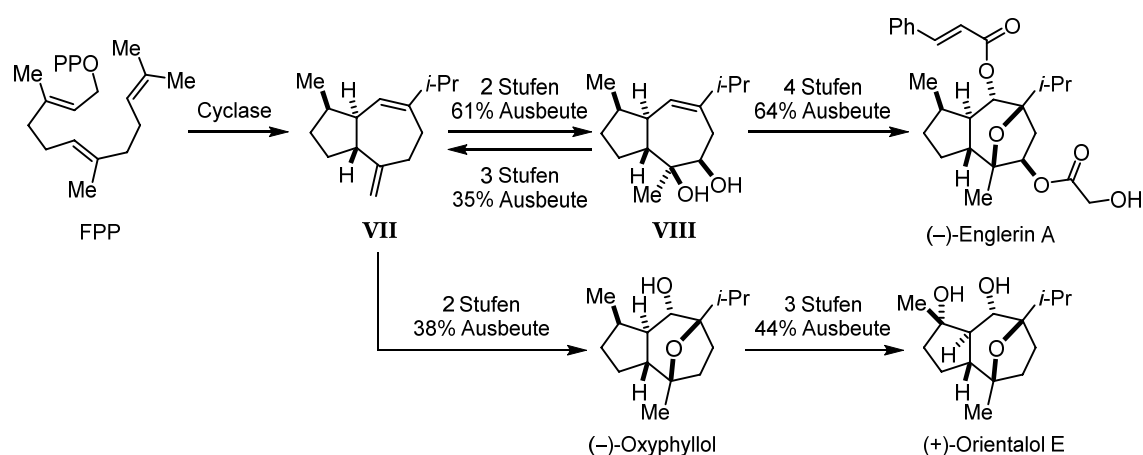
Beginnend von (*S*)-Isophorol, welches durch enzymatische Racematspaltung erhalten wurde, konnte das 1,3,3-Trimethylcyclohexyl-Fragment **II** in vier Schritten und 45% Ausbeute synthetisiert werden. Mit

Hilfe einer IRELAND–CLAISEN-Umlagerung konnte zwar die quaternäre Stereozentrum installiert werden, jedoch wurde das benachbarte Stereozentrum mit der unerwünschten Konfiguration aufgebaut, sodass eine spätere C9-Epimerisierung von Nöten war.

Nach der erfolgreichen Kupplung der beiden Fragmente **II** und **III**, wurden die beiden primären Alkohole des Intermediates **IV** simultan eliminiert, um den Vorläufer **V** für die anschließende Ringschlussmetathese zu erhalten. An dieser Stelle konnte die C9-Epimerisierung erfolgreich durchgeführt werden. Anschließend wurde der β -Ketoester **VI** in den Methyl-substituierten α,β -ungesättigten Ester überführt, wobei in diesem Schritt auch das anellierte Laktonacetal gebildet wurde. Abschließend konnte (+)-Darwinolid durch säurekatalysierte Transacetalisierung erhalten werden.

Das zweite Teilthema dieser Arbeit befasste sich mit dem Sesquiterpenoid (-)-Englerin A, welches 2009 von BEUTLER et al. aus dem Stamm des afrikanischen Baums *Phyllanthus engleri* isoliert wurde und eine hohe wachstumshemmende Wirkung gegenüber Nierenkrebszellen aufweist.^[3] Seit der erstmaligen Synthese des unnatürlichen Enantiomers durch die Arbeitsgruppe um CHRISTMANN wurden bereits zahlreiche Synthesen und biologischen Untersuchungen durchgeführt.^[4] Im Rahmen dieser Arbeit sollte ein neuartiger semisynthetischer Zugang zu (-)-Englerin A geschaffen werden und zusätzlich neue Derivate dargestellt werden, um deren Struktur-Aktivitäts-Beziehung zu untersuchen.

Zunächst wurde das Guaia-6,10(14)-dien (**VII**) in drei Stufen ausgehend von Diol-Intermediat **VIII** der (-)-Englerin A-Synthese nach CHRISTMANN synthetisiert (Schema 2).^[5]



Schema 2. Semisynthese von (-)-Englerin A, (-)-Oxyphyllol und (+)-Orientalol E ausgehend vom Biosyntheseprodukt Guaia-6,10(14)-dien (**VII**). Dien **VII** wurde zusätzlich in drei Stufen aus dem Diol **VIII** dargestellt, um durch Vergleich der optischen Rotationswerte die absolute Konfiguration des Produkts **VII** der Inkubation von FPP mit einer mutierten Sesquiterpen-Cyclase des Pilzes *Fusarium fujikuroi* zu bestimmen.

Die Arbeitsgruppe um DICKSCHAT untersuchte die Inkubation von Farnesylpyrophosphat (FPP) mit einer mutierten Sesquiterpen-Cyclase aus dem pathogenen Pilz *Fusarium fujikuroi* und konnte daraus

ebenfalls das Guaia-6,10(14)-dien **VII** isolieren.^[6] Durch den Vergleich der optischen Rotationswerte konnte die absolute Konfiguration eindeutig bestimmen werden. Mit Hilfe von ²H- und ¹³C-markierten FPP-Isotopomeren wurde der Biosynthesemechanismus dieser Cyclase aufgeklärt.

Der Arbeitsgruppe um LIU gelang es, das Guaia-6,10(14)-dien **VII** durch metabolisches Engineering des Mevalonatwegs in *Escherichia coli* bzw. *Saccharomyces cerevisiae* im Grammaßstab zu produzieren, was dessen Einsatz als Startmaterial für eine kurze Semisyntese von (-)-Englerin A ermöglichte (Schema 2). Durch Isomerisierung der exocyclischen Doppelbindung und anschließende regio- und stereoselektive Sharpless-Dihydroxylierung des daraus resultierenden trisubstituierten Alkens, konnte das Diol-Intermediat **VIII** der (-)-Englerin A-Synthese von CHRISTMANN et al. erhalten werden.^[5] In vier weiteren Schritten gelang die Synthese von (-)-Englerin A nach einer in der Arbeitsgruppe um CHRISTMANN optimierten Strategie.^[7]

Außerdem konnte das Guaia-6,10(14)-dien **VII** auch als Startmaterial für die Synthese zweier weiterer Sesquiterpenoide verwendet werden. Die Semisyntese von (-)-Oxyphyllol gelang in zwei Schritten durch zweifache stereoselektive Epoxidierung und anschließende selektive Epoxidöffnungen. Nach einer literaturbekannten Vorschrift konnte (-)-Oxyphyllol in drei Stufen in (+)-Orientalol E umgewandelt werden.^[8]

Außerdem konnten, aufbauend auf der bestehende Synthese nach CHRISTMANN insgesamt sieben neue (-)-Englerin A Derivate synthetisiert werden (Abbildung 1).

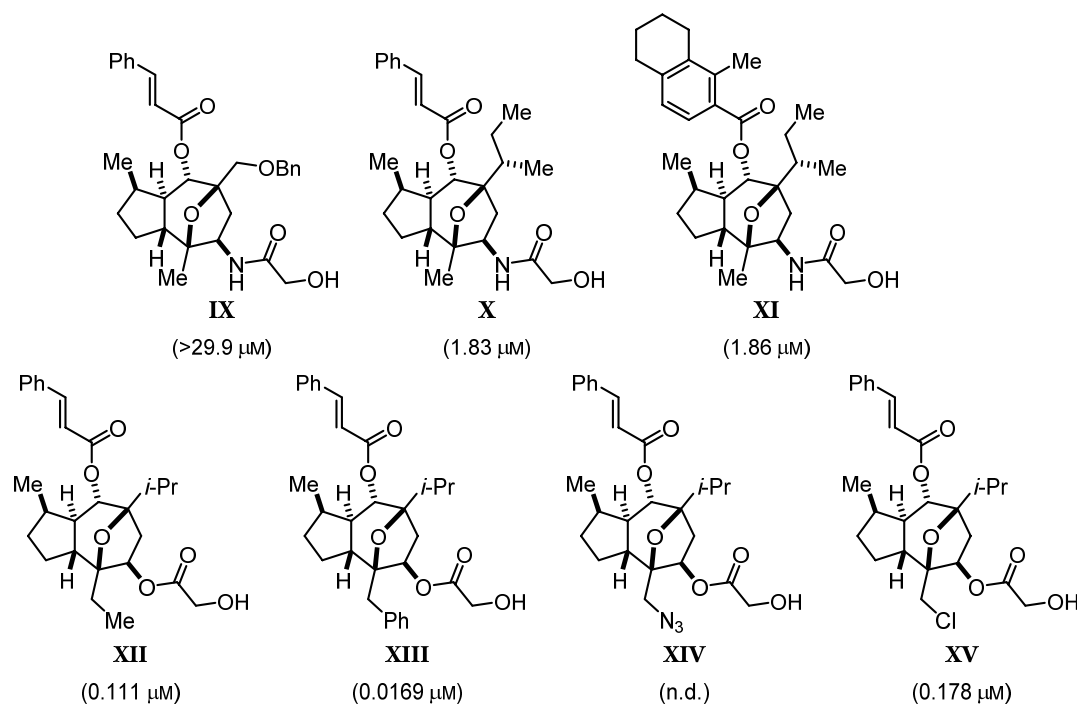


Abbildung 1. Synthetisierte (-)-Englerin A-Derivate. In Klammern: Inhibierung der Zellproliferation in der Nierenkrebszelllinie A498 (vgl. (-)-Englerin A: $\text{IC}_{50} = 0.049 \mu\text{M}$).

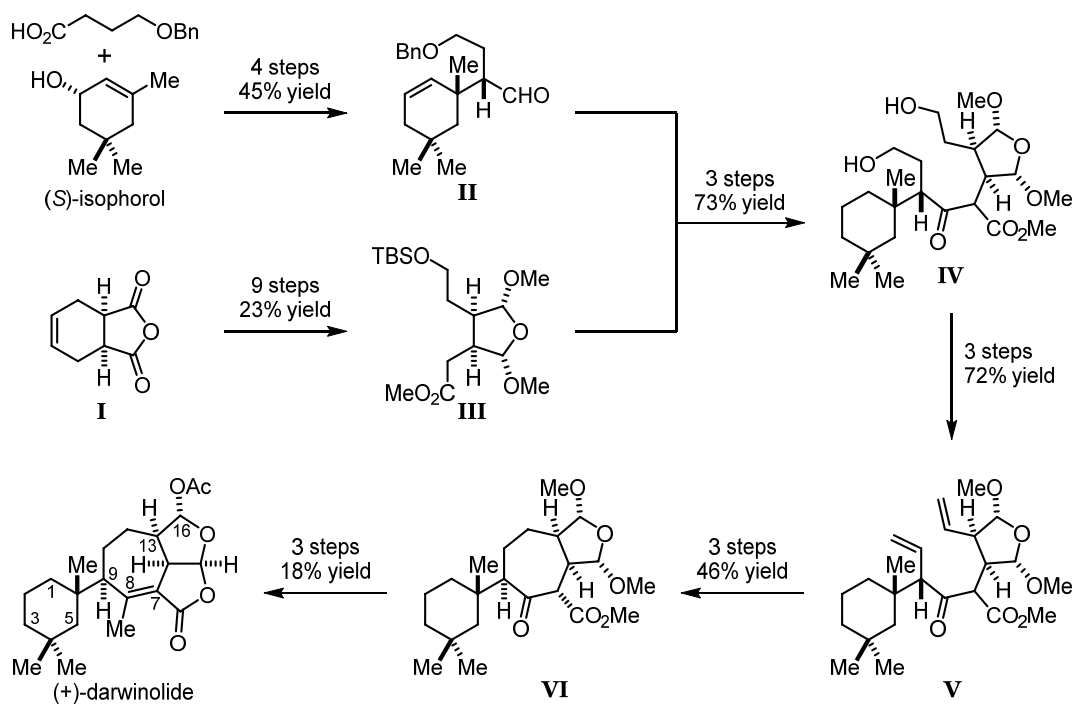
C9-Glykolamid-Derivate mit Benzyloxymethyl (**IX**) und (*S*)-*sec*-Butyl-Substituenten (**X** und **XI**) an Stelle der *iso*-Propyl-Gruppe an C7 wurden dargestellt. Diese weisen zwar eine erhöhte metabolische Stabilität im Vergleich zu den C9-Glykolat-Estern auf, jedoch einhergehend mit einer deutlichen Verringerung der inhibitorischen Aktivität.

Des Weiteren wurde die C10-Methyl-Gruppe erstmals derivatisiert. Durch die nukleophile Öffnung eines exocyclischen Epoxids konnten vier Derivate (**XII** – **XV**) gewonnen werden. Während die Ethyl- und Chloromethyl-Derivate (**XII** und **XV**) etwas niedrigere Aktivitäten aufweisen, ist das Benzyl-Derivat **XIII** fast dreimal aktiver als (-)-Englerin A. Das Azidomethyl-Derivat **XIV** wurde noch nicht untersucht.

Abstract

In the context of this thesis, two natural product synthesis projects were conducted. The first topic was the total synthesis of the rearranged diterpenoid (+)-darwinolide (**1**). This natural product was isolated from the Antarctic sponge *Dendrilla membranosa* in 2016 by BAKER et al.^[1] Darwinolide exhibits an inhibitory activity against the biofilm-phase of methicillin-resistant *Staphylococcus aureus* bacteria that is four times higher than the inhibition of the planktonic cells of the same strain. Intrigued by this unique biological profile, a synthesis of (+)-darwinolide was planned.

The first synthesis of (+)-darwinolide was successfully accomplished with 21 steps in the longest linear sequence and an overall yield of 1% (Scheme 1).^[2] The synthesis featured a convergent approach to install the C7–C8 bond in the central seven-membered ring by aldol addition of ester **III** to aldehyde **II**. The ester fragment **III** was obtained in 9 steps and 23% yield from commercially available *meso* anhydride **I**. The key-step in its synthesis was a highly enantioselective organocatalytic desymmetrization of a *meso* diol. The synthesis of the 1,3,3-trimethylcyclohexyl fragment **II** was achieved in 4 steps and 45% yield starting from the chiral (*S*)-isophorol that was obtained by enzymatic resolution. An IRELAND-CLAISEN rearrangement installed the stereo configuration of the quaternary center but favored the undesired configuration at the adjacent stereogenic center. Therefore, a late-stage epimerization at C9 was required.

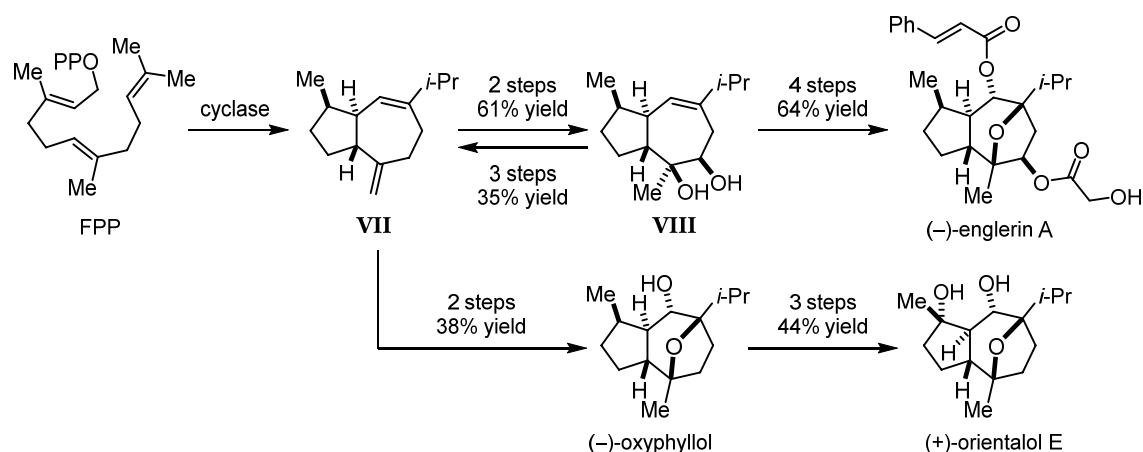


Scheme 1. Summary of the first total synthesis of (+)-darwinolide.

After the successful aldol fragment coupling, the two primary alcohols of intermediate **IV** were simultaneously eliminated to yield the metathesis precursor **V**. An olefin metathesis closed the seven-membered ring and at this stage, the C9 epimerization was possible. The β -keto ester **VI** was transformed into the tetrasubstituted olefin and coincidentally the fused lactone acetal was formed. Finally, an acid-catalyzed transacetalization yielded (+)-darwinolide.

The second project of this thesis concerned the sesquiterpenoid (-)-englerin A which was isolated from the root bark of the East African plant *Phyllanthus engleri* by BEUTLER et al. in 2009.^[3] (-)-Englerin A is a highly potent and selective inhibitor of renal carcinoma cell growth. After the first synthesis of the unnatural enantiomer by the group of CHRISTMANN,^[4] several other syntheses and biological studies have been reported. In the context of this thesis a novel semisynthetic access to (-)-englerin A should be found and new analogs should be synthesized.

At first, the guaia-6,10(14)-diene (**VII**) was synthesized in 3 steps starting from the diol intermediate **VIII** of CHRISTMANN's (-)-englerin A synthesis (Scheme 2).^[5] The group of DICKSCHAT studied the incubation of farnesyl pyrophosphate (FPP) with a mutated sesquiterpene cyclase from the plant pathogenic fungus *Fusarium fujikuroi* and isolated guaia-6,10(14)-diene **VII**. By comparison of the optical rotation values, the absolute configuration of guaia-6,10(14)-diene **VII** was confirmed. The biosynthetic mechanism for this sesquiterpene cyclase was elucidated by studying ²H and ¹³C-labelled FPP isotopomers.^[6]



Scheme 2. Semisynthesis of (-)-englerin A, (-)-oxyphyllol and (+)-orientalol E, starting from the biosynthesis product guaia-6,10(14)-diene **VII**. The diene **VII** was also synthesized starting from diol **VIII** in order to determine the absolute configuration of the product **VII** obtained by incubation of FPP with sesquiterpene cyclase 5 for *Fusarium fujikuroi*.^[6]

The group of LIU was able to produce the guaia-6,10(14)-diene (**VII**) on gram scale by genetic engineering of the mevalonate pathway in *Escherichia coli* and *Saccharomyces cerevisiae*. This enabled the use of guaia-6,10(14)-diene **VII** as a starting material for a concise semisynthesis of (-)-englerin A (Scheme 2). The isomerization of the exocyclic double bond into the internal position and the subsequent regio- and diastereoselective dihydroxylation afforded the diol intermediate **VIII** of CHRISTMANN's (-)-englerin A synthesis. Finally, a four-step sequence, previously optimized in the CHRISTMANN group, was applied to synthesize (-)-englerin A.^[7]

Furthermore, guaia-6,10(14)-diene **VII** proved to be a viable starting material also for the synthesis of the two related sesquiterpene natural products (-)-oxyphyllol and (+)-orientalol E. The synthesis of (-)-oxyphyllol was achieved in only two steps by diastereoselective bisepoxidation and subsequent one-pot regioselective hydride addition and transannular epoxide opening. Starting from (-)-oxyphyllol, (+)-orientalol was obtained in three more steps, applying a literature known procedure.^[8]

Additionally, the established total synthesis of (-)-englerin A was applied to synthesize new (-)-englerin A analogs (Figure 1).

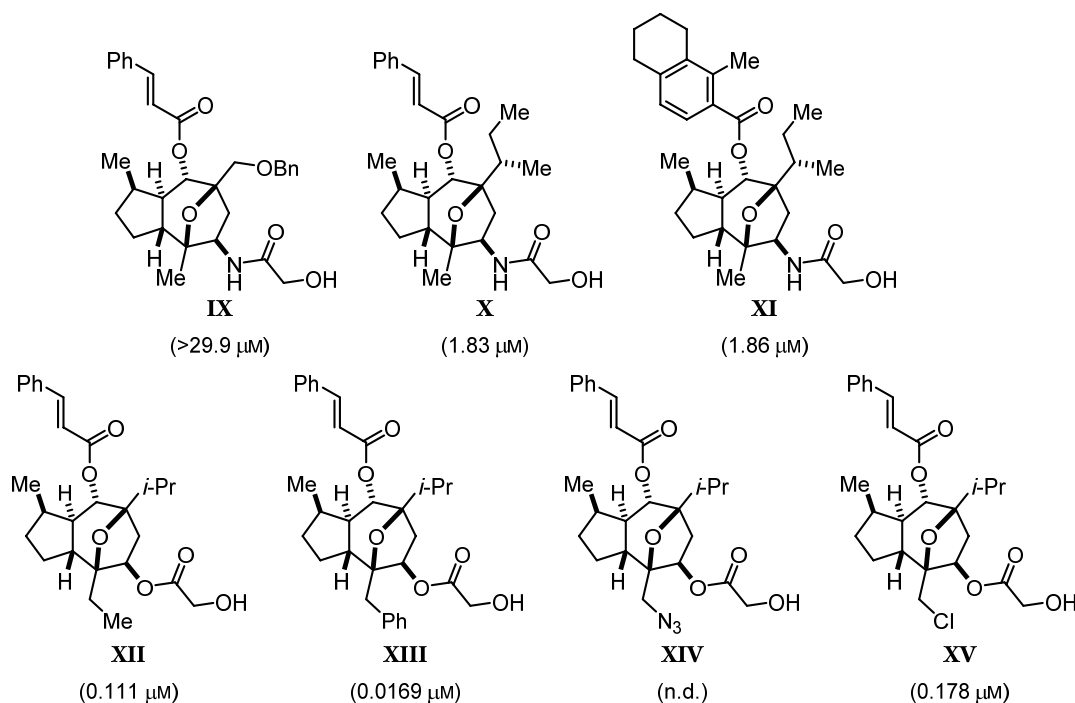


Figure 1. Synthesized (-)-englerin A analogs. Inhibition of cell proliferation in RCC line A498 (IC_{50}) in brackets, cf. (-)-englerin A: $IC_{50} = 0.049 \mu M$.

Since the C9 glycolate ester is metabolically unstable but essential for the biological activity, amide analogs bearing benzyloxymethyl (**IX**) and (*S*)-*sec*-butyl (**X** and **XI**) groups at C7 were synthesized. They exhibited a higher metabolic stability but were significantly less active than (-)-englerin A.

Furthermore, the C10 methyl group was subjected to functionalization for the first time. The ethyl (**XII**), benzyl (**XIII**), azidomethyl (**XIV**), and chloromethyl (**XV**) C10 analogs were obtained by nucleophilic opening of an exocyclic epoxide. The benzyl analog **XIII** is almost three-times more potent than (-)-englerin A and the ethyl and chloromethyl functionalities are also well tolerated. The azide analog **XIV** was not tested for its inhibitory activity, yet.

1 Motivation

1.1 Natural Products as Lead Structures in Drug Discovery

Over the course of three billion years, nature has developed a nearly endless diversity of secondary metabolites that are produced to protect organisms from predators, to help them to survive under extreme environmental conditions, or to ensure reproduction by attracting sexual partners. The majority of those secondary metabolites are comparably small molecules like terpenoids, alkaloids, or polyketides, that are referred to as natural products by medicinal chemists.^[9]

For millennia, humans have been utilizing the functional diversity of natural products as flavors and fragrances or for the treatment of diseases. While traditional medicine focused on the application of plants and crude plant extracts, modern pharmacology started to study their active ingredients. Early discoveries in the 19th century included the painkillers morphine and codeine from *Papaver somniferum* or the anti-malaria agent quinine from *Cinchona* species.^[10]

Until the middle of the 20th century, almost exclusively plant-derived natural products were used as drugs. Commencing with the discovery of penicillin in the 1930s, microbial sources developed into the main source for natural products in drug discovery. Since 2000, half of all approved natural product-based drugs and more than 60% of the new entities were based on bacterial or fungal sources (Figure 2).^[11] Microbial natural products are especially important as antibacterial agents, representing 69% of all antibiotics and 97% of the natural product based ones.

Despite decades of research, the surface of natural diversity has hardly been scratched. The pharmacological investigations of the terrestrial flora elucidated only about 6% of all plant species. Since the exploration of the marine environment just started in 1970s, due to advances in deep sea techniques, this source of natural products has barely been studied.^[12]

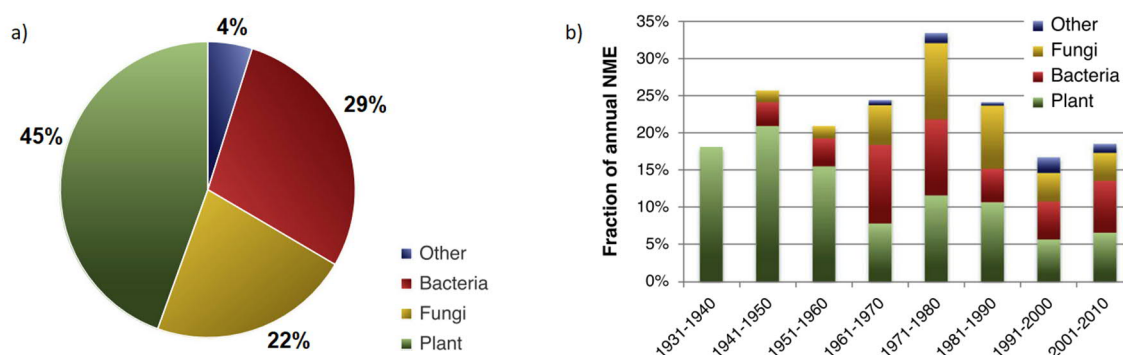


Figure 2. Natural product-based FDA-approved new molecular entities (NME): a) Cumulative percentage by environmental source; b) Fraction of annual NME separated by environmental source over time.^[11]

Analysis of the approved drugs by source highlights the importance of natural products. Just 35% of all small-molecule drugs are completely synthetic in origin. The other two thirds consist equally of natural product-derived drugs and synthetic drugs that either mimic natural products or possess pharmacophores that are directly derived from natural products (Figure 3a).^[10]

If one studies the number of approved drugs per year closely, it stands out that the average productivity of the pharmaceutical industry has declined from a peak in the 1980s until the middle of the 2000s (Figure 3b). This trend might be rationalized with a shift of focus in drug discovery, in favor of new chemical techniques that allows for high-throughput screening and the generation of large molecular libraries.

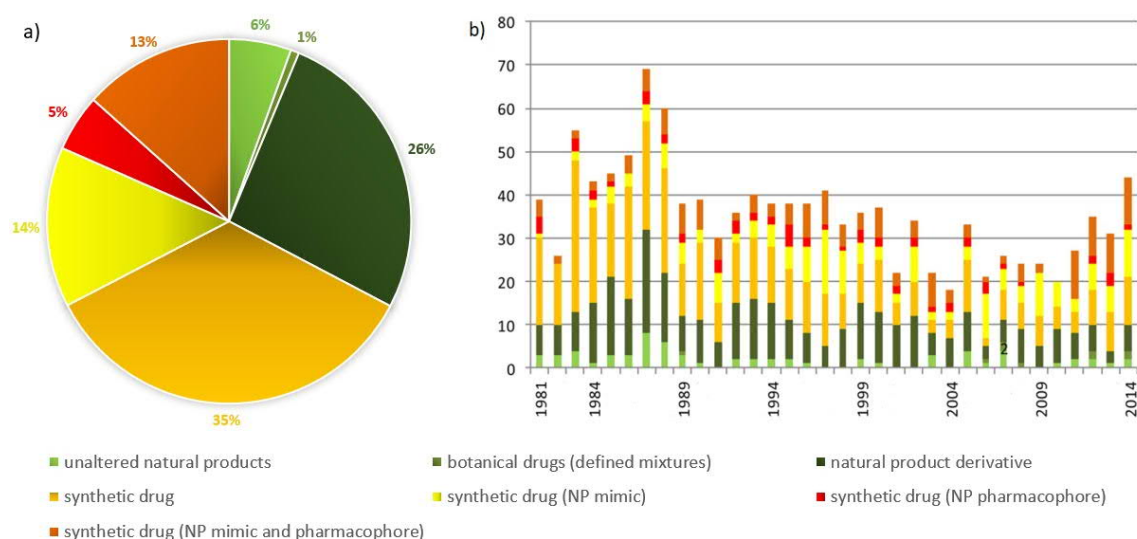


Figure 3. Statistics of all small-molecule drugs approved by the FDA from 1981 – 2014: a) Percentage by source, illustrating that 65% of the drugs are at least partially derived from natural products; b) Number of approved drugs by source per year, showing a downward trend in production from the 1980s until the 2000s.^[10]

The initial emphasis in the use of such *de novo* combinatorial chemistry approaches in drug discovery was to generate as many new compounds as possible by cross-coupling of different building blocks. The inefficiency of this approach is illustrated by the fact that only two drugs resulted directly from combinatorial chemistry (Figure 4b), the anti-cancer agent sorafenib (Nexavar[®]) and the genetic disorder-inhibitor ataluren (Translarna[®]).^[10] Early combinatorial libraries covered only a limited bioactive chemical space, since these structures are mostly aromatic and two-dimensional (Figure 4a). In contrast, natural products possess much more structural versatility, which allows them to selectively interact with molecular targets.^[13] In order to achieve a broader coverage of the bioactive chemical space, the focus shifted to smaller libraries of more complex, natural product-like structures, with an emphasis on building block-, functional group-, stereochemical and skeletal diversity.^[14]

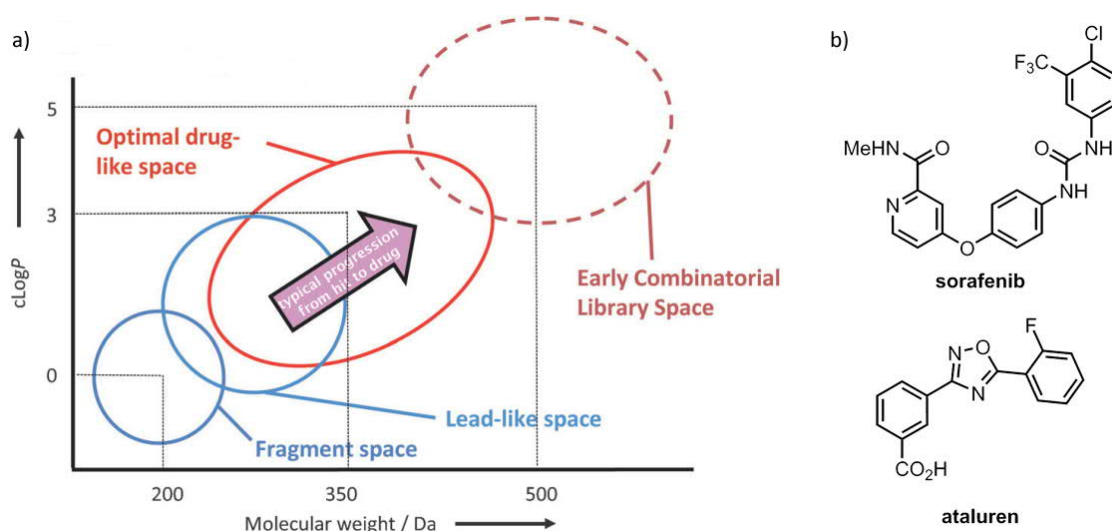


Figure 4. a) Analysis of the chemical space covered by early combinatorial libraries compared to the drug-like space;^[15] b) Structure of sorafenib and ataluren, the only two drugs derived from combinatorial chemistry.

Nowadays, the application of innovative technologies supports the discovery of molecular targets and the modelling of molecular interactions. This allows for the prediction of pharmacokinetic and pharmacodynamic features and parameters, which should result in better designed lead structures.^[16] As a result, the output of drug discovery programs has increased over the last few years to a record-breaking number of new approved drugs in 2018.^[17]

Also in natural product-based drug discovery, new frontiers have emerged due to the rapid evolution of genomic technologies. This permits the isolation and expression of biosynthetic cassettes, microbes, marine invertebrates and plant endophytes, leading to the discovery of previously unrecognized secondary metabolites from known microbial sources. The genomic information obtained this way can also support the identification of molecular targets.^[18]

1.2 Natural Product Synthesis in Drug Development

The major drawback for the application of natural products in drug discovery is their often tedious and low yielding isolation and the limited supply from natural sources. This can be a serious limiting factor in the preclinical and clinical development of naturally derived drugs. Natural product synthesis provides an important tool to obtain larger quantities of the compounds for screening and drug development purposes. Furthermore, the natural occurring compounds are often not selective and active enough towards a desired biological target. Total synthesis offers the possibility to identify more potent and sometimes structurally simpler natural product analogs by introducing precise functional modifications. An impressive example is the marine-derived anti-tumor agent halichondrin B (Figure 5). Synthetic

studies revealed that only one half of the molecule possesses its biological activity. This resulted in the development of the completely synthetic, structurally simplified anti-cancer drug eribulin (Halaven®).^[19]

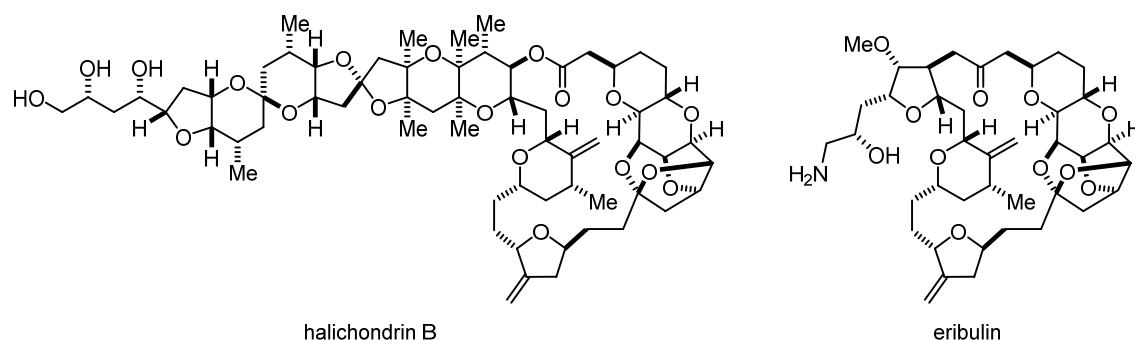
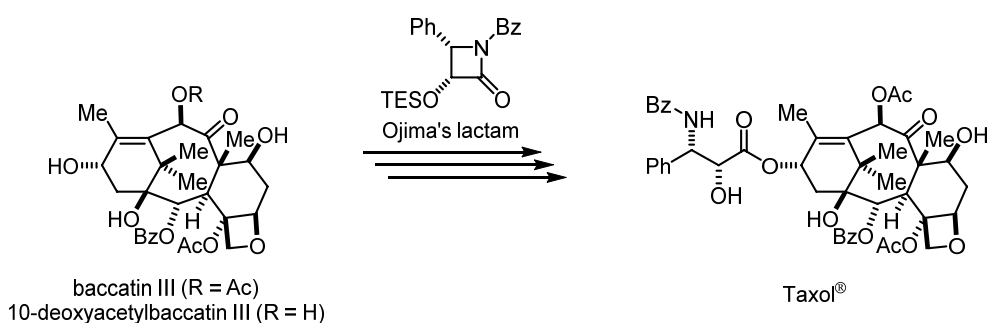


Figure 5. Structures of the marine natural product halichondrin B and the derived synthetic anti-tumor drug eribulin.

Although the total synthesis of complex natural products is an important process in drug discovery, since it offers the possibility for structure-activity relationship studies, sometimes it does not provide sufficient amounts for clinical studies and drug production. This issue can be solved by a semisynthetic approach, where an advanced intermediate is produced biosynthetically and converted into the final product by chemical transformations. A prime example for this approach is the anti-cancer agent paclitaxel (Taxol®) which was isolated from the bark of the Pacific yew *Taxus brevifolia*. Since the isolates of the natural product did not cover the worldwide demand of Taxol® and a total synthesis was not feasible on an industrial scale, a semisynthetic route was developed.^[20] The starting material 10-deoxygenylbaccatin III is isolated from the European yew *Taxus baccata* in large quantities. Recently, the bioproduction of baccatin III in the transgenic fungus *Flammulina velutipes* expressing the 10-deoxygenylbaccatin III-10 β -O-acetyltransferase gene was reported.^[21] Both compounds can be transformed into Taxol® in more than 50% yield and a maximum of four steps using Ojima's lactam for the tail addition (Scheme 3), whereas the shortest total synthesis requires 37 steps.^[22] This highlights the advantage of a semisynthesis over total synthesis in industrial production. However, the possibilities for derivatization in semisynthetic approaches is fairly limited and late-stage functionalization is a very complex issue.



Scheme 3. Semisynthetic access to the anti-cancer drug Taxol®.^[22a]

In the context of this thesis, both semi and total synthesis should be applied to obtain two highly biological active natural products (Figure 6).

The first project covers the synthesis of the biofilm-penetrating anti-MRSA agent (+)-darwinolide. Since this rearranged diterpenoid was only isolated in 2016, no synthesis has been reported until this thesis. Therefore, the first total synthetic access should offer the possibility to study the structural basis of darwinolide's unprecedented biological activity and its unknown mechanism-of-action.

In the second project, a well-established synthetic route towards the highly selective and active renal cancer inhibitor (-)-englerin A will be utilized to synthesize new analogs and perform structure-activity relationship studies. Furthermore, collaborations with two biosynthesis groups should result in a concise semisynthetic access to (-)-englerin A that would allow for the large-scale product of this promising drug-candidate.

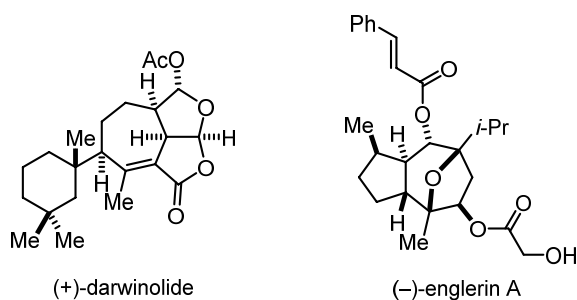


Figure 6. Structures of (+)-darwinolide and (-)-englerin A, the scientific goals of this thesis.

2 (+)-Darwinolide – A Biofilm-Penetrating Anti-MRSA Agent

2.1 Introduction

2.1.1 Methicillin-resistant *Staphylococcus Aureus* – A Global Health Risk

Due to the massive use of antibiotics since the middle of the 20th century, an increased amount of multi-drug resistant bacterial infections has occurred, which represents one of the major global healthcare problems nowadays.^[23] These germs include highly infectious strains of *Pseudomonas*, *Escherichia coli*, *Klebsiella pneumoniae* bacteria and especially methicillin-resistant *Staphylococcus Aureus* (MRSA). About one third of the global population is colonized by the gram-positive bacterium *Staphylococcus Aureus* (*S. Aureus*) and more than one percent of the people are carrying MRSA.^[24] Interestingly, the percentage of invasive MRSA isolates in European countries differs dramatically (0.9% in the Netherlands vs. 56% in Romania)^[25] and correlates with the frequency of antibiotics application.^[26] The majority of *S. Aureus* infections is asymptomatic but in case of an invasive infection the symptoms range from skin and soft tissue inflammation, pyomyositis to life-threatening diseases like endocarditis, pneumonia and sepsis.^[27] In the USA, approximately 100 000 invasive infections with MRSA were noted in 2005 which led to more than 18 500 deaths.^[28] This number is even higher than the annual AIDS death rate (17 000).^[29] Hospitals are the main site of MRSA infections, due to the colonization of medical equipment like catheters, the occurrence of open wounds and the generally weakened immune system of the patients.^[30] Further sites of infections include sport facilities and crowded places in general as well as livestock and agriculture, where the wide-spread use of antibiotics enhanced the number of resistant germs. Therefore, the risk of MRSA infections that could transfer to human is increased.^[31] Methicillin was discovered in 1959 to be the first β -lactamase-stable antibiotic,^[32] but just two years later, the first methicillin-resistant *S. Aureus* strains were isolated in Great Britain.^[33] Nowadays other β -lactam antibiotics like oxacillin, flucloxacillin or cefazolin are used as the standard treatment of methicillin-sensitive *S. Aureus* (MSSA) infections (Figure 7c). However, MRSA bacteria are resistant to all kinds of β -lactam antibiotics, since their antimicrobial mode-of-action, the inhibition of bacterial cell wall synthesis, is prevented.^[34] The cell wall in gram-positive bacteria consists of a network of peptidoglycan-strands formed by *N*-acetylmuramic acid (NAM) and *N*-acetylglucosamine (NAG), which are linked by two oligopeptides via a pentaglycine bridge (Figure 7a).^[35] Cross-linking of the two oligopeptides is facilitated by a transpeptidase, the penicillin-binding protein II (PBPIIa).^[36] β -Lactam antibiotics permanently bind to the active site of the PBPIIa and thus inactivate the transpeptidase activity that is critical for the cell wall synthesis and bacterial growth (Figure 7b). The resistance to β -lactam antibiotics

is genetically based and mediated by the Staphylococcal cassette chromosome mec (SCCmec), a genomic island that contains the resistance gene *mecA*.^[37] A mutation of the PBPIIa caused by *mecA* inhibits the binding of the antibiotics to the active site and therefore their antimicrobial activity. The SCCmec might originate from a different *Staphylococcus* species (*S. Sciuri*) by horizontal-gene transfer to *S. Aureus* and its acquisition in MSSA resulted in the formation of MRSA bacteria.^[38] Since SCCmec expresses different genotypes, a number of different MRSA lineages exist with various resistance rates and types.

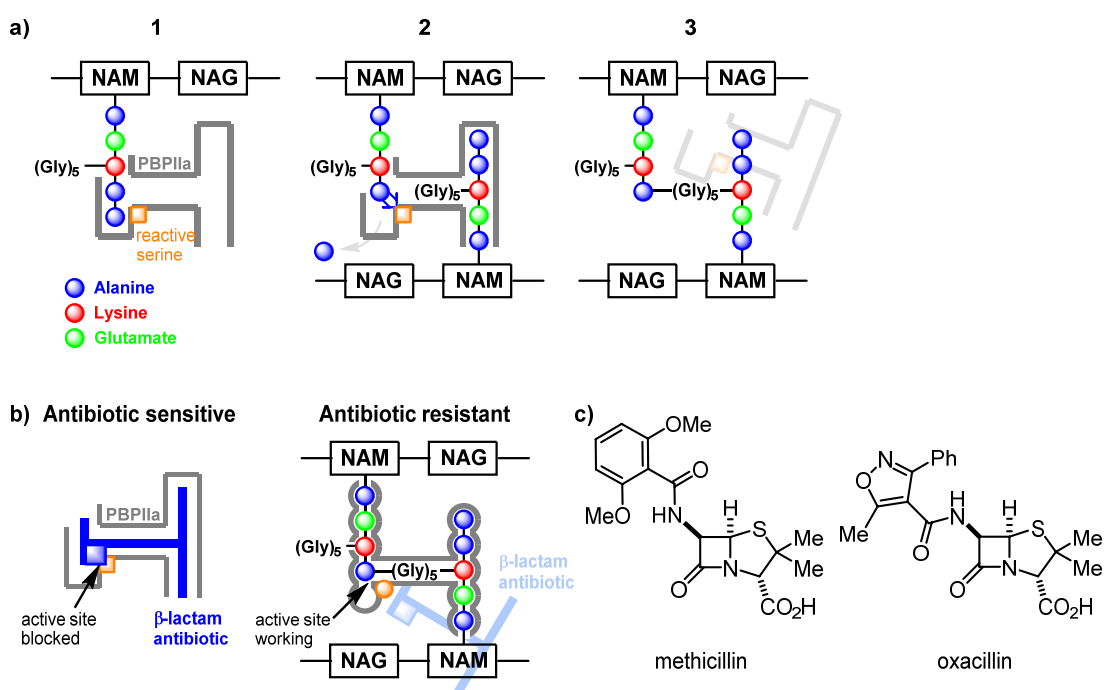


Figure 7. a) Bacterial cell wall synthesis: (1) A peptidoglycan-strand consisting of *N*-acetylmuramic acid (NAM) and *N*-acetylglucosamine (NAG) approaches the active site of the penicillin binding protein (PBPIIa); (2) The oligopeptide side-chain binds to the reactive serine by cleaving the terminal D-alanine, (3) Two peptidoglycan-strands are connected via a pentaglycine bridge (Gly)₅ and the PBPIIa diffuses off; b) β-Lactam antibiotics resistance mechanism; c) Structure of β-lactam antibiotics methicillin and oxacillin.

In most cases of MRSA infections, vancomycin or daptomycin are recommended for its treatment (Figure 8).^[39] However, these antimicrobial agents have some significant limitations. Vancomycin for example poorly penetrates lung tissue and the onset bactericidal activity is relatively low.^[40] Its mode of action is similar to β-lactam antibiotics, since it also inhibits the cell wall synthesis. Vancomycin is able to form hydrogen bonds to the D-alanyl-D-alanine terminus of the oligopeptide moiety and thus inhibits the cross-linking of the peptidoglycan-strands.^[41] An increasing number of partially (vancomycin-intermediate *S. Aureus*, VISA)^[42] or completely vancomycin-resistant *S. Aureus* (VRSA)^[43] has been reported lately. The minimum inhibitory concentration (MIC) has slowly increased since the 1990s, which results in higher doses required to maintain efficacy.^[44] One resistance mechanism against

vancomycin results from an alteration of the terminal amino acid sequence which reduces the affinity of vancomycin significantly due to the loss of hydrogen bonding interactions.^[45]

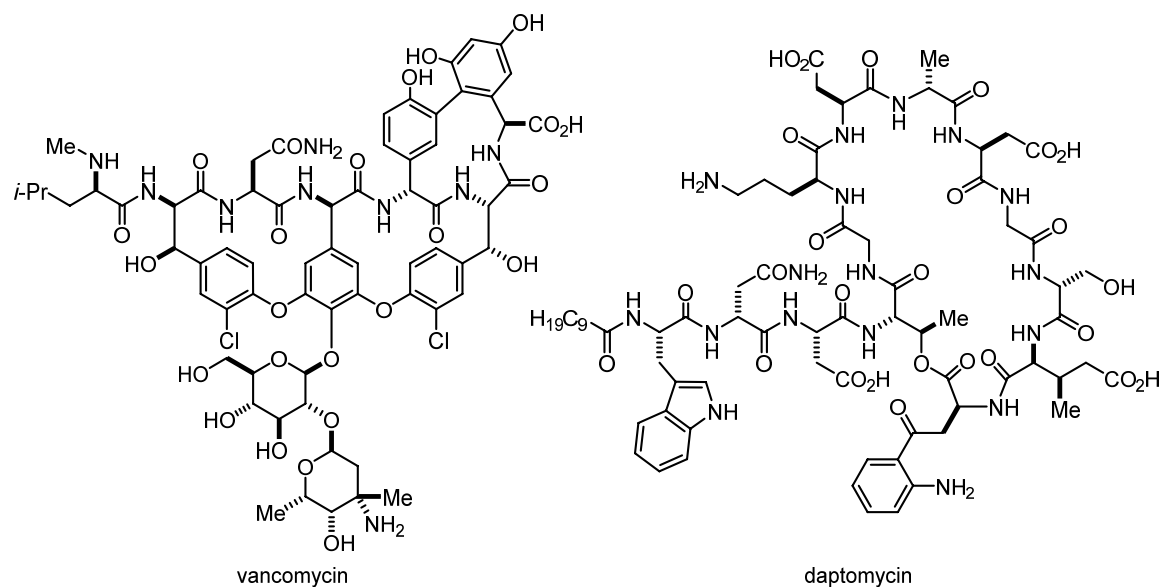


Figure 8. Structures of vancomycin and daptomycin – the standard antibiotics for the treatment of MRSA infections.

If the therapy with vancomycin fails, the treatment with daptomycin is recommended.^[39] Daptomycin was shown to be more effective than vancomycin for the treatment of some MRSA infections and resistances have rarely been reported with daptomycin, yet.^[46] However, there is evidence that a prior treatment with vancomycin could cause cross-resistance to daptomycin.^[47] The mechanism-of-action is different to other antibiotics, as daptomycin does not cause cell lysis. Daptomycin is incorporated into the cell membrane but not into the cell wall and creates holes in the membrane that leak calcium-ions.^[48] Thus, the resulting loss of membrane potential inhibits bacterial peptide-, DNA and RNA-synthesis and therefore leads to cell death.

Alternative therapeutic strategies have been studied, for example the use of different antibiotics like ceftaroline, linezolid or teicoplanin.^[49] Another option is a combination therapy, where vancomycin or daptomycin is applied together with β -lactam antibiotics, resulting in reduction of treatment time and persistent bacteria.^[50]

However, there is still no efficient treatment for all kinds of MRSA infections and the ongoing evolution of resistances towards common antimicrobial agents makes the development of new anti-MRSA agents a highly important issue.

2.1.2 Microbial Biofilms

A biofilm is defined as an aggregation of microorganisms that irreversibly adhere to each other and in most cases to a surface (Figure 9). The microbial cells are embedded within a self-produced matrix of extracellular polymeric substances (EPS).^[51] Although biofilms usually form at solid surfaces exposed to an aqueous environment, virtually every non-sterile surface can potentially be colonized by biofilms. They can thrive under extreme conditions like hot springs and frozen glaciers as well as very acidic or basic media.^[52] In human environments biofilms are growing for example in showers, at boat hulls and inside water pipes, causing clogging, biofouling and corrosion. Biofilms in the human body are involved in several infectious diseases like periodontitis, tooth decay, bacterial vaginosis, sinusitis, middle-ear infections, osteomyelitis, Lyme disease, endocarditis and cystic fibrosis.^[53] In chronic wound infections, biofilms are the main reason for their persistence and possible bacteremia. Moreover, biofilms are involved in device-associated infections as they colonize catheters, implants and other medical instruments. Especially, plastic devices are at risk due to the affinity of microorganisms to colonize surfaces containing biomaterials.

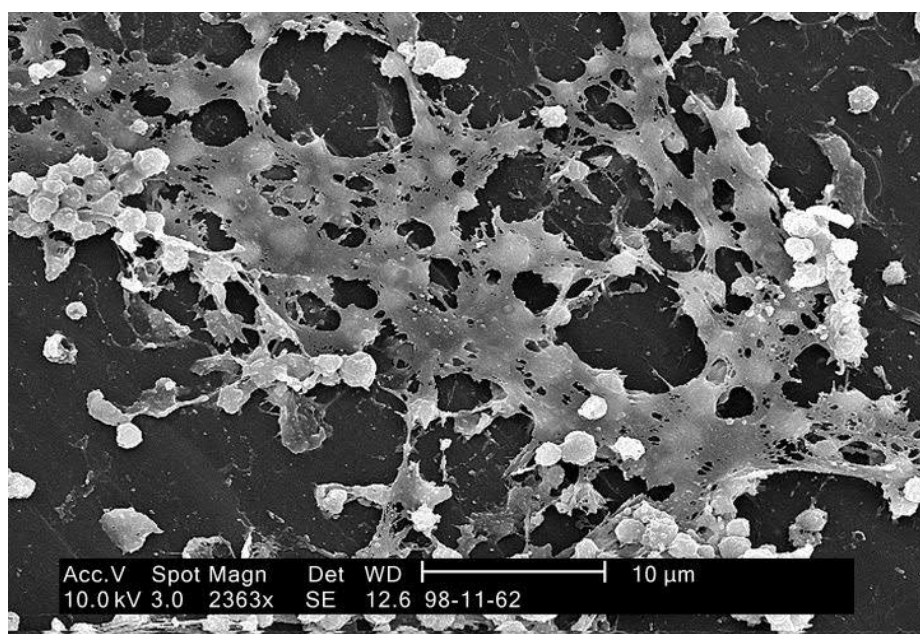


Figure 9. Electron Micrograph of a *S. Aureus* Biofilm.

Biofilm consist of less than 10% microorganisms (bacteria, fungi, algae, archaea etc.) in the dry mass. The remaining 90% are a highly hydrated matrix consisting of extracellular polymeric material (polysaccharides, proteins, nucleic acids and lipids).^[54] This EPS matrix provides the mechanical stability of the biofilm, mediates its adhesion to the surface and forms a three-dimensional network that permanently immobilizes the biofilm cells. Furthermore, the matrix facilitates horizontal transfer of

resistance genes and acts as an external digesting system by trapping extracellular enzymes and keeping them in close proximity. Bacteria within a biofilm have significantly different properties than the free-floating so-called planktonic cells. The dense and protected environment allows them to cooperate and interact, resulting in an increased resistance to detergents and antibiotics. Due to a decreased growth rate and a reduced metabolism of the bacteria within the biofilms, antimicrobial agents have very little effect. The formation of biofilms is generally described as a sequence of five stages (Figure 10).^[55] In the first two stages, the planktonic microorganisms attach to a surface by Van-der-Waals and hydrophobic interactions and subsequently adhere permanently to the surface. Stage three and four involve the growth and maturation of the biofilm by a combination of cell division and incorporation of external materials. Bacterial biofilms typically consist mainly of polysaccharide but also additional materials like soil particles, minerals and blood compounds are enclosed into the matrix at this stage. In the final stage, the fully established biofilm changes in shape and size and thereby releases cells from the biofilm. This dispersal results in the spread and colonization of new surfaces and therefore accounts for the virulence of biofilm-associated infections. The dispersed cells possess a unique phenotype and therefore significantly different properties than both planktonic and biofilm cells. Dispersed cells were found to be highly virulent against macrophages and *Caenorhabditis elegans*. In contrast to planktonic cells, the dispersed cells are lacking siderophores, resulting in a higher sensitivity to iron stress.^[56]

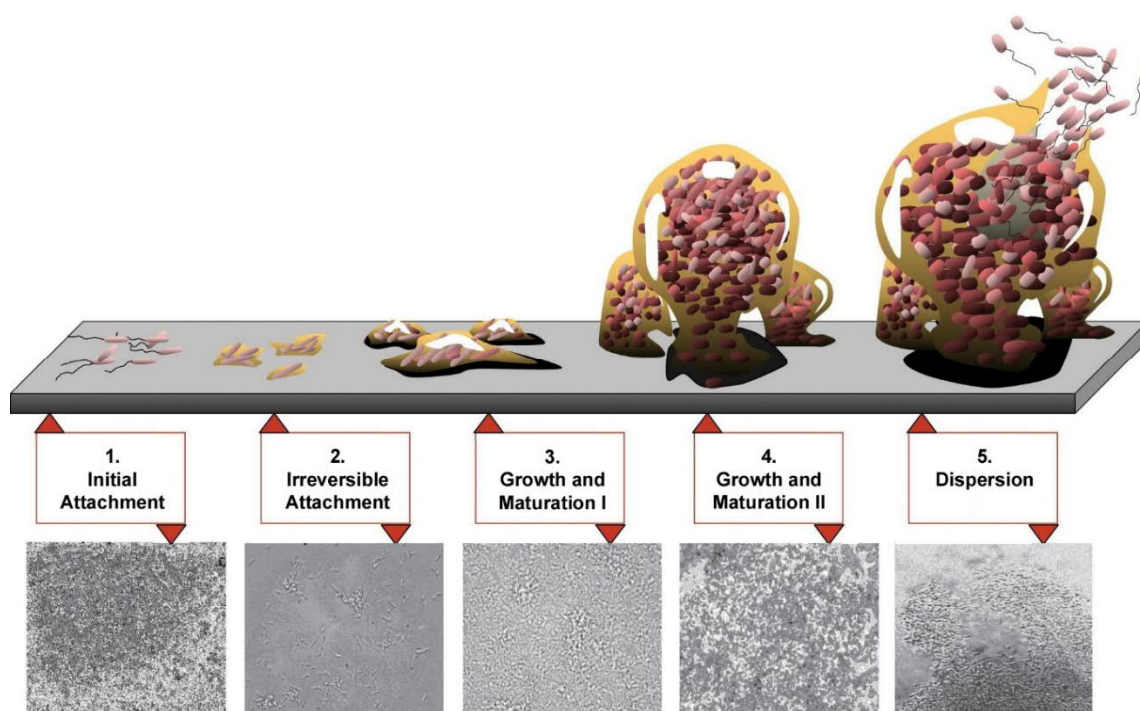


Figure 10. Five stage of biofilm formation: Schematic depiction and the associated photomicrograph of a developing *Pseudomonas aeruginosa* biofilm.^[55b]

While the majority of concepts against biofilms are based on the prevention of the initial attachment by modifying the surface (e.g. bactericidal or bacteriostatic coating, silver nanoparticles and small molecule inhibitors like calcium chelators), the dispersal process has not attracted so much attention.^[57] However, some enzymes like dispersin B, DNase I, Proteinase K and Lysostaphin have been described to degrade the EPS matrix and thus facilitate the dispersal of biofilms. This might find application in the development of anti-biofilm agents, although the *in vivo* efficacy of those enzymatic treatments is not well established and might cause adverse side reactions.^[58] Further biofilm inhibition strategies include small molecules like the fatty acid messenger *cis*-2-decenoic acid that induces dispersion of several gram-positive and gram-negative bacterial biofilms.^[59] Biofilm disassembly could also be triggered by a mixture of D-amino acids, that is implemented into the peptidoglycans and thus results in the release of the amylose fibers that link the cells.^[60] Alternative strategies like immunotherapy or bacteriophage therapy are still at an early stage in their development but the initial results are quite promising.^[57]

In conclusion, the significance of biofilms in infectious diseases has often not been recognized in the past and *in vitro* studies of planktonic bacteria do not represent the microbiology of biofilms very well. Therefore, there is still no validated strategy in place to treat infections that are caused by bacterial biofilms other than the complete removal of the infected tissue. However, this could be difficult, as biofilms are very heterogeneous, and a remaining small colony of microorganisms might lead to persistent infections. Thus, the development of an anti-biofilm specific agent is urgently required and of great public interest.

2.1.3 Darwinolide – Isolation and Biological Profile

In 2016, the group of BAKER extracted the Antarctic sponge *Dendrilla membranosa*, a member of the Darwinellidae family and isolated four natural products.^[1] Besides the previously reported natural products aplysulphurin,^[61] tetrahydroaplysulphurin,^[62] and membranolide,^[63] they also isolated the rearranged diterpene darwinolide (Figure 11). Its structure features a unique tricyclic core consisting of a [3.3.0]dioxabicyclopentanone fused to a cycloheptene. This unprecedented scaffold is linked to a 1,3,3-trimethylcyclohexyl moiety. The structure and absolute configuration of darwinolide was established unambiguously by single crystal X-ray analysis.

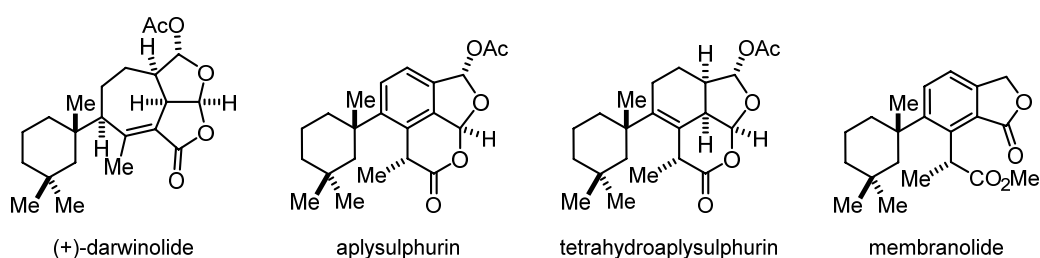
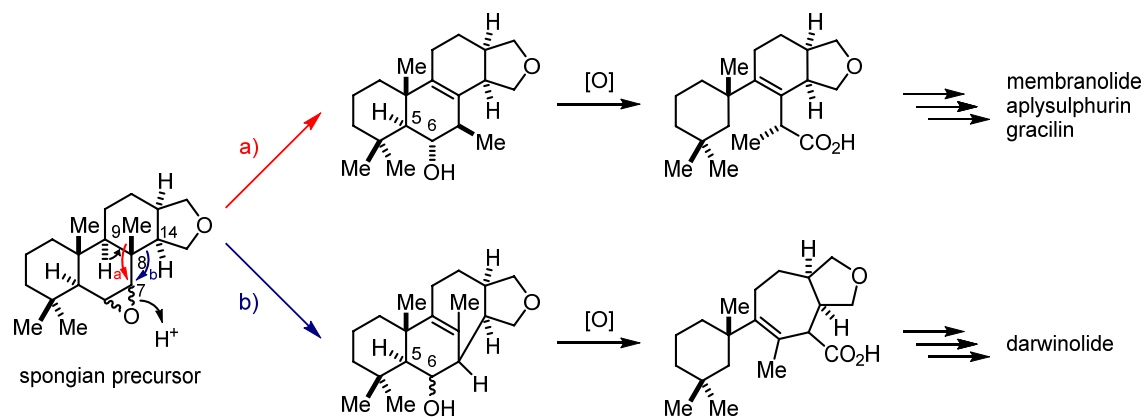


Figure 11. Structures of the natural products isolated from *Dendrilla membranosa* by BAKER et al.^[1]

Darwinolide was screened for activity against a clinical strain of a highly methicillin-resistant *S. aureus*. In a broth dilution assay darwinolide's minimal inhibitory concentration (MIC) was determined to be 132.9 μM . After darwinolide was washed out, only 1.6% of the treated bacteria were able to recover overnight. This indicated that darwinolide is cytotoxic rather than cytostatic. A biofilm of the same MRSA strain was established in vitro and an IC₅₀ value of 33.2 μM against this biofilm was determined. There is no treatment for MRSA biofilms available as a positive control, but the comparison with the literature revealed other more active biofilm inhibitors.^[64] However, in all precedented examples the planktonic cells were significantly more sensitive than those within a biofilm. Therefore, the four-fold selectivity of darwinolide for MRSA biofilms over planktonic cells is unique and combined with a low mammalian cytotoxicity (IC₅₀ = 73.4 μM against J774 macrophage cell line) makes darwinolide a promising candidate for the development of novel anti-biofilm specific antibiotics.

A biosynthetic proposal by BAKER et al.^[1] traced darwinolide and the other isolated diterpenes from *Dendrilla membranosa* back to a common spongian precursor (Scheme 4).^[65] A concerted cascade starting with the abstraction of the proton at C9 could either lead to a 1,2-methyl shift from C8 to C7 opening the α -epoxide (pathway a)^[65] or a rearrangement of C8–C14 bond might open the β -epoxide (pathway b). The second pathway might as well involve one or more carbocation intermediates to accommodate the stereochemical requirements of orbital orientation. Oxidative cleavage of the C5–C6

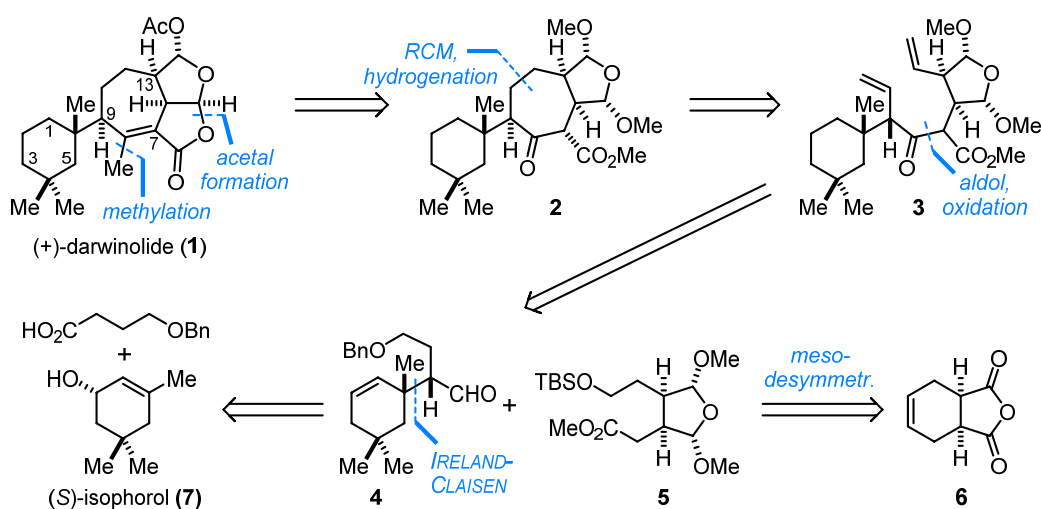
bond and further oxidative transformations could lead to the diterpene natural products membranulide, aplysulphurin and gracillin via pathway a or to darwinolide via pathway b.



Scheme 4. Possible biosynthetic pathway to the *Dendrilla membranosa* diterpene metabolites proposed by BAKER et al.^[65,1]

2.2 Scientific Goal

Intrigued by its promising biological profile and the unique structure, a total synthesis of (+)-darwinolide (**1**) was planned (Scheme 5). Since the fused lactone acetal is supposedly labile, its installation at the final stage was envisaged and the β -methyl-substituted α,β -unsaturated lactone was traced back to β -keto ester **2**. The two adjacent methylene groups within the seven-membered ring should allow for an olefin metathesis/hydrogenation transform leading to diene **3**. These terminal alkenes are envisaged to result from simultaneous eliminations of two primary alcohols. A convergent aldol disconnection of β -keto ester **3** leads to the equally complex aldehyde **4** and ester **5**. The quaternary stereocenter in aldehyde **4** can be installed by IRELAND-CLAISEN rearrangement of the ester derived from (*S*)-isophorol (**7**) and 4-(benzyloxy)butyric acid. Since this reaction would introduce the undesired stereo configuration adjacent to the aldehyde, a late stage epimerization at C9 was envisaged. Finally, the local symmetry of fragment **5** suggested a desymmetrization approach leading to the commercially available *meso* anhydride **6**.



Scheme 5. Retrosynthetic analysis for the total synthesis of (+)-darwinolide (**1**).

2.3 Publication

2.3.1 Synthesis of (+)-Darwinolide, a Biofilm-Penetrating Anti-MRSA Agent

THOMAS SIEMON, SIMON STEINHAEUER, MATHIAS CHRISTMANN*

Angew. Chem. Int. Ed. **2019**, *58*, 1120 – 1122. (DOI: 10.1002/anie.201813142)

Angew. Chem. **2019**, *131*, 1132 – 1134. (DOI: 10.1002/ange.201813142)

Permission granted for reproduction in print and electronic format for the purpose of this dissertation, by: *Angew. Chem. Int. Ed.* **2019**, *58*, 1120 – 1122, <http://dx.doi.org/10.1002/anie.201813142>.

Copyright: **2019** Wiley-VCH Verlag GmbH & Co. KGaA, Weinheim

Abstract: Darwinolide, a recently identified marine natural product from the Antarctic sponge *Dendrilla membranosa*, was previously shown to exhibit promising activity against the biofilm phase of methicillin-resistant *Staphylococcus aureus*. Its challenging tetracyclic rearranged spongian diterpenoid structure links a trimethylcyclohexyl subunit to a seven-membered core with two fused tetrahydrofuran units. Herein, we describe the first synthesis of (+)-darwinolide, which features a convergent aldol fragment coupling, an Ireland–Claisen rearrangement, and an organocatalytic desymmetrization as the key steps. Our results provide a foundation for the development of novel antibiofilm-specific antibiotics.

Authors Contribution:

T. SIEMON developed the synthetic strategy in cooperation with M. CHRISTMANN. All reactions were carried out and the analytic data (NMR, IR, HRMS, melting point, optical rotation) were collected and analyzed by T. SIEMON. The crystals for the X-ray diffraction analysis were provided by T. SIEMON and the co-author (S. STEINHAEUER) carried out the X-ray analysis. The draft for the manuscript was provided by T. SIEMON and revised by M. CHRISTMANN.



Synthesis of (+)-Darwinolide, a Biofilm-Penetrating Anti-MRSA Agent

Thomas Siemon, Simon Steinhauer, and Mathias Christmann*

Abstract: Darwinolide, a recently identified marine natural product from the Antarctic sponge *Dendrilla membranosa*, was previously shown to exhibit promising activity against the biofilm phase of methicillin-resistant *Staphylococcus aureus*. Its challenging tetracyclic rearranged spongian diterpenoid structure links a trimethylcyclohexyl subunit to a seven-membered core with two fused tetrahydrofuran units. Herein, we describe the first synthesis of (+)-darwinolide, which features a convergent aldol fragment coupling, an Ireland–Claisen rearrangement, and an organocatalytic desymmetrization as the key steps. Our results provide a foundation for the development of novel antibiofilm-specific antibiotics.

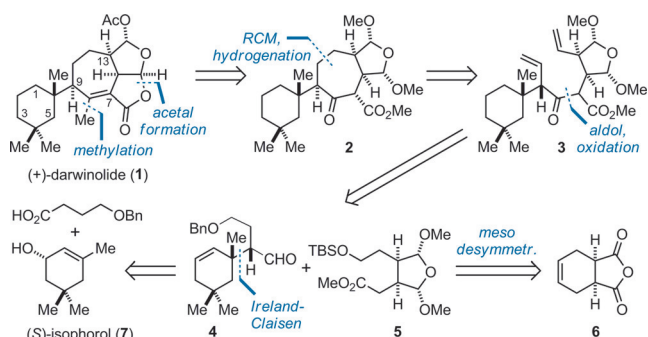
The vast majority of bacterial infections are considered to involve the formation of biofilms,^[1] an assemblage of microbial cells embedded within a self-produced extracellular polymeric matrix irreversibly attached to a surface. Chronical and persistent diseases such as osteomyelitis, rhinosinusitis, endocarditis, otitis media, and especially nosocomial infections are associated with biofilms of *Staphylococcus aureus*.^[2,3] Biofilm infections are resistant to conventional antimicrobial treatment,^[4] and low levels of β -lactam antibiotics may even induce the formation of biofilms in *S. aureus*.^[5] Thus the development of new antibiofilm agents for the treatment of drug resistant bacterial infections remains a priority.

In 2016, Baker and co-workers reported the isolation of the rearranged spongian diterpenoid darwinolide (**1**) from the Antarctic sponge *Dendrilla membranosa*.^[6] Darwinolide displays cytotoxic activity against a clinical strain of a highly methicillin-resistant *S. aureus* (MRSA) with a minimal inhibitory concentration (MIC) of 132.9 μM . An in vitro established biofilm of the same MRSA strain was inhibited with an IC_{50} value of 33.2 μM . This unique fourfold selectivity for MRSA biofilms over planktonic cells coupled with a low mammalian cytotoxicity (IC_{50} = 73.4 μM against J774 macrophage cell line) makes darwinolide a promising candidate for the development of novel antibiofilm-specific antibiotics.

Darwinolide's structure features a [3.3.0]dioxabicyclooctanone^[7] fused to a cycloheptene. This unprecedented tricyclic core is linked to a trimethylcyclohexyl moiety and was

suggested to result from a ring-expansion rearrangement of a common spongian precursor.^[6] The structure and absolute configuration of darwinolide were established unambiguously by single-crystal X-ray analysis.

Intrigued by its unique structure and the promising biological profile, we embarked on a total synthesis of **1**. As outlined in our retrosynthetic analysis (Scheme 1), we decided to construct the supposedly labile fused lactone acetal at the final stage of the synthesis while the tetrasubstituted double bond was traced back to a β -keto ester (**2**).



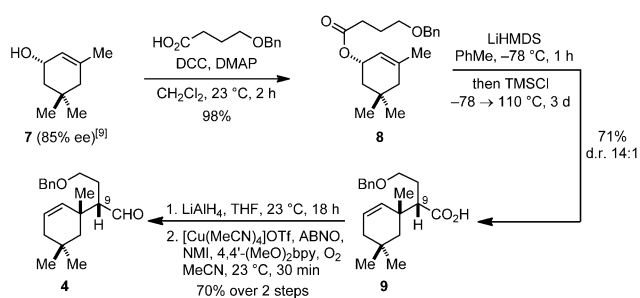
Scheme 1. Retrosynthetic analysis. RCM = ring-closing metathesis.

The two adjacent methylene groups within the seven-membered ring should allow for an olefin metathesis/hydrogenation process, leading to precursor **3**. The terminal alkenes in **3** were envisaged to result from a simultaneous elimination of two primary alcohols. A convergent aldol disconnection of β -keto ester **3** leads to the equally complex aldehyde **4** and ester **5**. The key step in the synthesis of the 1,3,3-trimethylcyclohexyl fragment **4** is an Ireland–Claisen rearrangement of the ester derived from 4-(benzyloxy)butyric acid and (*S*)-isophorol (**7**). Finally, the local symmetry of fragment **5** suggested a desymmetrization approach, leading back to the commercially available *meso* anhydride **6**.

Our synthesis started with a Steglich esterification^[8] of 4-(benzyloxy)butanoic acid and (*S*)-isophorol (**7**; Scheme 2), which was available in 85% *ee* by enzymatic resolution of the commercially available racemic alcohol.^[9] An Ireland–Claisen rearrangement^[10] of ester **8** proceeded with a yield of 71% to afford isomer **9** in a diastereomeric ratio of 14:1. As the stereogenic center adjacent to the carboxylic acid possesses the undesired configuration, an epimerization was required at a later stage. Interestingly, having the undesired configuration at C9 came as a blessing in disguise as it turned out to be beneficial in the subsequent aldol step. Reduction of the carboxylic acid **9** and subsequent copper-catalyzed

[*] M. Sc. T. Siemon, Dr. S. Steinhauer, Prof. Dr. M. Christmann
Freie Universität Berlin
Institute of Chemistry and Biochemistry
Takustr. 3, 14195 Berlin (Germany)
E-mail: mathias.christmann@fu-berlin.de

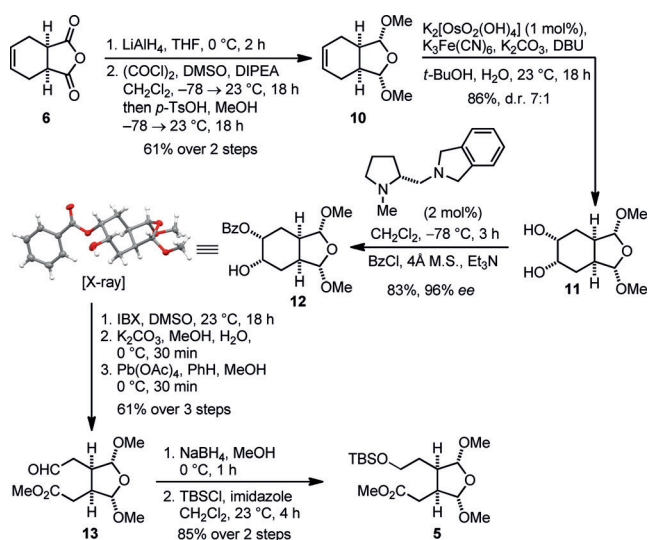
Supporting information and the ORCID identification number(s) for the author(s) of this article can be found under:
<https://doi.org/10.1002/anie.201813142>.



Scheme 2. Construction of the 1,3,3-trimethylcyclohexyl fragment **4**. ABNO = 9-azabicyclo[3.3.1]nonane *N*-oxyl, Bn = benzyl, bpy = 2,2'-bipyridine, DCC = dicyclohexyl carbodiimide, DMAP = 4-(dimethylamino)pyridine, LiHMDS = lithium hexamethyldisilazide, NMI = *N*-methylimidazole, TMS = trimethylsilyl.

aerobic oxidation under Stahl's conditions^[11] gave access to aldehyde **4** in 70% over two steps.

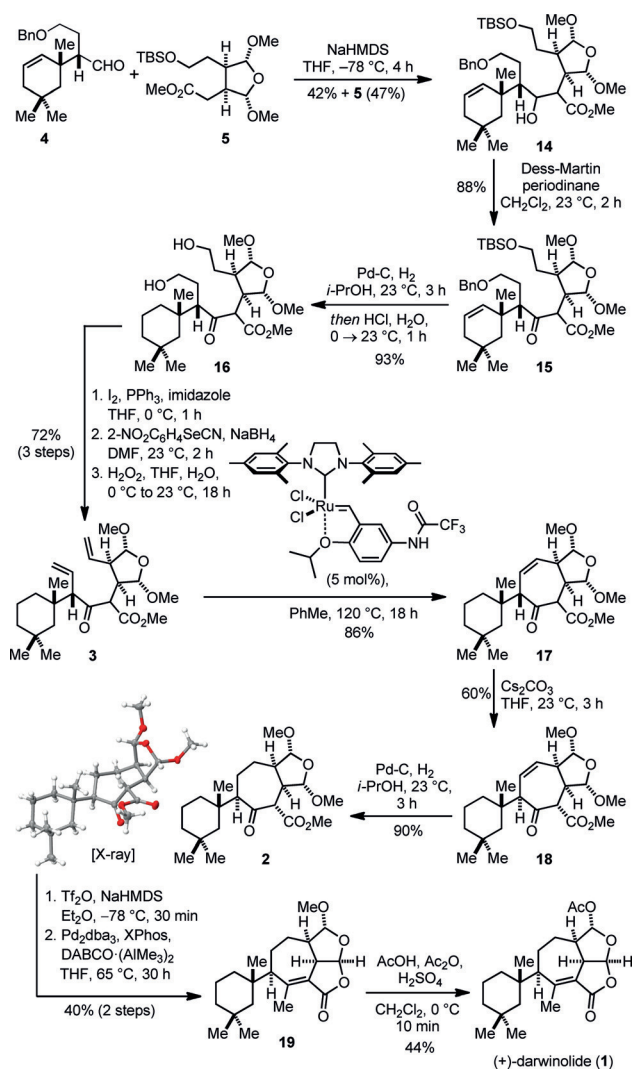
The synthesis of the tetrahydrofuran fragment **5** began with the reduction of the commercially available anhydride **6** with LiAlH₄ (Scheme 3). A one-pot procedure for the synthesis of bis-acetal **10** involved a Swern oxidation^[12] to the dialdehyde followed by an acid-catalyzed bis-acetalization. Dihydroxylation under Sharpless's conditions^[13] proceeded smoothly to give **11** in 86% yield and a diastereomeric ratio of 7:1 in favor of an attack from the convex face. Under Upjohn conditions (K₂[OsO₂(OH)₄], NMO, citric acid),^[14] an even better stereoselectivity (17:1 d.r.) could be achieved, but the yield was lower (65%) and the isolation troublesome. Desymmetrization of *meso*-diol **11** was accomplished using 2 mol % of Oriyama's proline-derived catalyst.^[15] Monobenzoate **12** was obtained in 83% yield and with excellent enantioselectivity (96% *ee*). The absolute configuration of **12** was confirmed by single-crystal X-ray analysis. A sequence of IBX oxidation, saponification, and Criegee oxidation^[16] of an α -hydroxy ketone intermediate with Pb(OAc)₄ afforded



Scheme 3. Synthesis of methyl ester **5** by a desymmetrization approach.^[22] Bz = benzoyl, DBU = 1,8-diazabicyclo[5.4.0]undecane, DIPEA = diisopropylethylamine, IBX = 2-iodoxybenzoic acid, M.S. = molecular sieves, *p*-Ts = *para*-toluenesulfonyl, TBS = *tert*-butyldimethylsilyl.

aldehyde **13** in 61% yield over three steps. After reduction with NaBH₄, protection of the primary hydroxy group as a benzyl moiety was possible but suffered from unsatisfactory yields. As a viable alternative, we obtained *tert*-butyldimethylsilyl ether **5** in 85% yield over two steps.

With aldehyde **4** and ester **5** in hand, an aldol reaction was performed (Scheme 4). While the transformation proceeded cleanly, full conversion could not be achieved. Interestingly, the aldol reaction of the (desired) C9 epimer was rather sluggish. Starting material **5** could be recovered in 47%, thus β -hydroxy ester **14** was obtained as a single diastereomer in 78% yield after four cycles. The configurations of the newly formed stereogenic centers were not determined as they were inconsequential for the final product. After a Dess–Martin oxidation^[17] of **14** to ketone **15**, the olefin was reduced and the protecting groups were removed by hydrogenolysis and the subsequent acidic workup, respectively, to give diol **16** in 93% yield. A direct elimination under Sharpless–Grieco conditions^[18] was unsuccessful, but a three-step sequence could be



Scheme 4. Formation of the central seven-membered ring and conclusion of the total synthesis of darwinolide.^[22] DABCO = 1,4-diazabicyclo[2.2.2]octane, dba = dibenzylideneacetone, Tf = trifluoromethanesulfonyl.

established in which both alcohols were eliminated simultaneously in 72% overall yield. The diol **16** was first transformed into the diiodide under Appel conditions, which was then treated with sodium 2-nitrophenylselenide generated in situ from 2-nitrophenylselenocyanate and NaBH₄.^[19] Upon oxidation with H₂O₂, diene **3** was obtained. A ring-closing metathesis^[20] was carried out with Umicore's M71SIMEs catalyst to generate the central seven-membered core structure **17** in 86% yield.

Epimerization at C9 was accomplished under basic conditions to afford the thermodynamically favored β-keto ester **18**. While the C11/C12 alkene certainly increases the acidity at the C9 position, alkene migration was not observed. After hydrogenation of the double bond, the correct configuration of the core structure **2** was confirmed by single-crystal X-ray analysis. Subsequently, β-keto ester **2** was transformed into the corresponding vinyl triflate. In the following methylation, the best results were obtained with Woodward's cross-coupling procedure,^[21] using Pd₂dba₃ and XPhos as precatalysts and a 2:1 adduct of Me₃Al and 1,4-diazabicyclo-[2.2.2]octane (DABCO) as the methyl source. Under these conditions, we also observed the formation of the fused lactone acetal moiety, which led to the tricycle **19** in 40% yield over two steps. Finally, (+)-darwinolide (**1**) was obtained by trans-acetalization with AcOH, Ac₂O, and H₂SO₄.

In conclusion, we have achieved the first synthesis of darwinolide in 21 steps in the longest linear sequence with an overall yield of 1.4%. Our synthetic approach offers the possibility to explore the structural basis of darwinolide's unique biological profile through the generation of analogues featuring deep-seated modifications.

Acknowledgements

We thank Umicore N.V. for the donation of the metathesis catalyst M71SIMEs. We thank Malte Brie (HU Berlin) and Jonas Genz (FU Berlin) for synthetic and Christiane Groneberg (FU Berlin) for analytical support.

Conflict of interest

The authors declare no conflict of interest.

Keywords: antibiotics · darwinolide · marine natural products · terpenoids · total synthesis

How to cite: *Angew. Chem. Int. Ed.* **2019**, *58*, 1120–1122
Angew. Chem. **2019**, *131*, 1132–1134

[1] C. A. Fux, J. W. Costerton, P. S. Stewart, P. Stoodley, *Trends Microbiol.* **2005**, *13*, 34.

- [2] J. W. Costerton, P. S. Stewart, E. P. Greenberg, *Science* **1999**, *284*, 1318.
- [3] A. S. Lynch, G. T. Robertson, *Annu. Rev. Med.* **2008**, *59*, 415.
- [4] U. Römling, C. Balsalobre, *J. Intern. Med.* **2012**, *272*, 541.
- [5] J. B. Kaplan, E. A. Izano, P. Gopal, M. T. Karwacki, S. Kim, J. L. Bose, K. W. Bayles, A. R. Horswill, *mBio* **2012**, *3*, e00198-12.
- [6] J. L. von Salm, C. G. Witowski, R. M. Fleeman, J. B. McClintock, C. D. Amsler, L. N. Shaw, B. J. Baker, *Org. Lett.* **2016**, *18*, 2596.
- [7] For selected syntheses of rearranged spongian diterpenoids, see: a) Y. Slutskyy, C. R. Jamison, P. Zhao, J. Lee, Y. H. Rhee, L. E. Overman, *J. Am. Chem. Soc.* **2017**, *139*, 7192; b) A. D. Lebsack, L. E. Overman, R. J. Valentekovich, *J. Am. Chem. Soc.* **2001**, *123*, 4851; c) T. P. Brady, S. H. Kim, K. Wen, E. A. Theodorakis, *Angew. Chem. Int. Ed.* **2004**, *43*, 739; *Angew. Chem.* **2004**, *116*, 757; d) E. J. Corey, M. A. Letavic, *J. Am. Chem. Soc.* **1995**, *117*, 9616; e) D. J. Tao, Y. Slutskyy, L. E. Overman, *J. Am. Chem. Soc.* **2016**, *138*, 2186; f) M. J. Schnermann, L. E. Overman, *J. Am. Chem. Soc.* **2011**, *133*, 16425; g) M. R. Garnsey, Y. Slutskyy, C. R. Jamison, P. Zhao, J. Lee, Y. H. Rhee, L. E. Overman, *J. Org. Chem.* **2018**, *83*, 6958.
- [8] B. Neises, W. Steglich, *Angew. Chem. Int. Ed. Engl.* **1978**, *17*, 522; *Angew. Chem.* **1978**, *90*, 556.
- [9] a) K. Winska, C. Wawrzenczyk, *Pol. J. Chem.* **2007**, *81*, 1887; b) K. Winska, C. Wawrzenczyk, J. Kula, PL209581 (B1), **2011**.
- [10] a) R. E. Ireland, R. H. Mueller, *J. Am. Chem. Soc.* **1972**, *94*, 5897; b) R. E. Ireland, R. H. Mueller, A. K. Willard, *J. Am. Chem. Soc.* **1976**, *98*, 2868.
- [11] J. E. Steves, S. S. Stahl, *J. Am. Chem. Soc.* **2013**, *135*, 15742.
- [12] K. Omura, D. Swern, *Tetrahedron* **1978**, *34*, 1651.
- [13] H. C. Kolb, M. S. VanNieuwenhze, K. B. Sharpless, *Chem. Rev.* **1994**, *94*, 2483.
- [14] a) V. VanRheenen, R. C. Kelly, D. Y. Cha, *Tetrahedron Lett.* **1976**, *17*, 1973; b) P. Dupau, R. Epple, A. A. Thomas, V. V. Fokin, K. B. Sharpless, *Adv. Synth. Catal.* **2002**, *344*, 421.
- [15] a) T. Oriyama, K. Imai, T. Hosoya, T. Sano, *Tetrahedron Lett.* **1998**, *39*, 397; b) T. Oriyama, K. Imai, T. Sano, T. Hosoya, *Tetrahedron Lett.* **1998**, *39*, 3529.
- [16] a) R. Criegee, *Ber. Dtsch. Chem. Ges. A/B* **1931**, *64*, 260; b) E. Baer, *J. Am. Chem. Soc.* **1940**, *62*, 1597.
- [17] D. B. Dess, J. C. Martin, *J. Org. Chem.* **1983**, *48*, 4155.
- [18] a) K. B. Sharpless, M. W. Young, *J. Org. Chem.* **1975**, *40*, 947; b) P. A. Grieco, S. Gilman, M. Nishizawa, *J. Org. Chem.* **1976**, *41*, 1485.
- [19] a) D. Liotta, U. Sunay, H. Santiesteban, W. Markiewicz, *J. Org. Chem.* **1981**, *46*, 2605; b) K. B. Sharpless, R. F. Lauer, *J. Am. Chem. Soc.* **1973**, *95*, 2697.
- [20] a) R. H. Grubbs, A. G. Wenzel, D. J. O'Leary, E. Khosravi, *Handbook of Metathesis*, Wiley-VCH, Weinheim, **2015**; b) J. Cossy, S. Arseniyadis, C. Meyer, *Metathesis in Natural Product Synthesis*, Wiley-VCH, Weinheim, **2010**.
- [21] T. Cooper, A. Novak, L. D. Humphreys, M. D. Walker, S. Woodward, *Adv. Synth. Catal.* **2006**, *348*, 686.
- [22] CCDC 1879212 and 1879213 (**12** and **2**) contain the supplementary crystallographic data for this paper. These data can be obtained free of charge from The Cambridge Crystallographic Data Centre.

Manuscript received: November 16, 2018

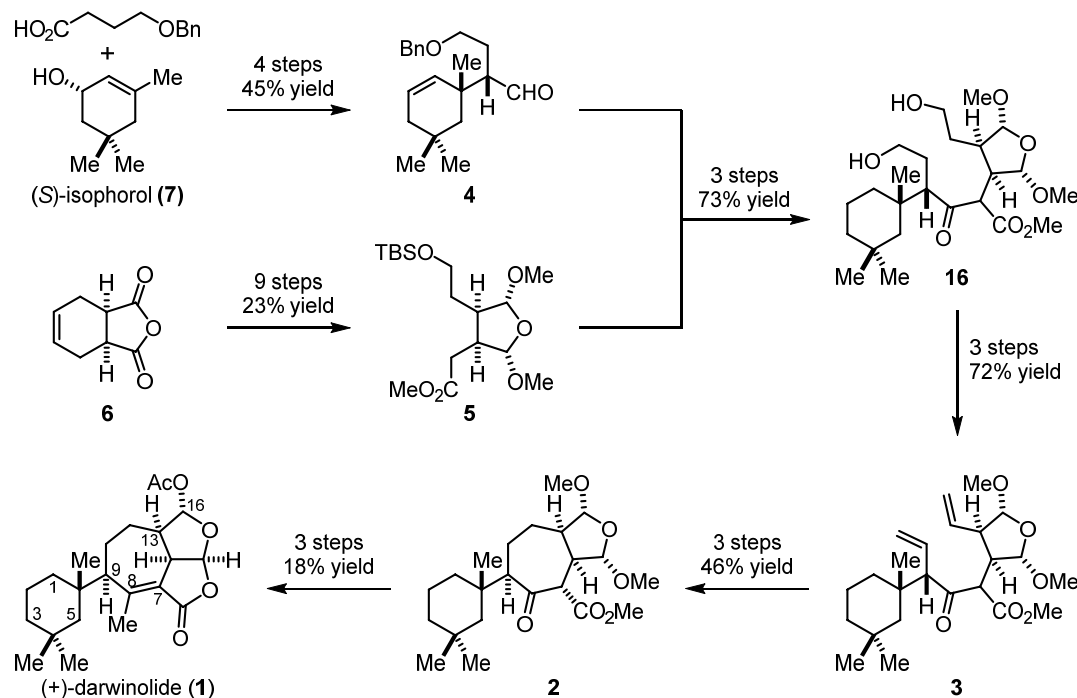
Accepted manuscript online: November 19, 2018

Version of record online: December 18, 2018

2.4 Summary and Outlook

In summary, the synthesis of (+)-darwinolide was successfully accomplished with 21 steps in the longest linear sequence and an overall yield of 1% (Scheme 6). In order to achieve a convergent synthesis, two equally complex fragments (**4** and **5**) were synthesized. The ester fragment **5** was obtained in 9 steps and 23% yield from commercially available *meso* anhydride **6**. A highly enantioselective organocatalytic desymmetrization of a *meso* diol was the key-step in its synthesis. The synthesis of the 1,3,3-trimethylcyclohexyl fragment **4** was achieved in 4 steps and 45% yield starting from the chiral (*S*)-isophorol that was obtained by enzymatic resolution. An IRELAND-CLAISEN rearrangement installed the stereo configuration of the quaternary center but favored the undesired configuration at the adjacent stereogenic center. Therefore, a late-stage epimerization at C9 was required.

The C7–C8 bond in the central seven-membered ring was installed by Aldol addition of ester **5** and aldehyde **4**. After an oxidation to the β -keto ester and the deprotection of the two primary alcohols, the intermediate **16** was transformed into the metathesis precursor **3** by simultaneous elimination of both alcohols. An olefin metathesis closed the seven-membered ring and at this stage, the C9 epimerization was possible. The β -keto ester **2** was transformed into the tetrasubstituted olefin and coincidentally the fused lactone acetal was formed. Finally, an acid-catalyzed transacetalization yielded (+)-darwinolide.



Scheme 6. Summary of the synthesis of (+)-darwinolide.

The synthesis provides several starting points for late stage derivatization opening a straightforward access to a representative substrate library for structure-activity relationship studies. For example, several C16 analogs could be synthesized by introducing different ester moieties. Starting from β -keto ester **2**, the vinyl triflate intermediate would allow the introduction of different substituents at C8 by transition metal-catalyzed cross-coupling. The C9 epimer of darwinolide was readily available by this synthetic route and its biological activity is currently investigated. If it exhibits a similar activity as (+)-darwinolide, the epimerization step could be avoided in future studies.

Altogether, these studies might give an insight into darwinolide's yet unknown mechanism-of-action and serve as a starting point in the development of an anti-biofilm specific antibiotic.

3 (-)-Englerin A – A Highly Active and Selective Inhibitor of Renal Cancer Cell Growth

3.1 Introduction

3.1.1 Renal Cancer

In 2018, more than 175 000 deaths were caused by kidney cancer worldwide and over 400 000 new cases have been recognized.^[66] The main types of kidney cancer are renal cell carcinoma (RCC), transitional cell carcinoma and nephroblastoma. RCC account for more than 90% of all kidney cancer diseases in adults.^[67] They originate in the proximal convoluted tubule, the section of the nephron that follows on the glomerular capsule, where the blood is filtered (Figure 12).

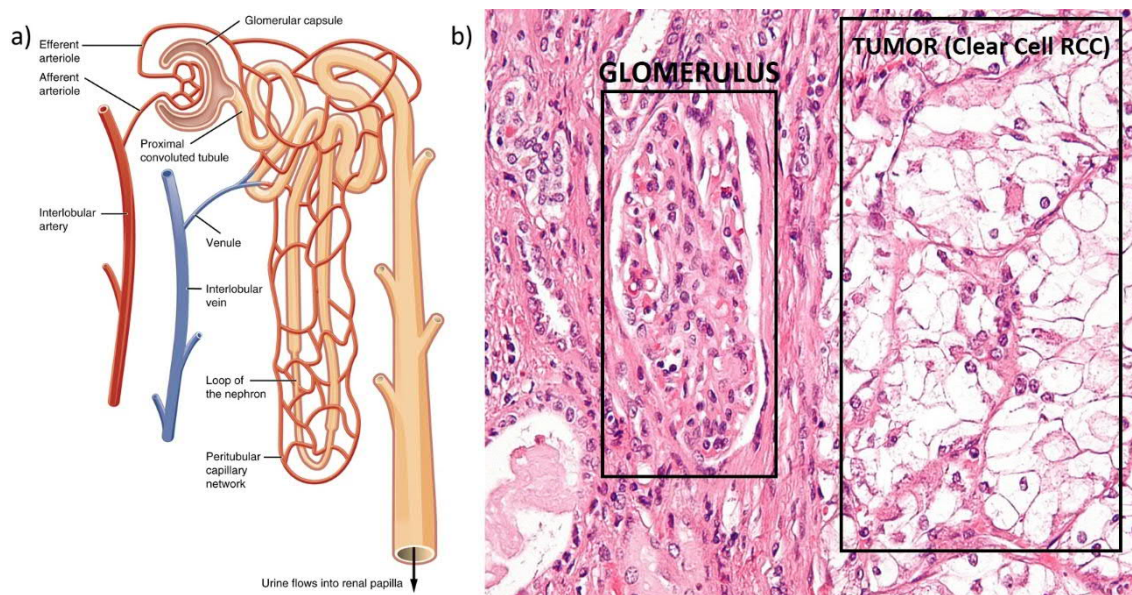


Figure 12. a) Schematic depiction of the blood flow in the nephron; b) High magnification micrograph of a clear cell RCC.^[68]

RCCs are often asymptomatic until an advanced, more severe stage. Therefore, up to 30% of all patients diagnosed with RCC are already metastatic.^[69] The average survival time with metastatic RCC is less than two years and only 10% of the patients survive more than 5 years.^[70]

The standard treatment of RCC is usually the partial or complete surgical removal of the kidney. Roughly 90% of the patients can be cured this way, if the cancer is not metastatic.^[71] However, if the tumor is small and not invasive, active surveillance, which means the monitoring of the RCC progression by various diagnostic methods can avoid surgery.^[72] Another alternative to surgery is a percutaneous ablative therapy. Hereby, radiologists can localize the tumor by image-guidance and destroy it either by heat (radiofrequency ablation) or by cold (cryoablation).^[73] This method can be used if the tumor is small

and if surgery is not feasible. Chemo- and radiotherapy are not successful in most cases of RCC.^[69] However, immuno- and antiangiogenic therapy have developed as viable methods for the treatment of advanced RCCs. Cancer cells are often able to evade the immune systems and thus grow in an unregulated fashion. The application of immune-stimulating agents (cytokines) has evolved as a suitable treatment. The first cytokines interleukin-II and interferon- α have resulted in a moderate cancer regression of up to 20%, but severe side effects have led to their abandoning.^[74] Over the last decade, novel immunotherapeutic agents have emerged. A combination therapy of the two monoclonal antibodies nivolumab (Opdivo®) and ipilimumab (Yervoy®) as well as a combination of the monoclonal antibody pembrolizumab (Keytruda®) with the kinase inhibitor axitinib (Inlyta®) are recommended as first-line treatments for patients with intermediate to poor risk diseases.^[74] In most cases, the prior removal of the primary tumor is advisable. Vascular endothelial growth factor (VEGF)-targeted therapy is suggested as a follow-up to a progressing immunotherapy.^[74] Such a targeted angiogenic therapy with VEGF inhibitors like bevacizumab (Avastin®), axitinib (Inlyta®) or sorafenib (Nexavar®) can also be performed as a single first-line treatment.^[74] Since RCC diseases are progressing very individually, it is impossible to define a general strategy for its treatment. However, immune- and targeted-therapy have contributed to an improvement in overall survival time of patients with metastatic RCC from under one year in 2008 up to 22 months five years later.^[75,70b] This trend illustrates the potential that targeted drugs provide and the necessity to develop novel anti-cancer agents.

3.1.2 Isolation and Biological Evaluation of (-)-Englerin A

In 2009, BEUTLER and coworkers performed a screening campaign for selective inhibitors against RCC by testing 34 plant extracts in the NCI 60-cell panel.^[3] Filtration with respect to their specificity for RCC lines found extracts from the East African plant *Phyllanthus engleri* to exhibit unprecedented activity and selective against those cells. A bioassay-guided fractionation of the root bark of *Phyllanthus engleri* yielded the sesquiterpene (-)-englerin A as the active compound. The cell growth inhibition induced by (-)-englerin A in RCC lines was in the nanomolar range ($GI_{50} = 1 - 87$ nM), whereas most of the other cells in the panel had GI_{50} values higher than 10 μ M.

The guaiane-type structure of (-)-englerin A consists of a *trans*-fused bicyclo[5.3.0]decane bearing an oxo-bridge between C7 and C10 in the seven-membered ring. Englerin A possesses a cinnamate ester at C6 and a glycolate ester at C9. The structurally related englerin B does not contain this glycolic acid ester and exhibits low inhibitory activity, suggesting that the glycolate moiety is essential for the biological activity (Figure 13). The absolute configuration of the natural product was established through the first

synthesis of the unnatural enantiomer (+)-englerin A by the CHRISTMANN group.^[4] (+)-Englerin A was later tested and did not show any significant biological activity.^[5]

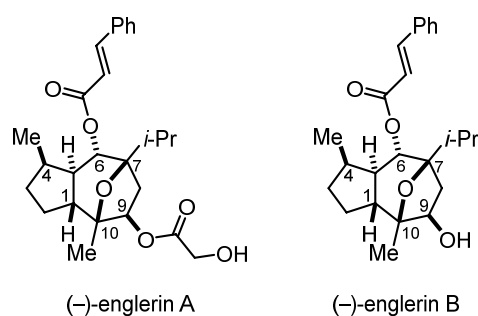


Figure 13. Structures of (-)-englerin A and B.

Intrigued by the promising biological activity of (-)-englerin A, studies towards its mode of action were conducted. Protein kinase C-theta (PKC θ) was identified as a target in the RCC line 786-0 by the group of NECKERS.^[76] Englerin was suggested to directly activate the PKC θ which results in phosphorylation of the insulin receptor substrate 1 (IRS1) and transcription factor HSF1, leading simultaneously to glucose addiction of the cells while inhibition of its transport. However, PKC θ cannot be found in the RCC A498 which displayed the highest sensitivity for (-)-englerin A. Therefore, PKC θ could not be the primary target for englerin A. WALDMANN et al. identified the transient receptor potential canonical (TRPC) channels 4 and 5 as targets for (-)-englerin A.^[77] Those non-selective cation channels are located in the plasma membrane of the cells and usually form homo- or heterotetrameric structures. Englerin was found to selectively bind to the externally exposed site of the TRPC4-channels and potently activate an influx of calcium ions that finally leads to cell death by overloading. TRPC5-channels are targeted as well but are rarely expressed in RCC cells.

BEECH and coworkers later revealed that in heterotetrameric TRPC4/1 channels an influx of sodium instead of calcium ions is induced by (-)-englerin A.^[78] In TRPC1 channels the influx of calcium ions is suppressed, resulting in a relatively small non-toxic cytosolic calcium ion elevation. In contrast, the cytosolic sodium ion concentration is increased, which leads to a stimulation of Na⁺/K⁺-ATPase. The authors suggest that insufficient Na⁺/K⁺-ATPase activity in some cells causes the sodium ion accumulation that finally leads to cell death. (-)-Englerin A was also reported to induce cytotoxicity by sodium ion influx through heterotetrameric TRPC4/1 channels in synovial sarcoma cells.^[79]

The xanthine derivative Pico145 was identified as a specific and highly potent inhibitor for englerin A-activated TRPC1/4/5 channels in the picomolar range (Figure 14).^[80] This tool compound might be pivotal for the further development of a renal cancer therapeutic agent. Another intriguing lead structure is the glycol ether (-)-englerin A-derivative **20** that acts as a competitive antagonist of (-)-englerin A in

homomeric TRPC5 channels.^[81] This englerin analog possesses little to no agonistic activity towards TRPC1/4/5 channels, but inhibits the englerin A-mediated channel opening. In contrast, TRPC4/5 channels activated by different cofactors (Gd^{3+} for TRPC5 and sphingosine-1-phosphate for TRPC4) were not inhibited but potentiated by compound **20**, probably due to a conformational change in the channels. These results might provide future insights into the actual binding side of (-)-englerin A, and compound **20** might also find application as an antidote to englerin poisoning.

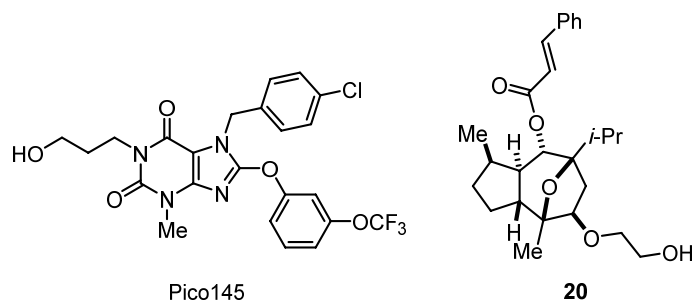


Figure 14. Structures of the TRPC1/4/5 inhibitor Pico145 and the competitive (-)-englerin A antagonist **20**.

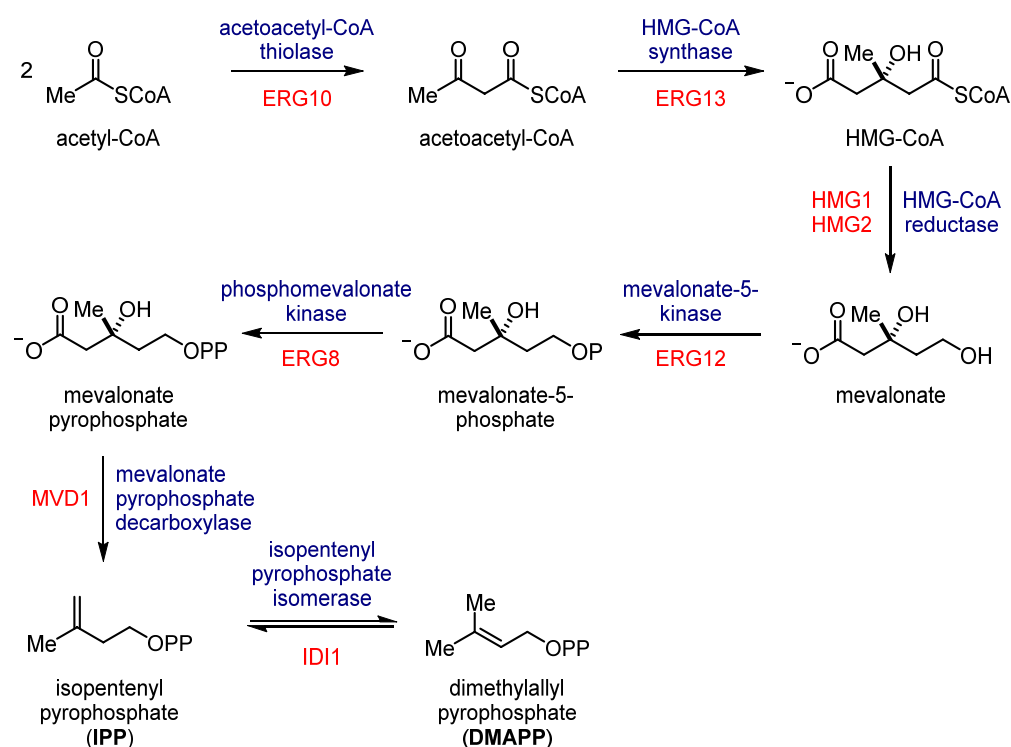
The critical challenge in the development of an anti-cancer drug based on (-)-englerin A is the translation of the highly promising *in vitro* activity into *in vivo* studies. Although, initial results displayed the successful inhibition of xenograft tumor growth in nude mice,^[76] further studies revealed unacceptable toxicity of englerin A.^[82] Rats and nude mice administered with various doses (1 – 10 mg/kg) of (-)-englerin A intravenously or intraperitoneally died or had to be euthanized. However, later studies revealed that intraperitoneal doses up to 2 mg/kg were tolerated in wild type mice.^[83] Although the locomotor activity was significantly affected, all mice recovered completely after about one hour. Knockout experiments with mice having disrupted TRPC4 or TRPC5 genes revealed that both contribute to the adverse effects. Knockout of both TRPC4 and TRPC5 completely protects against the adverse reaction of englerin A. The same could be observed, if the antagonist Pico145 was pre-administered before the injection of englerin A. Since no significant amount of englerin A could be found in the brain, a peripheral mechanism is likely to cause the adverse reaction. Although the underlying mechanism is unclear, these results indicate that the adverse effect is caused by an on-target event. Therefore, the potential of (-)-englerin A as lead structure in anti-cancer drug research must be questioned, although the development of a TRPC4-selective agonist might still result in an anti-cancer agent. Thus, the further research on englerin's mechanism of action is still of great importance.

3.1.3 Biosynthesis of (-)-Englerin A

3.1.3.1 Biosynthesis of Terpenes

Terpenes are biosynthetically derived from isopentenyl pyrophosphate (IPP) and its isomer dimethylallyl pyrophosphate (DMAPP). There are two independent metabolic pathways that produce these terpenoid precursors, the mevalonate (MVA) pathway and the 2-*C*-methyl-D-erythritol 4-phosphate (MEP) pathway.^[84] The MEP pathway only takes place in the plastid organelles of plants and algae, as well as in most bacteria and protozoa, while higher developed eukaryotes, archaea and some bacteria use the MVA pathway to produce IPP and DMAPP (Scheme 7).^[85]

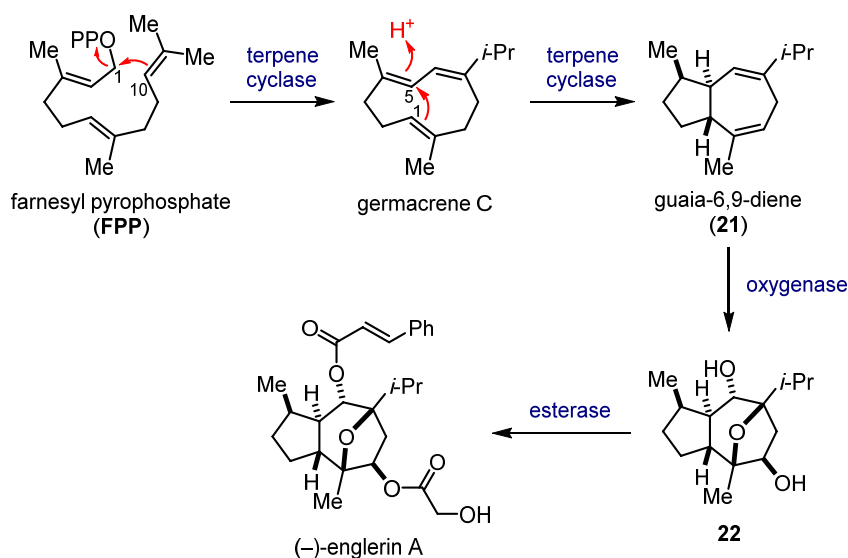
The initial condensation of two molecules acetyl-CoA in the MVA pathway is followed by a second condensation with acetyl-CoA to produce (*S*)-3-hydroxy-3-methyl-glutaryl-CoA (HMG-CoA).^[86] Subsequently, in the rate-determining step, HMG-CoA is reduced to (*R*)-mevalonate by NADPH. In eukaryotes, two consecutive ATP-consuming phosphorylation steps at the mevalonate 5-OH are followed by decarboxylation to yield IPP. In the final step, IPP is isomerized to DMAPP. Terpenoids are formed by condensation of these two building blocks. Farnesyl pyrophosphate (FPP) for example, the precursor for sesquiterpenoids, is synthesized from two molecules IPP and one molecule DMAPP.



Scheme 7. Biosynthesis of terpenes in Eukaryotes via the mevalonate pathway. Blue: Enzymes catalyzing these transformations. Red: Genes encoding for these transformations in *Saccharomyces cerevisiae*.^[87]

3.1.3.2 Proposed Biosynthetic Pathways towards (-)-Englerin A

CHRISTMANN et al. proposed the biosynthesis of (-)-englerin A to proceed via guaia-6,9-diene **21** (Scheme 8).^[88] Oxidation of diene **21** would lead to diol **22** which would afford (-)-englerin A after esterification. Since guaia-6,9-diene (**21**) is not literature known, their synthesis had to start from *cis,trans*-nepetalactone (see chapter 3.1.4.1).

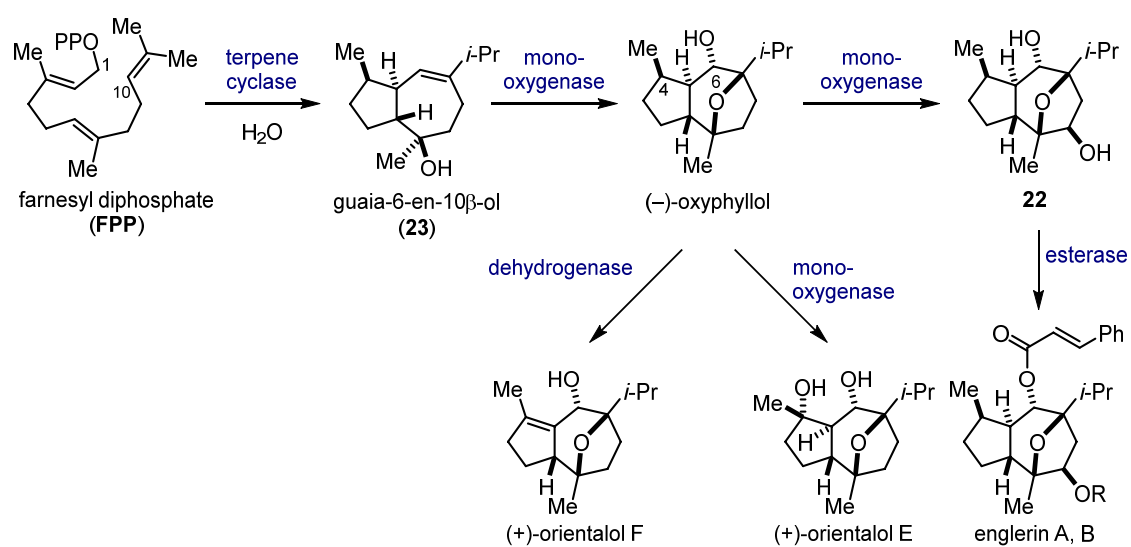


Scheme 8. Proposed biosynthesis of (-)-englerin A by CHRISTMANN et al.^[88]

Biosynthetically guaia-6,9-diene would result from cyclization of FPP. These cyclization pathways are usually initiated by 1,10-cyclization of FPP. A following hydride shift and deprotonation would lead to germacrene C, a common intermediate in sesquiterpene biosynthesis. Another cyclization (C1–C5) would give access to the bicyclic guaiane scaffold and deprotonation might result in guaia-6,9-diene.

Another biosynthetic hypothesis was proposed by SUN and LIN et al.^[89] They suggest that oxyphyllol is a crucial intermediate in the biosynthesis of both englerin A and B as well as orientalol E and F. Oxyphyllol was isolated from roots of the East Asian plant *Phyllanthus oxyphyllus*, the same genus as englerin A and B, in 2003 by SUTTHIVAIYAKIT et al.^[90] Its originally assigned structure was revised in the context of the synthesis by SUN and LIN et al. with respect to the stereogenic centers at C4 and C6. Both the two sesquiterpenes orientalol E and F were isolated in 2003 by PENG et al. from the rhizome of *Alisma orientalis*, a plant widely cultivated in China and Japan and applied in traditional Chinese medicine.^[91] A significant biological activity for either of the three sesquiterpenes is not known to date.

The hypothesis by SUN and LIN et al. proposed that cyclization of FPP would lead to guai-6-en-10 β -ol (**23**), a known natural product^[92] which might be a reasonable precursor of oxyphyllol (Scheme 9). Enzymatic C–H-oxidation might either lead to orientalol E or to diol **22** which is esterified to give englerin A and B. Dehydrogenation of oxyphyllol would afford orientalol F.



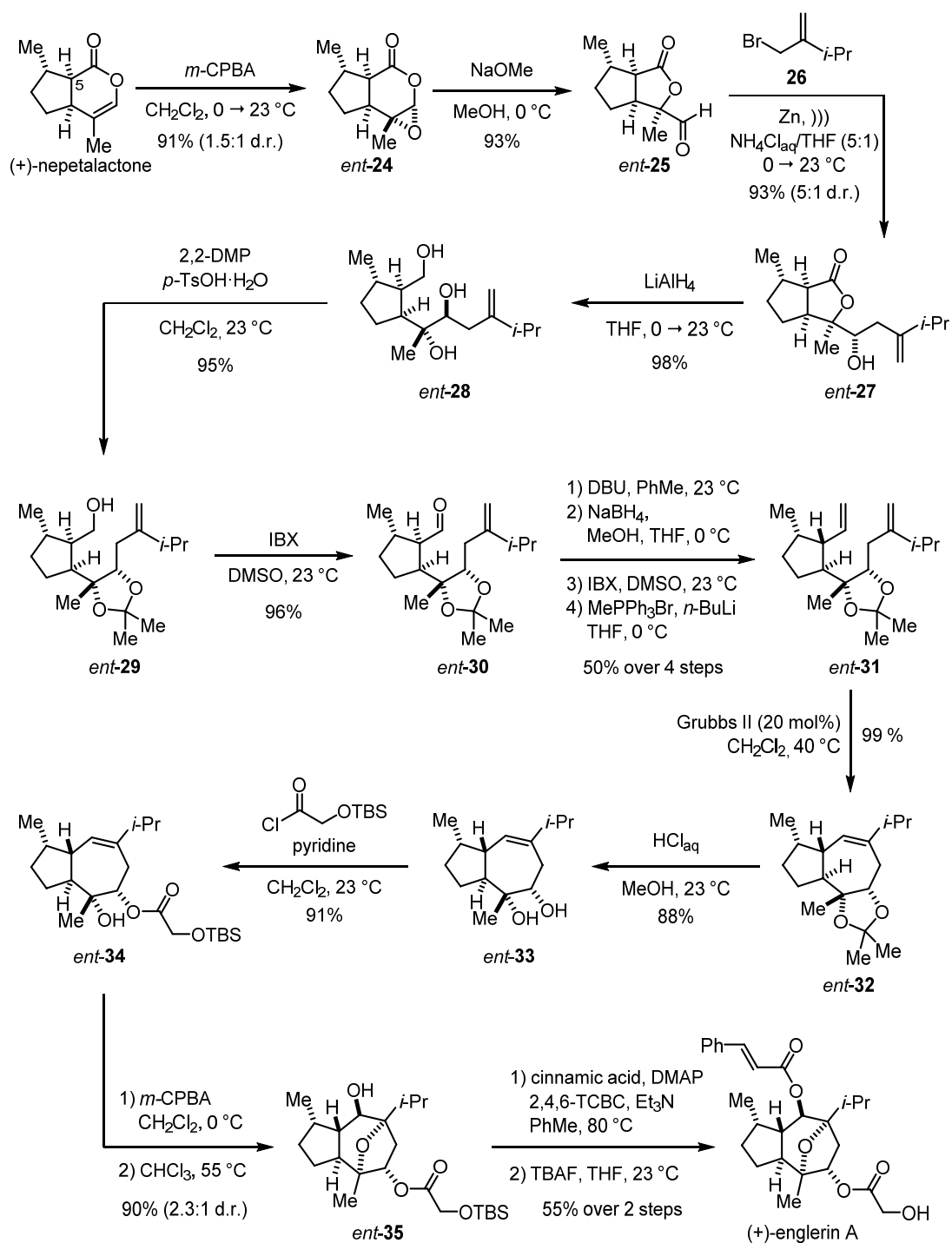
Scheme 9. Proposed biosynthetic pathway for oxyphyllol, englerin A and B and orientalol E and F by SUN and LIN et al.^[89]

3.1.4 Syntheses of Englerin A

Since its isolation, more than 20 total and formal syntheses of englerin A and analogs thereof have been reported. Ring-closing metathesis^[5,93] turned out to be a reliable method for the construction of the englerin scaffold. Yet, the majority of synthetic strategies employed cycloadditions including gold-catalyzed [2+2+2] cycloaddition,^[94] 1,3-dipolar [3+2] cycloaddition,^[95a-95c,8,95d] rhodium-^[96] and platinum-^[97] catalyzed [4+3] cycloaddition, as well as transition-metal free [4+3] cycloadditions.^[89,98] Alternatively the core structure could be installed by a sequence of conjugate MICHAEL addition and samarium(II) iodide-induced reductive coupling,^[99] intramolecular HECK-reaction,^[100] NAZAROV cyclization^[101] and oxy-COPE rearrangement.^[102] The following part will provide a detailed description of the englerin A syntheses by CHRISTMANN et al.^[4,5] and sum up the key steps in the other syntheses.

3.1.4.1 Synthesis of (+)-Englerin A by CHRISTMANN

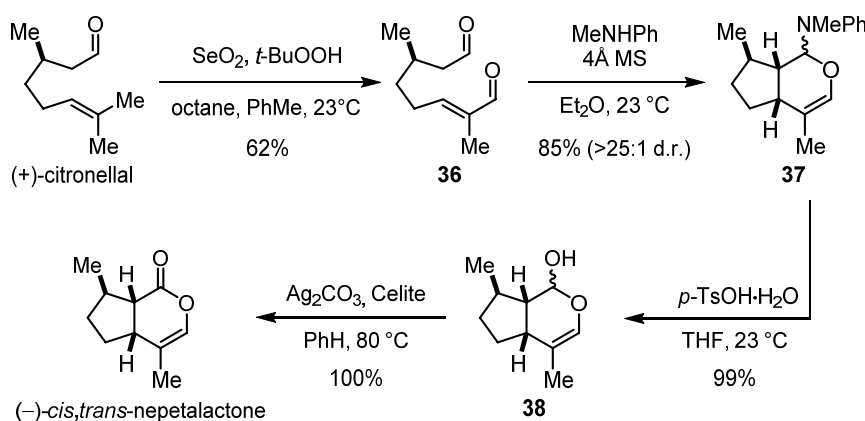
The first total synthesis of englerin A was accomplished by the CHRISTMANN group in the same year as the isolation was published.^[4] Starting from (+)-*cis,trans*-nepetalactone, the main ingredients of catnip (*nepeta cataria*), a moderately diastereoselective epoxidation (d.r. 1.5:1) and a subsequent base-induced ring contraction resulted in the formation of formyl lactone *ent*-**25** (Scheme 10). A BARBIER reaction with allyl bromide **26** afforded the homoallyl alcohol *ent*-**27** in excellent yield of 93% and good diastereoselectivity of 5:1. Global reduction of lactone *ent*-**27** with lithium aluminum hydride gave triol *ent*-**28** and the vicinal 1,2-diol was protected as an acetonide. The primary alcohol *ent*-**29** was oxidized to yield aldehyde *ent*-**30**, which was subsequently isomerized with 1,8-Diazabicyclo[5.4.0]undec-7-ene (DBU) to give the desired epimer at the α -position of the aldehyde in a diastereomeric ratio of 3:1. Since a separation of both diastereomers proved unsuccessful at this stage, a sequence of reduction, separation and re-oxidation was applied, followed by WITTIG olefination to yield the metathesis precursor *ent*-**31**. Ring-closing metathesis with 20 mol% of GRUBBS-II-catalyst completed the formation of cycloheptene *ent*-**32** in quantitative yield. Subsequently, acetonide deprotection under acidic conditions and a regioselective esterification of the resulting secondary alcohol with 2-(*tert*-butyldimethylsilyl)oxyacetyl chloride were carried out. The cycloalkene *ent*-**34** was epoxidized with *meta*-chloroperbenzoic acid (*m*-CPBA) in moderate diastereoselectivity of 2.3:1. Surprisingly, under heating in chloroform a transannular epoxide-opening by the attack of the tertiary alcohol directly formed the oxo-bridge. Finally, a YAMAGUCHI esterification with cinnamic acid and silyl ether cleavage gave access to englerin A. By comparison of the optical rotation values with the literature, the synthesized product was identified to be the unnatural enantiomer (+)-englerin A, clarifying the previously unknown absolute configuration, alongside. The synthesis of (+)-englerin A was accomplished in 17 steps and an overall yield of 5%.



Scheme 10. Synthesis of (+)-englerin A by Christmann et al.^[4]

3.1.4.2 Improved Synthesis of (-)-Englerin A by CHRISTMANN

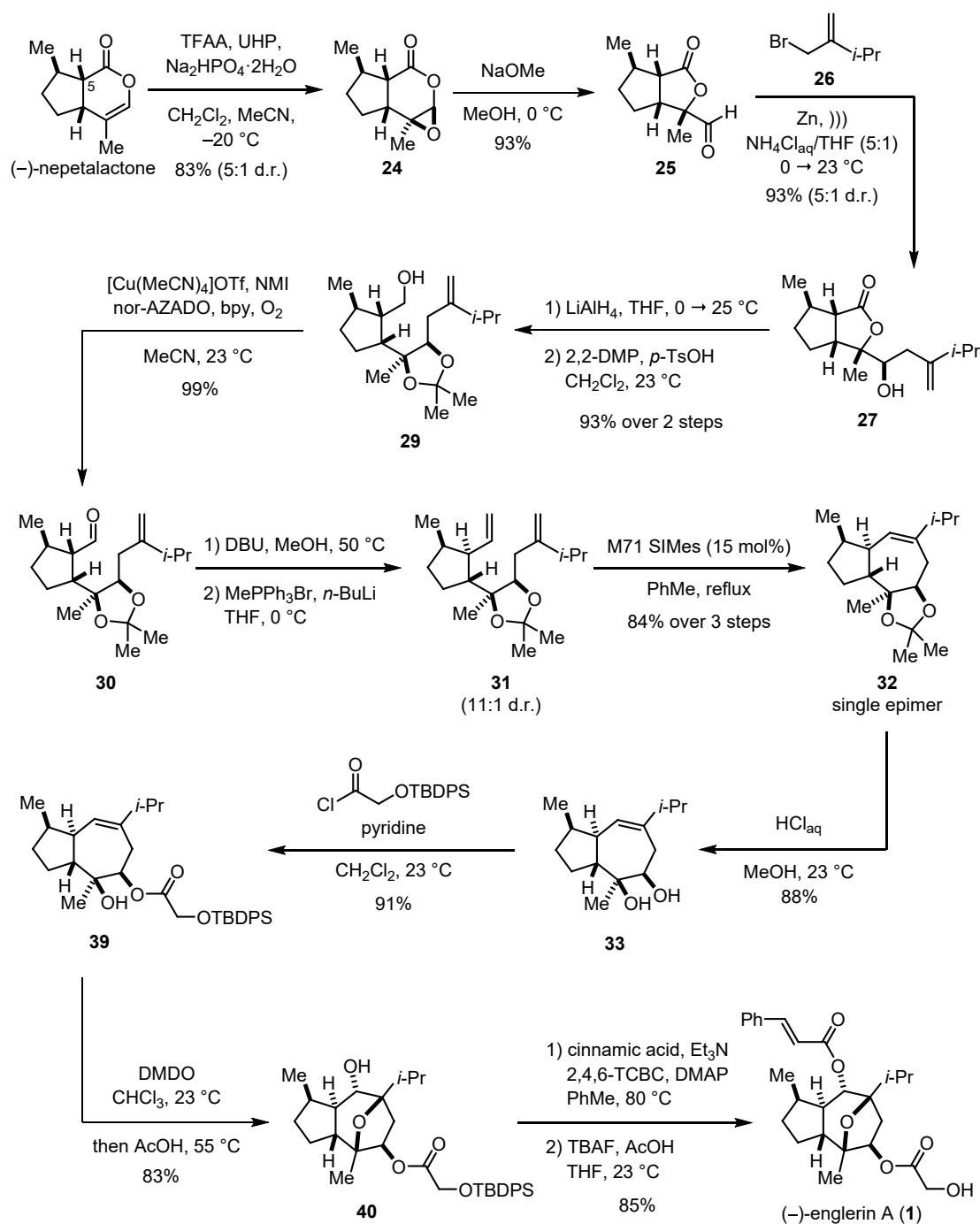
In 2011, the CHRISTMANN group reported a synthesis of (-)-englerin A applying a similar route as described above for the synthesis of unnatural enantiomer (+)-englerin A.^[5] Later on, this synthesis was further improved and the following part will provide a summary of these results.^[103,7] As the starting material (-)-*cis,trans*-nepetalactone was not available from natural sources, a four step sequence starting from (+)-citronellal was applied following SCHREIBER's protocol (Scheme 11).^[104] The RILEY oxidation of citronellal resulted in the formation of enal **36**, which was cyclized with *N*-methylaniline to give aminal **37**. After hydrolysis to the lactol **38**, a FETIZON oxidation using silver carbonate gave access to (-)-*cis,trans*-nepetalactone in 52% yield over 4 steps.



Scheme 11. Synthesis of (-)-*cis,trans*-nepetalactone starting from (+)-citronellal.

The epoxidation of nepetalactone was improved by applying trifluoroperacetic acid prepared in situ from trifluoroacetic anhydride and urea hydrogen peroxide resulting in a diastereomeric ratio of 5:1 (cf. *m*-CPBA 1.5:1). Application of a copper(I)-catalyzed aerobic oxidation of alcohol **29** avoided the necessity to use stoichiometric amounts of oxidant. The yield for the sequence leading to the metathesis product **32** could be raised to 84% over 3 steps (cf. 50% over 5 steps) mainly by optimizing the epimerization of aldehyde **30** to a diastereomeric ratio of 11:1 by changing the solvent from toluene to methanol. Ring-closing-metathesis with 15 mol% of UMICORE's catalyst M71 SIMes successfully separated both epimers, as the undesired epimer did not undergo metathesis, saving the separation sequence (Scheme 12). Epoxidation of cycloheptene **39** with DMDO and the subsequent addition of acetic acid formed the oxo-bridged scaffold **40** in a one-pot reaction as a single diastereomer. YAMAGUCHI-esterification with cinnamic acid and subsequent silyl ether cleavage gave access to (-)-englerin A in 85% yield over 2 steps.

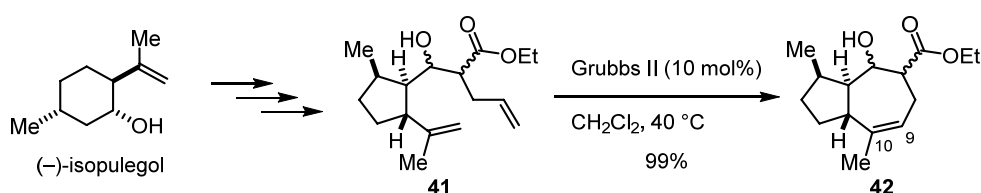
In summary, the synthesis of (-)-englerin A could be achieved in 14 steps and 22% overall yield starting from (-)-*cis,trans*-nepetalactone or 18 steps and 11% yield if counted from (+)-citronellal.



Scheme 12. Improved synthesis of (-)-englerin A by Christmann et al.

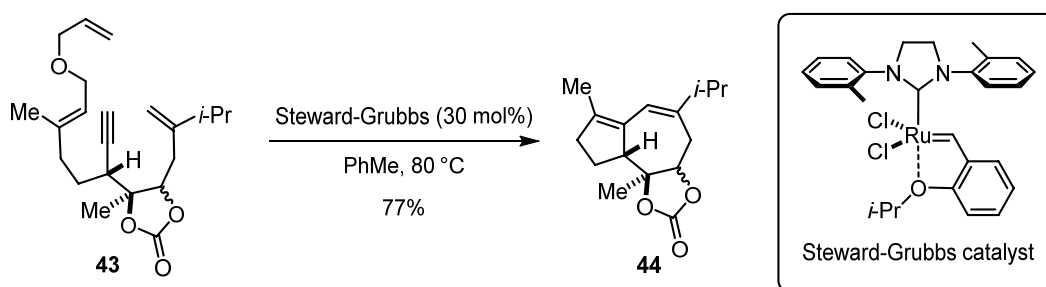
3.1.4.3 Further Syntheses Applying Ring-Closing Metathesis

Ring-closing metathesis was applied by five groups as the key-step for the cyclization of the cycloheptene ring. As in the CHRISTMANN synthesis,^[5] the group of HATAKEYAMA^[93a] performed a C6–C7 connection by olefin metathesis and the endgame was quite similar as well. The cyclopentane was constructed by intramolecular epoxide opening. Although this synthesis was 24 steps long, the overall yield was surprisingly high with 14%. The groups of METZ^[93c] and SHEN^[93d] made the retrosynthetic disconnection between C9 and C10. METZ' synthesis started from (-)-isopulegol and after the metathesis, diastereoselective epoxidation and dihydroxylation installed the correct oxidation state (Scheme 13). (-)-Englerin A was synthesized over 14 steps in 5.2% total yield. The synthesis of SHEN used (*R*)-(-)-carvone as a starting material and afforded a total yield of 4.3% over 18 steps.



Scheme 13. Ring-closing metathesis in the (-)-englerin A synthesis by METZ et al.^[93c]

A different approach was chosen by PARKER et al.^[93b] who performed a relay-enyne-metathesis that cyclized the bicyclo[5.3.0]decane scaffold in a single step (Scheme 14). This formal synthesis of (-)-englerin A started from geraniol and the chirality was introduced by SHARPLESS epoxidation.



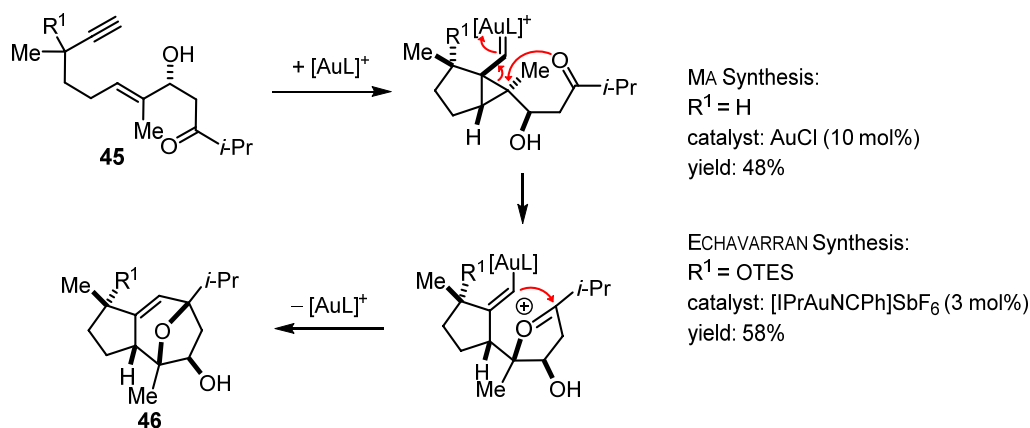
Scheme 14. Relay-enyne-metathesis in the formal (-)-englerin A synthesis by PARKER et al.^[93b]

3.1.4.4 Syntheses of Englerin A Based on Cycloadditions

Besides ring-closing metathesis, the majority of englerin syntheses are based on cycloadditions including gold-catalyzed [2+2+2] cycloaddition,^[94] 1,3-dipolar [3+2] cycloaddition,^[95a-95c,8,95d] rhodium-^[96] and platinum-^[97] catalyzed [4+3] cycloaddition, as well as transitions-metal free [4+3] cycloadditions.^[89,98] The following part will provide a systematic discussion of the different types of cycloadditions performed.

Gold-Catalyzed [2+2+2] Cycloaddition

The groups of MA and ECHAVARRAN both reported a gold-catalyzed cyclization of an enyne to build up the tricyclic englerin scaffold (Scheme 15).^[94] While the MA synthesis started from the chiral building block (+)-citronellal the synthesis of ECHAVARRAN used geraniol as the starting material and introduced the chirality via SHARPLESS asymmetric epoxidation and DENMARK aldol reaction. The precursor **45** for the key [2+2+2] cyclization differs only in the substituent at the C4-position. Both cyclizations construct the tricyclic scaffold **46** diastereoselectively with yields of 48% and 58%, respectively. The two syntheses have similar overall yields (ECHAVARRAN: 7.4%, MA: 8.1%) and the same step count (16 steps), but the MA synthesis is protecting group free and avoids the use of enantioselective transformations with expensive chiral catalysts.



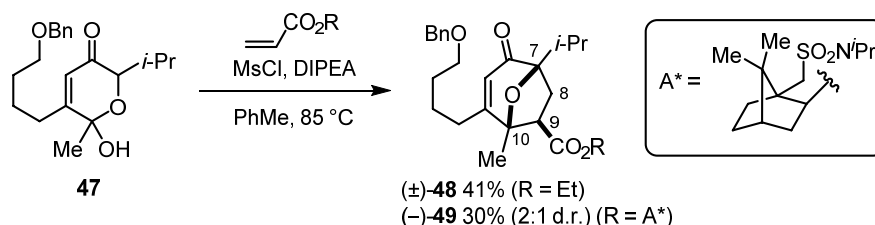
Scheme 15. Gold-catalyzed-[2+2+2]-cycloaddition reported by MA et al. and ECHAVARRAN et al.^[94]

1,3-Dipolar [3+2] Cycloaddition

The retrosynthetic fragmentation of the oxo-bridged cycloheptane results in two possible cycloaddition pathways. Cleavage of the C7–C8 and C9–C10 bonds allows for a 1,3-dipolar [3+2] cycloaddition approach. The first such synthesis of racemic englerin A was reported by the group of NICOLAOU and CHEN (Scheme 16).^[95a] Treatment of lactol **47** with mesyl chloride resulted in the formation of an oxopyrylium intermediate that undergoes cycloaddition with ethyl acrylate to afford racemic cycloadduct **48** in 41% yield. Using a chiral sulfonamide acrylate (A*) instead, resulted in a moderately

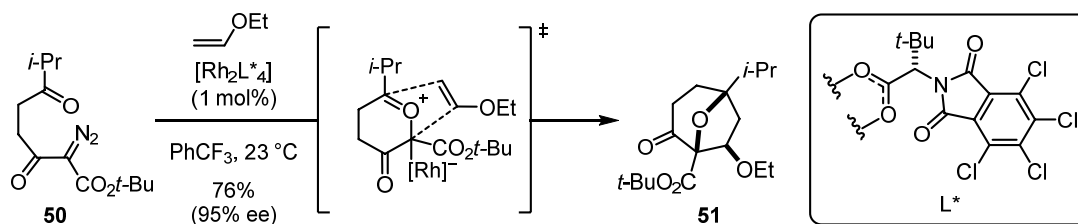
diastereoselective cycloaddition (2:1 d.r.) and gave access to a formal asymmetric synthesis. The construction of the englerin scaffold was completed by aldol condensation to form the five-membered ring. Overall, a synthesis of racemic englerin A was achieved in 21 steps and 1.7% yield.

A similar approach was presented by TCHABANENKO et al., who performed a 1,3-dipolar [3+2] cycloaddition of a pyrylium ylide with vinyl acetate in a sealed tube at 180 °C.^[95d]



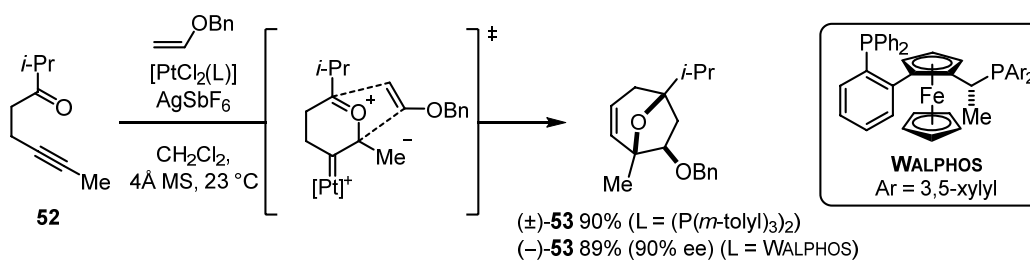
Scheme 16. Key 1,3-dipolar [3+2] cycloaddition from the NICOLAOU/CHEN synthesis.^[95a]

Inverse electron-demand metal-catalyzed [3+2] cycloadditions of carbonyl ylides with electron-rich vinyl ethers were performed by the groups of HASHIMOTO/ANADA and IWASAWA.^[95b,95c] The HASHIMOTO/ANADA approach utilized a rhodium-catalyzed cycloaddition of the carbonyl ylide derived from 2-diazo-3,6-diketoester **50** with vinyl ethyl ether (Scheme 17). Application of a *tert*-leucine derived chiral rhodium-catalyst resulted in good yield of 76% and excellent enantioselectivity of 95%. A similar aldol condensation as in the NICOLAOU/CHEN synthesis constructed the tricyclic framework and finally gave access to (-)-englerin A in 25 steps and 5.2% overall yield.



Scheme 17. Rhodium-catalyzed [3+2] cycloaddition reported by ANADA/HASHIMOTO et al.^[95b]

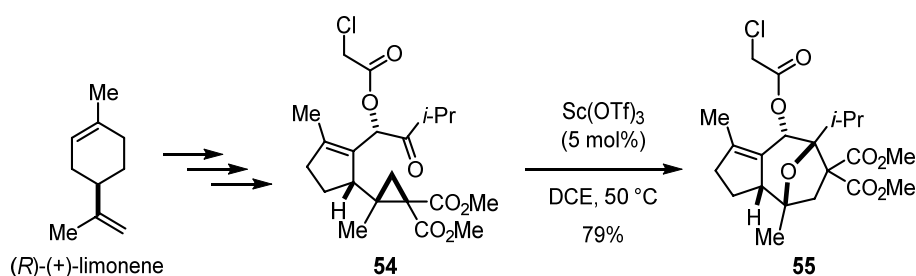
IWASAWA et al. applied a diastereoselective platinum-catalyzed carbonyl ylide [3+2] cycloaddition with benzyl vinyl ether starting from acyclic ketoalkyne **52** in their synthesis of racemic englerin A (Scheme 18).^[95c]



Scheme 18. Platinum-catalyzed [3+2] cycloaddition reported by IWASAWA et al.^[95c]

They previously described an enantioselective version of this transformation using the chiral WALPHOS ligand to obtain the oxo-bridged cycloheptene **53** with 90% enantiomeric excess.^[105] Hence, this approach represents a formal asymmetric synthesis.

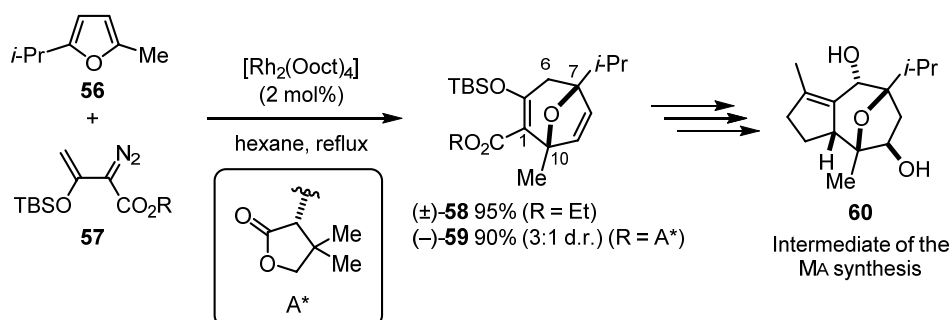
The group of WANG presented a different approach towards a [3+2] cycloaddition (Scheme 19).^[8] Starting from (+)-limonene, a hydroxyl-directed stereo- and regioselective intramolecular cyclopropanation afforded intermediate **54**. A formal [3+2] intramolecular cross cycloaddition catalyzed by scandium triflate gave access to the tricyclic scaffold **55**. This synthetic approach delivers (-)-englerin A in 20 steps and 1.5% overall yield. Additionally, they also achieve the synthesis of the related guaiane-type sesquiterpenes (-)-oxyphyllol, (+)-orientalol E and F applying a very similar procedure as presented by SUN and LIN^[89] (for details see Scheme 22).



Scheme 19. Formal [3+2] intramolecular cross cycloaddition reported by WANG et al.^[8]

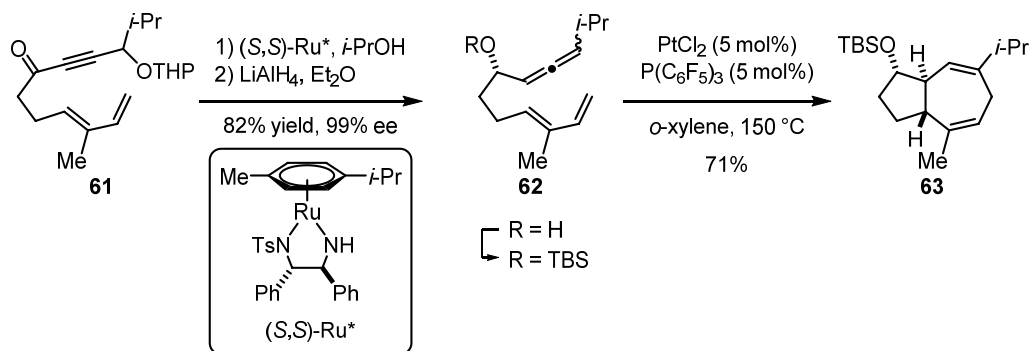
[4+3] Cycloaddition Strategies

Beside the [3+2] cycloaddition approach, a second cycloaddition pathway is possible installing the C1–C10 and the C6–C7 bonds by a [4+3] cycloaddition. THEODORAKIS and coworkers presented a rhodium-induced [4+3] cycloaddition of 2-isopropyl-5-methylfuran **56** with diazo ester **57** (Scheme 20).^[96] Applying lactone **A*** as a chiral auxiliary allowed for the cycloaddition with 90% yield and a moderate diastereomeric ratio of 3:1. The synthesis of the tricyclic scaffold was concluded by aldol condensation to give the cyclopentene intermediate **60** previously reported by MA et al.^[94a] Thus, it represents a formal enantioselective synthesis of (-)-englerin A.



Scheme 20. Rhodium-catalyzed [4+3] cycloaddition described by THEODORAKIS et al.^[96]

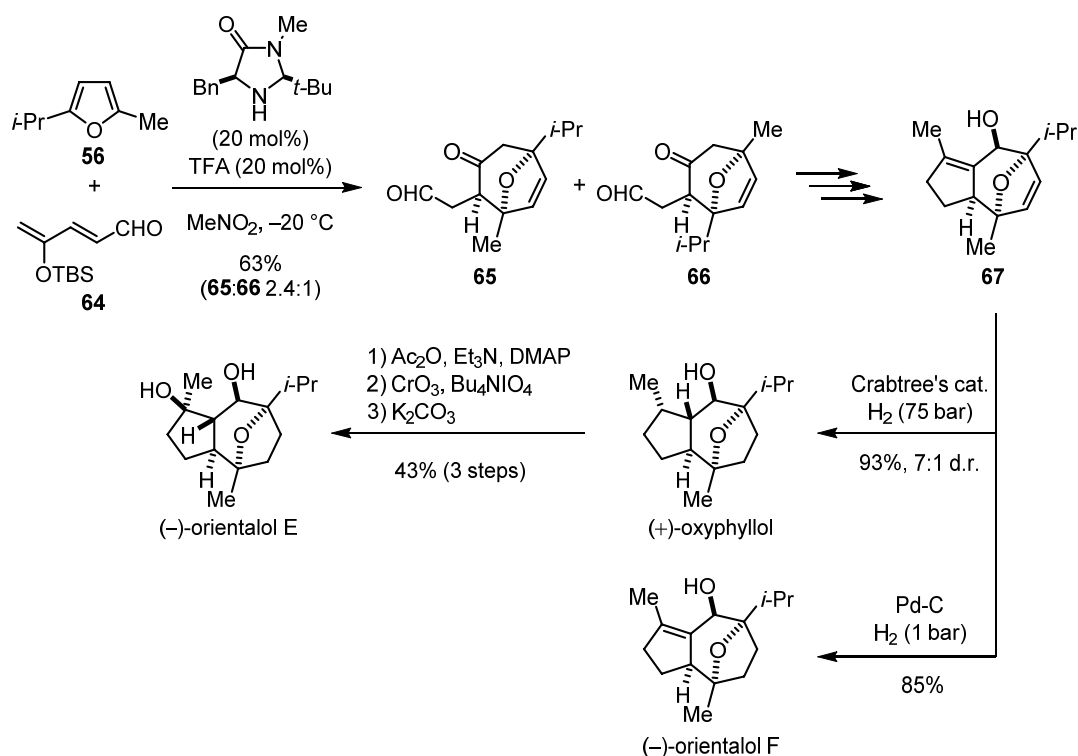
LÓPEZ and MASCAREÑAS et al. reported an approach that constructed the *trans*-fused guaiane scaffold in a single-step by an intramolecular platinum-catalyzed [4+3] cycloaddition of a diene with an allene (**62**, Scheme 21).^[97] The chirality of the starting material **62** was introduced by highly enantioselective ruthenium-catalyzed transfer hydrogenation with 99% ee. Finally, regio- and diastereoselective dihydroxylation followed by epoxidation and transannular epoxide opening afforded englerin's tricyclic scaffold. Overall, the synthesis of (-)-englerin A was achieved in 17 steps with 10% yield.



Scheme 21. Platinum-catalyzed allenediene [4+3] Cycloaddition reported by LOPEZ et al.^[97]

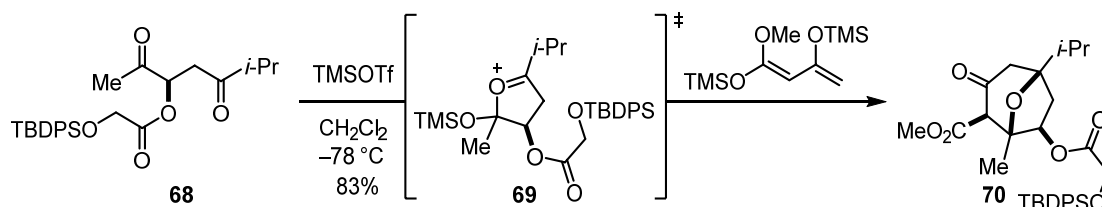
Beside the discussed transition metal-catalyzed [4+3] cycloadditions, there are also reports of transition metal-free approaches. SUN and LIN et al. presented an organocatalytic [4+3] cycloaddition of dienal **64** with 2-isopropyl-5-methylfuran (**56**) using 20 mol% of MACMILLAN's imidazolidinone catalyst (Scheme 22).^[89] The cycloadduct was obtained as a scarcely separable mixture of regioisomers (**65** and **66**) with a ratio of 2.4:1 in favor of the desired one (**65**), but with the wrong absolute configuration. An aldol condensation delivered the tricyclic intermediate **67** which was applied to synthesize (+)-englerin A and the related sesquiterpenoids (+)-oxyphyllol and (-)-orientalol E and F.

The synthesis of (-)-orientalol F was achieved by regioselective hydrogenation of diene-intermediate **67** with palladium on activated charcoal and atmospheric hydrogen pressure. Using CRABTREE's catalyst and a high hydrogen pressure (75 bar), both alkenes could be hydrogenated affording (+)-oxyphyllol. A three-step sequence consisting of acetylation, C-H-oxidation and saponification allowed for the transformation of oxyphyllol into (-)-orientalol E. The synthesis of (+)-englerin A was concluded as well, starting from intermediate **67** in five more steps, resulting altogether in a 14 steps synthesis of the unnatural enantiomer, that delivers 0.9% overall yield.



Scheme 22. Organocatalytic [4+3] cycloaddition approach towards the englerin scaffold and the subsequent synthesis of (+)-oxyphyllol and (-)-orientalol E/F reported by SUN and LIN et al.^[89]

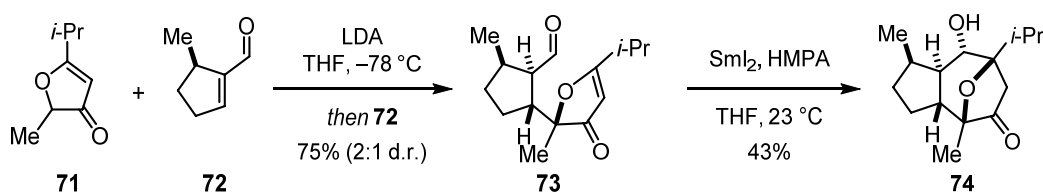
Just recently, PLIETKER et al. reported a [4+3] cycloaddition of a β -ketoester-derived bis-silylenolether with a 1,4-diketone (Scheme 23).^[98b] The cycloadduct **70** is formed regio- and stereoselectively by trimethylsilyl triflate-mediated tandem double MUKAIYAMA-aldol additions to the in situ formed cyclic oxonium species **69** of the 1,4-diketone **68**. The chiral starting material **68** was obtained by a moderately enantioselective organocatalytic decarboxylative aldol reaction with 60% ee from methylglyoxal. Finally, the five-membered ring was formed by HECK-reaction. This concise approach allowed for the synthesis of (-)-englerin A in 12 steps and 10% overall yield.



Scheme 23. TMSOTf-mediated [4+3] cycloaddition reported by PLIETKER et al.^[98b]

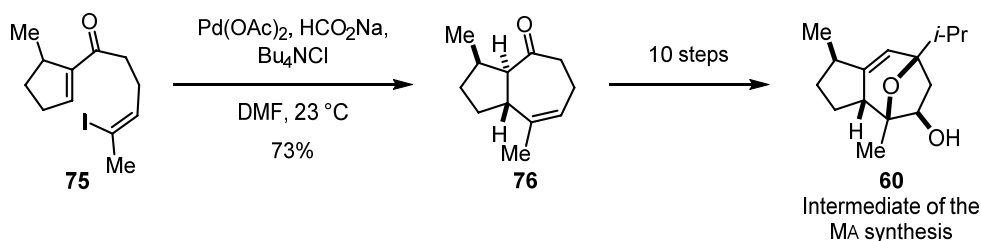
3.1.4.5 Further Synthetic Strategies

Although ring-closing metatheses and cycloadditions represent by far the most applied strategies towards the synthesis of englerin A, some alternative strategies have been reported as well. One of the most elegant entries into englerin's structure was presented by CHAIN et al. (Scheme 24).^[99] The scaffold was constructed in just two steps with most of the functionalities already in place. First a MICHAEL addition of a 3-furanone-derived enolate (**71**) with an α,β -unsaturated aldehyde (**72**) formed the C1–C10 bond and subsequently a samarium(II) iodide-mediated reductive carbonyl-alkene cyclization concluded the tricyclic englerin scaffold **74**. With just 8 steps and 8.5% overall yield, this synthesis represents the shortest route towards (-)-englerin A to date.



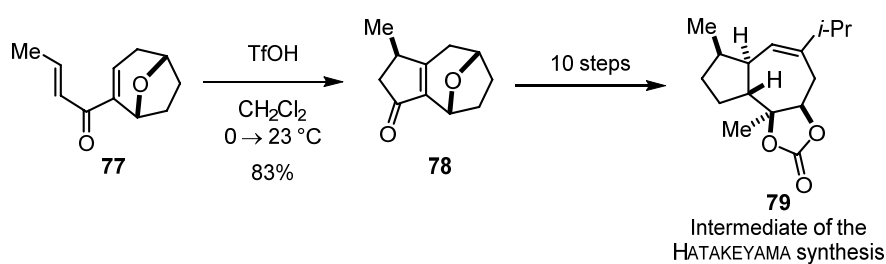
Scheme 24. MICHAEL addition/reductive coupling sequence reported by CHAIN et al.^[99]

Several englerin syntheses applied intramolecular HECK-reactions to close the five-membered ring after installing the oxo-bridged cycloheptane by cycloadditions.^[89,98] The group of COOK used a reductive intramolecular HECK-cyclization of vinyl iodide **75** to form the *trans*-fused hydroazulene core (**76**, Scheme 25).^[100] Ten more steps are necessary to achieve a formal synthesis of (-)-englerin A by reaching an intermediate of the MA synthesis (**60**).^[94a]



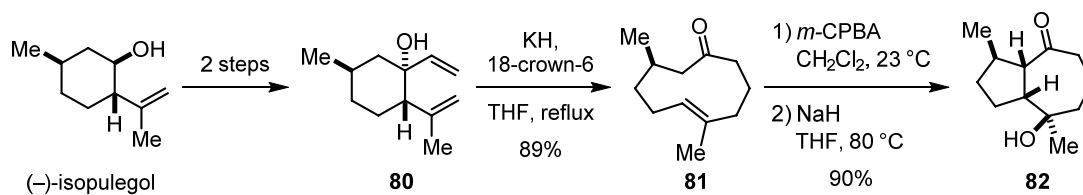
Scheme 25. Reductive HECK-cyclization approach by COOK et al.^[100]

A NAZAROV cyclization was the key-step in the synthesis of IWABUCHI et al. forming the five-membered ring (Scheme 26).^[101] Although this approach allows for the synthesis of the tricyclic framework **78** in just six steps, a lot of additional transformations are necessary to reach an intermediate of the HATAKEYAMA synthesis (**79**),^[93a] thus representing a relatively lengthy formal synthesis of (-)-englerin A.



Scheme 26. NAZAROV cyclization approach reported by IWABUCHI et al.^[101]

The group of MAIER reported a synthesis of 9-deoxy-englerin A starting from (–)-isopulegol using an oxy-COPE rearrangement and a transannular epoxide opening as key steps for the formation of the guaiane-skeleton (**82**, Scheme 27). Overall, this approach allowed for the synthesis of 9-deoxy-englerin A in 15 steps and 13% yield, but subsequent biological studies revealed no inhibitory activity, confirming the necessity of the C9-glycolate for the biological activity.



Scheme 27. Oxy-COPE rearrangement approach in the synthesis of 9-deoxy-englerin A by MAIER et al.^[102]

3.1.5 Structure-Activity-Relationship Studies of (-)-Englerin A

The structure-activity-relationship (SAR) of (-)-englerin A has been widely studied by several groups. Thereby, some structural features proved to be essential for the biological activity of englerin A. While (-)-englerin A is highly active against RCC lines, the unnatural enantiomer (+)-englerin A,^[5] as well as the glycolate lacking (-)-englerin B do not possess any significant inhibitory activity.^[3] Likewise, the radical simplification of the carbon skeleton (**83**),^[106] removal of the five-membered ring (**84**),^[96b] the C4-methyl group (**85**)^[107] or the C9-side chain (**86**)^[102] did not result in significantly active analogs (Figure 15). Mimicking englerin's structure by linking the cinnamate and glycolate side chains to the diol derivatives of the monoterpenes borneol (**87** and **88**) and fenchol (**89**) did not result in biologically active compounds either.^[108]

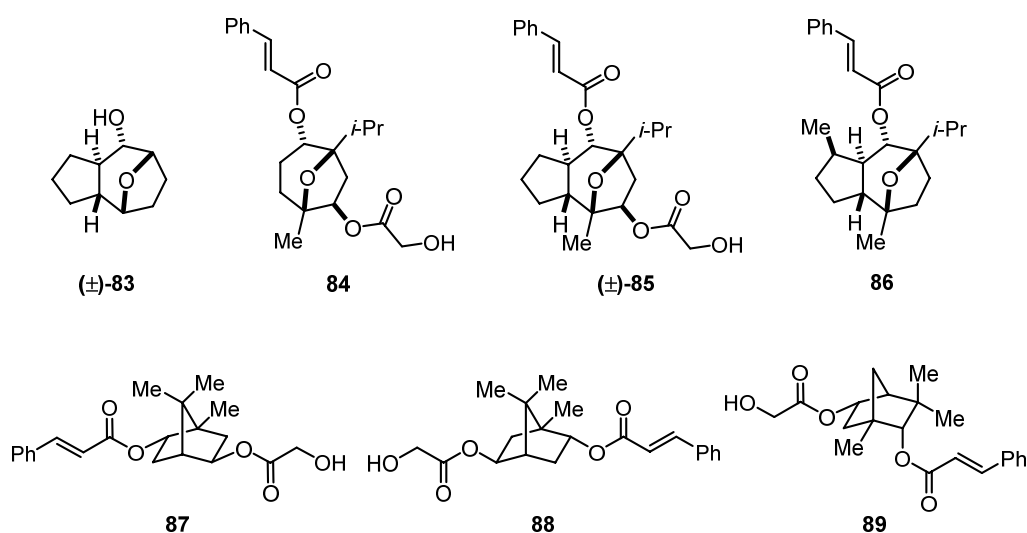


Figure 15. Activity lacking englerin analogs with a radically modified core structure.^[102,96b,106-108]

On the other hand, PARKER et al. showed that displacement of the C4-methyl group with the sterically more demanding isopropyl group increased the inhibitory activity against the RCC line A498 (Table 1, entry 4).^[109] The same is true for the C7-isopropyl group. CHRISTMANN et al. figured out that smaller substituents at this position decrease the inhibitory activity significantly (entries 5 and 6).^[5] In contrast, the analog bearing a more bulky (*S*)-*sec*-butyl group exhibits a five-fold increase in inhibitory activity (entry 8).^[110] The group of ECHAVARRAN confirmed this trend by presenting analogs with cyclopropyl, phenyl or cyclohexyl substituents in the C7-position, although these derivatives possess a double bond in the cyclopentane ring (entries 11 – 13).^[111] Compared to the isopropyl analog (entry 10) the more sterically demanding cyclohexyl derivative (entry 13) exhibits a higher activity. Interestingly, the cyclopropyl analog (entry 11) in ECHAVARRAN's studies even exhibits a higher inhibitory activity against the RCC line A498 than the cyclopropyl analog (entry 7) from CHRISTMANN's studies.^[103] To achieve a

better comparability of different SAR-studies, a relative inhibitory activity against the RCC line A498 is given by dividing the inhibitory activity (IC_{50} or GI_{50}) reported for (-)-englerin A in the respective publications by the activity of the analogs. Thus, a value above 1 signals an analog with a higher activity than (-)-englerin A.

Table 1. SAR-studies elucidating the influence of the C4-methyl and the C7-isopropyl group.^[5,110,103,111,109]



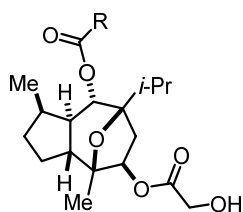
entry	R ¹	R ²	activity ^a	entry	R	activity ^{a,[111]}
1	Me	<i>i</i> -Pr	1	10	<i>i</i> -Pr	0.29
2	H	<i>i</i> -Pr	0.08 ^[109]	11	<i>c</i> -Pr	0.10
3	Et	<i>i</i> -Pr	0.26 ^[109]	12	Ph	0.11
4	<i>i</i> -Pr	<i>i</i> -Pr	1.23 ^[109]	13	<i>c</i> -hexyl	0.47
5	Me	Me	<0.01 ^[5]			
6	Me	Et	0.05 ^[5]			
7	Me	<i>c</i> -Pr	0.03 ^[103]			
8	Me	(<i>S</i>)- <i>s</i> -Bu	5.00 ^[110]			
9	Me	CH ₂ OBn	0.75 ^[110]			

a) Relative inhibitory activity against RCC line A498 (activity of (-)-englerin A divided by the activity of the analog).

The cinnamate ester proved to be readily accessible to modifications that increase englerin's potency as demonstrated in independent SAR studies from the CHRISTMANN and CHEN group (Table 2).^[112,5] The CHEN group synthesized racemic englerin A analogs, of whom only the 4-fluorocinnamate analog (entry 2) displayed a slightly higher antiproliferative activity against the RCC line A498 than (±)-englerin A. Interestingly, in the studies of CHRISTMANN the same, enantiopure analog showed a significantly lower activity. Two more derivatives, the cyclopropyl and the β-methyl cinnamate (entries 3 and 4) exhibited increased potency in another RCC line (UO31) but lower activity towards A498. The CHRISTMANN group synthesized a total of 21 cinnamate analogs. This first generation of analogs revealed three structural features, the (*E*)-β-methylcinnamate (entry 4), cyclohexylacrylate (entry 5) and 2-naphthoate (entry 6) to exhibit up to twice the activity of (-)-englerin A against the RCC line A498. Further studies in the CHRISTMANN group combined those structural features, resulting in analogs with

nanomolar potency (entries 7 – 11) especially those containing a 5,6,7,8-tetrahydro-2-naphthoate (entry 9) or a methyl group at C1-position of the naphthyl group (entry 10) with a three-fold increased potency.^[113] The analog that contained both these structural features (entry 11) even exhibited a five-fold increased cytotoxic activity compared to (-)-englerin A and therefore represents the analog with the highest reported activity to date.

Table 2. Selected cinnamate analogs and their inhibitory activity relative to englerin A in the RCC line A498.



First generation of analogs			Second generation of analogs		
entry	R	activity ^a	entry	R	activity ^{a,[113]}
1		1	7		0.86
2		0.06 ^[5] 1.40 ^[112]	8		1.02
3		0.92 ^[112]	9		3.72
4		1.73 ^[5] 0.52 ^[112]	10		3.04
5		1.80 ^[5]	11		5.06
6		1.88 ^[5]			


a) Relative inhibitory activity against RCC line A498 (activity of (-)-englerin A divided by the activity of the analog).

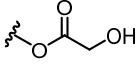
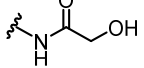
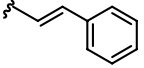
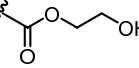
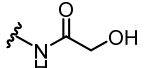
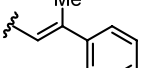
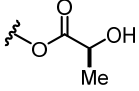
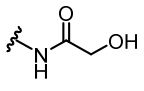
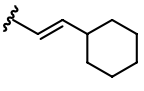
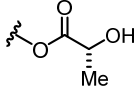
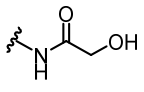
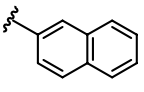
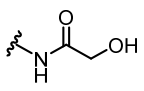
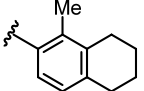
The glycolate ester was shown to be essential for the inhibitory activity of (-)-englerin A. However, its metabolic stability is a major issue. In vitro test indicated that englerin A is stable in the plasma of dogs and humans but in rat and mice plasma there was virtually no englerin A found anymore 90 minutes after the addition.^[82] On the other hand, a high concentration of englerin B was detected, suggesting a rapid metabolism. Thus, both the inhibitory activity as well as the metabolic stability were studied.

In both the CHEN and the CHRISTMANN studies, the antiproliferative activity of the glycolate ester was examined as well. CHEN introduced an inverse ester analog that exhibits almost the same potency as

englerin A (Table 3, entry 2). Furthermore, a (*S*)-lactate derivative was presented that shows twice the activity of englerin A (entry 3). These results could not be confirmed by CHRISTMANN's studies. Both the (*S*)- and the (*R*)-lactate analogs were synthesized, and both possessed a significantly lower activity (entry 3 and 4).^[113] Interestingly, the (*R*)-lactate was three times more active than the (*S*)-lactate. In conclusion, improvement of the inhibitory activity by varying the glycolate ester proved unsuccessful.

Table 3. Selected glycolate analogs and their inhibitory activity relative to englerin A in the RCC line A498.



entry	R ¹	activity ^a	entry	R ¹	R ²	activity ^a
1		1	5			0.06 ^[114]
2		0.93 ^[112]	6			<0.01 ^[114]
3		2.27 ^[112] 0.04 ^[113]	7			<0.01 ^[114]
4		0.12 ^[113]	8			<0.01 ^[114]
			9			0.03 ^[7]

a) Relative inhibitory activity against RCC line A498 (activity of (-)-englerin A divided by the activity of the analog).

In order to suppress the issue of metabolic instability, the group of CHAIN and the group of CHRISTMANN independently synthesized glycolate amide analogs.^[103,114,7] Although those derivatives exhibit significantly lower inhibitory activity (entries 5 – 9), pharmacokinetic evaluation in mice showed a good oral bioavailability and a much higher metabolic stability. Interestingly, variation of the cinnamate side chain (entries 6 – 9), which resulted in more potent analogs when bearing a glycolate ester at C9 (cf. Table 2, entries 4 – 6), was not well tolerated for the amide analogs.

The group of SCHNEIDER designed englerin analogs by computational de novo design (Figure 16). The resulting two low-molecular weight englerin A mimetics **90** and **91** were synthesized and exhibit nanomolar binding affinities and antagonistic efficiency towards transient receptor potential melastatin 8 (TRPM8) ion channels.^[115]

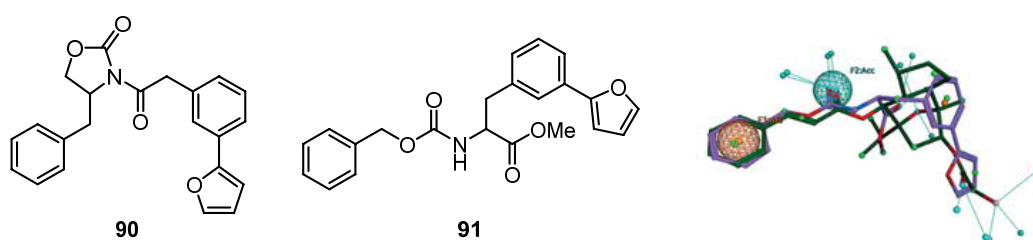


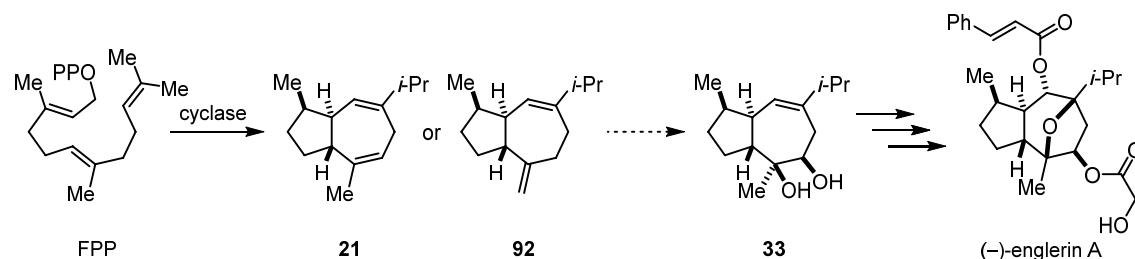
Figure 16. Computational de novo design of low-molecular weight englerin A mimetics. Comparison of the low-energy conformations of (-)-englerin A (green) and analog **91** (purple).

In conclusion, the extensive SAR-studies by various groups have resulted in ten analogs that undoubtedly exhibit a higher inhibitory activity than (-)-englerin A. Especially the modification of the cinnamate ester proved to be viable, resulting in analogs with up to five-fold enhanced antiproliferative activity. Furthermore, the displacement of the C4-methyl and the C7-isopropyl group with sterically more demanding substituents is beneficial for englerin's potency as well. Modifications of the glycolate ester only revealed the crucial role this side chain possesses, as no analog was found, that is undoubtedly more active. However, implementation of glycolate amide analogs at least solves the metabolic instability issues of the glycolate ester, albeit these derivatives are significantly less active.

3.2 Scientific Goal

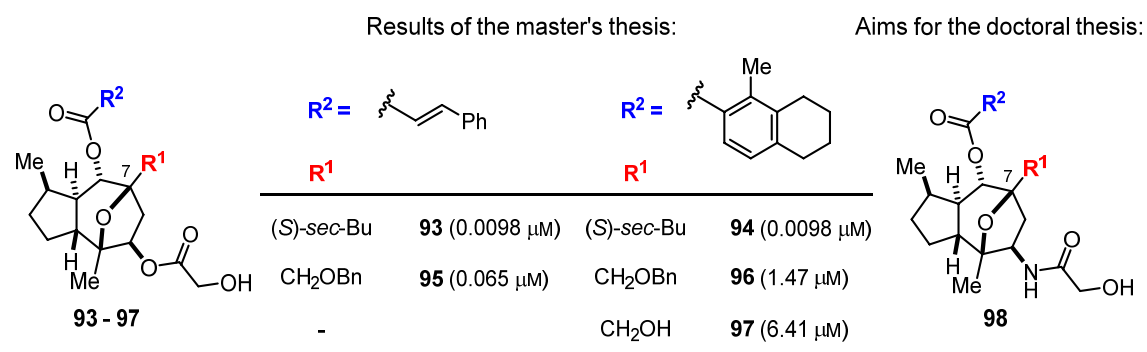
In collaboration with two biosynthesis groups, we aimed for a semisynthetic access to (-)-englerin A. The group of DICKSCHAT studies enzymatic mechanisms of terpene cyclases from fungi and bacteria by *in vitro* incubation with isotope-labeled isoprenoid substrates.^[116] LIU and coworkers have developed a platform, that allows for a high yield production of terpenoids, as well as for the mining of novel terpenoids by systematic engineering of metabolic pathways.^[117] In this context, a semisynthesis of (-)-englerin A was envisaged, based on a biosynthetically produced starting material.

Two potential precursors, guaia-6,9-diene (**21**) and guaia-6,10(14)-diene (**92**), should be synthesized starting from the diol intermediate **33** of CHRISTMANN's (-)-englerin A synthesis (Scheme 28). These guaianes should serve as a reference for the identification of suitable biosynthetic building blocks and as starting materials for studies aiming for the synthesis of (-)-englerin A.



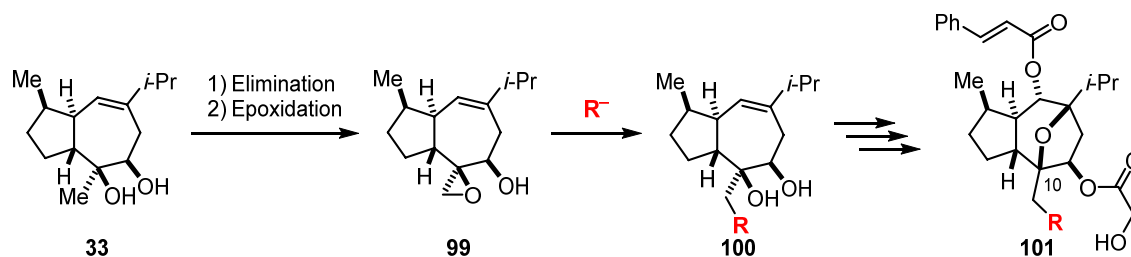
Scheme 28. Proposed semisynthetic pathway towards (-)-englerin A.

Another goal of this thesis was the synthesis of new (-)-englerin A analogs and studies of their structure-activity relationship. In the course of my master's thesis, I synthesized analogs bearing a (*S*)-sec-butyl (**93** and **94**), benzyloxymethyl (**95** and **96**), or hydroxymethyl group (**97**) instead of the isopropyl group at C7 (Scheme 29).^[110] Since the glycolate ester at C9 is metabolically instable, the amide analogs should be synthesized using a route that was previously developed in the CHRISTMANN group.^[103,7]



Scheme 29. Planned synthesis of amide analogs bearing the C7 side chains introduced during the master's thesis. Inhibition of cell proliferation in RCC line A498 (IC₅₀ in brackets, cf. (-)-englerin A: IC₅₀ = 0.045 μM).

The methyl group at C10 has never been subject to any SAR study. A functionalization would be possible by eliminating the tertiary alcohol of diol intermediate **33**, performing an epoxidation of the resulting alkene and opening this epoxide (**99**) with various nucleophiles (Scheme 30). This would lead back to a diol intermediate (**100**), that can be transformed into englerin A analogs (**101**).



Scheme 30. Planned synthesis of novel C10 analogs.

3.3 Publications

3.3.1 Mechanistic Characterisation of Two Sesquiterpene Cyclases from the Plant Pathogenic Fungus *Fusarium fujikuroi*

IMMO BURKHARDT, THOMAS SIEMON, MATTHIAS HENROT, LENA STUDT, SARAH RÖSLER, BETTINA TUDZYNSKI, MATHIAS CHRISTMANN,* AND JEROEN S. DICKSCHAT*

Angew. Chem. Int. Ed. **2016**, *55*, 8748 – 8751. (DOI: 10.1002/anie.201603782)

Angew. Chem. **2016**, *128*, 8890 – 8893. (DOI: 10.1002/ange.201603782)

Permission granted for reproduction in print and electronic format for the purpose of this dissertation, by: *Angew. Chem. Int. Ed.* **2016**, *55*, 8748 – 8751, [http:// dx.doi.org/10.1002/anie.201603782](http://dx.doi.org/10.1002/anie.201603782).

Copyright: **2016** Wiley-VCH Verlag GmbH & Co. KGaA, Weinheim

Abstract: Two sesquiterpene cyclases from *Fusarium fujikuroi* were expressed in *Escherichia coli* and purified. The first enzyme was inactive because of a critical mutation, but activity was restored by sequence correction through site-directed mutagenesis. The mutated enzyme and two naturally functional homologues from other fusaria converted farnesyl diphosphate into guaia-6,10(14)-diene. The second enzyme produced eremophilene. The absolute configuration of guaia-6,10(14)-diene was elucidated by enantioselective synthesis, while that of eremophilene was evident from the sign of its optical rotation and is opposite to that in plants but the same as in *Sorangium cellulosum*. The mechanisms of both terpene cyclases were studied with various ¹³C- and ²H-labelled FPP isotopomers.

Author Contribution:

T. SIEMON performed the synthesis of compound **1** and provided the analytic data (NMR, HRMS, IR, optical rotation) for this compound and the synthetic intermediates **5**. Samples of the synthetic compounds were provided to the co-authors as a reference for their studies. The part of the manuscript concerning the enantioselective synthesis of compound **1** was written by T. SIEMON, M. HENROT and M. CHRISTMANN.

Natural Products

International Edition: DOI: 10.1002/anie.201603782

German Edition: DOI: 10.1002/ange.201603782

Mechanistic Characterisation of Two Sesquiterpene Cyclases from the Plant Pathogenic Fungus *Fusarium fujikuroi*

Immo Burkhardt, Thomas Siemon, Matthias Henrot, Lena Studt, Sarah Rösler, Bettina Tudzynski, Mathias Christmann,* and Jeroen S. Dickschat*

Abstract: Two sesquiterpene cyclases from *Fusarium fujikuroi* were expressed in *Escherichia coli* and purified. The first enzyme was inactive because of a critical mutation, but activity was restored by sequence correction through site-directed mutagenesis. The mutated enzyme and two naturally functional homologues from other fusaria converted farnesyl diphosphate into guaia-6,10(14)-diene. The second enzyme produced eremophilene. The absolute configuration of guaia-6,10(14)-diene was elucidated by enantioselective synthesis, while that of eremophilene was evident from the sign of its optical rotation and is opposite to that in plants but the same as in *Sorangium cellulosum*. The mechanisms of both terpene cyclases were studied with various ¹³C- and ²H-labelled FPP isotopomers.

The rice pathogenic fungus *Fusarium fujikuroi* causes severe crop losses in agriculture through the production of mycotoxins, including the fumonisins, fusarins, fusaric acid, and moniliformin.^[1] Furthermore, large amounts of gibberellins, an important class of plant hormones that derive from the diterpene *ent*-kaurene, are produced by the fungus.^[2] In plants, gibberellins regulate processes such as stem and leaf growth, flowering, fruiting, and seed germination. Their overproduction by fusaria causes out-of-control growth and development in infected plants that is known as the “foolish seedling” or “bakanae” disease. The distantly related *F. sporotrichioides* makes a family of mycotoxins derived from trichodiene, the trichothecenes.^[3] These compounds are absent in *F. fujikuroi* and related species because the biosynthetic genes, including a trichodiene synthase gene,

are missing in their genomes. Instead, the *F. fujikuroi* genome houses a bifunctional *ent*-copalyl diphosphate synthase/*ent*-kaurene synthase (CPS/KS) for gibberellin biosynthesis,^[4] a lanosterol synthase, a phytoene synthase for neurosporoxanthin biosynthesis,^[5] and nine sesquiterpene cyclases (STC1–9).^[6] Only two of these have been characterized as (+)-koraol (STC4) and (–)- α -acorenol synthases (STC6),^[7] but knowledge about the products of the other STCs is important because it may lead to the identification of undiscovered mycotoxins that are potentially involved in plant pathogenicity. Herein, we describe the identification of the products from STC5 (FFUJ11739) and STC3 (FFUJ04067) and their mechanistic characterization by isotopic labelling techniques.^[8]

Two uncharacterized STCs from *F. fujikuroi* (STC5 and STC3) were investigated through the construction of overexpression mutants. The mutants were analyzed for the production of terpenes by capturing their volatiles on charcoal filters followed by GC/MS analysis.^[9] Although quantitative reverse transcription (RT)-PCR revealed higher expressions of the terpene cyclase genes, none of the mutants showed production of a new terpene compared to the wildtype, possibly because of oxidative modifications by other enzymes with genes that are clustered with the terpene cyclase genes (Figure S1 in the Supporting Information). Reverse transcription of the corresponding mRNA and amplification of the cDNA by PCR allowed gene cloning into the yeast-to-*E. coli* shuttle vector pYE-Express through homologous recombination.^[10] The proteins were expressed, purified, and incubated with geranyl (GPP), farnesyl (FPP), and geranylgeranyl (GGPP) diphosphate, followed by GC/MS analysis of the formed products.

STC5 yielded no product from any of the tested substrates, presumably because of a critically mutated gene that leads to an asparagine to lysine exchange in the NSE triad that usually displays a ND(L,I,V)XSXXXE sequence in functional terpene cyclases (Figure S2).^[11] Two STC5 homologues from *F. mangiferae* and *F. proliferatum* with intact NSE triads both yielded a sesquiterpene from FPP (Figures S3 and S4A), while no products were observed for GPP or GGPP. Sequence correction of *F. fujikuroi* STC5 through K288N mutation restored activity and gave the same product. A preparative-scale incubation of 60 mg FPP with *F. mangiferae* STC5 allowed the isolation of 1 mg (4%) of the pure compound. Its structure was established by one- and two-dimensional NMR techniques (Table S1 in the Supporting Information). The ¹³C-NMR spectra revealed fifteen signals (three methyl groups, four sp³ methylene and four sp³ methine carbons, two olefinic quarternary carbons, one olefinic

[*] I. Burkhardt, Prof. Dr. J. S. Dickschat

Kekulé-Institut für Organische Chemie und Biochemie
Rheinische Friedrich-Wilhelms-Universität Bonn
Gerhard-Domagk-Straße 1, 53121 Bonn (Germany)
E-mail: dickschat@uni-bonn.deT. Siemon, Dr. M. Henrot, Prof. Dr. M. Christmann
Institut für Chemie und Biochemie – Organische Chemie
Freie Universität Berlin, Takustraße 3, 14195 Berlin (Germany)Dr. L. Studt, S. Rösler, Prof. Dr. B. Tudzynski
Institut für Biologie und Biotechnologie der Pflanzen
Westfälische Wilhelms-Universität Münster
Schlossplatz 8, 48143 Münster (Germany)Dr. L. Studt
Institut für Angewandte Genetik und Zellbiologie
Universität für Bodenkultur Wien
Konrad-Lorenz-Straße 24/1, 3430 Tulln an der Donau (Austria)Supporting information and the ORCID identification number(s) for the author(s) of this article can be found under <http://dx.doi.org/10.1002/anie.201603782>.

methylene, and one olefinic CH), suggesting a bicyclic system. The $^1\text{H-NMR}$ signals for the directly coupled hydrogens were assigned from the HMQC spectrum and $^1\text{H},^1\text{H-COSY}$ showed three contiguous spin systems (C1-2-3-4(-15)-5-6, C11(-13)-12 and C8-9, Figure 1A). HMBC correlations from H11, H12, and H13 to C7 indicated a C7–C11 bond, while

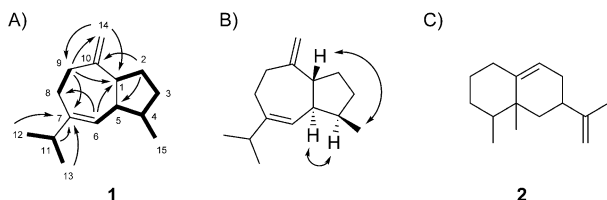
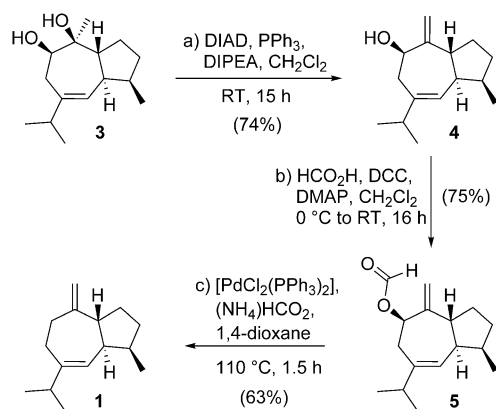


Figure 1. Structures of the enzyme products. A) Contiguous spin systems of **1** determined by $^1\text{H},^1\text{H-COSY}$ (bold) and key HMBC correlations (arrows); B) key NOESY correlations for **1** (double headed arrows); C) structure of **2**.

cross-peaks from H8 and H9 to C7 and H6 to C8 revealed a C6-7-8 linkage. Correlations from H14 to C1 and C9, from H9 to C1 and C14, and from H2 to C10 placed C10 between C1 and C9. The ring closure from C1 to C5 was evident from cross-peaks between H2 and C5 and between H6 and C1, resulting in the planar structure of guaia-6,10(14)-diene (**1**). Key NOESY correlations between H1–H15 and H4–H5 suggested a *trans*-guaiane (Figure 1B).

The absolute configuration of **1** was elucidated through enantioselective synthesis starting with diol **3**, a well-characterized intermediate from our englerin synthesis (Scheme 1).^[12] Using a Mitsunobu protocol,^[13] selective

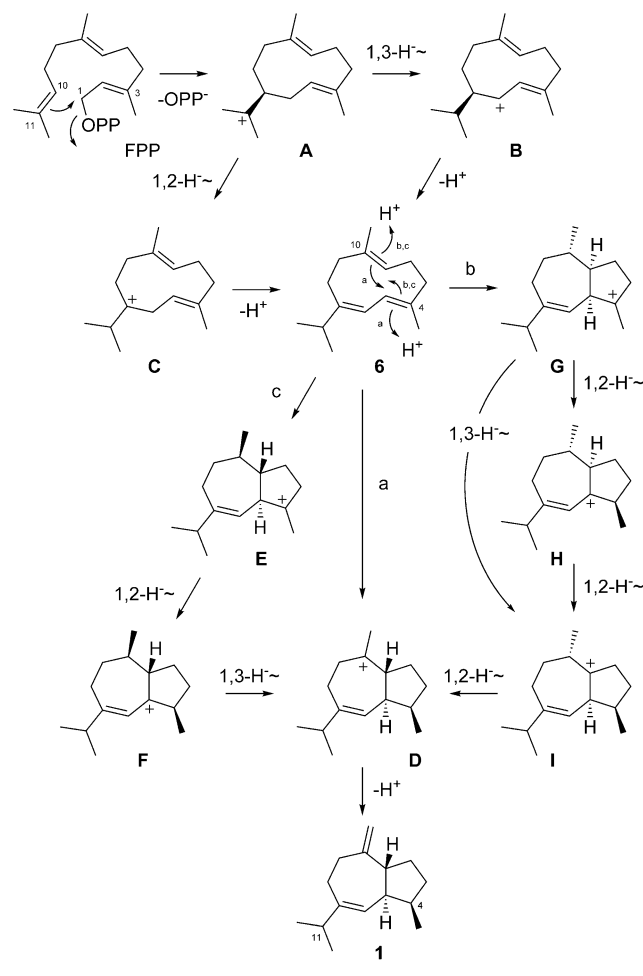


Scheme 1. Enantioselective synthesis of (1*R*,4*R*,5*S*)-**1**.

elimination of the tertiary alcohol afforded exocyclic alkene **4** in 74% yield (notably, a natural product with identical spectroscopic data yet a different structure was published).^[14] The secondary alcohol was converted into the corresponding formate **5** through Steglich esterification.^[15] Pd-catalyzed hydrogenolysis^[16] of the allylic formate afforded (1*R*,4*R*,5*S*)-**1** in 63% yield with an optical rotation of $[\alpha]_{\text{D}}^{22.8} = -22.2$ (*c* 0.15, CH_2Cl_2), while the optical rotation of the enzyme product was $[\alpha]_{\text{D}}^{22.0} = -19.3$ (*c* 0.15, CH_2Cl_2), thus confirming

their identity. A compound with identical spectroscopic data but incompletely assigned configuration was reported from the soft coral *Nephtea chabrollei*.^[17]

Several mechanisms for FPP cyclization to **1** can be proposed (Scheme 2). The initial 1,10-cyclization of FPP to the (*E,E*)-germacradienyl cation (**A**) may be followed by a 1,3-hydride shift to **B** or a 1,2-hydride migration to **C** and



Scheme 2. Proposed cyclization mechanisms for the biosynthesis of **1**.

deprotonation to germacrene **C** (**6**). Reprotonation at C4 of **6** and cyclization (path a) can give rise to **D** that yields **1** upon deprotonation. Alternatively, **6** may be cyclized by C10 reprotonation to **G**, followed by three sequential 1,2-hydride shifts via **H** and **I** to **D** (path b). Cation **I** is also accessible from **G** by 1,3-hydride migration. Finally, C10 reprotonation of **6** may initiate a cyclization to **E**, a stereoisomer of **G**, which produces **D** by a sequence of a 1,2- and a 1,3-hydride transfer (path c). The proposed mechanisms were experimentally tested through the enzymatic conversion of labelled FPP isotopomers.^[18] (1,1- $^2\text{H}_2$,11- ^{13}C)FPP resulted in labelled **1** that exhibited a singlet at $\delta = 37.8$ ppm for C11 in the $^{13}\text{C-NMR}$, thus indicating that no deuterium was attached to this carbon atom (Figure 2A). In conclusion, the conversion of **A** into **6** does not proceed by a 1,3-hydride shift via **B**. GC/MS analysis of the product revealed the loss of one deuterium by

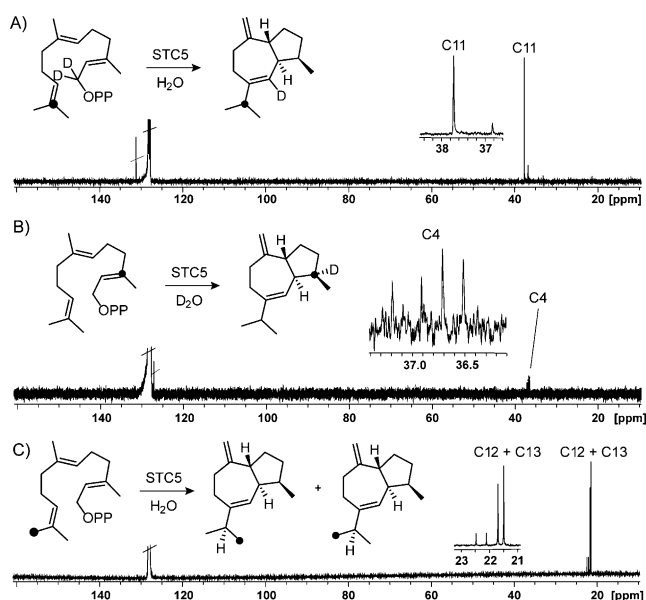
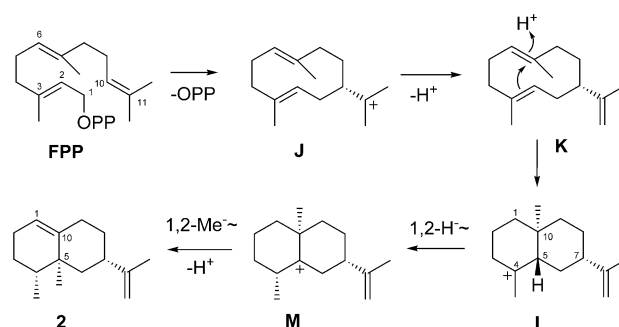


Figure 2. Enzymatic mechanism of STC5. ^{13}C -NMR spectrum of A) (6- ^2H ,11- ^{13}C)-**1** obtained from (1,1- $^2\text{H}_2$,11- ^{13}C)FPP, B) (4- ^2H ,4- ^{13}C)-**1** from (3- ^{13}C)FPP in D_2O , C) mixture of (12- ^{13}C)-**1** and (13- ^{13}C)-**1** obtained from (13- ^{13}C)FPP. Black dots indicate ^{13}C -labelled carbons.

a molecular ion at m/z 206, as is expected for the pathway via **C** (Figure S4B). Enzymatic conversion of (10- ^2H)FPP^[19] yielded a product with an increased molecular mass of m/z 205 in its mass spectrum, but still the same base peak ion at m/z 161 as unlabeled **1** (Figure S4C). Since this fragment ion arises through isopropyl cleavage, the deuterium labelling in the terpene obtained from (10- ^2H)FPP can be localized in the isopropyl group, thus corroborating the 1,2-hydride shift from **A** to **C**. To distinguish between the options for the reprotonation of **6**, incubation experiments in D_2O were performed.^[20] Incubation of (3- ^{13}C)FPP in D_2O yielded a triplet for C4 of **1** at $\delta = 36.7$ ppm ($\Delta\delta = -0.5$ ppm, $^1J_{\text{C,D}} = 20.1$ Hz), thus indicating that deuterium was connected to C4 (Figure 2B). This finding is in agreement with the conversion of **6** into **D** and **1** via pathway a, but not via pathways b or c. The singlet at $\delta = 37.2$ ppm indicated that a portion of the labelled material was not deuterated at C4 because the incubation buffer contained residual water, as was also evident from GC/MS analysis of the sample (Figure S4D). To exclude the possibility that a minor fraction of **6** may react via pathway b or c to cation **D**, (2- ^{13}C)FPP and (6- ^{13}C)FPP were enzymatically converted in D_2O , yielding (^2H ,5- ^{13}C)-**1** and (^2H ,1- ^{13}C)-**1**, which only exhibited singlets for C5 and C1 (Figure S5), while deuterium uptake was evident from the mass spectra (Figures S4E and S4F). In conclusion, pathway a is the only one that is relevant for the reaction from **6** to **D**. An incubation experiment with (13- ^{13}C)FPP resulted in amplified ^{13}C signals for both C12 and C13 (Figure 2C), thus indicating that the isopropyl group in cation **A** is not conformationally fixed but can freely rotate prior to the 1,2-hydride shift to **C**.

Incubation of STC3 with FPP yielded a sesquiterpene, while GPP and GGPP were not accepted. GC/MS analysis (Figure S6A) suggested the structure of valencene or eremo-

philene, but it was not possible to clearly assign one of these structures. A large-scale incubation of 50 mg FPP yielded 4.6 mg (19%) of the pure sesquiterpene with ^1H - and ^{13}C -NMR data matching those of eremophilene (**2**; Table S1).^[21] Determination of the rotary power as $[\alpha]_{\text{D}}^{20.8} = +86.1$ (c 0.36, CHCl_3) (lit.: $[\alpha]_{\text{D}}^{25} = +131.7$ (c 1.0, CHCl_3))^[21] pointed to the opposite enantiomer to in plants and the coral *Plexaurella fusifera*,^[22] but the same as in the myxobacterium *Sorangium cellulosum*.^[21] The proposed biosynthesis of **2** (Scheme 3)



Scheme 3. Proposed cyclization mechanism for the biosynthesis of **2**.

starts with a 1,10-cyclization of FPP to the (*E,E*)-germacradienyl cation **J**, followed by deprotonation to germacrene **A** (**K**). Cyclization upon reprotonation at C6 leads to the cation **L**, and subsequent 1,2-hydride and 1,2-methyl migrations and deprotonation yield **2**. The 1,2-hydride shift to **M** was shown by enzymatic conversion of (2- ^2H ,3- ^{13}C)FPP, which resulted in a triplet at $\delta = 36.6$ ppm ($\Delta\delta = -0.5$ ppm, $^1J_{\text{C,D}} = 19.0$ Hz) in the ^{13}C -NMR spectrum of **2**, thus indicating the connection of deuterium to C4 (Figure 3A). A singlet for the non-deuterated compound is also visible at $\delta = 37.1$ ppm as a result of the deuteration grade of the substrate (86% by MS, Figure S6B). The reprotonation in **K** occurs at the same carbon atom from which a proton is lost in the final step. To test whether it is the same or another proton that is first introduced and then lost, an enzymatic conversion of FPP in D_2O was conducted. Indeed GC/MS analysis of the product gave no evidence for any deuterium uptake from D_2O (Figure S6C). Finally, the

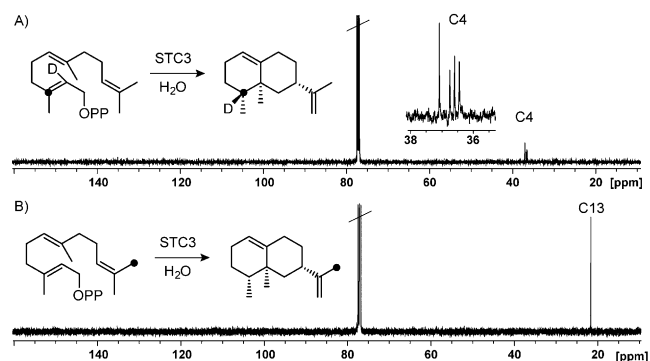


Figure 3. Enzymatic mechanism of STC3. ^{13}C -NMR spectra of A) (4- ^2H ,4- ^{13}C)-**2** obtained from (2- ^2H ,3- ^{13}C)FPP, B) (13- ^{13}C)-**2** obtained from (13- ^{13}C)FPP. Black dots indicate ^{13}C -labelled carbons.

stereochemical fate of the terminal methyl groups of FPP was followed by enzymatic conversion of (13-¹³C)FPP, which resulted in the incorporation of labelling only into the methyl group C13 and not C12 of **2** (Figure 3B). In contrast to STC5, STC3 shows a strict stereochemical course in this aspect, as previously described for several other terpene cyclases.^[18a,23]

In summary we have identified STC3 and STC5 from *F. fujikuroi* as (+)-eremophilene and (–)-guaia-6,10(14)-diene synthases. STC5 in *F. fujikuroi* was only active after a sequence correction in the mutated NSE triad, while homologues from *F. proliferatum* and *F. mangiferae* are naturally functional. The biosynthesis of both compounds was investigated in detail to show the stereospecific course of the cyclizations, reprotonations, and hydride shifts. A detailed investigation of the multilayer regulation of the STC5 gene cluster by pathway-specific and epigenetic processes in *F. fujikuroi* is currently in progress.

Acknowledgments

This work was funded by the DFG (DI1536/7-1, TU101/16-3).

Keywords: enzyme mechanisms · *Fusarium fujikuroi* · isotopic labelling · NMR spectroscopy · terpenes

How to cite: *Angew. Chem. Int. Ed.* **2016**, *55*, 8748–8751
Angew. Chem. **2016**, *128*, 8890–8893

- [1] a) M. Jestoi, *Crit. Rev. Food Sci. Nutr.* **2008**, *48*, 21; b) E. M. Niehaus, K. Kleigrew, P. Wiemann, L. Studt, C. M. Sieber, L. R. Connolly, M. Freitag, U. Güldener, B. Tudzynski, H.-U. Humpf, *Chem. Biol.* **2013**, *20*, 1055; c) L. Studt, S. Janevska, E. M. Niehaus, I. Burkhardt, B. Arndt, C. M. Sieber, H.-U. Humpf, J. S. Dickschat, B. Tudzynski, *Environ. Microbiol.* **2016**, *18*, 936.
- [2] C. Bömke, B. Tudzynski, *Phytochemistry* **2009**, *70*, 1876.
- [3] M. Kimura, T. Tokai, N. Takahashi-Ando, S. Ohsato, M. Fujimura, *Biosci. Biotechnol. Biochem.* **2007**, *71*, 2105.
- [4] B. Tudzynski, H. Kawaide, Y. Kamiya, *Curr. Genet.* **1998**, *34*, 234.
- [5] P. Linnemannstöns, M. M. Prado, R. Fernandez-Martin, B. Tudzynski, J. Avalos, *Mol. Genet. Genomics* **2002**, *267*, 593.
- [6] P. Wiemann, C. M. Sieber, K. W. von Barga, L. Studt, E. M. Niehaus, J. J. Espino, K. Huß, C. B. Michielse, S. Albermann, S. V. Bergner, et al., *PLoS Pathog.* **2013**, *9*, e1003475.
- [7] a) N. L. Brock, K. Huss, B. Tudzynski, J. S. Dickschat, *ChemBioChem* **2013**, *14*, 311; b) C. A. Citron, N. L. Brock, B. Tudzynski, J. S. Dickschat, *Chem. Commun.* **2014**, *50*, 5224.
- [8] J. Rinkel, J. S. Dickschat, *Beilstein J. Org. Chem.* **2015**, *11*, 2493.
- [9] a) K. Grob, F. Zürcher, *J. Chromatogr. A* **1976**, *117*, 285; b) J. S. Dickschat, *Nat. Prod. Rep.* **2014**, *31*, 838; c) C. A. Citron, P. Rabe, J. S. Dickschat, *J. Nat. Prod.* **2012**, *75*, 1765.
- [10] J. S. Dickschat, K. A. K. Pahirulzaman, P. Rabe, T. A. Klapschinski, *ChemBioChem* **2014**, *15*, 810.
- [11] a) M. Seemann, G. Zhai, J.-W. de Kraker, C. M. Paschall, D. W. Christianson, D. E. Cane, *J. Am. Chem. Soc.* **2002**, *124*, 7681; b) J. S. Dickschat, *Nat. Prod. Rep.* **2016**, *33*, 87.
- [12] a) M. Willot, L. Radtke, D. Könnig, R. Fröhlich, V. H. Gessner, C. Strohmman, M. Christmann, *Angew. Chem. Int. Ed.* **2009**, *48*, 9105; *Angew. Chem.* **2009**, *121*, 9269; b) L. Radtke, M. Willot, H. Y. Sun, S. Ziegler, S. Sauerland, C. Strohmman, R. Fröhlich, P. Habenberger, H. Waldmann, M. Christmann, *Angew. Chem. Int. Ed.* **2011**, *50*, 3998; *Angew. Chem.* **2011**, *123*, 4084.
- [13] A. F. Barrero, E. J. Alvarez-Manzaneda, R. Chahboun, *Tetrahedron Lett.* **2000**, *41*, 1959.
- [14] Q. Wang, D. Chen, *Helv. Chim. Acta* **2007**, *90*, 2432.
- [15] B. Neises, W. Steglich, *Angew. Chem. Int. Ed. Engl.* **1978**, *17*, 522; *Angew. Chem.* **1978**, *90*, 556.
- [16] J. Tsuji, T. Yamakawa, *Tetrahedron Lett.* **1979**, *20*, 613.
- [17] M. Rama Rao, K. V. Sridevi, U. Venkatesham, T. Prabhaker Rao, S. S. Lee, Y. Venkatesvarlu, *J. Chem. Res.* **2000**, 245.
- [18] a) P. Rabe, L. Barra, J. Rinkel, R. Riclea, C. A. Citron, T. A. Klapschinski, A. Janusko, J. S. Dickschat, *Angew. Chem. Int. Ed.* **2015**, *54*, 13448; *Angew. Chem.* **2015**, *127*, 13649; b) D. E. Cane, J. S. Oliver, P. H. M. Harrison, C. Abell, B. R. Hubbard, C. T. Kane, R. Lattman, *J. Am. Chem. Soc.* **1990**, *112*, 4513; c) J. A. Faraldos, S. Wu, J. Chappell, R. M. Coates, *J. Am. Chem. Soc.* **2010**, *132*, 2998.
- [19] C. A. Citron, P. Rabe, L. Barra, C. Nakano, T. Hoshino, J. S. Dickschat, *Eur. J. Org. Chem.* **2014**, 7684.
- [20] a) P. Rabe, K. A. K. Pahirulzaman, J. S. Dickschat, *Angew. Chem. Int. Ed.* **2015**, *54*, 6041; *Angew. Chem.* **2015**, *127*, 6139; b) P. Rabe, J. Rinkel, T. A. Klapschinski, L. Barra, J. S. Dickschat, *Org. Biomol. Chem.* **2016**, *14*, 158; c) P. Rabe, A. Janusko, B. Goldfuss, J. S. Dickschat, *ChemBioChem* **2016**, *17*, 146.
- [21] A. Schiffrin, T. T. B. Ly, N. Günnewich, J. Zapp, V. Thiel, S. Schulz, F. Hannemann, Y. Khatri, R. Bernhardt, *ChemBioChem* **2015**, *16*, 337.
- [22] a) J. Hochmannová, V. Herout, *Collect. Czech. Chem. Commun.* **1964**, *29*, 2369; b) J. L. Frenz-Ross, J. J. Enticknap, R. G. Kerr, *Mar. Biotechnol.* **2008**, *10*, 572.
- [23] a) F. C. Baker, C. J. W. Brooks, S. A. Hutchinson, *J. Chem. Soc. Chem. Commun.* **1975**, 293b; b) D. E. Cane, P. C. Prabhakaran, J. S. Oliver, D. B. McIlwaine, *J. Am. Chem. Soc.* **1990**, *112*, 3209; c) C.-M. Wang, R. Hopson, X. Lin, D. E. Cane, *J. Am. Chem. Soc.* **2009**, *131*, 8360; d) N. L. Brock, S. R. Ravella, S. Schulz, J. S. Dickschat, *Angew. Chem. Int. Ed.* **2013**, *52*, 2100; *Angew. Chem.* **2013**, *125*, 2154.

Received: April 19, 2016

Published online: June 13, 2016

3.3.2 Microbe Engineering of Guaia-6,10(14)-diene as a Building Block for the Semisynthetic Production of Plant-Derived (-)-Englerin A

THOMAS SIEMON,^a ZHANGQIAN WANG,^a GUANGKAI BIAN,^a TOBIAS SEITZ, ZILING YE, YAN LU, SHU CHENG, YUNKUN DING, ZIXIN DENG, TIANGANG LIU* AND MATHIAS CHRISTMANN*

a) These authors contributed equally to this work.

The following part has been submitted to:

J. Am. Chem. Soc. **2020**

Herein, a preprint version of this article is published.

Permission for the reproduction of the preprint version of this article is granted by:

Copyright © 2020 American Chemical Society.

Abstract: Herein, we report the semisynthetic production of the potent transient receptor potential canonical (TRPC) channel agonist (-)-englerin A (EA), using guaia-6,10(14)-diene as the starting material. Guaia-6,10(14)-diene was systematically engineered in *Escherichia coli* and *Saccharomyces cerevisiae* using the CRISPR/Cas9 system and produced with high titers. This opened the possibility for a very short chemical synthesis of EA and the two related guaianes (-)-oxyphyllol and (+)-orientalol E. The potentially scalable approach combines the advantages of synthetic biology and chemical synthesis and provides an efficient and economical method for producing EA and its analogues.

Author Contribution: T. Siemon performed the chemical synthesis of compound **4**, (-)-oxyphyllol (**10**) and (+)-orientalol E (**11**) and all intermediates. The analytic data (NMR, HRMS, IR, optical rotation) for these compounds were collected and analyzed by T. Siemon. The conversion of compound **4** to (-)-englerin A (EA) was performed and reported by T. Seitz.^[7] The introduction of the manuscript and the chemical synthesis part were written by T. Siemon and M. Christmann, in collaboration with T. Liu.

Microbe Engineering of Guaia-6,10(14)-diene as a Building Block for the Semisynthetic Production of Plant-Derived (-)-Englerin A

Thomas Siemon,^{1,5} Zhangqian Wang,^{2,5} Guangkai Bian,^{2,5} Tobias Seitz,¹ Ziling Ye,³ Yan Lu,² Shu Cheng,² Yunkun Ding,² Zixin Deng,^{2,4} Tiangang Liu*^{2,4} and Mathias Christmann*¹

¹Institute of Chemistry and Biochemistry, Freie Universität Berlin, Berlin, Germany. ²Key Laboratory of Combinatorial Biosynthesis and Drug Discovery, Ministry of Education and School of Pharmaceutical Sciences, Wuhan University, Wuhan, China. ³J1 Biotech Co., Ltd., Wuhan, China. ⁴Hubei Engineering Laboratory for Synthetic Microbiology, Wuhan Institute of Biotechnology, Wuhan, China. ⁵These authors contributed equally to this work. *e-mail: liutg@whu.edu.cn or mathias.christmann@fu-berlin.de

Abstract: Herein, we report the semisynthetic production of the potent transient receptor potential canonical (TRPC) channel agonist (-)-englerin A (EA), using guaia-6,10(14)-diene as the starting material. Guaia-6,10(14)-diene was systematically engineered in *Escherichia coli* and *Saccharomyces cerevisiae* using the CRISPR/Cas9 system and produced with high titers. This opened the possibility for a very short chemical synthesis of EA and the two related guaianes (-)-oxyphyllol and (+)-orientalol E. The potentially scalable approach combines the advantages of synthetic biology and chemical synthesis and provides an efficient and economical method for producing EA and its analogues.

From the beginnings of mankind, extracts from Nature have been used to deliver medical benefit to those in need.¹ As therapeutics moved from mixtures to constitutionally and stereochemically defined molecular entities, there has been a growing demand to access active pharmaceutical ingredients in high purity and on scale. Extraction from the natural host has traditionally been in competition with chemical synthesis. While extraction from plants may be harmful to the environment or suffer from low titers, multistep chemical synthesis may require large amounts of potentially harmful solvents and toxic reagents. In recent years, the progress in molecular biology and the development of the CRISPR/Cas9 system have allowed for the engineering of microbial pathways to produce biopharmaceuticals.² However, biotechnological processes are often optimized towards defined products and usually do not allow the flexibility that chemical synthesis offers. Therefore, a biomimetic semisynthesis can provide a viable alternative by combining the benefits of synthetic biology and chemical synthesis.

Terpenoid natural products are a prime example for such a strategy as they represent some of the most potent modulators of biological processes and their biosynthesis is rather straightforward. The initial cyclization of oligoprenyls is followed by oxidation and optional post-functionalization processes such as esterifications or glycosylations. Each step in this sequence adds a layer of complexity towards the optimal binding to the protein of interest (**Fig. 1**).

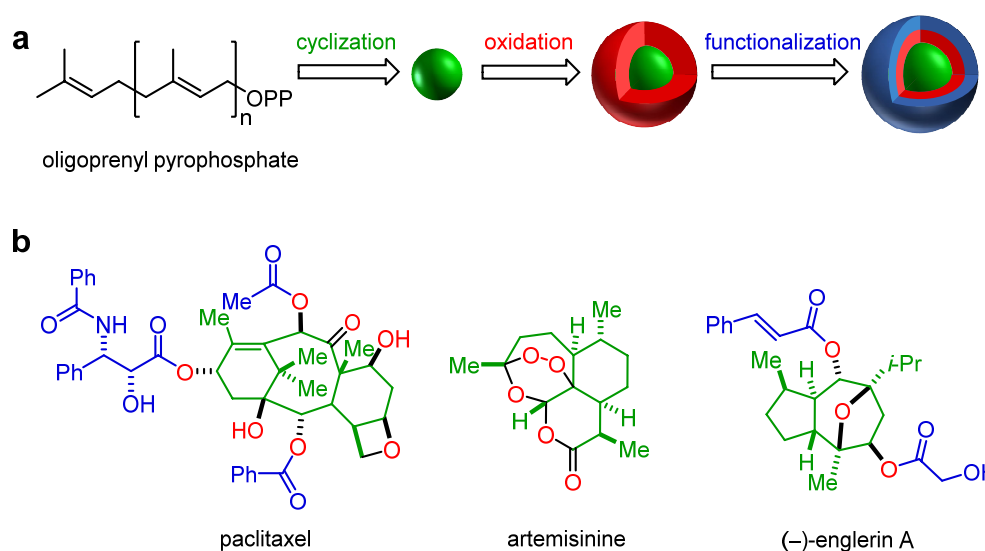


Figure 1. Assembly of bioactive terpenoids. a) Nature's blueprint for complex terpenoid synthesis. b) Three examples of bioactive natural products with layered complexity.

Mimicking this blueprint from nature, biology can provide the core scaffold, while synthetic chemists are able to manipulate the outer spheres. This strategy has been successfully applied for the commercial production of paclitaxel by using leaf extracted baccatin III as the starting core material,³ and by using the engineered microbe-produced artemisinic acid as the starting material for the semisynthesis of artemisinin.⁴ Herein, we describe the fusion of yeast biotechnology with chemical synthesis to provide a straightforward access to the potent transient receptor potential canonical (TRPC) channel agonist (-)-englerin A (EA).

In 2009, a screening campaign by Beutler and coworkers found extracts from the root bark of the East African plant *Phyllanthus engleri* to selectively inhibit the growth of Renal cell carcinoma with nanomolar activity and the guaiane-type sesquiterpenoid EA was isolated as the active principle.⁵ The cellular target of EA was identified as the non-selective TRPC ion channels 1/4/5. EA selectively binds to the externally exposed site of those channels and induces a Ca^{2+} - or Na^{+} -ion influx that finally leads to cell death by overloading.⁶⁻⁷

Intrigued by its promising bioactivity and appealing molecular architecture, more than 20 different total or formal syntheses of EA have been developed.⁸⁻¹² However, these multistep syntheses are often tedious and cannot meet the demand for a stable large-scale production. Therefore, a concise semisynthetic approach towards EA, starting from a biotechnologically derived advanced intermediate presents a viable alternative. To demonstrate the potential of this strategy for diversification in the chemical synthesis stage, two other guaianes (-)-oxyphyllol and (+)-orientalol E, have been synthesized from the same microbial-produced starting material guaia-6,10(14)-diene (**1**).

Since the enzymes involved in the biosynthetic pathway of EA in *P. engleri* remain unclear, it is important to first identify the building blocks for EA. It has been reported that sesquiterpene cyclase STC5 from the filamentous fungus *Fusarium fujikuroi* can produce guaiane-type hydrocarbon sesquiterpene scaffold guaia-6,10(14)-diene (**1**).¹³ This compound might be useful as a starting material for a scalable semisynthesis of EA.

In recent years, we have developed a platform for the biosynthesis of terpenoids, that allows for the production of large amounts of farnesene, taxadiene, and lycopenes, as well as for the genome mining of novel sesqui-, di-, and sesterterpenes.¹⁴ This technology was applied to screen for guaia-6,10(14)-diene cyclases with high catalytic activity. Sesquiterpene cyclases of filamentous fungi were systematically evaluated and screened (**Supplementary Fig. 1**). *Escherichia coli* C1 (*E. coli* BL21(DE3)/pMH1/pFZ81), harboring an engineered mevalonate (MVA) pathway, has been widely used for efficient overproduction and genome mining of terpenoids¹⁴⁻¹⁵; this platform was selected for functional verification of terpene cyclase (**Fig. 2a**). Plasmids pGB218, pSC52, pSC54, and pSC56, which harbor the farnesyl pyrophosphate synthase (FPPS), sesquiterpene cyclases, and an additional copy of Idi, were constructed and transformed into *E. coli* C1 to generate mutants *E. coli* G1–G4 (**Supplementary Fig. 2**). Subsequently, *in vivo* fermentation was carried out and the production of guaia-6,10(14)-diene was detected by gas chromatography mass spectrometry (GC/MS) analysis. The data showed that in addition to STC5, three sesquiterpene cyclases, FgJ02895, FpN62905, and FmM7560 from *F. graminearum* J1-012, *F. proliferatum* NRRL 62905, and *F. mangiferae* MRC 7560, respectively, were potent guaia-6,10(14)-diene cyclases. Finally, the production of guaia-6,10(14)-diene (**1**) was further confirmed by *in vitro* assay and nuclear magnetic resonance (NMR) analysis (**Supplementary Fig. 3**, **Supplementary Table 4** and **Supplementary Figs. 5a-g**)¹³. Additionally, *E. coli* G1 showed the highest catalytic efficiency with a titer of 48.8 mg/L at the shaking flask fermentation level, indicating that FgJ02895 is a suitable candidate for further engineering (**Fig. 2b**).

To acquire a sufficient amount of guaia-6,10(14)-diene for chemical synthesis of EA, the upstream MVA pathway and downstream guaia-6,10(14)-diene forming pathway were balanced by integrating an additional copy of *FgJ02895* into pGB218 to generate plasmid pSC61. The resulting data showed that guaia-6,10(14)-diene was increased by 1.28-fold with a titer of 62.3 mg/L in *E. coli* G5. Finally, production of guaia-6,10(14)-diene was further increased by 9.6-fold and up to 468 mg/L in 5-L fed-batch fermentation of *E. coli* G5 (**Fig. 2e**). Based on these results, 0.8 g of guaia-6,10(14)-diene were purified for chemical synthesis of (-)-EA.

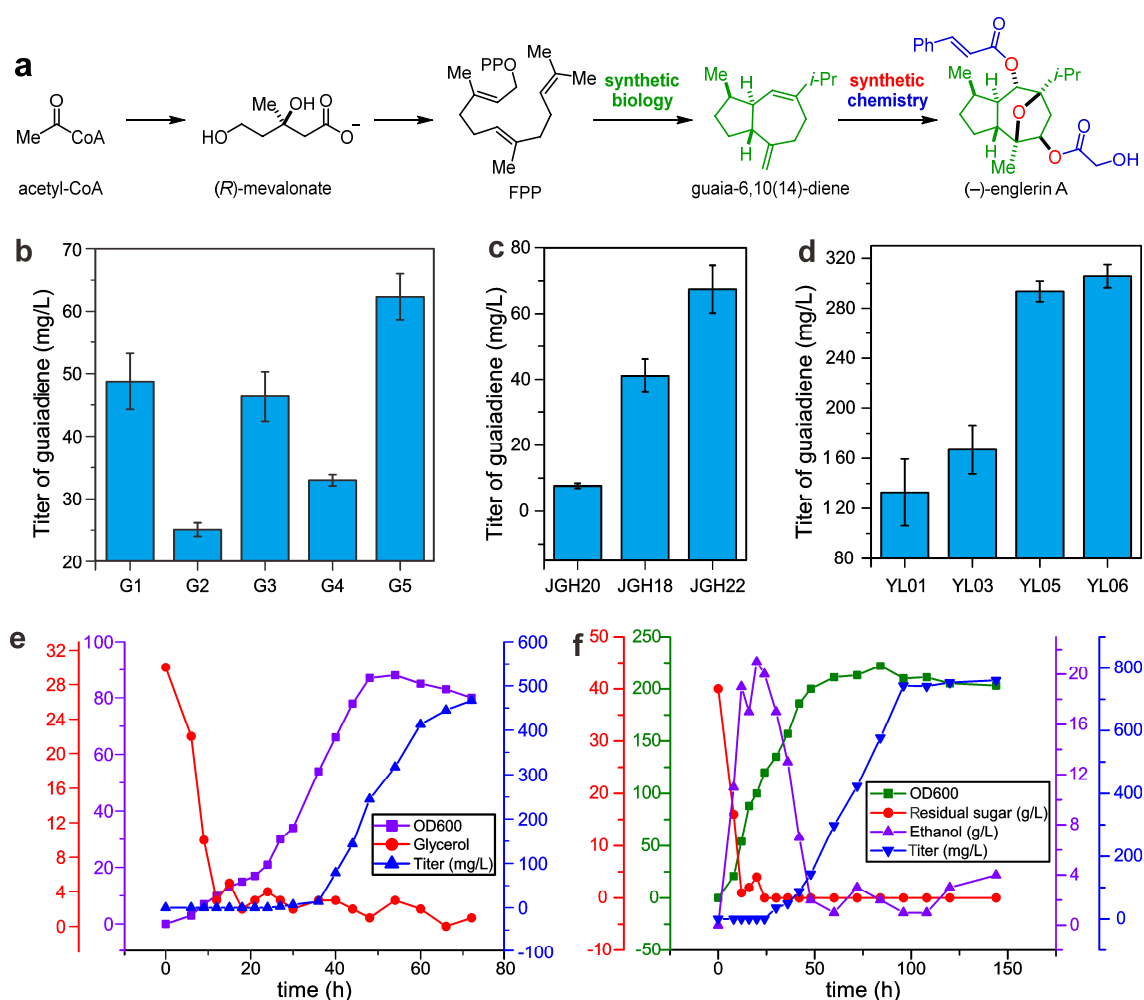


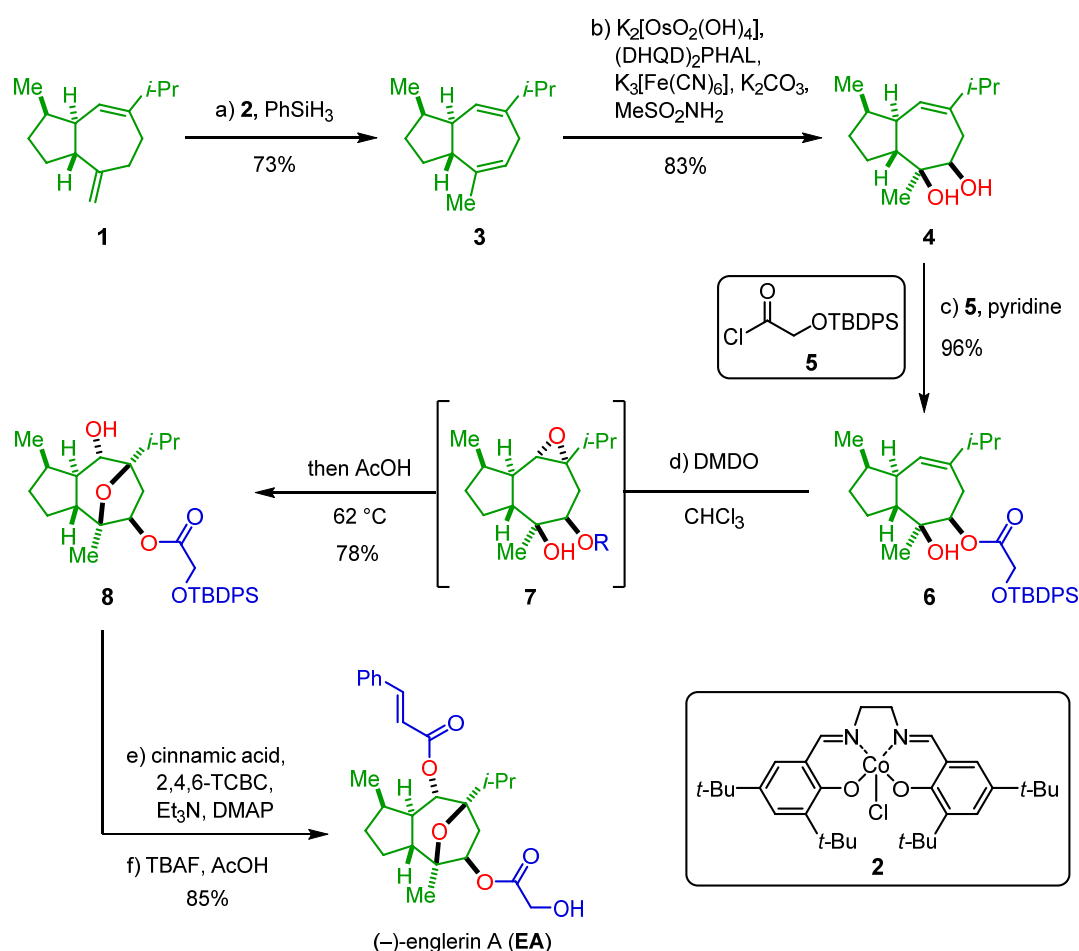
Figure 2. Production of guaia-6,10(14)-diene in *E. coli* and *S. cerevisiae*. **a**) Semisynthetic production of (-)-englerin A by using synthetic biology produced guaia-6,10(14)-diene via the MVA pathway. **b**) Guaia-6,10(14)-diene produced by *E. coli* G1-G5 in shaking flasks. **c**) Efficiency of yeast precursor-providing platform YZL141 and JCR27. **d**) Increased titer of guaia-6,10(14)-diene in JCR27 step by step. **e**) Guaia-6,10(14)-diene production of *E. coli* G5 in 5-L fed-batch fermentation. **f**) Guaia-6,10(14)-diene production of *S. cerevisiae* YL06 in 5-L fed-batch fermentation.

To meet the potential high demand for guaia-6,10(14)-diene (**1**) for a scalable synthesis and production of EA and its analogues with pharmaceutical quality, *S. cerevisiae* was selected for further engineering. The MVA pathway was systematically engineered, a series of mutants were constructed, and the titer of guaia-6,10(14)-diene was gradually increased (**Supplementary Figs. 3 and 4**). First, as a proof of concept, downstream ERG20 (FPP synthase) and FgI02895 were overexpressed in the previously engineered terpenoid precursor-providing platform *S. cerevisiae* YZL141,¹⁶ and guaia-6,10(14)-diene was produced by the resulting strain JGH20 with a titer of 7.68 mg/L in shaking flasks. To increase the metabolic flux towards terpene synthesis, and based on previous work related to metabolic engineering of the MVA pathway,^{4,15} additional copies of *ERG10*, *ERG13*, *ERG12*, *ERG8*, *tHMG1*, *MVD1*, and *IDI* in the MVA pathway were systematically engineered by the CRISPR/Cas9

system, and the efficient precursor-providing platform *S. cerevisiae* JCR27 was established. Next, downstream *ERG20* and *FgJ02895* were integrated into JCR27 and the titer of guaia-6,10(14)-diene was increased by 5.4-fold to 41.4 mg/L in the resulting strain JGH18. In parallel, strain JGH22 (with codon optimized *gJ02895-Sc* and *ERG20*) was constructed and the titer was further increased to 67.5 mg/L (**Fig. 2c**). Considering that tHMG1 is the rate-limiting step in the MVA pathway¹⁵ and an increase in the copy number of *FgJ02895* can increase the titer of guaia-6,10(14)-diene, strain YL01 (JGH22 with an additional copy of *FgJ02895-Sc* and *tHMG1*) was generated with a titer of 132.8 mg/L. One and two additional copies of *FgJ02895-Sc* were sequentially integrated and strains YL03 and YL05 were constructed with titers of 166.9 and 170.2 mg/L, respectively. Finally, to decrease production costs, *GAL80* in YL05 was deleted to eliminate the requirement for galactose and the resulting strain YL06 was generated with a titer of 292.9 mg/L (**Fig. 2d**). The production of guaia-6,10(14)-diene was further increased up to 0.8 g/L in 5-L fed-batch fermentation of *S. cerevisiae* YL06 (**Fig. 2f**).

The efficient production of guaia-6,10(14)-diene (**1**) enabled the development of a short synthetic route towards EA. Following Shenvi's protocol¹⁷ using catalytic amounts of cobalt-catalyst **2** and phenylsilane the exocyclic double bond of diene **1** was selectively isomerized to give the trisubstituted olefin **3** in 73% yield (**Scheme 1**). Dihydroxylation using Upjohn conditions¹⁸ as performed in the englerin synthesis by Lopez et al.¹⁹ was difficult, as their substrate possessed a bulky silylether at the C4-position which guided the regio- and stereoselectivity. Fortunately, this issue was solved by performing Sharpless asymmetric dihydroxylation with (DHQD)₂PHAL²⁰ as a chiral ligand to afford diol **4** in 83% yield as a single diastereomer.

One of the major issues in our first-generation synthesis of the unnatural enantiomer (+)-EA was the low diastereoselectivity in the epoxidation of the trisubstituted olefin with *m*-CPBA (2.3:1 d.r.).¹⁰ This issue was overcome in this second-generation synthesis by installing a (*tert*-butyldimethyl)silyl ether at C9, resulting in an increased diastereomeric ratio (5.4:1 d.r.).⁹ To avoid additional protecting group manipulations, glycolate **6** was synthesized using acid chloride **5** and subsequently screened with different epoxidizing agents. Dimethyldioxirane (DMDO) in chloroform²¹⁻²² gave epoxide **7** as a single diastereomer. A direct one-pot transannular opening of epoxide **7** was achieved by adding acetic acid and heating to 62°C to afford the tricyclic intermediate **8** in 75% yield. The use of standard DMDO solution in acetone led to longer reaction times and lower yields. Yamaguchi esterification of alcohol **8** with cinnamic acid followed by desilylation using a buffered TBAF solution afforded (-)-EA in 85% yield in 2 steps. In conclusion, this approach allows for a concise synthesis of (-)-EA in only 6 steps with an overall yield of 38% starting from guaia-6,10(14)-diene (**1**).

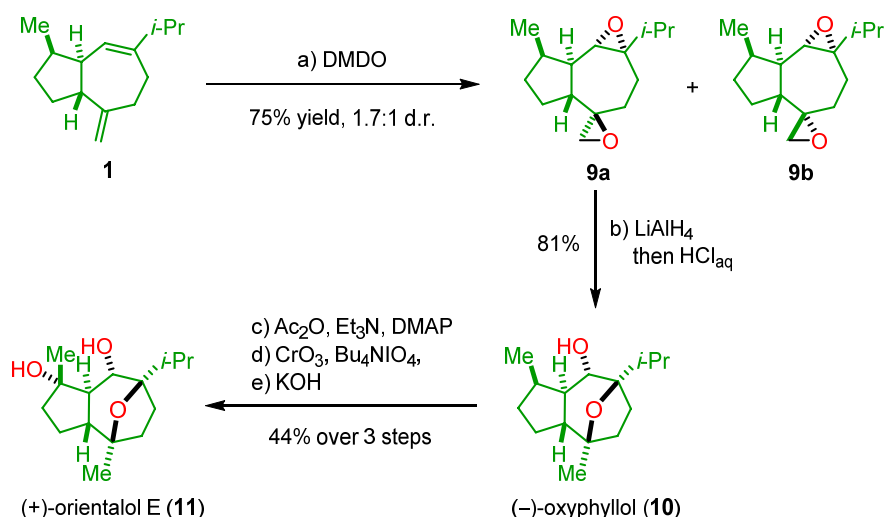


Scheme 1. Concise Synthesis of (-)-Englerin A. Conditions: (a) **2** (5 mol%), PhSiH₃ (5 mol%), PhH, 23 °C, 18 h, 73%; (b) K₂[OsO₂(OH)₄] (10 mol%), hydroquinidine 1,4-phthalazinediyl diether ((DHQD)₂PHAL, 20 mol%), K₃[Fe(CN)₆], K₂CO₃, MeSO₂NH₂, *t*-BuOH, H₂O (1:1), 23 °C, 3 d, 83%; (c) **5**, pyridine, CH₂Cl₂, 23 °C, 1.5 h, 96%, (d) DMDO, CHCl₃, 23 °C, 16 h, then AcOH, 62 °C, 17 h, 78% (single diastereomer); (e) cinnamic acid, 2,4,6-trichlorobenzoyl chloride, Et₃N, 4-dimethylaminopyridine, CH₂Cl₂, 23 °C, 5 h; (f) tetrabutylammonium fluoride, AcOH (40 mol%), THF, 23 °C, 1.5 h, 85% over 2 steps.

The potential of **1** as a building block was further demonstrated by the synthesis of two other guaianes. (-)-Oxyphyllol (**10**) and (+)-orientalol E (**11**) were isolated from *Phyllanthus oxyphyllus*²³ and *Alisma orientalis*,²⁴ respectively, but their biological activities have not been studied, in detail. In the context of their englerin syntheses, Sun and Lin et al.,²⁵ Wang et al.,¹¹ and Metz et al.²⁶ reported the syntheses or formal syntheses of these two natural products.

A two-step synthesis of (-)-oxyphyllol was performed by epoxidizing **1** using an excess of DMDO (**Scheme 2**). The bisepoxides **9a** and **9b** were obtained in 75% yield with a diastereomeric ratio of 1.7:1 for the exocyclic epoxide, while the trisubstituted olefin was epoxidized with high diastereoselectivity. Opening of the exocyclic epoxide with lithium aluminum hydride and acidic workup gave (-)-oxyphyllol in 81% yield. Applying a three-step sequence similar to that reported by Sun and Lin et al.²⁵ and

Wang et al.¹¹ allowed for the conversion of (-)-oxyphyllol (**10**) into (+)-orientalol E (**11**) by acetylation, C–H-oxidation, and saponification in 44% yield.



Scheme 2. Synthesis of (-)-Oxyphyllol and Formal Synthesis of (+)-Orientalol E. Conditions: (a) DMSO, acetone, 0 °C, 30 min, 75% (1.7:1 d.r.); (b) LiAlH₄, Et₂O, 0 °C, 1 h, then HCl_{aq}, 0 °C, 15 min, 81%; (c) Ac₂O, Et₃N, DMAP, 23 °C, 16 h; (d) CrO₃, Bu₄NIO₄, CH₂Cl₂, MeCN, -30 °C → 0 °C, 45 min; (e) KOH, MeOH, 50 °C, 3 h, 44% over 3 steps.

In summary, we report a conceptionally new synthetic route towards EA involving synthetic biology and chemical synthesis. Guaia-6,10(14)-diene cyclase from filamentous fungi was employed as an alternative to introduce the missing enzymes and provide a building block for semisynthesis of plant sesquiterpenoid EA. In the biotechnological processes, overproduction of guaia-6,10(14)-diene in *E. coli* and *S. cerevisiae* were realized with titers of 0.5 and 0.8 g/L in fed-batch fermentation, respectively. The production of sufficient starting material enabled a highly efficient synthesis of EA in only 6 steps with 38% overall yield, representing the shortest route and highest yielding synthesis to date. Additionally, this route allows for short syntheses of two related sesquiterpenoids, (-)-oxyphyllol and (+)-orientalol E.

The interplay between synthetic biology and chemical synthesis was key in providing a straightforward and scalable access to EA and two other guaiane terpenes. Synthetic biology offered a direct entry into the three-dimensional carbon framework using the power of terpene cyclases. Synthetic chemistry on the other hand allowed for a rapid scaffold diversification by adding additional layers of complexity onto the carbocyclic core. We anticipate that this synergistic approach will become a general tool to cast the chemical space of biologically active terpene natural products.

References

- 1 Lemke, T. L. & Williams, D. A. *Foye's Principles of Medicinal Chemistry*. (Wolters Kluwer Health/Lippincott Williams & Wilkins, 2012).
- 2 Jinek, M. *et al.* A Programmable Dual-RNA-Guided DNA Endonuclease in Adaptive Bacterial Immunity. *Science* **337**, 816-821 (2012).
- 3 Malik, S. *et al.* Production of the anticancer drug taxol in *Taxus baccata* suspension cultures: a review. *Process Biochem.* **46**, 23-34 (2011).
- 4 Paddon, C. J. *et al.* High-level semi-synthetic production of the potent antimalarial artemisinin. *Nature* **496**, 528-532 (2013).
- 5 Ratnayake, R., Covell, D., Ransom, T. T., Gustafson, K. R. & Beutler, J. A. Englerin A, a selective inhibitor of renal cancer cell growth, from *Phyllanthus engleri*. *Org. Lett.* **11**, 57-60 (2009).
- 6 Akbulut, Y. *et al.* (-)-Englerin A is a potent and selective activator of TRPC4 and TRPC5 calcium channels. *Angew. Chem. Int. Ed.* **54**, 3787-3791 (2015).
- 7 Ludlow, M. J. *et al.* (-)-Englerin A-evoked Cytotoxicity Is Mediated by Na⁺ Influx and Counteracted by Na⁺/K⁺-ATPase. *J. Biol. Chem.* **292**, 723-731 (2017).
- 8 Wu, Z. *et al.* Englerins: A Comprehensive Review. *J. Nat. Prod.* **80**, 771-781 (2017).
- 9 Willot, M. *et al.* Total synthesis and absolute configuration of the guaiane sesquiterpene englerin A. *Angew. Chem. Int. Ed.* **48**, 9105-9108 (2009).
- 10 Radtke, L. *et al.* Total synthesis and biological evaluation of (-)-englerin A and B: synthesis of analogues with improved activity profile. *Angew. Chem. Int. Ed.* **50**, 3998-4002 (2011).
- 11 Liu, P. *et al.* Total Syntheses of (-)-Englerins A/B, (+)-Orientalols E/F, and (-)-Oxyphyllol. *Org. Lett.* **20**, 2517-2521 (2018).
- 12 Guo, L. & Plietker, B. β -Ketoesters as Mono- or Bisnucleophiles: A Concise Enantioselective Total Synthesis of (-)-Englerin A and B. *Angew. Chem. Int. Ed.* **58**, 8346-8350 (2019).
- 13 Burkhardt, I. *et al.* Mechanistic characterisation of two sesquiterpene cyclases from the plant pathogenic fungus *Fusarium fujikuroi*. *Angew. Chem. Int. Ed.* **55**, 8748-8751 (2016).
- 14 Bian, G., Deng, Z. & Liu, T. Strategies for terpenoid overproduction and new terpenoid discovery. *Curr. Opin. Biotechnol.* **48**, 234-241 (2017).
- 15 Zhu, F. *et al.* In vitro reconstitution of mevalonate pathway and targeted engineering of farnesene overproduction in *Escherichia coli*. *Biotechnol. Bioeng.* **111**, 1396-1405 (2014).
- 16 Bian, G. *et al.* Metabolic Engineering-Based Rapid Characterization of a Sesquiterpene Cyclase and the Skeletons of Fusariumdiene and Fusagramineol from *Fusarium graminearum*. *Org. Lett.* **20**, 1626-1629 (2018).
- 17 Crossley, S. W., Barabé, F. & Shenvi, R. A. Simple, chemoselective, catalytic olefin isomerization. *J. Am. Chem. Soc.* **136**, 16788-16791 (2014).
- 18 VanRheenen, V., Kelly, R. & Cha, D. Y. An improved catalytic OsO₄ oxidation of olefins to cis-1,2-glycols using tertiary amine oxides as the oxidant. *Tetrahedron Lett.* **17**, 1973-1976 (1976).
- 19 Nelson, R., Gulías, M., Mascareñas, J. L. & López, F. Concise, Enantioselective, and Versatile Synthesis of (-)-Englerin A Based on a Platinum-Catalyzed [4C+ 3C] Cycloaddition of Allenedienes. *Angew. Chem. Int. Ed.* **55**, 14359-14363 (2016).
- 20 Sharpless, K. B. *et al.* The osmium-catalyzed asymmetric dihydroxylation: a new ligand class and a process improvement. *J. Org. Chem.* **57**, 2768-2771 (1992).
- 21 Ferrer, M., Gibert, M., Sánchez-Baeza, F. & Messegue, A. Easy availability of more concentrated and versatile dimethyldioxirane solutions. *Tetrahedron Lett.* **37**, 3585-3586 (1996).
- 22 Murray, R. W. & Singh, M. Synthesis of Epoxides Using Dimethyldioxirane: trans-Stilbene Oxide. *Org. Synth.*, 91-91 (1997).

- 23 Sutthivaiyakit, S., Nakorn, N. N., Kraus, W. & Sutthivaiyakit, P. A novel 29-nor-3, 4-seco-friedelane triterpene and a new guaiane sesquiterpene from the roots of *Phyllanthus oxyphyllus*. *Tetrahedron* **59**, 9991-9995 (2003).
- 24 Peng, G.-P., Tian, G., Huang, X.-F. & Lou, F.-C. Guaiane-type sesquiterpenoids from *Alisma orientalis*. *Phytochemistry* **63**, 877-881 (2003).
- 25 Wang, J., Chen, S.-G., Sun, B.-F., Lin, G.-Q. & Shang, Y.-J. Collective total synthesis of englerin A and B, orientalol E and F, and oxyphyllol: application of the organocatalytic 4+3 cycloaddition reaction. *Chem. Eur. J.* **19**, 2539–2547 (2013).
- 26 Zahel, M. & Metz, P. A concise enantioselective synthesis of the guaiane sesquiterpene (-)-oxyphyllol. *Beilstein J. Org. Chem.* **9**, 2028–2032 (2013).

Acknowledgements

This work was financially supported by funding from J1 Biotech Co., Ltd., and grants from the National Key R&D Program of China (2018YFA0900400), the National Natural Science Foundation of China (31670090 and 31800032), the Medical Science Advancement Program (Clinical Medicine) of Wuhan University (TFLC2018002).

3.4 Unpublished Results

3.4.1 Synthesis of aza-Englerin A Analogs

Extensive SAR studies have shown that the glycolate ester at C9 is essential for the inhibitory activity of (-)-englerin A (cf. chapter 3.1.5). However, its metabolic instability is a major concern for further studies of (-)-englerin A as an anti-cancer drug. Therefore, alternative substitution patterns have been studied and the group of CHAIN reported amide analogs that were stable and orally bioavailable but less active.^[114] Simultaneously, a very similar strategy was developed in the CHRISTMANN group.^[103,7] This approach should be applied in order to develop metabolically stable and more potent aza-englerin A analogs. In the context of my master's thesis, the synthesis of englerin A analogs bearing an (*S*)-*sec*-butyl, benzyloxymethyl, or hydroxymethyl group (**93** – **97**) instead of the isopropyl group at C7 was accomplished (Figure 17).^[110] The side chains were introduced during the BARBIER reaction following the improved protocol for CHRISTMANN's (-)-englerin A synthesis as described in chapter 3.1.4.2. SAR-studies revealed that the (*S*)-*sec*-butyl analogs **93** and **94** exhibit a five-fold increase in inhibitory activity against the RCC line A498 compared to (-)-englerin A. Interestingly, for the benzyloxymethyl analogs, only the C6 cinnamate ester analog **95** possesses a similar potency as (-)-englerin A. However, the 1-methyl-5,6,7,8-tetrahydronaphthoate substituent at C6 which induces a huge increase in activity for the C7 isopropyl analogs is not well tolerated in analog **96**. The hydroxymethyl group **97** results in an even lower inhibitory activity.

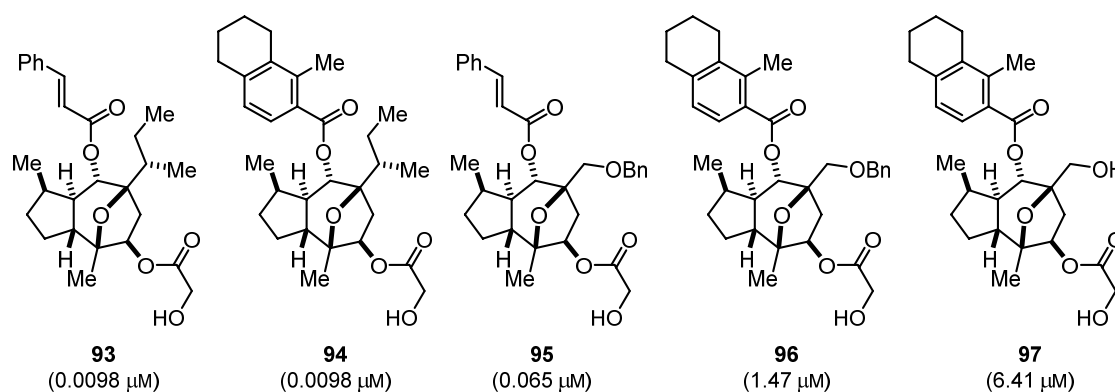
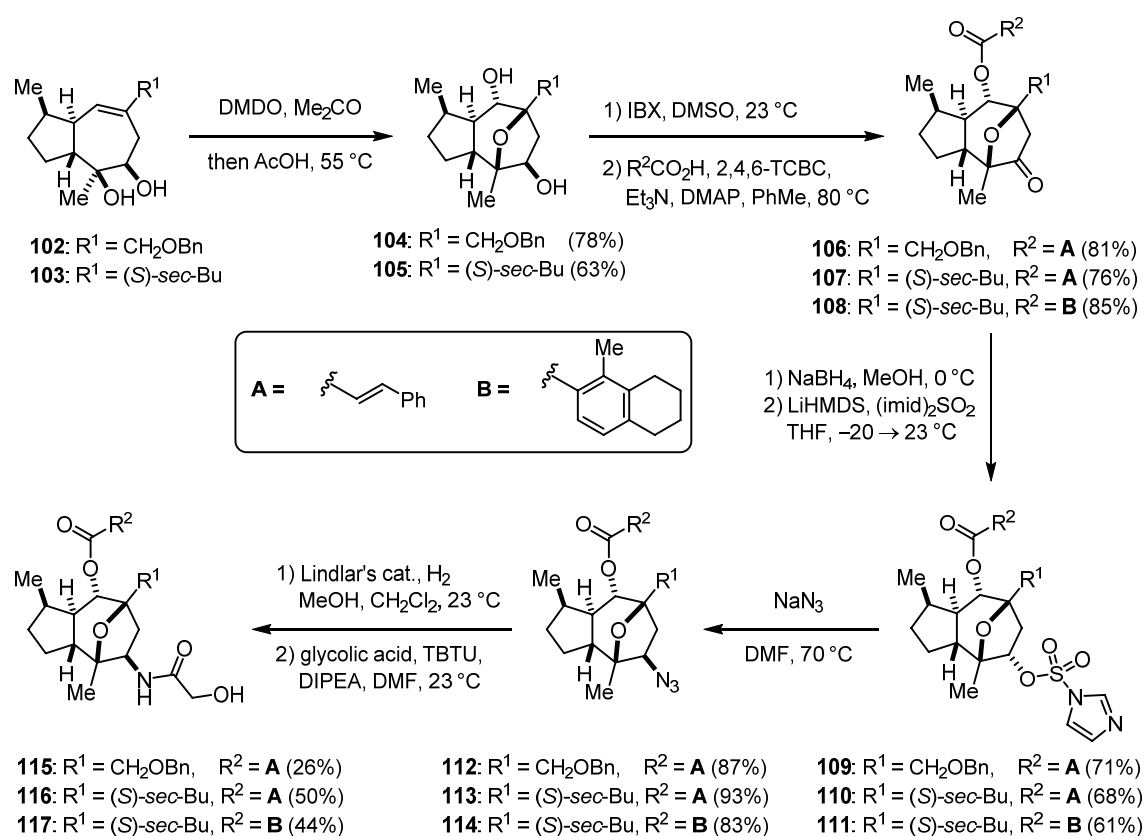


Figure 17. Englerin A analogs bearing an (*S*)-*sec*-butyl, benzyloxymethyl, and hydroxymethyl group at C7, synthesized during the master's thesis. Inhibition of cell proliferation in RCC line A498 (IC_{50} in brackets, cf. (-)-englerin A: IC_{50} = 0.049 μM).

In the course of this synthesis, the diol intermediates **102** and **103** were obtained. These intermediates served as a starting point for the synthesis of aza-englerin A analogs (Scheme 31). In a one-pot procedure, the trisubstituted alkenes were stereoselectively epoxidized with dimethyldioxirane (DMDO) and an acid-mediated transannular epoxide opening yielded the diols **104** and **105** in moderate to good yield.

The less hindered secondary alcohol at C9 was oxidized to the ketone and the remaining alcohol was esterified with cinnamic acid (**A**) or 1-methyl-5,6,7,8-tetrahydro-2-naphthoic acid (**B**) applying YAMAGUCHI's protocol.^[118] Due to a lack of material, for the benzyloxymethyl derivative only the cinnamate ester was synthesized. Diastereoselective reduction of the ketones **106** – **108** with sodium borohydride yielded the secondary alcohols that were transformed to the imidazolyl sulfonates **109** – **111**. Nucleophilic substitution with sodium azide under inversion of stereoconfiguration resulted in the desired C9 azide epimers **112** – **114**. Chemoselective reduction with LINDLAR's catalyst under a hydrogen atmosphere afforded the amine that was directly converted to the aza-englerin analogs **115** – **117** using the peptide coupling agent TBTU and glycolic acid.^[119]



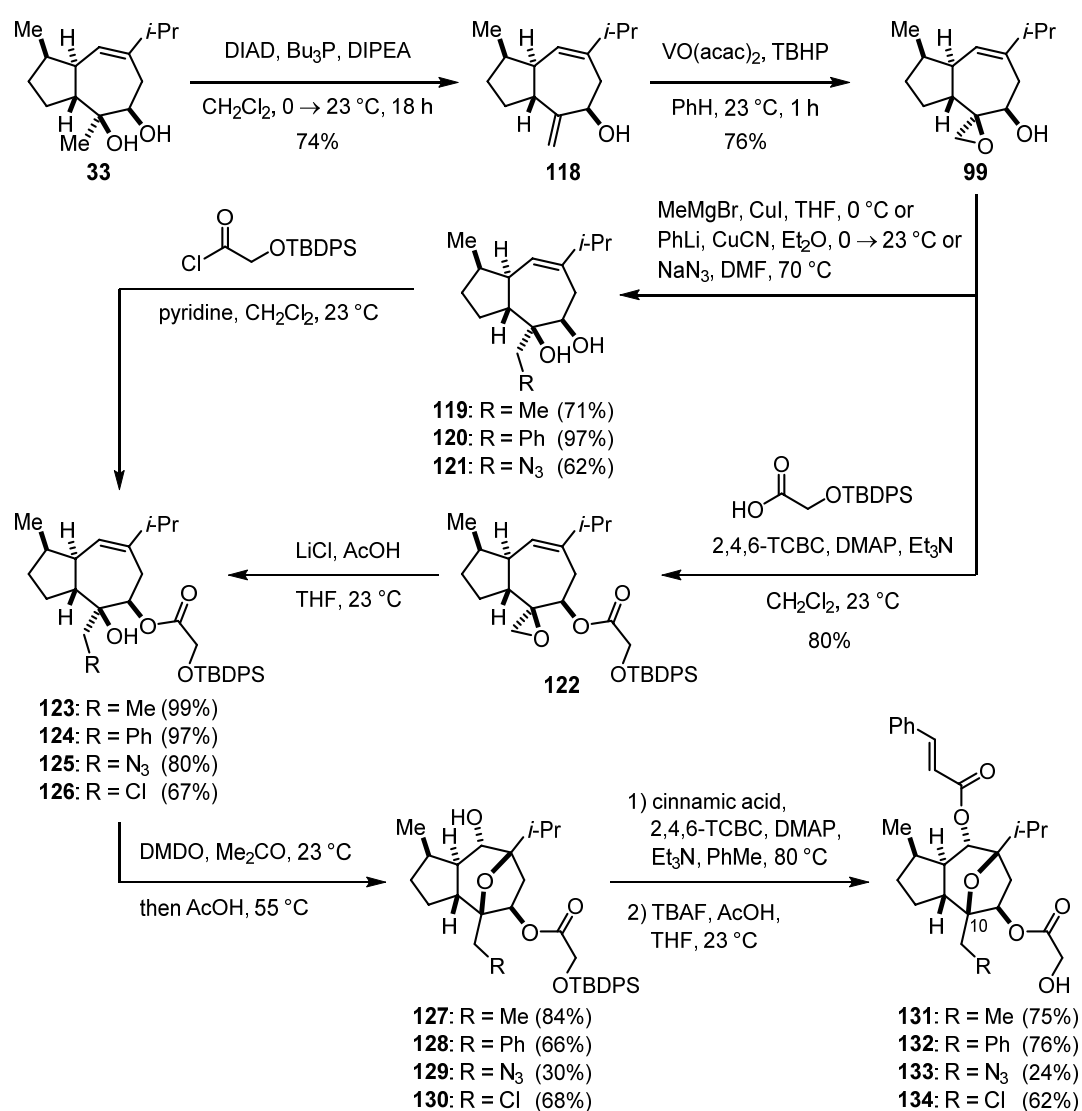
Scheme 31. Synthesis of aza-englerin A analogs bearing (benzyloxy)methyl and (*S*)-*sec*-butyl substituents at C7.

The synthesized analogs were tested for their inhibitory activity on the cell proliferation in the RCC line A498 and for their stability in mouse plasma by the Lead Discovery Center GmbH. The (*S*)-*sec*-butyl analogs **116** (IC₅₀ = 1.83 μM) and **117** (IC₅₀ = 1.86 μM) exhibited a significantly lower inhibitory activity than (-)-englerin A (IC₅₀ = 0.049 μM) and the benzyloxymethyl analog **115** did not show any activity up to a concentration of 29.9 μM. Thus, the C9 glycolate amide functionality was not well tolerated for these analogs, especially when compared to the (*S*)-*sec*-butyl analogs **93** and **94** (IC₅₀ = 0.0098 μM for each) with a glycolate ester at C9. However, the metabolic stability in mouse plasma was significantly higher for

all tested analogs compared to (-)-englerin A. Therefore, the aim of synthesizing metabolically more stable analogs was accomplished, albeit accompanied by a significant decrease of inhibitory activity.

3.4.2 Synthesis of C10 Methyl Analogs of (-)-Englerin A

Since the C10 methyl group has never been subject to any SAR study, the question arises if a modification at this position is tolerated or might be even beneficial. Only the radically simplified englerin core lacking all methyl and the *iso*-propyl group has been reported.^[106] Starting from the diol intermediate **33** of CHRISTMANN's (-)-englerin A synthesis, a straightforward access towards C10 analogs is possible (Scheme 32).



Scheme 32. Synthesis of (-)-englerin A analogs bearing various functionalities at the C10 methyl group.

As previously reported in Chapter 3.3.1, the tertiary alcohol of diol intermediate **33** undergoes elimination under MITSUNOBU conditions (Scheme 32).^[6] Subsequently, a vanadium-catalyzed

hydroxyl-directed epoxidation afforded the exocyclic epoxide **99** diastereoselectively in 76% yield.^[120] Several nucleophiles were applied to open the epoxide resulting in 1,2-diols **119** – **121**. The addition of methyl and phenyl cuprates as well as sodium azide proceeded smoothly, giving good to excellent yields. For the addition of lithium chloride under acidic conditions, the secondary alcohol **99** was esterified using YAMAGUCHI's protocol prior to the epoxide opening.^[118] The 1,2-diols **119** – **121** were selectively esterified at the less hindered secondary alcohol with 2-((*tert*-butyldiphenylsilyl)oxy)acetyl chloride in excellent yields. Subsequently, a one-pot epoxidation and acid-mediated transannular epoxide opening sequence gave access to the oxo-bridge products **127** – **130**. Finally, the Yamaguchi esterification with cinnamic acid and the silyl ether cleavage using a buffered TBAF solution afforded the (-)-englerin A analogs **131** – **134**.

The synthesized analogs, except for the azidomethyl analog **133**, were subjected to structure-activity relationship studies for their inhibitory activity on the cell proliferation in the RCC line A498 by the Lead Discovery Center GmbH. For the azidomethyl analog **133** the yields over the last three steps were so low that further studies were abandoned. Likewise, the envisioned conversion into the corresponding amine and the copper-catalyzed Click reaction for possible bio-affinity labeling experiments could not be performed.

The biological studies revealed that the C10 modification was generally well tolerated with only a moderate drop in activity for the ethyl and chloromethyl analogs **131** ($IC_{50} = 111$ nM) and **134** ($IC_{50} = 178$ nM) compared to (-)-englerin A ($IC_{50} = 49$ nM). The C10 benzyl analog **132** even exhibits an almost three-fold increase in activity ($IC_{50} = 16.9$ nM). Therefore, this analog represents one of the most potent (-)-englerin A derivatives.

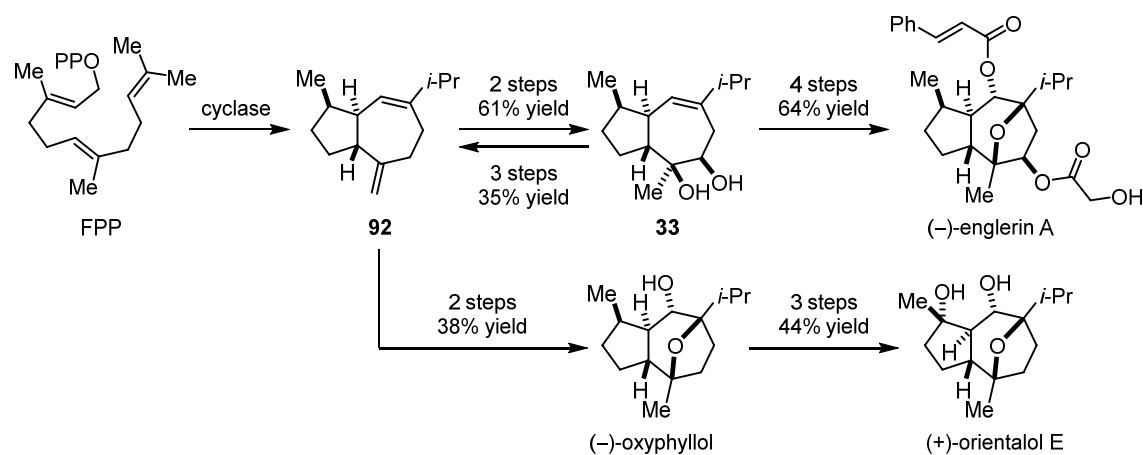
3.5 Summary and Outlook

Ten years after the isolation of (-)-englerin A and the initial synthesis of the unnatural enantiomer by the CHRISTMANN group, this thesis has added another new chapter to the topic. The collaboration with two biosynthesis groups resulted in a six-step semisynthesis of (-)-englerin A.

At first, the guaia-6,10(14)-diene **92** was synthesized in 3 steps starting from the diol intermediate **33** of CHRISTMANN's (-)-englerin A synthesis (Scheme 33). By comparison of the optical rotation values, the absolute configuration of diene **92** produced by incubation of farnesyl pyrophosphate (FPP) with sesquiterpene cyclase 5 from the plant pathogenic fungus *Fusarium fujikuroi* was confirmed. The group of DICKSCHAT elucidated the biosynthetic mechanism for this sesquiterpene cyclase by studying ²H and ¹³C-labelled FPP isotopomers.^[6]

The group of LIU was able to produce the guaia-6,10(14)-diene **92** on gram scale by metabolic engineering of the mevalonate pathway in *E. coli* and *S. cerevisiae*. This enabled the use of diene **92** as a starting material for a concise semisynthesis of (-)-englerin A. The isomerization of the exocyclic double bond into the internal position and the subsequent regio- and diastereoselective dihydroxylation afforded the diol intermediate **33** of CHRISTMANN's (-)-englerin A synthesis. Finally, a four-step sequence, previously optimized in the CHRISTMANN group, was applied to synthesize (-)-englerin A.^[7]

Furthermore, guaia-6,10(14)-diene **92** proved to be a viable starting material for the synthesis of the two related sesquiterpene natural products (-)-oxyphyllol and (+)-orientalol E as well. The synthesis of (-)-oxyphyllol was achieved in only two steps by diastereoselective bisepoxidation and subsequent one-pot regioselective hydride addition and transannular epoxide opening. Starting from (-)-oxyphyllol, (+)-orientalol was obtained in three more steps, applying a literature known procedure.^[8,9]



Scheme 33. Semisynthesis of (-)-englerin A, (-)-oxyphyllol and (+)-orientalol E, starting from the biosynthesis product guaia-6,10(14)-diene **92**. The diene **92** was also synthesized starting from diol **33** in order to determine the absolute configuration of the product **92** obtained by incubation of FPP with sesquiterpene cyclase 5 for *Fusarium fujikuroi*.^[6]

In summary, this concise semisynthetic approach allowed for syntheses of the sesquiterpene natural products (-)-englerin A, (-)-oxyphyllol and (+)-orientalol E starting from the biosynthetically produced guaia-6,10(14)-diene **92**. The (-)-englerin A semisynthesis represents the shortest and highest yielding access with six steps and 38% overall yield.

Additionally, the established total synthesis of (-)-englerin A was applied to synthesize new (-)-englerin A analogs (Figure 18). Since the C9 glycolate ester is metabolically instable but essential for the biological activity, amide analogs have been synthesized. Applying a procedure previously developed in the CHRISTMANN group, the aza-englerin A analogs **109** – **111** bearing (*S*)-*sec*-butyl and benzyloxy-methyl groups at C7 were synthesized.

Furthermore, the C10 methyl group was subjected to functionalization for the first time. The ethyl (**131**), benzyl (**132**), azidomethyl (**133**), and chloromethyl (**134**) C10 analogs were obtained by opening of an exocyclic epoxide.

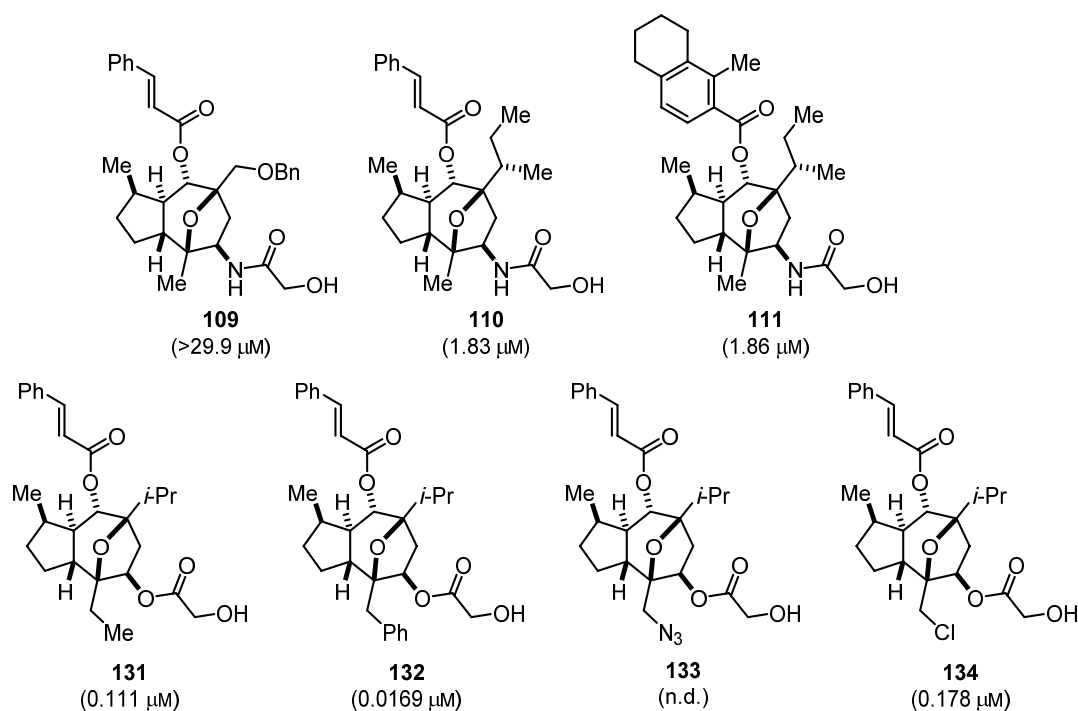


Figure 18. Synthesized (-)-englerin A analogs. Inhibition of cell proliferation (-) in RCC line A498 (IC_{50}) in brackets, cf. (-)-englerin A: IC_{50} = 0.049 μM .

Structure-activity relationship studies, elucidating the inhibitory activity against the RCC line A498 and the metabolic stability in mouse plasma, revealed that the aza-englerin A analogs (**109** – **111**) are significantly less active but possess a higher metabolic stability than (-)-englerin A (Figure 18). In contrast, the functionalization at the C10 methyl group was well tolerated. The inhibitory activity for the ethyl and chloromethyl analogs (**131** and **134**) was slightly decreased, but the benzyl analog **132** was almost three-times more potent than (-)-englerin A. Since the azidomethyl analog **133** was only

obtained in very small quantities, the biological evaluation and further synthetic transformations into the amine or a 1,2,3-triazole were abandoned. However, the derivatization at the C10 methyl group seems to be very promising and the benzyl analog **132** represents one of the most potent (–)-englerin A analogs.

4 List of References and Illustration Credits

4.1 References

- [1] J. L. von Salm, C. G. Witowski, R. M. Fleeman, J. B. McClintock, C. D. Amsler, L. N. Shaw, B. J. Baker, *Org. Lett.* **2016**, *18*, 2596.
- [2] T. Siemon, S. Steinhauer, M. Christmann, *Angew. Chem. Int. Ed.* **2019**, *58*, 1120.
- [3] R. Ratnayake, D. Covell, T. T. Ransom, K. R. Gustafson, J. A. Beutler, *Org. Lett.* **2009**, *11*, 57.
- [4] M. Willot, L. Radtke, D. Könnig, R. Fröhlich, V. H. Gessner, C. Strohmam, M. Christmann, *Angew. Chem. Int. Ed.* **2009**, *48*, 9105.
- [5] L. Radtke, M. Willot, H. Sun, S. Ziegler, S. Sauerland, C. Strohmam, R. Fröhlich, P. Habenberger, H. Waldmann, M. Christmann, *Angew. Chem. Int. Ed.* **2011**, *50*, 3998.
- [6] I. Burkhardt, T. Siemon, M. Henrot, L. Studt, S. Rösler, B. Tudzynski, M. Christmann, J. S. Dickschat, *Angew. Chem. Int. Ed.* **2016**, *55*, 8748.
- [7] Tobias Seitz, *PhD Thesis*, Freie Universität Berlin, **2017**.
- [8] P. Liu, Y. Cui, K. Chen, X. Zhou, W. Pan, J. Ren, Z. Wang, *Org. Lett.* **2018**, *20*, 2517.
- [9] D. A. Williams, T. L. Lemke, *Foye's principles of medicinal chemistry*, Lippincott Williams & Wilkins, Philadelphia, **2002**.
- [10] D. J. Newman, G. M. Cragg, *J. Nat. Prod.* **2016**, *79*, 629.
- [11] E. Patridge, P. Gareiss, M. S. Kinch, D. Hoyer, *Drug Discov. Today* **2016**, *21*, 204.
- [12] G. M. Cragg, D. J. Newman, *Biochim. Biophys. Acta, Gen. Subj.* **2013**, *1830*, 3670.
- [13] M. Feher, J. M. Schmidt, *J. Chem. Inf. Comput. Sci.* **2003**, *43*, 218.
- [14] W. R.J.D. Galloway, A. Isidro-Llobet, D. R. Spring, *Nature Comm.* **2010**, *1*, 80.
- [15] A. Nadin, C. Hattotuwigama, I. Churcher, *Angew. Chem. Int. Ed.* **2012**, *51*, 1114.
- [16] N. E. Thomford, D. A. Senthebane, A. Rowe, D. Munro, P. Seele, A. Maroyi, K. Dzobo, *Int. J. Mol. Sci.* **2018**, *19*.
- [17] A. Mullard, *Nature Rev. Drug Discov.* **2019**, *18*, 85.
- [18] L.-A. Giddings, D. J. Newman, *Bioactive Compounds from Extremophiles*, Springer, Heidelberg, **2015**.
- [19] M. J. Yu, W. Zheng, B. M. Seletsky, B. A. Littlefield, Y. Kishi, *Annu. Rep. Med. Chem.* **2011**, *46*, 227.
- [20] K. V. Rao, *Pharm. Res.* **1993**, *10*, 521.
- [21] F. Han, L.-Z. Kang, X.-L. Zeng, Z.-W. Ye, L.-Q. Guo, J.-F. Lin, *J. Sci. Food Agric.* **2014**, *94*, 2376.
- [22] a) I. Ojima, I. Habus, M. Zhao, M. Zucco, Y. H. Park, C. M. Sun, T. Brigaud, *Tetrahedron* **1992**, *48*, 6985; b) P. A. Wender, N. F. Badham, S. P. Conway, P. E. Floreancig, T. E. Glass, J. B. Houze, N. E. Krauss, D. Lee, D. G. Marquess, P. L. McGrane, W. Meng, M. G. Natchus, A. J. Shuker, J. C. Sutton, R. E. Taylor, *J. Am. Chem. Soc.* **1997**, *119*, 2757.
- [23] World Health Organization, **2014**, *WHO Antimicrobial Resistance: Global Report on Surveillance*, <https://www.who.int/drugresistance/documents/surveillancereport/en/>. Accessed 29.06.2019.
- [24] C. D. Salgado, B. M. Farr, D. P. Calfee, *Clin. Infect Dis.* **2003**, *36*, 131.

- [25] European Centre for Disease Prevention and Control, **2015**, *Antimicrobial Surveillance in Europe 2014*,
<https://ecdc.europa.eu/sites/portal/files/media/en/publications/Publications/antimicrobial-resistance-europe-2014.pdf>. Accessed 29.06.2019.
- [26] European Centre for Disease Prevention and Control, *Annual epidemiological report - Antimicrobial resistance and healthcare-associated infections 2014*,
<https://ecdc.europa.eu/sites/portal/files/media/en/publications/Publications/antimicrobial-resistance-annual-epidemiological-report.pdf>. Accessed 29.06.2019.
- [27] A. Hassoun, P. K. Linden, B. Friedman, *Critical care* **2017**, *21*, 211.
- [28] R. M. Klevens, M. A. Morrison, J. Nadle, S. Petit, K. Gershman, S. Ray, L. H. Harrison, R. Lynfield, G. Dumyati, J. M. Townes, A. S. Craig, E. R. Zell, G. E. Fosheim, L. K. McDougal, R. B. Carey, S. K. Fridkin, *JAMA* **2007**, *298*, 1763.
- [29] Centers for Disease Control and Prevention, **2007**, *HIV/AIDS Surveillance Report 2005*,
https://www.cdc.gov/hiv/pdf/statistics_2005_hiv_surveillance_report_vol_17.pdf. Accessed 29.06.2019.
- [30] A. S. Lee, H. de Lencastre, J. Garau, J. Kluytmans, S. Malhotra-Kumar, A. Peschel, S. Harbarth, *Nat. Rev. Dis. Primers* **2018**, *4*, 18033.
- [31] a) P. L. Mehndiratta, P. Bhalla, *Indian J. Med. Res.* **2014**, *140*, 339; b) S. Gopal, K. C. Divya, *Vet. World* **2017**, *10*, 311.
- [32] a) E. T. Knudsen, G. N. Rolinson, *Lancet* **1959**, *274*, 1105; b) E. T. Knudsen, G. N. Rolinson, *Br. Med. J.* **1960**, *2*, 700.
- [33] M. P. Jevons, *Br. Med. J.* **1961**, *1*, 124.
- [34] F. D. Lowy, *J. Clin. Invest.* **2003**, *111*, 1265.
- [35] G. Seltmann, O. Holst, *The Bacterial Cell Wall*, Springer, Berlin, Heidelberg, **2002**.
- [36] E. Sauvage, F. Kerff, M. Terrak, J. A. Ayala, P. Charlier, *FEMS Microbiol. Rev.* **2008**, *32*, 234.
- [37] A. Pantosti, A. Sanchini, M. Monaco, *Future Microbiol.* **2007**, *2*, 323.
- [38] S. W. Wu, H. de Lencastre, A. Tomasz, *J. Bacteriol.* **2001**, *183*, 2417.
- [39] C. Liu, A. Bayer, S. E. Cosgrove, R. S. Daum, S. K. Fridkin, R. J. Gorwitz, S. L. Kaplan, A. W. Karchmer, D. P. Levine, B. E. Murray, M. J. Rybak, D. A. Talan, H. F. Chambers, *Clin. Infect Dis.* **2011**, *52*, 285.
- [40] R. Kullar, S. L. Davis, D. P. Levine, M. J. Rybak, *Clin. Infect Dis.* **2011**, *52*, 975.
- [41] J. R. Knox, R. F. Pratt, *Antimicrob. Agents. Chemother.* **1990**, *34*, 1342.
- [42] T. L. Smith, M. L. Pearson, K. R. Wilcox, C. Cruz, M. V. Lancaster, B. Robinson-Dunn, F. C. Tenover, M. J. Zervos, J. D. Band, E. White, W. R. Jarvis, *N. Engl. J. Med.* **1999**, *340*, 493.
- [43] a) I. M. Gould, R. Cauda, S. Esposito, F. Gudiol, T. Mazzei, J. Garau, *Int. J. Antimicrob. Agents* **2011**, *37*, 202; b) J. H. Han, P. H. Edelstein, E. Lautenbach, *J. Antimicrob. Chemother.* **2012**, *67*, 2346.
- [44] M. Rybak, B. Lomaestro, J. C. Rotschafer, R. Moellering, W. Craig, M. Billeter, J. R. Dalovisio, D. P. Levine, *Am. J. Health Syst. Pharm.* **2009**, *66*, 82.
- [45] J. Pootoolal, J. Neu, G. D. Wright, *Annu. Rev. Pharmacol. Toxicol.* **2002**, *42*, 381.
- [46] S. L. Davis, P. S. McKinnon, L. M. Hall, G. Delgado, W. Rose, R. F. Wilson, M. J. Rybak, *Pharmacotherapy* **2007**, *27*, 1611.

- [47] a) G. Sakoulas, J. Alder, C. Thauvin-Eliopoulos, R. C. Moellering, G. M. Eliopoulos, *Antimicrob. Agents. Chemother.* **2006**, *50*, 1581; b) P. A. Moise, M. Amodio-Groton, M. Rashid, K. C. Lamp, H. L. Hoffman-Roberts, G. Sakoulas, M. J. Yoon, S. Schweitzer, A. Rastogi, *Antimicrob. Agents. Chemother.* **2013**, *57*, 1192.
- [48] J. Pogliano, N. Pogliano, J. A. Silverman, *J. Bacteriol.* **2012**, *194*, 4494.
- [49] T. L. Holland, C. Arnold, V. G. Fowler, *JAMA* **2014**, *312*, 1330.
- [50] a) J. S. Davis et al., *Clin. Infect Dis.* **2016**, *62*, 173; b) I. Shafiq, Z. P. Bulman, S. L. Spitznogle, J. E. Osorio, I. S. Reilly, A. J. Lesse, G. I. Parameswaran, K. A. Mergenhagen, B. T. Tsuji, *Infect. Dis. (Lond.)* **2017**, *49*, 410.
- [51] C. A. Fux, J. W. Costerton, P. S. Stewart, P. Stoodley, *Trends Microbiol.* **2005**, *13*, 34.
- [52] L. Hall-Stoodley, J. W. Costerton, P. Stoodley, *Nature Rev. Microbiol.* **2004**, *2*, 95.
- [53] A. S. Lynch, G. T. Robertson, *Annu. Rev. Med.* **2008**, *59*, 415.
- [54] H.-C. Flemming, J. Wingender, *Nature Rev. Microbiol.* **2010**, *8*, 623.
- [55] a) P. Stoodley, K. Sauer, D. G. Davies, J. W. Costerton, *Annu. Rev. Microbiol.* **2002**, *56*, 187; b) D. Monroe, *PLoS Biol.* **2007**, *5*, e307.
- [56] S. L. Chua, Y. Liu, J. K. H. Yam, Y. Chen, R. M. Vejborg, B. G. C. Tan, S. Kjelleberg, T. Tolker-Nielsen, M. Givskov, L. Yang, *Nature Comm.* **2014**, *5*, 4462.
- [57] P. Y. Chung, Y. S. Toh, *Pathog. Dis.* **2014**, *70*, 231.
- [58] M. Chen, Q. Yu, H. Sun, *Int. J. Mol. Sci.* **2013**, *14*, 18488.
- [59] D. G. Davies, C. N. H. Marques, *J. Bacteriol.* **2009**, *191*, 1393.
- [60] I. Kolodkin-Gal, D. Romero, S. Cao, J. Clardy, R. Kolter, R. Losick, *Science* **2010**, *328*, 627.
- [61] P. Karuso, B. W. Skelton, W. C. Taylor, A. H. White, *Aust. J. Chem.* **1984**, *37*, 1081.
- [62] P. Karuso, P. R. Bergquist, R. C. Cambie, J. S. Buckleton, G. R. Clark, C. E.F. Rickard, *Aust. J. Chem.* **1986**, *39*, 1643.
- [63] T. F. Molinski, D. J. Faulkner, *J. Org. Chem.* **1987**, *52*, 296.
- [64] R. Fleeman, T. M. LaVoi, R. G. Santos, A. Morales, A. Nefzi, G. S. Welmaker, J. L. Medina-Franco, M. A. Giulianotti, R. A. Houghten, L. N. Shaw, *J. Med. Chem.* **2015**, *58*, 3340.
- [65] R. A. Keyzers, P. T. Northcote, M. T. Davies-Coleman, *Nat. Prod. Rep.* **2006**, *23*, 321.
- [66] F. Bray, J. Ferlay, I. Soerjomataram, R. L. Siegel, L. A. Torre, A. Jemal, *CA Cancer J. Clin.* **2018**, *68*, 394.
- [67] A. Sánchez-Gastaldo, E. Kempf, A. González Del Alba, I. Duran, *Cancer Treat. Rev.* **2017**, *60*, 77.
- [68] J. G. Betts, P. DeSaix, E. Johnson, J. E. Johnson, O. Korol, D. H. Kruse, B. Poe, J. A. Wise, M. Womble, K. A. Young, **2017**, *Anatomy and physiology*, <https://cnx.org/contents/FPtK1z mh@15.5:719EIHui@8/25-3-Gross-Anatomy-of-the-Kidney>. Accessed 19.07.2019.
- [69] H. T. Cohen, F. J. McGovern, *N. Engl. J. Med.* **2005**, *353*, 2477.
- [70] a) S. Patil, J. Manola, P. Elson, S. Negrier, B. Escudier, T. Eisen, M. Atkins, R. Bukowski, R. J. Motzer, *J. Urol.* **2012**, *188*, 2095; b) S. Buti, M. Bersanelli, A. Sikokis, F. Maines, F. Facchinetti, E. Bria, A. Ardizzoni, G. Tortora, F. Massari, *Anticancer drugs* **2013**, *24*, 535.
- [71] B. I. Rini, W. K. Rathmell, P. Godley, *Curr. Opin. Oncol.* **2008**, *20*, 300.

- [72] M. C. Smaldone, D. Canter, A. Kutikov, R. G. Uzzo in *Renal Cell Carcinoma: Clinical Management* (Eds.: S. C. Campbell, B. I. Rini), Humana Press, Totowa, NJ, **2013**, pp. 167–194.
- [73] Matin, Ahrar in *Renal Cell Carcinoma: Clinical Management* (Eds.: S. C. Campbell, B. I. Rini), Humana Press, Totowa, NJ, **2013**, pp. 155–166.
- [74] D. George, E. Jonasch, *Immunotherapy of renal cell carcinoma*, <https://www.uptodate.com/contents/immunotherapy-of-renal-cell-carcinoma#H38>. Accessed 19.07.2019.
- [75] K. Gupta, J. D. Miller, J. Z. Li, M. W. Russell, C. Charbonneau, *Cancer Treat. Rev.* **2008**, *34*, 193.
- [76] C. Sourbier, B. T. Scroggins, R. Ratnayake, T. L. Prince, S. Lee, M.-J. Lee, P. L. Nagy, Y. H. Lee, J. B. Trepel, J. A. Beutler, W. M. Linehan, L. Neckers, *Cancer cell* **2013**, *23*, 228.
- [77] Y. Akbulut, H. J. Gaunt, K. Muraki, M. J. Ludlow, M. S. Amer, A. Bruns, N. S. Vasudev, L. Radtke, M. Willot, S. Hahn, T. Seitz, S. Ziegler, M. Christmann, D. J. Beech, H. Waldmann, *Angew. Chem. Int. Ed.* **2015**, *54*, 3787.
- [78] M. J. Ludlow, H. J. Gaunt, H. N. Rubaiy, K. E. Musialowski, N. M. Blythe, N. S. Vasudev, K. Muraki, D. J. Beech, *J. Biol. Chem.* **2017**, *292*, 723.
- [79] K. Muraki, K. Ohnishi, A. Takezawa, H. Suzuki, N. Hatano, Y. Muraki, N. Hamzah, R. Foster, H. Waldmann, P. Nussbaumer, M. Christmann, R. S. Bon, D. J. Beech, *Sci. Rep.* **2017**, *7*, No. 16988.
- [80] H. N. Rubaiy, M. J. Ludlow, M. Henrot, H. J. Gaunt, K. Miteva, S. Y. Cheung, Y. Tanahashi, N. Hamzah, K. E. Musialowski, N. M. Blythe, H. L. Appleby, M. A. Bailey, L. McKeown, R. Taylor, R. Foster, H. Waldmann, P. Nussbaumer, M. Christmann, R. S. Bon, K. Muraki, D. J. Beech, *J. Biol. Chem.* **2017**, *292*, 8158.
- [81] H. N. Rubaiy, T. Seitz, S. Hahn, A. Choidas, P. Habenberger, B. Klebl, K. Dinkel, P. Nussbaumer, H. Waldmann, M. Christmann, D. J. Beech, *Br. J. Pharmacol.* **2018**, *175*, 830.
- [82] C. Carson, P. Raman, J. Tullai, L. Xu, M. Henault, E. Thomas, S. Yeola, J. Lao, M. McPate, J. M. Verkuyl, G. Marsh, J. Sarber, A. Amaral, S. Bailey, D. Lubicka, H. Pham, N. Miranda, J. Ding, H.-M. Tang, H. Ju, P. Tranter, N. Ji, P. Krastel, R. K. Jain, A. M. Schumacher, J. J. Loureiro, E. George, G. Berellini, N. T. Ross, S. M. Bushell, G. Erdemli, J. M. Solomon, *PLoS one* **2015**, *10*, e0127498.
- [83] S. Y. Cheung, M. Henrot, M. Al-Saad, M. Baumann, H. Muller, A. Unger, H. N. Rubaiy, I. Mathar, K. Dinkel, P. Nussbaumer, B. Klebl, M. Freichel, B. Rode, S. Trainor, S. J. Clapcote, M. Christmann, H. Waldmann, S. K. Abbas, D. J. Beech, N. S. Vasudev, *Oncotarget* **2018**, *9*, 29634.
- [84] a) W. N. Hunter, *J. Biol. Chem.* **2007**, *282*, 21573; b) I. Buhaescu, H. Izzedine, *Clin. Biochem.* **2007**, *40*, 575.
- [85] M. Rohmer, *Nat. Prod. Rep.* **1999**, *16*, 565.
- [86] J. L. Goldstein, M. S. Brown, *Nature* **1990**, *343*, 425.
- [87] K. Kuranda, J. François, G. Palamarczyk, *FEMS Yeast Res.* **2010**, *10*, 14.
- [88] M. Willot, M. Christmann, *Nat. Chem.* **2010**, *2*, 519.
- [89] J. Wang, S.-G. Chen, B.-F. Sun, G.-Q. Lin, Y.-J. Shang, *Chem. Eur. J.* **2013**, *19*, 2539.
- [90] S. Sutthivaiyakit, N. N. Nakorn, W. Kraus, P. Sutthivaiyakit, *Tetrahedron* **2003**, *59*, 9991.
- [91] G.-P. Peng, G. Tian, X.-F. Huang, F.-C. Lou, *Phytochemistry* **2003**, *63*, 877.
- [92] J. H. G. Lago, C. B. Brochini, N. F. Roque, *Phytochemistry* **2000**, *55*, 727.

- [93] For further englerin syntheses applying ring-closing metathesis, see: a) K. Takahashi, K. Komine, Y. Yokoi, J. Ishihara, S. Hatakeyama, *J. Org. Chem.* **2012**, *77*, 7364; b) J. Lee, K. A. Parker, *Org. Lett.* **2012**, *14*, 2682; c) M. Zahel, A. Kessberg, P. Metz, *Angew. Chem. Int. Ed.* **2013**, *52*, 5390; d) J. Zhang, S. Zheng, W. Peng, Z. Shen, *Tetrahedron Lett.* **2014**, *55*, 1339.
- [94] For englerin syntheses applying gold-catalyzed [2+2+2]-cycloaddition, see: a) Q. Zhou, X. Chen, D. Ma, *Angew. Chem. Int. Ed.* **2010**, *49*, 3513; b) K. Molawi, N. Delpont, A. M. Echavarren, *Angew. Chem. Int. Ed.* **2010**, *49*, 3517.
- [95] For englerin syntheses applying [3+2]-cycloaddition, see: a) K. C. Nicolaou, Q. Kang, S. Y. Ng, D. Y.-K. Chen, *J. Am. Chem. Soc.* **2010**, *132*, 8219; b) T. Hanari, N. Shimada, Y. Kurosaki, N. Thrimurtulu, H. Nambu, M. Anada, S. Hashimoto, *Chem. Eur. J.* **2015**, *21*, 11671; c) H. Kusama, A. Tazawa, K. Ishida, N. Iwasawa, *Chem. Asien. J.* **2016**, *11*, 64; d) C. Reagan, G. Trevitt, K. Tchabanenko, *Eur. J. Org. Chem.* **2019**, *2019*, 1027.
- [96] a) J. Xu, E. J. E. Caro-Diaz, E. A. Theodorakis, *Org. Lett.* **2010**, *12*, 3708; b) J. Xu, E. J. E. Caro-Diaz, A. Batova, S. D. E. Sullivan, E. A. Theodorakis, *Chem. Asien. J.* **2012**, *7*, 1052.
- [97] R. Nelson, M. Gulías, J. L. Mascareñas, F. López, *Angew. Chem. Int. Ed.* **2016**, *55*, 14359.
- [98] a) S. Hagihara, K. Hanaya, T. Sugai, M. Shoji, *J. Antibiot.* **2018**, *71*, 257; b) B. Plietker, L. Guo, *Angew. Chem. Int. Ed.* **2019**.
- [99] Z. Li, M. Nakashige, W. J. Chain, *J. Am. Chem. Soc.* **2011**, *133*, 6553.
- [100] P. Gao, S. P. Cook, *Org. Lett.* **2012**, *14*, 3340.
- [101] K. Morisaki, Y. Sasano, T. Koseki, T. Shibuta, N. Kanoh, W.-H. Chiou, Y. Iwabuchi, *Org. Lett.* **2017**, *19*, 5142.
- [102] D. B. Ushakov, V. Navickas, M. Ströbele, C. Maichle-Mössmer, F. Sasse, M. E. Maier, *Org. Lett.* **2011**, *13*, 2090.
- [103] Sven Hahn, *PhD Thesis*, Freie Universität Berlin, **2016**.
- [104] S. L. Schreiber, H. V. Meyers, K. B. Wiberg, *J. Am. Chem. Soc.* **1986**, *108*, 8274.
- [105] K. Ishida, H. Kusama, N. Iwasawa, *J. Am. Chem. Soc.* **2010**, *132*, 8842.
- [106] H. Abe, A. Tezuka, T. Kobayashi, H. Ito, *Heterocycles* **2014**, *88*, 651.
- [107] L. Dong, X.-Z. Jiao, X.-Y. Liu, C.-S. Tian, X.-Y. Li, Y.-Y. Yao, P. Xie, *J. Asian. Nat. Prod. Res.* **2014**, *16*, 629.
- [108] M. J. Acerson, B. S. Bingham, C. A. Allred, M. B. Andrus, *Tetrahedron Lett.* **2015**, *56*, 3277.
- [109] D. C. Elliott, J. A. Beutler, K. A. Parker, *ACS Med. Chem. Lett.* **2017**, *8*, 746.
- [110] T. Siemon, *Master's Thesis*, Freie Universität Berlin, **2015**.
- [111] L. López-Suárez, L. Riesgo, F. Bravo, T. T. Ransom, J. A. Beutler, A. M. Echavarren, *ChemMedChem* **2016**, *11*, 1003.
- [112] K. P. Chan, D. Y.-K. Chen, *ChemMedChem* **2011**, *6*, 420.
- [113] Lea Radtke, *PhD Thesis*, Technische Universität Dortmund, **2012**.
- [114] D. M. Fash, C. J. Peer, Z. Li, I. J. Talisman, S. Hayavi, F. J. Sulzmaier, J. W. Ramos, C. Sourbier, L. Neckers, W. D. Figg, J. A. Beutler, W. J. Chain, *Bioorg. Med. Chem. Lett.* **2016**, *26*, 2641.
- [115] L. Friedrich, T. Rodrigues, C. S. Neuhaus, P. Schneider, G. Schneider, *Angew. Chem. Int. Ed.* **2016**, *55*, 6789.
- [116] J. S. Dickschat, *Eur. J. Org. Chem.* **2017**, *2017*, 4872.
- [117] G. Bian, Z. Deng, T. Liu, *Curr. Opin. Biotechnol.* **2017**, *48*, 234.

List of References and Illustration Credits

- [118] J. Inanaga, K. Hirata, H. Saeki, T. Katsuki, M. Yamaguchi, *Bull. Chem. Soc. Jpn.* **1979**, *52*, 1989.
- [119] P. G. Reddy, T. V. Pratap, G. D. K. Kumar, S. K. Mohanty, S. Baskaran, *Eur. J. Org. Chem.* **2002**, *2002*, 3740.
- [120] E. D. Mihelich, K. Daniels, D. J. Eickhoff, *J. Am. Chem. Soc.* **1981**, *103*, 7690.

4.2 Illustration Credits

Figure 2, p. 1

Reprinted with permission from (E. Patridge, P. Gareiss, M. S. Kinch, D. Hoyer, *Drug Discov. Today* **2016**, *21*, 204.) © 2015 Elsevier Ltd. (License No.: 4653670291923).

Figure 3, p. 2

D. J. Newman, G. M. Cragg, *J. Nat. Prod.* **2016**, *79*, 629. © 2016 American Chemical Society and American Society of Pharmacognosy.

Figure 4, p. 3

Reprinted with permission from (A. Nadin, C. Hattotuwigama, I. Churcher, *Angew. Chem. Int. Ed.* **2012**, *51*, 1114.) © 2012 Wiley-VCH Verlag GmbH & Co. KGaA, Weinheim (License No.: 4653670798992)

Figure 7, p. 8

Drawn using ChemDraw Professional 16.0.

Figure 9, p. 10

Downloaded for free from: <https://pixnio.com/science/microscopy-images/staphylococcus-aureus/biofilm-formation-found-inside-the-lumen-of-an-indwelling-catheter-being-secreted-by-staphylococcus-aureus-bacteria> (Accessed 02.07.2019). Photo credit to Rodney M. Donlan, Ph.D., Janice Carr, USCDCP.

Figure 10, p. 11

Adapted from D. Monroe, *PLoS Biol.* **2007**, *5*, e307. © 2007 Don Monroe.

Figure 12, p. 23

a) Reprinted with permission from (J. G. Betts, P. DeSaix, E. Johnson, J. E. Johnson, O. Korol, D. H. Kruse, B. Poe, J. A. Wise, M. Womble, K. A. Young, 2017, *Anatomy and physiology*, <https://cnx.org/contents/FPtK1zmf@15.5:7l9EIHui@8/25-3-Gross-Anatomy-of-the-Kidney>. (Accessed 19.07.2019.)) © 2012 Rice University.

b) Downloaded and adapted for free from https://commons.wikimedia.org/wiki/File:Clear_cell_renal_cell_carcinoma_high_mag_cropped.jpg (Accessed 19.07.2019).

Figure 16, p. 46

Reprinted with permission from (L. Friedrich, T. Rodrigues, C. S. Neuhaus, P. Schneider, G. Schneider, *Angew. Chem. Int. Ed.* **2016**, *55*, 6789.) © 2016 Wiley-VCH Verlag GmbH & Co. KGaA, Weinheim (License No.: 4653681446026).

Appendix

Supporting Information – Synthesis of (+)-Darwinolide



Supporting Information

Synthesis of (+)-Darwinolide, a Biofilm-Penetrating Anti-MRSA Agent

*Thomas Siemon, Simon Steinhauer, and Mathias Christmann**

anie_201813142_sm_miscellaneous_information.pdf

General Working Methods

The analytical data was obtained with the help of the following equipment.

NMR spectroscopy

^1H and ^{13}C NMR spectra were acquired on a JEOL ECX 400 (400 MHz), JEOL ECP 500/ Bruker Avance 500 (500 MHz) and a Bruker Avance 700 (700 MHz) in CDCl_3 or CD_3OD as a solvent. The chemical shifts were reported relative to CDCl_3 ($\delta = ^1\text{H}$: 7.26 ppm, ^{13}C : 77.16 ppm) or CD_3OD ($\delta = ^1\text{H}$: 3.31 ppm, ^{13}C : 49.00 ppm). The multiplicities of the signals are described using the following abbreviations: s = singlet, d = doublet, t = triplet, q = quartet, m = multiplet, br = broad and combinations thereof.

The spectra were evaluated with the software MestReNova 10.

Mass spectra were obtained on a ESI-FTICR-MS: Ionspec QFT-7 (Agilent/Varian).

IR: spectra were measured on a JASCO FT/IR-4100 Spectrometer. Characteristic absorption bands are displayed in wavenumbers $\tilde{\nu}$ in cm^{-1} and were analyzed with the software Spectral Manager from JASCO.

Melting points were measured on a Thermovar from the company Reichert and are not corrected.

Enantiomeric excess was determined by chiral HPLC using Agilent Technologies 1200 series equipped with Chiralpak[®] IC or by chiral GC using Agilent 7890B equipped with Lipodex E column.

Optical rotation measurements were performed on a P-2000 polarimeter from Jasco in a 10 cm optical-path length cell with the frequency of the NaD line measured at the temperature and concentration (in g/100 mL) indicated.

Crystal data were collected on a Bruker D8 Venture diffractometer with a Photon 100 CMOS detector with $\text{CuK}\alpha$ radiation.

Chromatography Reaction progress was monitored by thin layer chromatography on aluminum backed silica gel plates (silica gel 60 F 254 from E. Merck), visualizing with UV light ($\lambda = 254 \text{ nm}$). The plates were developed using vanillin dip solution (170 mL methanol, 20.0 mL conc. acetic acid, 10.0 mL conc. sulfuric acid with 1.0 g vanillin), KMnO_4 dip solution (3.0 g potassium permanganate, 5.0 mL NaOH-solution (5 w/w), 300 mL dest. water) or an anisaldehyde solution (450 mL ethanol, 25.0 mL anisaldehyde, 25.0 mL conc. sulfuric acid, 8.0 mL acetic acid).

Flash chromatography was performed using silica gel M60 from Macherey & Nagel (particle size: 40 – 63 μm).

Reagents and Solvents Reactions with air or moisture-sensitive substances were, if not otherwise indicated, carried out under an argon atmosphere with the help of the Schlenk

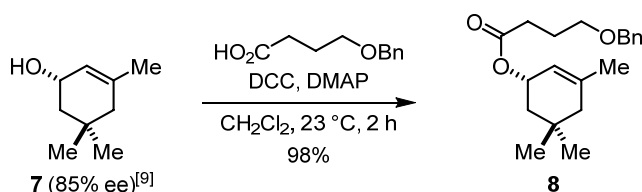
technique. All other reagents and solvents were used as purchased from commercial suppliers unless otherwise noted. Anhydrous solvents were purified with the solvent purification system MB-SPS-800 (Braun). The solvents (diethyl ether, ethyl acetate, pentane and dichloromethane) used for column chromatography and work up were purified from commercially available technical grade solvents by distillation under reduced pressure with the help of rotatory evaporators (Heidolph or IKA) at 40 °C water bath temperature.

(*S*)-Isophorol was obtained in 85% *ee* by enzymatic resolution of racemic 3,5,5-trimethylcyclohex-2-en-1-ol using *Candida Rugosa* lipase.^[1] 4-Benzyloxybutanoic acid was synthesized from γ -butyrolactone according to the literature.^[2] DABAL-Me₃ was obtained by the reaction of 1,4-diazabicyclo[2.2.2]octane and trimethylaluminium.^[3]

Compound names are derived from Chemdraw and are not necessarily identical with the IUPAC nomenclature.

Experimental Procedure

(*S*)-3,5,5-Trimethylcyclohex-2-en-1-yl 4-(benzyloxy)butanoate (**8**)



An oven-dried 500 mL round-bottom-flask equipped with a Teflon-coated magnetic stirring bar was charged with alcohol **7** (7.04 g, 50.2 mmol, 1.0 equiv.) and dry CH₂Cl₂ (250 mL). 4-(benzyloxy)butanoic acid (13.7 g, 70.3 mmol, 1.4 equiv.), *N,N'*-dicyclohexyl-carbodiimide (15.5 g, 75.3 mmol, 1.5 equiv.) and 4-(dimethylamino)pyridine (613 mg, 5.02 mmol, 0.1 equiv.) were added at 23 °C. The reaction mixture was stirred under an atmosphere of argon for 18 h and afterwards the solvent was removed under reduced pressure. The residue was taken up in Et₂O (200 mL) and filtered through a sintered glass funnel. The filtrate was concentrated under reduced pressure and purified by column chromatography (SiO₂, pentane/Et₂O 15:1) to afford ester **8** (15.5 g, 98%) as a colorless oil.

$[\alpha]_{\text{D}}^{27} = -47.2^\circ$ ($c = 0.79$, CHCl₃).

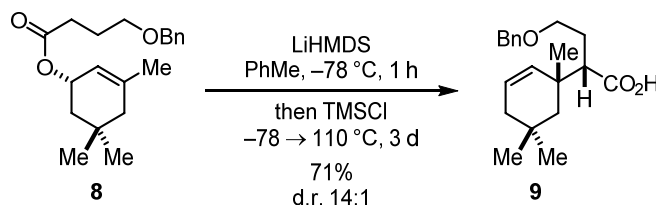
¹H NMR (500 MHz, CDCl₃): δ [ppm] = 7.36 – 7.31 (m, 4H), 7.31 – 7.25 (m, 1H), 5.38 – 5.36 (m, 1H), 5.36 – 5.32 (m, 1H), 4.50 (s, 2H), 3.51 (t, $J = 6.2$ Hz, 2H), 2.42 (t, $J = 7.4$ Hz, 2H), 1.95 (tt, $J = 7.5, 6.2$ Hz, 2H), 1.87 (d, $J = 17.3$ Hz, 1H), 1.73 (dd, $J = 12.8, 6.0$ Hz, 1H), 1.69 (s, 3H), 1.38 (dd, $J = 12.9, 7.9$ Hz, 1H), 1.67 (d, $J = 17.3$ Hz, 1H), 1.00 (s, 3H), 0.94 (s, 3H).

^{13}C NMR (126 MHz, CDCl_3): δ [ppm] = 172.9, 138.2, 137.9, 128.0, 127.3, 127.2, 119.0, 72.6, 69.6, 68.9, 43.7, 40.4, 31.2, 30.3, 30.1, 26.7, 24.9, 23.4.

HRMS (ESI): m/z calcd for $\text{C}_{20}\text{H}_{28}\text{O}_3\text{Na}$ $[\text{M}+\text{Na}]^+$: 339.1930; found: 339.1939.

IR (ATR): $\tilde{\nu}$ = 2952, 2929, 2869, 2361, 2336, 1728, 1454, 1365, 1256, 1173, 1110, 1077, 1025, 972, 944, 761, 751, 739, 700, 686, 668 cm^{-1} .

(S)-4-(Benzyloxy)-2-((R)-1,5,5-trimethylcyclohex-2-en-1-yl)butanoic acid (9)



An oven-dried 500 mL three-necked-flask equipped with a reflux condenser, a Schlenk adapter, a dropping funnel and a Teflon-coated magnetic stirring bar was charged with 1,1,1,3,3,3-hexamethyldisilazane (18.0 mL, 86.9 mmol, 2.5 equiv.) and dry PhMe (50 mL) under an atmosphere of argon. *n*-BuLi (2.5 M in hexane, 27.8 mL, 69.5 mmol, 2.0 equiv.) was added at -78 °C and the solution was warmed to 23 °C over 30 min. After re-cooling to -78 °C, a solution of ester **8** (11.0 g, 34.8 mmol, 1.0 equiv.) in dry PhMe (100 mL) was added and the mixture was stirred at -78 °C for 1 h. Chlorotrimethylsilane (8.80 mL, 69.5 mmol, 2.0 equiv.) was added and after another 15 min at -78 °C, the reaction mixture was refluxed for 3 d. HCl (1 M aq., 200 mL) was added at 0 °C and the aqueous phase was extracted with Et_2O (3 x 200 mL). The combined organic phases were dried over Na_2SO_4 , filtered and concentrated under reduced pressure. Column chromatography (SiO_2 , pentane/ Et_2O 8:1 + 0.7% HCO_2H) afforded the acid **9** (7.89 g, 71%, 14:1 d.r.) as a colorless oil.

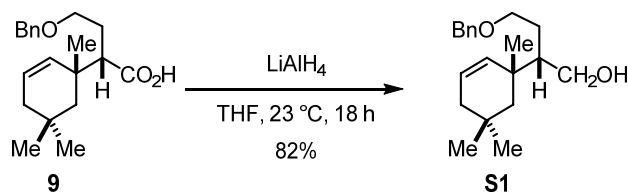
$[\alpha]_{\text{D}}^{24} = +3.00^\circ$ ($c = 0.90$, CHCl_3).

^1H NMR (500 MHz, CDCl_3): δ [ppm] = 10.72 (br s, 1H), 7.41 – 7.25 (m, 5H), 5.73 (ddd, $J = 10.1, 5.5, 2.6$ Hz, 1H), 5.32 (d, $J = 10.1$ Hz, 1H), 4.52 (d, $J = 12.1$ Hz, 1H), 4.49 (d, $J = 12.1$ Hz, 1H), 3.53 – 3.43 (m, 2H), 2.38 (dd, $J = 11.3, 2.3$ Hz, 1H), 1.98 (ddt, $J = 13.8, 11.6, 5.9$ Hz, 1H), 1.82 (dtd, $J = 13.9, 7.0, 2.5$ Hz, 1H), 1.77 (t, $J = 2.8$ Hz, 1H), 1.75 (dt, $J = 5.5, 1.6$ Hz, 1H), 1.62 (d, $J = 14.2$ Hz, 1H), 1.34 (d, $J = 14.2$ Hz, 1H), 1.19 (s, 3H), 0.99 (s, 6H).

^{13}C NMR (126 MHz, CDCl_3): δ [ppm] = 179.8, 138.3, 133.4, 128.4, 127.6, 127.5, 126.2, 73.0, 69.1, 53.6, 43.9, 38.3, 38.2, 32.6, 30.0, 28.2 (2C), 26.3.

HRMS (ESI): m/z calcd for $\text{C}_{20}\text{H}_{28}\text{O}_3\text{Na}$ $[\text{M}+\text{Na}]^+$: 339.1930; found: 339.1931.

IR (ATR): $\tilde{\nu}$ = 2950, 2923, 2870, 1730, 1701, 1455, 1364, 1254, 1111, 859, 844, 750, 738, 727, 714, 697, 671, 659 cm^{-1} .

(S)-4-(benzyloxy)-2-((R)-1,5,5-trimethylcyclohex-2-en-1-yl)butan-1-ol (S1)

An oven-dried 500 mL Schlenk flask equipped with a Teflon-coated magnetic stirring bar was charged with LiAlH₄ (2.30 g, 61.5 mmol, 3.0 equiv.) and dry THF (70 mL). A solution of acid **9** (6.50 g, 20.5 mmol, 1.0 equiv) in dry THF (30 mL) was added slowly at 0 °C. After warming to 23 °C the suspension was stirred for 18 h. The reaction mixture was diluted with Et₂O (50 mL) and HCl (1 M aq., 50 mL) was added dropwise at 0 °C. The suspension was filtered through sand and the aqueous phase was extracted with Et₂O (3 x 100 mL). The combined organic phases were washed with brine (100 mL), dried over Na₂SO₄, filtered and concentrated under reduced pressure. Column chromatography (SiO₂, pentane/Et₂O 4:1) afforded alcohol **S1** (5.07 g, 82%) as a colorless oil.

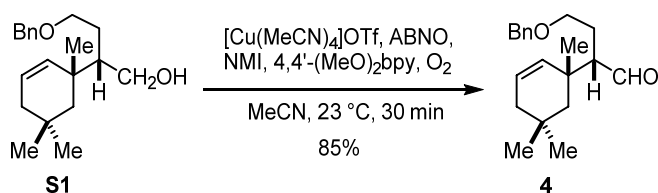
$[\alpha]_{\text{D}}^{24} = +25.4^{\circ}$ ($c = 0.75$, CHCl₃).

¹H NMR (500 MHz, CDCl₃): δ [ppm] = 7.38 – 7.27 (m, 5H), 5.63 (ddd, $J = 10.2, 5.6, 2.6$ Hz, 1H), 5.32 (d, $J = 10.1$ Hz, 1H), 4.53 (s, 2H), 3.83 (td, $J = 7.8, 4.0$ Hz, 1H), 3.63 (dt, $J = 9.5, 4.8$ Hz, 1H), 3.47 – 3.39 (m, 2H), 3.26 – 3.21 (m, 1H), 1.87 – 1.80 (m, 1H), 1.75 – 1.65 (m, 2H), 1.61 – 1.51 (m, 1H), 1.38 (d, $J = 13.8$ Hz, 1H), 1.36 – 1.30 (m, 1H), 1.15 (d, $J = 14.3$ Hz, 1H), 1.13 (s, 3H), 0.95 (s, 3H), 0.93 (s, 3H).

¹³C NMR (126 MHz, CDCl₃): δ [ppm] = 137.8, 134.9, 128.6, 128.0 (2C), 125.0, 73.4, 71.1, 63.7, 52.1, 44.2, 38.9, 38.5, 33.1, 30.1, 29.9, 28.2, 26.9.

HRMS (ESI): m/z calcd for C₂₀H₃₀O₂Na [M+Na]⁺: 325.2138; found: 325.2154.

IR (ATR): $\tilde{\nu} = 3440, 3011, 2950, 2867, 1496, 1476, 1455, 1363, 1289, 1263, 1206, 1092, 1029, 994, 731, 697, 680$ cm⁻¹.

(S)-4-(benzyloxy)-2-((R)-1,5,5-trimethylcyclohex-2-en-1-yl)butanal (4)

A 100 mL round-bottom-flask equipped with a Teflon-coated magnetic stirring bar was charged with alcohol **S1** (5.50 g, 18.2 mmol, 1.0 equiv.), [Cu(MeCN)₄]OTf (685 mg, 1.82 mmol, 0.1 equiv.), 9-Aza-bicyclo[3.3.1]nonane *N*-oxyl (25.5 mg, 180 μ mol, 0.01 equiv.), *N*-methylimidazole

(0.29 mL, 3.64 mmol, 0.2 equiv.), 4,4'-dimethoxy-2,2'-bipyridine (394 mg, 1.82 mmol, 0.1 equiv.) and MeCN (50 mL). The atmosphere was exchanged to O₂ by three times evacuating and flushing with O₂. The reaction mixture was stirred at 23 °C for 30 min und an O₂ atmosphere and HCl (1 M aq., 20 mL) was added. The aqueous phase was extracted with Et₂O (3 x 50 mL). The combined organic phases were dried over Na₂SO₄, filtered and concentrated under reduced pressure. Column chromatography (SiO₂, pentane/Et₂O 30:1) afforded aldehyde **4** (4.64 g, 85%) as a colorless oil.

$[\alpha]_D^{24} = +1.00^\circ$ ($c = 1.4$, CHCl₃).

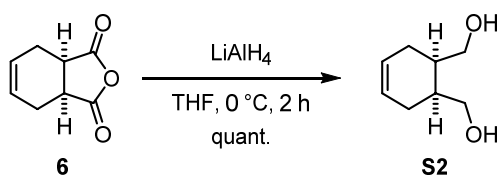
¹H NMR (400 MHz, CDCl₃): δ [ppm] = 9.71 (d, $J = 4.5$ Hz, 1H), 7.36 – 7.25 (m, 5H), 5.72 (ddd, $J = 10.2, 5.4, 2.9$ Hz, 1H), 5.35 (d, $J = 10.1$ Hz, 1H), 4.45 (d, $J = 12.0$ Hz, 1H), 4.41 (d, $J = 12.0$ Hz, 1H), 3.44 – 3.34 (m, 2H), 2.15 (ddd, $J = 10.8, 4.3, 2.2$ Hz, 1H), 2.07 – 1.97 (m, 1H), 1.82 – 1.71 (m, 3H), 1.58 (d, $J = 13.6$ Hz, 1H), 1.27 (d, $J = 14.0$ Hz, 1H), 1.18 (s, 3H), 0.97 (s, 3H), 0.95 (s, 3H).

¹³C NMR (176 MHz, CDCl₃): δ [ppm] = 205.9, 138.3, 132.5, 128.4, 127.7, 127.6, 126.3, 73.0, 68.9, 60.3, 44.7, 38.7, 38.2, 32.7, 29.8, 28.1, 26.7, 25.3.

HRMS (ESI): m/z calcd for C₂₀H₂₈O₂Na [M+Na]⁺: 323.1981; found: 323.1993.

IR (ATR): $\tilde{\nu} = 3013, 2951, 2867, 1717, 1496, 1477, 1455, 1363, 1290, 1265, 1209, 1101, 1028, 993, 935, 906, 731, 698$ cm⁻¹.

cis-4-Cyclohexene-1,2-dimethanol (**S2**)

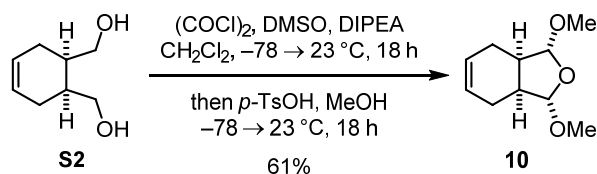


An oven-dried 1 L Schlenk flask equipped with a Teflon-coated magnetic stirring bar was charged with LiAlH₄ (15.2 g, 400 mmol, 2.0 equiv.) and dry THF (500 mL). Anhydride **6** (30.4 g, 200 mmol, 1.0 equiv.) was added in portions at 0 °C and the resulting suspension was stirred at 23 °C for 2 h. The reaction mixture was cooled to 0 °C and diluted with Et₂O (100 mL). H₂O (18 mL), NaOH (10% aq, 30 mL) and again H₂O (45 mL) were added dropwise at 0 °C. The suspension was warmed to 23 °C for 15 min and MgSO₄ was added. After 10 min, the precipitation was filtered off and the filtrate was diluted with brine (250 mL). The aqueous phase was extracted with EtOAc (3 x 300 mL) and the combined organic phases were dried over Na₂SO₄, filtered and concentrated under reduced pressure. Diol **S2** (28.1 g, 99%) was obtained as a colorless oil and used without further purification.

^1H NMR (400 MHz, CDCl_3): δ [ppm] = 5.60 (s, 2H), 3.71 (dd, J = 11.0, 6.8 Hz, 1H), 3.57 (dd, J = 11.0, 3.6 Hz, 2H), 3.27 (br. s, 2H), 2.21 – 1.96 (m, 6H).

The spectral data are in accordance with the literature.^[4]

***meso*-(1*R*,3*S*,3*aS*,7*aR*)-1,3-Dimethoxy-1,3,3*a*,4,7,7*a*-hexahydroisobenzofuran (10)**



An oven-dried 2 L three-necked-flask equipped with a mechanical stirrer, a Schlenk adapter and a dropping funnel was charged with oxalyl chloride (50.8 mL, 593 mmol, 3.0 equiv.) and dry CH_2Cl_2 (350 mL) under an atmosphere of argon. Dry DMSO (84.2 mL, 1.19 mol, 6.0 equiv.) was added at -78°C over a period of 45 min. After stirring for 15 min at -78°C , a solution of diol **S2** (28.1 g, 198 mmol, 1.0 equiv.) in dry CH_2Cl_2 (500 mL) was added dropwise over 1 h. The solution was further stirred at -78°C for 1 h and *N,N*-diisopropylethylamine (252 mL, 1.48 mol, 7.5 equiv.) was added over a period of 30 min. The reaction mixture was stirred at -78°C for 2 h and stored at -28°C for 16 h. After an additional 2 h at -78°C , a solution of *p*-toluenesulfonic acid monohydrate (140 g, 736 mmol, 3.7 equiv.) in MeOH (300 mL) was added. The solution was stirred at 23°C for 18 h and NH_4Cl (sat. aq., 300 mL) was added at 0°C . The aqueous phase was extracted with CH_2Cl_2 (3 x 250 mL). The combined organic phases were concentrated under reduced pressure. The residue was dissolved in EtOAc (500 mL) and washed with brine (2 x 200 mL). The organic phase was dried over Na_2SO_4 , filtered and concentrated under reduced pressure. Purification by column chromatography (SiO_2 , pentane/ Et_2O 15:1) to afford bisacetal **10** (22.1 g, 61%) as a colorless oil.

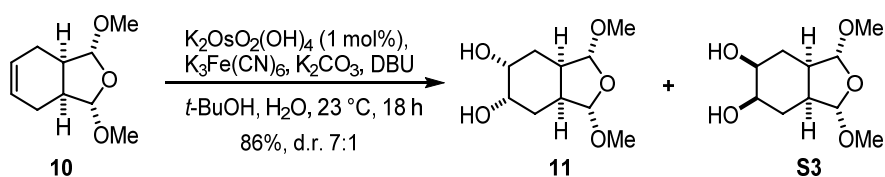
^1H NMR (500 MHz, CDCl_3): δ [ppm] = 5.68 (t, J = 1.6 Hz, 2H), 4.70 (d, J = 3.0 Hz, 2H), 3.41 (s, 6H), 2.46 – 2.35 (m, 2H), 2.28 – 2.15 (m, 2H), 1.98 – 1.86 (m, 2H).

^{13}C NMR (126 MHz, CDCl_3): δ [ppm] = 125.1, 110.4, 55.7, 39.3, 23.1.

HRMS (ESI): m/z calcd for $\text{C}_{10}\text{H}_{16}\text{O}_3\text{Na}$ [$\text{M}+\text{Na}$] $^+$: 207.0991; found: 207.0989.

IR (ATR): $\tilde{\nu}$ = 3026, 2952, 2894, 2843, 2362, 1727, 1659, 1440, 1389, 1306, 1252, 1208, 1191, 1123, 1099, 1087, 1040, 999, 968, 921, 884, 846, 803, 758, 738 cm^{-1} .

meso-(1R,3S,3aS,5S,6R,7aR)-1,3-Dimethoxyoctahydroisobenzofuran-5,6-diol (11**) and meso-(1R,3S,3aS,5R,6S,7aR)-1,3-Dimethoxyoctahydroisobenzofuran-5,6-diol (**S3**)**



A 500 mL round-bottom-flask equipped with a Teflon-coated magnetic stirring bar was charged with bisacetal **10** (22.1 g, 120 mmol, 1 equiv.), *tert*-butanol (150 mL) and H_2O (150 mL). $K_2OsO_2(OH)_4$ (442 mg, 1.20 mmol, 0.01 equiv.), $K_3Fe(CN)_6$ (119 g, 360 mmol, 3.0 equiv.), K_2CO_3 (49.7 g, 360 mmol, 3.0 equiv.) and 1,8-diazabicyclo[5.4.0]undec-7-ene (17.9 mL, 120 mmol, 1.0 equiv.) were added and the reaction mixture was stirred at 23 °C for 18 h. $Na_2S_2O_5$ (ca. 50 g) was added in portions at 0 °C and the mixture was concentrated under reduced pressure. The residue was taken up in EtOAc (500 mL) and the solids were filtered and washed with EtOAc (500 mL) and CH_2Cl_2 (200 mL). The filtrate was concentrated under reduced pressure and column chromatography (SiO_2 , $CH_2Cl_2/MeOH$ 30:1) afforded diol **11** (19.7 g, 76%) as a colorless crystalline solid and diols **S3** (2.8 g, 10%) as a colorless oil.

Diol 11:

m.p.: 138 °C.

1H NMR (700 MHz, MeOH- d_4): δ [ppm] = 4.82 – 4.79 (m, 2H), 3.80 – 3.77 (m, 2H), 3.40 (s, 6H), 2.44 – 2.39 (m, 2H), 1.97 – 1.91 (m, 2H), 1.57 – 1.52 (m, 2H).

^{13}C NMR (176 MHz, MeOH- d_4): δ [ppm] = 109.2, 68.0, 54.4, 40.2, 27.7.

HRMS (ESI): m/z calcd for $C_{10}H_{18}O_5Na$ [$M+Na$] $^+$: 241,1046; found: 241.1064.

IR (ATR): $\tilde{\nu}$ = 3381, 2956, 2933, 2924, 2883, 2862, 1449, 1395, 1370, 1351, 1338, 1309, 1262, 1225, 1211, 1190, 1135, 1113, 1072, 1047, 1025, 996, 974, 939, 923, 887, 812, 726, 706 cm^{-1} .

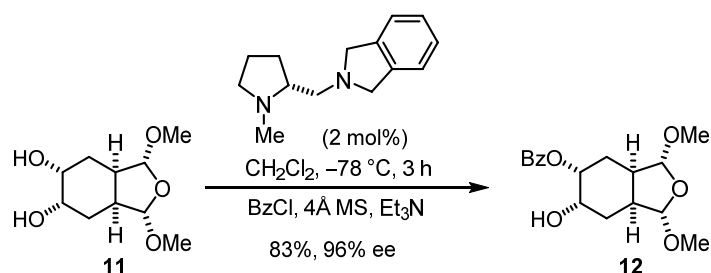
Diol S3:

1H NMR (700 MHz, $CDCl_3$): δ [ppm] = 4.98 (s, 2H), 3.76 – 3.72 (m, 2H), 3.37 (s, 6H), 3.05 – 2.94 (m, 2H), 2.27 – 2.21 (m, 3H), 1.87 – 1.82 (m, 3H), 1.69 – 1.60 (m, 2H).

^{13}C NMR (176 MHz, $CDCl_3$) δ 109.6, 69.4, 55.5, 41.5, 27.6.

HRMS (ESI): m/z calcd for $C_{10}H_{18}O_5Na$ [$M+Na$] $^+$: 241,1046; found: 241.1058.

IR (ATR): $\tilde{\nu}$ = 3424, 2929, 2834, 1444, 1393, 1328, 1304, 1276, 1233, 1194, 1154, 1096, 1065, 1036, 1006, 990, 966, 933, 882, 852, 784, 734, 703, 679, 657 cm^{-1} .

(1*S*,3*R*,3*aR*,5*R*,6*S*,7*aS*)-6-Hydroxy-1,3-dimethoxyoctahydroisobenzofuran-5-yl benzoate (12**)**

An oven-dried 1 L Schlenk flask equipped with a Teflon-coated magnetic stirring bar was charged with (*R*)-2-((1-methylpyrrolidin-2-yl)methyl)isoindoline (147 mg, 0.678 mmol, 0.02 equiv.), 4 Å molecular sieves (4.40 g) and CH₂Cl₂ (150 mL). Subsequently, triethylamine (4.70 mL, 33.9 mmol, 1.0 equiv.), a solution of *meso*-diol **11** (7.40 g, 33.9 mmol, 1.0 equiv.) in CH₂Cl₂ (200 mL) and a solution benzoyl chloride (5.90 mL, 50.8 mmol, 1.5 equiv.) in CH₂Cl₂ (50 mL) were added dropwise at -78 °C. After stirring at -78 °C for 3 h, NH₄Cl (sat. aq., 100 mL) was added and the aqueous phase was extracted with CH₂Cl₂ (3 x 150 mL). The combined organic phases were dried over Na₂SO₄, filtered and concentrated under reduced pressure. Purification by column chromatography (SiO₂, pentane/EtOAc 2:1 → 1:2) afforded ester **12** (9.08 g, 83%, 96% *ee*) as a colorless crystalline solid.

$[\alpha]_{\text{D}}^{28} = +3.95^{\circ}$ ($c = 1.68$, CHCl₃).

m.p.: 107 °C.

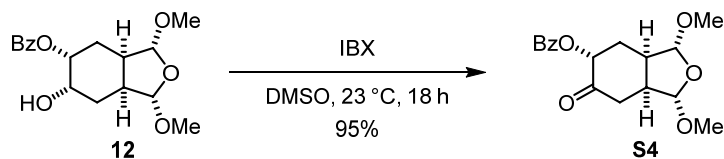
¹H NMR (400 MHz, CDCl₃): δ [ppm] = 8.05 – 8.02 (m, 2H), 7.59 – 7.57 (m, 1H), 7.46 – 7.43 (m, 2H), 5.27 (dt, $J = 8.1, 3.1$ Hz, 1H), 4.84 (t, $J = 3.0$ Hz, 2H), 4.05 (dt, $J = 8.4, 3.1$ Hz, 1H), 3.44 (s, 6H), 2.65 – 2.58 (m, 1H), 2.57 – 2.50 (m, 1H), 2.23 (ddd, $J = 14.1, 7.9, 6.0$ Hz, 1H), 2.04 (ddd, $J = 14.3, 8.4, 6.1$ Hz, 1H), 1.84 – 1.68 (m, 2H).

¹³C NMR (101 MHz, CDCl₃): δ [ppm] = 166.4, 133.5, 130.1, 129.8, 128.6, 109.2, 109.0, 72.5, 67.5, 55.9, 55.8, 40.7, 40.4, 28.7, 25.9.

HRMS (ESI): m/z calcd for C₁₇H₂₂O₆Na [M+Na]⁺: 345.1308; found: 345.1316.

IR (ATR): $\tilde{\nu} = 3471, 2931, 2833, 1713, 1602, 1584, 1449, 1395, 1379, 1352, 1314, 1273, 1206, 1179, 1098, 1071, 1048, 1025, 994, 974, 942, 923, 897, 854, 806, 713$ cm⁻¹.

HPLC: *ee* was determined by HPLC analysis (Chiralpak® IC, 30% *i*PrOH/hexane, 0.9 mL/min, 49 bar, 270.4 nm), retention time: $t_{\text{major}} = 10.16$ min, $t_{\text{minor}} = 27.46$ min, *ee* = 96%.

(1*S*,3*R*,3*aR*,5*R*,7*aS*)-1,3-Dimethoxy-6-oxooctahydroisobenzofuran-5-yl benzoate (S4**)**

An oven-dried 250 mL round-bottom-flask equipped with a Teflon-coated magnetic stirring bar was charged with alcohol **12** (9.05 g, 28.1 mmol, 1.0 equiv.) and dry DMSO (30 mL) under an atmosphere of argon. 2-Iodoxybenzoic acid (11.8 g, 42.1 mmol, 1.5 equiv.) was added at 23 °C and the reaction mixture was stirred for 18 h. H₂O (50 mL) was added dropwise and the resulting suspension was filtered through sand. The filtrate was extracted with EtOAc (3 x 50 mL) and the combined organic phases were washed with brine (2 x 50 mL), dried over Na₂SO₄, filtered and concentrated under reduced pressure. Purification by column chromatography (SiO₂, pentane/EtOAc 2:1) afforded ketone **S4** (8.55 g, 95%) as a colorless crystalline solid.

$[\alpha]_D^{27} = +15.3^\circ$ ($c = 1.90$, CHCl₃).

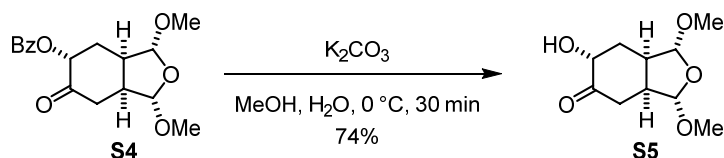
m.p.: 75 °C.

¹H NMR (500 MHz, CDCl₃): δ [ppm] = 8.09 – 8.04 (m, 2H), 7.60 – 7.55 (m, 1H), 7.45 (t, $J = 7.9$ Hz, 2H), 5.47 (dd, $J = 11.4, 5.9$ Hz, 1H), 5.22 (d, $J = 4.9$ Hz, 1H), 4.75 (s, 1H), 3.51 (s, 3H), 3.41 (s, 3H), 2.84 (dt, $J = 10.8, 5.9$ Hz, 1H), 2.72 (dd, $J = 27.6, 10.0$ Hz, 2H), 2.52 – 2.43 (m, 2H), 2.33 (ddd, $J = 13.8, 11.2, 5.8$ Hz, 1H).

¹³C NMR (126 MHz, CDCl₃): δ [ppm] = 203.5, 165.6, 133.5, 130.0, 129.4, 128.6, 109.3, 109.0, 73.7, 56.5, 55.4, 46.4, 41.5, 39.3, 30.7.

HRMS (ESI): m/z calcd for C₁₇H₂₀O₆Na [M+Na]⁺: 343,1152; found: 343.1161.

IR (ATR): $\tilde{\nu} = 2956, 2925, 2854, 1738, 1452, 1373, 1267, 1240, 1102, 1074, 1047, 1007, 962, 940, 916, 712$ cm⁻¹.

(1*R*,3*S*,3*aS*,6*R*,7*aR*)-6-Hydroxy-1,3-dimethoxyhexahydroisobenzofuran-5(3*H*)-one (S5**)**

A 250 mL round-bottom-flask equipped with a Teflon-coated magnetic stirring bar was charged with ester **S4** (7.89 g, 24.6 mmol, 1.0 equiv.), MeOH (75 mL) and H₂O (10 mL). K₂CO₃ was added at 0 °C and the solution was stirred at 0 °C for 30 min. The reaction mixture was diluted with H₂O (50 mL) and extracted with CH₂Cl₂ (5 x 50 mL). The combined organic phases were dried over Na₂SO₄, filtered and concentrated under reduced pressure. Purification by column

chromatography (SiO₂, pentane/EtOAc 1:1) afforded α -hydroxy ketone **S5** (3.94 g, 74%) as a colorless crystalline solid.

m.p.: 86 °C.

$[\alpha]_D^{29} = +11.3^\circ$ ($c = 0.59$, CHCl₃).

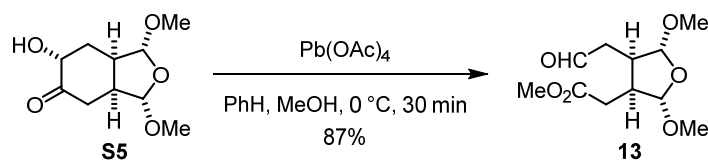
¹H NMR (500 MHz, CDCl₃): δ [ppm] = 5.20 (d, $J = 5.5$ Hz, 1H), 4.70 (s, 1H), 4.28 (dd, $J = 11.7, 6.4$ Hz, 1H), 3.52 (s, 3H), 3.40 (s, 3H), 2.76 – 2.70 (m, 1H), 2.70 – 2.62 (m, 2H), 2.56 (ddd, $J = 14.2, 6.9, 2.3$ Hz, 1H), 2.42 – 2.32 (m, 1H), 1.85 (ddd, $J = 14.1, 12.2, 6.0$ Hz, 1H).

¹³C NMR (126 MHz, CDCl₃): δ [ppm] = 210.2, 109.4, 109.2, 71.6, 56.7, 55.2, 46.9, 41.7, 38.7, 33.8.

HRMS (ESI): m/z calcd for C₁₀H₁₆O₅ [M+H]⁺: 217.1073; found: 217.1064.

IR (ATR): $\tilde{\nu} = 3439, 2932, 2835, 1721, 1446, 1391, 1239, 1186, 1094, 1075, 1041, 995, 957, 937, 912, 797, 716$ cm⁻¹.

Methyl 2-((2*S*,3*S*,4*R*,5*R*)-2,5-dimethoxy-4-(2-oxoethyl)tetrahydrofuran-3-yl)acetate (**13**)



An oven-dried 250 mL round-bottom-flask equipped with a Teflon-coated magnetic stirring bar was charged with α -hydroxy ketone **S5** (3.29 g, 15.2 mmol, 1.0 equiv.), benzene (75 mL) and MeOH (15 mL). Pb(OAc)₄ (6.75 g, 15.2 mmol, 1.0 equiv.) was added at 0 °C and the solution was stirred at 0 °C for 30 min. Na₂S₂O₅ (2.90 g) was added and after 10 min the reaction mixture was filtered through sand. The filtrate was concentrated under reduced pressure and purified by column chromatography (SiO₂, pentane/EtOAc 2:1) to afford methyl ester **13** (3.24 g, 87%) as a colorless oil.

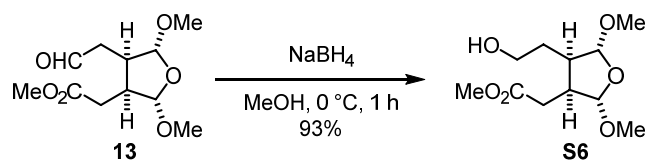
$[\alpha]_D^{23} = -10.5^\circ$ ($c = 0.24$, CHCl₃).

¹H NMR (500 MHz, CDCl₃): δ [ppm] = 9.70 (t, $J = 1.7$ Hz, 1H), 4.75 (d, $J = 3.1$ Hz, 1H), 4.71 (d, $J = 3.5$ Hz, 1H), 3.64 (s, 3H), 3.37 (s, 6H), 2.91 (ddd, $J = 15.4, 6.9, 3.5$ Hz, 1H), 2.82 (ddd, $J = 15.1, 7.8, 3.0$ Hz, 1H), 2.50 (ddd, $J = 17.0, 6.9, 1.5$ Hz, 1H), 2.42 (ddd, $J = 17.0, 8.5, 1.9$ Hz, 1H), 2.29 (d, $J = 7.8$ Hz, 1H), 2.29 (d, $J = 7.8$ Hz, 1H).

¹³C NMR (126 MHz, CDCl₃): δ [ppm] = 200.3, 172.1, 109.2, 109.1, 55.7, 55.6, 52.0, 43.0, 41.2, 40.8, 31.9.

HRMS (ESI): m/z calcd for C₁₁H₁₈O₆Na [M+Na]⁺: 269.0995; found: 269.0988.

IR (ATR): $\tilde{\nu} = 2990, 2953, 2838, 2359, 2322, 1732, 1685, 1541, 1523, 1508, 1472, 1456, 1438, 1418, 1388, 1362, 1339, 1260, 1198, 1171, 1100, 1050, 994, 941, 798$ cm⁻¹.

Methyl 2-((2*S*,3*S*,4*R*,5*R*)-4-(2-hydroxyethyl)-2,5-dimethoxytetrahydrofuran-3-yl)acetate (S6**)**

An oven-dried 250 mL round-bottom-flask equipped with a Teflon-coated magnetic stirring bar was charged with aldehyde **13** (3.93 g, 15.9 mmol, 1.0 equiv.) and MeOH (75 mL). Sodium borohydride (907 mg, 23.9 mmol, 1.5 equiv.) was added at 0 °C. After stirring at 0 °C for 1 h, the reaction mixture was treated with NH₄Cl (sat. aq., 50 mL). The aqueous phase was extracted with CH₂Cl₂ (5 x 50 mL) and the combined organic phases were dried over Na₂SO₄, filtered and concentrated under reduced pressure. Purification by column chromatography (SiO₂, pentane/EtOAc 1:1.5) afforded alcohol **S6** (3.67 g, 93%) as a colorless oil.

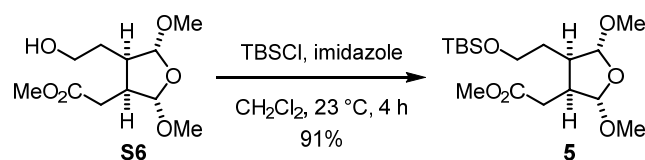
$[\alpha]_{\text{D}}^{23} = -18.5^\circ$ ($c = 0.31$, CHCl₃).

¹H NMR (400 MHz, CDCl₃): δ [ppm] = 4.84 (d, $J = 5.4$ Hz, 1H), 4.79 (s, 1H), 3.73 – 3.66 (m, 2H), 3.69 (s, 3H), 3.46 (s, 3H), 3.39 (s, 3H), 2.75 – 2.67 (m, 1H), 2.63 – 2.50 (m, 1H), 2.42 (dd, $J = 16.0, 5.6$ Hz, 1H), 2.23 (dd, $J = 16.0, 10.0$ Hz, 1H), 2.10 (t, $J = 6.2$ Hz, 1H), 1.74 – 1.65 (m, 1H), 1.62 – 1.52 (m, 1H).

¹³C NMR (126 MHz, CDCl₃): δ [ppm] = 172.7, 110.2, 108.7, 61.9, 56.1, 55.1, 52.0, 44.7, 43.4, 31.9, 29.8.

HRMS (ESI): m/z calcd for C₁₁H₂₀O₆Na [M+Na]⁺: 271.1152; found: 271.1140.

IR (ATR): $\tilde{\nu} = 3449, 2952, 2915, 2844, 2363, 2322, 1734, 1541, 1508, 1438, 1396, 1261, 1171, 1099, 1052, 986, 942, 771$ cm⁻¹.

Methyl-2-((2*S*,3*S*,4*R*,5*R*)-4-(2-((tert-butyldimethylsilyl)oxy)ethyl)-2,5-dimethoxytetrahydrofuran-3-yl)acetate (5**)**

An oven-dried 250 mL round-bottom-flask equipped with a Teflon-coated magnetic stirring bar was charged with alcohol **S6** (1.05 g, 4.23 mmol, 1.0 equiv.) and CH₂Cl₂ (20 mL). Tert-butyldimethylsilyl chloride (1.30 g, 8.46 mmol, 2.0 equiv.) and imidazole (431 mg, 6.34 mmol, 1.5 equiv.) were added and the reaction mixture was stirred for 4 h at 23 °C. The reaction was terminated by the addition of NH₄Cl (sat. aq., 50 mL) and the aqueous phase was extracted with CH₂Cl₂ (3 x 50 mL). The combined organic phases were dried over Na₂SO₄, filtered and concentrated under reduced

pressure. Purification by column chromatography (SiO₂, pentane/Et₂O 4:1) afforded silyl ether **5** (1.40 g, 91%) as a colorless oil.

$[\alpha]_D^{23} = -5.90^\circ$ ($c = 0.80$, CHCl₃).

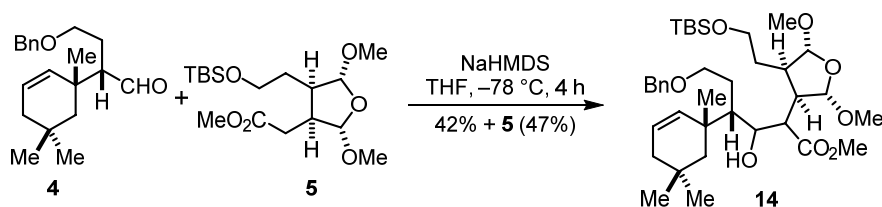
¹H NMR (700 MHz, CDCl₃): δ [ppm] = 4.77 (s, 1H), 4.77 (d, $J = 6.6$ Hz, 1H), 3.68 (s, 3H), 3.67 – 3.64 (m, 1H), 3.61 (dt, $J = 10.3, 6.9$ Hz, 1H), 3.41 (s, 3H), 3.39 (s, 3H), 2.73 (tdd, $J = 9.7, 5.9, 2.2$ Hz, 1H), 2.48 (dd, $J = 15.8, 5.9$ Hz, 1H), 2.45 (dtd, $J = 8.6, 6.8, 4.3$ Hz, 1H), 2.24 (dd, $J = 15.8, 10.0$ Hz, 1H), 1.61 (dq, $J = 13.9, 7.0$ Hz, 1H), 1.56 – 1.50 (m, 1H), 0.88 (s, 9H), 0.04 (s, 6H).

¹³C NMR (176 MHz, CDCl₃): δ [ppm] = 172.8, 110.2, 109.1, 62.3, 55.9, 55.3, 51.9, 43.8, 43.4, 32.0, 29.9, 26.1, 18.4, –5.3 (2C).

HRMS (ESI): m/z calcd for C₁₇H₃₄O₆SiNa [M+Na]⁺: 385.2017; found: 385.2021.

IR (ATR): $\tilde{\nu} = 2952, 2928, 2857, 1739, 1471, 1438, 1388, 1362, 1254, 1196, 1167, 1099, 1053, 993, 944, 834, 811, 776, 739, 713, 701, 681, 671, 661$ cm⁻¹.

Methyl (4S)-6-(benzyloxy)-2-((2S,3R,4R,5R)-4-(2-((tert-butyldimethylsilyl)oxy)ethyl)-2,5-dimethoxytetrahydrofuran-3-yl)-3-hydroxy-4-((R)-1,5,5-trimethylcyclohex-2-en-1-yl)hexanoate (14**)**



An oven-dried 250 mL Schlenk flask equipped with a Teflon-coated magnetic stirring bar was charged with sodium bis(trimethylsilyl)amide (2 M in THF, 2.60 mL, 5.30 mmol, 1.0 equiv.) and dry THF (20 mL). A solution of methyl ester **5** (1.91 g, 5.26 mmol, 1.0 equiv.) in dry THF (15 mL) was added at –78 °C. After stirring at –78 °C for 1 h, a solution of aldehyde **4** (2.20 g, 7.28 mmol, 1.38 equiv.) in dry THF (15 mL) was added and the reaction mixture was stirred at –78 °C for 3 h. The reaction was terminated by the addition of NH₄Cl (sat. aq., 50 mL) and the aqueous phase was extracted with EtOAc (3 x 50 mL). The combined organic phases were washed with brine (50 mL), dried over Na₂SO₄, filtered and concentrated under reduced pressure. Purification by column chromatography (SiO₂, pentane/Et₂O 5:1 → 2:1) afforded β -hydroxy ester **14** (1.46 g, 42%) as a colorless oil. The methyl ester **5** (900 mg, 2.48 mmol) and aldehyde **4** (1.40 g, 4.65 mmol) were reisolated and reused. After three repetitions using the same starting materials, a combined yield for β -hydroxy ester **14** of 78% (2.73 g) was isolated.

$[\alpha]_D^{23} = +0.39^\circ$ ($c = 3.07$, CHCl₃).

¹H NMR (700 MHz, CDCl₃): δ [ppm] = 7.34 – 7.30 (m, 5H), 5.63 (ddd, $J = 10.2, 6.0, 2.2$ Hz, 1H), 5.33 (d, $J = 10.2$ Hz, 1H), 4.90 (d, $J = 6.5$ Hz, 1H), 4.83 (s, 1H), 4.49 (d, $J = 12.1$ Hz, 1H), 4.45 (d, $J =$

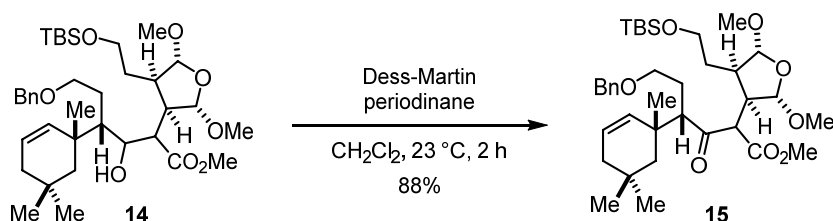
12.1 Hz, 1H), 4.05 (dt, $J = 6.7, 3.3$ Hz, 1H), 3.59 (s, 3H), 3.59 – 3.55 (m, 2H), 3.48 (s, 3H), 3.46 – 3.43 (m, 1H), 3.36 (s, 3H), 3.36 – 3.34 (m, 1H), 3.07 (dt, $J = 12.5, 6.5$ Hz, 1H), 2.74 (d, $J = 6.7$ Hz, 1H), 2.59 (dd, $J = 11.9, 3.8$ Hz, 1H), 2.26 (ddd, $J = 12.0, 6.7, 2.7$ Hz, 1H), 1.85 – 1.79 (m, 1H), 1.79 – 1.76 (m, 1H), 1.71 – 1.67 (m, 1H), 1.58 (d, $J = 14.0$ Hz, 1H), 1.61 – 1.50 (m, 2H), 1.46 – 1.43 (m, 1H), 1.25 (ddt, $J = 14.2, 12.0, 5.9$ Hz, 1H), 1.19 (d, $J = 14.0$ Hz, 1H), 1.07 (s, 3H), 0.95 (s, 6H), 0.88 (s, 9H), 0.03 (s, 6H).

^{13}C NMR (176 MHz, CDCl_3): δ [ppm] = 173.0, 138.6, 134.4, 128.3, 127.6, 127.4, 125.2, 108.1, 107.7, 72.7, 71.5, 69.4, 61.7, 55.8, 54.7, 51.7, 51.0, 49.3, 45.3, 44.8, 44.6, 39.9, 38.4, 33.0, 30.0, 29.1, 28.4, 26.6, 25.9, 25.4, 18.3, -5.4, -5.5.

HRMS (ESI): m/z calcd for $\text{C}_{37}\text{H}_{62}\text{O}_8\text{SiNa}$ $[\text{M}+\text{Na}]^+$: 685.4106; found: 685.4102.

IR (ATR): $\tilde{\nu} = 3526, 2951, 2929, 2903, 2858, 1734, 1541, 1507, 1457, 1362, 1253, 1211, 1161, 1096, 1008, 984, 961, 835, 776, 735$ cm^{-1} .

Methyl (4S)-6-(benzyloxy)-2-((2S,3R,4R,5R)-4-(2-((tert-butyldimethylsilyl)oxy)ethyl)-2,5-dimethoxytetrahydrofuran-3-yl)-3-oxo-4-((R)-1,5,5-trimethylcyclohex-2-en-1-yl)hexanoate (15)



An oven-dried 50 mL round-bottom-flask equipped with a Teflon-coated magnetic stirring bar was charged with alcohol **14** (744 mg, 1.12 mmol, 1.0 equiv.) and CH_2Cl_2 (7 mL). Dess-Martin periodinane (953 mg, 2.24 mmol, 2.0 equiv.) was added at 0 °C. The reaction mixture was warmed to 23 °C and stirred for 2 h. Direct purification of the reaction mixture by column chromatography (SiO_2 , pentane/ Et_2O 6:1) afforded ketone **15** (655 mg, 88%) as a colorless oil.

$[\alpha]_{\text{D}}^{21} = +64.7^\circ$ ($c = 3.66, \text{CHCl}_3$).

^1H NMR (500 MHz, CDCl_3): δ [ppm] = 7.37 – 7.20 (m, 5H), 5.69 (ddd, $J = 10.1, 5.2, 3.1$ Hz, 1H), 5.26 (d, $J = 10.1$ Hz, 1H), 4.79 (dd, $J = 15.6, 3.5$ Hz, 2H), 4.40 (d, $J = 12.2$ Hz, 1H), 4.37 (d, $J = 12.2$ Hz, 1H), 3.89 (d, $J = 11.5$ Hz, 1H), 3.62 – 3.51 (m, 2H), 3.53 (s, 3H), 3.39 (s, 3H), 3.37 (s, 3H), 3.35 – 3.24 (m, 1H), 3.19 (ddd, $J = 9.5, 7.2, 5.7$ Hz, 1H), 3.12 (dt, $J = 9.6, 7.0$ Hz, 1H), 2.92 (dd, $J = 10.3, 2.0$ Hz, 1H), 2.43 (ddt, $J = 10.7, 7.0, 3.7$ Hz, 1H), 2.11 – 1.97 (m, 1H), 1.80 (dt, $J = 17.0, 2.7$ Hz, 1H), 1.72 (dd, $J = 16.9, 5.2$ Hz, 1H), 1.65 (dtd, $J = 14.4, 7.2, 2.0$ Hz, 1H), 1.59 (d, $J = 14.2$ Hz, 1H),

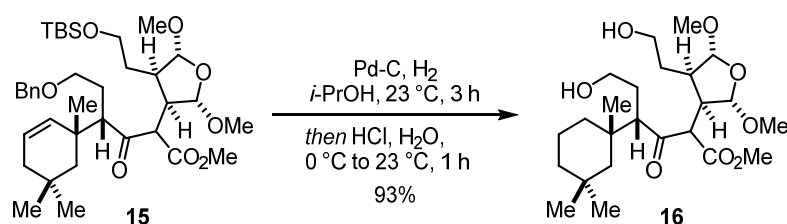
1.52 – 1.44 (m, 1H), 1.44 – 1.35 (m, 1H), 1.18 (d, $J = 14.1$ Hz, 1H), 1.08 (s, 3H), 1.00 (s, 3H), 0.94 (s, 3H), 0.87 (s, 9H), 0.02 (s, 6H).

^{13}C NMR (126 MHz, CDCl_3): δ [ppm] = 205.0, 168.2, 138.5, 133.7, 128.4 (2C), 127.7 (2C), 127.6, 126.0, 108.9, 107.7, 72.5, 68.6, 61.9, 61.4, 56.9, 55.4, 54.7, 52.6, 45.3, 45.2, 43.3, 40.1, 38.4, 31.8, 30.1, 29.8, 29.2, 27.5, 26.0 (3C), 25.8, 18.4, -5.3 (2C).

HRMS (ESI): m/z calcd for $\text{C}_{37}\text{H}_{60}\text{O}_8\text{SiNa}$ $[\text{M}+\text{Na}]^+$: 683.3949; found: 683.3969.

IR (ATR): $\tilde{\nu} = 2951, 2931, 2859, 1745, 1714, 1455, 1362, 1254, 1194, 1101, 1011, 945, 907, 835, 778, 737, 712, 702, 690, 681, 671, 659$ cm^{-1} .

Methyl (4S)-6-hydroxy-2-((2S,3R,4R,5R)-4-(2-hydroxyethyl)-2,5-dimethoxytetrahydrofuran-3-yl)-3-oxo-4-((S)-1,3,3-trimethylcyclohexyl)hexanoate (16)



A 50 mL round-bottom-flask equipped with a Teflon-coated magnetic stirring bar was charged with compound **15** (655 mg, 990 μmol , 1.0 equiv.), Pd/C (5%, 211 mg, 100 μmol , 0.1 equiv.) and *i*-PrOH (5 mL). The atmosphere was exchanged to H_2 by three times evacuating and flushing with H_2 (1 atm). After stirring at 23 $^\circ\text{C}$ for 3 h, HCl (1 M aq., 2.50 mL, 2.50 mmol, 2.5 equiv.) was added at 0 $^\circ\text{C}$. The reaction mixture was stirred at 23 $^\circ\text{C}$ for 1 h and filtered through Celite[®]. The filtrate was treated with NaHCO_3 (sat. aq., 10 mL) and the aqueous phase was extracted with CH_2Cl_2 (3 x 15 mL). The combined organic phases were dried over Na_2SO_4 , filtered and concentrated under reduced pressure. Purification by column chromatography (SiO_2 , pentane/EtOAc 1:4) afforded diol **16** (422 mg, 93%) as a colorless oil.

$[\alpha]_{\text{D}}^{24} = +89.5^\circ$ ($c = 1.86$, CHCl_3).

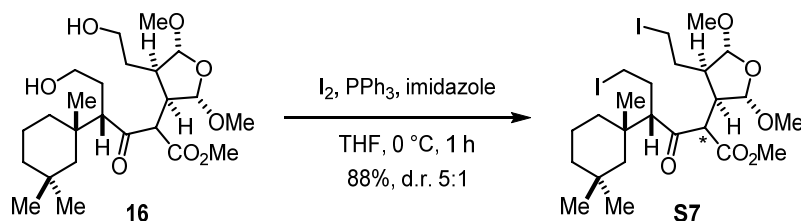
^1H NMR (700 MHz, CDCl_3): δ [ppm] = 4.82 (d, $J = 5.3$ Hz, 1H), 4.71 (d, $J = 1.4$ Hz, 1H), 3.78 (d, $J = 11.5$ Hz, 1H), 3.75 (s, 3H), 3.67 – 3.58 (m, 2H), 3.44 (s, 3H), 3.41 (dt, $J = 10.9, 5.3$ Hz, 1H), 3.37 (s, 3H), 3.20 (ddd, $J = 11.5, 6.8, 1.4$ Hz, 1H), 3.16 (ddd, $J = 11.0, 8.8, 5.3$ Hz, 1H), 2.96 (d, $J = 9.9$ Hz, 1H), 2.65 – 2.58 (m, 1H), 2.26 (s, 1H), 1.89 (ddt, $J = 13.9, 11.3, 5.1$ Hz, 1H), 1.74 – 1.62 (m, 1H), 1.64 – 1.54 (m, 3H), 1.50 – 1.42 (m, 1H), 1.42 – 1.32 (m, 3H), 1.29 (d, $J = 14.1$ Hz, 1H), 1.27 – 1.24 (m, 1H), 1.21 – 1.14 (m, 1H), 1.18 (d, $J = 13.6$ Hz, 1H), 0.95 (s, 3H), 0.94 (s, 3H), 0.94 (s, 3H).

^{13}C NMR (176 MHz, CDCl_3): δ [ppm] = 206.1, 168.9, 109.4, 107.4, 62.2, 61.6, 60.8, 57.1, 55.9, 54.8, 53.0, 49.8, 46.7, 43.1, 39.1, 38.4, 37.6, 33.4, 31.1, 30.0, 29.3, 21.4, 19.1.

HRMS (ESI): m/z calcd for $C_{24}H_{42}O_8Na$ $[M+Na]^+$: 481.2772; found: 481.2794.

IR (ATR): $\tilde{\nu}$ = 3456, 2950, 2927, 1743, 1708, 1387, 1267, 1192, 1143, 1102, 1059, 1011, 944, 905, 842, 790, 763, 749, 727 cm^{-1} .

Methyl (4*S*)-6-iodo-2-((2*S*,3*R*,4*R*,5*R*)-4-(2-iodoethyl)-2,5-dimethoxytetrahydrofuran-3-yl)-3-oxo-4-((*S*)-1,3,3-trimethylcyclohexyl)hexanoate (S7**)**



An oven-dried 50 mL round-bottom-flask equipped with a Teflon-coated magnetic stirring bar was charged with diol **16** (420 mg, 920 μ mol, 1.0 equiv.), triphenylphosphine (959 mg, 3.66 mmol, 4.0 equiv.), imidazole (374 mg, 5.49 mmol, 6.0 equiv.) and dry THF (4.5 mL) at 0 °C. After 10 min iodine (930 mg, 3.66 mmol, 4.0 equiv.) was added and the reaction mixture was stirred at 0 °C for 1 h. The solvent was removed under reduced pressure and the residue was purified by column chromatography (SiO_2 , pentane/Et₂O 6:1) to afford diiodide **S7** (455 mg, 73%) and its C7-epimer (91 mg, 15%) as colorless oils, respectively.

Major epimer:

$[\alpha]_D^{23} = +41.6^\circ$ ($c = 0.90$, $CHCl_3$).

¹H NMR (700 MHz, $CDCl_3$): δ [ppm] = 4.72 (d, $J = 4.4$ Hz, 1H), 4.69 (d, $J = 2.5$ Hz, 1H), 3.84 (s, 3H), 3.77 (d, $J = 11.3$ Hz, 1H), 3.41 (s, 3H), 3.36 (s, 3H), 3.24 (ddd, $J = 11.3, 6.7, 2.5$ Hz, 1H), 3.16 (ddd, $J = 9.4, 9.3, 5.8$ Hz, 1H), 3.02 (td, $J = 9.2, 7.4$ Hz, 1H), 2.97 (td, $J = 9.2, 4.6$ Hz, 1H), 2.73 (dd, $J = 10.7, 1.9$ Hz, 1H), 2.58 (dt, $J = 9.6, 8.2$ Hz, 1H), 2.50 – 2.45 (m, 1H), 2.34 – 2.27 (m, 1H), 1.94 (dtd, $J = 14.1, 8.5, 1.9$ Hz, 1H), 1.90 – 1.85 (m, 2H), 1.60 – 1.54 (m, 2H), 1.40 – 1.34 (m, 2H), 1.30 (d, $J = 13.7$ Hz, 1H), 1.28 – 1.23 (m, 1H), 1.18 – 1.12 (m, 1H), 1.13 (d, $J = 13.8$ Hz, 1H), 0.96 (s, 3H), 0.94 (s, 3H), 0.94 (s, 3H).

¹³C NMR (176 MHz, $CDCl_3$): δ [ppm] = 204.5, 168.3, 108.6, 107.6, 62.8, 62.2, 55.9, 55.0, 53.6, 49.8, 47.2, 45.8, 39.1, 38.9, 37.6, 34.3, 31.8, 31.5, 31.2, 28.7, 21.2, 19.1, 3.7, 2.7.

HRMS (ESI): m/z calcd for $C_{24}H_{40}I_2O_6Na$ $[M+Na]^+$: 701.0806; found: 701.0828.

IR (ATR): $\tilde{\nu}$ = 2949, 295, 2844, 1740, 1709, 1435, 1386, 1246, 1196, 1156, 1102, 1034, 1002, 956, 917, 756, 700, 660 cm^{-1} .

Minor epimer:

$[\alpha]_D^{24} = -36.9^\circ$ ($c = 0.79$, $CHCl_3$).

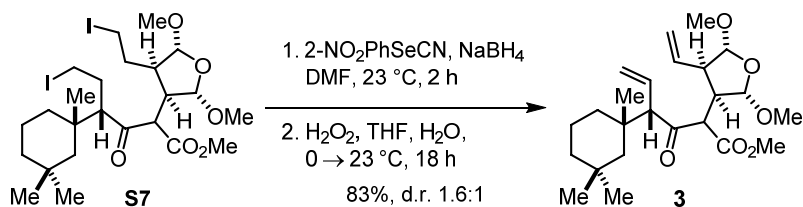
^1H NMR (700 MHz CDCl_3): δ [ppm] = 5.24 (d, J = 2.9 Hz, 1H), 4.71 (d, J = 3.7 Hz, 1H), 3.72 (s, 3H), 3.68 (d, J = 4.9 Hz, 1H), 3.40 (s, 3H), 3.40 – 3.33 (m, 3H), 3.29 (ddd, J = 9.9, 8.1, 4.9 Hz, 1H), 3.24 (ddd, J = 9.9, 9.1, 5.1 Hz, 1H), 3.10 (ddd, J = 9.9, 8.7, 7.2 Hz, 1H), 2.93 (ddd, J = 9.9, 8.7, 7.6 Hz, 1H), 2.79 (ddd, J = 7.8, 4.9, 2.8 Hz, 1H), 2.59 – 2.55 (m, 1H), 2.51 (dd, J = 8.7, 3.2 Hz, 1H), 2.15 – 2.05 (m, 2H), 2.04 – 1.98 (m, 1H), 1.97 – 1.90 (m, 1H), 1.58 – 1.52 (m, 1H), 1.48 (dt, J = 14.0, 3.9 Hz, 1H), 1.40 – 1.33 (m, 3H), 1.25 (td, J = 12.4, 4.0 Hz, 1H), 1.12 – 1.06 (m, 2H), 1.03 (s, 3H), 0.96 (s, 3H), 0.91 (s, 3H).

^{13}C NMR (176 MHz, CDCl_3): δ [ppm] = 206.7, 168.2, 108.9, 106.4, 64.9, 58.0, 55.6, 55.5, 52.6, 49.4, 47.5, 46.6, 39.0, 38.3, 36.2, 35.0, 31.8, 31.7, 31.0, 28.0, 21.4, 18.9, 5.5, 2.5.

HRMS (ESI): m/z calcd for $\text{C}_{24}\text{H}_{40}\text{I}_2\text{O}_6\text{Na}$ $[\text{M}+\text{Na}]^+$: 701.0806; found: 701.0788.

IR (ATR): $\tilde{\nu}$ = 2951, 2924, 2868, 1746, 1714, 1458, 1385, 1246, 1195, 1156, 1103, 1036, 991, 956 cm^{-1} .

Methyl (4*S*)-2-((2*S*,3*R*,4*R*,5*R*)-2,5-dimethoxy-4-vinyltetrahydrofuran-3-yl)-3-oxo-4-((*S*)-1,3,3-trimethylcyclohexyl)hex-5-enoate (3**)**



An oven-dried 50 mL round-bottom-flask equipped with a Teflon-coated magnetic stirring bar was charged with 2-nitrophenylselenocyanate (450 mg, 1.98 mmol, 3.0 equiv.) and dry DMF (6.0 mL). NaBH_4 (94.8 mg, 2.51 mmol, 3.8 equiv.) was added and the mixture was stirred for 1 h at 23 °C under an atmosphere of argon. This solution was added to diiodide **7** (major epimer, 448 mg, 0.66 mmol, 1.0 equiv.) and the reaction mixture was stirred at 23 °C for 2 h. NaHCO_3 (sat. aq., 10 mL) was added at 0 °C and the aqueous phase was extracted with Et_2O (3 x 15 mL). The combined organic phases were washed with brine (10 mL), dried over Na_2SO_4 , filtered and concentrated under reduced pressure. The crude product was dissolved in THF (6.0 mL) and H_2O_2 (30% aq., 0.54 mL, 5.30 mmol, 8.0 equiv.) was added at 0 °C. The reaction was stirred for 18 h at 23 °C and terminated by the addition of NaHCO_3 (sat. aq., 10 mL). The aqueous phase was extracted with Et_2O (3 x 10 mL) and the combined organic phases were washed with brine (15 mL), dried over Na_2SO_4 , filtered and concentrated under reduced pressure. Purification by column chromatography (SiO_2 , pentane/ Et_2O 10:1) afforded diene **3** (233 mg, 83%, mixture of diastereomers 1.6:1 d.r.) as a colorless oil.

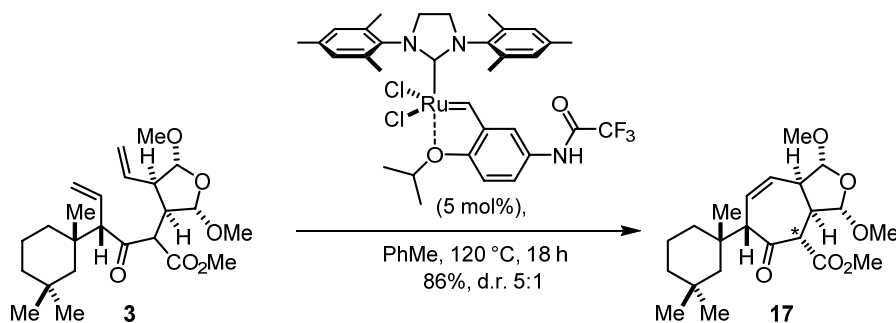
^1H NMR (700 MHz, CDCl_3): δ [ppm] major epimer = 5.75 (dt, $J = 17.1, 10.0$ Hz, 1H), 5.60 (dt, $J = 17.0, 10.2$ Hz, 1H), 5.15 (dd, $J = 10.1, 1.7$ Hz, 1H), 5.12 (dd, $J = 10.4, 1.7$ Hz, 1H), 5.09 (d, $J = 16.8$ Hz, 1H), 4.99 (dd, $J = 17.1, 1.7$ Hz, 1H), 4.83 (d, $J = 4.1$ Hz, 1H), 4.77 (d, $J = 2.2$ Hz, 1H), 3.62 (d, $J = 11.5$ Hz, 1H), 3.57 (s, 3H), 3.39 (s, 3H), 3.38 (s, 3H), 3.30 – 3.26 (m, 2H), 3.09 (tt, $J = 7.2, 2.3$ Hz, 1H), 1.56 – 1.52 (m, 1H), 1.51 – 1.47 (m, 1H), 1.36 – 1.33 (m, 1H), 1.36 – 1.27 (m, 3H), 1.28 (d, $J = 14.0$ Hz, 1H), 1.08 (s, 3H), 1.04 (d, $J = 14.0$ Hz, 1H), 0.94 (s, 3H), 0.89 (s, 3H); δ [ppm] minor epimer = 5.54 (dt, $J = 16.9, 10.0$ Hz, 1H), 5.43 (dt, $J = 17.1, 10.2$ Hz, 1H), 5.24 (dd, $J = 10.0, 1.6$ Hz, 1H), 5.19 (dd, $J = 17.0, 1.5$ Hz, 1H), 5.04 (dd, $J = 10.3, 1.7$ Hz, 1H), 5.00 (dd, $J = 17.1, 1.6$ Hz, 1H), 4.90 (d, $J = 6.2$ Hz, 1H), 4.68 (s, 1H), 3.68 (s, 3H), 3.59 (d, $J = 11.1$ Hz, 1H), 3.38 (s, 3H), 3.36 (s, 3H), 3.10 – 3.07 (m, 1H), 3.05 (dt, $J = 11.0, 6.5$ Hz, 1H), 2.93 (d, $J = 10.1$ Hz, 1H), 1.60 – 1.46 (m, 2H), 1.39 (dt, $J = 13.9, 4.1$ Hz, 1H), 1.37 – 1.21 (m, 3H), 1.09 (s, 3H), 1.07 – 1.00 (m, 2H), 0.93 (s, 3H), 0.86 (s, 3H).

^{13}C NMR (176 MHz, CDCl_3): δ [ppm] major epimer = 203.5, 168.0, 134.4, 133.4, 119.6 (2C), 108.5 (2C), 67.9, 61.5, 55.4, 55.2, 52.3, 52.2, 48.8, 45.7, 39.3, 38.9, 35.7, 34.8, 31.0, 28.3, 22.2, 19.0; δ [ppm] minor epimer = 201.6, 169.0, 133.7, 133.1, 121.9, 120.0, 108.4, 108.2, 68.9, 57.8, 56.3, 54.9, 52.4, 51.7, 48.7, 45.2, 39.4, 37.3, 35.1, 34.7, 30.9, 28.5, 22.8, 19.0.

HRMS (ESI): m/z calcd for $\text{C}_{24}\text{H}_{38}\text{O}_6\text{Na}$ [$\text{M}+\text{Na}$] $^+$: 445.2560; found: 445.2578.

IR (ATR): $\tilde{\nu} = 2950, 2925, 2871, 2851, 2360, 2338, 1747, 1716, 1627, 1509, 1457, 1436, 1386, 1348, 1261, 1237, 1196, 1165, 1038, 995, 952, 924, 741, 718, 698, 682, 670, 652\text{ cm}^{-1}$.

Methyl (1*R*,3*S*,3*aR*,6*S*,8*aR*)-1,3-dimethoxy-5-oxo-6-((*S*)-1,3,3-trimethylcyclohexyl)-3,3*a*,4,5,6,8*a*-hexahydro-1*H*-cyclohepta[*c*]furan-4-carboxylate (17)



An oven-dried 10 mL round-bottom-flask equipped with a Teflon-coated magnetic stirring bar was charged with diene **3** (215 mg, 510 μmol , 1.0 equiv.), Umicore M71SIMes (18.7 mg, 25.4 μmol , 0.05 equiv.) and dry PhMe (2.0 mL) under an atmosphere of argon. The reaction mixture was heated to 120 °C in a sealed flask for 18 h. The solvent was removed under reduced pressure and purification by column chromatography (SiO_2 , pentane/ Et_2O 5:1) afforded olefin **17** (172 mg, 86%, mixture of diastereomers 5:1 d.r.) as a colorless oil.

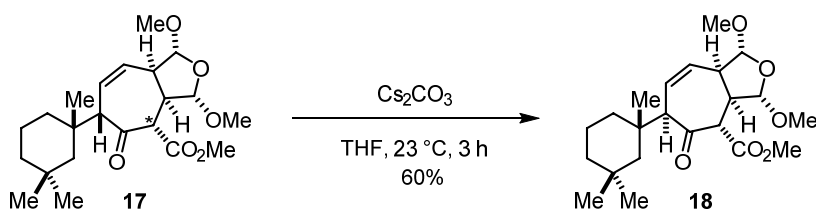
^1H NMR (700 MHz, CDCl_3): δ [ppm] major epimer = 5.94 (ddd, $J = 11.4, 6.9, 2.6$ Hz, 1H), 5.67 (ddd, $J = 11.4, 4.8, 1.5$ Hz, 1H), 4.91 – 4.87 (m, 1H), 4.88 (s, 1H), 3.84 (d, $J = 10.5$ Hz, 1H), 3.72 (s, 3H), 3.41 (s, 3H), 3.37 (s, 3H), 3.29 (ddd, $J = 10.6, 7.7, 5.4$ Hz, 1H), 3.06 – 3.02 (m, 2H), 1.84 – 1.79 (m, 1H), 1.56 – 1.53 (m, 1H), 1.46 – 1.40 (m, 2H), 1.34 – 1.28 (m, 1H), 1.31 (d, $J = 13.5$ Hz, 1H), 1.16 (d, $J = 13.7$ Hz, 1H), 1.13 – 1.09 (m, 1H), 1.10 (s, 3H), 0.95 (s, 3H), 0.90 (s, 3H); δ [ppm] minor epimer = 6.09 (ddd, $J = 11.9, 9.0, 2.8$ Hz, 1H), 5.98 (dd, $J = 11.9, 3.0$ Hz, 1H), 5.37 (s, 1H), 4.91 – 4.87 (m, 1H), 4.09 (d, $J = 4.7$ Hz, 1H), 3.72 (s, 3H), 3.44 (s, 3H), 3.39 (s, 3H), 3.18 (td, $J = 9.5, 3.5$ Hz, 1H), 3.12 – 3.06 (m, 2H), 1.77 (d, $J = 14.1$ Hz, 1H), 1.59 – 1.51 (m, 2H), 1.46 – 1.40 (m, 1H), 1.36 (d, $J = 13.9$ Hz, 1H), 1.34 – 1.28 (m, 2H), 1.08 (s, 3H), 1.04 – 1.03 (m, 1H), 0.96 (s, 3H), 0.89 (s, 3H).

^{13}C NMR (176 MHz, CDCl_3): δ [ppm] major epimer = 202.9, 168.6, 129.5, 128.7, 110.8, 109.4, 66.1, 57.5, 55.7, 54.9, 52.5, 48.4, 48.3, 45.5, 39.5, 38.9, 36.0, 33.9, 31.0, 29.2, 22.2, 19.1. δ [ppm] minor epimer = 206.2, 170.1, 168.6, 129.9, 129.7, 112.5, 108.5, 62.1, 57.3, 56.0, 55.9, 52.4, 50.4, 49.0, 45.6, 39.3, 38.6, 36.3, 33.0, 31.2, 23.5, 19.1.

HRMS (ESI): m/z calcd for $\text{C}_{22}\text{H}_{34}\text{O}_6\text{Na}$ $[\text{M}+\text{Na}]^+$: 417.2247; found: 417.2262.

IR (ATR): $\tilde{\nu} = 2948, 2923, 2865, 2844, 2359, 1757, 1715, 1438, 1382, 1250, 1193, 1167, 1102, 1035, 988, 958, 806, 759, 734, 697, 669, 655$ cm^{-1} .

Methyl(1*R*,3*S*,3*aR*,4*S*,6*R*,8*aR*)-1,3-dimethoxy-5-oxo-6-((*S*)-1,3,3-trimethylcyclohexyl)-3*a*,4,5,6,8*a*-hexahydro-1*H*-cyclohepta[*c*]furan-4-carboxylate (18**)**



A 10 mL round-bottom-flask equipped with a Teflon-coated magnetic stirring bar was charged with ketone **17** (5:1 d.r., 27.2 mg, 68.9 μmol , 1.0 equiv.), Cs_2CO_3 (46.0 mg, 141 μmol , 2.0 equiv.) and THF (0.5 mL). The mixture was stirred for 3 h at 23 °C and the reaction was terminated by the addition of NH_4Cl (sat. aq., 5 mL). The aqueous phase was extracted with CH_2Cl_2 (3 x 5 mL) and the combined organic phases were dried over Na_2SO_4 , filtered and concentrated under reduced pressure. Purification by column chromatography (SiO_2 , pentane/ Et_2O 6:1) afforded ketone **18** (16.3 mg, 60%, single diastereomer) as a colorless oil.

$[\alpha]_{\text{D}}^{25} = +87.4^\circ$ ($c = 0.37$, CHCl_3).

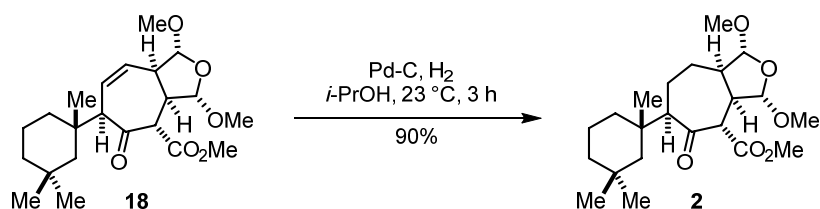
^1H NMR (700 MHz, CDCl_3): δ [ppm] = 5.74 (dt, J = 11.1, 3.1 Hz, 1H), 5.70 (dt, J = 11.1, 2.8 Hz, 1H), 4.87 (d, J = 3.3 Hz, 1H), 4.77 (d, J = 2.6 Hz, 1H), 3.75 (s, 3H), 3.71 (d, J = 11.1 Hz, 1H), 3.43 (s, 3H), 3.39 (s, 3H), 3.29 (dt, J = 4.4, 2.3 Hz, 1H), 3.26 – 3.19 (m, 2H), 1.54 – 1.50 (m, 2H), 1.46 (dt, J = 13.3, 4.3 Hz, 1H), 1.34 (d, J = 13.1 Hz, 1H), 1.31 – 1.23 (m, 2H), 1.17 – 1.06 (m, 2H), 1.15 (s, 3H), 0.96 (s, 3H), 0.89 (s, 3H).

^{13}C NMR (151 MHz, CDCl_3): δ [ppm] = 202.5, 169.2, 129.2, 126.3, 110.0, 109.3, 62.4, 58.0, 55.8, 55.3, 52.5, 48.4, 47.1, 46.9, 39.2, 36.4, 36.1, 34.3, 30.8, 28.5, 22.2, 18.6.

HRMS (ESI): m/z calcd for $\text{C}_{22}\text{H}_{34}\text{O}_6\text{Na}$ [$\text{M}+\text{Na}$] $^+$: 417.2247; found: 417.2255.

IR (ATR): $\tilde{\nu}$ = 2924, 2845, 1751, 1714, 1461, 1437, 1384, 1248, 1195, 1104, 1058, 1024, 993, 957, 911, 859, 801, 716 cm^{-1} .

Methyl (1*R*,3*S*,3*aR*,4*S*,6*R*,8*aR*)-1,3-dimethoxy-5-oxo-6-((*S*)-1,3,3-trimethylcyclohexyl) octahydro-1*H*-cyclohepta[*c*]furan-4-carboxylate (2**)**



A 10 mL round-bottom-flask equipped with a Teflon-coated magnetic stirring bar was charged with olefin **18** (27.0 mg, 68.0 μmol , 1.0 equiv.), Pd/C (5% Pd, 14.5 mg, 6.80 μmol , 0.1 equiv.) and *i*-PrOH (0.6 mL). The atmosphere was exchange to H_2 by three times evacuating and flushing with H_2 (1 atm). After stirring at 23 $^\circ\text{C}$ for 2 h under an atmosphere of H_2 , the mixture was filtered through Celite $^\circledR$. The filtrate was concentrated under reduced pressure and purification by column chromatography (SiO_2 , pentane/ Et_2O 3:1) afforded ketone **2** (24.2 mg, 90%) as a colorless crystalline solid.

m.p.: 111 $^\circ\text{C}$.

$[\alpha]_{\text{D}}^{25} = +43.8^\circ$ (c = 0.30, CHCl_3).

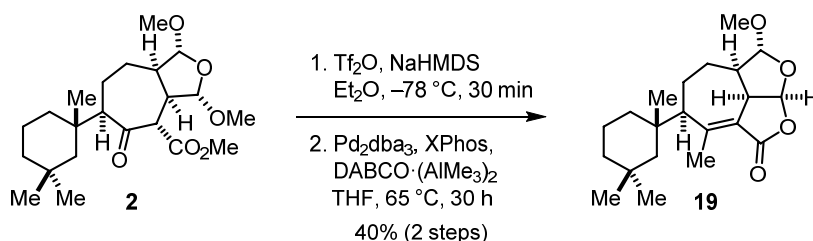
^1H NMR (700 MHz, CDCl_3): δ [ppm] = 4.91 (d, J = 5.7 Hz, 1H), 4.68 (s, 1H), 3.73 (s, 3H), 3.55 (d, J = 12.7 Hz, 1H), 3.47 (s, 3H), 3.37 (s, 3H), 2.85 (dd, J = 12.7, 7.7 Hz, 1H), 2.64 (ddd, J = 11.4, 5.7, 2.9 Hz, 1H), 2.43 (dd, J = 11.1, 5.7 Hz, 1H), 1.80 – 1.74 (m, 2H), 1.71 – 1.60 (m, 2H), 1.55 – 1.52 (m, 1H), 1.47 – 1.42 (m, 2H), 1.36 (d, J = 13.0 Hz, 1H), 1.26 – 1.19 (m, 3H), 1.14 (s, 3H), 1.09 – 1.02 (m, 2H), 0.96 (s, 3H), 0.87 (s, 3H).

^{13}C NMR (176 MHz, CDCl_3): δ [ppm] = 207.5, 169.0, 110.5, 108.5, 64.8, 57.7, 56.6, 54.9, 52.3, 48.7, 48.4, 44.4, 39.2, 36.8, 36.3, 35.0, 30.7, 28.0, 24.4, 21.5, 19.9, 18.6.

HRMS (ESI): m/z calcd for $\text{C}_{22}\text{H}_{36}\text{O}_6\text{Na}$ [$\text{M}+\text{Na}$] $^+$: 419.2404; found: 419.2418.

IR (ATR): $\tilde{\nu}$ = 2950, 2925, 2868, 2845, 1751, 1713, 1458, 1385, 1293, 1248, 1229, 1202, 1167, 1104, 1029, 995, 954 cm^{-1} .

(2a*S*,2a¹*R*,4*R*,4a*R*,7*R*)-4-methoxy-8-methyl-7-((*S*)-1,3,3-trimethylcyclohexyl)-2a¹,4,4a,5,6,7-hexahydro-2,3-dioxacyclopenta[*cd*]azulen-1(2a*H*)-one (19)



An oven-dried 10 mL round-bottom-flask equipped with a Teflon-coated magnetic stirring bar was charged with ketone **2** (9.8 mg, 25 μmol , 1.0 equiv.) and dry Et_2O (0.7 mL). Sodium bis(trimethylsilyl)amide (2 M in THF, 0.02 mL, 40 μmol , 1.6 equiv.) was added at -78°C and the solution was stirred at -78°C for 1 h. After the addition of freshly distilled trifluoromethanesulfonic anhydride (13 μL , 74 μmol , 3.0 equiv.), the reaction was stirred at -78°C for another 30 min and terminated by the addition of NaHCO_3 (sat. aq., 5 mL). The aqueous phase was extracted with Et_2O (3 x 5 mL). The combined organic phases were washed with NaHCO_3 (sat. aq., 5 mL) and brine (5 mL), dried over Na_2SO_4 , filtered and concentrated under reduced pressure to a volume of 1 mL. Column chromatography (SiO_2 , pentane/ Et_2O 5:1) afforded the corresponding vinyl triflate, which was directly used for the next reaction step. The solvent was exchange to dry THF (0.5 mL) and tris(dibenzylideneacetone)dipalladium(0) (2.3 mg, 2.5 μmol , 0.1 equiv.), 2-Dicyclohexylphosphino-2',4',6'-triisopropylbiphenyl (XPhos, 2.4 mg, 5.0 μmol , 0.2 equiv.) and bis(trimethylaluminum)-1,4-diazabicyclo[2.2.2]octane adduct (19 mg, 74 μmol , 3.0 equiv.) were added under an atmosphere of argon. The reaction was heated in a sealed flask at 65°C for 30 h and terminated by the addition of HCl (1 M aq., 3 mL). The aqueous phase was extracted with Et_2O (5 x 3 mL) and the combined organic phases were dried over Na_2SO_4 , filtered and concentrated under reduced pressure. Purification by column chromatography (SiO_2 , pentane/ Et_2O 8:1) afforded lactone **19** (3.8 mg, containing 10% methyl ester, 40%) as a colorless oil.

$[\alpha]_{\text{D}}^{22} = -4.60^\circ$ ($c = 0.19$, CHCl_3).

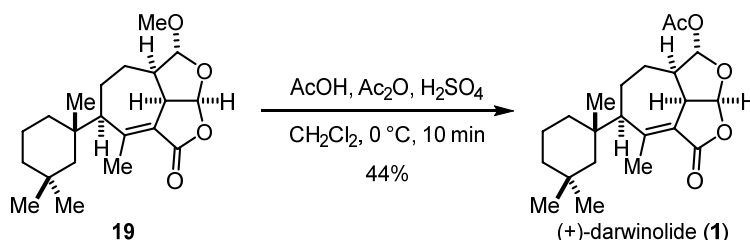
$^1\text{H NMR}$ (700 MHz, CDCl_3): δ [ppm] = 5.95 (d, $J = 6.5$ Hz, 1H), 4.70 (d, $J = 2.1$ Hz, 1H), 3.84 (ddd, $J = 9.5, 6.5, 2.1$ Hz, 1H), 3.39 (s, 3H), 2.37 (d, $J = 2.4$ Hz, 3H), 2.13 – 2.07 (m, 2H), 1.83 – 1.77 (m, 1H), 1.61 – 1.56 (m, 2H), 1.53 – 1.46 (m, 2H), 1.42 – 1.33 (m, 4H), 1.31 – 1.27 (m, 1H), 1.17 – 1.13 (m, 1H), 1.12 (s, 3H), 1.11 – 1.04 (m, 3H), 0.97 (s, 3H), 0.85 (s, 3H).

^{13}C NMR (176 MHz, CDCl_3): δ [ppm] = 168.2, 158.7, 120.4, 111.3, 102.9, 57.1, 55.7, 50.5, 45.6, 43.0, 39.3, 38.6, 36.0, 33.9, 30.8, 28.6, 25.7, 22.2, 19.4, 18.7, 15.6.

HRMS (ESI): m/z calcd for $\text{C}_{21}\text{H}_{32}\text{O}_4\text{Na}$ $[\text{M}+\text{Na}]^+$: 371.2193; found: 371.2211.

IR (ATR): $\tilde{\nu}$ = 2924, 2863, 1758, 1636, 1459, 1386, 1243, 1212, 1106, 1043, 1006, 974, 949, 801, 789, 777, 713 cm^{-1} .

Darwinolide (1)



A 10 mL round-bottom-flask equipped with a Teflon-coated magnetic stirring bar was charged with acetal **19** (1.7 mg, 4.9 μmol , 1.0 equiv.) and CH_2Cl_2 (0.2 mL). Acetic anhydride (3.4 μL , 33 μmol , 6.8 equiv.), acetic acid (1.9 μL , 33 μmol , 6.8 equiv.) and sulfuric acid (conc., 1.0 μL , 19 μmol , 3.8 equiv.) were added at 0 $^\circ\text{C}$. The reaction was stirred at 0 $^\circ\text{C}$ for 10 min and terminated by the addition of NaHCO_3 (sat. aq., 2 mL). The aqueous phase was extracted with CH_2Cl_2 (3 x 3 mL) and the combined organic phases were dried over Na_2SO_4 , filtered and concentrated under reduced pressure. Purification by preparative thin layer chromatography (SiO_2 , pentane/ Et_2O 1.5:1) afforded darwinolide **1** (0.8 mg, 44%) as a colorless solid.

$[\alpha]_{\text{D}}^{22} = +20.7^\circ$ ($c = 0.07$, CHCl_3).

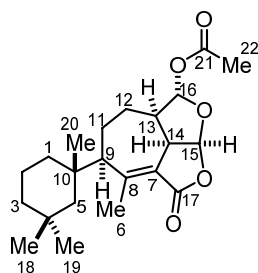
^1H NMR (700 MHz, CDCl_3): δ [ppm] = 6.07 (d, $J = 6.6$ Hz, 1H), 5.94 (s, 1H), 3.93 (ddd, $J = 9.5, 6.8, 2.4$ Hz, 1H), 2.39 (d, $J = 2.3$ Hz, 3H), 2.26 – 2.22 (m, 1H), 2.11 – 2.08 (m, 1H), 2.08 (s, 3H), 1.92 (dd, $J = 13.3, 6.7$ Hz, 1H), 1.66 – 1.58 (m, 2H), 1.54 – 1.46 (m, 2H), 1.44 – 1.35 (m, 2H), 1.39 (d, $J = 13.9$ Hz, 1H), 1.22 – 1.14 (m, 1H), 1.14 (s, 3H), 1.09 (d, $J = 13.9$ Hz, 1H), 1.12 – 1.04 (m, 2H), 0.98 (s, 3H), 0.86 (s, 3H).

^{13}C NMR (176 MHz, CDCl_3): δ [ppm] = 169.7, 167.7, 159.4, 119.5, 104.0, 103.8, 57.3, 50.5, 45.1, 43.2, 39.2, 38.6, 36.0, 33.9, 30.8, 28.5, 25.6, 22.2, 21.2, 19.3, 18.7, 15.6.

HRMS (ESI): m/z calcd for $\text{C}_{22}\text{H}_{32}\text{O}_5\text{Na}$ $[\text{M}+\text{Na}]^+$: 399.2142; found: 399.2131.

IR (ATR): $\tilde{\nu}$ = 2923, 2852, 1758, 1636, 1457, 1239, 984, 953, 857, 798, 787, 772 cm^{-1} .

Comparison of NMR data:



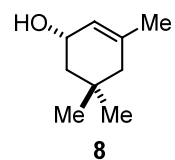
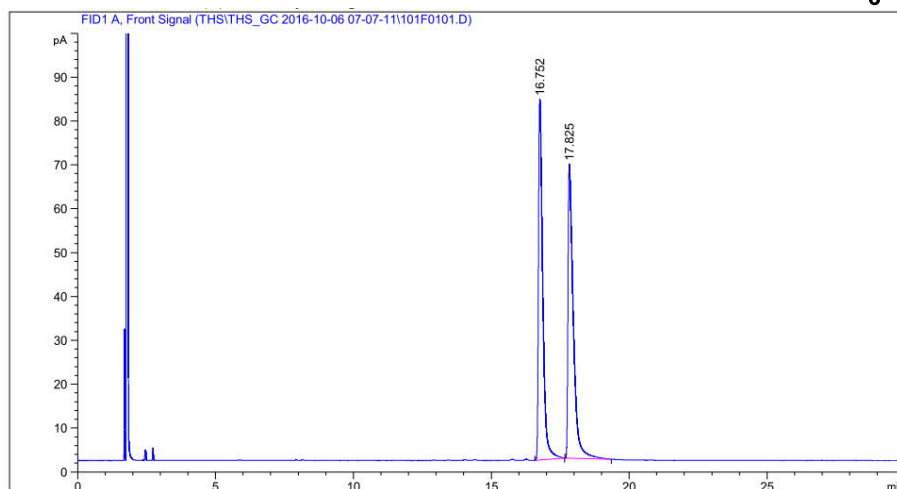
No.	¹³ C NMR Isolation 125 MHz [ppm]	¹³ C NMR Synthetic 176 MHz [ppm]	Δ [ppm]
1	38.6	38.6	0
2	18.7	18.7	0
3	39.2	39.2	0
4	30.8	30.8	0
5	50.5	50.5	0
6	15.6	15.6	0
7	119.5	119.5	0
8	159.5	159.4	0.1
9	57.3	57.3	0
10	36.0	36.0	0
11	19.2	19.3	0.1
12	25.6	25.6	0
13	43.2	43.2	0
14	45.1	45.1	0
15	103.9	103.9	0
16	103.8	103.8	0
17	167.7	167.7	0
18	33.9	33.9	0
19	28.5	28.5	0
20	22.1	22.2	0.1
21	169.7	169.7	0
22	21.2	21.2	0

Appendix

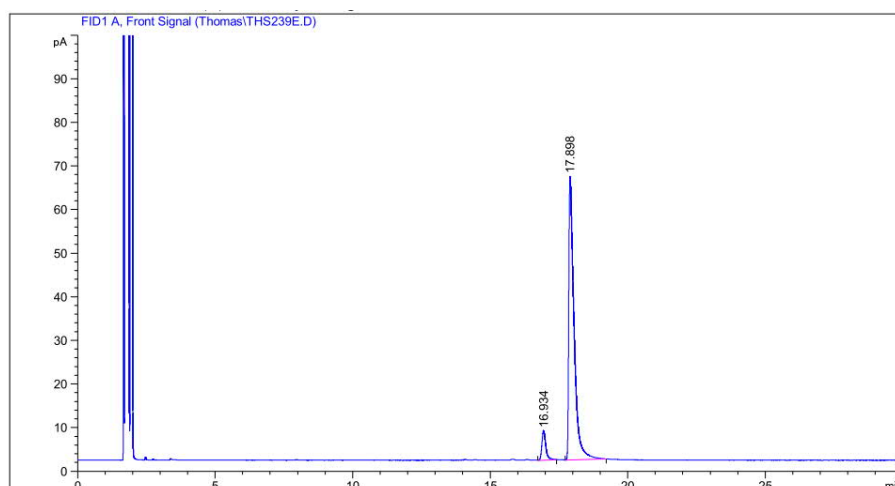
No.	¹ H NMR Isolation (<i>J</i> in Hz) 500 MHz [ppm]	¹ H NMR Synthetic (<i>J</i> in Hz) 700 MHz [ppm]	Δ [ppm]
1	1.08 m; 1.54 m	1.08 m, 1.54 m	0
2	1.50 m; 1.59 m	1.50 m; 1.59 m	0
3	1.11 m; 1.37 m	1.11 m; 1.37 m	0
5	1.08 d (14.1); 1.38 d (14.1)	1.09 d (13.9); 1.39 d (13.9)	0.01
6	2.39 d (2.3)	2.39 d (2.3)	0
9	2.08 m	2.09 m	0.01
11	1.42 m; 1.64 m	1.42 m, 1.64 m	0
12	1.92 m; 1.19 m	1.92 m, 1.19 m	0
13	2.24 m	2.24 m	0
14	3.93 tt (7.0, 2.4)	3.93 ddd (9.5, 6.8, 2.4)	0
15	6.07 d (7.0)	6.07 d (6.6)	0
16	5.93 s	5.94 s	0.01
18	0.86 s	0.86 s	0
19	0.98 s	0.98 s	0
20	1.14 s	1.14 s	0
22	2.08 s	2.08 s	0

GC Data

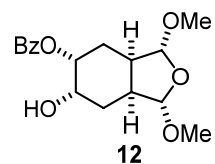
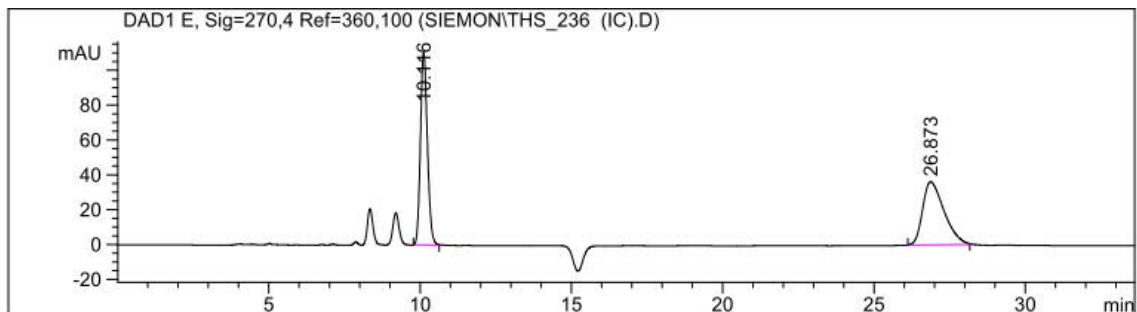
Lipodex E: isotherm 85 °C, 2 µL/min, split ratio 50:1, FID 200 °C.

**Racemic Mixture:**

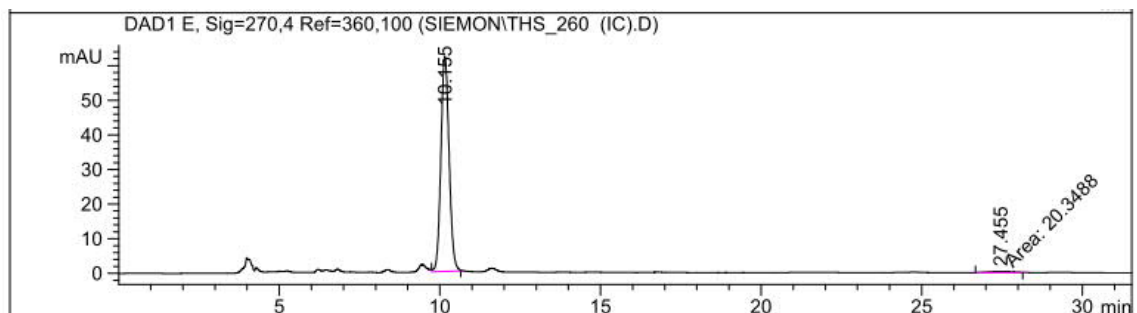
RetTime [min]	Type	Width [min]	Area [pA*s]	Area %
16.752	BB	0.1447	885.56256	49.74771
17.825	BB	0.1724	894.54449	50.25229

Enantioenriched:

RetTime [min]	Type	Width [min]	Area [pA*s]	Area %
16.934	BB	0.1370	66.61150	7.14637
17.898	BB	0.1760	865.49060	92.85363

HPLC DataChiralpak® IC; 20 °C; 30% *i*PrOH/hexane; 0.9 mL/min; 49 bar, 270.4 nm.**Racemic Mixture:**

RetTime [min]	Type	Width [min]	Area [mAU*s]	Height [mAU]	Area %
10.116	BB	0.2459	1758.69519	110.35031	49.6877
26.873	BB	0.7553	1780.80298	36.23899	50.3123

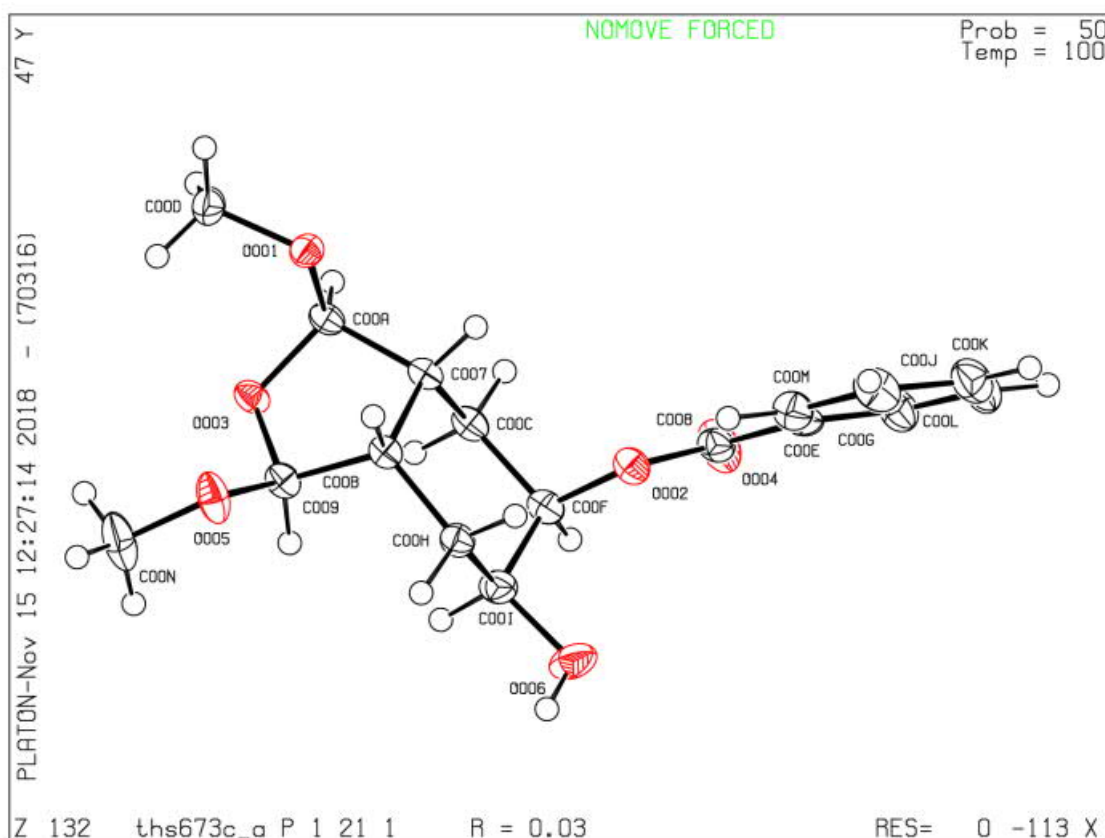
Enantioenriched:

RetTime [min]	Type	Width [min]	Area [mAU*s]	Height [mAU]	Area %
10.155	VB	0.2746	1100.35095	62.12405	98.1843
27.455	MM	0.9373	20.34881	3.61848e-1	1.8157

Crystallographic Data

Crystal data for monobenzoate **12** ($M = 322.36$ g/mol):

monoclinic; space group: $P 1 21 1$; $a = 12.4774(6)$ Å, $b = 5.4579(3)$ Å, $c = 12.6279(6)$ Å, $\alpha = 90^\circ$, $\beta = 111.525(2)^\circ$, $\gamma = 90^\circ$, $V = 799.99(7)$ Å³, $Z = 2$, $T = 100$ K, $\mu(\text{CuK}\alpha) = 1.54178$ mm⁻¹, $\rho_{\text{calc}} = 1.338$ g/cm³, 13823 reflections measured ($3.808^\circ \leq 2\theta \leq 68.407^\circ$), 2886 unique ($R_{\text{int}} = 0.0740$, $R_{\text{sigma}} = 0.0371$) which were used in all calculations. The final R_1 was 0.0328 ($I > 2\sigma(I)$) and wR_2 was 0.0758.

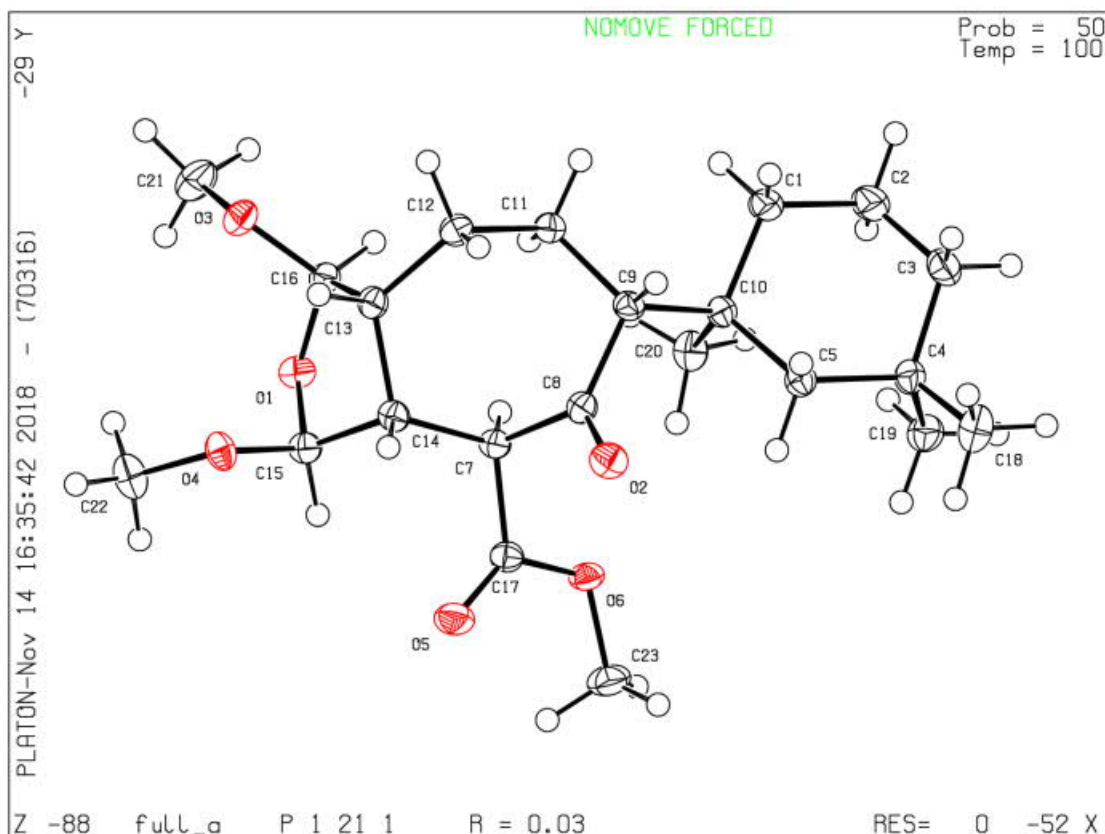


CCDC 1879212 contains the supplementary crystallographic data for this structure. These data can be obtained free of charge from The Cambridge Crystallographic Data Center via www.ccdc.cam.ac.uk/structures.

Appendix

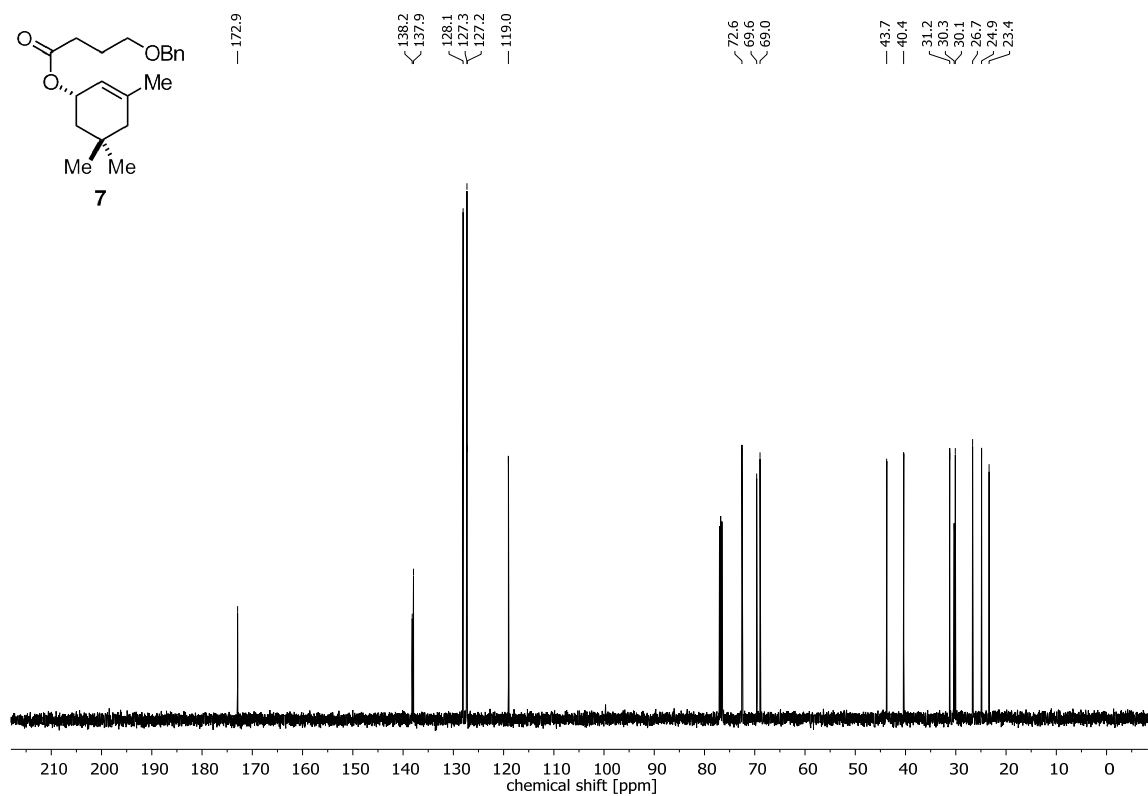
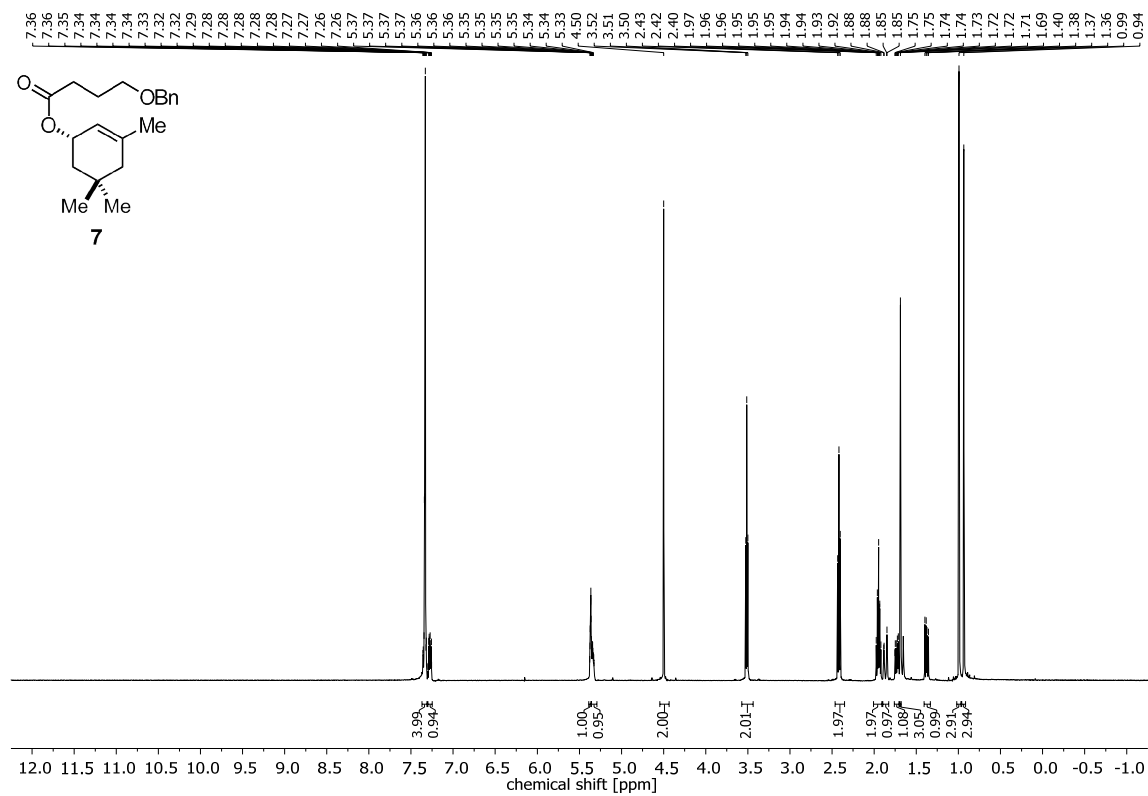
Crystal data for β -keto ester **2** (396.52 g/mol):

monoclinic, space group P 1 21 1, $a = 7.4891(3) \text{ \AA}$, $b = 17.3135(7) \text{ \AA}$, $c = 8.4426(4) \text{ \AA}$, $\alpha = 90^\circ$, $\beta = 93.848(2)^\circ$, $\gamma = 90^\circ$, $V = 1092.22(8) \text{ \AA}^3$, $Z = 2$, $T = 100 \text{ K}$, $\mu(\text{CuK}\alpha) = 1.54178 \text{ mm}^{-1}$, $\rho_{\text{calc}} = 1.206 \text{ g/cm}^3$, 18521 reflections measured ($5.109^\circ \leq 2\theta \leq 74.355^\circ$), 4407 unique ($R_{\text{int}} = 0.0815$, $R_{\text{sigma}} = 0.0369$) which were used in all calculations. The final R_1 was 0.0335 ($I > 2\sigma(I)$) and wR_2 was 0.0836.

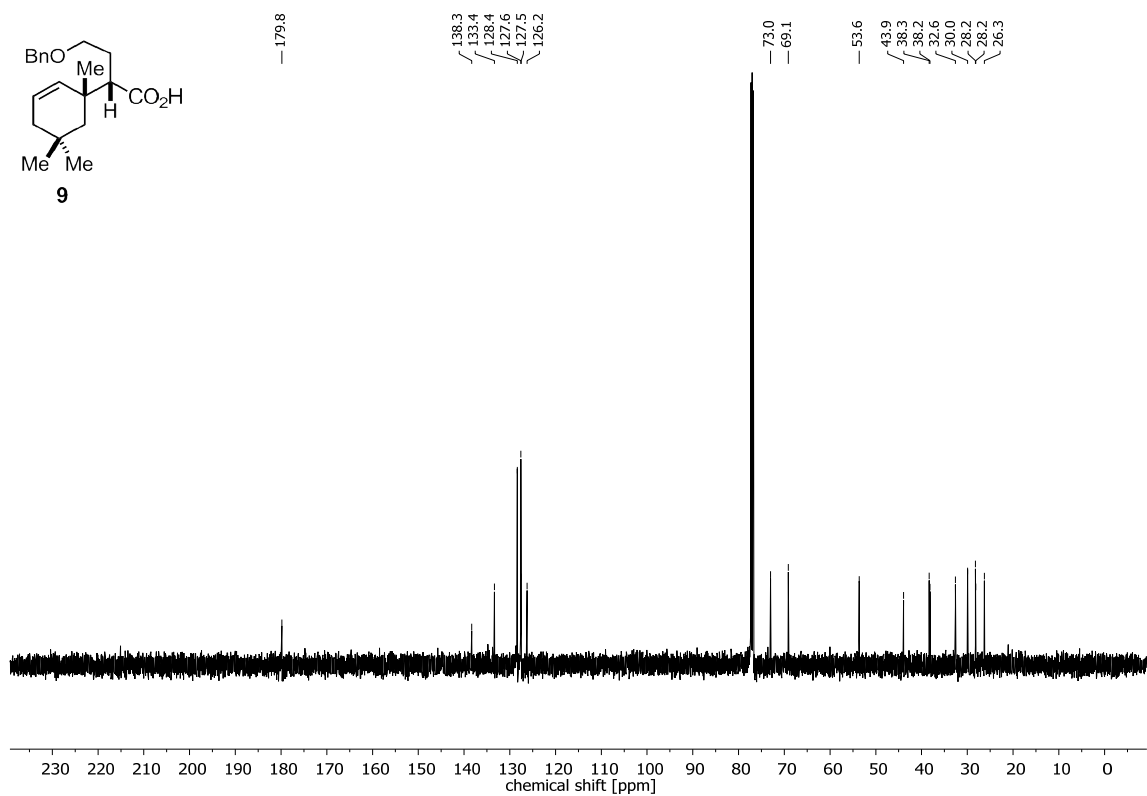
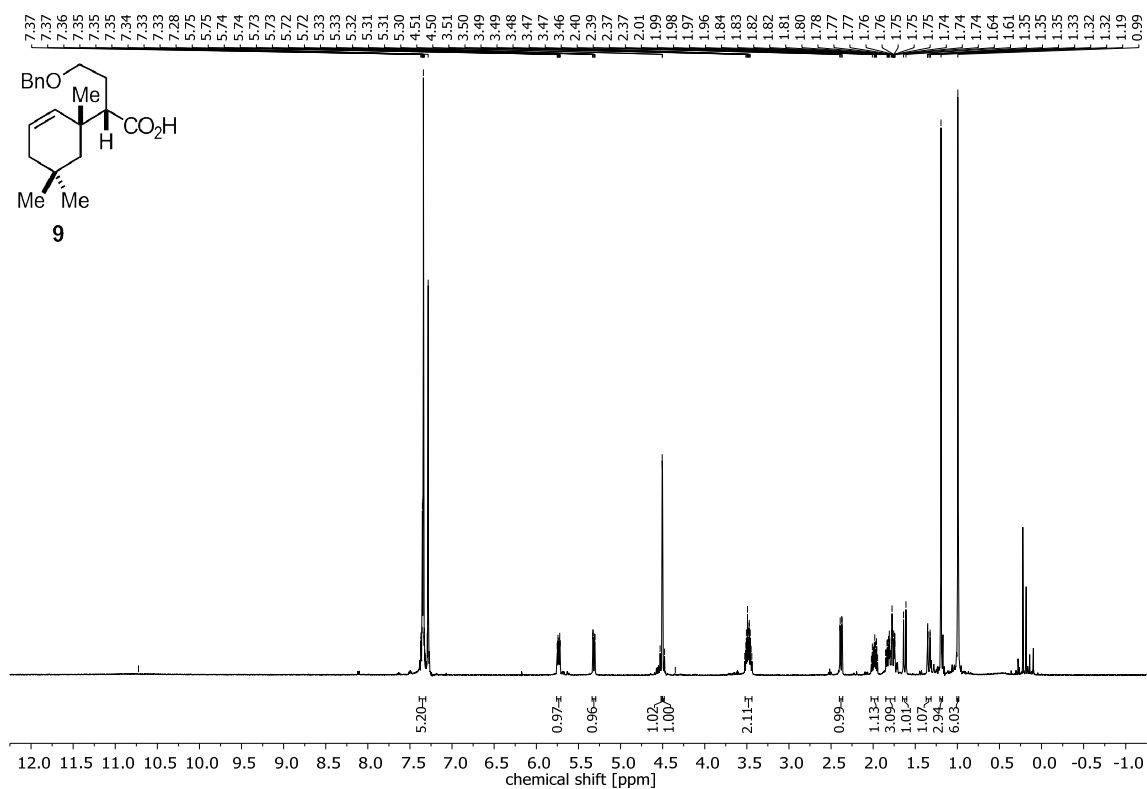


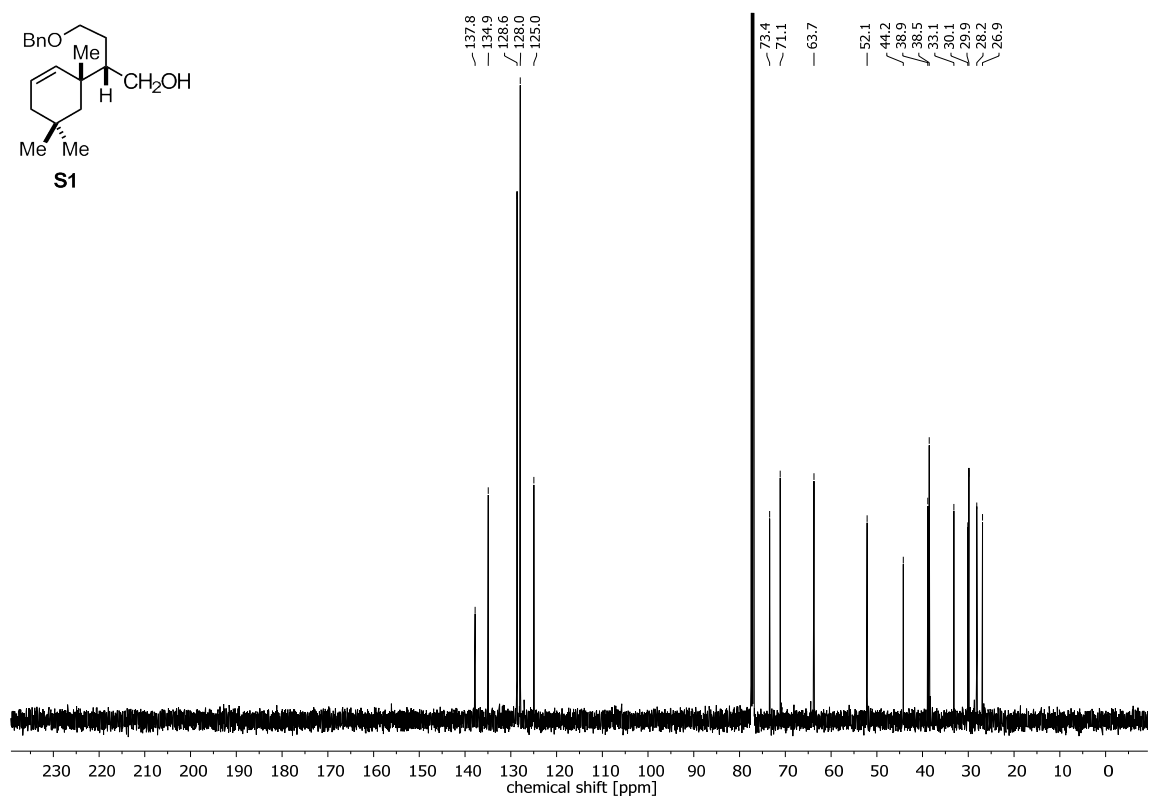
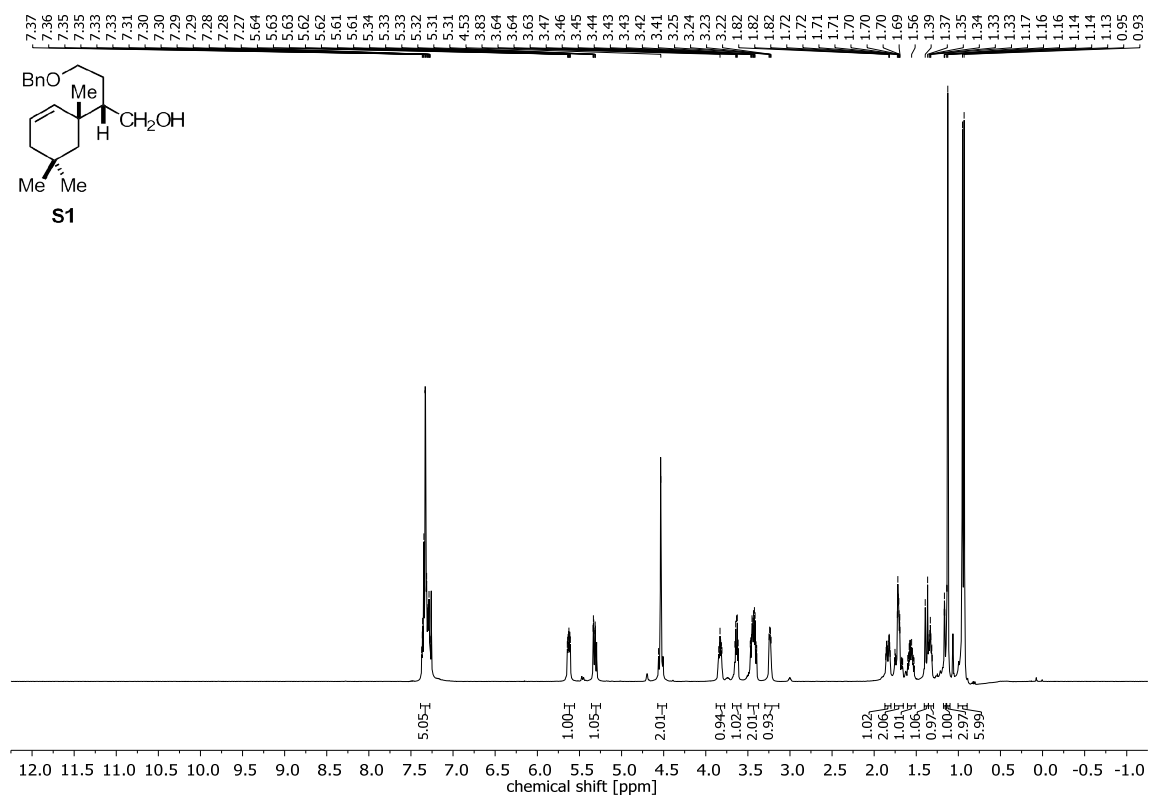
CCDC 1879213 contains the supplementary crystallographic data for this structure. These data can be obtained free of charge from The Cambridge Crystallographic Data Center via www.ccdc.cam.ac.uk/structures.

NMR Spectra

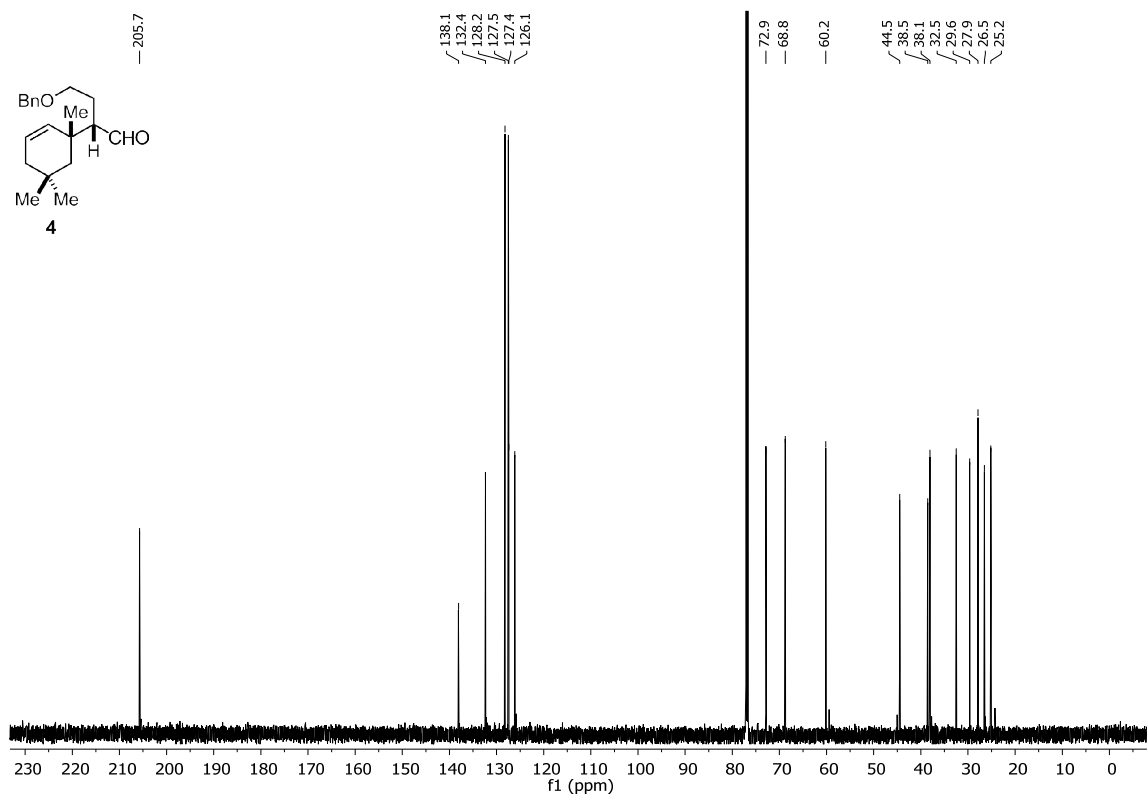
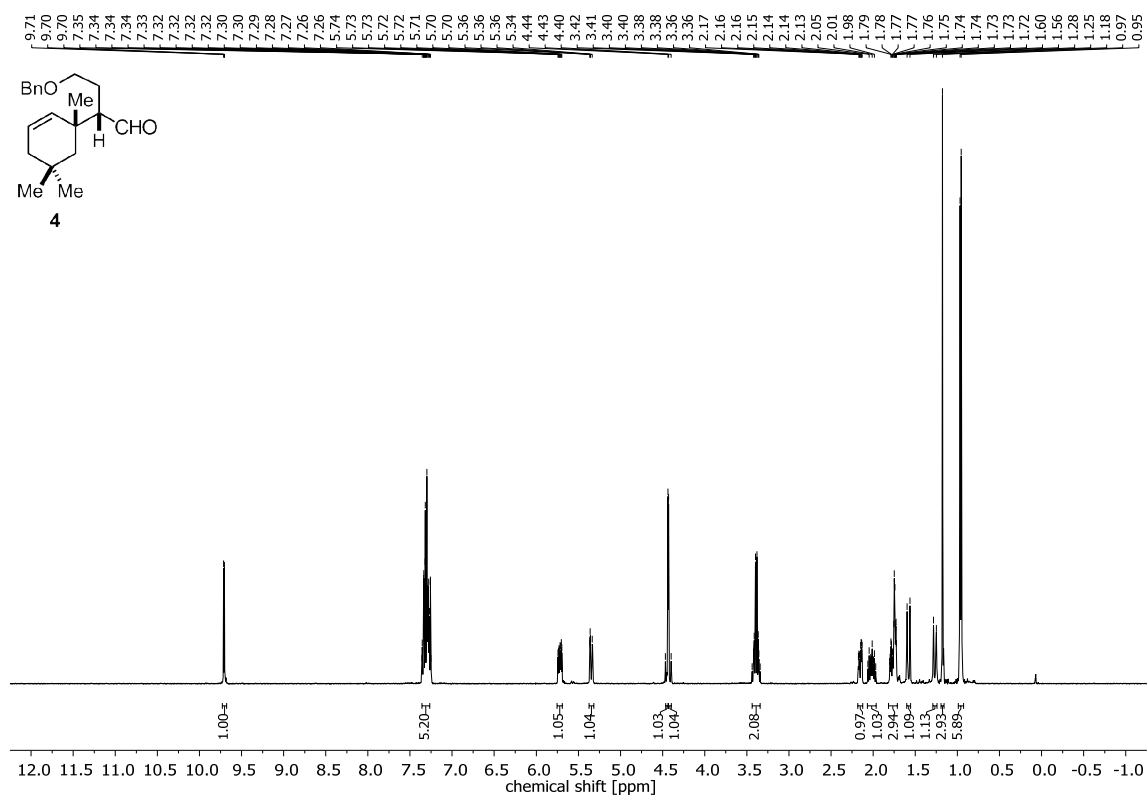


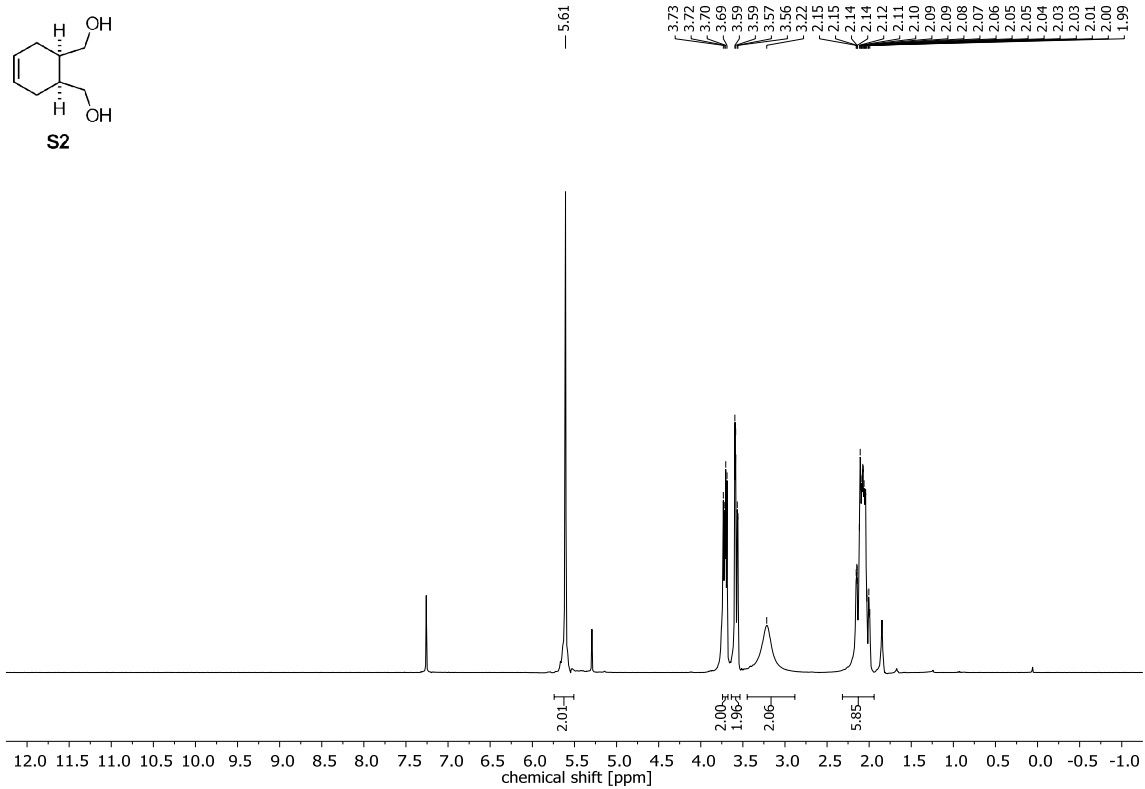
Appendix



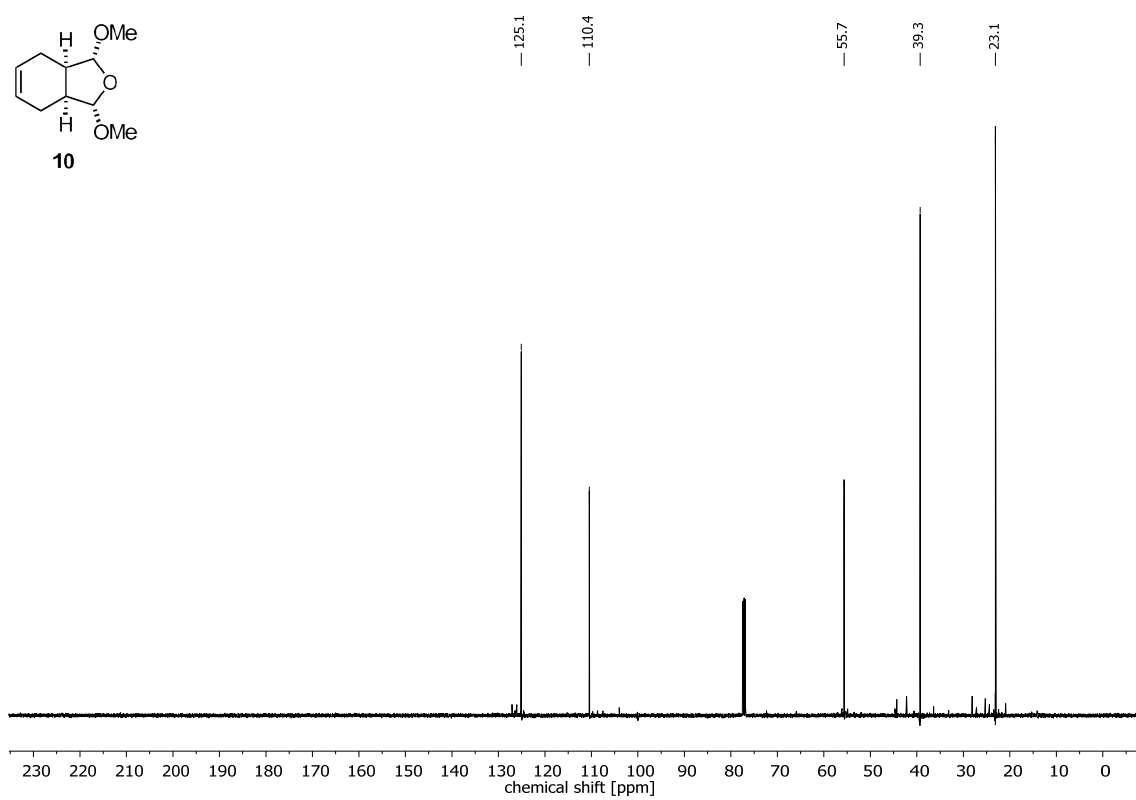
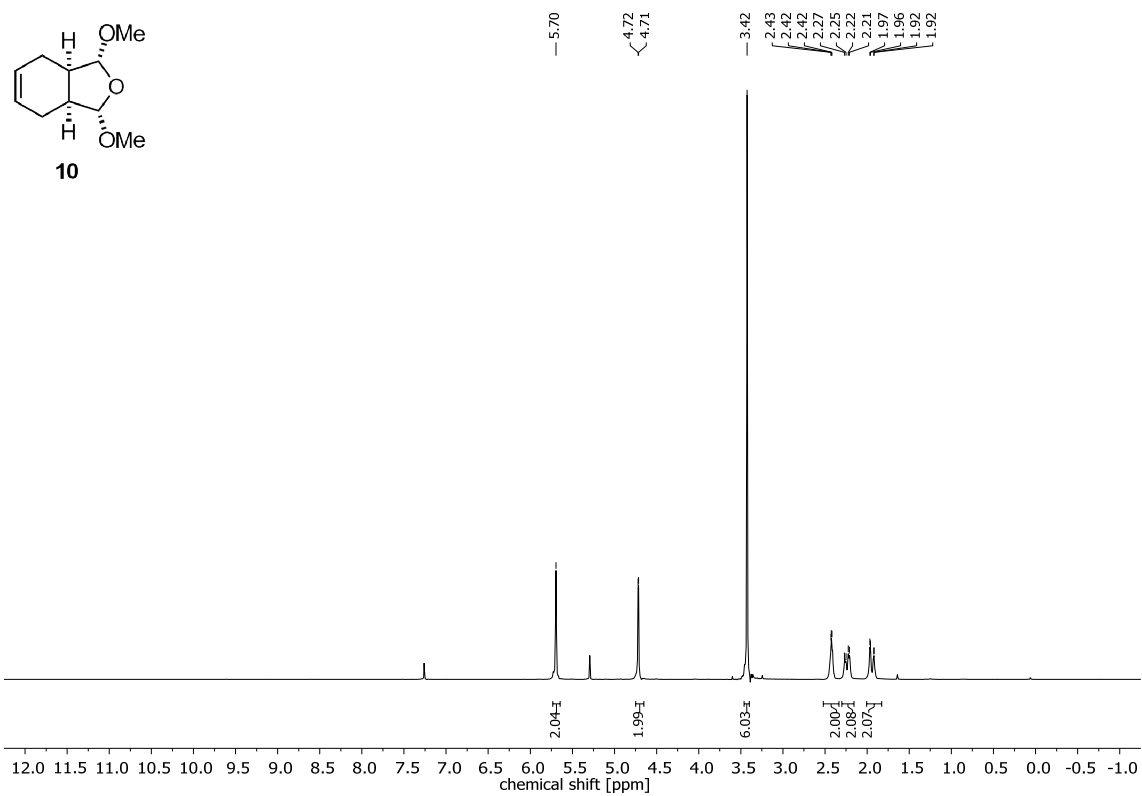


Appendix

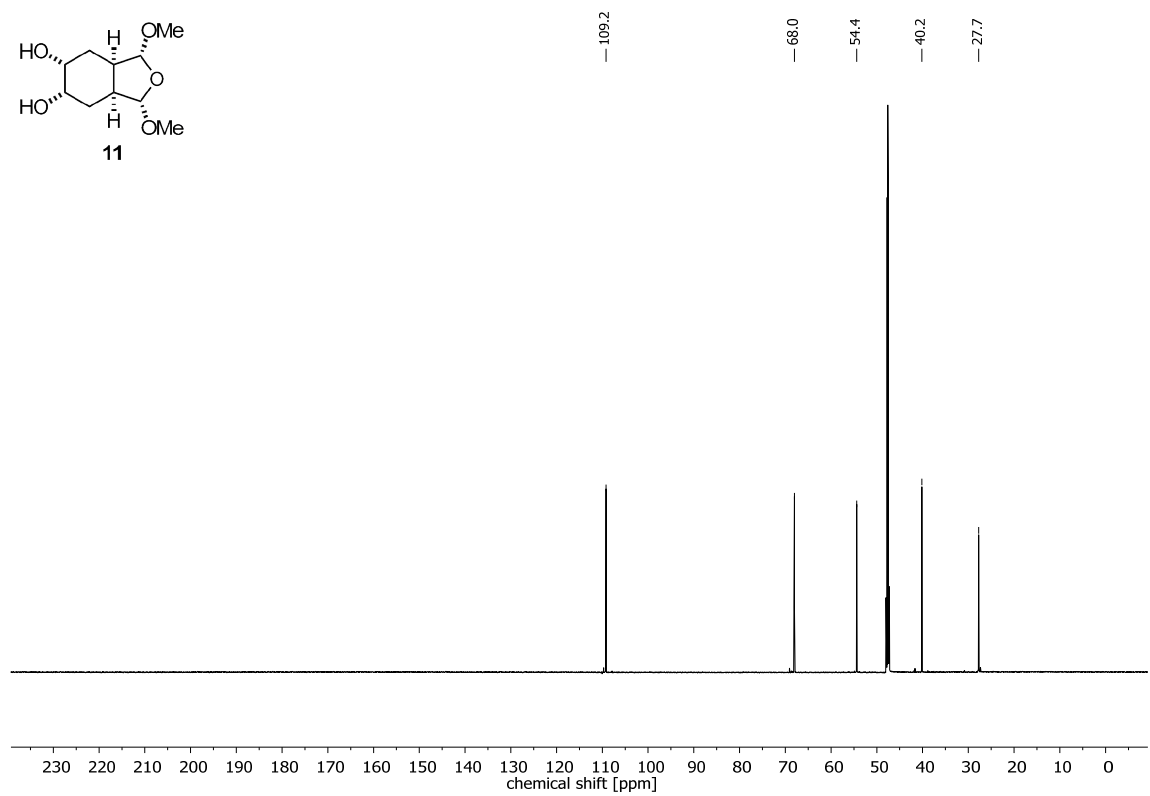
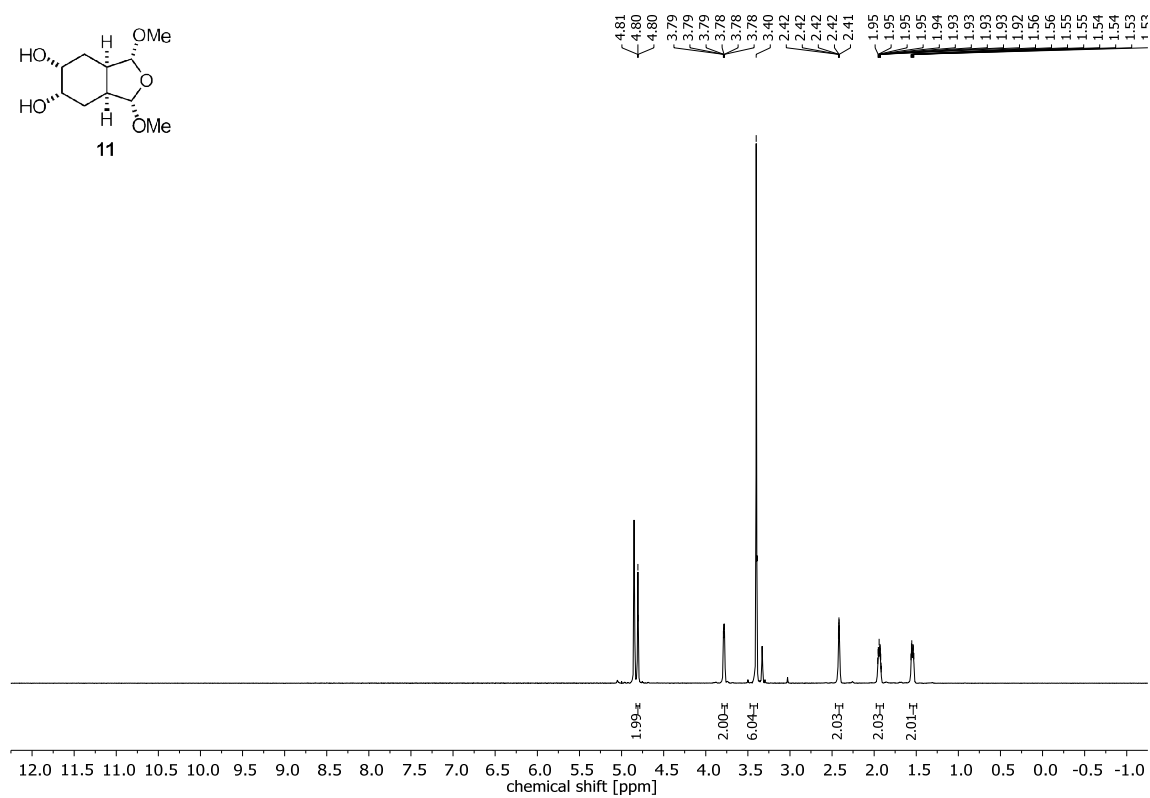




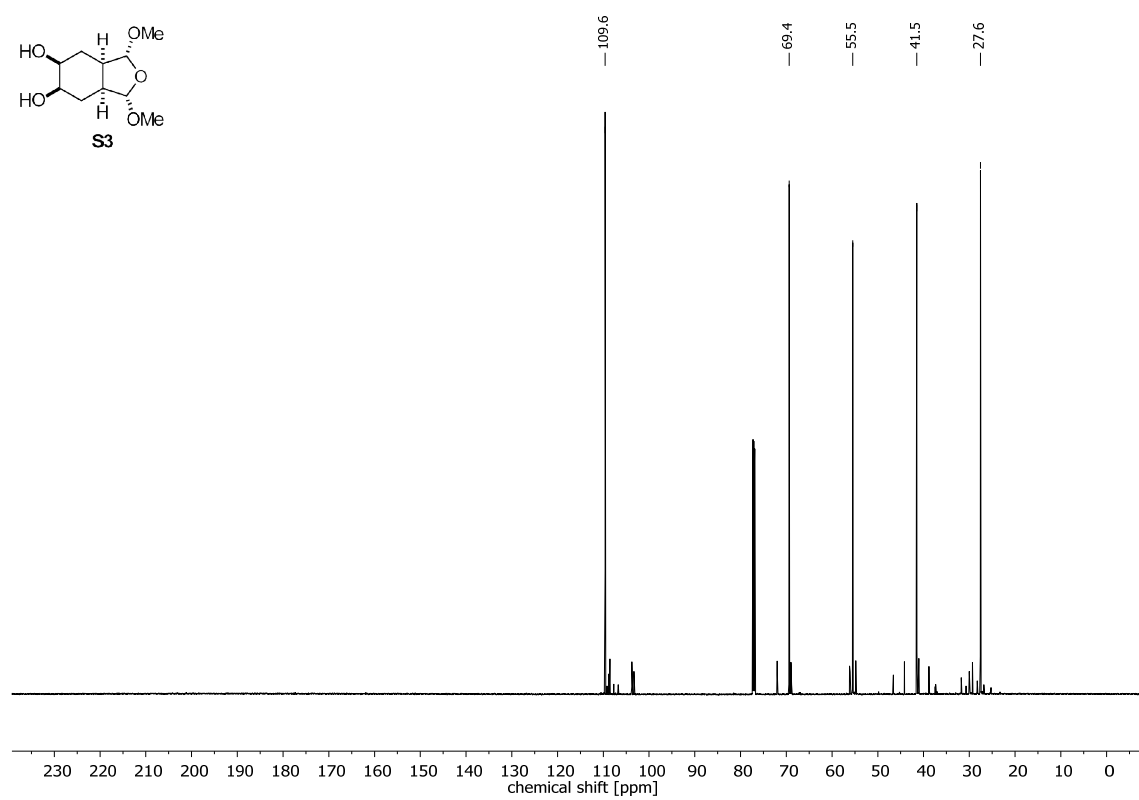
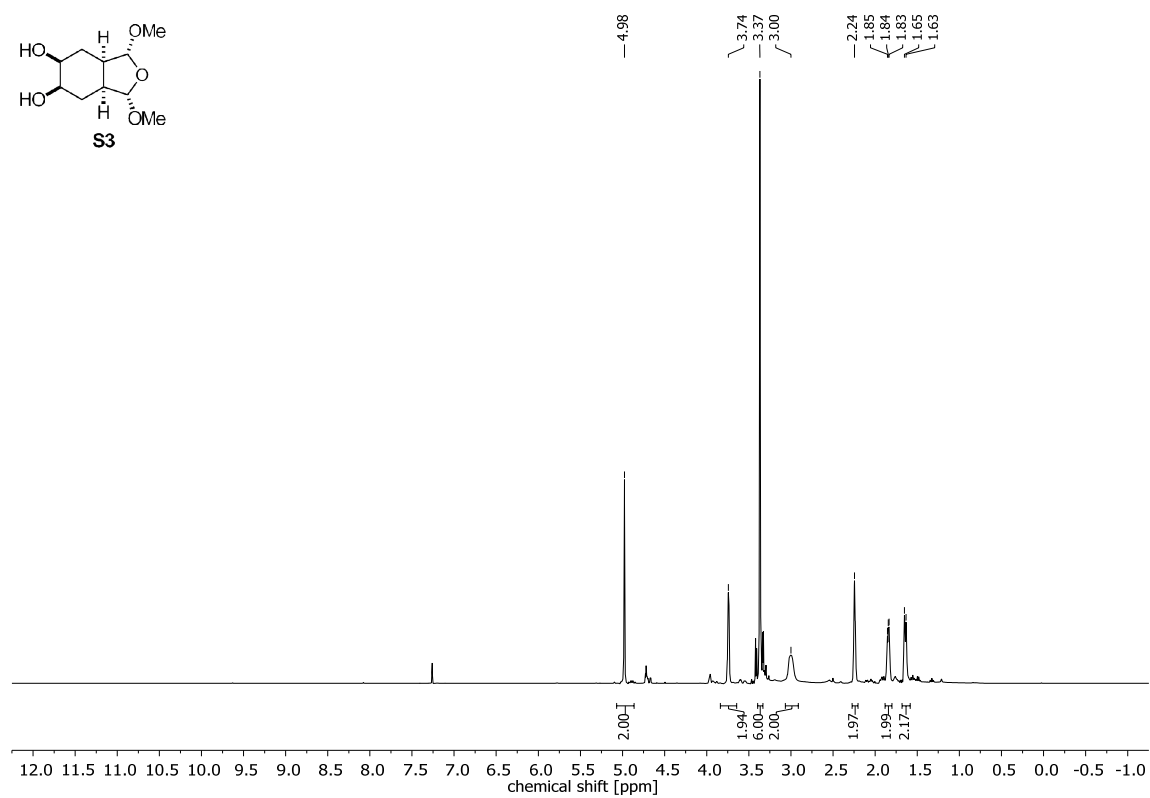
Appendix



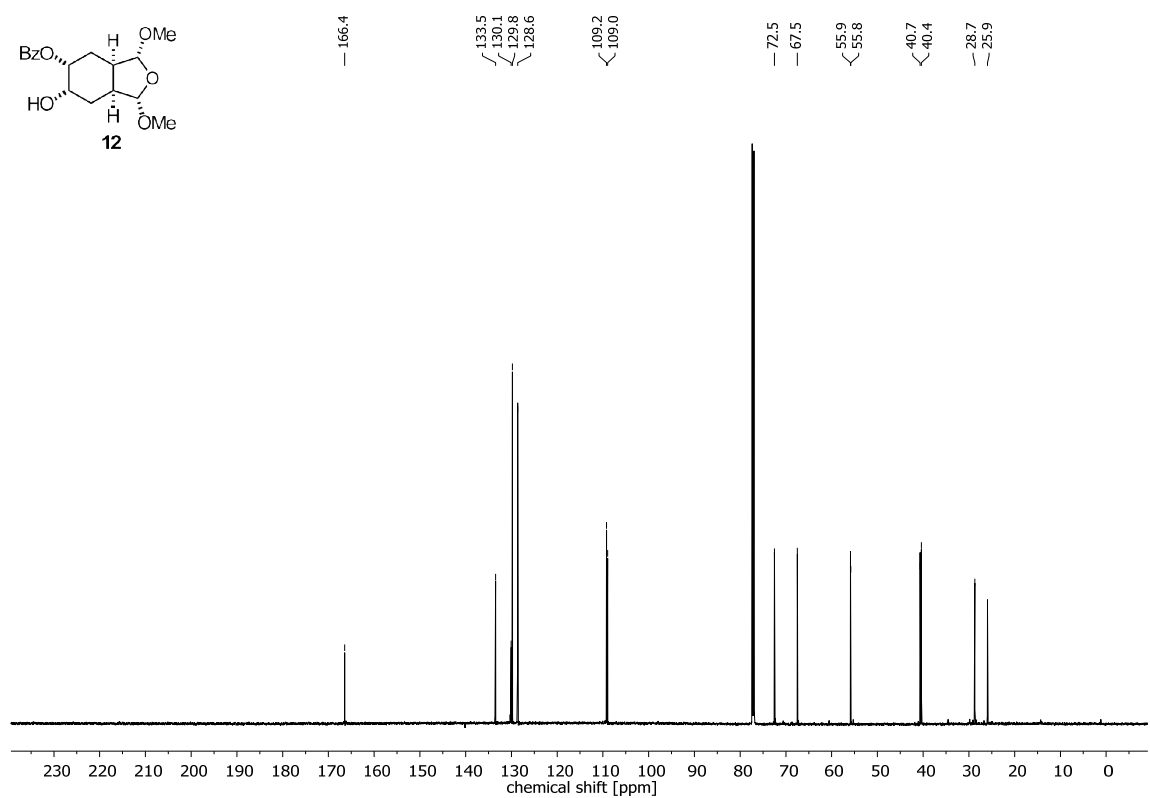
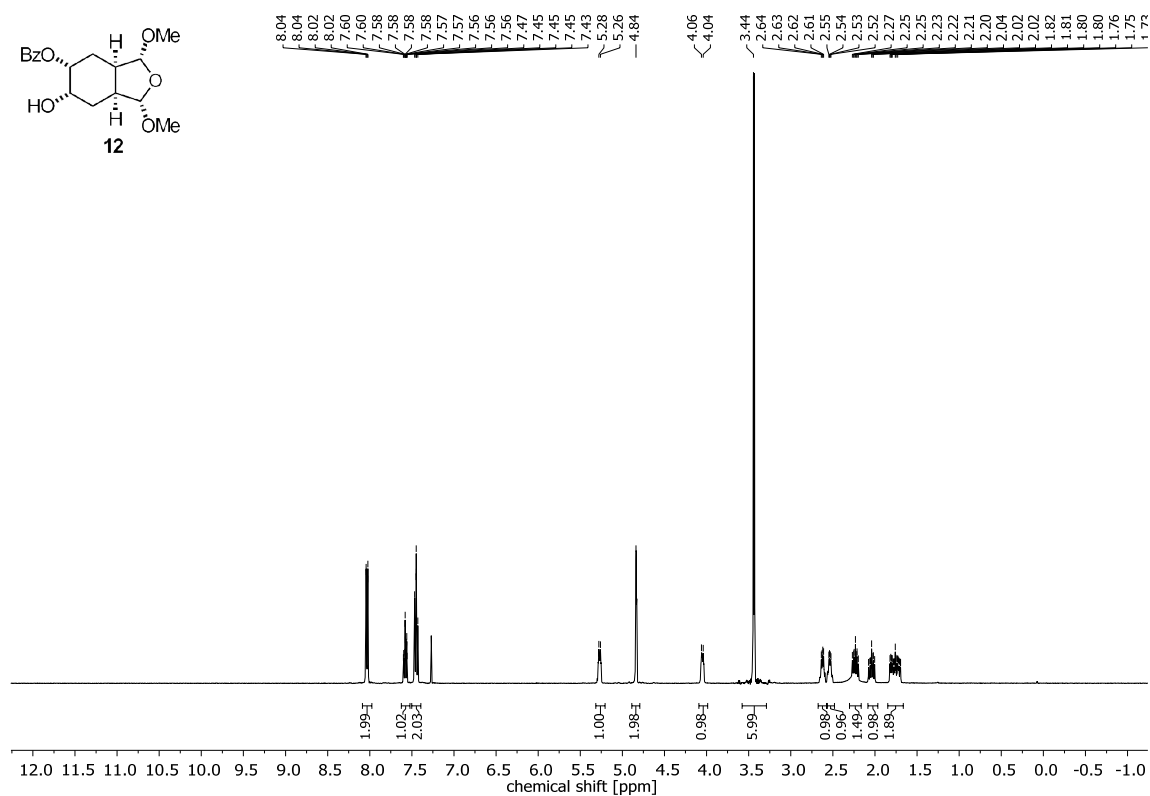
Supporting Information – Synthesis of (+)-Darwinolide



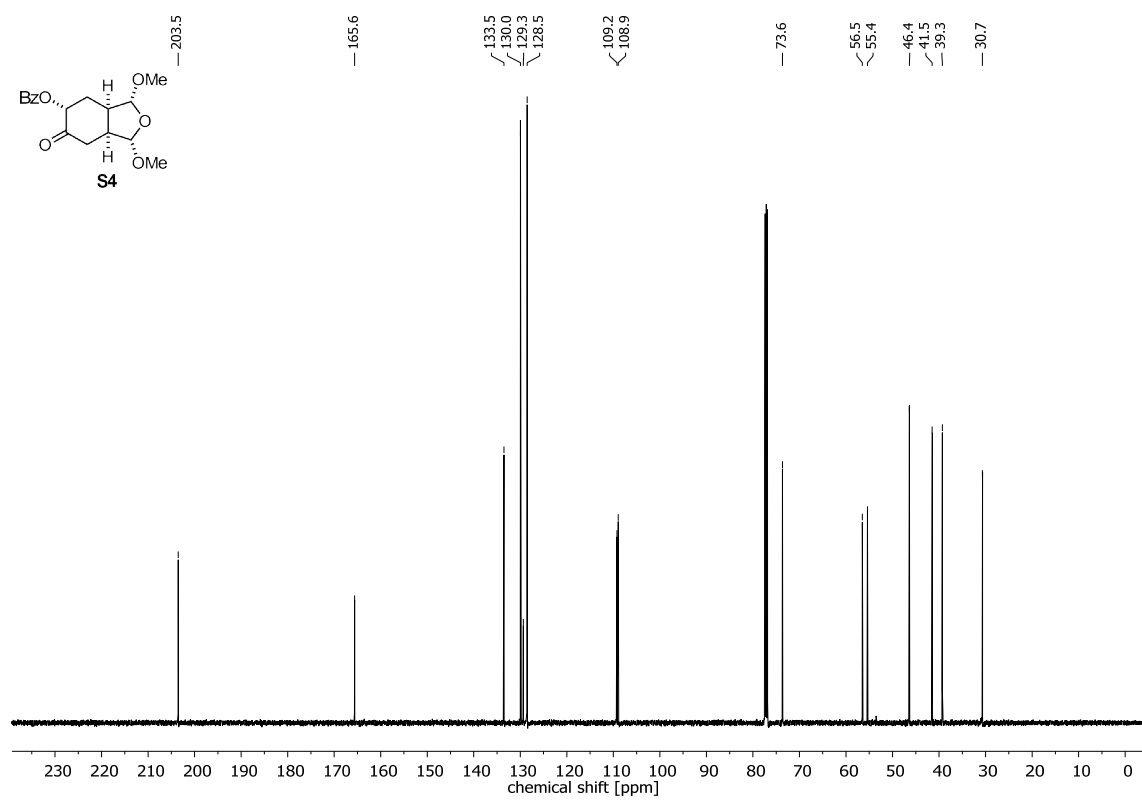
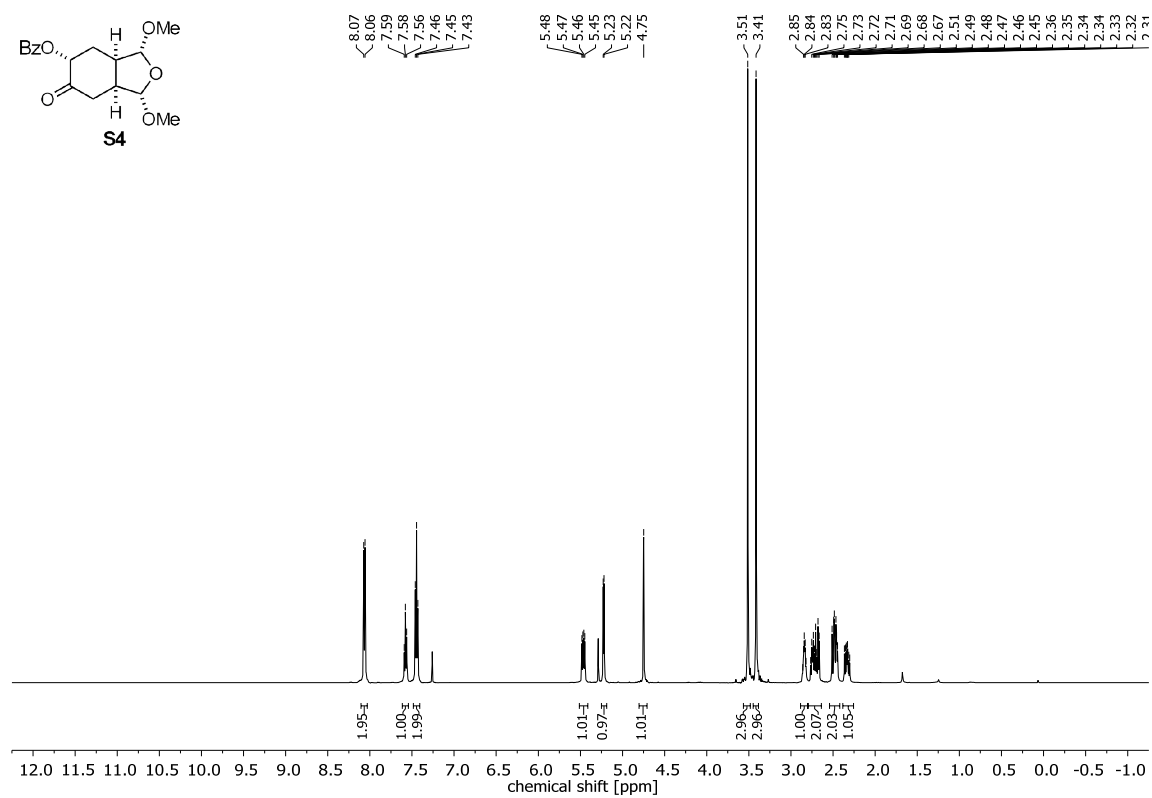
Appendix



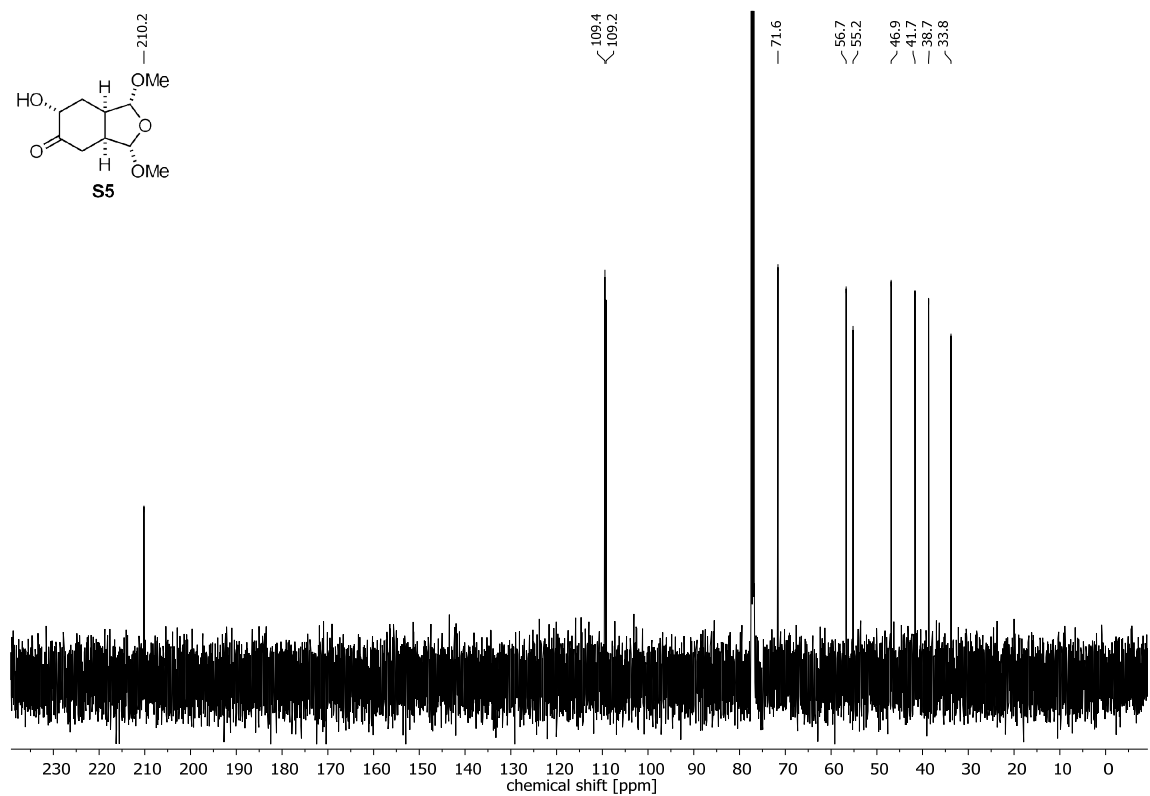
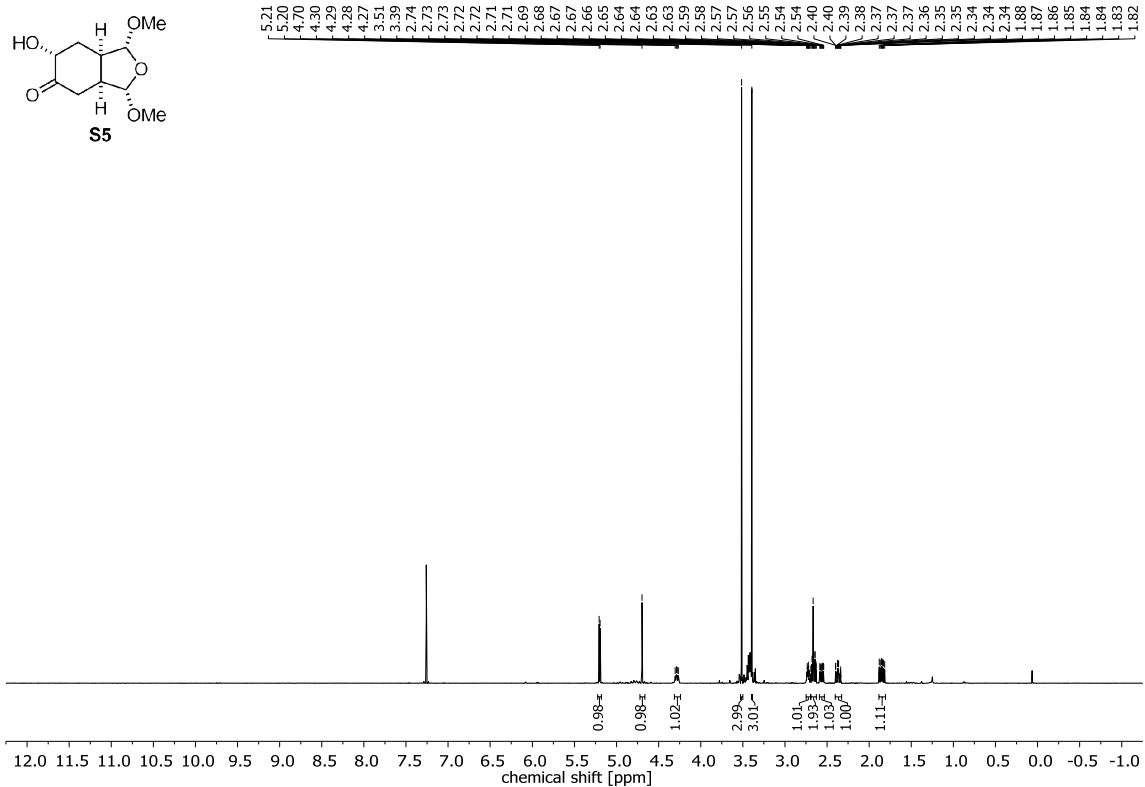
Supporting Information – Synthesis of (+)-Darwinolide



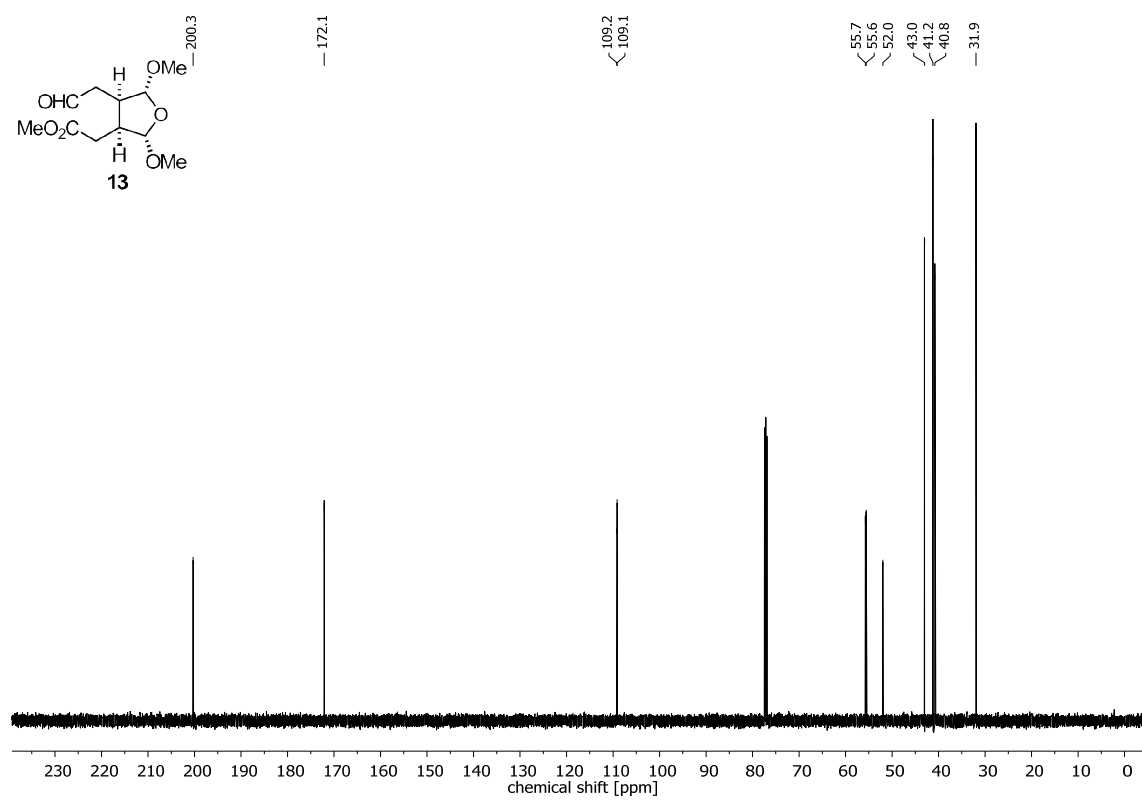
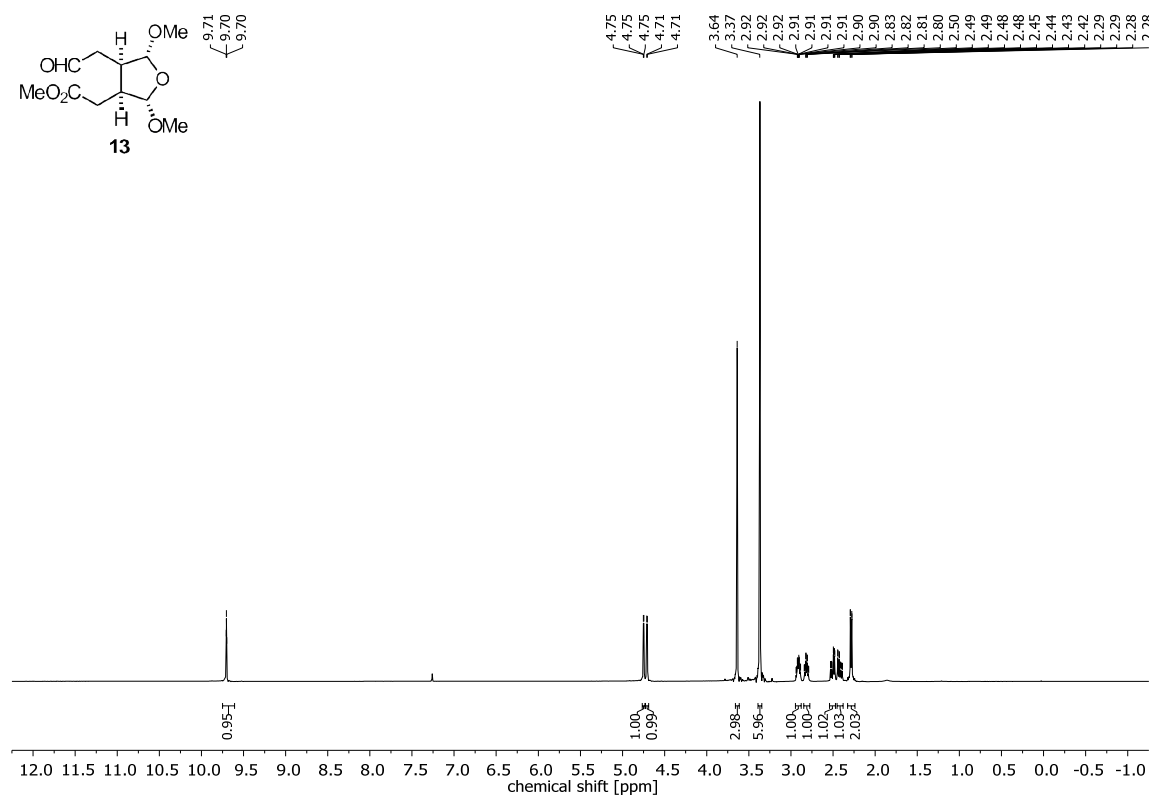
Appendix



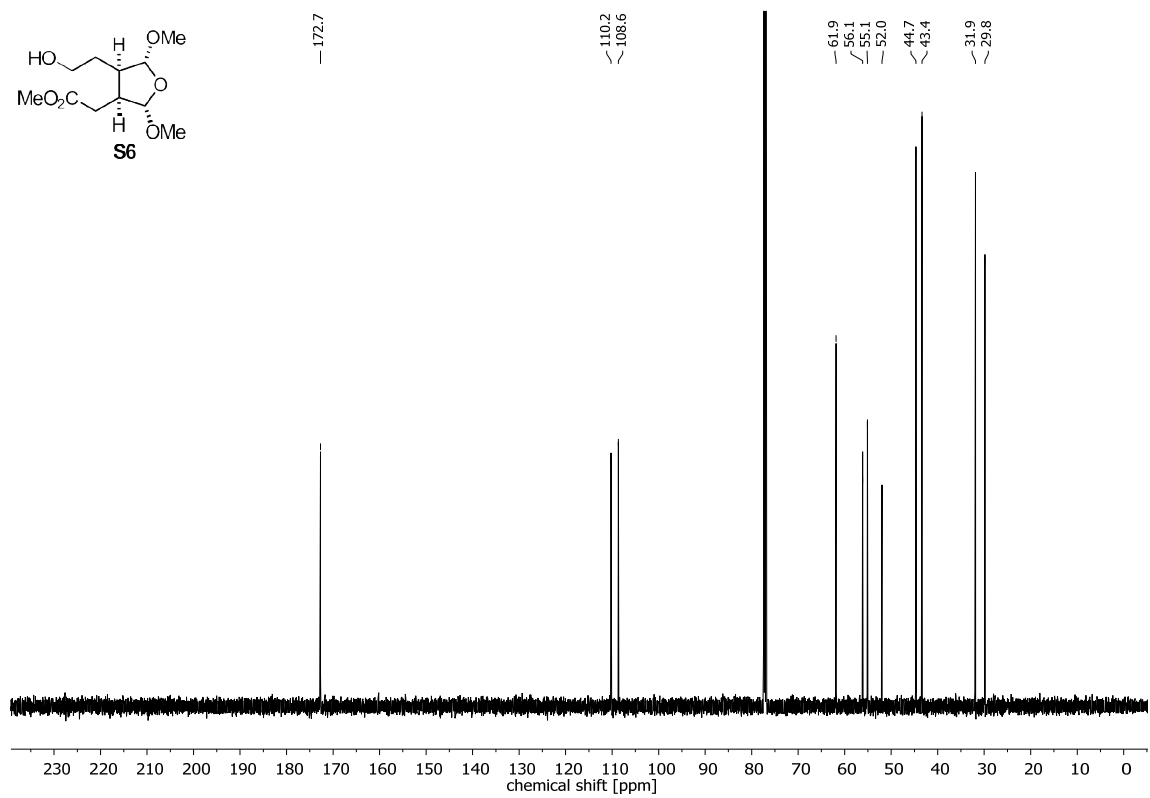
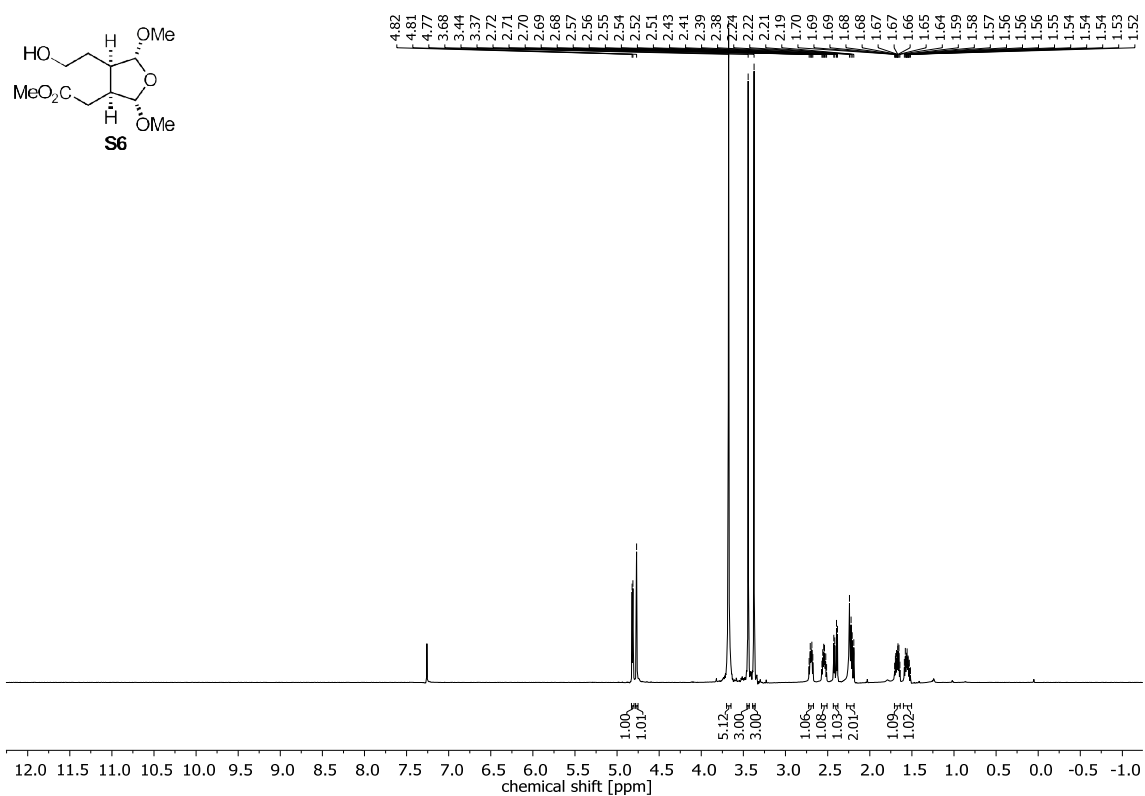
Supporting Information – Synthesis of (+)-Darwinolide



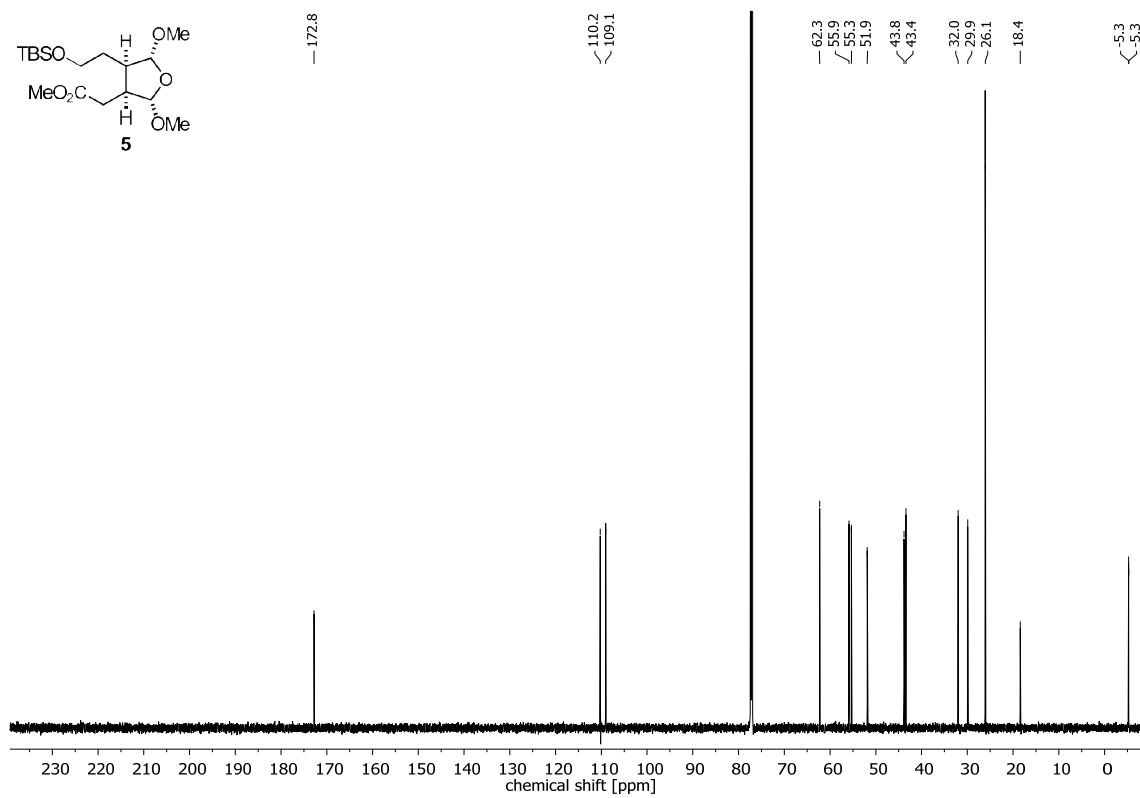
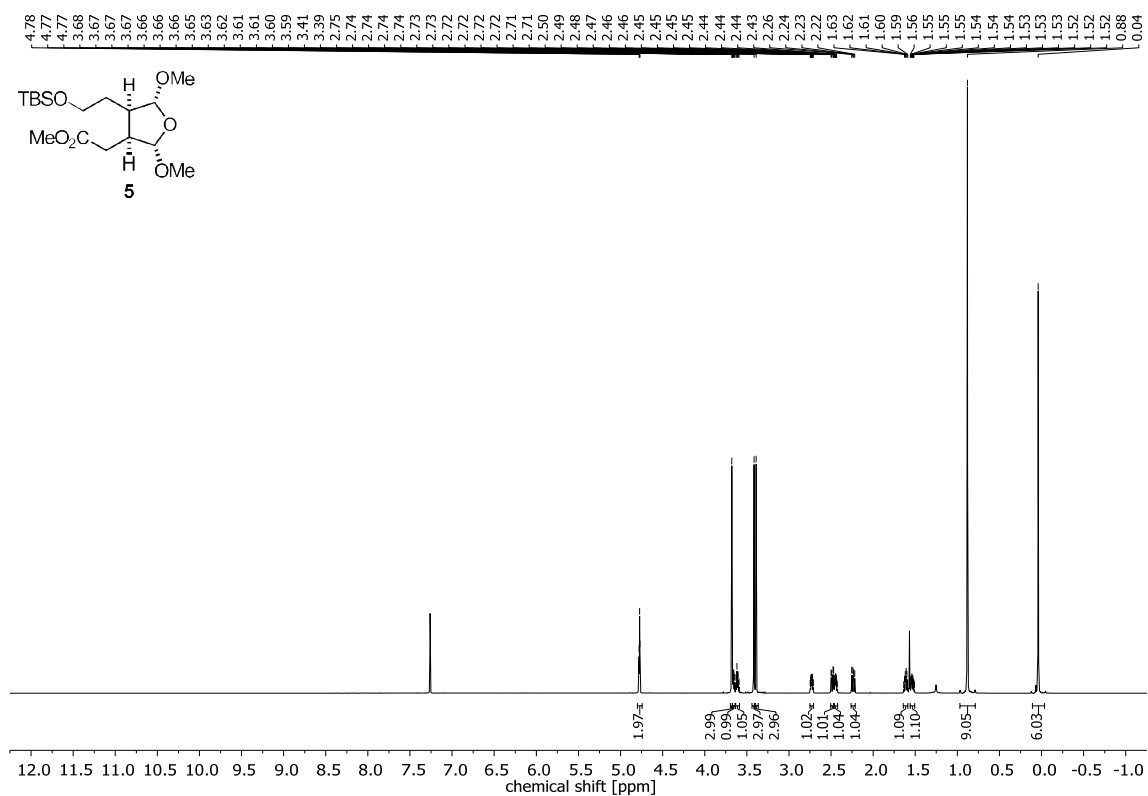
Appendix



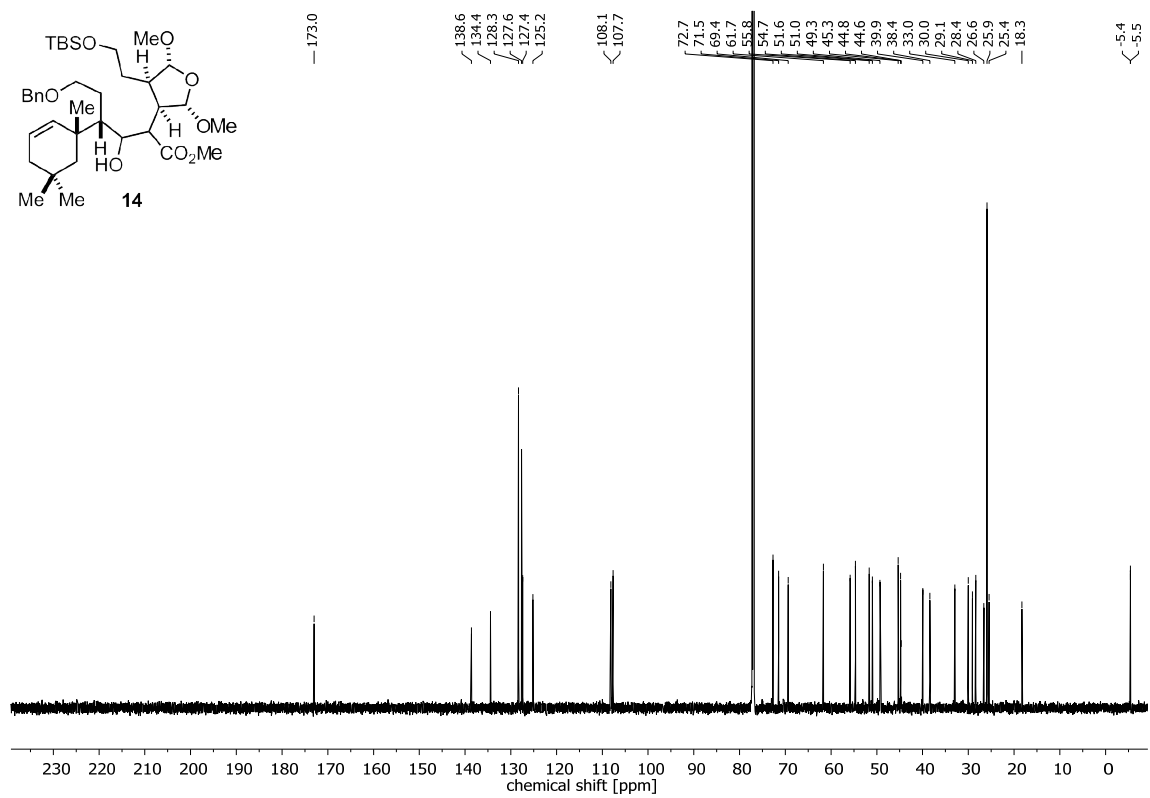
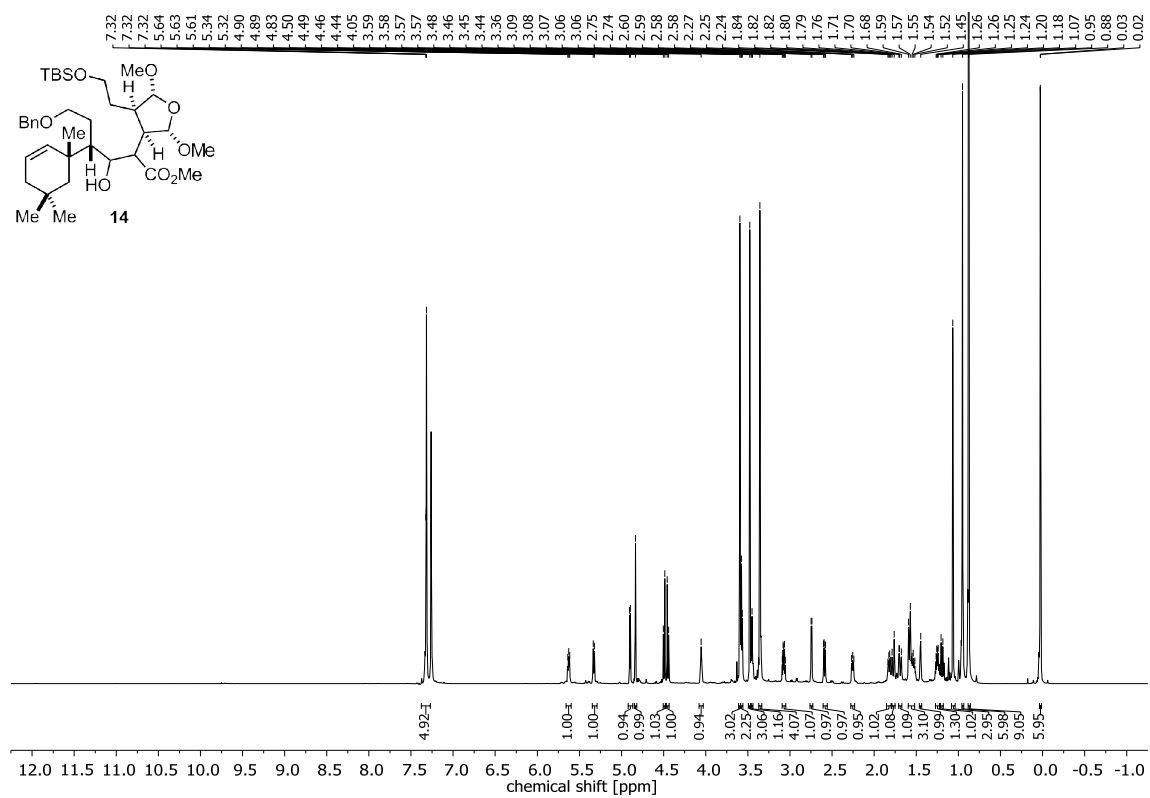
Supporting Information – Synthesis of (+)-Darwinolide



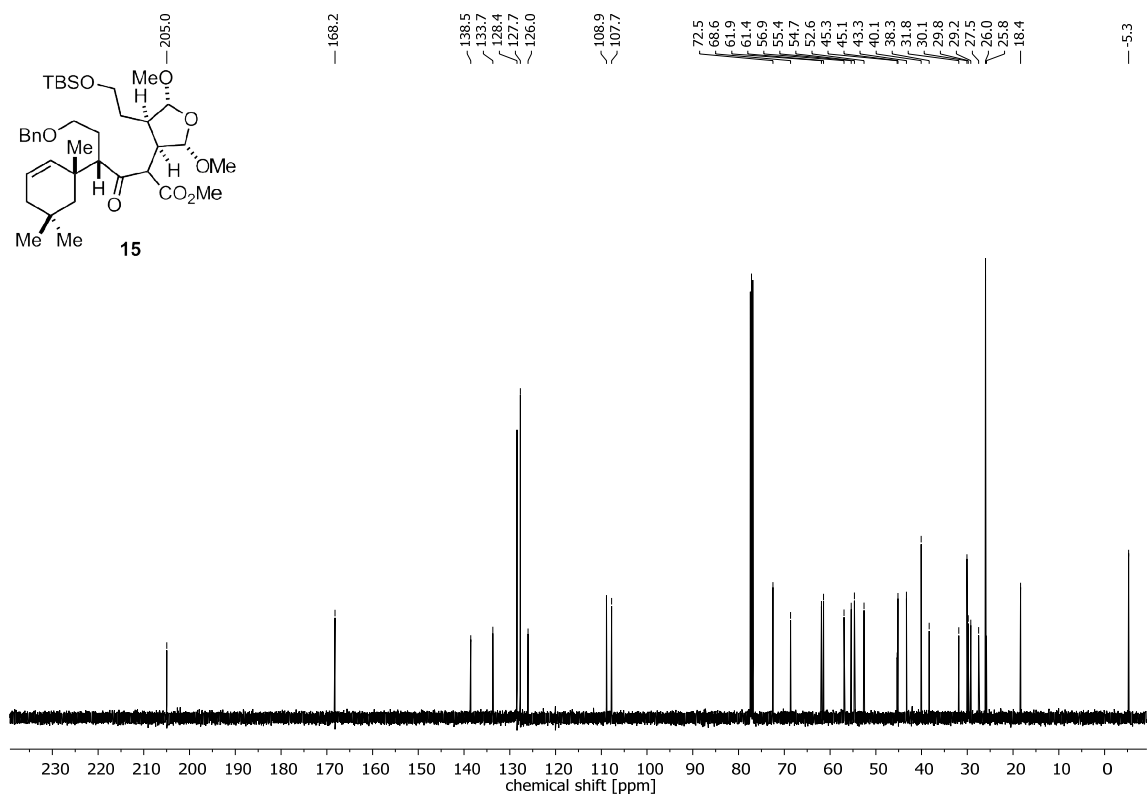
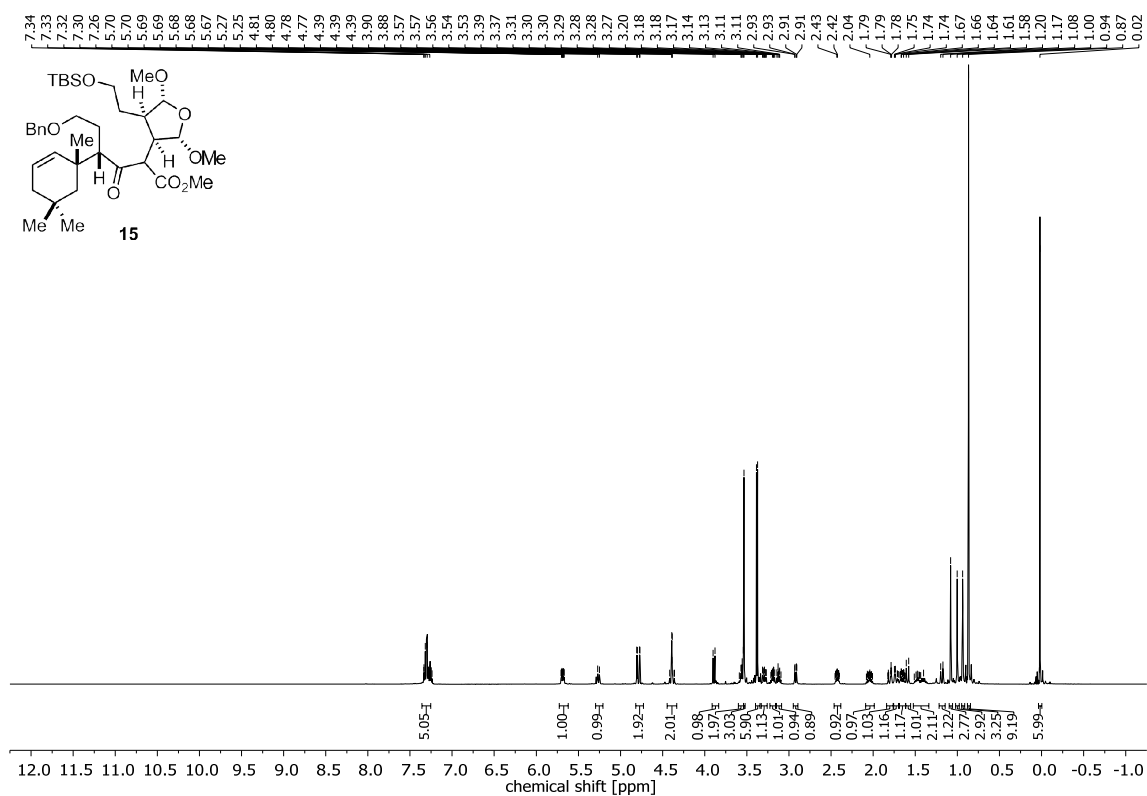
Appendix



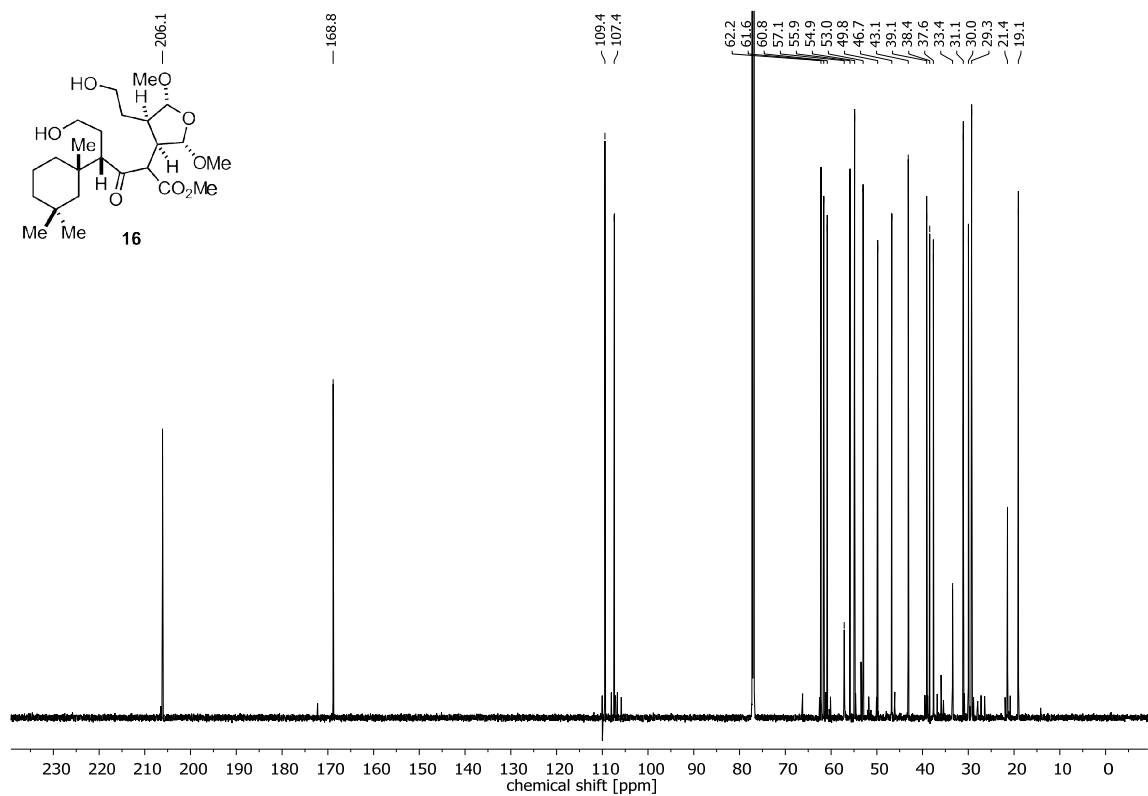
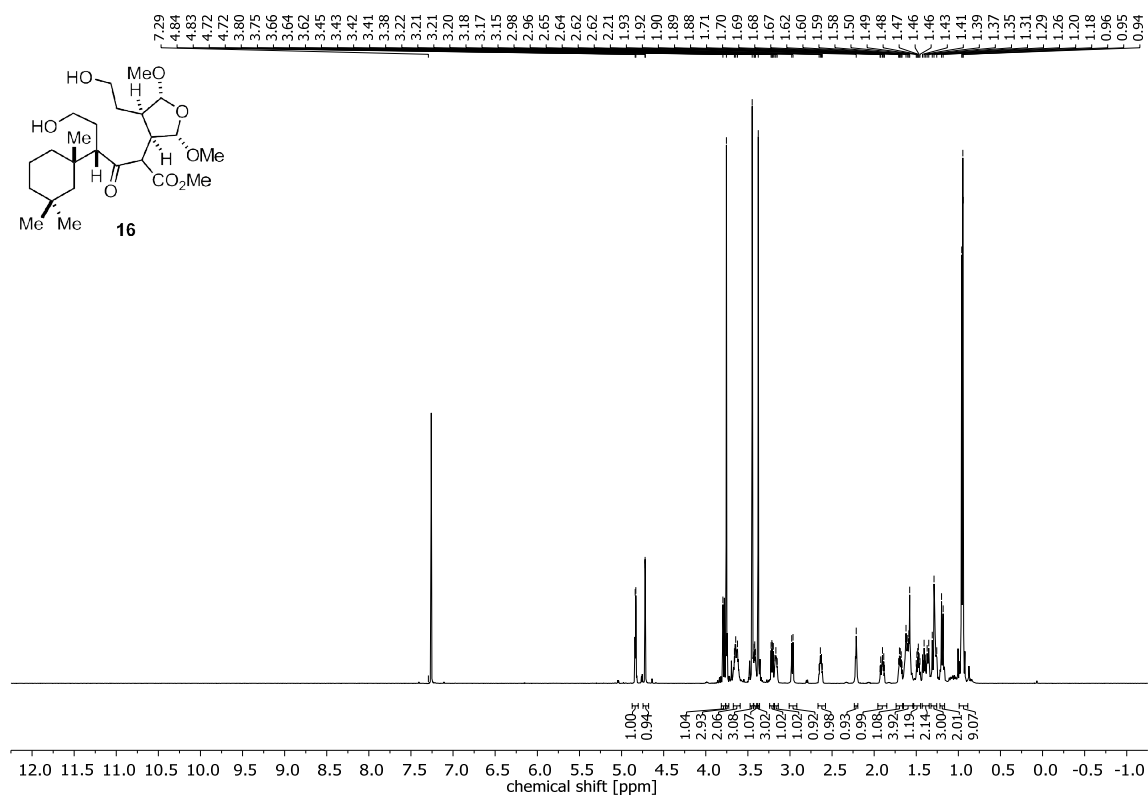
Supporting Information – Synthesis of (+)-Darwinolide



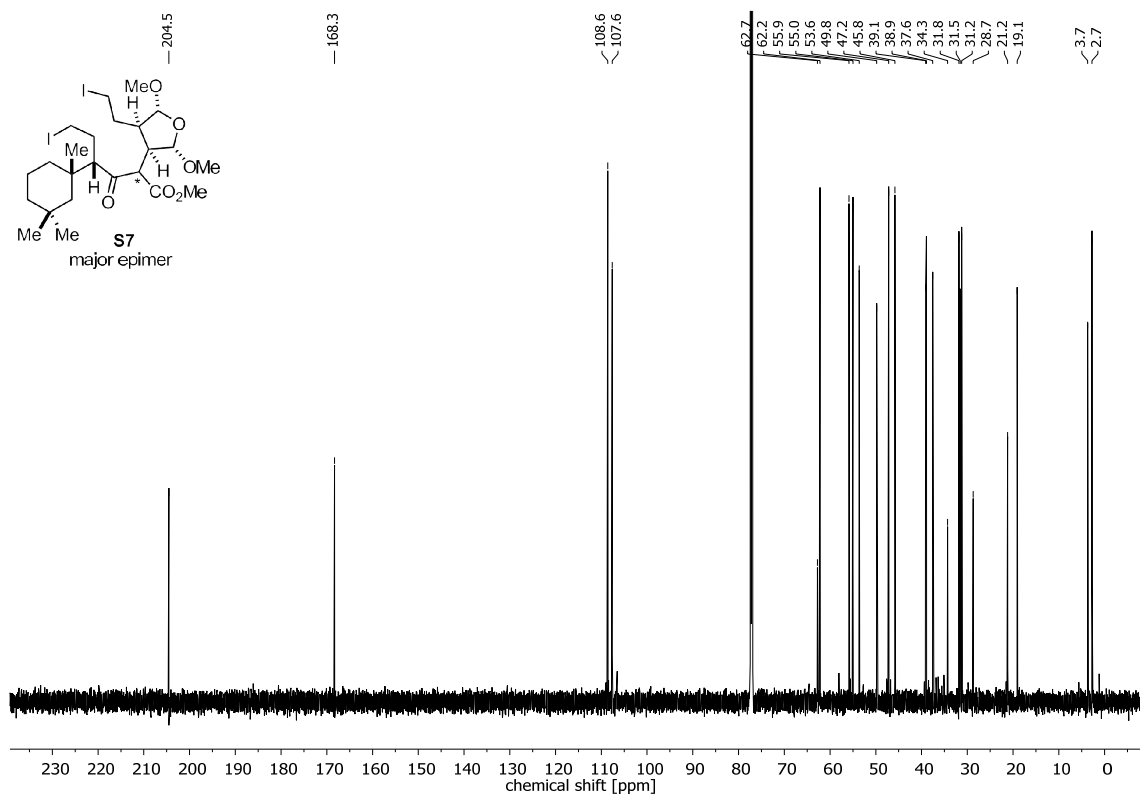
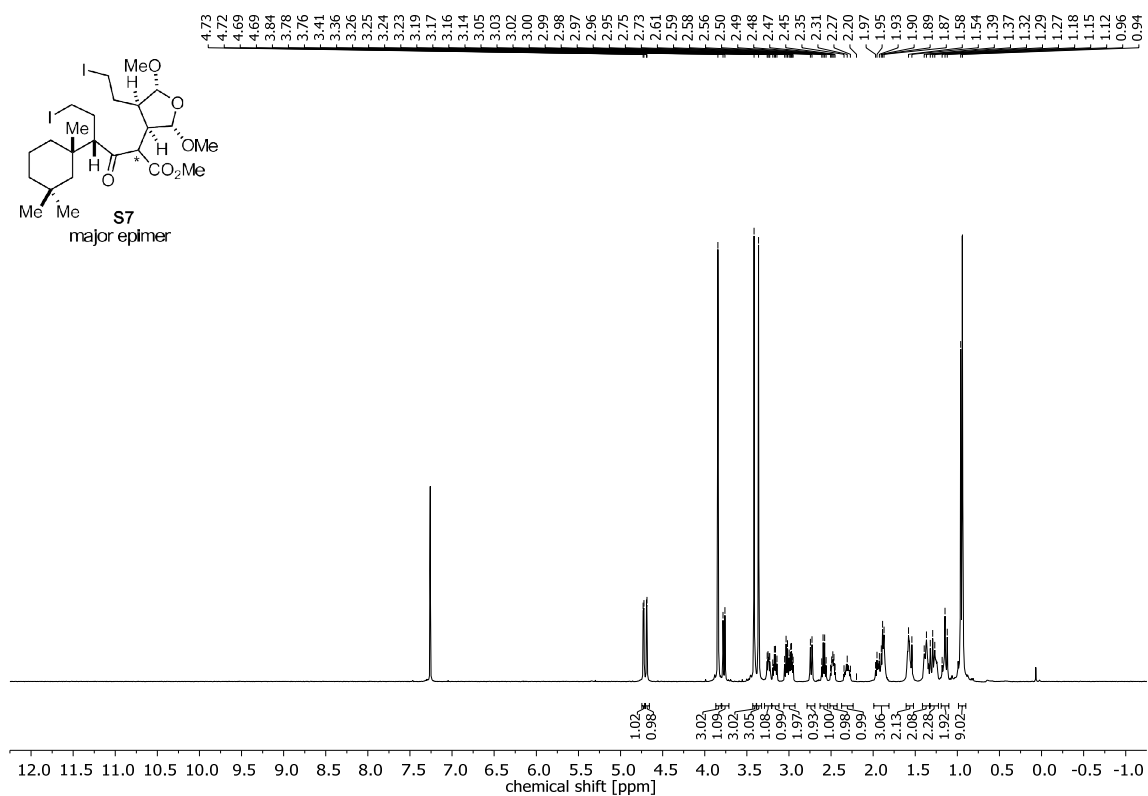
Appendix



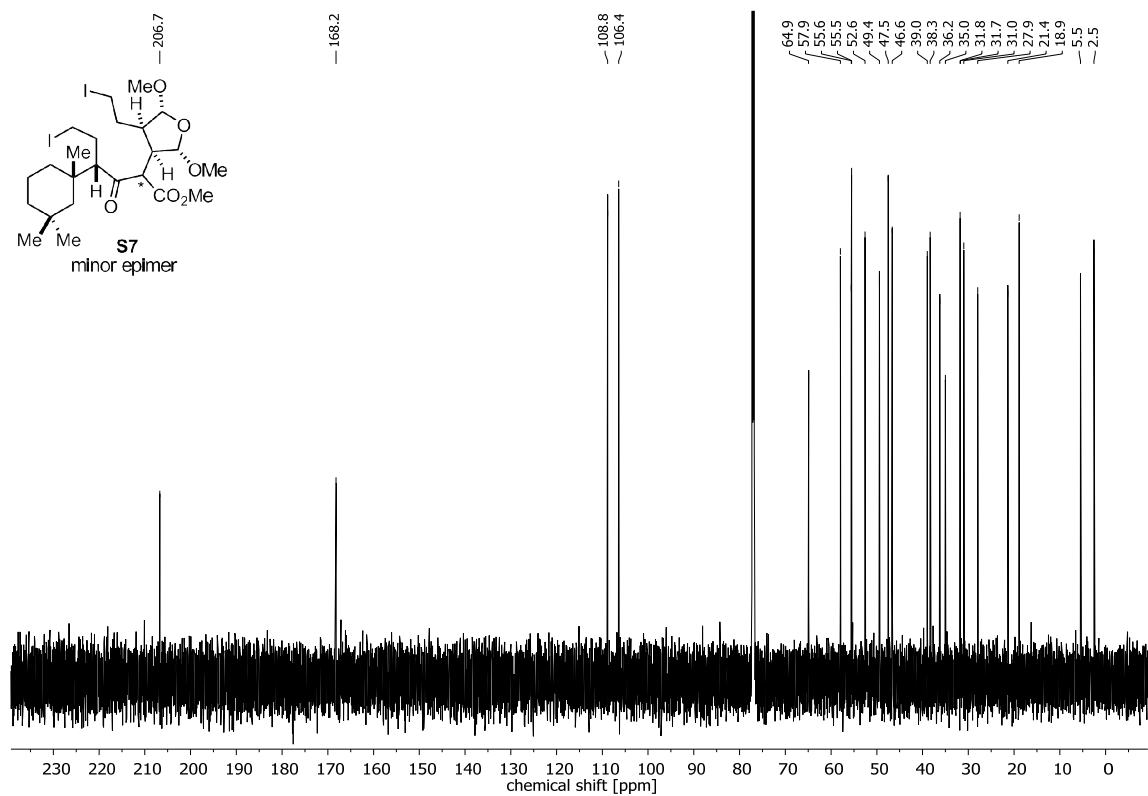
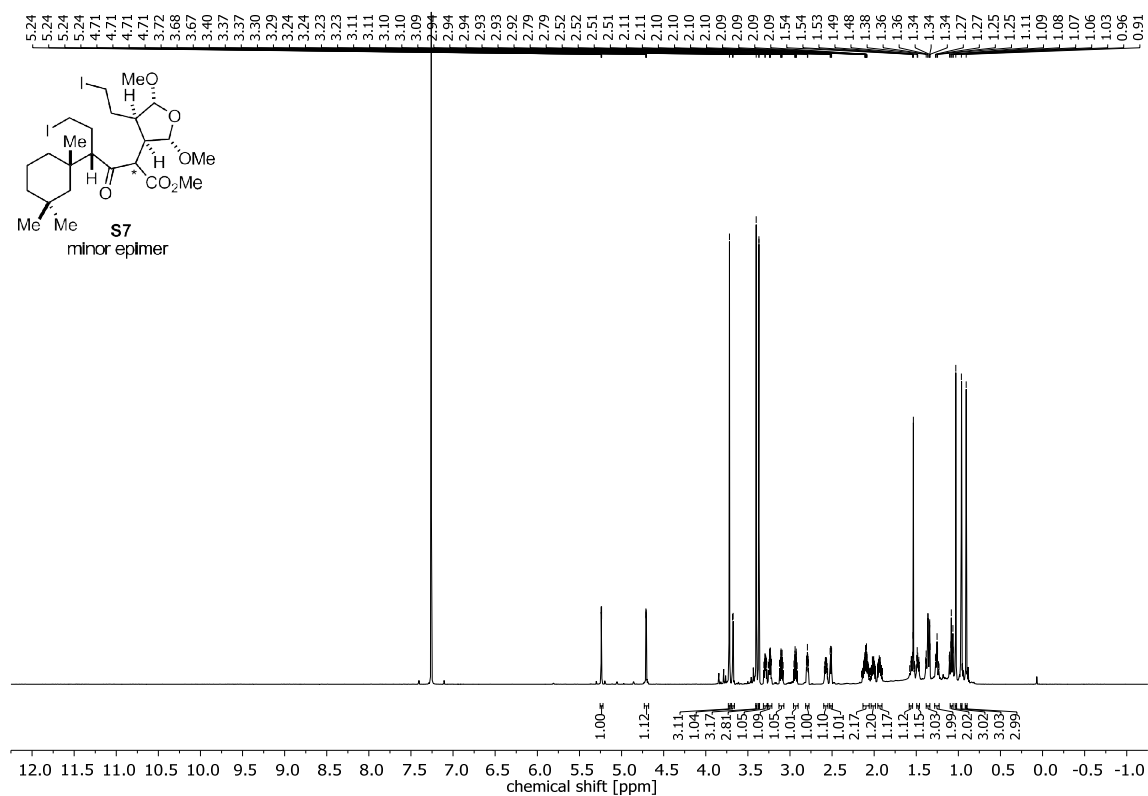
Supporting Information – Synthesis of (+)-Darwinolide



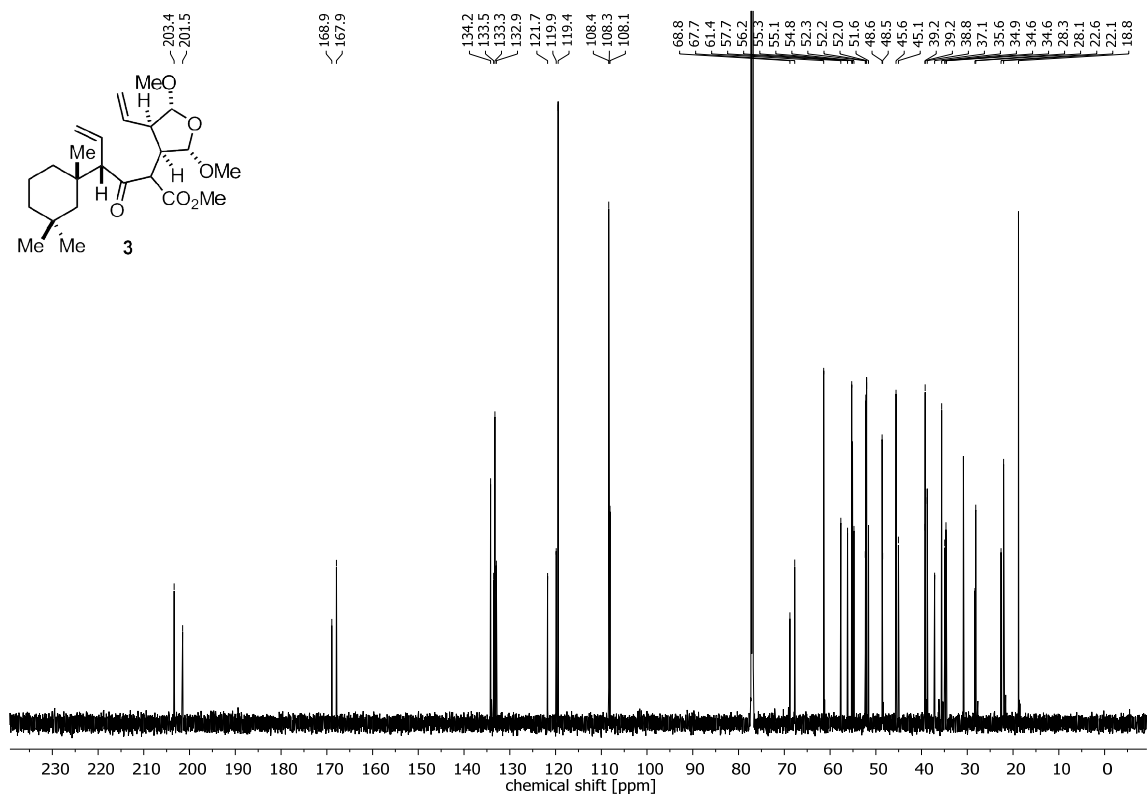
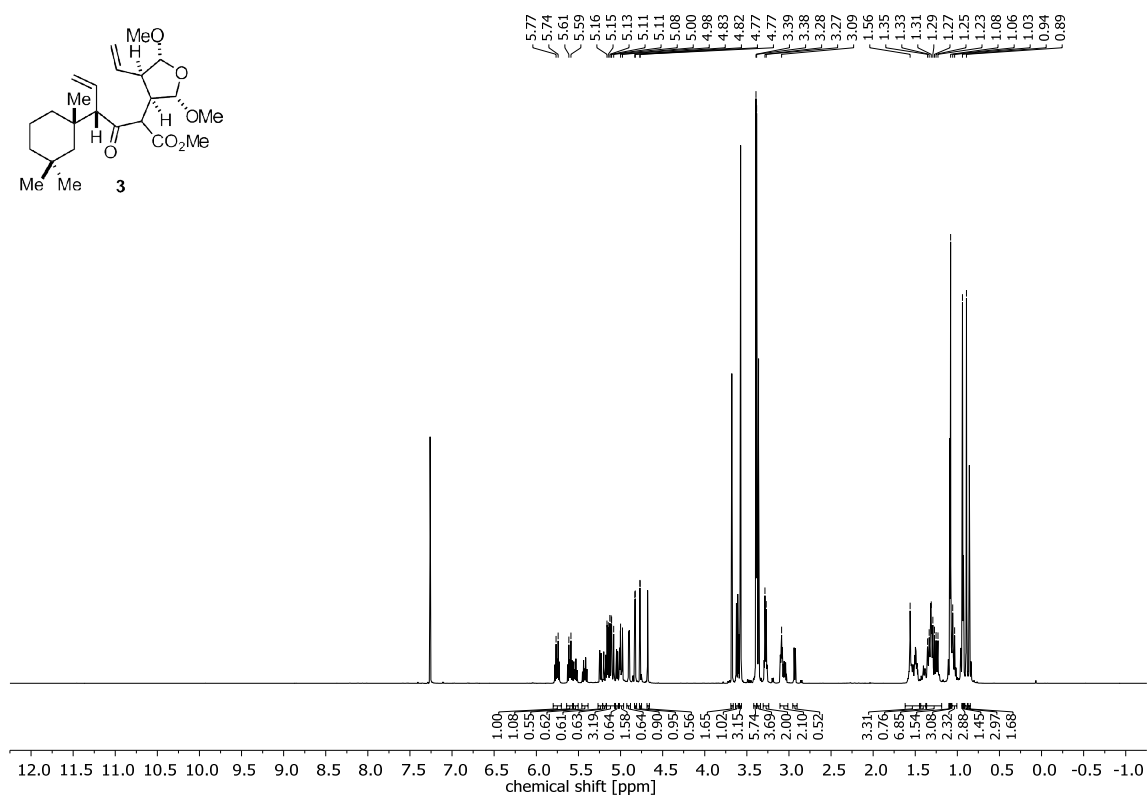
Appendix



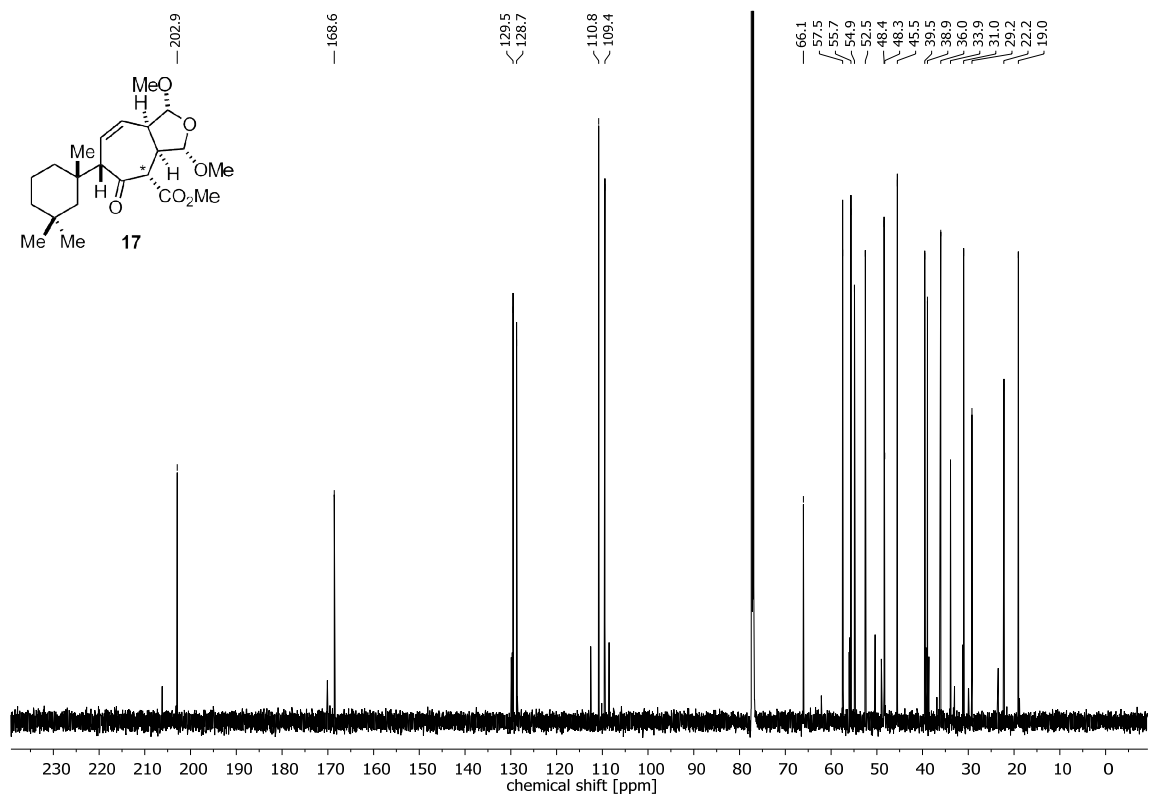
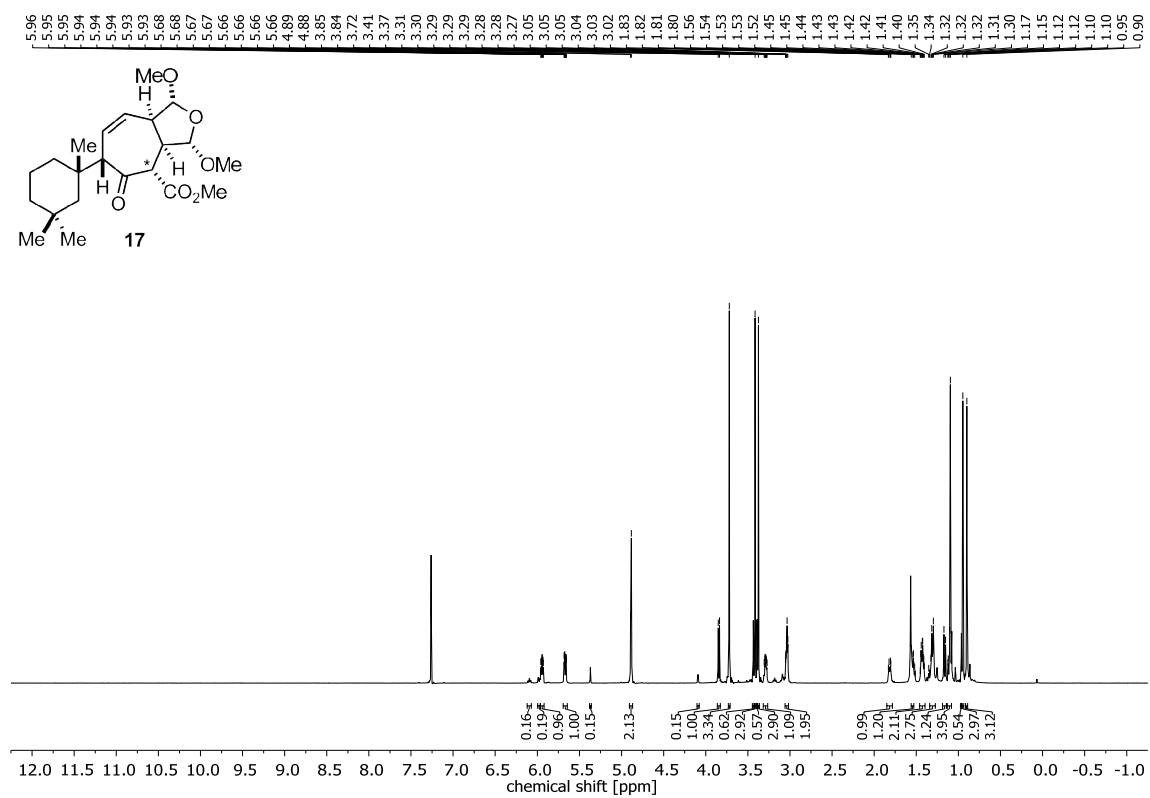
Supporting Information – Synthesis of (+)-Darwinolide



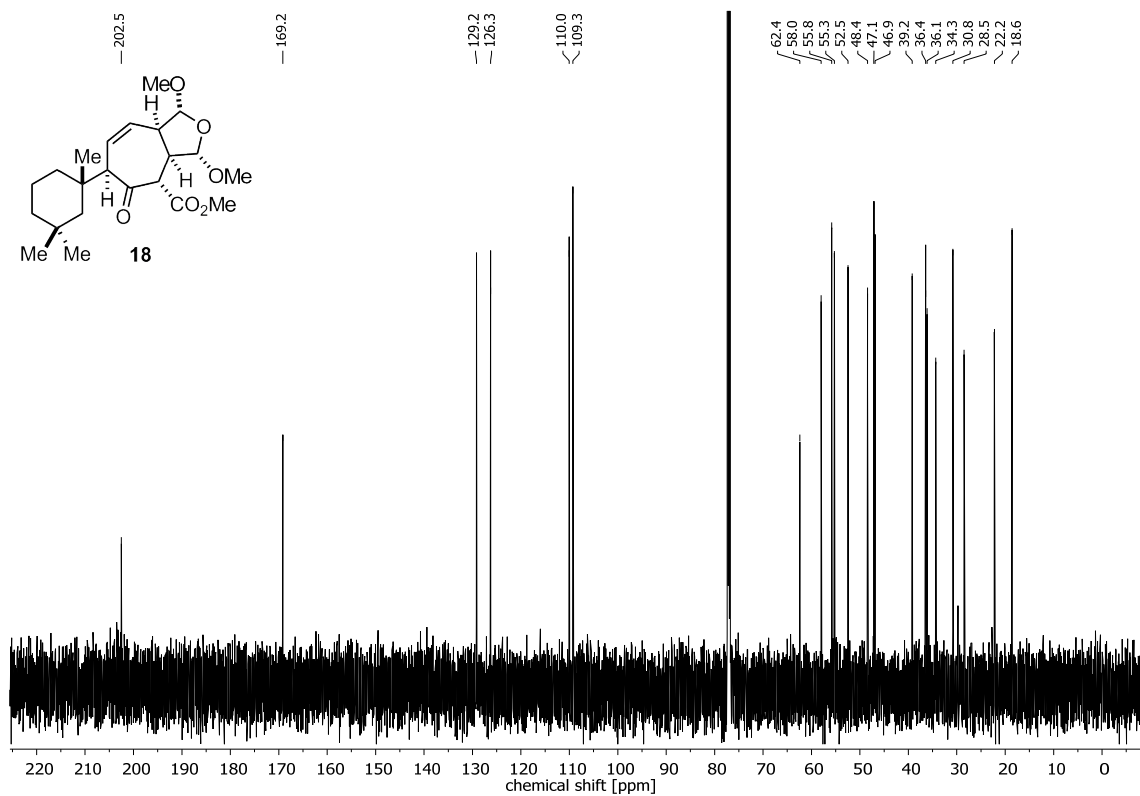
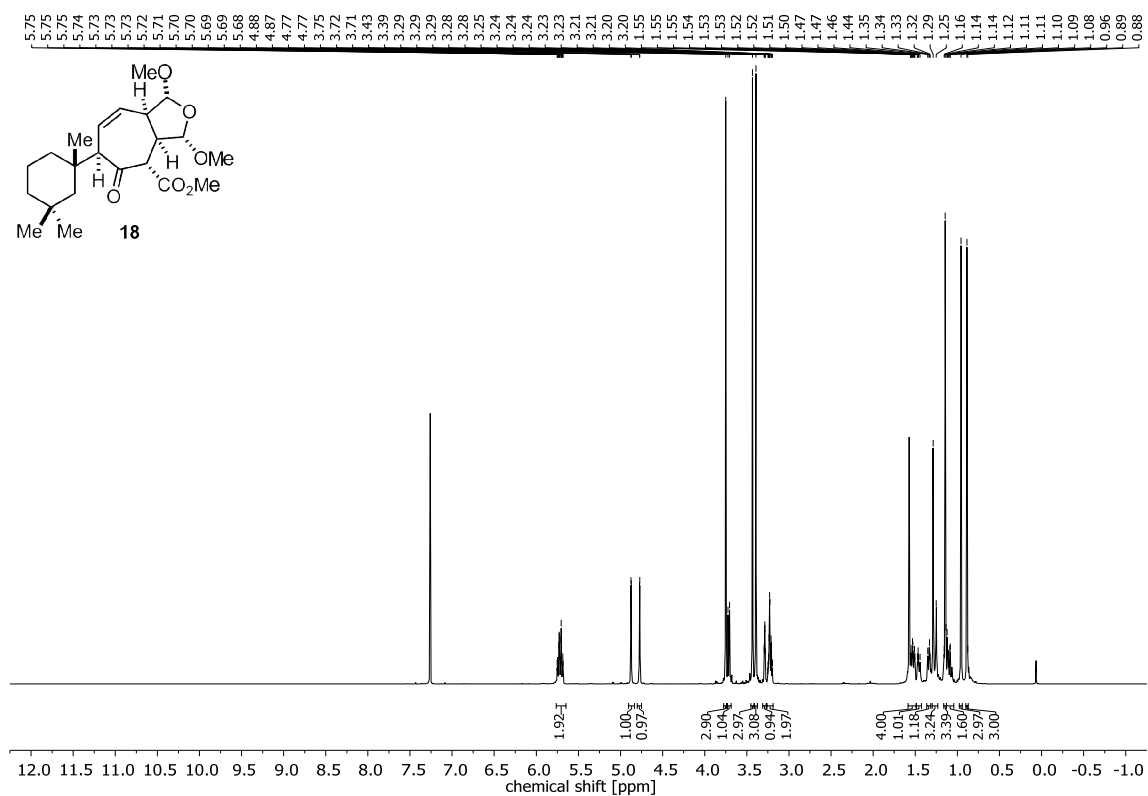
Appendix



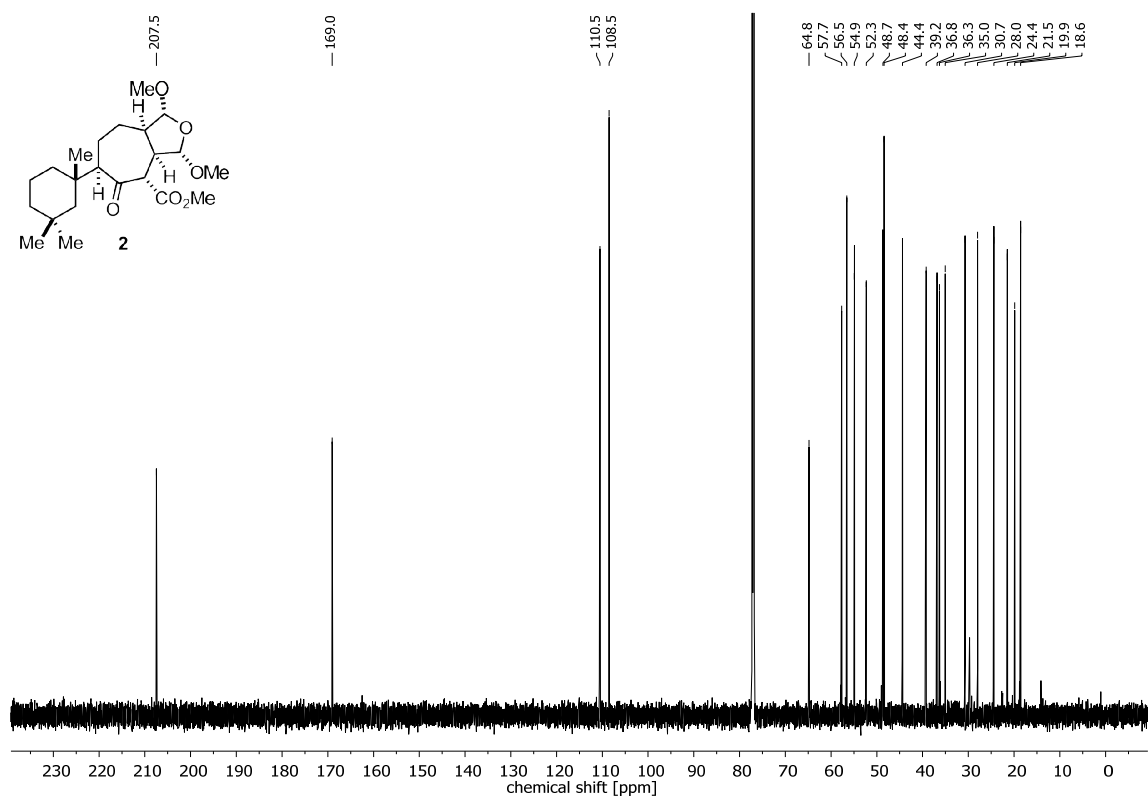
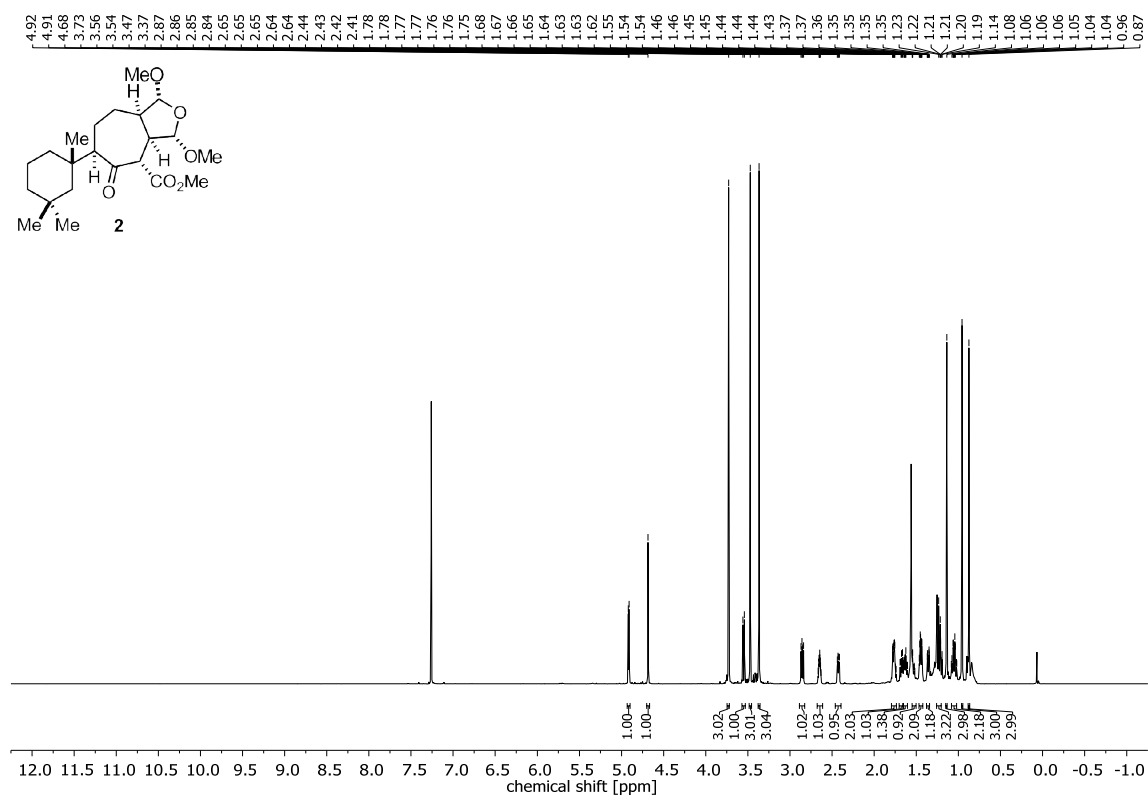
Supporting Information – Synthesis of (+)-Darwinolide



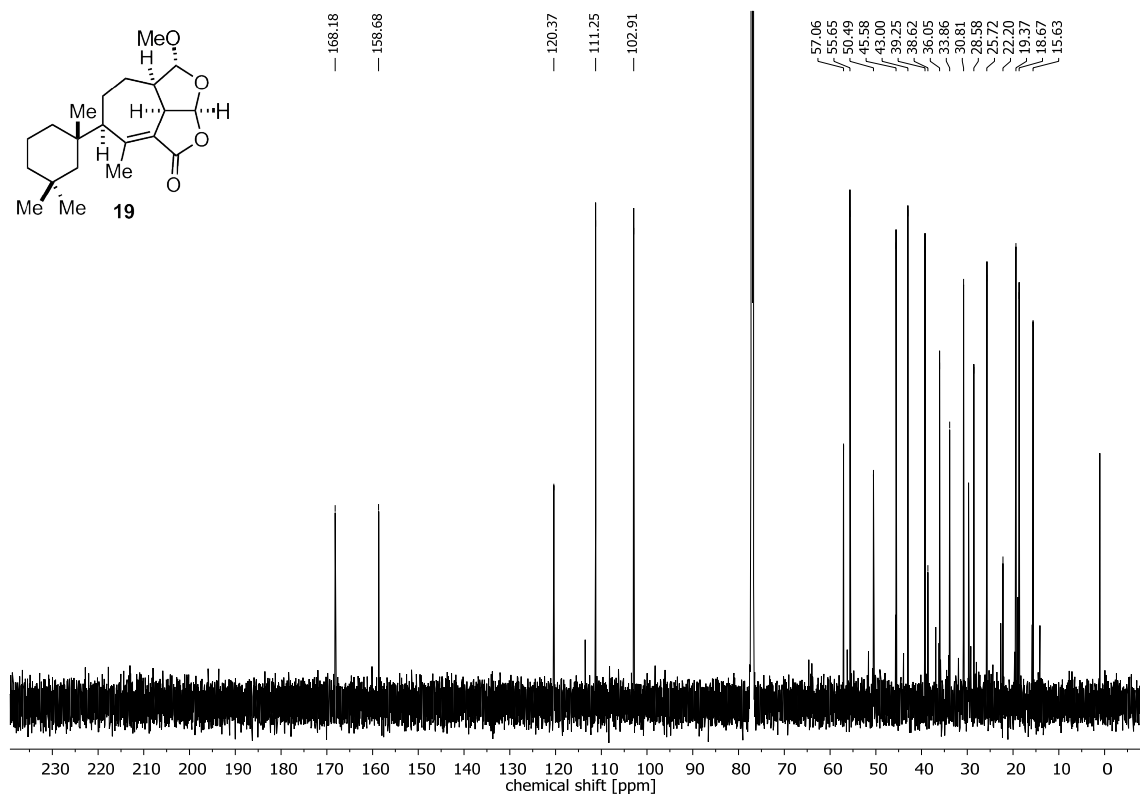
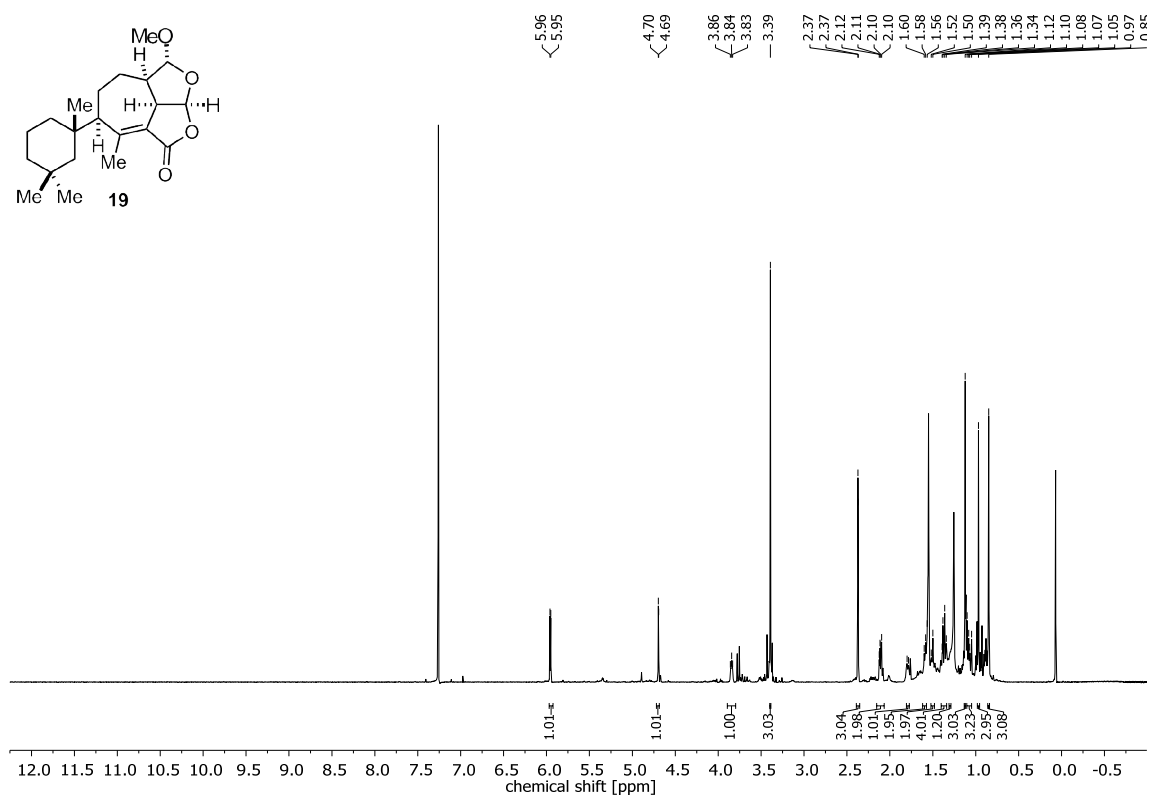
Appendix



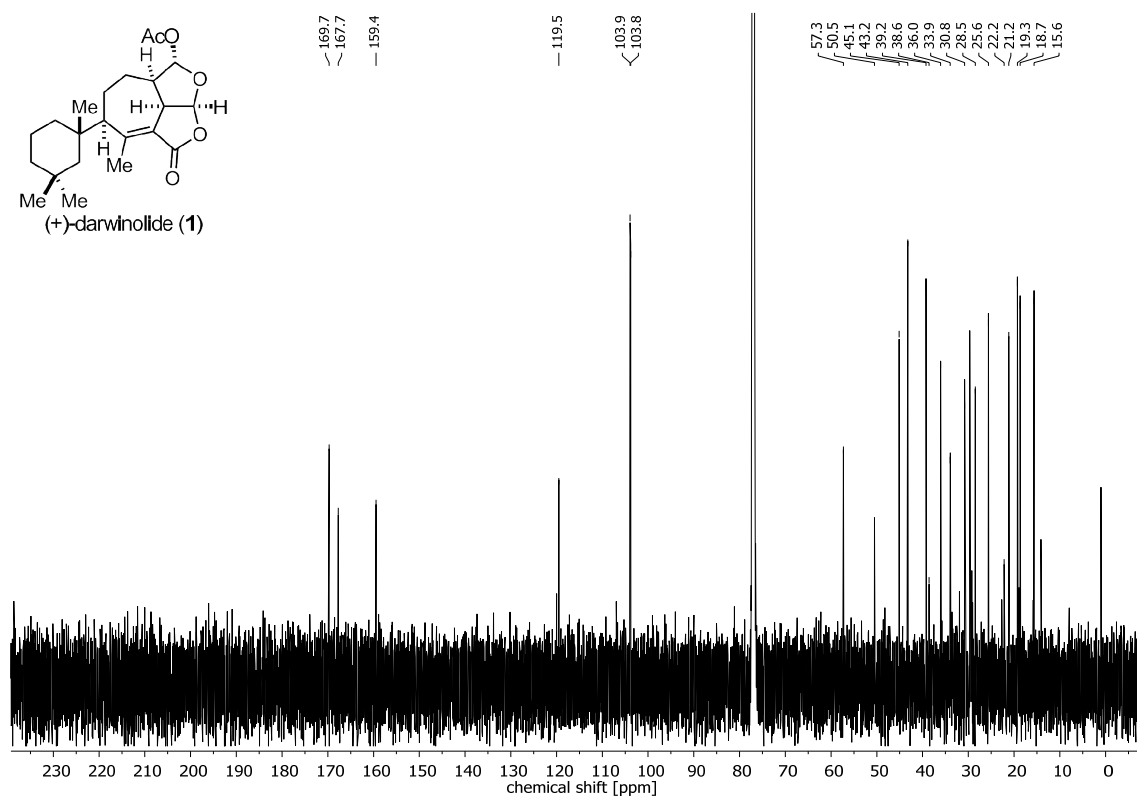
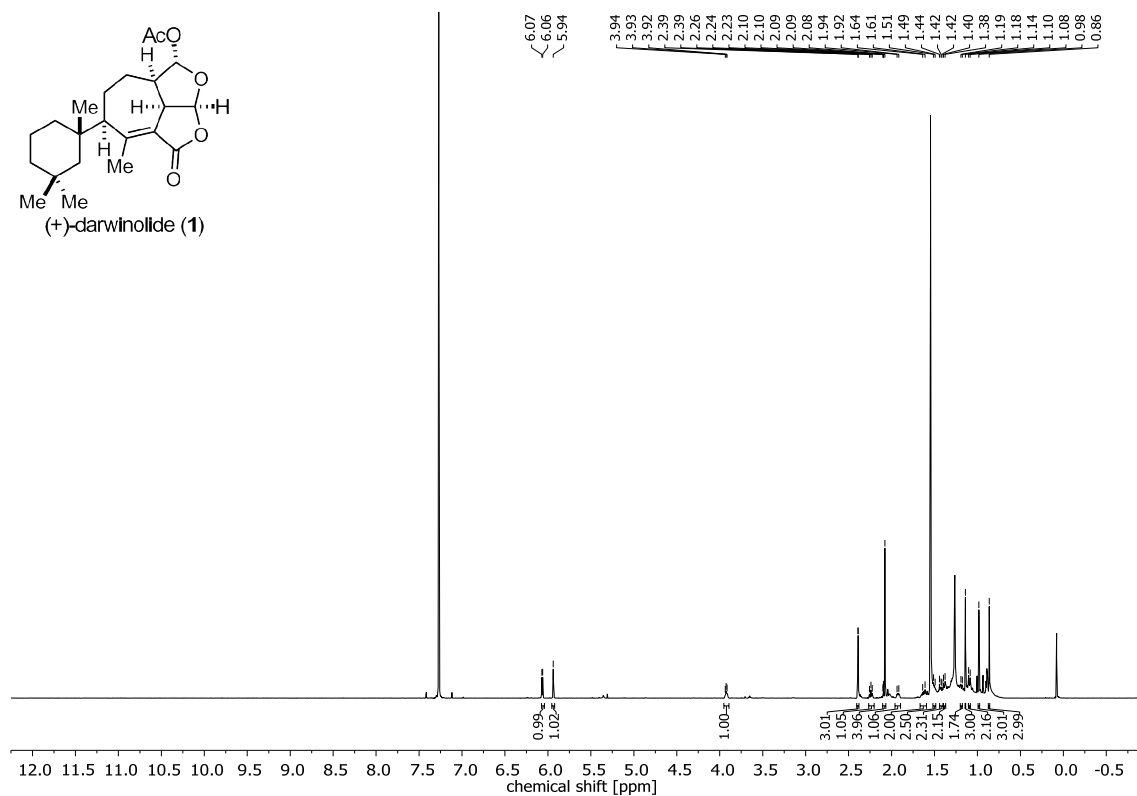
Supporting Information – Synthesis of (+)-Darwinolide



Appendix



Supporting Information – Synthesis of (+)-Darwinolide



Literature

- [1] a) K. Winska, C. Wawrzenczyk, *Pol. J. Chem.* **2007**, *81*, 1887; b) K. Winska, C. Wawrzenczyk, J. Kula, PL209581, (B1), **2011**.
- [2] J. A. Lafontaine, D. P. Provencal, C. Gardelli, J. W. Leahy, *J. Org. Chem.* **2003**, *68*, 4215.
- [3] K. Biswas, O. Prieto, P. J. Goldsmith, S. Woodward, *Angew. Chem. Int. Ed.* **2005**, *44*, 2232.
- [4] M. Ito, A. Osaku, A. Shiibashi, T. Ikariya, *Org. Lett.* **2007**, *9*, 1821.

Supporting Information–Terpene Cyclase Characterization



Supporting Information

Mechanistic Characterisation of Two Sesquiterpene Cyclases from the Plant Pathogenic Fungus *Fusarium fujikuroi*

Immo Burkhardt, Thomas Siemon, Matthias Henrot, Lena Studt, Sarah Rösler, Bettina Tudzynski, Mathias Christmann, and Jeroen S. Dickschat**

anie_201603782_sm_miscellaneous_information.pdf

Table 1. NMR data of enzyme products **1** recorded in C₆D₆ and **2** in CDCl₃.

C ^[a]	1		2	
	¹³ C	¹ H ^[b]	¹³ C	¹ H ^[b]
1	48.09 (CH)	2.33 (m)	120.6 (C _q)	5.34 (m)
2	28.1 (CH ₂)	1.77 (m)	25.6 (CH ₂)	2.04 (m), 1.96 (m)
3	33.2 (CH ₂)	1.76 (m), 1.20 (m)	27.2 (CH ₂)	1.49 (m)
4	37.2 (CH)	2.14 (m)	37.1 (CH)	1.53 (m)
5	48.07 (CH)	2.35 (m)	38.2 (C _q)	-
6	124.4 (CH)	5.66 (br d, <i>J</i> =2.8)	39.9 (CH ₂)	1.54 (m)
7	148.7 (C _q)	-	38.6 (CH)	2.04 (m)
8	30.4 (CH ₂)	2.14 (m), 2.00 (m)	30.2 (CH ₂)	1.68 (m)
9	37.81 (CH ₂)	2.51 (dd, <i>J</i> =12.5, 8.7), 2.04 (m)	28.5 (CH ₂)	2.39 (m), 1.96 (m)
10	154.6 (C _q)	-	144.2 (C _q)	-
11	37.80 (CH)	2.20 (sept, <i>J</i> =6.8)	150.2 (C _q)	-
12	21.7 (CH ₃)	0.98 (d, <i>J</i> =6.8)	108.4 (CH ₂)	4.73 (br s Z-H), 4.70 (br s, E-H)
13	21.5 (CH ₃)	0.99 (d, <i>J</i> =6.9)	21.7 (CH ₃)	1.73 (s)
14	106.7 (CH ₂)	4.85 (br s, E-H), 4.83 (br s, Z-H)	20.4 (CH ₃)	0.92 (s)
15	17.3 (CH ₃)	0.91 (d, <i>J</i> =7.1)	16.2 (CH ₃)	0.87 (d, <i>J</i> =6.6)

[a] Carbon numbering as shown in Figure 1 of main text. [b] Coupling constants *J* in Hz, multiplicities: m=multiplett, s=singlet, d=doublet, sept=septet, br=broad.

Primer used in this study

Overhangs for cloning and mutation sites are highlighted in bold.

Designation	Sequence
GPD-Ff-STC3-F	TACCCCGCTTGAGCAGAC ATATGATTGCGACTATAAACGGAGACAC
GPD-Ff-STC3-R	CGGATAACAATTTACACAGGAAACAGC TACAAGACGAACTGGTTGAAGGAGC
GPD-Ff-STC5-F	TACCCCGCTTGAGCAGAC ATATGGTCAAATTTGATAGTGGTTCTGAGTCCG
GPD-Ff-STC5-R	GCGGATAACAATTTACACAGGAAACAGC ATACTACTAACGATTTCGATCTGGAACC
GPD-dia-for	CATCTTCCCATCCAAGAACC
Invitro_STC3_F	GGCAGCCATATGGCTAGCATGACTGGTGGAA TGATTGCGACTATAAACGGAGACAC
Invitro_STC3_R	GGCAGCCATATGGCTAGCATGACTGGTGGAT CACACAGCAATAGGTTCCAAATCTG
Invitro_FfSTC5_F	GGCAGCCATATGGCTAGCATGACTGGTGGAA TGGTCAAATTTGATAGTGGTTCTGAGTCC
Invitro_FfSTC5_R	TCTCAGTGGTGGTGGTGGTGGTGGTGGTGG CTCGAGTTTACAACGCTGCCATCTTCTTTGG
Invitro_FmanSTC5_F	GCCATATGGCTAGCATGACTGGTGGAA TGGTCAAATTCGATAGTGGTTC
Invitro_FmanSTC5_R	TCTCAGTGGTGGTGGTGGTGGTGGTGGTGG CTCGAGTTTACAACGCTGCCATCTTCTTTGG
Invitro_FpET1STC5_F	GGCAGCCATATGGCTAGCATGACTGGTGGAA TGGTCAAATTTGATAGTGGTTCTGAG
Invitro_FpET1STC5_R	TCTCAGTGGTGGTGGTGGTGGTGGTGGTGG CTCGAGTTTACAACGCTGCCATCTTCTTTGG
STC5-Mut-F	CAGATCCTGTTAGTCAATGACATTCTCTCC
STC5-Mut-R	GGAGAGAATGTCATTGACTAACAGGATCTG

General synthetic and analytical methods

Chemicals were purchased from Acros Organics (Geel, Belgium) or Sigma Aldrich Chemie GmbH (Steinheim, Germany) and used without purification. Thin-layer chromatography was performed with 0.2 mm precoated plastic sheets Polygram® Sil G/UV254 (Machery-Nagel). Column chromatography was carried out using Merck silica gel 60 (70-200 mesh). ¹H NMR and ¹³C NMR spectra were recorded on Bruker AV I (400 MHz), AV III HD Prodigy (500 MHz) and AV III HD Cryo (700 MHz) spectrometers, and were referenced against CDCl₃ (δ = 7.26 ppm) and C₆D₆ (δ = 7.16 ppm) for ¹H-NMR and CDCl₃ (δ = 77.01 ppm) and C₆D₆ (δ = 128.06 ppm) for ¹³C-NMR. GC- MS analyses were carried out with a HP 7890B gas chromatograph connected to a HP 5977A inert mass detector fitted with parameters were (1) inlet pressure, 77.1 kPa, He 23.3 mL min⁻¹, (2) injection volume, 2 μ L, (3) transfer line, 250 °C, and (4) electron energy 70 eV. The GC was programmed as follows: 5 min at 50 °C increasing at 10 °C min⁻¹ to 320 °C, and operated in split mode (50:1, 60 s valve time). The carrier gas was He at 1 mL min⁻¹. Retention indices (I) were determined from a homologous series of n-alkanes (C₈-C₄₀). Optical rotary powers were recorded on a Krüss P8000 Polarimeter.

Strains and culture conditions

F. fujikuroi IMI58289 wild type as well as *STC3* and *STC5* overexpression strains were grown on CM agar medium for 3-5 days and directly subjected to headspace analysis as previously described.^[1]

Overexpression of *STC3* and *STC5*

For the generation of the *STC3* and *STC5* overexpression vectors pOE::*FfSTC3* and pOE::*FfSTC5* the respective genes were amplified using the primer pairs GPD-Ff-*STC3*-F//R and GPD-*STC5*-F//R. The amplicons were cloned into the vector pgpd_gen,^[2] containing the geneticin-resistance cassette^[3] and the constitutive *gpd* promoter amplified from *pveAgfp*^[4] by yeast recombination cloning.^[5] Plasmid DNA was extracted from yeast by using the GeneJET Plasmid Miniprep Kit (Fermentas/Thermo Scientific), amplified in *Escherichia coli* and sequenced using the BigDye Terminator v3.1 cycle sequencing kit according to the manufacturer's instructions.

Generation of in vitro expression vectors

The cDNA fragments of the *STC* genes were amplified by using primer pairs Invitro_*STC3*_F//R, Invitro_*FfSTC5*_F//R, Invitro_*FmSTC5*_F//R and Invitro_*FpET1STC5*_F//R, respectively. The fragments were cloned into the yeast-to-*E. coli* shuttle vector pYE-Express by homologous recombination as previously described.^[6] Sequence correction of *F. fujikuroi STC5* by construction of a K288N mutant was done by amplifying two overlapping fragments of *FfSTC5* with the primer pairs Invitro_*FfSTC5*_F//*STC5*-Mut-R and *STC5*-Mut-F//Invitro_*FfSTC5*_R and subsequent cloning into the vector pYE-Express. Correct assembly of the generated plasmids was verified by restriction and sequencing.

Fungal transformations

Preparation of protoplasts and transformation of *F. fujikuroi* was carried out as described.^[4] For overexpression of *STC3* and *STC5* genes, the mutant strain SG139/ Δ *ffsc6*/ Δ *ffsc4*^[1] with deletions of the terpene cyclases for the gibberellin, acorenol and koraiol biosynthesis was transformed with 10 μ g of either vector pOE::*FfSTC5* or pOE::*FfSTC3*. Transformed protoplasts were regenerated in selection agar containing geneticin (100 μ g mL⁻¹). Integration of pOE::*FfSTC3* and pOE::*FfSTC5* was verified by diagnostic PCR using the primer pairs GPD-dia-for//GPD-Ff-*STC3*-R and GPD-dia-for//GPD-Ff-*STC5*-R, respectively. Overexpression of the genes *STC3* and *STC5* was verified by Northern blot analyses.

Transformation of *E. coli*, expression and purification of recombinant enzyme

E. coli BL21 was transformed with the expression plasmids by electroporation and the obtained transformants were precultured in 2YT liquid medium (16 g tryptone, 10 g yeast extract, 5 g NaCl, 1L water, 50 µg/L Kanamycin, pH 7.2, 35 mL) overnight. An aliquot from these cultures was used to inoculate expression cultures in 2YT liquid medium (8 L, 50 µg/L Kanamycin), which were grown to an OD₆₀₀ = 0.4 at 37 °C and 160 rpm and subsequently cooled to 18 °C for 30 minutes. Expression was induced by addition of IPTG (400 µM) and continued at 18 °C and 160 rpm overnight. Cells were harvested by centrifugation at 5.100 g for 1 hour. The obtained cell pellets were resuspended in 15 mL lysis buffer (20 mM Na₂HPO₄, 0.5 M NaCl, 20 mM imidazole, 1 mM MgCl₂, pH 7.0) for 1 L of harvested culture and ultra-sonicated on ice for 7 x 60 seconds. The water soluble fraction was obtained by centrifugation at 12.900 g for 2 x 10 minutes and filtration through a 20 µm cellulose filter. The target enzyme was purified in two 60 mL portions via Ni²⁺-NTA-affinity chromatography with Ni²⁺-NTA superflow (Novagen, 30 mL) using binding buffer (20 mM Na₂HPO₄, 0.5 M NaCl, 20 mM imidazole, 1 mM MgCl₂, pH 7) for 2 x 20 mL washings and elution buffer (20 mM Na₂HPO₄, 0.5 M NaCl, 500 mM imidazole, 1 mM MgCl₂, pH 7) for 2 x 25 mL elutions. All wash and elution fractions were checked by SDS-PAGE.

Incubation of purified enzyme and product isolation on preparative scale

Product of STC 5:

Incubation was performed using the collected pure enzyme fractions (100 mL) mixed with 50 mL 30 % (v/v) glycerine. This solution was stirred at 200 rpm and 28 °C while 50 mL of water containing 1 mg/mL FPP were added dropwise over 1 hour using a syringe pump. Incubation was continued at 28 °C and 160 rpm overnight. The reaction mixture was extracted with 3 x 100 mL pentane and the combined organic layers were dried over MgSO₄ and concentrated in vacuo. Purification of the crude Product (15.1 mg) via repeated column chromatography on silica gel (100 % pentane, 7 °C) yielded 1 mg of (–)-guaia-6,10(14)-diene (**1**).

Product of STC 3:

Incubation was performed using the collected pure enzyme fractions (100 mL) diluted with 20 mL of water containing 3 mg/mL FPP at 28 °C and 160 rpm overnight. The reaction mixture was extracted with 3 x 60 mL pentane and the combined organic layers were dried over MgSO₄ and concentrated in vacuo. Purification of the crude product (9.6 mg) via column chromatography on silica gel (100% pentane, 7 °C) yielded 4.6 mg of (+)-eremophilene (**2**).

Expression and purification of recombinant enzyme on analytical scale in H₂O

An aliquot of preculture was used to inoculate expression cultures in 2YT liquid medium (500 mL, 50 µg/L Kanamycin), which were grown to an OD₆₀₀ = 0.4 at 37 °C and 160 rpm and subsequently cooled to 18 °C for 30 minutes. Expression was induced by addition of IPTG (400 µM) and continued at 18 °C and 160 rpm overnight. Cells were harvested by centrifugation at 5.100 g for 1 hour. The obtained cell pellets were resuspended in 10 mL lysis buffer (20 mM Na₂HPO₄, 0.5 M NaCl, 20 mM imidazole, 1 mM MgCl₂, pH 7.0) for 500 mL of harvested culture and ultra-sonicated on ice for 7 x 30 seconds. The water soluble fraction was obtained by centrifugation at 12.900 g for 2 x 10 minutes and filtration through a 20 µm cellulose filter. The target enzyme was purified via Ni²⁺-NTA-affinity chromatography with Ni²⁺-NTA superflow (Novagen, 5 mL) using binding buffer (20 mM Na₂HPO₄, 0.5 M NaCl, 20 mM imidazole, 1 mM MgCl₂, pH 7) for 2 x 10 mL washings and elution buffer (20 mM Na₂HPO₄, 0.5 M NaCl, 500 mM imidazole, 1 mM MgCl₂, pH 7) for 2 x 10 mL elutions. All wash and elution fractions were checked by SDS-PAGE.

Expression and purification of recombinant enzyme on analytical scale in D₂O

An aliquot of preculture was used to inoculate expression cultures in 2YT liquid medium (500 mL, 50 µg/L Kanamycin), which were grown to an OD₆₀₀ = 0.4 at 37 °C and 160 rpm and subsequently cooled to 18 °C for 30 minutes. Expression was induced by addition of IPTG (400 µM) and continued at 18 °C and 160 rpm overnight. Cells were harvested by centrifugation at 5.100 g for 1 hour. The obtained cell pellets were resuspended in 10 mL lysis buffer (20 mM Na₂HPO₄, 0.5 M NaCl, 20 mM imidazole, 1 mM MgCl₂, pH 7.0) for 500 mL of harvested culture and ultra-sonicated on ice for 7 x 30 seconds. The water soluble fraction was obtained by centrifugation at 12.900 g for 2 x 10 minutes and filtration through a 20 µm cellulose filter. The target enzyme was purified via Ni²⁺-NTA-affinity chromatography with Ni²⁺-NTA superflow (Novagen, 5 mL) using binding buffer (20 mM Na₂HPO₄, 0.5 M NaCl, 20 mM imidazole, 1 mM MgCl₂, pH 7) for 2 x 10 mL washings, D₂O binding buffer (D₂O, 20 mM Na₂HPO₄, 0.5 M NaCl, 20 mM imidazole, 1 mM MgCl₂, pH 7) for 1 x 5 mL washings and D₂O elution buffer (D₂O, 20 mM Na₂HPO₄, 0.5 M NaCl, 500 mM imidazole, 1 mM MgCl₂, pH 7) for 2 x 5 mL elutions. All wash and elution fractions were checked by SDS-PAGE.

Incubations of purified enzyme on analytical scale

The pure enzyme fractions were concentrated by centrifugation using Vivaspin20 tubes (Sartorius stedim, Göttingen) to volume of 3 mL and was mixed with 4 mL 1 mg/mL FPP solution (in H₂O or D₂O for the respective experiments) and incubated at 28 °C and 160 rpm overnight. The reaction mixture was extracted with 2 x 0.5 mL C₆D₆ or CDCl₃, dried over MgSO₄ and analyzed directly by NMR and GC/MS.

Analytical data of isolated compounds

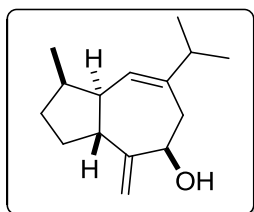
(-)-Guaia-6,10(14)-diene (1): $R_f = 0.97$ (pentane); GC: (HP5-MS) $I = 1495$; $[\alpha]_D^{22.0} = -19.3$ ($c = 0.15$, CH_2Cl_2), MS (EI 70 ev): m/z (%) = 204 (63), 189 (31), 175 (6), 161 (100), 147 (20), 133 (44), 121 (44), 120 (15), 119 (48), 107 (26), 106 (10), 105 (60), 95 (14), 94 (15), 93 (27), 92 (10), 91 (56), 81 (31), 79 (25), 77 (9), 69 (8), 67 (16), 65 (5), 55 (13), 41 (14); HREIMS: calculated for $[\text{C}_{15}\text{H}_{24}]^+$ 204,1873, found 204.1875.

(+)-Eremophilene (2): $R_f = 0.78$ (pentane); GC: (HP5-MS) $I = 1368$; $[\alpha]_D^{22.0} = +86.1$ ($c = 0.15$, CHCl_3); MS (EI 70 ev): m/z (%) = 204 (48), 189 (38), 175 (11), 161 (100), 147 (46), 135 (35), 134 (25), 121 (35), 120 (22), 119 (73), 108 (50), 107 (79), 106 (74), 94 (38), 93 (87), 92 (66), 80 (38), 79 (64), 78 (26), 69 (16), 67 (25), 65 (11), 55 (30), 43 (8), 41 (36), 39 (9); HREIMS: calculated for $[\text{C}_{15}\text{H}_{24}]^+$ 204,1873, found 204.1872.

NMR-data are listed in the main text (Table 1).

Synthetic procedures

Compound 4



Chemical Formula: $\text{C}_{15}\text{H}_{24}\text{O}$
Molecular Weight: 220,3505

A solution of DIAD (22.7 μL , 23.3 mg, 0.116 mmol, 1.1 equiv) in dry CH_2Cl_2 (0.5 mL) was added at 0 °C under an argon atmosphere with a syringe pump over 1 h to a stirred solution of **3** (25 mg, 0.105 mmol, 1 equiv), DIPEA (27 μL , 20.3 mg, 0.158 mmol, 1.5 equiv) and PBU_3 (40 μL , 32 mg, 0.158 mmol, 1.5 equiv) in dry CH_2Cl_2 (0.5 mL). The mixture was allowed to stir at 20 °C overnight. The mixture was then concentrated *in vacuo* and the residue was purified by column chromatography (SiO_2 , pentane/ Et_2O , 20:1) to afford the desired product **4** (17 mg, 74 %) as a colorless oil.

$R_f = 0.17$ (pentane/ Et_2O , 20:1; vanillin);

$[\alpha]_D^{22} = -78.0$ ($c = 0.33$, MeOH);

$^1\text{H NMR}$ (700 MHz, CDCl_3): δ [ppm] = 5.70 (d, $J = 3.1$ Hz, 1H), 4.97 (s, 1H), 4.83 (s, 1H), 4.40 (d, $J = 8.4$ Hz, 1H), 2.61 – 2.51 (m, 2H), 2.31 – 2.18 (m, 4H), 1.94 – 1.88 (m, 1H), 1.88 – 1.82

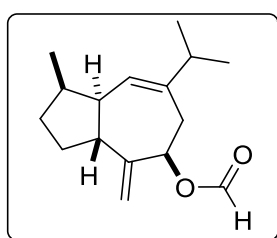
(m, 1H), 1.75 – 1.68 (m, 1H), 1.35 – 1.30 (m, 1H), 1.02 (d, $J = 6.8$ Hz, 3H), 1.02 (d, $J = 6.8$ Hz, 3H), 0.95 (d, $J = 6.8$ Hz, 3H);

^{13}C NMR (175 MHz, CDCl_3): δ [ppm] = 155.8, 142.7, 125.5, 107.2, 73.0, 48.3, 42.3, 37.8, 37.5, 36.7, 32.6, 27.5, 21.5 (2C), 17.3;

IR (v/cm^{-1} , neat): 3376, 2955, 2928, 2870, 1638, 1459, 1378, 1262, 1045, 898;

HRMS (ESI): m/z calculated for $\text{C}_{15}\text{H}_{24}\text{NaO}$ [$\text{M}+\text{Na}$] $^+$: 243.1719, found: 243.1720.

Compound 5



Chemical Formula: $\text{C}_{16}\text{H}_{24}\text{O}_2$
Molecular Weight: 248,3660

To a stirred solution of alcohol **3** (10 mg, 45.4 μmol , 1 equiv) in dry CH_2Cl_2 (0.5 mL) was added formic acid (5.9 μL , 152 μmol , 3.3 equiv), DCC (28.1 mg, 136 μmol , 3.0 equiv) and DMAP (1.0 mg, 8.2 μmol , 0.2 equiv) at 0 °C under an argon atmosphere. After 16 h of stirring at 20 °C, the reaction mixture was filtered through sand. The filtrate was concentrated *in vacuo* and the residue was purified by column chromatography (SiO_2 , pentane/ Et_2O 200:1) to afford formate **5** (8.5 mg, 75%) as a colorless oil.

$R_f = 0.80$ (pentane/ Et_2O , 20:1; vanillin);

$[\alpha]_D^{20.4} = -43.3$ ($c = 0.5$, CHCl_3);

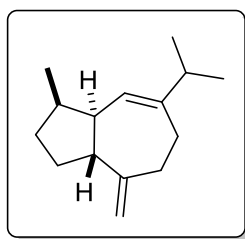
^1H NMR (700 MHz, CDCl_3): δ [ppm] = 8.07 (s, 1H), 5.68 – 5.64 (m, 2H), 5.02 (s, 1H), 4.94 (s, 1H), 2.65 (dd, $J = 15.6, 8.6$ Hz, 1H), 2.63 – 2.52 (m, 1H), 2.32 – 2.21 (m, 3H), 2.24 (d, $J = 15.6$ Hz, 1H), 1.95 – 1.88 (m, 1H), 1.88 – 1.82 (m, 1H), 1.73 – 1.67 (m, 1H), 1.38 – 1.27 (m, 1H), 0.98 (d, $J = 7.1$ Hz, 3H), 0.97 (d, $J = 7.1$ Hz, 3H), 0.94 (d, $J = 6.7$ Hz, 3H);

^{13}C NMR (176 MHz, CDCl_3): δ [ppm] = 160.6, 150.9, 142.4, 125.1, 109.9, 74.9, 48.4, 43.1, 37.6, 36.9, 34.8, 32.8, 27.8, 21.6, 21.5, 17.3;

IR (v/cm^{-1} , neat): 2956, 2927, 2870, 1725, 1171;

HRMS (ESI): m/z calculated for $\text{C}_{16}\text{H}_{24}\text{NaO}_2$ [$\text{M}+\text{Na}$] $^+$: 271.1669, found: 271.1671.

Compound 1



Chemical Formula: C₁₅H₂₄
Molecular Weight: 204,3570

A mixture of formate **5** (10.5 mg, 42.3 μmol, 1 equiv), PdCl₂(PPh₃)₂ (3.0 mg, 4.23 μmol, 0.1 equiv) and ammonium formate (6.7 mg, 106 μmol, 2.5 equiv) in 1,4-dioxane (0.85 mL) was stirred at 110 °C for 1.5 h under an argon atmosphere. H₂O (5 mL) was added at room temperature and the aqueous phase was extracted with pentane (3 x 5 mL). The combined organic phases were washed with saturated aqueous NaHCO₃ solution and brine, dried over Na₂SO₄ and concentrated *in vacuo*. The residue was purified by column chromatography (SiO₂, pentane) to afford the terpene **1** (5.4 mg, 63%) as a colorless oil.

R_f = 0.95 (pentane; vanillin);

[α]_D^{22.8} = -22.2 (c = 0.15, CH₂Cl₂);

¹H NMR (700 MHz, C₆D₆): δ [ppm] = 5.66 (d, J = 2.2 Hz, 1H), 4.84 (d, J = 11.5 Hz, 2H), 2.51 (dd, J = 13.2, 8.7 Hz, 1H), 2.40 – 2.27 (m, 2H), 2.20 (hept, J = 6.7 Hz, 1H), 2.15 – 2.09 (m, 1H), 2.14 (d, J = 8.7 Hz, 1H), 2.08 – 1.97 (m, 2H), 1.83 – 1.68 (m, 3H), 1.27 – 1.16 (m, 1H), 0.99 (d, J = 6.7 Hz, 3H), 0.98 (d, J = 6.7 Hz, 3H), 0.91 (d, J = 7.0 Hz, 3H);

¹³C NMR (176 MHz, C₆D₆): δ [ppm] = 154.3, 148.4, 124.2, 106.5, 47.8, 47.8, 37.5, 37.5, 36.9, 32.9, 30.1, 27.8, 21.4, 21.2, 17.0;

IR (ν/cm⁻¹, neat): 2956, 2927, 2868;

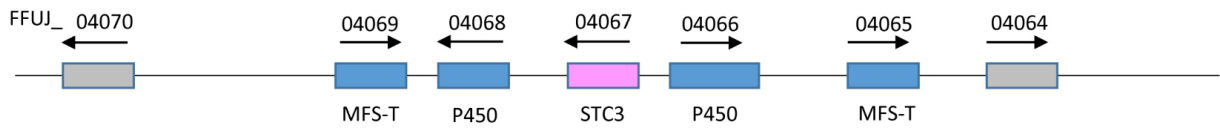
References

- [1] N. L. Brock, K. Huss, B. Tudzynski, J. S. Dickschat, *ChemBioChem* **2013**, *14*, 311-314.
- [2] L. Studt, F. J. Schmidt, L. Jahn, C. M. K. Sieber, L. R. Connolly, E.-M. Niehaus et al., *Appl. Environ. Microbiol.* **2013**, *79*, 7719-7734.
- [3] B. H. Bluhm, H. Kim, R. E. Butchko, C. P. Woloshuk, *Mol. Plant Pathol.* **2008**, *9*, 203-211.
- [4] P. Wiemann, D. W. Brown, K. Kleigrew, J. W. Bok, N. P. Keller, H.-U. Humpf, B. Tudzynski, *Mol. Microbiol.* **2010**, *77*, 972-999.

- [5] J. Schumacher, *Fungal Genet. Biol.* **2012**, *49*, 483-497.
- [6] J. S. Dickschat, K. A. K. Pahirulzaman, P. Rabe, T. A. Klapschinski, *ChemBioChem* **2014**, *15*, 810-814.

A

STC3 gene cluster



B

STC5 gene cluster

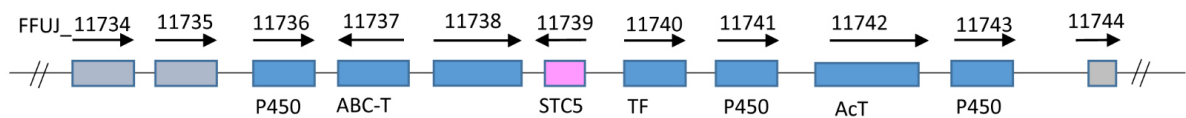


Figure 1. The putative STC3 and STC5 gene clusters. A) Putative *STC3* cluster genes (*FFUJ_11736* through *FFUJ_11743*) and B) putative *STC5* cluster genes (*FFUJ_04065* through *FFUJ_04069*) are depicted as blue boxes, genes directly upstream (*FFUJ_04070*) and downstream (*FFUJ_*, *FFUJ_04064*) of the cluster are shown in grey. The terpene cyclase genes are highlighted in purple. Arrows indicate direction of translation. Abbreviations: P450 – cytochrome P450 monooxygenase; TF – transcription factor; ABC-T – ABC-transporter; MFS-T – MFS-type transporter; AcT – acetyl transferase domain.

270 280 290 300 310

A) HPLVFEIMIIMSDQILLV**K**DILSYEKDLRLGVDHNMVRLLK

B) HPLVFEIMIIMSDQILLV**N**DILSYEKDLRLGVDHNMVRLLK

C) HPLVFEIMVIMSDQILLV**N**DILSYEKDLRLGVDHNMVRLLK

Figure 2. Partial amino acid sequences (positions 270 – 310) displaying the naturally occurring critical mutation at position 288 in STC5 of *Fusarium fujikuroi*. A) *Fusarium fujikuroi* STC5, B) *Fusarium fujikuroi* STC5 corrected by site-directed mutagenesis, C) *Fusarium mangiferae* STC5.

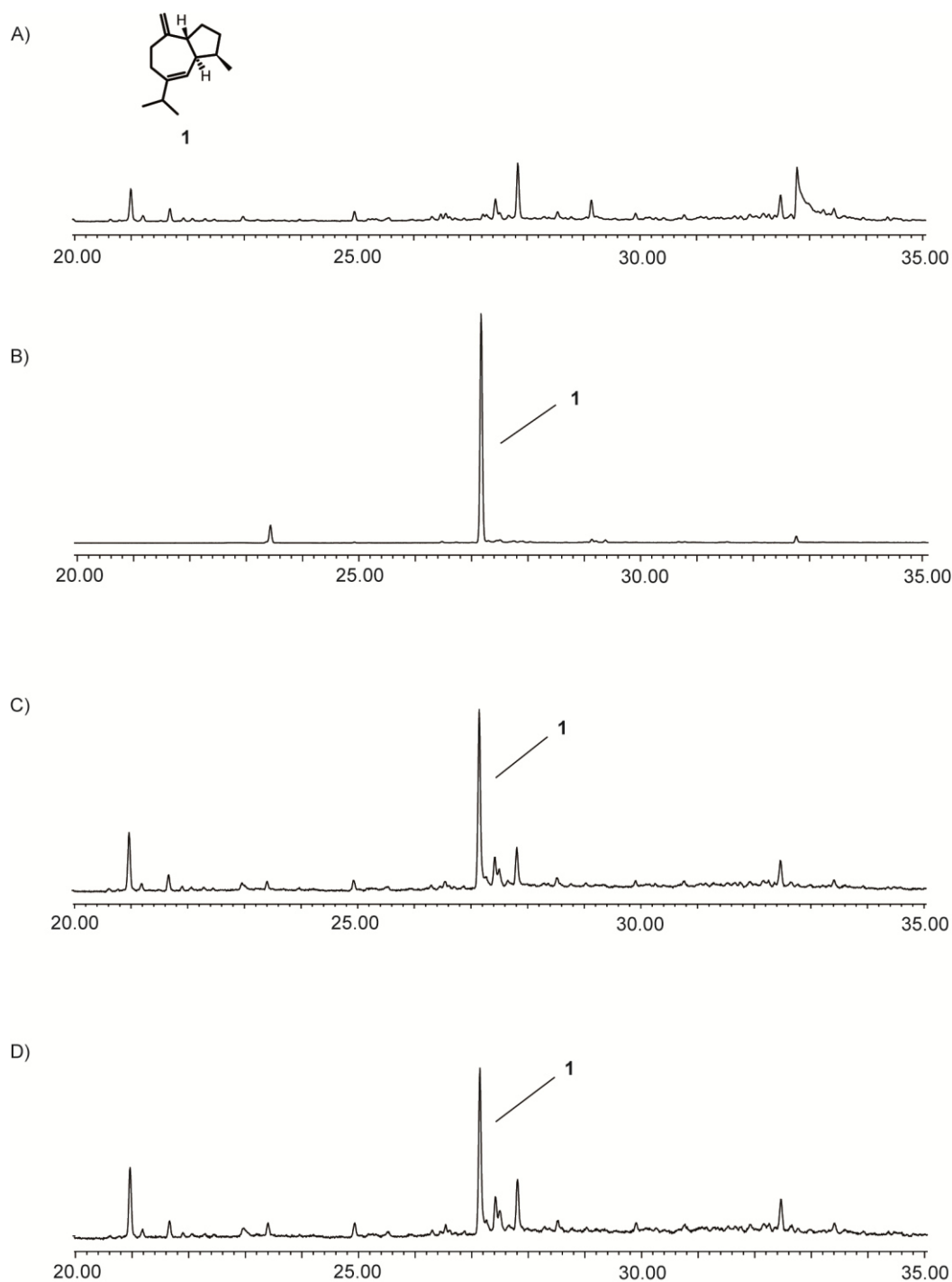


Figure 3. Total ion chromatograms of extracts obtained from incubation experiments of FPP with A) STC5 from *F. fujikuroi*, B) STC5 from *F. mangiferae*, C) STC5 from *F. proliferatum*, D) STC5 from *F. fujikuroi* with corrected sequence. While the original STC5 from *F. fujikuroi* is inactive, all other three enzymes produced selectively (–)-guaia-6,10(14)-diene (**1**).

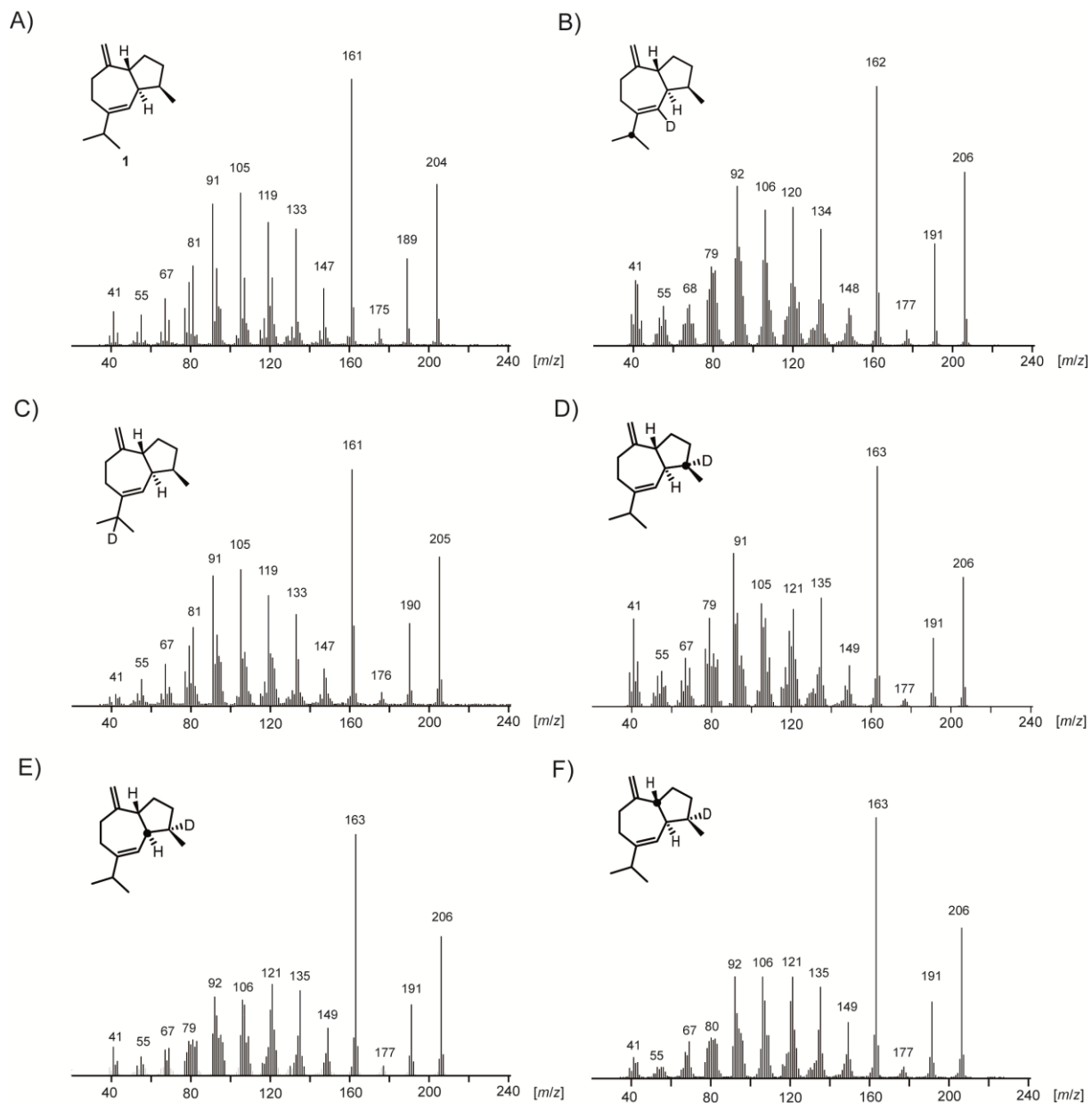


Figure 4. Mass spectra of products enzymatically formed by STC5 from incubations with A) FPP, B) (1,1- $^2\text{H}_2$,11- ^{13}C)-FPP, C) ($^{10}\text{H}_2$)-FPP, D) (3- ^{13}C)-FPP in D_2O , E) (2- ^{13}C)-FPP in D_2O , F) (6- ^{13}C)-FPP in D_2O . Black dots indicate ^{13}C -labelled carbons.

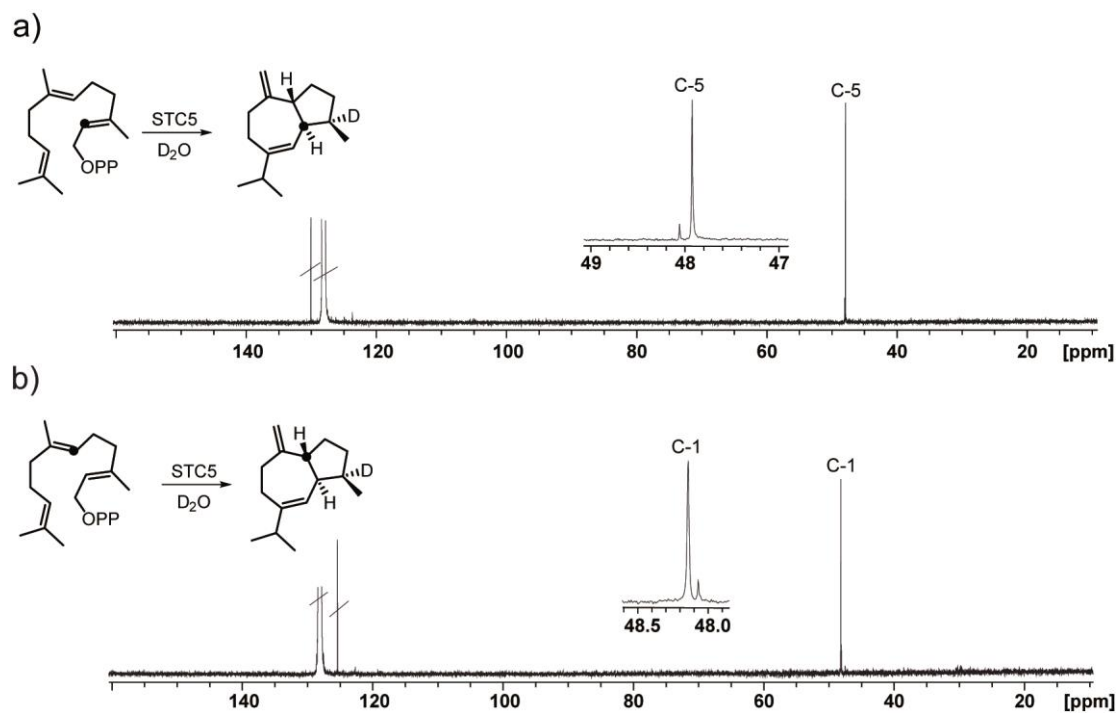


Figure 5. Enzyme mechanistic investigations. ^{13}C -NMR spectrum of A) (4- ^2H ,5- ^{13}C)-1 obtained from (6- ^{13}C)FPP in D_2O , B) (4- ^2H ,1- ^{13}C)-1 obtained from (2- ^{13}C)FPP in D_2O . Black dots indicate ^{13}C -labelled carbons.

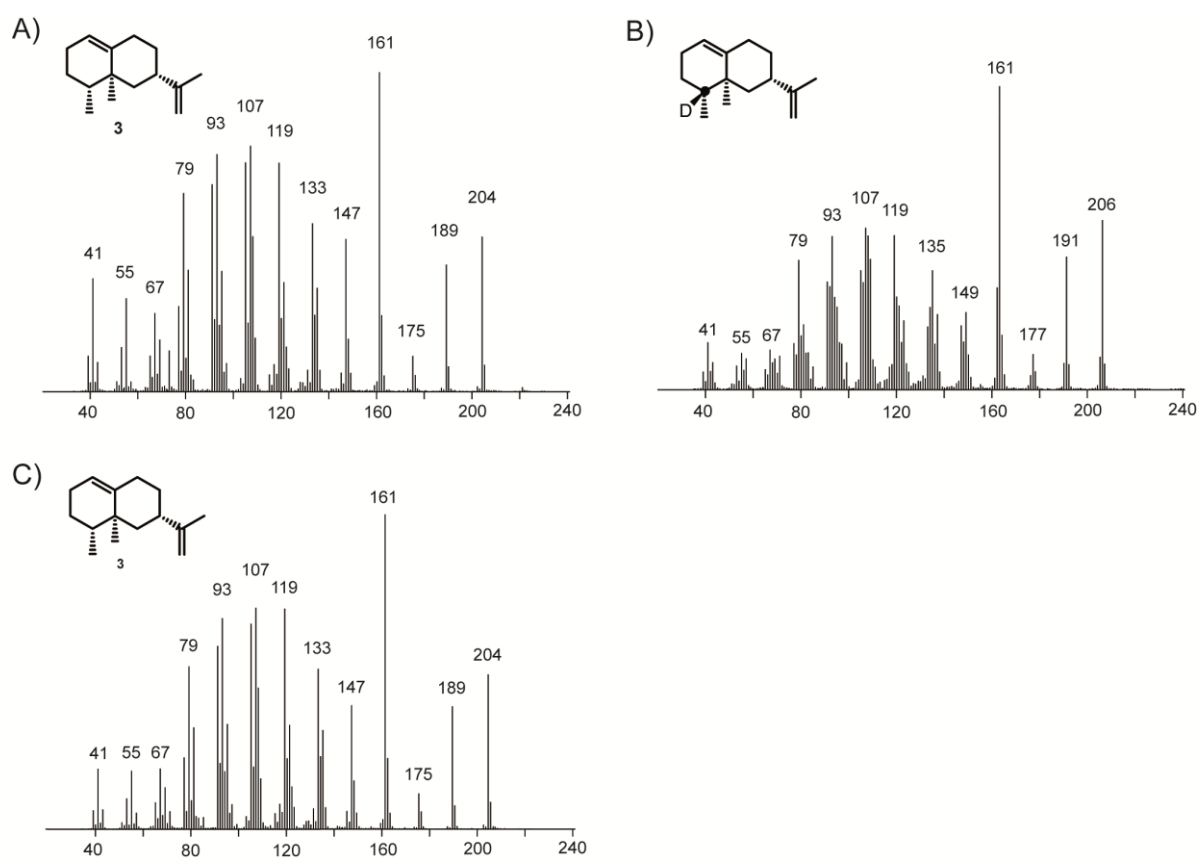


Figure 6. Mass spectra of products enzymatically formed by *Fusarium fujikuroi* STC3 from incubations with A) FPP, B) FPP in D_2O , C) $(2-^2H-3-^{13}C)$ -FPP. Black dots indicate ^{13}C -labelled carbons.

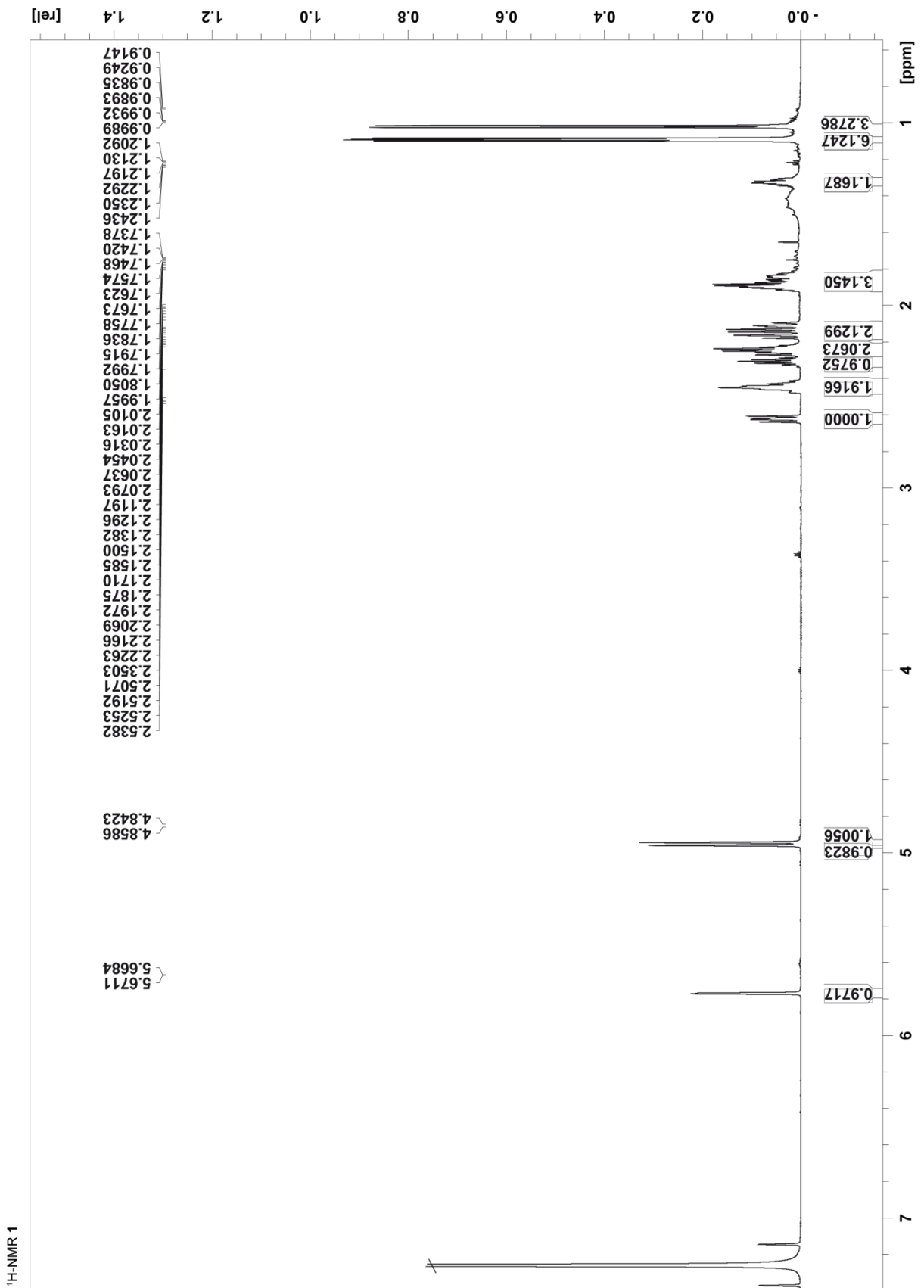


Figure 7. ¹H-NMR spectrum of enzymatically formed compound **1**.

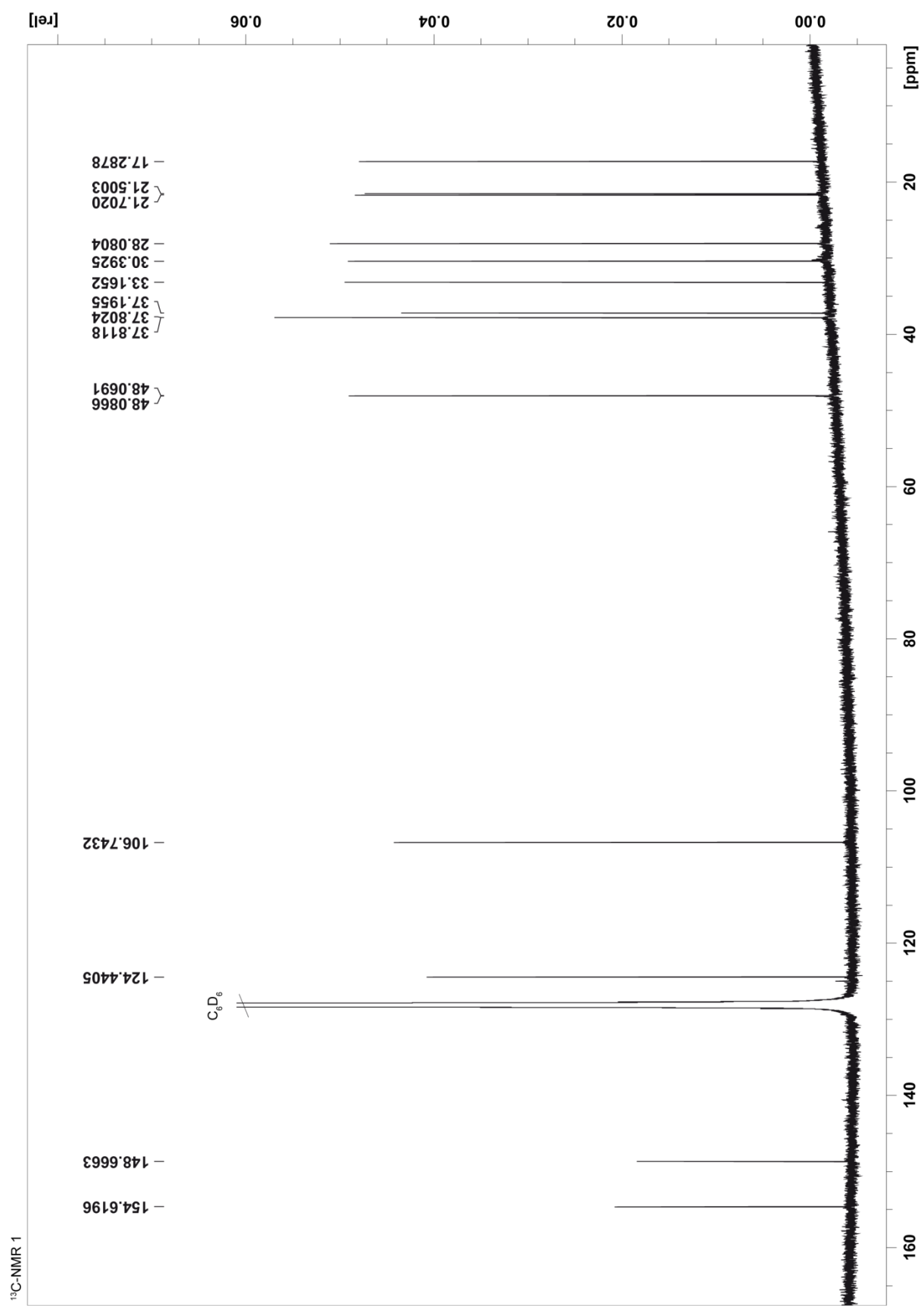


Figure 8. ¹³C-NMR spectrum of enzymatically formed compound 1.

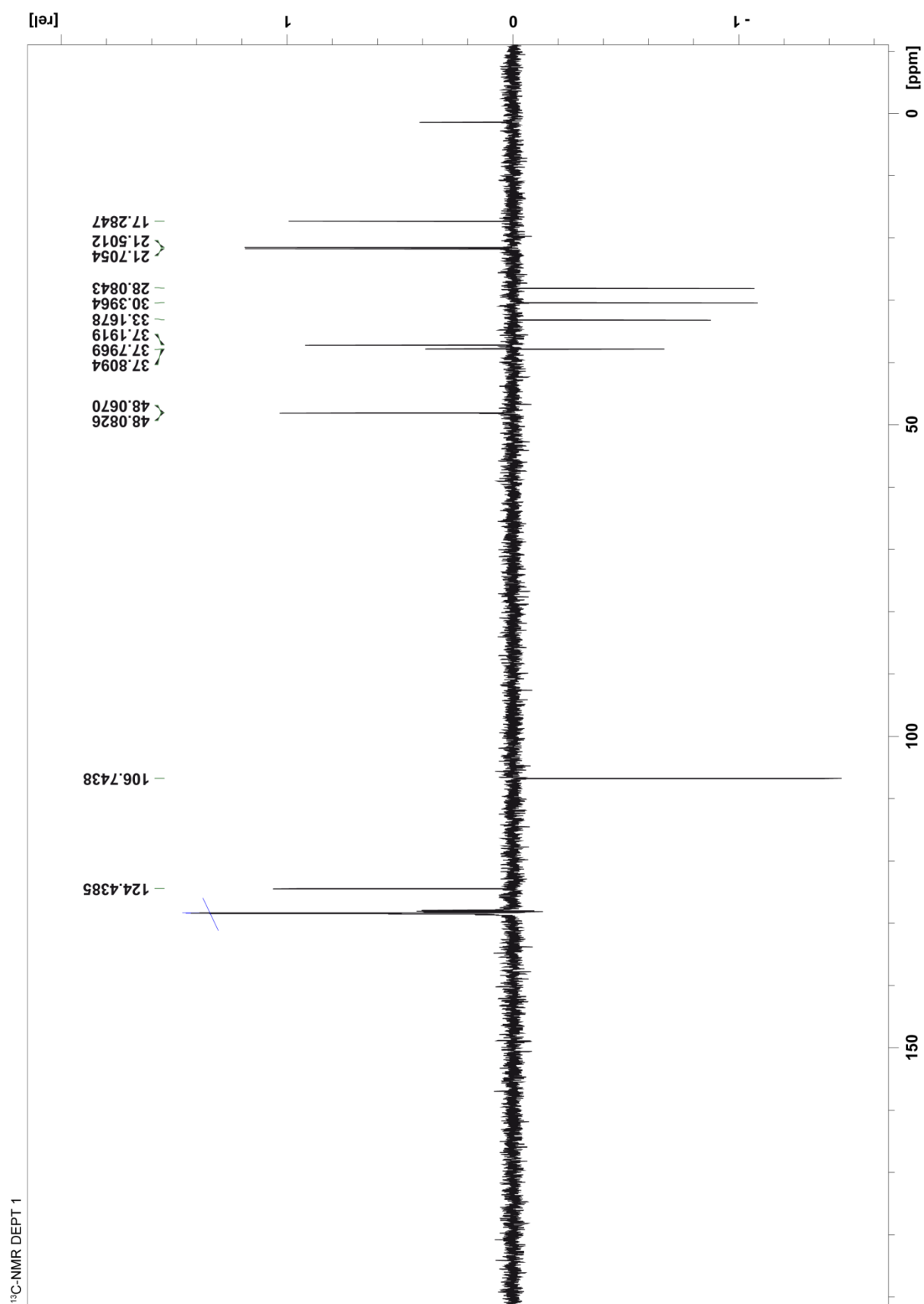


Figure 9. ¹³C-DEPT spectrum of enzymatically formed compound **1**.

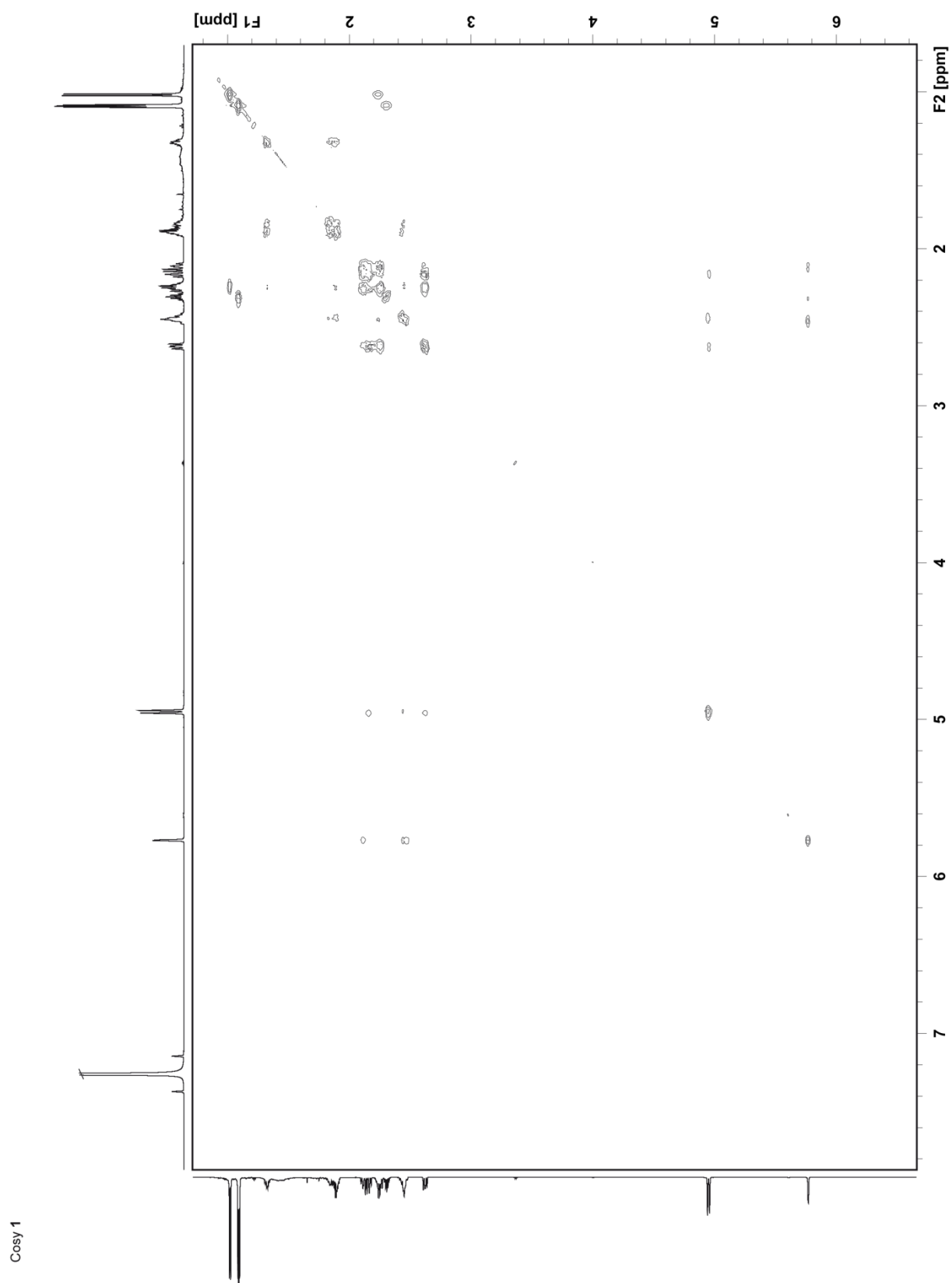


Figure 10. ^1H , ^1H -COSY of enzymatically formed compound **1**.

$^1\text{H}, ^{13}\text{C}$ -HSQC 1

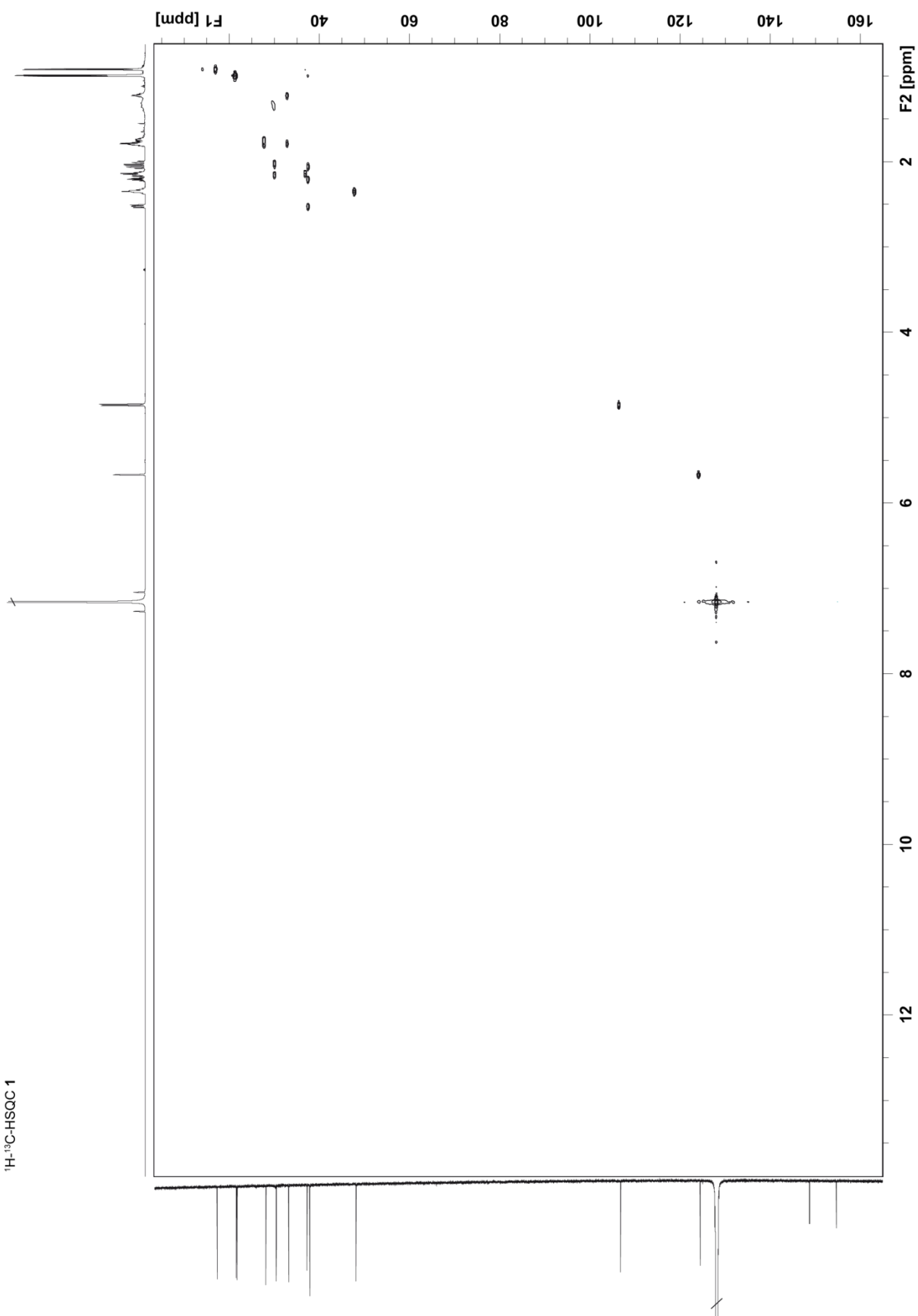


Figure 11. $^1\text{H}, ^{13}\text{C}$ -HMOC spectrum of enzymatically formed compound **1**.

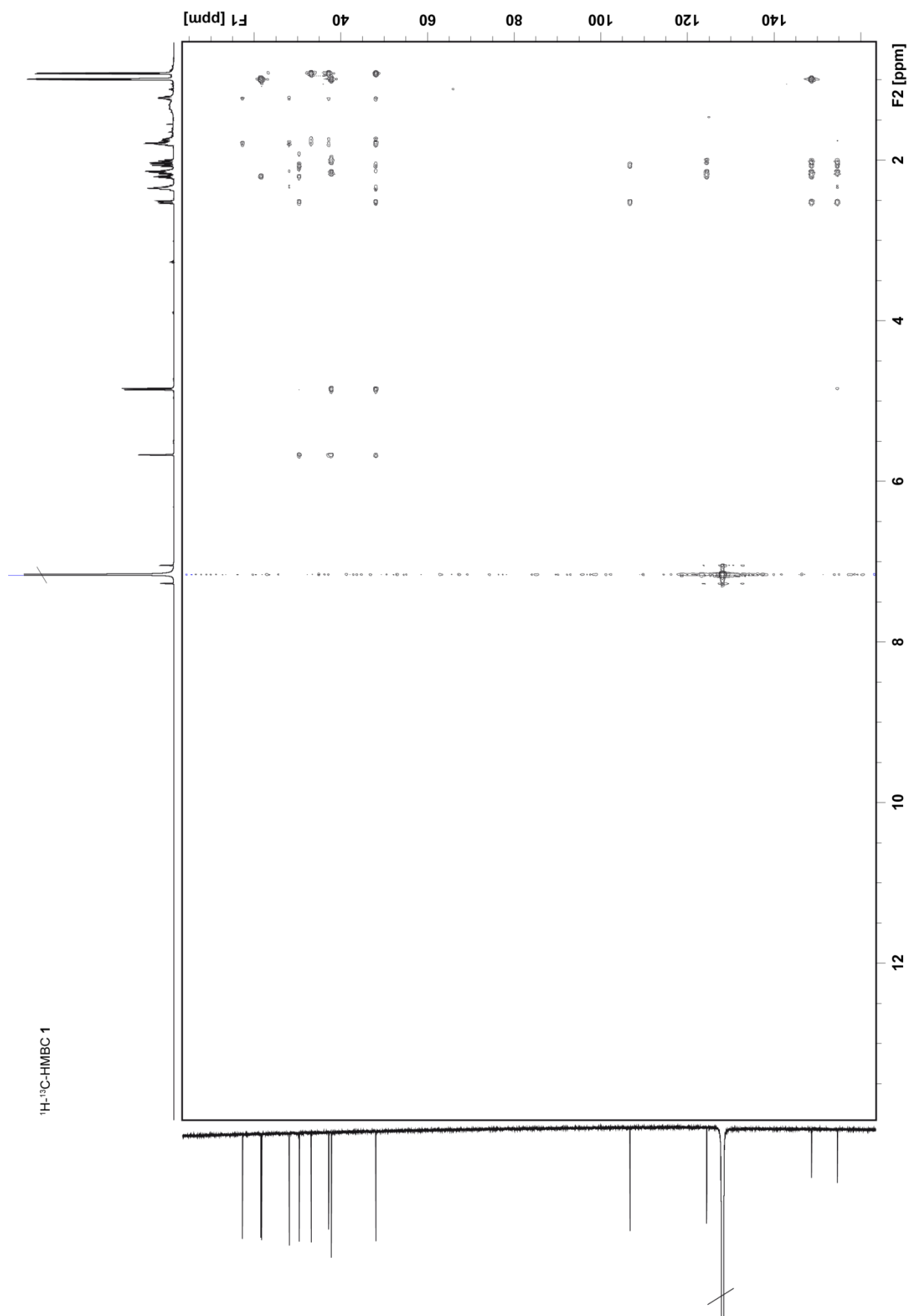


Figure 12. ^1H , ^{13}C -HMBC NMR spectrum of enzymatically formed compound **1**.

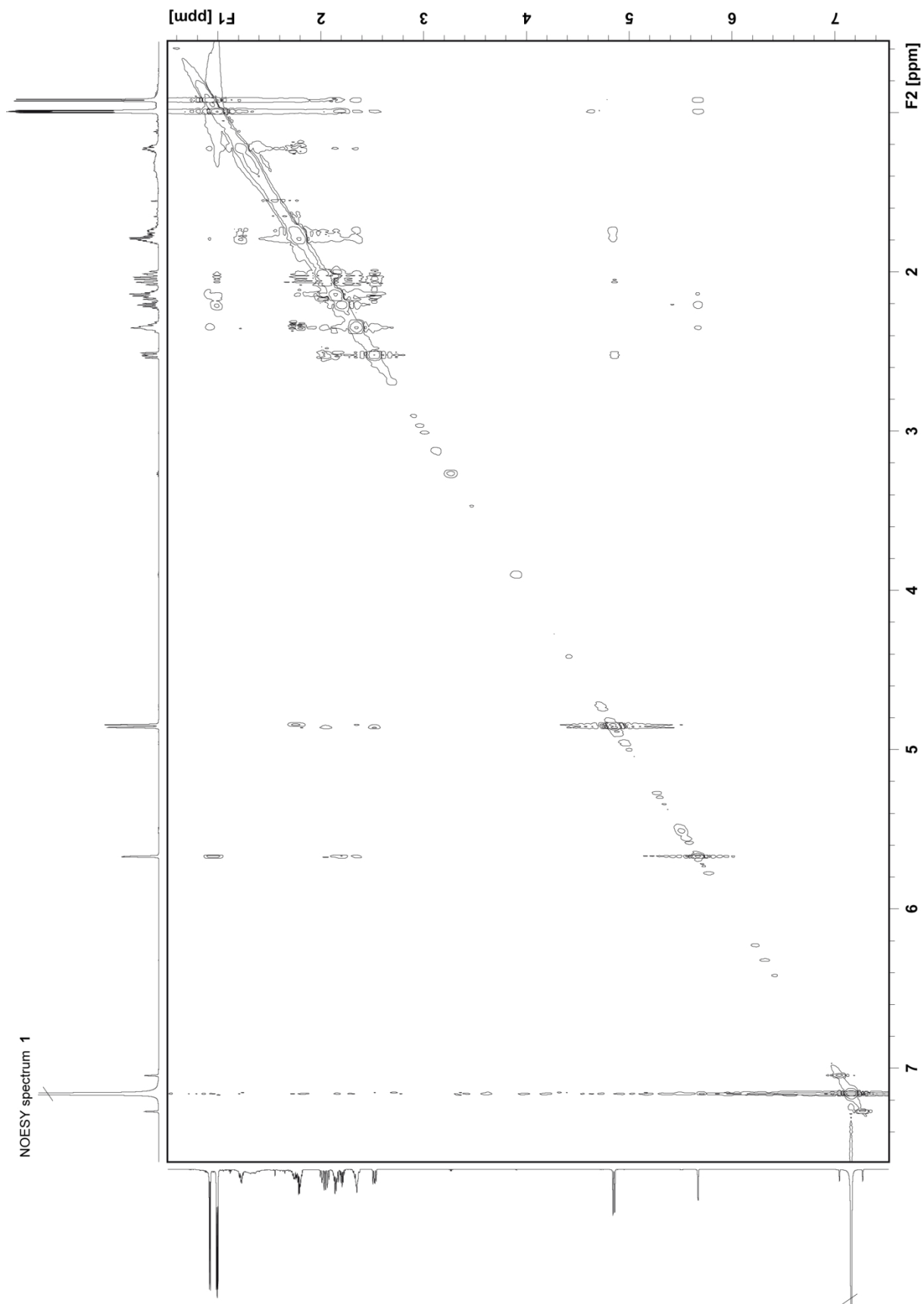


Figure 13. ^1H , ^1H -NOESY spectrum of enzymatically formed compound **1**.

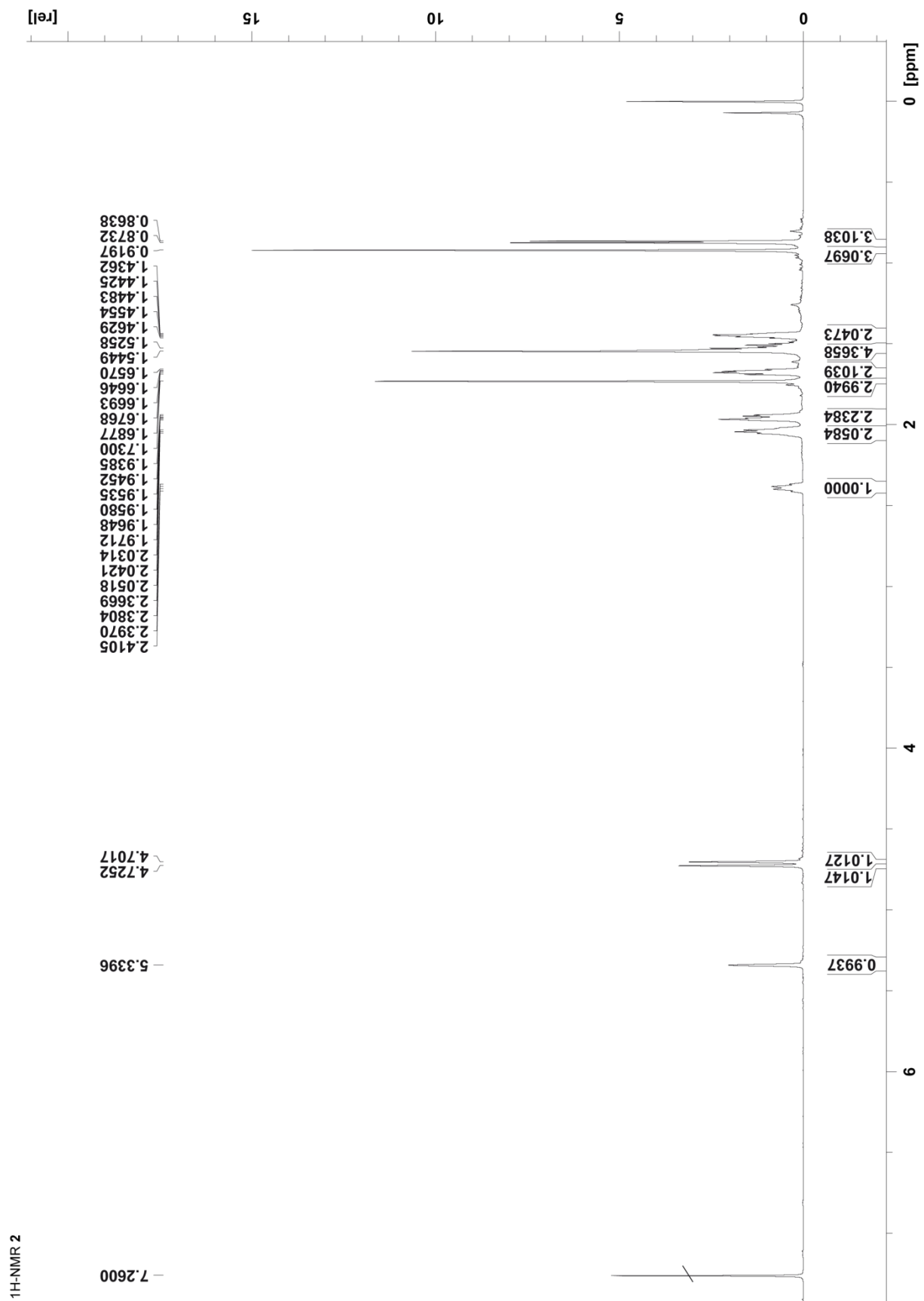


Figure 14. $^1\text{H-NMR}$ spectrum of enzymatically formed compound **2**.

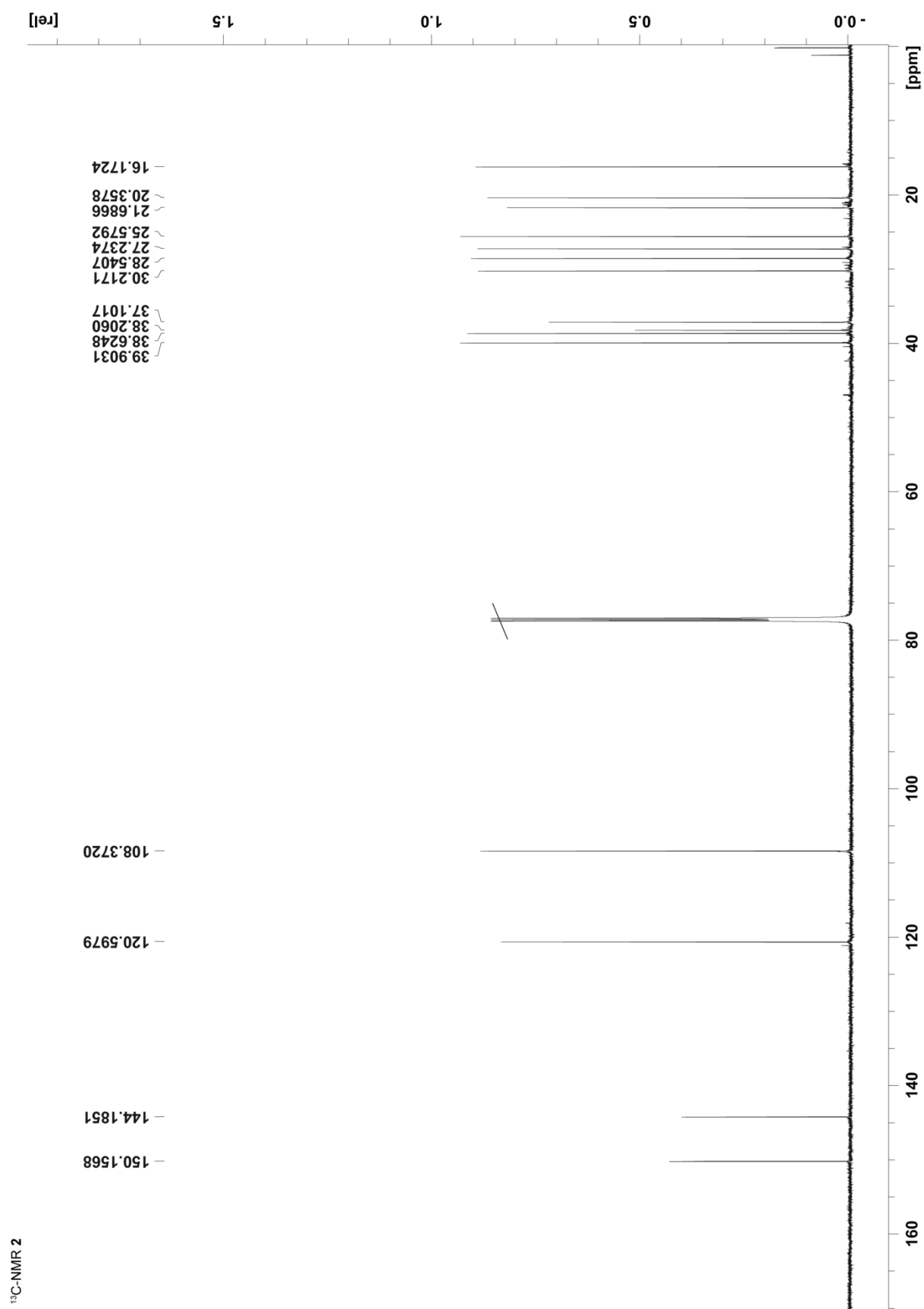


Figure 15. ¹³C-NMR spectrum of enzymatically formed compound 2.

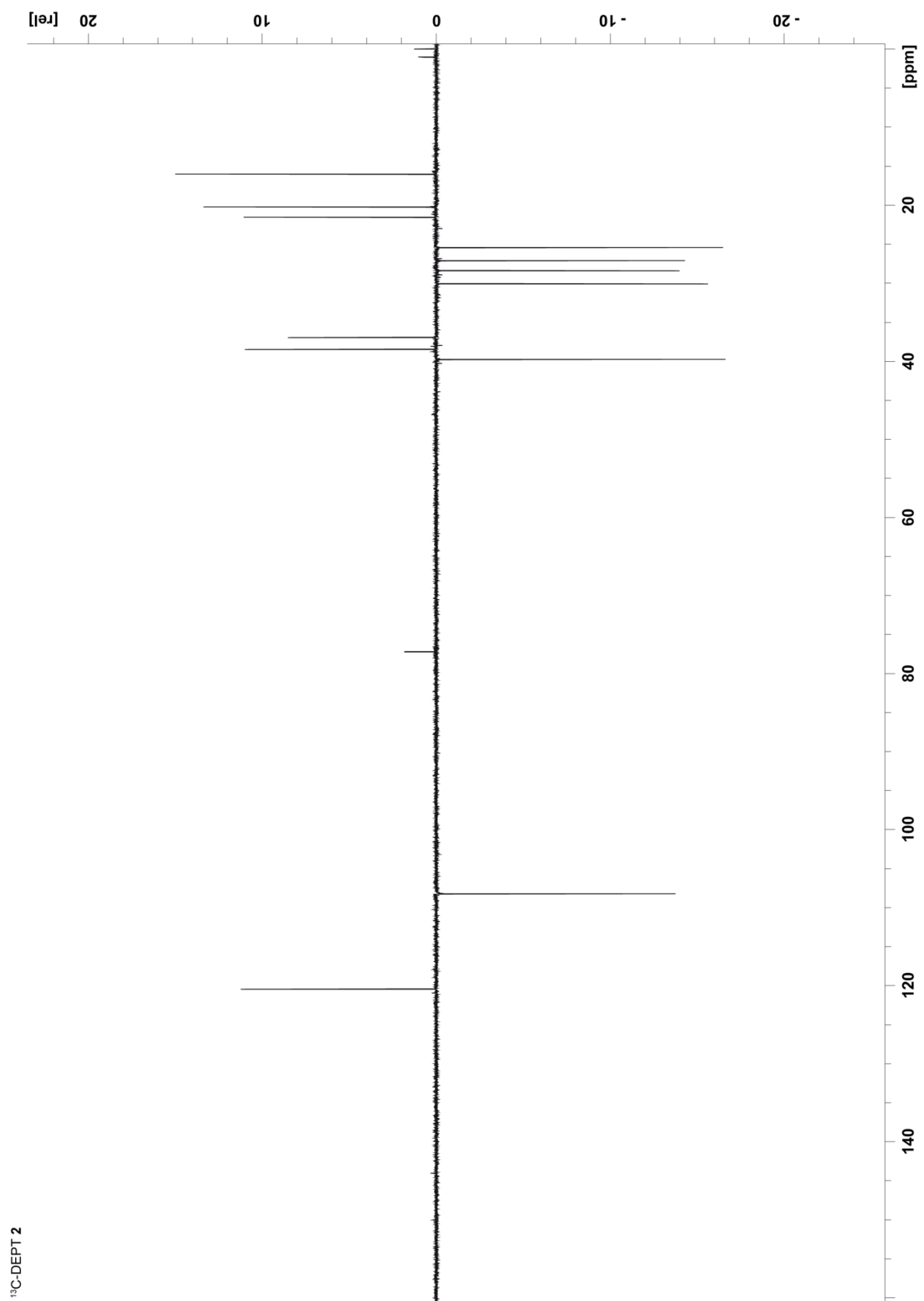


Figure 16. ^{13}C -DEPT spectrum of enzymatically formed compound **2**.

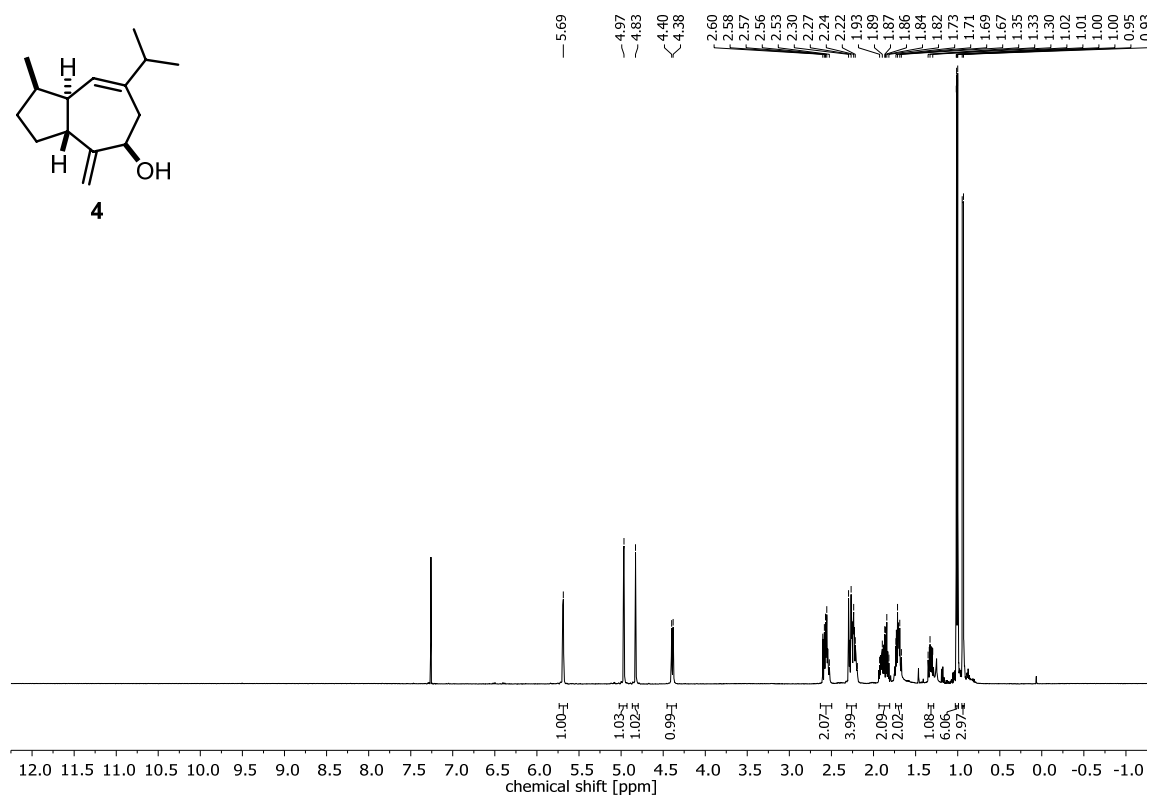


Figure 17. $^1\text{H-NMR}$ spectrum of synthetic compound 4.

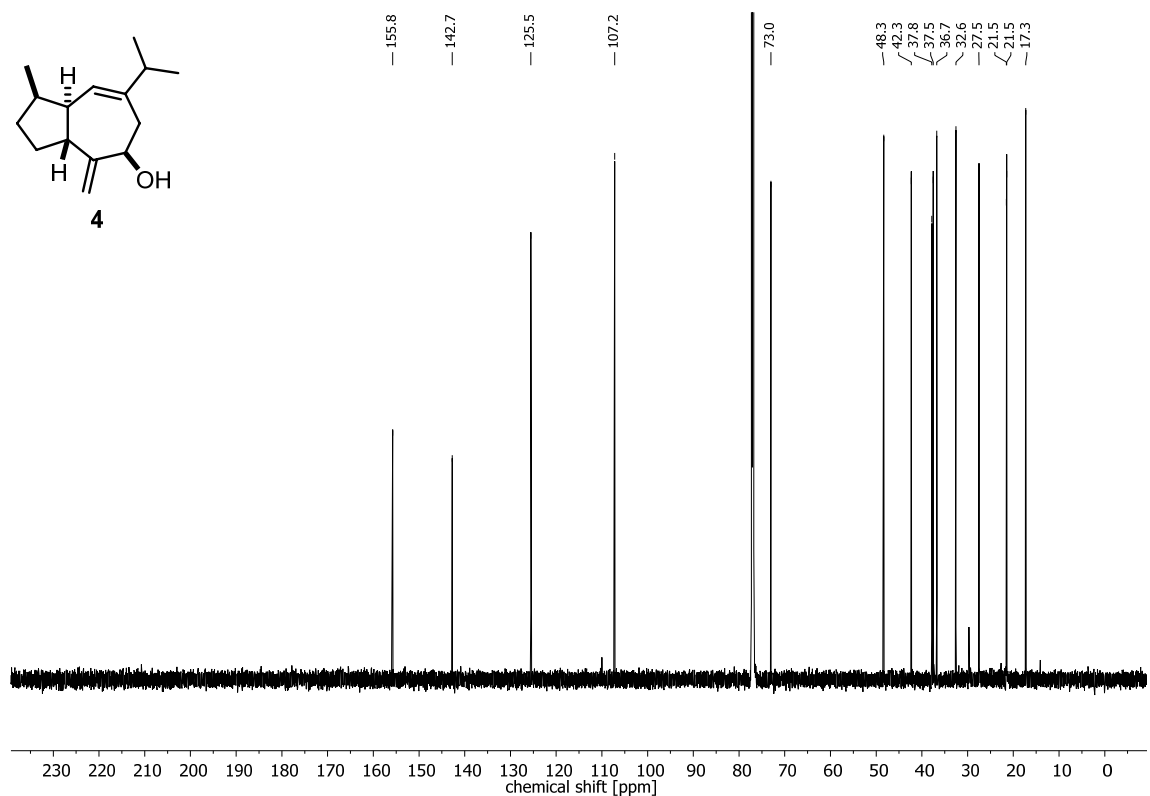


Figure 18. $^{13}\text{C-NMR}$ spectrum of synthetic compound 4.

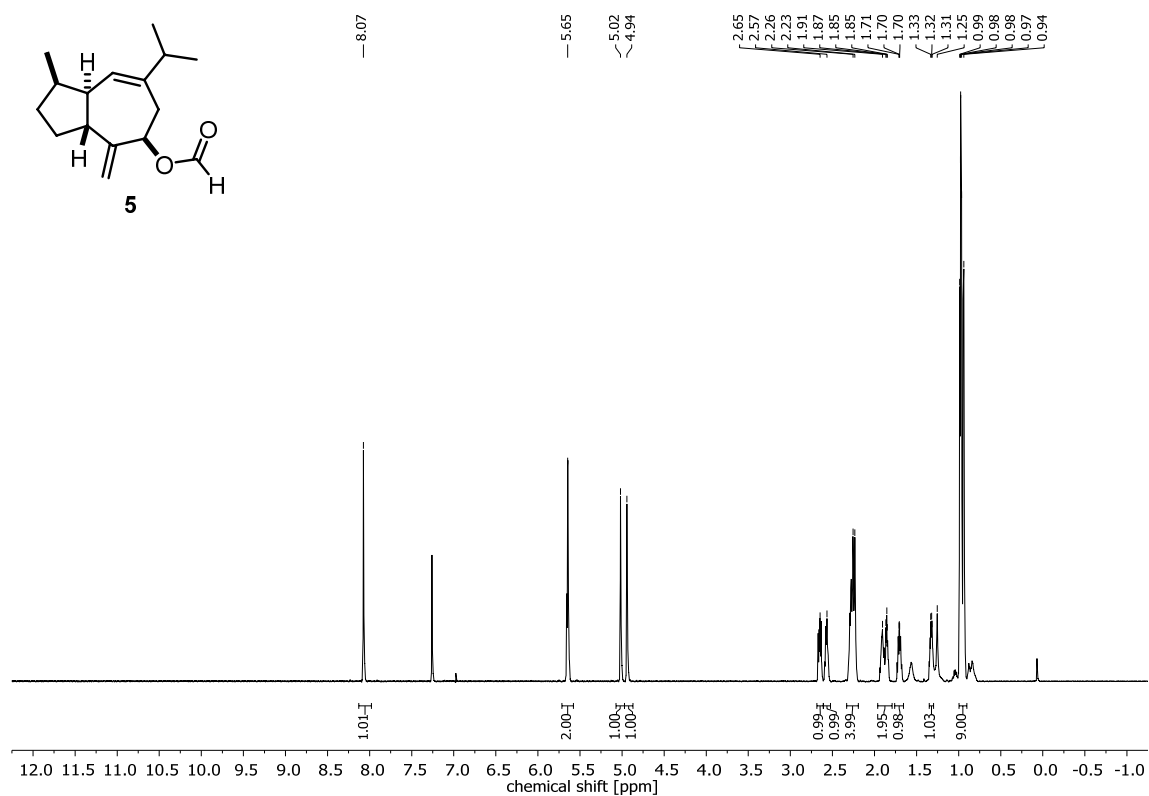


Figure 19. $^1\text{H-NMR}$ spectrum of synthetic compound 5.

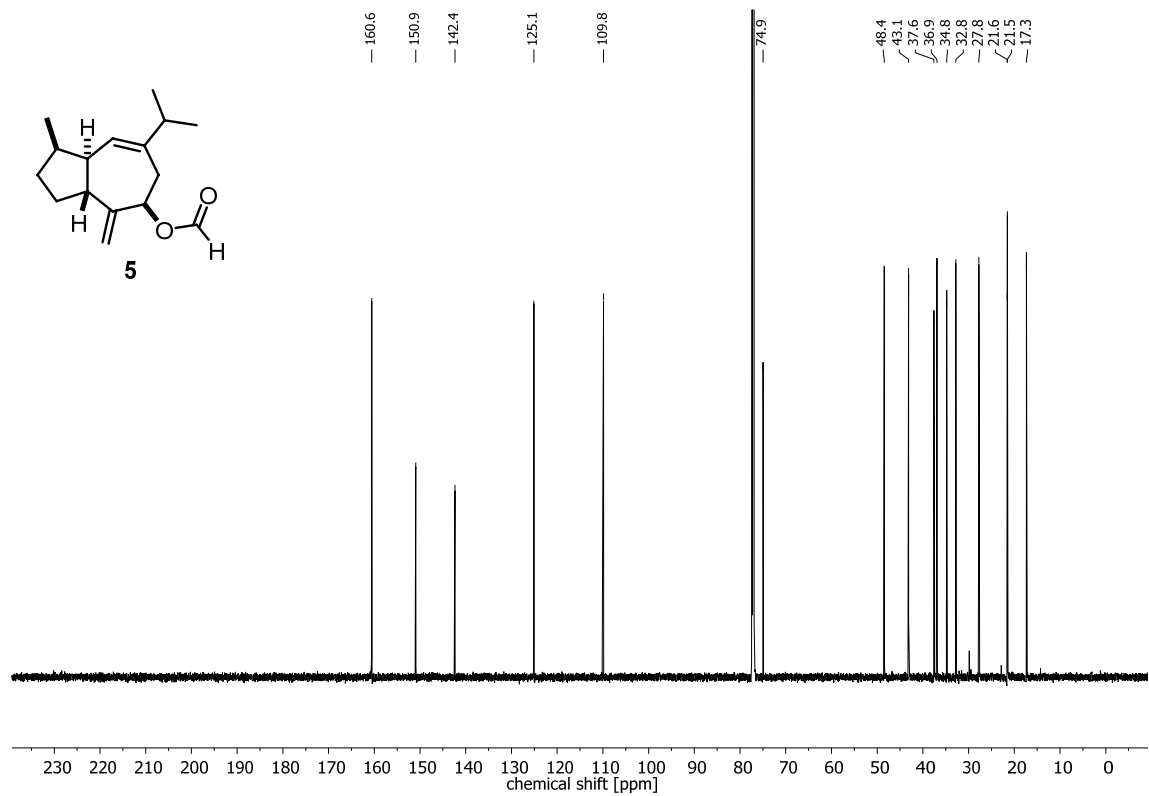
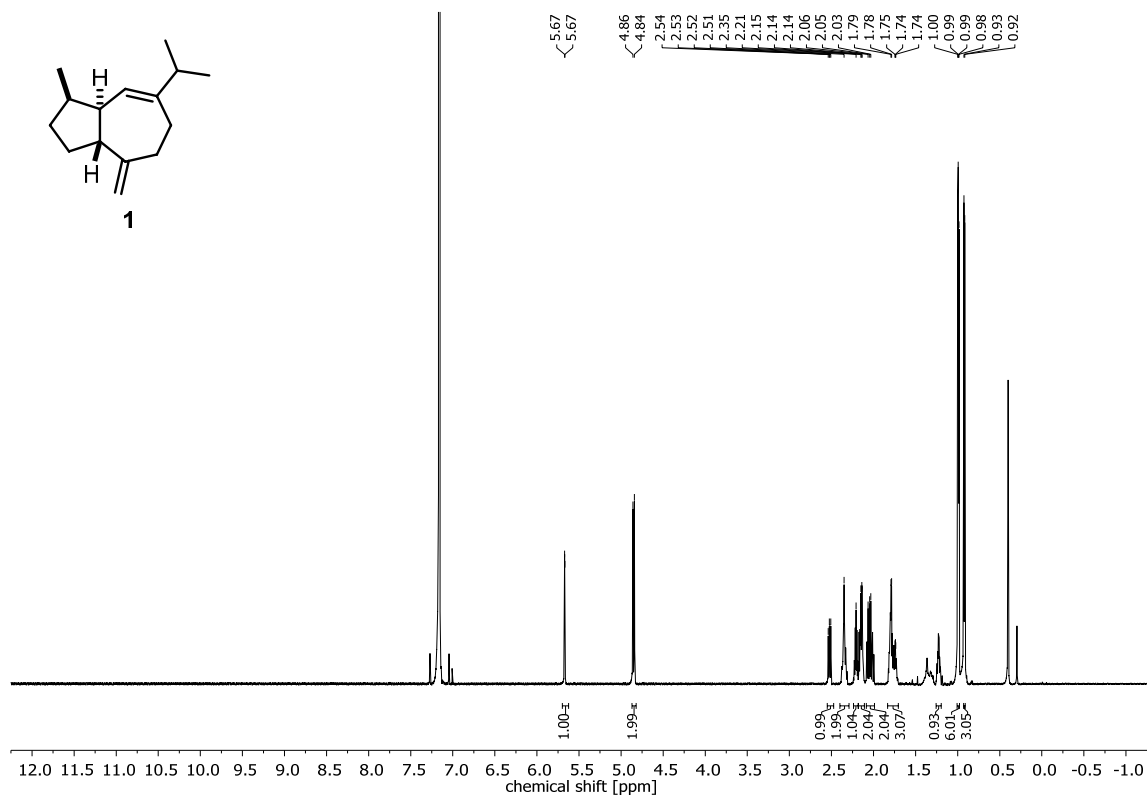
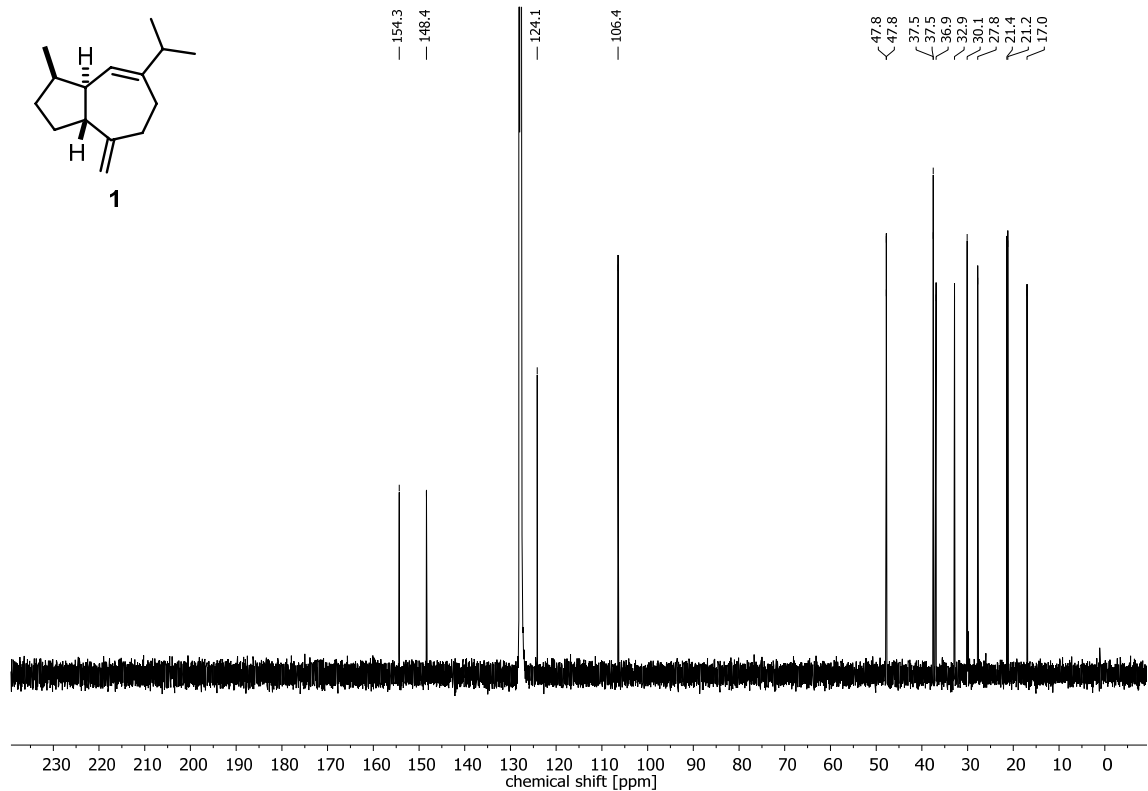


Figure 20. $^{13}\text{C-NMR}$ spectrum of synthetic compound 5.

Figure 21. $^1\text{H-NMR}$ spectrum of synthetic compound **1**.Figure 22. $^{13}\text{C-NMR}$ spectrum of synthetic compound **1**.

Supporting Information – Semisynthesis of (–)-Englerin A

Microbe Engineering of Guaia-6,10(14)-diene as a Building Block for the Semisynthetic Production of Plant-Derived (–)-Englerin A

Thomas Siemon,^{1,5} Zhangqian Wang,^{2,5} Guangkai Bian,^{2,5} Tobias Seitz,¹ Ziling Ye,³ Yan Lu,² Shu Cheng,² Yunkun Ding,² Zixin Deng,^{2,4} Tiangang Liu^{*,2,4} and Mathias Christmann^{*,1}

¹Institute of Chemistry and Biochemistry, Freie Universität Berlin, Berlin, Germany. ²Key Laboratory of Combinatorial Biosynthesis and Drug Discovery, Ministry of Education and School of Pharmaceutical Sciences, Wuhan University, Wuhan, China. ³J1 Biotech Co., Ltd., Wuhan, China. ⁴Hubei Engineering Laboratory for Synthetic Microbiology, Wuhan Institute of Biotechnology, Wuhan, China. ⁵These authors contributed equally to this work. *e-mail: mathias.christmann@fu-berlin.de, liutg@whu.edu.cn.

General Working Methods

The analytical data was obtained with the help of the following equipment.

NMR spectroscopy

^1H and ^{13}C NMR spectra were acquired on a JEOL ECX 400 (400 MHz), JEOL ECP 500/ Bruker Avance 500 (500 MHz) and a Bruker Avance 700 (700 MHz) in CDCl_3 or CD_3OD as a solvent. The chemical shifts were reported relative to CDCl_3 ($\delta = ^1\text{H}$: 7.26 ppm, ^{13}C : 77.16 ppm), C_6D_6 ($\delta = ^1\text{H}$: 7.16 ppm, ^{13}C : 128.06 ppm) or CD_3OD ($\delta = ^1\text{H}$: 3.31 ppm, ^{13}C : 49.00 ppm). The multiplicities of the signals are described using the following abbreviations: s = singlet, d = doublet, t = triplet, q = quartet, hept = heptet, m = multiplet, br = broad and combinations thereof.

The spectra were evaluated with the software MestReNova 10.

Mass spectra were obtained on an ESI-FTICR-MS: Ionspec QFT-7 (Agilent/Varian).

IR: spectra were measured on a JASCO FT/IR-4100 Spectrometer. Characteristic absorption bands are displayed in wavenumbers $\tilde{\nu}$ in cm^{-1} and were analyzed with the software Spectral Manager from JASCO.

Optical rotation measurements were performed on a P-2000 polarimeter from Jasco in a 10 cm optical-path length cell with the frequency of the NaD line measured at the temperature and concentration (in g/100 mL) indicated.

Chromatography Reaction progress was monitored by thin layer chromatography on aluminum backed silica gel plates (silica gel 60 F 254 from E. Merck), visualizing with UV light ($\lambda = 254$ nm). The plates were developed using vanillin dip solution (170 mL methanol, 20.0 mL conc. acetic acid, 10.0 mL conc. sulfuric acid with 1.0 g vanillin) or an anisaldehyde solution (450 mL ethanol, 25.0 mL anisaldehyde, 25.0 mL conc. sulfuric acid, 8.0 mL acetic acid).

Flash chromatography was performed using silica gel M60 from Macherey & Nagel (particle size: 40 – 63 μm).

Reagents and Solvents Reactions with air or moisture-sensitive substances were, if not otherwise indicated, carried out under an argon atmosphere with the help of the Schlenk technique. All other reagents and solvents were used as purchased from commercial suppliers unless otherwise noted. Anhydrous solvents were purified with the solvent purification system MB-SPS-800 (Braun). The solvents (diethyl ether, ethyl acetate, pentane and dichloromethane) used for column chromatography and work up were purified from commercially available technical grade solvents by distillation under reduced pressure with the help of rotatory evaporators (Heidolph or IKA) at 40 °C water bath temperature.

Benzene was degassed by bubbling argon through the solution for 10 min. The 2-((tert-butylidiphenylsilyl)oxy)acetyl chloride could be prepared from glycolic acid via a literature known procedure.^[1] DMDO was prepared as a solution in CHCl₃ via the known method.^[2]

Online Methods

Plasmids, strains, and culture conditions. All primers used for cloning are listed in **Supplementary Table 1**. All plasmids (**Supplementary Table 2**) were constructed by the restriction enzyme digestion/ligation method,^[3] Golden gate method,^[4] Gibson method^[5] or yeast assembly method.^[6] All strains are summarized in **Supplementary Table 3**. *Escherichia coli* DH10B was used for plasmid construction and amplification. *Escherichia coli* BL21 (DE3) was used for protein expression and guaia-6,10(14)-diene overproduction. *Saccharomyces cerevisiae* CEN.PK2-1D (accession number: 30000B) was used for in vivo plasmid assembly and cultivation in YPD medium. *S. cerevisiae* YZL141^[7] and *Saccharomyces cerevisiae* JCR27 were constructed as platforms for guaia-6,10(14)-diene overproduction. Filamentous fungi *Fusarium graminearum* J1-012^[8] was used for RNA extraction and amplification of *FgJ02895*.

Phylogenetic analysis of sesquiterpene synthases of filamentous fungi origin. The characterized and the putative sesquiterpene cyclases were gathered for phylogenetic analysis. The evolutionary history was inferred by using the Maximum Likelihood method based on the Poisson correction model. The tree with the highest log likelihood (-6934.43) is shown. Initial tree(s) for the heuristic search were obtained automatically by applying Neighbor-Join and BioNJ algorithms to a matrix of pairwise distances estimated using a JTT model, and then selecting the topology with superior log likelihood value. The analysis involved 126 amino acid sequences. All positions containing gaps and missing data were eliminated. There was a total of 48 positions in the final dataset. Evolutionary analyses were conducted in MEGA7.^[9] The data (**Supplementary Fig. 1**) showed that guaia-6,10(14)-diene cyclase STC5, together with three putative sesquiterpene cyclases, *FgJ02895*, *FpN62905*, and *FmM7560*, clustered in the same branch, which indicated that these three sesquiterpene cyclases maybe function as guaia-6,10(14)-diene cyclase.

Experimental Procedure

Cloning, expression, and purification of *FgJ02895*. The total RNA of *F. graminearum* J1-012 was extracted and cDNA was synthesized as described previously.^[10] To verify the function of *FgJ02895*, the coding sequence of *FgJ02895* was amplified from the cDNA library of *F. graminearum* J1-012 by using primer pair P1/P2, followed digested with *NdeI/XhoI* and insert into pET28a to generate pGB150.

Ten milliliters of overnight cultures of *E. coli* BL21(DE3) with pGB150 (*N-terminal his6-tag_FgJ02895*) were inoculated into 2-L flasks containing 1 L LB medium supplemented with 50 mg/L kanamycin and grown at 37 °C. When the OD600 reached 0.6–0.8, IPTG (0.1 mM) was added. After induction at 16 °C for 24 h, the cultures were harvested and resuspended in 40 mL of buffer A (50 mM Tris–Cl, 300 mM NaCl, 4 mM β-mercaptoethanol, pH 7.6). *FgJ02895* was then purified as described previously.^[11]

In vitro enzyme assays and GC/MS detection. Enzymes assays were carried out as described previously.^[8] Reactions were carried out using 100 μM FPP as a substrate, 2 mM Mg²⁺, 10% glycerol, and 10 μM *FgJ02895* in 200 μL 50 mM Tris–HCl buffer (pH 7.6) at 30 °C for 2 h. The products were extracted with an equal volume of hexane and then detected and analyzed by GC/MS (**Supplementary Figure 1**).

For GC/MS detection, the organic layer was centrifuged at 10,000 ×g for 5 min and diluted with hexane by 100-fold. The samples were injected into TRACE TR-5MS column (30 m × 0.25 mm × 0.25 μm). The oven temperature was set to 80 °C for 1 min, increased to 220 °C at a rate of 10 °C/min, and held at 220 °C for 15 min. The temperatures of the injector and transfer lines were maintained at 230 °C and 240 °C, respectively.

Plasmids construction and overproduction of guaia-6,10(14)-diene in *E. coli*. To achieve high expression in *E. coli*, *FgJ02895* was codon optimized as *FgJ02895-Ec*. Next, *FgJ02895-Ec* was amplified by the primer pair P3/P4 and inserted into pET21a to generate pGB216. The *XbaI/XhoI*-digested fragment (*FPPS-Idi*) of pGB308^[8] was inserted into pGB216 (*SpeI/XhoI* digested) to generate pGB218. STC5 of *F. fujikuroi* IMI58289 was amplified by the primer pair P5/P6 and insert into pET21a to generate pSC51. The *XbaI/XhoI*-digested fragment *FPPS-Idi* was inserted into pET21a-STC5 (*SpeI/XhoI* digested) to generate pSC52. FpN62905 of *F. proliferatum* NRRL 62905 was amplified by the primer pair P7/P8 and inserted into pET21a to generate pSC53. Using the same strategy, the *XbaI/XhoI*-digested fragment *FPPS-Idi* was inserted into pET21a-FpN62905 (*SpeI/XhoI* digested) to generate pSC54. FmM7560 of *F. mangiferae* MRC 7560 was

amplified by the primer pair P9/P10 and inserted into pET21a to generate pSC55. Using the same strategy, the *XbaI/XhoI*-digested fragment *FPPS-Idi* was inserted into pET21a-FmM7560 (*SpeI/XhoI*-digested) to generate pSC56. To increase the expression level of *FgJ02895-Ec*, *FgJ02895-Ec* and the plasmid backbone of pGB218 was amplified by the primer pairs P11/P12 and P13/P14, respectively. These two fragments were digested with *AscI* and then assembled to generate pSC61.

To realize the overproduction of guaia-6,10(14)-diene in *E. coli*, plasmids pGB218, pSC52, pSC54, pSC56, and pSC61 were transformed into *E. coli* C1(BL21(DE3)/pMH1/pFZ81) to generate *E. coli* G1-G5, respectively (**Supplementary Figure 3**). These *E. coli* strains were grown at 37 °C with 100 mg/L ampicillin, 50 mg/L kanamycin, and 34 mg/L chloramphenicol in 500-mL flasks containing 200 mL LB medium. When the OD₆₀₀ reached 0.6–0.8, IPTG (0.1 mM) was added. After induction at 16 °C for 24 h, the cultures were overlaid with 10% *n*-decane and cultivated at 28 °C for an additional 3 days. Experiments were repeated three times. Next, the organic layer was collected for GC/MS detection and titer calculation. The purified guaia-6,10(14)-diene was selected to generate a standard curve with appropriate dilution factors and averaged for three replicate analyses.

Plasmids for overproduction of guaia-6,10(14)-diene in *S. cerevisiae*. To establish an efficient precursor (IPP and DMAPP)-providing a platform to facilitate overproduction of guaia-6,10(14)-diene in *S. cerevisiae*, a series of plasmids was constructed and the MVA pathway was enhanced. The cassettes “XII-2 right-pRS426 backbone-XII-2 right” and *hygR* were amplified from pZY403 (unpublished data) by the primer pairs P15/P16 and P17/P18, respectively; the *cas9* expression cassette was amplified from p43802 by the primer pair P19/P20. Finally, these three fragments were assembled by the yeast assembly method to generate pZY600. To enhance the expression level of the mevalonate pathway in *S. cerevisiae*, plasmids pZY412, pZY413, and pZY414 were constructed. The backbone of pRS426 was amplified with the primer pair P21/P22; the left and right recombination arms of chrXII-4 of *S. cerevisiae* were amplified with the primer pairs P23/P24 and P25/P26; *T_{ADH1}*, *MVD1*, and *P_{GAL7}-T_{GAL10}* were amplified with primer pairs P27/P28, P29/P30, and P31/P32, respectively; *ERG10*, *P_{GAL10}-P_{GAL1}*, *IDI1* and *T_{CYC1}* were amplified with the primer pairs P33/P34, P35/P36, P37/P38, and P39/P40, respectively. Finally, the above amplified ten fragments were assembled to generate pZY412. The backbone of pRS426 was amplified with the primer pair P41/P42; the left and right recombination arms of ChrXI-3 of *S. cerevisiae* were amplified with the primer pairs P43/P44 and P45/P46; *T_{CYC1}*, *ERG8*, and *P_{GAL1}-P_{GAL10}* were amplified with the primer pairs P47/P48, P49/P50, and P51/P52, respectively; *tHMG1*, *T_{GAL10}*

P_{GAL7}, *ERG12*, and *T_{ADH1}* were amplified with the primer pairs P53/P54, P55/P56, P57/P58, and P59/P60, respectively. Finally, the above amplified ten fragments were assembled to generate pZY413. The backbone of pRS426 was amplified with the primer pair P61/P62; the left and right recombination arms for CRISPR integration were amplified from *S. cerevisiae* with the primer pairs P63/P64 and P65/P66; *tHMG1-T_{tHMG1}*, *P_{GAL1}-P_{GAL10}*, and *ERG13-T_{CYC1}* were amplified with the primer pairs P67/P68, P69/P70, and P71/P72, respectively. Finally, the above amplified six fragments were assembled to generate pZY414.

To overproduce guaia-6,10(14)-diene in *S. cerevisiae*. The cassettes with the left and right *LEU2* homologous arm, *T_{CYC1}*, and backbone of pRS426 were amplified from pZY516 (unpublished data) with the primer pair P73/P74; *ERG20(FPPS)* together with *tERG20* was amplified with the primer pair P75/P76; the cDNA sequence of FgJ02895 and adjacent *P_{GAL1}-P_{GAL10}* were amplified by the primer pairs P77/78 and P79/P80, respectively. Finally, the above-mentioned four fragments were assembled to generate pYH320. To facilitate gene expression in *S. cerevisiae*, *FgJ02895* was codon-optimized as *FgJ02895-Sc*. The plasmid backbone was amplified from pYH320 with the primer pair P75/P81 and *FgJ02895-Sc* and adjacent *P_{GAL1}-P_{GAL10}* were amplified by the primer pairs P82/83 and P80/P84, respectively. These three fragments were assembled to generate pYH322. To further enhance metabolic flux of the MVA pathway and expression level of *FgJ02895-Sc*, plasmids pYL05, pYL05, and pYL07 were constructed. The backbone of pRS426 was amplified by the primer pair P85/P86; the left and right recombination arms of *URA3* of *S. cerevisiae* were amplified with the primer pairs P87/P88 and P89/P90; the selection markers *HIS3*, *tCYC1*, and *tPGK1* of *S. cerevisiae* were amplified by the primer pairs P91/P92, P93/P94, and P95/P96, respectively; the cassette *P_{GAL1}-P_{GAL10}-tHMG1* was amplified from pZY141 by the primer pair P97/P98; *FgJ02895-Sc* was amplified from pYH320 with the primer pair P99/P100; finally these eight fragments were assembled to generate pYL05. The backbone of pRS426 was amplified by the primer pair P101/P102; the left and right recombination arms of *HIS3* of *S. cerevisiae* were amplified with the primer pairs P103/P104 and P105/P106; *T_{CPS1}*, *P_{GAL1}-P_{GAL10}*, and *T_{ADH1}* of *S. cerevisiae* were amplified by the primer pairs P107/P108, P109/P110, and P111/P112, respectively; the selection marker *TRP* was amplified from pRS424 with the primer P113/P114; *FgJ02895-Sc* was amplified from pYH320 with the primer pair P115/P116; these eight fragments were assembled to generate pYL06. The backbone of pRS426 was amplified by the primer pair P117/P118; the left and right recombination arms of *YPRCdelta15* were amplified with the primer pairs P119/P120 and P121/P122; *T_{GPM1}* and *PGK1* of *S. cerevisiae* were amplified by the primer pairs P123/P124 and P125/P126, respectively; cassette *P_{GAL1}-P_{GAL10}-FgJ02895-Sc*

was amplified from pYL05 by the primer pair P127/P128. Finally, these six fragments were assembled to generate pYL07.

Plasmids pZY412, pZY413, pZY414, and pYL07 were constructed for CRISPR/Cas9-mediated integration, and the corresponding gRNA plasmid was produced as follows. The backbone of p43803 was amplified using the primer pairs P129/P130 and P131/P132, and then assembled to generate pZY606. Similarly, the backbone of p43803 was amplified using the primer pairs P130/P133 and P131/P134, and then assembled to generate pZY607; the backbone of p43803 was amplified using the primer pairs P130/P135 and P131/P136, and then assembled to generate pZY608; the backbone of p43803 was amplified using the primer pairs P130/P137 and P131/P138, and then assembled to generate pZY623.

Overproduction of guaia-6,10(14)-diene in *S. cerevisiae*. To overproduce of guaia-6,10(14)-diene in *S. cerevisiae*, pYH320 was linearized and integrated into the *LEU2* site of *S. cerevisiae* YZL141^[7] to generate *S. cerevisiae* JGH18. To enhance metabolic flux of the MVA pathway, pZY600 with Cas9 protein was integrated into the *ChrXII-2* site of *S. cerevisiae* CEN.PK2-1D to generate *S. cerevisiae* JCR1. Followed, using pZY607, the linearized pZY413 (Δ *ChrXI-3::ERG8_P_{GAL1}P_{GAL10}tHMG1_P_{GAL7}ERG12*) was integrated into the *ChrXI-3* site of mutant JCR1 to generate *S. cerevisiae* JCR23. Using pZY608, the linearized pZY414 (Δ *ChrX-3::P_{GAL1}ERG13_P_{GAL10}tHMG1*) was integrated into the *ChrX-3* site of mutant JCR23 to generate *S. cerevisiae* JCR25. Next, using pZY606, the linearized pZY412 (Δ *ChrXII-4::IDI1_P_{GAL1}P_{GAL10}ERG10_P_{GAL7}MVD1*) was integrated into the *ChrXII-4* site of mutant JCR25 to generate *S. cerevisiae* JCR27. After enhancing metabolic flux of the MVA pathway, pYH320 was linearized and integrated into the *LEU2* site of mutant JCR27 to generate *S. cerevisiae* JGH20. Plasmid pYH322 with the *FgJ02895-Sc* was also integrated into the *LEU2* site of mutant JCR27 to generate *S. cerevisiae* JGH22 to evaluate the guaia-6,10(14)-diene production efficiency. To further increase the titer of guaia-6,10(14)-diene, plasmid pLY05 with *tHMG1* and *FgJ02895-Sc* was linearized and integrated into the *URA3* site of mutant JGH22 to generate *S. cerevisiae* YL01; plasmid pLY06 with *FgJ02895-Sc* was linearized and integrated into the *HIS3* site of mutant YL01 to generate *S. cerevisiae* YL03; plasmid pLY07 with *FgJ02895-Sc* was linearized and integrated into the *YPRCdelta15* site of mutant YL03 to generate *S. cerevisiae* YL05. To replenish the *URA3* selection marker, the *GAL80* left and right homologous arms and *URA3* selection marker were amplified with the primer pairs P129/P130, P131/P132, and P133/P134, respectively. These three fragments were co-transformed into *S. cerevisiae* YL05 to generate *S. cerevisiae* YL06.

For shaking-flask fermentation of guaia-6,10(14)-diene, recombinant yeast mutants were inoculated into 5 mL of YPD (1% yeast extract, 2% tryptone, and 2% glucose) medium and cultured at 30 °C on a rotary shaker (220 rpm) overnight. The seed broth was inoculated into 45 mL YPDH (YPD medium with 1% galactose) medium to a final density of 0.1 (OD600). The culture was overlaid with 5 mL *n*-decane and cultivated at 30 °C for 72 h. Experiments were repeated three times. The organic layer was collected for GC/MS detection.

Fed-batch fermentation of guaia-6,10(14)-diene-producing strains in *E. coli* and *S. cerevisiae*.

Escherichia coli G2 and *S. cerevisiae* YL06 were selected for fed-batch fermentation as previously described with some modifications.^[12,13] For guaia-6,10(14)-diene overproduction in *E. coli*, single colonies of mutant *E. coli* G2 were grown in 5 mL LB medium overnight at 30 °C in a rotary shaker at 220 rpm as the seed culture, after which 1% of the seed culture was transferred into a 500-mL flask containing 200 mL LB and cultured at 30 °C with shaking at 220 rpm for 8–10 h. Next, 10% of the seed culture was inoculated into 2.5 L M9 medium (10 g/L (NH₄)₂SO₄, 8.5 g/L KH₂PO₄, 1 g/L MgSO₄·7H₂O, 0.5 g/L sodium citrate, 40 g/L glycerol, 0.063 g/L CaCl₂, 10 mL/L thiamine solution, 4.17 mL/L vitamins, and 4.17 mL/L metals solutions)^[14] in a 7-L fermenter for fed-batch fermentation at 30 °C, with the pH maintained at 7.2 using 9.9 N NH₄OH. The initial agitation was set to 250 rpm and increased gradually to 400 rpm to maintain the dissolved oxygen (DO) level above 20%. When the OD600 reached ~10, the culture was fed with sterile glycerol (fed solution: 500 g/L glycerol, 2 g/L MgSO₄·7H₂O) at a constant rate of 1 mL/min. When the OD600 reached 30, a final concentration of 0.25 mM IPTG was added and the production process was induced. One hour later, 5 mL antifoam L61 was added to control the foam and a 20% volume of IPM was added to facilitate accumulation of guaia-6,10(14)-diene. When the guaia-6,10(14)-diene concentration stopped increasing, fermentation was stopped.

For guaia-6,10(14)-diene overproduction in *S. cerevisiae*, fermentation media, trace metal solution, and vitamin solution were prepared as described previously.^[15,16] Single colonies of mutant *S. cerevisiae* YL06 were cultivated in 5 mL YPD medium for 20–24 h at 30 °C in a rotary shaker at 220 rpm as the seed culture, after which 1% of the seed culture was transferred into a 500-mL flask containing 250 mL YPD and cultured at 30 °C with shaking at 220 rpm for 16–20 h. Next, 30 mL trace metal solution (5.75 g/L ZnSO₄·7H₂O, 0.32 g/L MnCl₂·4H₂O, 0.47 g/L CoCl₂·6H₂O, 0.48 g/L Na₂MoO₄·2H₂O, 2.9 g/L CaCl₂·2H₂O, 2.8 g/L FeSO₄·7H₂O, and 80 mL/L 0.5 M EDTA, pH 8.0), 36 mL vitamin solution (0.05 g/L biotin, 1 g/L calcium pantothenate, 1 g/L nicotinic acid, 25 g/L myo-inositol, 1 g/L thiamine HCl, 1 g/L pyridoxal HCl, and 0.2 g/L p-aminobenzoic acid) and 10% of the seed culture were inoculated into 3 L LMG medium (40 g/L glucose, 15 g/L

(NH₄)₂SO₄, 6.2 g/L MgSO₄·7H₂O, 8 g/L KH₂PO₄, 5.9 g/L succinic acid, pH 5.0) in a 7-L fermenter for fed-batch fermentation at 30 °C, with the pH maintained at 5.0 using 2 M NaOH. During fermentation, the agitation speed increased gradually from 300 to 600 rpm and the airflow rate was maintained at 3 vvm with a DO above 20%. A two-stage fed-batch strategy was employed during the fermentation process. When glucose approached ~1 g/L in the batch culture, the first stage feeding solution (500 g/L glucose, 8 g/L KH₂PO₄, 6.2 g/L MgSO₄·7H₂O, 3.5 g/L K₂SO₄, 0.28 g/L Na₂SO₄, 10 mL trace metal solution, and 12 mL vitamin solution) was added and glucose was maintained at 1–2 g/L to enable rapid cell growth. When the OD reached 120, the first stage was stopped, and the culture was overlaid with a 20% volume of IPM to facilitate accumulation of guaia-6,10(14)-diene. When ethanol was decreased to 1–2 g/L, the second stage was started. The feeding solution ethanol was used to produce guaia-6,10(14)-diene, with the feeding rate adjusted to 7.56–20.16 mL/h to maintain an ethanol concentration of ~5 g/L. When the guaia-6,10(14)-diene concentration stopped increasing, fermentation was stopped.

Purification and structural characterization of guaia-6,10(14)-diene produced by FgJ02895.

When the fermentation procedure was finished, the organic layer of *n*-decane was collected and concentrated by atmospheric distillation in a round-bottom flask placed in an oil bath. The residue was subjected to column chromatography on a silica gel column (100 mesh, 60 cm × 5 cm i.d.) and eluted with a gradient solvent of hexane and ethyl acetate (10:0 to 9:1, v/v) to give five fractions. Further purification of guaia-6,10(14)-diene was performed by preparative HPLC using an Ultimate 3000 HPLC (Thermo Fisher Scientific, Waltham, MA, USA) equipped with a Waters Xterra RP C18 column (3.9 × 150 mm, 5 μm; Milford, MA, USA). The gradient was 0–5 min: 20% acetonitrile, 5–10 min: 20%–100% acetonitrile, 10–40 min: 100% acetonitrile, 40–45 min: 100%–20% acetonitrile at a flow rate of 1.5 mL/min with UV detection at λ = 210 nm, giving **1**. Product structures were determined by NMR analysis.

Table S1. Oligonucleotides for the construction of plasmids in this study.

Plasmid	Primer	Sequence (5'-3')
pGB150	P1	CCAGCATATGGTCAAATTCGACAGCAGTAG
	P2	ATATctcgagactagTCACAGCGCCGCCAAACTCTTTG
pGB216	P3	GCATCATATGGTTAAATTCGACAGCAGC
	P4	ATATctcgagactagTTACAGCGCCGCCAGGCTCTTC
pSC51	P5	GAGTCATATGGTCAAATTTGATAGTGGTTC
	P6	ATATctcgagactagTTACAACGCTGCCATCTTCTTTG
pSC53	P7	GCATcatATGGTCAAATTTGATAGTGGTTC
	P8	ATATctcgagactagTTACAACGCTGCCATCTTCTTTG
pSC55	P9	TACGCATATGGTCAAATTCGATAGTGGTTC
	P10	ATATctcgagactagTTACAACGCTGCCATCTTCTTTG
pSC61	P11	CGTAGAGGATCGGGCGCGCCtaatacgaactactatagggg
	P12	gggtgtctcgagACTAGTTACAGCGCCGCCAGGCTCT
	P13	gggtctgaggggtttttgGGCGCGCCCGATCCCGCgAAATTAATACG
	P14	ccctatagtgagtcgtattaGGCGCGCCCGATCCTCTACGCCGGACGC
pZY600	P15	GCTTGAGAAGGTTTTGGGACGCTCGAAGGCTTTAATTTGCccgccatccagtgctgaa
	P16	cattatacgaagtataaaggggtgtcgaacctgcagccataacggttacacggaag
	P17	cgggccctctactgctcctccgtgtaacgcgttatggctgcaggtcgacaaccc
	P18	AGTAAAAAGGAGTAGAAACATTTTGAAGCTATGAGCTcgttagtatcgaatcgacagc
	P19	ggtcgtatactgctgtcgattcgatacgaacAGCTCATAGCTTCAAATGTTTCTAC
	P20	aagggtctcgagagctcgttttcgacactggatggcggGCAAATTAAGCCTTCGAGC
pZY412	P21	aaaacttgattatctcatacctcattgatgGCGGCCGCAACAGTTGCGCAGCCTGAA
	P22	ctgaattagatcccgaagtcattgagtcGCGGCCGCTACTAGAGCTCCAGCTTTTGTTTC
	P23	CTAAAGGGAACAAAAGCTGGAGCTCTAGTAGCGGCCGCgactcaatgactcgggatct
	P24	CATGAGGTCGCTCTTATTGACCACCTCTACCGGctgaacaggaactaagtagctac
	P25	tagtgatcagatccactagtggaattcccattagagtagcaataaaag
	P26	GCCATTCAGGCTGCGCAACTGTTGCGGCCGCcatcaatggaggtatgagataaatcaag
	P27	cgtataaaatagccgctgtagctacttaagttcctgttcagCCGGTAGAGGTGTGGTCA
	P28	GACGCAAAGACTGGTCTACCAAAGGAATAAGCGAATTTCTTATGATTTATGATTTTAT
	P29	TAATAATAAAAATCATAAATCATAAGAAATTCGCTTATTCTTTGGTAGACCAGTCTTT
	P30	caacatgataaaaaaacagttgaatattccctcaaaaATGACCGTTTACACAGCATC
	P31	GGTAACGGATGCTGTGTAACGGTCATttttgaggaataatcaactgtttttttat
	P32	GGTGGTGCTTCTCTATTGTCATTGAAAAGATATGAttgccagcttactatcctct
	P33	atttcaagaaggatagtaagctggcaaaTCATATCTTTTCAATGACAATAGAGGAAG
	P34	aaaaaaaaagtaagaattttgaaaattcaataaaATGTCTCAGAACGTTTACATTGT
	P35	CGATACAATGTAACGTTCTGAGACATttatattgaatttcaaaaattctactttt

	P36	CATGGGGCATACTATTGTTGTCGGCAGTCATtatagtttttctccttgacgttaaagt
	P37	tatacctctatactttaacgtcaaggagaaaaactataATGACTGCCGACAACAATAG
	P38	tacatgatatcgacaaaggaaaagggcctgtTTATAGCATTCTATGAATTTGCCTGTC
	P39	CTGAAGTGGAAAATGACAGGCCAAATTCATAGAATGCTATAAacaggccccttttcttt
	P40	gaggcatcctttatttgactctaattgggaattgccactagtgatctgatcacc
pZY413	P41	cattcaagccattaagtatacccaacttaacGCGGCCGCAACAGTTGCCGAGCCTGAA
	P42	atggtttacaacccgaggattctctgcGCGGCCGCTACTAGAGCTCCAGCTTTTGTTCC
	P43	TCACTAAAGGGAACAAAAGCTGGAGCTCTAGTAGCGGCCGCgcagagaaatccctcggtt
	P44	gcttgagaaggtttgggacgctcgaaggcttaattgcaatcagacgcacgctgg
	P45	CATGAGGTCGCTCTTATTGACCACACCTCTACCGGttacgtggattgagccagcaatac
	P46	TTCGCCATTCAAGGCTGCGCAACTGTTGCGGCCGCgtaagttgggtataactaatggct
	P47	ttccgttttaggatattgacccaagcgtcgtctgattgcaaataaagccttcgac
	P48	TTAGGAAAGAAAAAGATCCGAAACTTATCTTGATAAATAAacaggccccttttcttt
	P49	acatgatatcgacaaaggaaaagggcctgtTTATTATCAAGATAAGTTTCCGGATCT
	P50	atatacctctatactttaacgtcaaggagaaaaactataATGTCAGAGTTGAGAGCCT
	P51	GCACTGAAGGCTCTCAACTCTGACATtatagtttttctccttgacgttaaagtataga
	P52	AATGACTGTTTTATTGGTTAAAACCATttatattgaattttcaaaaattctactttt
	P53	aaaaagtaagaattttgaaaattcaataaaATGGTTTTAACCAATAAACAGTCATT
	P54	gagtgcatatttcaagaaggatagtaagctggcaaaTTAGGATTTAATGCAGGTGACG
	P55	TTGAAAGATGGGTCGTCACCTGCATTAAATCCTAAttgccagcttactatccttct
	P56	tcccgtgcagaagtaagaacggtaatgacattttgagggaaatattcaactgtttt
	P57	tgataaaaaaaaaacagttgaatattccctcaaaaatgtcattaccgttctaactctg
	P58	TAATAATAAAAATCATAAATCATAAGAAATTCGCttatgaagtccatgtaaatctg
	P59	ccaggaacacgaattaccatggactcataaGCGAATTTCTTATGATTTATGATTTT
	P60	gtttaataatgatctgtattgctggctcaatccagtaaCCGGTAGAGGTGTGGTCAAT
pZY414	P61	gcccaacgcctttacatttatttcaaatgGCGGCCGCAACAGTTGCCGAGCCTGAATG
	P62	cctatctgtatgtgttaattgagGCGGCCGCTACTAGAGCTCCAGCTTTTGTTCC
	P63	GGAACAAAAGCTGGAGCTCTAGTAGCGGCCGCtcaaatcacacatacagataggtc
	P64	CTATGTGCGCCATCCGATAAATGTAGGAGCAATGAAGCtctctgtatgctcgctctgc
	P65	AAGGTTTTGGGACGCTCGAAGGCTTTAATTTGCccacttttcaatgaaacggatattga
	P66	GCCATTCAGGCTGCGCAACTGTTGCGGCCGCcattttgaaataaatgtaaaggcgtgg
	P67	taggcaagaagtaggcgagagccgacatacagagaGCTTCATTGCTCCTACATTTATCGG
	P68	agtaagaattttgaaaattcaataaaATGGTTTTAACCAATAAACAGTCATTTCTG
	P69	AAATGACTGTTTTATTGGTTAAAACCATttatattgaattttcaaaaattctactttt
	P70	ACACCAACAAAGTTTAGTTGAGAGTTTCATtatagtttttctccttgacgttaaagta
	P71	tctatactttaacgtcaaggagaaaaactataATGAAACTCTCAACTAACTTTGTTG
	P72	actagcatatcaatatccgtttcattgaaaagtgGCAAAATTAAGCCTTCGAGCGTC

Appendix

pYH320	P73	ACTAGTCCAAGGATTTTTTTTAAAAAGATTCTCTTTTTTTATGATATTTGTACATAAAC
	P74	CGCGAGAGTTGTTGATACCAAAGAGTTTGGCGGCGCTGTGAACAGGCCCTTTTCCTTT
	P75	ctttaacgtcaaggagaaaaaactataatgGCTTCAGAAAAAGAAATTAG
	P76	ATGTACAAATATCATAAAAAAGAGAATCTTTTTAAAAAAATCCTTGGACTAGTCACG
	P77	ATAACTAATTACATGATATCGACAAAGGAAAAGGGGCCTGTTACAGCGCCGCCAAACT
	P78	tccaaaaaaaagtaagaatTTTTgaaaattcaataaaATGGTCAAATTCGACAGCAG
	P79	AACTACTGCTGTGCAATTTGACCATttatattgaatTTTcaaaaattctactTTTT
	P80	CTAATTTCTTTTTCTGAAGCattatagTTTTTctccttgacgttaaag
pYH322	P81	CAAGAGAATTGTTGATTCCAAAATCATTGGCTGCATTATAAACAGGCCCTTTTCCTTT
	P82	aaaaaaagtaagaatTTTTgaaaattcaataaaATGGTTAAGTTTCGATTCTTCATCTT
	P83	ATTACATGATATCGACAAAGGAAAAGGGGCCTGTTTATAATGCAGCCAATGATTTTGA
	P84	AAGATGAAGAATCGAACTTAACCATttatattgaatTTTcaaaaattctactTTTT
pYL05	P85	cctctcgagagtagacattgcccTTaaacgGCGGCCGCACAGACAAGCTGTGACCGTC
	P86	gctcaaaaacctggaattatctcgTGCAGGCCGCGCTTTTGTCCCTTAGTGAGGG
	P87	TTAACCTCACTAAAGGGAACAAAAGCGCGGCCGCacgcagataattccaggattttg
	P88	CGACTCACTATAGGGCGAATTGGGTACcttctgctcaggttttg
	P89	GTTAATAAAGCTCGAAAATTCTGCGTTCGTTgtaaagcatgtataactcaaaat
	P90	CTCCCGGAGACGGTCACAGCTTGCTGTGCGGCCGCcgtttaagggcaaatgactctc
	P91	caaaaacctgcaggaaacgaagGTACCCAATTCGCCCTATAGTGAGTCG
	P92	CTTGAGAAGTTTTGGGACGCTCGAAGGCTTTAATTTGCTCACAGCTTGCTGTAAAGCG
	P93	TTGTCTGCTCCCGCATCCGCTTACAGACAAGCTGTGAGCAAATTAAGCCTTCGAGCG
	P94	GTTTGAAGATGGGTCCGTCACCTGCATTAAATCCTAAACAGGCCCTTTTCCTTTGTC
	P95	CCAAAATCATTGGCTGCATTATAAATTGAATTGAATTGAAATCGATAGATCAATTTTT
	P96	tgaagctctaatttgagtttagtatacatgcatTAACGAACGCAGAATTTTCG
	P97	TAATTACATGATATCGACAAAGGAAAAGGGGCCTGTTTAGGATTTAATGCAGGTGACGG
	P98	ATTCTGAAGATGAAGAATCGAACTTAACCATtatagTTTTTctccttgacgttaaagt
	P99	ctctactTTaacgtcaaggagaaaaaactataATGGTTAAGTTTCGATTCTTCATCTT
	P100	AAAAATTGATCTATCGATTTCAATTCATTCAATTTATAATGCAGCCAATGATTTTGA
pYL06	P101	tggatctattgtctgcatccactgacggttGCGGCCGCACAGACAAGCTGTGACCGTC
	P102	caagaaatgggtggctggacgttGCGGCCGCGCTTTTGTCCCTTAGTGAGGGTTAA
	P103	CAATTAACCCTCACTAAAGGGAACAAAAGCGCGGCCGCaaacgtccagccaccatttc
	P104	ATCCGCTTACAGACAAGCTGTGAttagtatattctcgaagaaatcacattactttat
	P105	TAAAAAAGAAAGTGTCAAATCAAGTGTCAAATaagagatggaggacgggaaaaag
	P106	AGCTCCCGGAGACGGTCACAGCTTGCTGTGCGGCCGCaaacgtcagtgatgcagac
	P107	TGAAGAATCGAACTTAACCATttatattgaatTTTcaaaaattctactTTTTTTTgg
	P108	TCTTTGACTATTCAATCATTGCGCtatagTTTTTctccttgacgttaaag
	P109	ctttaacgtcaaggagaaaaaactataGCGCAATGATTGAATAGTCAAAGA

Supporting Information – Semisynthesis of (-)-Englerin A

	P110	caactaacttttcccgtcctccatctcttATTTGACACTTGATTTGACACTTCTTTTT
	P111	CGCGTAATACGACTCACTATAGGGCGAATTGGGTACCCGGTAGAGGTGTGGTCAATAAG
	P112	GGCTGCATTATAAGCGAATTTCTTATGATTTATGATTTTTATTATTAATAAGTTATAA
	P113	ataaagtaatgtgatttctcgaagaatatactaaaTCACAGCTTGTCTGTAAGCGGAT
	P114	CATGAGGTGCGCTCTTATTGACCACACCTCTACCGGGTACCCAATTGCCCCTATAGTGAG
	P115	aaaaaaagtaagaattttgaaaattcaatataaATGGTTAAGTTTCGATTCTTCATCTT
	P116	TAATAATAAAAATCATAAATCATAAGAAATTCGCTTATAATGCAGCCAATGATTTTGG
pYL07	P117	GCGTTCATCGGTTTATTAGAAGCGCGGCCGCAACAGTTGCGCAGCCTGAATGGCGAATG
	P118	GGAATAACGTGATTTTTGTACCAAATTGCCGCGGCCGCTACTAGAGCTCCAGCTTTTGTTC
	P119	GAACAAAAGCTGGAGCTCTAGTAGCGGCCGCGCAATTTGGTACAAAAATCACGTTATCC
	P120	ACCAATTGCAAAGGGAAAAGCTGAATGGGCAGTTCGAATATTTGCGAAACCCTATGCTC
	P121	GTTTAATAACTCGAAAATTCTGCGTTCGTTAATGGAAGGTCGGGATGAGCATATAC
	P122	CATTCGCCATTCAGGCTGCGCAACTGTTGCGGCCGCGCTTCTAATAAACCGATGAACGC
	P123	AATTTCAAATCCGAACAACAGAGCATAGGGTTTCGCAAATATTCGAACTGCCATTGAG
	P124	aaagtaagaattttgaaaattcaatataaGTCTGAAGAATGAATGATTTGATGATTTTC
	P125	TGATTCCAAAATCATTGGCTGCATTATAAATTGAATTGAATTGAAATCGATAGATCAAT
	P126	GTATATGCTCATCCCGACCTTCCATTAACGAACGCAGAATTTTCGAGTTATTAAC
	P127	TCATCAAATCATTCTTCTCAGACTtatatgaaatttcaaaaatttctactttttt
	P128	AAAAAATTGATCTATCGATTTCAATTCAATTCAATTTATAATGCAGCCAATGATTTTGG
pZY606	P129	taaatgatcgctcaagaattgagtaaacGTTTTAGAGCTAGAAATAGCAAGTTAAAAT
	P130	gataaaggcatccccgattatattc
	P131	cacaaagtatgcaatcc
	P132	TTTCTAGCTCTAAAACgtttactcaattcttgaagcgatcatttatctttcactgcgga
pZY607	P133	taaatgatcatatgtctctaatttggaaGTTTTAGAGCTAGAAATAGCAAGTTAAAAT
	P134	TTTCTAGCTCTAAAACtccaaaattagagacatatgatcatttatctttcactgcgga
pZY608	P135	taaatgatcctaagtgtcccggttctaGTTTTAGAGCTAGAAATAGCAAGTTAAAAT
	P136	TTTCTAGCTCTAAAACtagaaacgaggacacattagatcatttatctttcactgcgga
pZY623	P127	taaatgatcTCTTGAATCAGTACATAGCGTTTTAGAGCTAGAAATAGCAAGTTAAAAT
	P128	TTTCTAGCTCTAAAACGCTATGTACTGATTCCAAGAgatcatttatctttcactgcgga
ΔGAL80 ::URA3	P129	caatggtctaggtagtgccattcg
	P130	CGACTCACTATAGGGCGAATTGGGTACgacgggagtgaaagaacgg
	P131	tccggttcttccactcccgctGTACCCAATTGCCCCTATAGTGAG
	P132	gccaaagcacagggaagatgctTCACAGCTTGTCTGTAAGCGGA
	P133	GCATCCGCTTACAGACAAGCTGTGAaagcatctgcctgtgctt
	P134	gagaccaccaagaatacagaagctattat

Table S2. Plasmids used in this study.

Plasmids	Description	Source
pMH1	<i>P_{Lac}: AtoB, ERG13, tHMG1, CM^R</i>	[17]
pFZ81	<i>P_{Lac}: ERG12, ERG8, MVD1, IDI, Kan^R</i>	[17]
pGB150	<i>P_{T7}: N-terminal his6-tag FgJ02895, Kan^R</i>	This work
pGB216	<i>P_{T7}: N-terminal his6-tag FgJ02895-Ec, Amp^R</i>	This work
pGB218	<i>P_{T7}: FgJ02895-Ec, FPPS, IDI</i>	This work
pSC52	<i>P_{T7}: STC5, FPPS, IDI</i>	This work
pSC54	<i>P_{T7}: FpN62905, FPPS, IDI</i>	This work
pSC56	<i>P_{T7}: FmM7560, FPPS, IDI</i>	This work
pSC61	<i>P_{T7}-FgJ02895(2X)-Ec-ispA-IDI</i>	This work
pZY412	<i>ChrXII-4Δ:: P_{GAL1}_IDI1, P_{GAL10}_ERG10, P_{GAL7}_MVD1</i>	This work
pZY413	<i>P_{GAL1}_ERG8, P_{GAL10}_tHMG1, P_{GAL7}_ERG12</i>	This work
pZY414	<i>ChrX-3Δ:: P_{GAL1}_ERG13, P_{GAL10}_tHMG1</i>	This work
pZY521	<i>GAL80Δ::URA3</i>	This work
pZY600	<i>ChrXII-2Δ:: HygR_P_{TEF1}_Cas9</i>	This work
pZY606	<i>gRNA_ChrXII-4</i>	This work
pZY607	<i>gRNA_ChrXI-3</i>	This work
pZY608	<i>gRNA_ChrX-3</i>	This work
pZY623	<i>gRNA_YPRCdelta15</i>	This work
pYH320	<i>ΔLEU2::URA3_PGAL10_FgJ02895, PGAL1_ERG20</i>	This work
pYH322	<i>ΔLEU2::URA3_PGAL10_FgJ02895-Sc, PGAL1_ERG20</i>	This work
pLY05	<i>URA3Δ::HIS3_P_{GAL1}_FgJ02895_P_{GAL10}_tHMG1</i>	This work
pLY06	<i>HISΔ::TRP1_P_{GAL10}_FgJ02895-Sc</i>	This work
pLY07	<i>YPRCdelta15Δ:: PGAL1_FgJ02895-Sc; GAL80Δ::URA3</i>	

Table S3. Strains used in this study.

Strains	Genome type	Source
<i>E. coli</i> BL21(DE3)	<i>E. coli</i> B <i>F-dcm ompT hsdSB(rB-mB-)gal</i>	Invitrogen
<i>E. coli</i> C1	<i>P_{Lac}-AtoB-ERG13-tHMG1; P_{Lac}-ERG12-ERG8-MVD1-Idi;</i>	[17]
<i>E. coli</i> G1	<i>P_{Lac}-AtoB-ERG13-tHMG1; P_{Lac}-ERG12-ERG8-MVD1-Idi; P_{T7}-FgJ02895-Ec-ispA-Idi;</i>	This work
<i>E. coli</i> G2	<i>P_{Lac}-AtoB-ERG13-tHMG1; P_{Lac}-ERG12-ERG8-MVD1-Idi; P_{T7}-FgJ02895(2X)-Ec-ispA-Idi;</i>	This work
<i>E. coli</i> G3	<i>P_{Lac}-AtoB-ERG13-tHMG1; P_{Lac}-ERG12-ERG8-MVD1-Idi; P_{T7}-FgJ02895-Ec-GSTGS-ispA-Idi;</i>	This work
<i>S. cerevisiae</i> CEN.PK2-1D	<i>MATα, ura3-52, trp1-289, leu2-3,112, his3Δ1, MAL2-8C, SUC2</i>	EUROSCARF
<i>S. cerevisiae</i> YZL141	<i>gal1Δ, gal7Δ, gal10Δ:: TRP1_P_{GAL10}-tHMG1</i>	[7]
<i>S. cerevisiae</i> JGH20	<i>gal1Δ, gal7Δ, gal10Δ:: TRP1_P_{GAL10}-tHMG1; ΔLEU2::URA3_P_{GAL10}-FgJ02895, P_{GAL1}-ERG20</i>	This work
<i>S. cerevisiae</i> JCR1	<i>ChrXII-2Δ:: HygR_P_{TEF1}-Cas9</i>	This work
<i>S. cerevisiae</i> JCR23	<i>ChrXII-2Δ:: HygR_P_{TEF1}-Cas9; ChrXI-3Δ:: P_{GAL1}-ERG8, P_{GAL10}-tHMG1, P_{GAL7}-ERG12</i>	This work
<i>S. cerevisiae</i> JCR25	<i>ChrXII-2Δ:: HygR_P_{TEF1}-Cas9; ChrXI-3Δ:: P_{GAL1}-ERG8, P_{GAL10}-tHMG1, P_{GAL7}-ERG12; ChrX-3Δ:: P_{GAL1}-ERG13, P_{GAL10}-tHMG1</i>	This work
<i>S. cerevisiae</i> JCR27	<i>ChrXII-2Δ:: HygR_P_{TEF1}-Cas9; ChrXI-3Δ:: P_{GAL1}-ERG8, P_{GAL10}-tHMG1, P_{GAL7}-ERG12; ChrX-3Δ:: P_{GAL1}-ERG13, P_{GAL10}-tHMG1; ChrXII-4Δ:: P_{GAL1}-IDI1, P_{GAL10}-ERG10, P_{GAL7}-MVD1</i>	This work
<i>S. cerevisiae</i> JGH18	<i>ChrXII-2Δ:: HygR_P_{TEF1}-Cas9; ChrXI-3Δ:: P_{GAL1}-ERG8, P_{GAL10}-tHMG1, P_{GAL7}-ERG12; ChrX-3Δ:: P_{GAL1}-ERG13, P_{GAL10}-tHMG1; ChrXII-4Δ:: P_{GAL1}-IDI1, P_{GAL10}-ERG10, P_{GAL7}-MVD1; ΔLEU2::URA3_P_{GAL10}-FgJ02895, P_{GAL1}-ERG20</i>	This work
<i>S. cerevisiae</i> JGH22	<i>ChrXII-2Δ:: HygR_P_{TEF1}-Cas9; ChrXI-3Δ:: P_{GAL1}-ERG8, P_{GAL10}-tHMG1, P_{GAL7}-ERG12; ChrX-3Δ:: P_{GAL1}-ERG13, P_{GAL10}-tHMG1; ChrXII-4Δ:: P_{GAL1}-IDI1, P_{GAL10}-ERG10, P_{GAL7}-MVD1; ΔLEU2::URA3_P_{GAL10}-FgJ02895-Sc, P_{GAL1}-ERG20</i>	This work
<i>S. cerevisiae</i> YL01	<i>ChrXII-2Δ:: HygR_P_{TEF1}-Cas9; ChrXI-3Δ:: P_{GAL1}-ERG8, P_{GAL10}-tHMG1, P_{GAL7}-ERG12; ChrX-3Δ:: P_{GAL1}-ERG13, P_{GAL10}-tHMG1; ChrXII-4Δ:: P_{GAL1}-IDI1, P_{GAL10}-ERG10, P_{GAL7}-MVD1; ΔLEU2::URA3_P_{GAL10}-FgJ02895-Sc, P_{GAL1}-ERG20; URA3Δ::HIS3_P_{GAL1}-FgJ02895_P_{GAL10}-tHMG1</i>	This work

Appendix

<p><i>S. cerevisiae</i> YL03</p>	<p><i>ChrXII-2Δ:: HygR_P_{TEF1}_Cas9; ChrXI-3Δ:: P_{GAL1}_ERG8, P_{GAL10}_tHMG1, P_{GAL7}_ERG12; ChrX-3Δ:: P_{GAL1}_ERG13, P_{GAL10}_tHMG1; ChrXII-4Δ:: P_{GAL1}_IDI1, P_{GAL10}_ERG10, P_{GAL7}_MVD1; ΔLEU2::URA3_P_{GAL10}_FgJ02895-Sc, P_{GAL1}_ERG20; URA3Δ::HIS3_P_{GAL1}_FgJ02895_ P_{GAL10}_tHMG1; HISΔ::TRP1_P_{GAL10}_FgJ02895-Sc</i></p>	<p>This work</p>
<p><i>S. cerevisiae</i> YL05</p>	<p><i>ChrXII-2Δ:: HygR_P_{TEF1}_Cas9; ChrXI-3Δ:: P_{GAL1}_ERG8, P_{GAL10}_tHMG1, P_{GAL7}_ERG12; ChrX-3Δ:: P_{GAL1}_ERG13, P_{GAL10}_tHMG1; ChrXII-4Δ:: P_{GAL1}_IDI1, P_{GAL10}_ERG10, P_{GAL7}_MVD1; ΔLEU2::URA3_P_{GAL10}_FgJ02895-Sc, P_{GAL1}_ERG20; URA3Δ::HIS3_P_{GAL1}_FgJ02895_ P_{GAL10}_tHMG1; HISΔ::TRP1_P_{GAL10}_FgJ02895-Sc; YPRCdelta15Δ:: P_{GAL1}_FgJ02895-Sc</i></p>	<p>This work</p>
<p><i>S. cerevisiae</i> YL06</p>	<p><i>ChrXII-2Δ:: HygR_P_{TEF1}_Cas9; ChrXI-3Δ:: P_{GAL1}_ERG8, P_{GAL10}_tHMG1, P_{GAL7}_ERG12; ChrX-3Δ:: P_{GAL1}_ERG13, P_{GAL10}_tHMG1; ChrXII-4Δ:: P_{GAL1}_IDI1, P_{GAL10}_ERG10, P_{GAL7}_MVD1; ΔLEU2::URA3_P_{GAL10}_FgJ02895-Sc, P_{GAL1}_ERG20; URA3Δ::HIS3_P_{GAL1}_FgJ02895_ P_{GAL10}_tHMG1; HISΔ:: TRP1_P_{GAL10}_FgJ02895-Sc; YPRCdelta15Δ:: P_{GAL1}_FgJ02895-Sc; GAL80Δ::URA3</i></p>	<p>This work</p>

>STC5 (*Fusarium fujikuroi* IMI58289)

MVKFDSGSESEMTNGDELHINSKHEVKSRMANGNGVHNVPDHDQFQDRAEMEV LIL
PDLFSSLMSVPARENPHYASVKADADEWISFVINADAKWASRNKRVDFTYLASIWAPD
CSAFALRTSADWNSWAFLFDDQFDEGHLSNDLEGAINIARTREIMEGTAPRYTADSE
HPIRYVFQTLCDRVKQNPEGFYAGKPSSERFYRRWMWAHELWYWEGLVAQVRTNVE
GRSFTRGPEEYLAMRRGSLGAYPALVNNEWAYGIDLPEEVADHPLVFEIMIIMSDQILL
VNDILSYEKDLRLGVDHNMVRLKAKGLSTQQAINVEGVMINNCYRRYYRALSELPCF
GEEADRALLGYLEVEKNHALGSLLWSYNTGRYFKSKEDGARVRKTRRELLIPKKMAAL*

>FpN62905 (*Fusarium proliferatum* NRRL 62905)

MVKFDSGSESEMTNGDELHINSKHEVKSRMANGNGVHNVPDHDQFQDRAEMEV LIL
PDLFSSLMSVPARENPHYASVKADADEWISSVINADAKWASRNKRVDFTYLASIWAPD
CSAFALRTSADWNSWAFLFDDQFDEGHLSNDLDGAINIARTREIMEGTAPRYTADSE
HPIRYVFQTLCDRVKQSPEGFYAGKPSSERFYRRWMWAHELWYWEGLVAQVRTNVEG
RSFTRGPEEYLAMRRGSLGAYPALVNNEWAYGIDLPEEVADHPLVFEIMVIMSDQILL
VNDILSYEKDLRLGVDHNMVRLKAKGLSTQQAINVEGVMINNCYRRYYRALSELPCF
GEEADRALLGYLEVEKNHALGSLLWSYKTGRYFKSKEDGARVRKTRRELLIPKKMAAL*

>FmM7560 (*Fusarium mangiferae* MRC 7560)

MVKFDSGSESEMTNGDEVHINTKHEVKSRMANGNGVHNVPDHDQFQDRAEMEV LIL
PDLFSSLMSVPARENPHYASVKADADEWISSVINADAKWASRNKRVDFTYLASIWAPD
CSAFALRTSADWNSWAFLFDDQFDEGHLSNDLDGAINIARTREIMEGTAPRYTADSE
HPIRYVFQTLCDRVKQSPEGFYAGKPSSDRFYRRWMWAHELWYWEGLVAQVRTNVE
GRSFTRGPEEYLAMRRGSLGAYPALVNNEWAYGIDLPEDVADHPLVFEIMVIMSDQIL
LVNDILSYEKDLRLGVDHNMVRLKAKGLSTQQAINVEGVMINNCYRRYYRALSELPC
FGEEADRALLGYLEVEKNHALGSLLWSYKTGRYFKSKEDGARVRKTRRELLIPKKMAAL

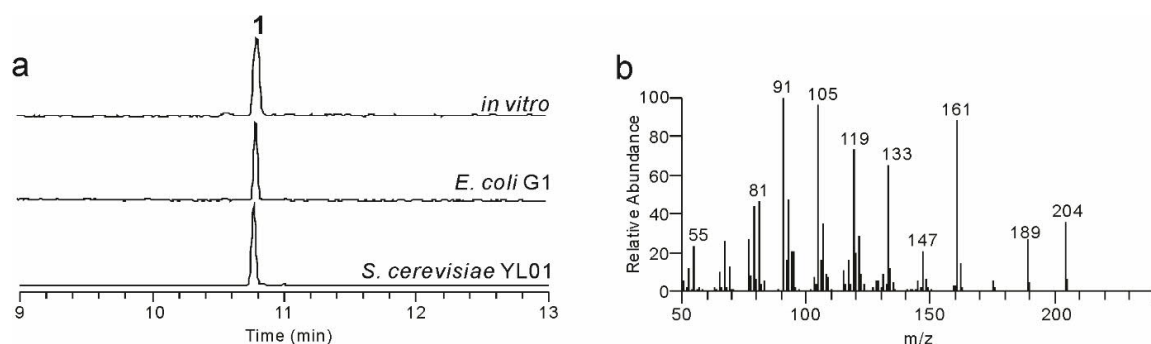
*

>FgJ02895 (*Fusarium graminearum* J1-012)

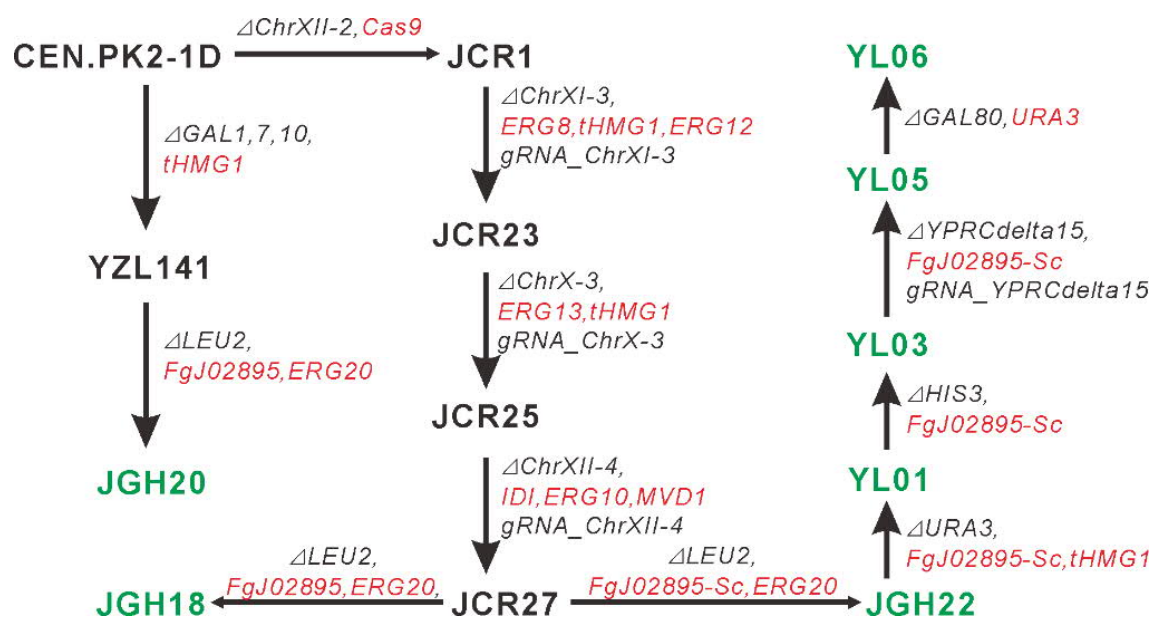
MVKFDSSSESEMTTGDEVYIDTKHEVKLKMKNNGVYNEPKHDQFQGRDEMEVLIL
PDLFSSLMSVPARENPNYASVKAEDDWISSVIKADADWTNRNKRVDFTYLANIWAP
DCSAFALRTSADWNSWAFLFDDQFDEGHLCNDLEGAISEIARTREIMEGTAPRYTADS
EHPIRYVFQTLCDRIKQSPEGFFIGKPSSDRFYKRWMWAHELWYQGLVDQVRTNVEG
RSYTRRPEEYMAMRRGSLGAYPALVNNEWAYGIDLPEEVADHPSVFEIMVIISDQILLV
NDILSYEKDLRLGVDHNMVRLKAKGHSTQQAINVEGVMINNCYRRYYRALSKLPCFG
EEADRALLGFLEVEKNHALGSLLWSYKTGRYFKSKEDGARVRKTRRELLIPKSLAAL*

Table S4. NMR data of guaia-6,10(14)-diene.

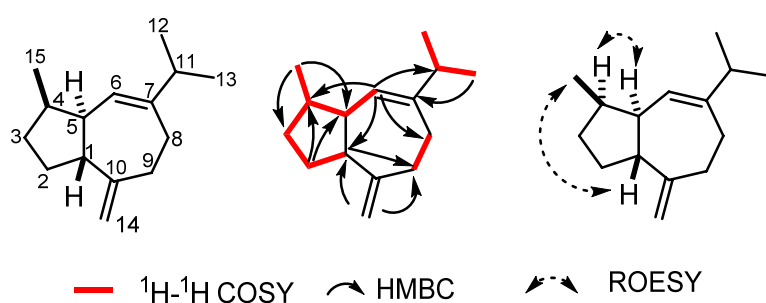
Nr.	¹³ C	¹ H	Intensity	Multiplicity	HMBC correlation	COSY correlation
	δ(ppm)	δ(ppm)				
1	47.7	2.29	1H	overlap	6, 9, 14	H-2b
2	27.6	1.81	1H	m	4, 10	H-1, H-3a
		1.71	1H			
3	32.9	1.85	1H	m	1	H-4a
		1.28	1H	m		
4	36.8	2.20	1H	overlap	1	H-15
5	47.6	2.28	1H	overlap		H-6
6	123.9	5.56	1H	br s	4, 8, 11	
7	148.5					
8	30.0	2.19	1H	overlap		H-9a
		1.98	1H	overlap		
9	37.4	2.47	1H	m	7, 14	H-8a
		1.99	1H	overlap		
10	155.0					
11	37.3	2.23	1H	m		H-12, H-13
12	21.5	0.98	3H	d (<i>J</i> = 3.9 Hz)	7, 11, 13	H-11
13	21.3	0.96	3H	d (<i>J</i> = 3.9 Hz)	7, 11, 12	H-11
14	106.0	4.69	1H	br s		
		4.67	1H	br s		
15	17.1	0.93	3H	d (<i>J</i> = 6.9 Hz)	3, 5	



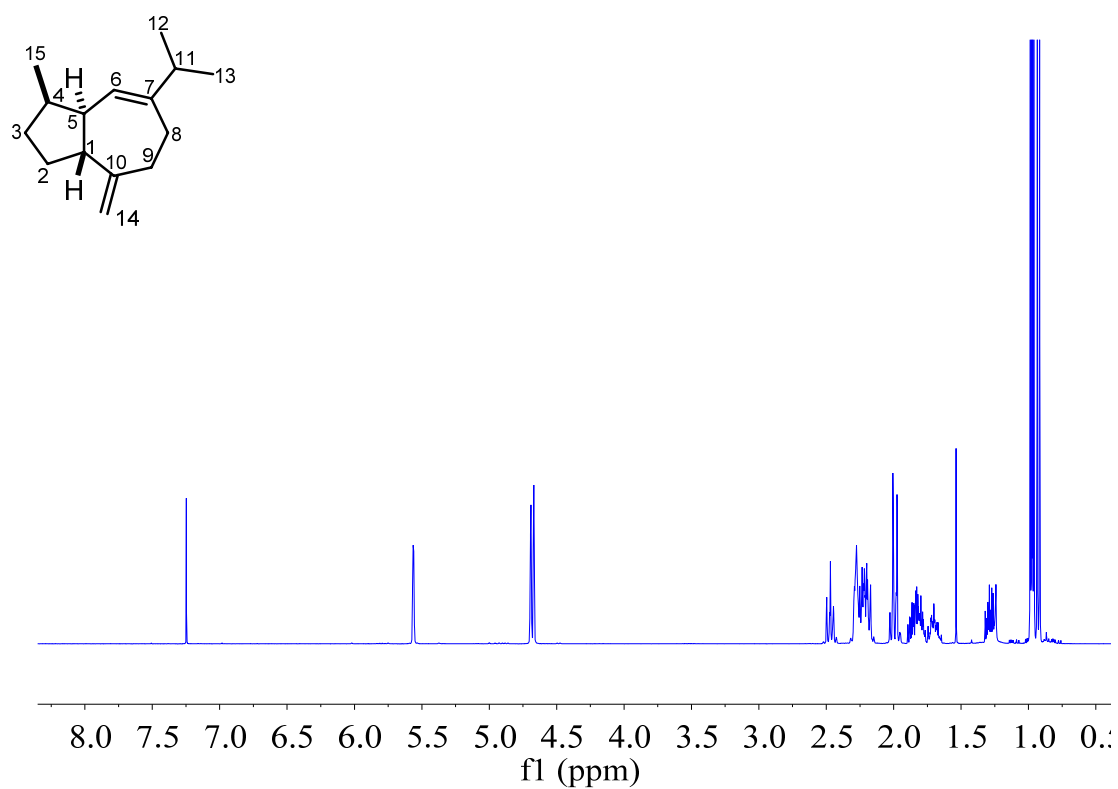
Supplementary Figure 3. *In vitro* assay and *in vivo* fermentation of guaia-6,10(14)-diene (1) in *E. coli* and *S. cerevisiae*. (a) GC/MS chromatogram of guaia-6,10(14)-diene produced by *in vitro* assay and *in vivo* fermentation; (b) mass spectra of guaia-6,10(14)-diene produced by FgJ02895.



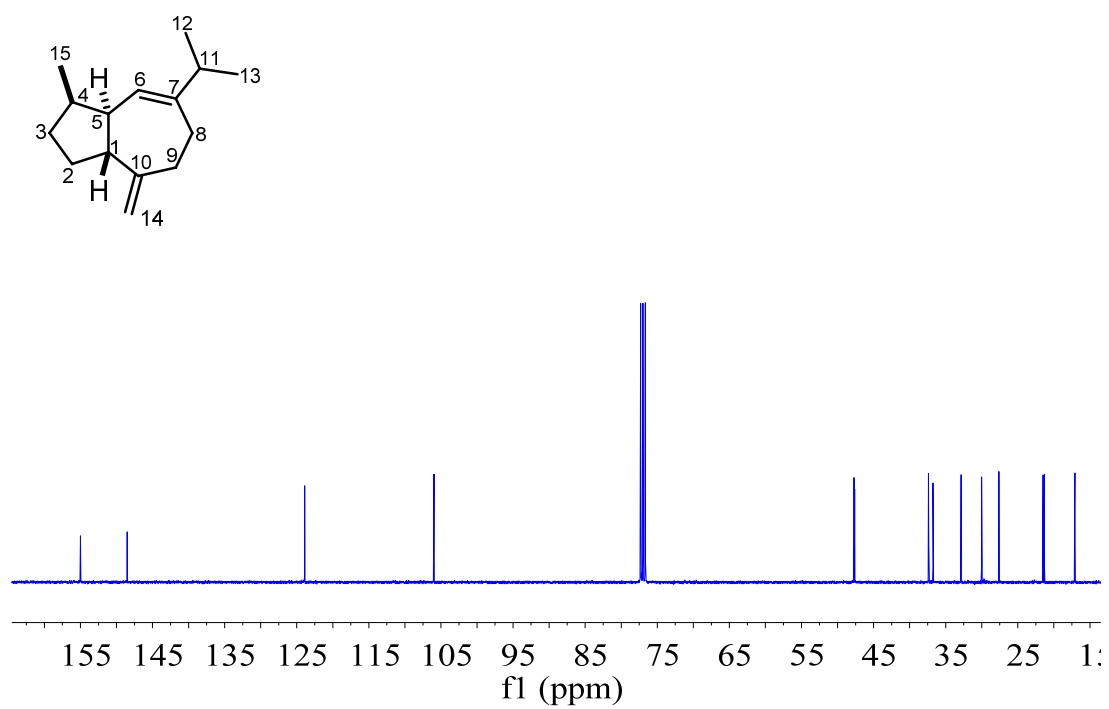
Supplementary Figure 4. Flowchart of *S. cerevisiae* mutant construction in this study.



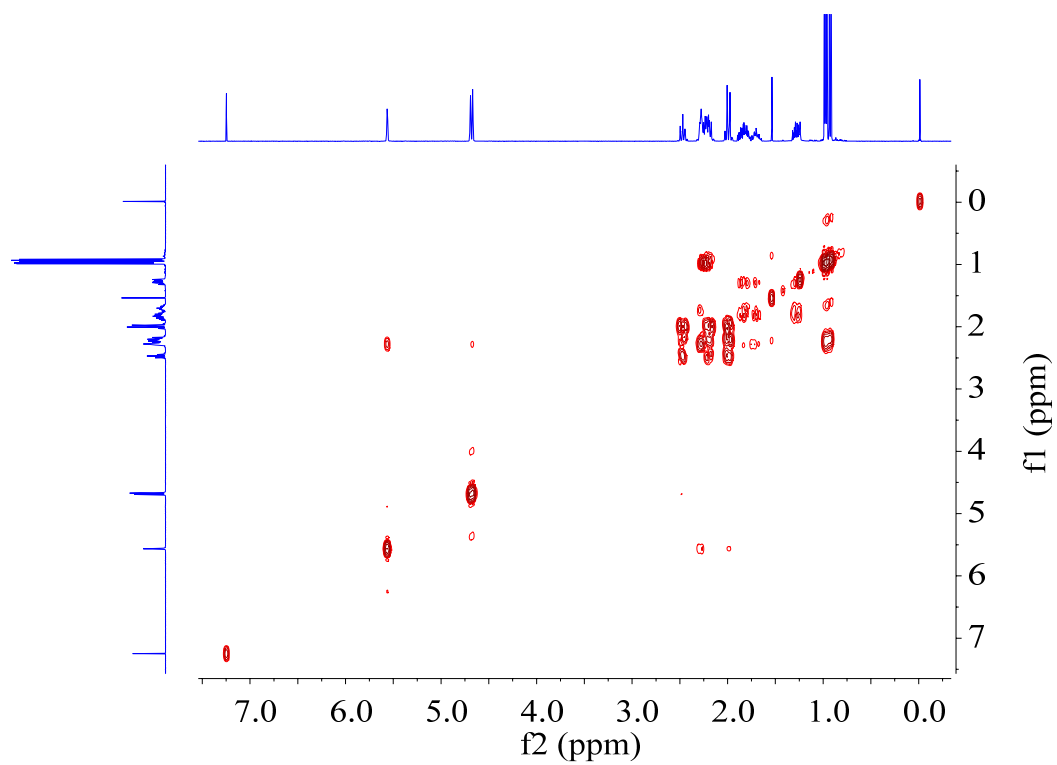
Supplementary Figure 5a. The relative configuration, ^1H - ^1H COSY, the key HMBC and NOESY correlations of compound **1** produced by *E. coli* G1.



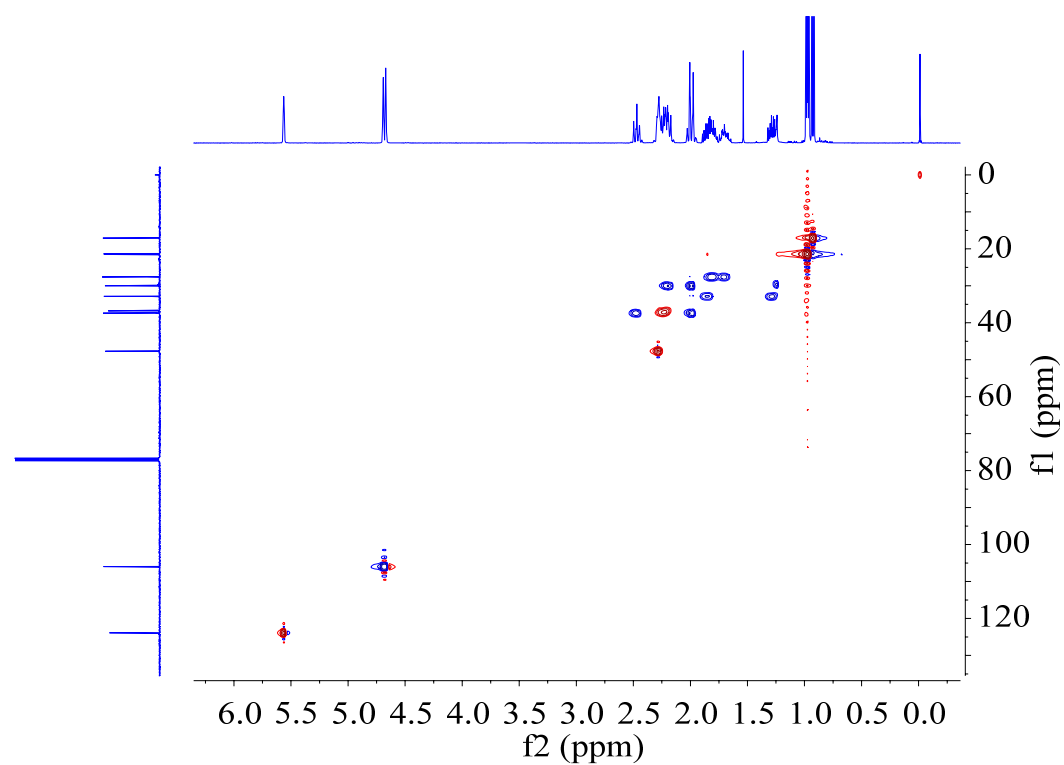
Supplementary Figure 5b. ^1H NMR spectrum of compound **1** produced by *E. coli* G1 (CDCl₃ at 400 MHz).



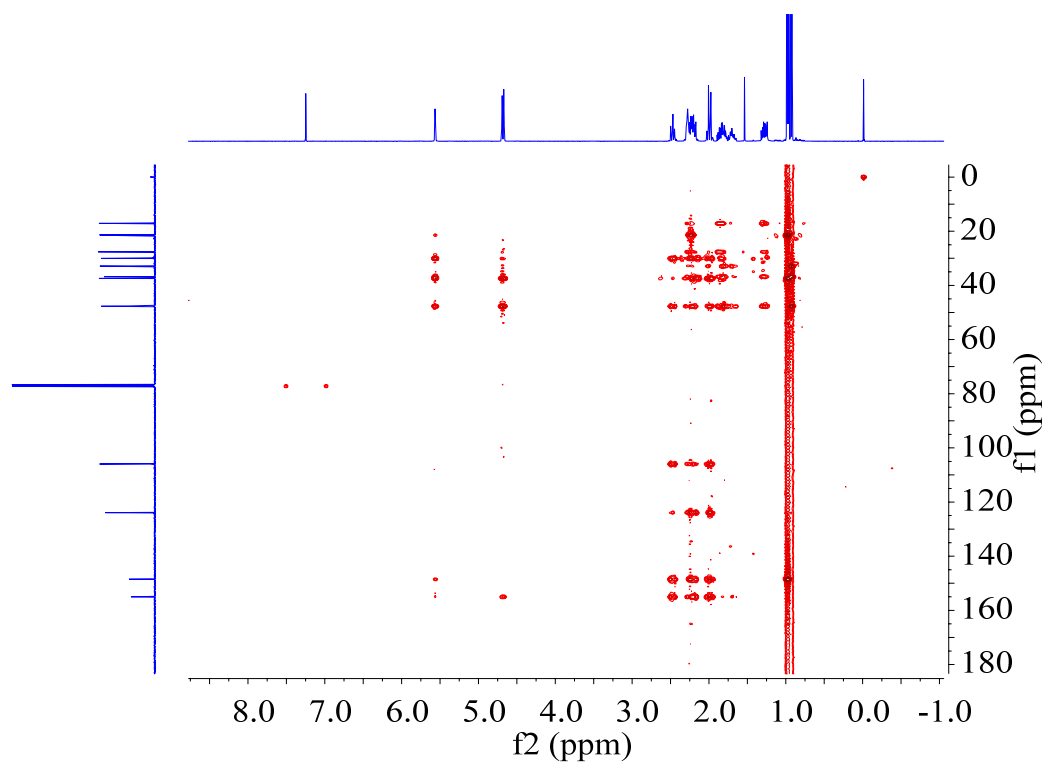
Supplementary Figure 5c. ^{13}C NMR spectrum of compound 1 produced by *E. coli* G1.



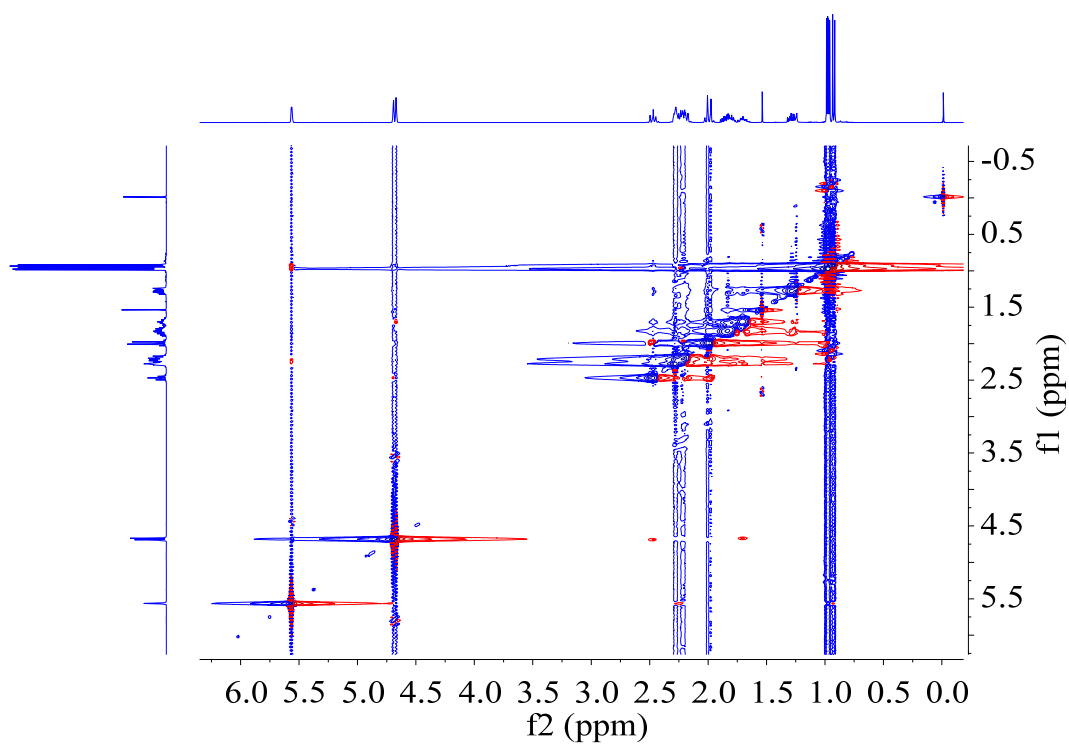
Supplementary Figure 5d. COSY spectrum of compound **2** produced by *E. coli* G1.



Supplementary Figure 5e. HSQC spectrum of compound **2** produced by *E. coli* G1.

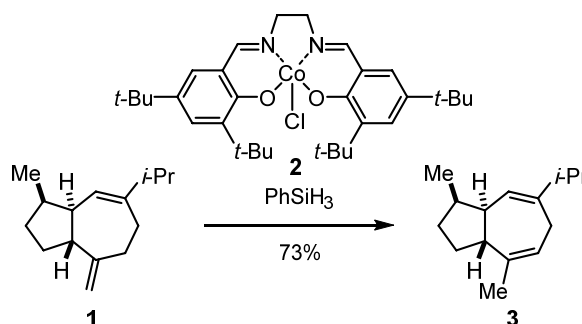


Supplementary Figure 5f. HMBC spectrum of compound **2** produced by *E. coli* G1.



Supplementary Figure 5g. ROESY spectrum of compound **2** produced by *E. coli* G1.

Synthetic Procedure



To a solution of alkene **1** (42.0 mg, 205 μmol , 1.0 equiv.) in degassed benzene (0.5 mL) was added a solution of cobalt-catalyst **2** (6.0 mg, 10.3 μmol , 5 mol%) in degassed benzene (0.5 mL) and phenylsilane (1.23 μL , 10.0 μmol , 5 mol%). The resulting red solution was stirred under argon atmosphere at 23 °C for 16 h. The reaction mixture was directly purified by column chromatography (silica gel, pentane) to afford alkene **3** (30.7 mg, 150 μmol , 73%) as a colorless oil.

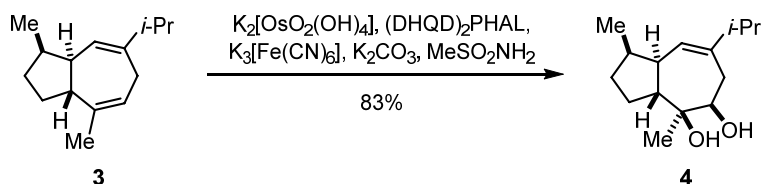
$[\alpha]_{\text{D}}^{28} = -15.5^\circ$ ($c = 0.63$, CH_2Cl_2).

$^1\text{H NMR}$ (700 MHz, C_6D_6): $\delta = 5.68$ (d, $J = 5.2$ Hz, 1H), 5.48 – 5.45 (m, 1H), 2.93 (d, $J = 17.0$ Hz, 1H), 2.64 (ddd, $J = 12.6, 7.8, 5.2$ Hz, 1H), 2.49 (dd, $J = 17.0, 7.6$ Hz, 1H), 2.43 – 2.35 (m, 1H), 2.22 (hept, $J = 6.8$ Hz, 1H), 2.19 – 2.12 (m, 1H), 1.86 – 1.78 (m, 2H), 1.66 (s, 3H), 1.34 – 1.28 (m, 1H), 1.17 – 1.12 (m, 1H), 1.03 (d, $J = 6.8$ Hz, 3H), 1.02 (d, $J = 6.8$ Hz, 3H), 0.94 (d, $J = 7.2$ Hz, 3H) ppm.

$^{13}\text{C NMR}$ (176 MHz, C_6D_6): $\delta = 146.9, 139.5, 122.3, 120.8, 45.5, 44.0, 36.8, 35.0, 31.6, 29.0, 28.9, 23.7, 21.3, 21.2, 18.0$ ppm.

IR (ATR): $\tilde{\nu} = 2958, 2936, 2870, 1712, 1461, 1380$ cm^{-1} .

HRMS (EI): m/z calcd for $\text{C}_{15}\text{H}_{24}$ $[\text{M}]^+$: 204,1873; found: 204.1884.

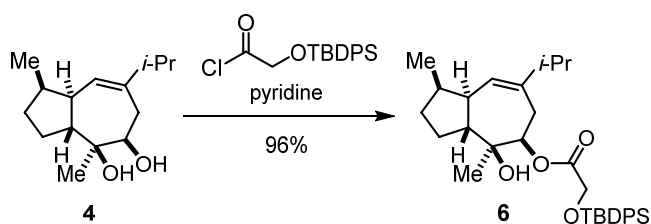


To a solution of **3** (5.2 mg, 25.4 μmol , 1.0 equiv.) in $t\text{-BuOH}$ (0.13 mL) and H_2O (0.13 mL) was added premixed $\text{K}_2\text{OsO}_2(\text{OH})_4$ (1.0 mg, 2.71 μmol , 10 mol%), $(\text{DHQD})_2\text{PHAL}$ (4.0 mg, 5.14 μmol , 0.20 mol%), $\text{K}_3\text{Fe}(\text{CN})_6$ (25.0 mg, 76.2 μmol , 3.0 equiv.), K_2CO_3 (10.5 mg, 76.2 μmol , 3.0 equiv.), MeSO_2NH_2 (2.4 mg, 25.4 μmol , 1.0 equiv.). The reaction mixture was stirred for 2 d at 23 °C. An excess of $\text{Na}_2\text{S}_2\text{O}_5$ was added and after 10 minutes of stirring, the aqueous phase was extracted with CH_2Cl_2 (4 x 3 mL). The combined organic phases were dried over Na_2SO_4 and the solvent

was removed under reduced pressure. The crude product was purified by column chromatography (silica gel, pentane/Et₂O, 1:1) to afford the product **4** (5.0 mg, 83%) as a colorless solid. The spectroscopical data are in accordance with the literature.^[18]

¹H NMR (400 MHz, CDCl₃): δ = 5.61 (t, *J* = 1.5 Hz, 1H), 3.56 (d, *J* = 8.6 Hz, 1H), 2.50 (ddd, *J* = 15.6, 8.6, 1.5 Hz, 1H), 2.29 – 2.14 (m, 4H), 2.05 – 1.96 (m, 2H), 1.89 – 1.58 (m, 4H), 1.44 – 1.35 (m, 1H), 1.20 (s, 3H), 1.00 (d, *J* = 6.8 Hz, 3H), 0.99 (d, *J* = 6.8 Hz, 3H), 0.88 (d, *J* = 6.7 Hz, 3H) ppm.

¹³C NMR (176 MHz, CDCl₃): δ = 142.8, 125.9, 76.4, 75.1, 46.3, 43.8, 37.7, 37.4, 33.2, 32.7, 23.9, 21.6, 21.6, 19.1, 15.5 ppm.



Diol **4** (20.0 mg, 84.0 μmol, 1 equiv.) and dry pyridine (22.3 μL, 277 μmol, 3.3 equiv.) were dissolved in CH₂Cl₂ (0.40 mL) and 2-((*tert*-butyldiphenylsilyloxy)acetyl chloride (83.8 mg, 252 μmol, 3 equiv.) was slowly added. The reaction mixture was stirred for 1.5 h at 23 °C. Water (15 mL) was added and the aqueous phase was extracted with CH₂Cl₂ (4 x 15 mL). The combined organic phases were dried over Na₂SO₄ and the solvent was removed under reduced pressure. The crude product purified by column chromatography (silica gel, pentane/Et₂O, 5:1) to afford ester **6** (42.9 mg, 80.2 μmol, 96%) as a colorless oil.

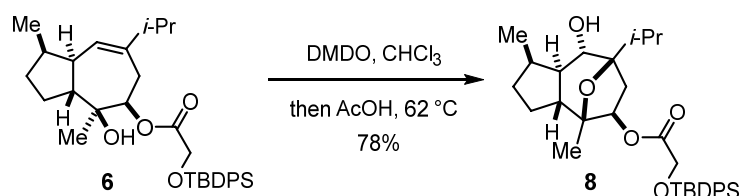
$[\alpha]_{\text{D}}^{20} = -20.2^\circ$ (*c* = 1.0, CHCl₃).

¹H NMR (700 MHz, CDCl₃): δ = 7.70 – 7.67 (m, 4H), 7.46 – 7.42 (m, 2H), 7.41 – 7.37 (m, 4H), 5.50 (d, *J* = 1.9 Hz, 1H), 4.83 (dd, *J* = 9.4, 1.3 Hz, 1H), 4.32 – 4.25 (m, 2H), 2.65 (ddd, *J* = 16.3, 9.3, 1.8 Hz, 1H), 2.26 – 2.22 (m, 1H), 2.21 – 2.13 (m, 3H), 1.94 (d, *J* = 16.2 Hz, 1H), 1.84 (s, 1H), 1.82 – 1.76 (m, 1H), 1.72 – 1.67 (m, 1H), 1.65 – 1.59 (m, 1H), 1.39 – 1.34 (m, 1H), 1.13 (s, 3H), 1.09 (s, 9H), 0.94 (d, *J* = 6.8 Hz, 3H), 0.92 (d, *J* = 6.8 Hz, 3H), 0.83 (d, *J* = 7.0 Hz, 3H) ppm.

¹³C NMR (176 MHz, CDCl₃): δ = 170.6, 143.0, 135.7, 132.8, 132.8, 130.1, 130.1, 128.0, 125.0, 78.5, 75.6, 62.7, 46.3, 43.8, 37.9, 37.4, 33.2, 30.0, 26.8, 23.8, 21.6, 21.4, 19.7, 19.3, 15.4 ppm.

IR (ATR): $\tilde{\nu}$ = 2957, 2931, 2858, 1760, 1463, 1428, 1381, 1362, 1288, 1205, 1139, 1114, 1035, 1013, 948, 823, 740, 703, 657 cm⁻¹.

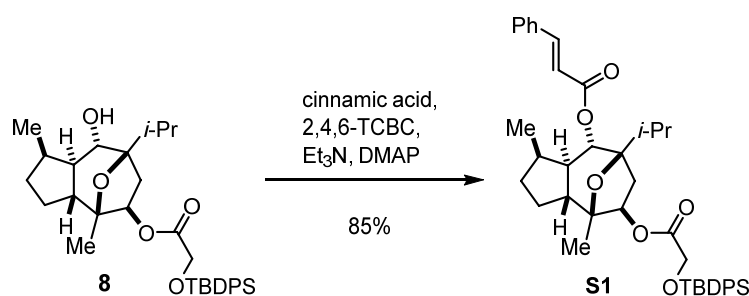
HRMS (ESI): *m/z* calcd for C₃₃H₄₆O₄SiNa [M+Na]⁺: 557.3063; found: 557.3060.



Ester **6** (11.6 mg, 22.0 μmol , 1.0 equiv.) was dissolved by the addition of DMSO (solution in CHCl_3 , 0.07 mol/L, 0.43 mL, 30.0 μmol , 1.4 equiv.) and the reaction mixture was stirred at 23 $^\circ\text{C}$ for 16 h. After the addition of acetic acid (20.0 μL , 271 μmol , 12.5 equiv.), the solution was stirred for another 17 h at 62 $^\circ\text{C}$. The solvent was removed under reduced pressure and purification by column chromatography (SiO_2 , pentane/ Et_2O 5:1 \rightarrow 2:1) afforded alcohol **8** (9.30 mg, 16.9 μmol , 78%) as a colorless oil. The spectroscopic data are in accordance with the literature.^[19]

^1H NMR (500 MHz, CDCl_3): δ = 7.71 – 7.66 (m, 4H), 7.46 – 7.41 (m, 2H), 7.41 – 7.36 (m, 4H), 5.07 (dd, J = 7.9, 2.9 Hz, 1H), 4.25 (s, 2H), 3.63 (d, J = 10.2 Hz, 1H), 2.40 (dd, J = 14.5, 7.9 Hz, 1H), 2.37 – 2.28 (m, 1H), 2.06 – 1.90 (m, 2H), 1.71 – 1.52 (m, 3H), 1.34 – 1.18 (m, 3H), 1.09 (s, 9H), 1.08 (s, 3H), 1.03 (d, J = 7.0 Hz, 3H), 1.01 (d, J = 6.8 Hz, 4H), 0.88 (d, J = 7.2 Hz, 3H) ppm.

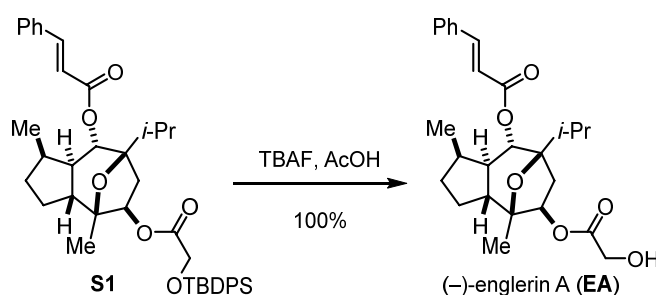
^{13}C NMR (126 MHz, CDCl_3): δ = 171.0, 135.7 (4C), 132.9, 132.8, 130.0 (2C), 127.9 (4C), 85.9, 84.5, 75.5, 70.8, 62.3, 48.0, 48.0, 38.5, 32.1, 31.4, 30.6, 26.7 (3C), 25.6, 19.3, 19.0, 18.3, 17.5, 16.9 ppm.



Triethylamine (13.0 μL , 93.7 μmol , 4.0 equiv.) and 2,4,6-trichlorobenzoyl chloride (8.06 μL , 52.0 μmol , 2.2 equiv.) were added to a solution of cinnamic acid (6.90 mg, 47.0 μmol , 2.0 equiv.) in CH_2Cl_2 (0.1 mL) at 23 $^\circ\text{C}$ and stirred for 1 h. The resulting suspension was added to a solution of **8** (12.9 mg, 23.4 μmol , 1.0 equiv.) and DMAP (7.40 mg, 60.9 μmol , 2.6 eq) in CH_2Cl_2 (0.2 mL) at 23 $^\circ\text{C}$. The solution was stirred for 24 h at 23 $^\circ\text{C}$. Sat. aqueous NaHCO_3 solution (3 mL) was added and the aqueous phase was extracted with Et_2O (3 x 15 mL). The combined organic phases were dried over Na_2SO_4 and the solvent was removed under reduced pressure. The crude product was purified by column chromatography (silica gel, pentane/ Et_2O , 12:1) to afford ester **S1** (13.5 mg, 19.8 μmol , 85%) as a colorless oil. The analytical data are in agreement with the literature data.^[19]

^1H NMR (700 MHz, CDCl_3): δ = 7.70 (d, J = 7.6 Hz, 4H), 7.66 (d, J = 16.0 Hz, 1H), 7.54 – 7.51 (m, 2H), 7.46 – 7.42 (m, 2H), 7.42 – 7.37 (m, 7H), 6.39 (d, J = 15.9 Hz, 1H), 5.14 (dd, J = 7.7, 2.4 Hz, 1H), 5.11 (d, J = 10.3 Hz, 1H), 4.30 – 4.24 (m, 2H), 2.61 (dd, J = 14.5, 7.9 Hz, 1H), 2.13 (h, J = 6.9 Hz, 1H), 1.97 – 1.90 (m, 1H), 1.85 (hept, J = 6.9 Hz, 1H), 1.78 – 1.69 (m, 3H), 1.55–1.51 (m, 1H), 1.30 – 1.22 (m, 3H), 1.12 (s, 3H), 1.10 (s, 9H), 0.98 (d, J = 6.8 Hz, 3H), 0.94 (t, J = 7.1 Hz, 6H) ppm.

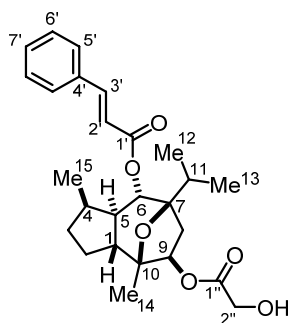
^{13}C NMR (176 MHz, CDCl_3): δ = 171.0, 165.6, 145.1, 135.6 (2C), 135.6 (2C), 134.3, 132.8, 132.8, 130.4, 129.9, 128.9 (2C), 128.1 (2C), 127.8 (2C), 127.8 (2C), 118.1, 85.4, 84.5, 75.4, 71.3, 62.3, 47.5, 46.9, 39.8, 32.9, 31.2, 31.0, 26.7 (3C), 24.6, 19.3, 18.9, 18.2, 17.5, 16.9 ppm.



Acetic acid (0.8 μL , 13.4 μmol , 1.0 equiv.) was added to a solution of **S1** (9.1 mg, 13.4 μmol , 1.0 equiv.) in THF (0.25 mL) at 23 $^{\circ}\text{C}$. Then a TBAF-solution (1 M in THF, 27.0 μL , 26.7 μmol , 2.0 equiv.) was added at 23 $^{\circ}\text{C}$ and the reaction mixture was stirred at this temperature for 1.5 h. Sat. aqueous NH_4Cl (4 mL) was added and the aqueous phase was extracted with Et_2O (3 x 10 mL). The combined organic phases were dried over Na_2SO_4 and the solvent was removed under reduced pressure. The crude product purified by column chromatography (silica gel, pentane– Et_2O , 2:1) to afford (-)-englerin A (**EA**, 5.90 mg, 13.3 μmol , 100%) as a colorless oil. The analytical data are in agreement with the literature data.^[20]

^1H NMR (700 MHz, CD_3OD): δ = 7.68 (d, J = 16.0 Hz, 1H), 7.62 – 7.59 (m, 2H), 7.41 – 7.38 (m, 3H), 6.50 (d, J = 16.0 Hz, 1H), 5.25 (dd, J = 8.0, 3.0 Hz, 1H), 5.11 (d, J = 10.5 Hz, 2H), 4.14 (s, 2H), 2.69 (dd, J = 14.5, 8.0 Hz, 1H), 2.16 – 2.09 (m, 1H), 2.03 – 1.96 (m, 1H), 1.89 – 1.82 (m, 2H), 1.79 – 1.71 (m, 2H), 1.69 – 1.63 (m, 1H), 1.36 – 1.24 (m, 3H), 1.18 (s, 3H), 1.00 (d, J = 6.8 Hz, 3H), 0.96 (d, J = 7.1 Hz, 3H), 0.92 (d, J = 7.1 Hz, 3H) ppm.

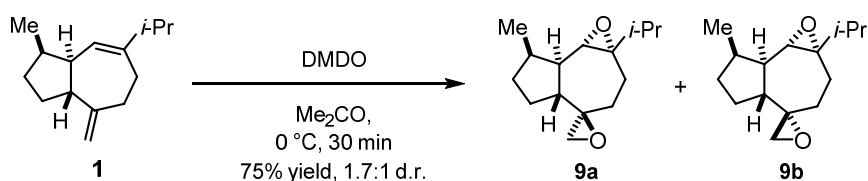
^{13}C NMR (176 MHz, CD_3OD): δ = 173.9, 167.3, 146.7, 135.6, 131.6, 130.0 (2C), 129.3 (2C), 118.8, 86.6, 86.0, 76.6, 72.5, 61.0, 48.9, 48.0, 40.7, 34.0, 32.4, 32.0, 25.5, 19.2, 18.5, 17.7, 17.2 ppm.

Table S5. Comparison of NMR data for EA with the literature.^[20]

(-)-englerin A (EA)

No	¹ H NMR (CD ₃ OD)			¹³ C NMR (CD ₃ OD)		
	δ_{obs} [ppm]	δ_{Lit} [ppm] ^[20]	Δ [ppm]	δ_{obs} [ppm]	δ_{Lit} [ppm] ^[20]	Δ [ppm]
1	1.79 – 1.71 (m) ^a	1.73 (m)	+0.02	48.9	48.9	0
2	1.79 – 1.71 (m) ^a	1.71 (m)	+0.04	25.5	25.5	0
	1.36 – 1.24 (m) ^a	1.30 (m)	0			
3	2.03 – 1.96 (m)	1.98 (m)	+0.01	32.0	32.0	0
	1.36 – 1.24 (m) ^a	1.25 (m)	-0.05			
4	2.16 – 2.09 (m)	2.12 (m)	0	32.4	32.4	0
5	1.69 – 1.63 (m)	1.63 (m)	+0.03	48.0	48.0	0
6	5.11 (d)	5.10 (d)	+0.01	72.5	72.4	+0.1
7				86.6	86.4	+0.2
8	2.69 (dd)	2.67 (dd)	+0.02	40.7	40.7	0
	1.89 – 1.82 (m) ^a	1.86 (dd)	0			
9	5.25 (dd)	5.23 (dd)	+0.02	76.6	76.6	0
10				86.0	86.0	0
11	1.89 – 1.82 (m) ^a	1.86 (m)	0	34.0	34.0	0
12	1.00 (d) ^b	1.00 (d) ^b	0	17.7	17.8	-0.1
13	0.96 (d) ^b	0.95 (d) ^b	+0.01	18.5	18.6	-0.1
14	1.18 (s)	1.18 (s)	0	19.2	19.3	-0.1
15	0.92 (d)	0.92 (d)	0	17.2	17.3	-0.1
1'				167.3	167.3	0
2'	6.50 (d)	6.50 (d)	0	118.8	118.8	0
3'	7.68 (d)	7.68 (d)	0	146.7	146.8	-0.1
4'				135.6	135.6	0
5'	7.62 - 7.59 (m)	7.61 (m)	0	129.3	129.3	0
6'	7.41 – 7.38 (m) ^a	7.40	0	130.0	130.1	-0.1
		(brdd) ^a				
7'	7.41 – 7.38 (m) ^a	7.40	0	131.6	131.6	0
		(brdd) ^a				
1''				173.9	173.9	0
2''	4.14 (s)	4.14 (brs)	0	61.0	61.0	0

^a overlapped signals; ^b chemical shifts in the same column may be interchangeable



Alkene **1** (12.3 mg, 60.0 μmol , 1.0 equiv.) was dissolved by the addition of DMDO solution (0.04 M in acetone, 3.9 mL, 180 μmol , 3.0 equiv.) and stirred at 23 $^\circ\text{C}$ for 2 h. The solvent was removed under reduced pressure and purification by column chromatography (silica gel, pentane/ Et_2O 9:1) afforded bisepoxide **9a** (6.7 mg, 28.3 μmol , 47%) and its epimer **9b** (4.0 mg, 16.9 μmol , 28%) as colorless oils, respectively.

9a:

$[\alpha]_{\text{D}}^{20} = -24.6^\circ$ ($c = 0.26$, CHCl_3).

$^1\text{H NMR}$ (700 MHz, CDCl_3): $\delta = 2.97$ (d, $J = 7.3$ Hz, 1H), 2.67 (dd, $J = 4.2, 2.1$ Hz, 1H), 2.47 (d, $J = 4.1$ Hz, 1H), 2.37 – 2.31 (m, 1H), 2.31 – 2.26 (m, 1H), 2.22 (ddd, $J = 14.9, 7.3, 1.6$ Hz, 1H), 2.01 (t, $J = 13.7$ Hz, 1H), 1.74 (dt, $J = 10.7, 7.5$ Hz, 1H), 1.66 – 1.57 (m, 3H), 1.46 (t, $J = 14.0$ Hz, 1H), 1.38 – 1.32 (m, 2H), 1.12 – 1.06 (m, 1H), 1.05 (d, $J = 7.1$ Hz, 3H), 1.03 (d, $J = 7.0$ Hz, 3H), 0.98 (d, $J = 6.8$ Hz, 3H) ppm.

$^{13}\text{C NMR}$ (176 MHz, CDCl_3): $\delta = 64.5, 62.4, 61.3, 49.3, 47.9, 45.3, 35.7, 35.0, 34.9, 34.7, 27.2, 23.7, 19.0, 17.8, 15.5$ ppm.

IR (ATR): $\tilde{\nu} = 2958, 2926, 2877, 2861, 1461, 1383, 1221, 1171, 1122, 1024, 963, 921, 899, 854, 814$ cm^{-1} .

HRMS (ESI): m/z calcd for $\text{C}_{15}\text{H}_{24}\text{O}_2\text{Na}$ $[\text{M}+\text{Na}]^+$: 259.1668; found: 259.1657.

9b:

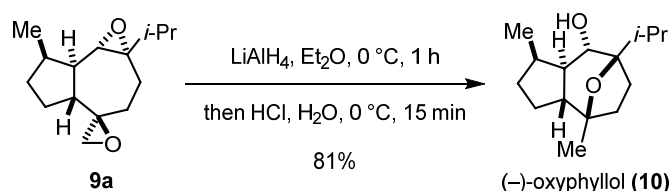
$[\alpha]_{\text{D}}^{20} = -12.0^\circ$ ($c = 0.26$, CHCl_3).

$^1\text{H NMR}$ (700 MHz, CDCl_3): $\delta = 2.98$ (d, $J = 7.5$ Hz, 1H), 2.73 (d, $J = 4.7$ Hz, 1H), 2.51 (d, $J = 4.7$ Hz, 1H), 2.36 – 2.23 (m, 1H), 2.20 (ddd, $J = 10.8, 9.7, 7.6$ Hz, 1H), 2.11 – 2.05 (m, 2H), 2.01 (ddd, $J = 14.8, 13.1, 1.7$ Hz, 1H), 1.81 – 1.72 (m, 2H), 1.61 (hept, $J = 6.7$ Hz, 1H), 1.47 – 1.42 (m, 1H), 1.35 (ddd, $J = 14.8, 6.8, 1.6$ Hz, 1H), 1.21 – 1.15 (m, 1H), 1.13 – 1.07 (m, 1H), 1.09 (d, $J = 7.2$ Hz, 3H), 1.03 (d, $J = 7.0$ Hz, 3H), 0.97 (d, $J = 6.8$ Hz, 3H) ppm.

$^{13}\text{C NMR}$ (176 MHz, CDCl_3): $\delta = 64.6, 61.9, 60.3, 54.3, 45.8, 45.2, 35.0, 34.7, 34.6, 33.9, 26.7, 25.0, 19.0, 17.8, 16.3$ ppm.

IR (ATR): $\tilde{\nu} = 2957, 2872, 1458, 1381, 953, 898, 841, 804$ cm^{-1} .

HRMS (ESI): m/z calcd for $\text{C}_{15}\text{H}_{24}\text{O}_2\text{Na}$ $[\text{M}+\text{Na}]^+$: 259.1668; found: 259.1658.



To a solution of bisepoxide **9a** (6.7 mg, 28.0 μmol , 1.0 equiv.) in Et_2O (0.3 mL) was added LiAlH_4 (2.2 mg, 57.0 μmol , 2.0 equiv.) at $0\text{ }^\circ\text{C}$. After stirring at $0\text{ }^\circ\text{C}$ for 30 min, aqueous HCl (1 M, 0.28 mL, 10 equiv.) was added and stirring was continued for another 15 min at $0\text{ }^\circ\text{C}$. The aqueous phase was extracted with EtOAc (4 x 5 mL). The combined organic phases were dried over Na_2SO_4 and the solvent was removed under reduced pressure. Purification by column chromatography (silica gel, pentane/ Et_2O 7:1) afforded (–)-oxyphyllol (**10**, 5.4 mg, 22.6 μmol , 81%) as colorless solid.

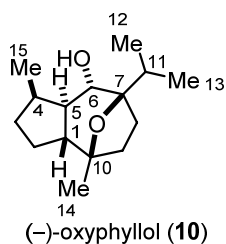
$[\alpha]_{\text{D}}^{23} = -37.1^\circ$ ($c = 0.36$, CHCl_3).

$^1\text{H NMR}$ (700 MHz, CDCl_3): $\delta = 3.69$ (d, $J = 10.3$ Hz, 1H), 2.34 – 2.22 (m, 1H), 1.98 (dddd, $J = 13.7$, 10.4, 8.5, 2.0 Hz, 1H), 1.92 (p, $J = 6.9$ Hz, 1H), 1.80 (ddd, $J = 12.8$, 9.6, 5.2 Hz, 1H), 1.74 – 1.64 (m, 2H), 1.62 – 1.56 (m, 2H), 1.41 – 1.34 (m, 2H), 1.22 (s, 3H), 1.17 (dtd, $J = 13.6$, 8.4, 2.8 Hz, 1H), 1.02 (d, $J = 7.0$ Hz, 3H), 1.02 (d, $J = 6.8$ Hz, 3H), 1.01 – 0.95 (m, 1H), 0.88 (d, $J = 7.2$ Hz, 3H) ppm.

$^{13}\text{C NMR}$ (176 MHz, CDCl_3): $\delta = 86.4$, 83.0, 71.8, 49.4, 48.7, 32.5, 31.7, 31.6, 30.5, 29.7, 29.2, 25.9, 24.3, 18.4, 17.5, 17.1 ppm.

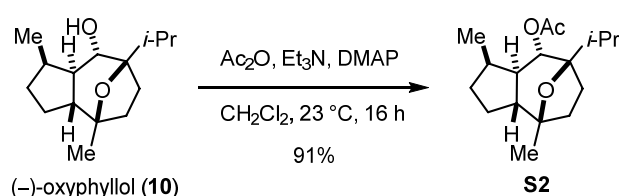
IR (ATR): $\tilde{\nu} = 3416$, 2956, 2870, 1467, 1379, 1308, 1261, 1104, 1064, 1046, 1025, 1006, 939 cm^{-1} .

HRMS (ESI): m/z calcd for $\text{C}_{15}\text{H}_{26}\text{O}_2\text{Na}$ $[\text{M}+\text{Na}]^+$: 261.1825; found: 261.1829.

Table S6. Comparison of NMR Data for (-)-Oxyphyllol with the literature.^[21]

No	¹ H NMR			¹³ C NMR		
	δ_{obs} [ppm]	δ_{Lit} [ppm] ^[21]	Δ [ppm]	δ_{obs} [ppm]	δ_{Lit} [ppm] ^[21]	Δ [ppm]
1	1.60 (m) ^a	1.61 (m)	-0.01	49.4	49.4	0
2	1.00 (m)	0.99 (m)	+0.01	25.9	25.9	0
3	1.60 (m) ^a	1.59 (m)	+0.01	31.7	31.6	+0.01
	1.17 (dtd)	1.16 (dddd)	+0.01			
4	1.98 (dddd)	1.97 (ddd)	+0.01	30.5	30.5	0
	2.28 (m)	2.28 (dddq)	0			
5	1.38 (m) ^a	1.38 (m) ^a	0	48.7	48.7	0
6	3.69 (d)	3.69 (d)	0	71.8	71.8	0
7				86.4	86.4	0
8	1.68 (m) ^a	1.66 (m)	+0.02	29.2	29.2	0
	1.80 (ddd)	1.78 (ddd)	+0.02			
9	1.38 (m) ^a	1.38 (m) ^a	0	31.7	31.7	0
	1.68 (m) ^a	1.71 (m)	-0.03			
10				83.0	83.0	0
11	1.92 (hept)	1.94 (qq)	-0.02	32.5	32.5	0
12	1.02 (d) ^b	1.01 (d) ^b	+0.01	17.5 ^b	17.5 ^b	0
13	1.02 (d) ^b	1.02 (d) ^b	0	18.4 ^b	18.4 ^b	0
14	1.22 (s)	1.22 (s)	0	24.3	24.3	0
15	0.88 (d)	0.88 (d)	0	17.1	17.0	+0.01

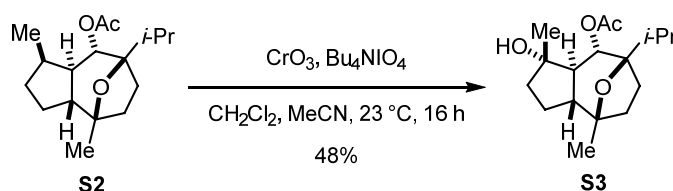
^a overlapped signals; ^b chemical shifts in the same column may be interchangeable



To a solution of (-)-oxyphyllol (**10**, 19.0 mg, 79.7 μmol , 1.0 equiv.) in CH_2Cl_2 (0.8 mL) was added acetic anhydride (70.0 μL , 741 μmol , 9.4 equiv.), Et_3N (110 μL , 794 μmol , 10.0 equiv.) and DMAP (9.7 mg, 79.7 μmol , 1.0 equiv.). The reaction mixture was stirred at 23 $^\circ\text{C}$ for 16 h and directly purified by column chromatography (silica gel, pentane/ Et_2O 20:1) to afford acetate **S2** (20.3 mg, 72.4 μmol , 91%) as a colorless oil. The analytic data are in accordance with the literature.^[22]

^1H NMR (600 MHz, CDCl_3): δ = 5.06 (d, J = 10.4 Hz, 1H), 2.12 – 2.07 (m, 1H), 2.05 (s, 3H), 1.99 – 1.90 (m, 2H), 1.86 – 1.74 (m, 4H), 1.68 – 1.62 (m, 1H), 1.57 (ddd, J = 12.9, 10.4, 6.5 Hz, 1H), 1.50 – 1.41 (m, 1H), 1.28 (s, 3H), 1.28 – 1.22 (m, 1H), 1.13 – 1.00 (m, 1H), 1.01 (d, J = 6.8 Hz, 3H), 0.96 (d, J = 7.1 Hz, 3H), 0.93 (d, J = 7.1 Hz, 3H) ppm.

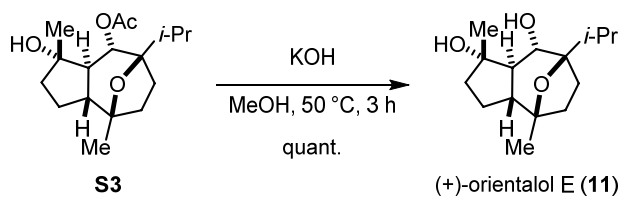
^{13}C NMR (151 MHz, CDCl_3): δ = 169.9, 85.9, 83.2, 72.6, 49.0, 47.4, 33.3, 31.5, 31.3, 31.2, 30.4, 25.0, 24.4, 21.5, 18.4, 17.6, 17.2 ppm.



Anhydrous chromium trioxide (35.6 mg, 356 μmol , 10.0 equiv.) was dissolved in MeCN (3 mL) and CH_2Cl_2 (1 mL). After stirring for 10 min at 23 $^\circ\text{C}$, the mixture was cooled to $-30\text{ }^\circ\text{C}$ and a solution of **S2** (10.1 mg, 35.6 μmol , 1.0 equiv.) in CH_2Cl_2 (1 mL) was added. A solution of Bu_4NIO_4 (154 mg, 356 μmol , 10.0 equiv.) in MeCN (3 mL) was added after 5 min and the resulting mixture was allowed to warm to 0 $^\circ\text{C}$ and stirred for another 45 min at this temperature. Sat. aqueous Na_2SO_3 was added and the aqueous phase was extracted with CH_2Cl_2 (3 x 10 mL). The combined organic phases were dried over Na_2SO_4 and the solvent was removed under reduced pressure. Purification by column chromatography (silica gel, pentane/ EtOAc 3:1) afforded alcohol **S3** (5.1 mg, 17.2 μmol , 48%) as a colorless oil. The analytic data are in accordance with the literature.^[22]

^1H NMR (700 MHz, CDCl_3): δ = 5.05 (d, J = 10.0 Hz, 1H), 2.03 (s, 3H), 2.05 – 2.00 (m, 1H), 1.87 (ddd, J = 12.6, 10.0, 4.4 Hz, 1H), 1.84 – 1.71 (m, 5H), 1.64 (td, J = 12.4, 6.9 Hz, 1H), 1.58 – 1.52 (m, 1H), 1.47 (td, J = 12.7, 5.2 Hz, 1H), 1.37 (s, 3H), 1.31 – 1.24 (m, 2H), 1.22 (s, 3H), 0.98 (d, J = 6.9 Hz, 3H), 0.93 (d, J = 7.1 Hz, 3H) ppm.

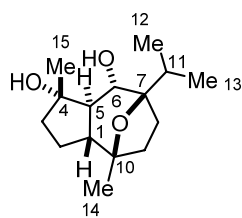
^{13}C NMR (176 MHz, CDCl_3): $\delta = 170.9, 85.8, 83.2, 78.9, 72.2, 53.0, 50.7, 40.2, 33.1, 31.5, 30.5, 25.1, 23.8, 23.0, 21.7, 18.4, 17.5$ ppm.



To a solution of acetate **S3** (1.0 mg, 3.94 μmol , 1.0 equiv.) in MeOH was added KOH (11.0 mg, 196 μmol , 50 equiv.) and the resulting suspension was stirred at 50 °C for 3 h. The solvent was removed under reduced pressure and the crude product was purified by column chromatography (silica gel, pentane/EtOAc 2:1) to afford (+)-orientalol E (**11**, 1.0 mg, 3.94 μmol , quant.) as a colorless oil. The spectral data are in accordance to the literature.^[23]

^1H NMR (700 MHz, CDCl_3): $\delta = 3.80$ (d, $J = 10.1$ Hz, 1H), 1.96 – 1.90 (m, 2H), 1.87 – 1.81 (m, 2H), 1.77 – 1.68 (m, 3H), 1.63 – 1.49 (m, 4H), 1.45 (td, $J = 12.7, 5.2$ Hz, 1H), 1.34 (s, 3H), 1.33 – 1.29 (m, 1H), 1.21 (s, 3H), 1.04 (d, $J = 7.1$ Hz, 3H), 1.03 (d, $J = 7.1$ Hz, 3H) ppm.

^{13}C NMR (176 MHz, CDCl_3): $\delta = 86.3, 83.0, 79.1, 72.0, 54.4, 50.4, 40.0, 32.4, 31.7, 29.0, 25.1, 23.7, 23.6, 18.2, 17.4$ ppm.

Table S7. Comparison of NMR Data for (+)-Orientalol E with the literature.^[23]

(+)–orientalol E (11)

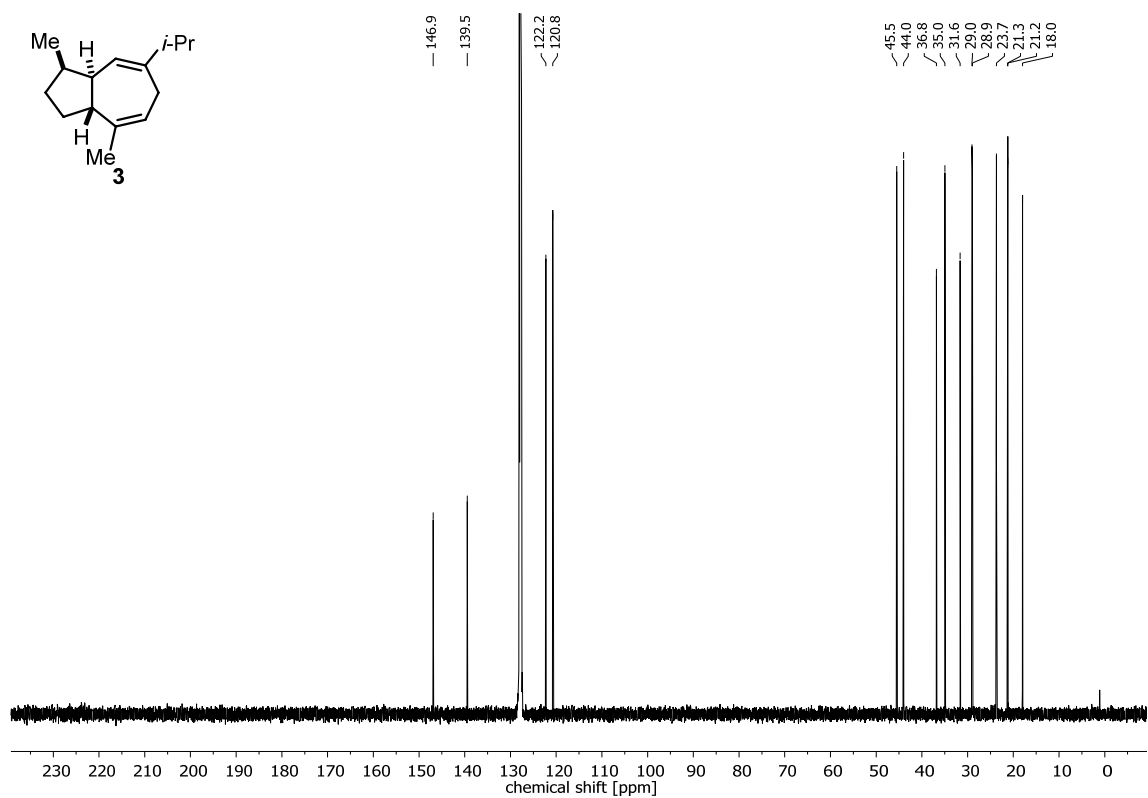
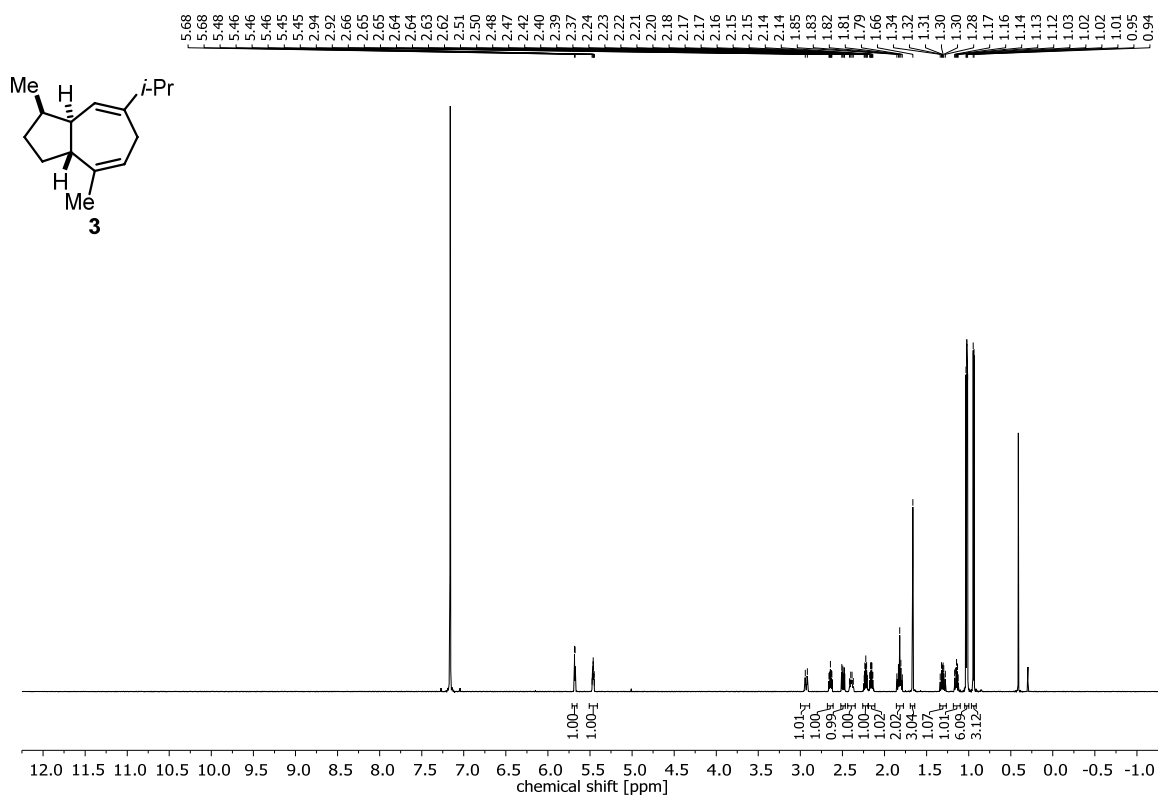
No	¹ H NMR			¹³ C NMR		
	δ_{obs} [ppm]	δ_{Lit} [ppm] ^[23]	Δ [ppm]	δ_{obs} [ppm]	δ_{Lit} [ppm] ^[23]	Δ [ppm]
1	1.72 (m) ^a	1.72	0	50.4	50.4	0
2		-		23.6	23.5	+0.1
3		-		40.0	40.1	-0.1
4		-		79.1	79.1	0
5	1.56 (m) ^a	1.57	-0.01	54.4	54.5	-0.1
6	3.80 (d)	3.80 (d)	0	72.0	72.1	-0.1
7				86.3	86.4	-0.1
8		-		29.0	29.0	0
9		-		31.7	31.8	-0.1
10				83.0	83.0	0
11	1.93 (m) ^a	1.95	-0.02	32.4	32.4	0
12	1.03 (d) ^b	1.03 (d) ^b	0	17.4	17.4 ^b	0
13	1.04 (d) ^b	1.04 (d) ^b	0	18.3	18.3 ^b	0
14	1.34 (s)	1.33 (s)	+0.01	25.1	25.1	0
15	1.21 (s)	1.21 (s)	0	23.7	23.6	+0.1

^a overlapped signals; ^b chemical shifts in the same column may be interchangeable

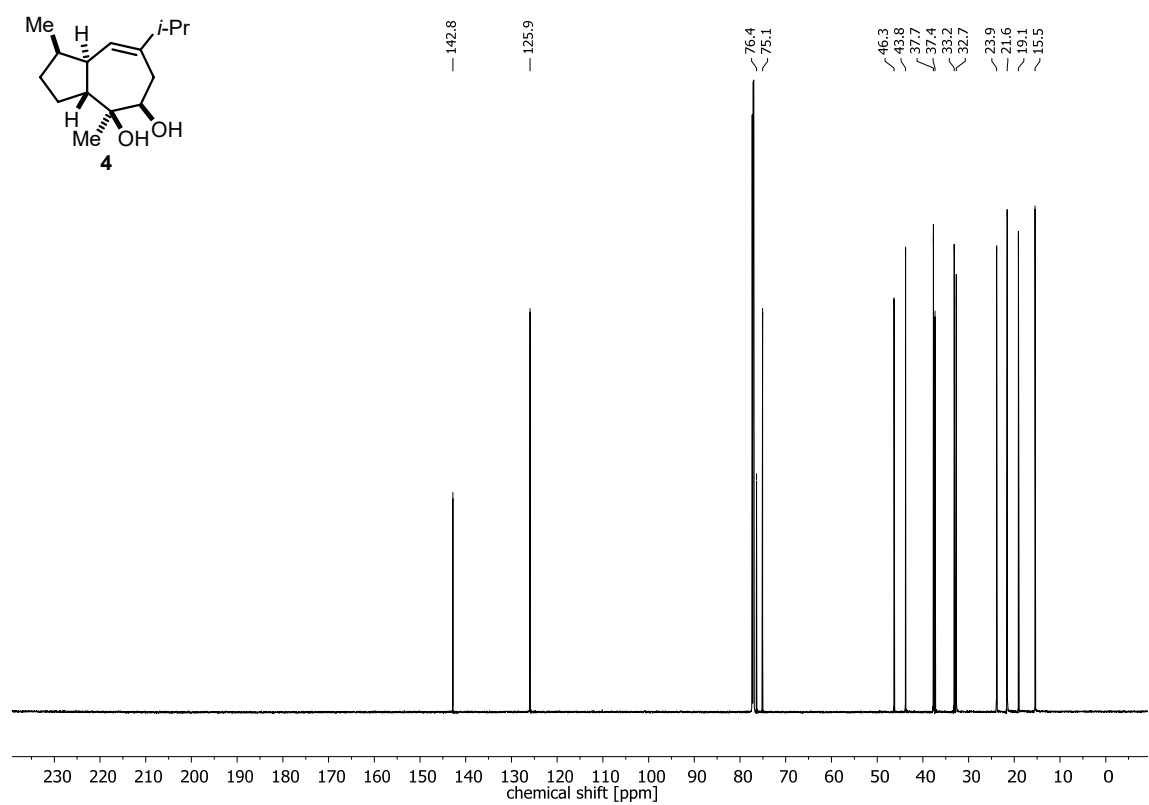
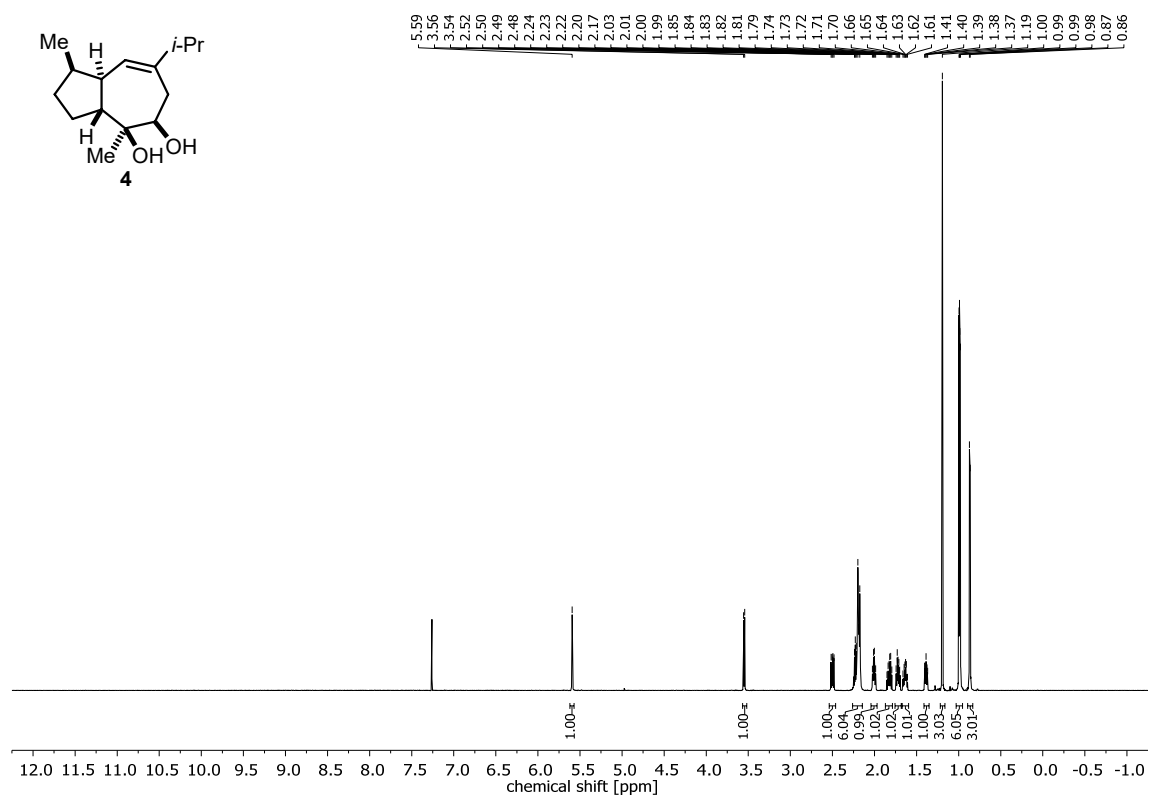
References

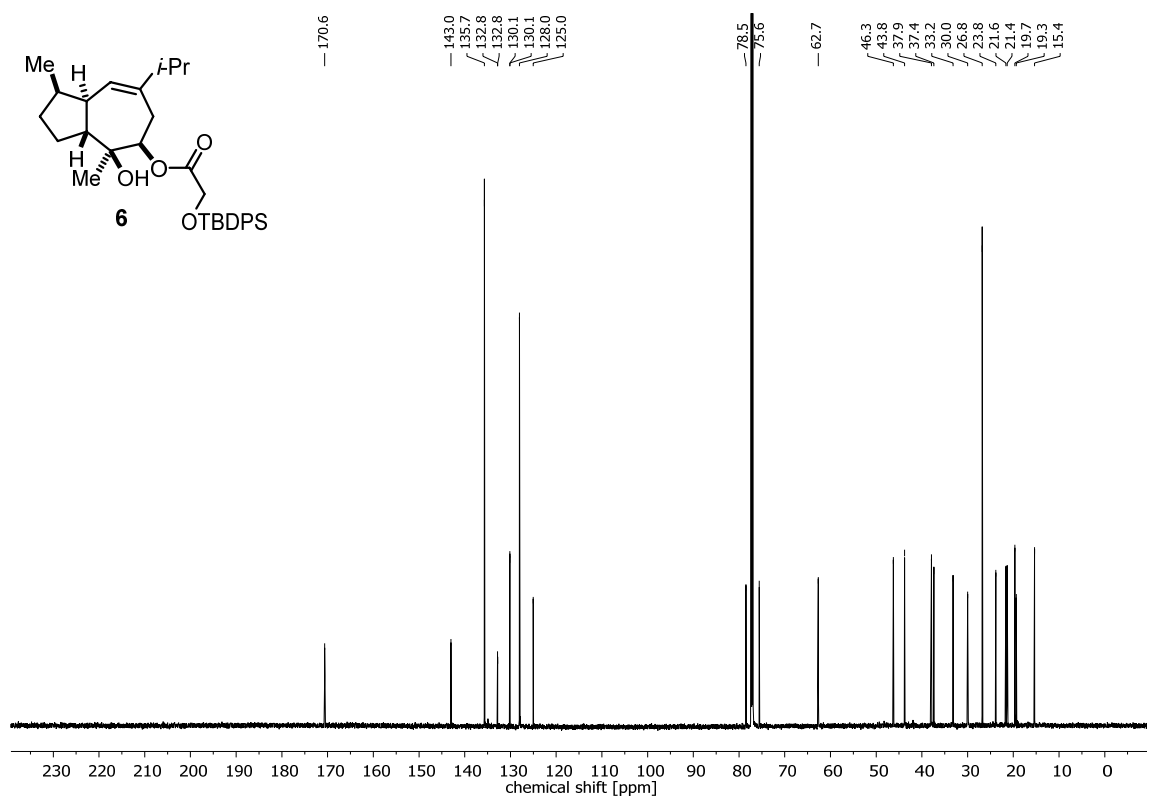
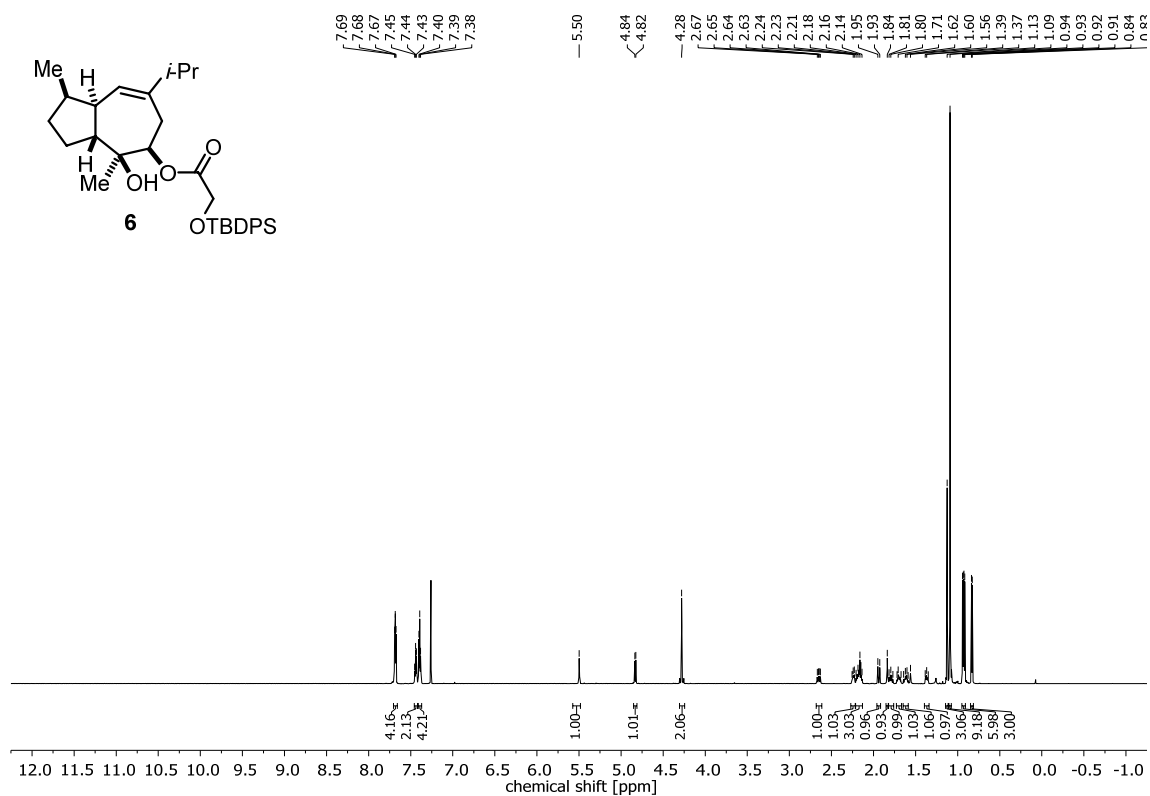
- [1] a) S. Fanjul, A. N. Hulme, *J. Org. Chem.* **2008**, *73*, 9788; b) W. Li, J. Gan, D. Ma, *Angew. Chem. Int. Ed.* **2009**, *48*, 8891.
- [2] a) M. Ferrer, M. Gibert, F. Sánchez-Baeza, A. Messeguer, *Tetrahedron Lett.* **1996**, *37*, 3585; b) R. W. Murray, M. Singh, *Org. Synth.* **1997**, *74*, 91.
- [3] M. R. Green, J. Sambrook, *A Laboratory Manual* 4th **2012**.
- [4] C. Engler, R. Gruetzner, R. Kandzia, S. Marillonnet, *PLoS One* **2009**, *4*, e5553.
- [5] D. G. Gibson, L. Young, R. Y. Chuang, J. C. Venter, C. A. Hutchison, H. O. Smith, *Nat. Methods* **2009**, *6*, 343.
- [6] D. G. Gibson, *Nucleic Acids Res.* **2009**, *37*, 6984.
- [7] G. Bian, A. Hou, Y. Yuan, B. Hu, S. Cheng, Z. Ye, Y. Di, Z. Deng, T. Liu, *Org. Lett.* **2018**, *20*, 1626.
- [8] G. Bian, Y. Han, A. Hou, Y. Yuan, X. Liu, Z. Deng, T. Liu, *Metab. Eng.* **2017**, *42*, 1.
- [9] S. Kumar, G. Stecher, K. Tamura, *Mol. Biol. Evol.* **2016**, *33*, 1870.
- [10] G. Bian, Y. Yuan, H. Tao, X. Shi, X. Zhong, Y. Han, S. Fu, C. Fang, Z. Deng, T. Liu, *Biotechnol. J.* **2017**, *12*, 1600697.
- [11] G. Bian, T. Ma, T. Liu, *Methods Enzymol.* **2018**, *608*, 97.
- [12] F. Zhu, L. Lu, S. Fu, X. Zhong, M. Hu, Z. Deng, T. Liu, *Process Biochem.* **2015**, *50*, 341.
- [13] T. Ma, B. Shi, Z. Ye, X. Li, M. Liu, Y. Chen, J. Xia, J. Nielsen, Z. Deng, T. Liu, *Metab. Eng.* **2019**, *52*, 134.
- [14] X. Lu, H. Vora, C. Khosla, *Metab. Eng.* **2008**, *10*, 333.
- [15] P. van Hoek, E. de Hulster, J. P. van Dijken, J. T. Pronk, *Biotechnol. Bioeng.* **2000**, *68*, 517.
- [16] C. J. Paddon, P. Westfall, D. Pitera, K. Benjamin, K. Fisher, D. McPhee, M. Leavell, A. Tai, A. Main, D. Eng, *Nature* **2013**, *496*, 528-532.
- [17] F. Zhu, X. Zhong, M. Hu, L. Lu, Z. Deng, T. Liu, *Biotechnol. Bioeng.* **2014**, *111*, 1396.
- [18] a) M. Willot, L. Radtke, D. Könnig, R. Fröhlich, V. H. Gessner, C. Strohmam, M. Christmann, *Angew. Chem. Int. Ed.* **2009**, *48*, 9105; b) L. Radtke, M. Willot, H. Sun, S. Ziegler, S. Sauerland, C. Strohmam, R. Fröhlich, P. Habenberger, H. Waldmann, M. Christmann, *Angew. Chem. Int. Ed.* **2011**, *50*, 3998.
- [19] K. Takahashi, K. Komine, Y. Yokoi, J. Ishihara, S. Hatakeyama, *J. Org. Chem.* **2012**, *77*, 7364.
- [20] R. Ratnayake, D. Covell, T. T. Ransom, K. R. Gustafson, J. A. Beutler, *Org. Lett.* **2009**, *11*, 57.
- [21] S. Sutthivaiyakit, N. N. Nakorn, W. Kraus, P. Sutthivaiyakit, *Tetrahedron* **2003**, *59*, 9991.
- [22] a) J. Wang, S.-G. Chen, B.-F. Sun, G.-Q. Lin, Y.-J. Shang, *Chem. Eur. J.* **2013**, *19*, 2539; b) P. Liu, Y. Cui, K. Chen, X. Zhou, W. Pan, J. Ren, Z. Wang, *Org. Lett.* **2018**, *20*, 2517.
- [23] G.-P. Peng, G. Tian, X.-F. Huang, F.-C. Lou, *Phytochemistry* **2003**, *63*, 877.

Supporting Information – Semisynthesis of (-)-Englerin A

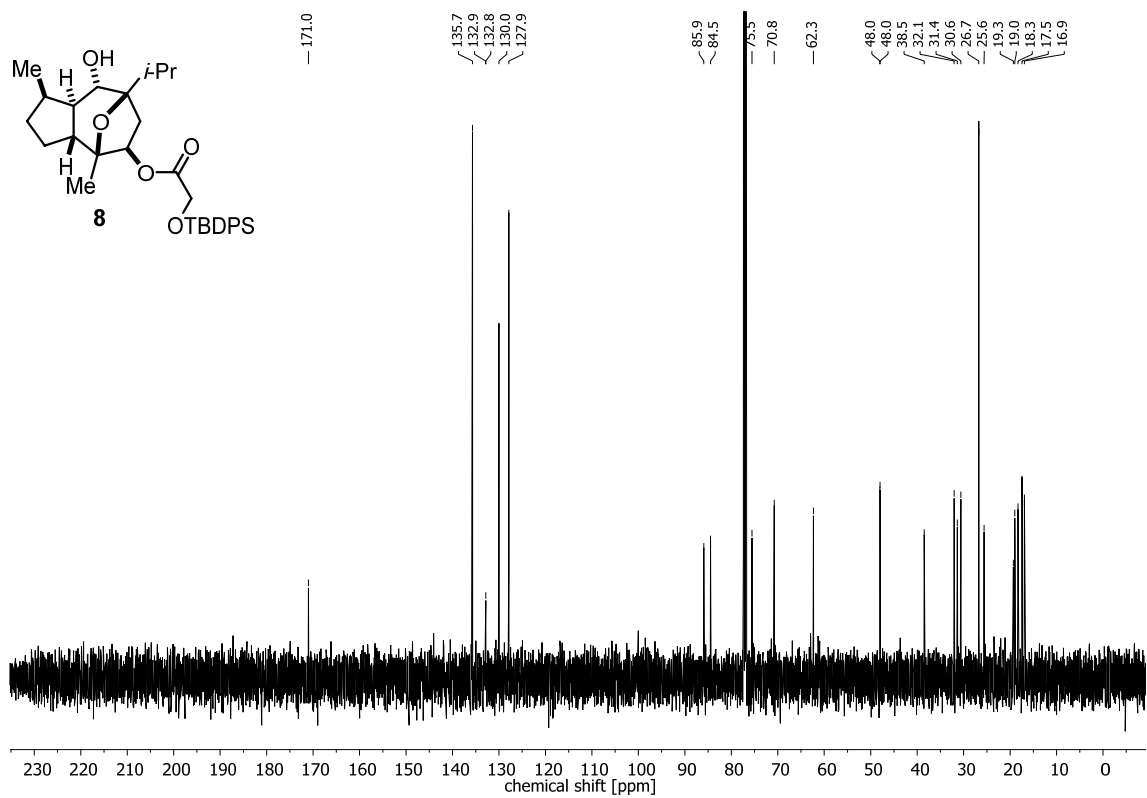
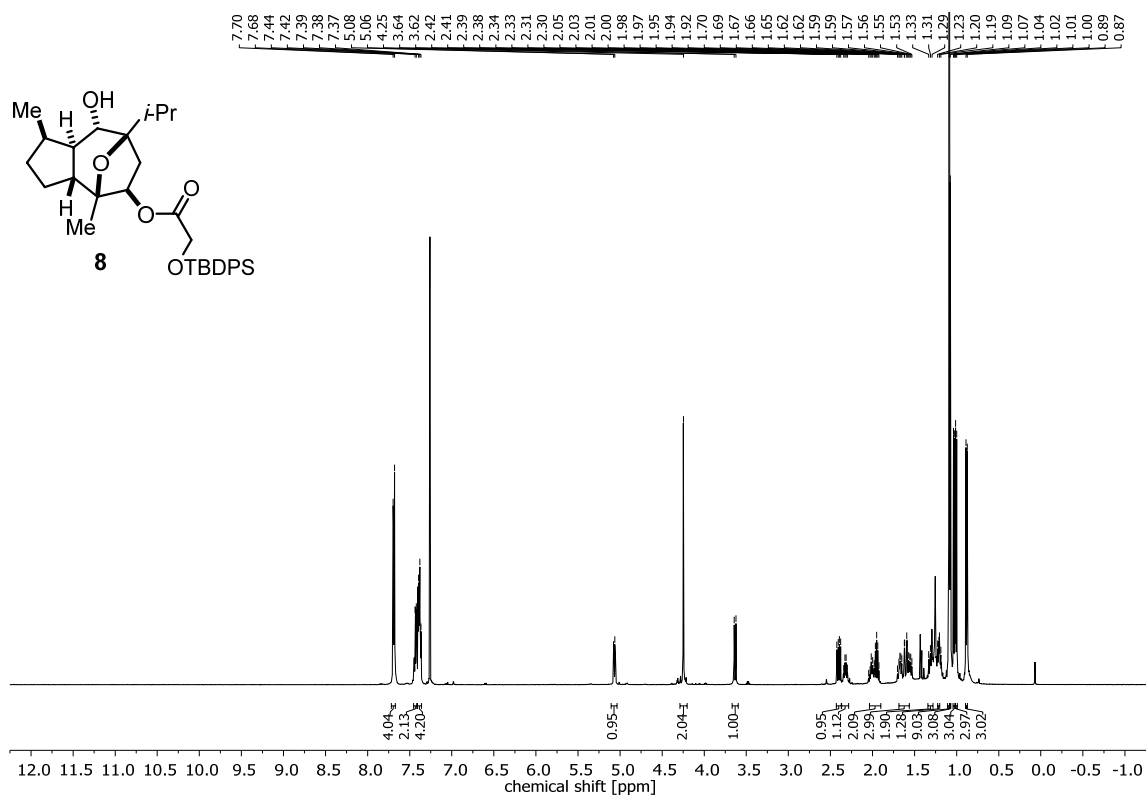


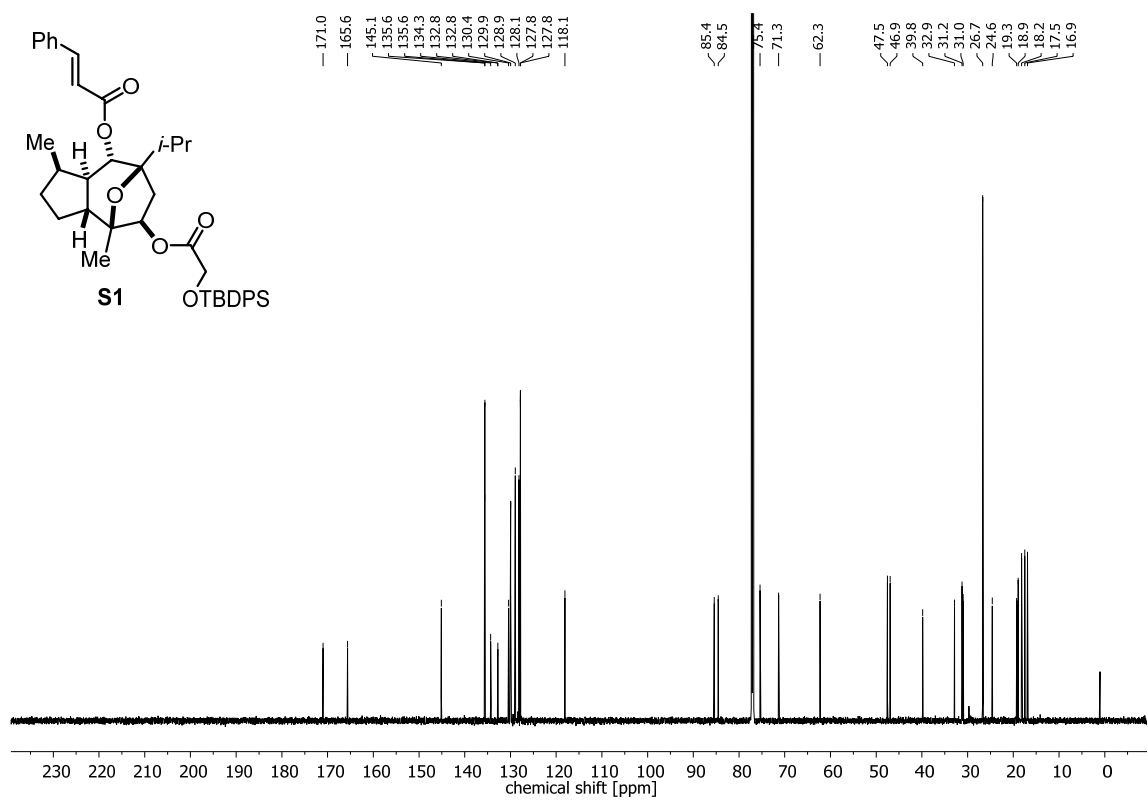
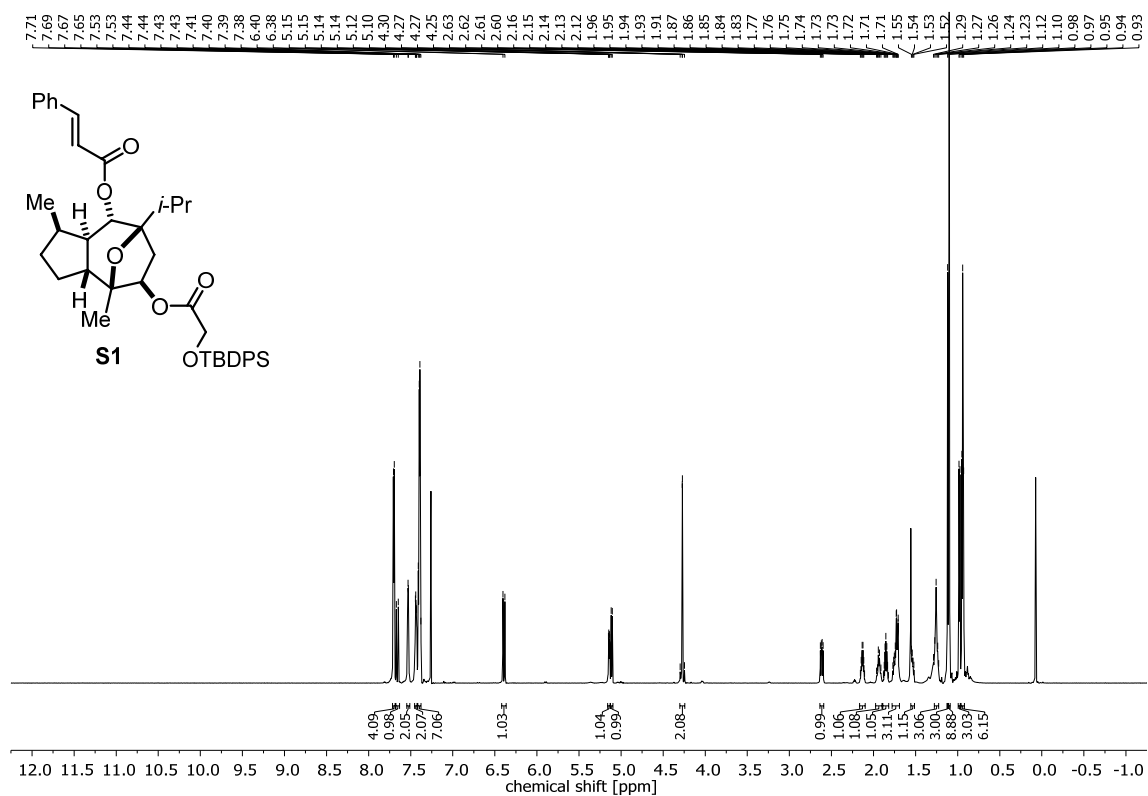
Appendix



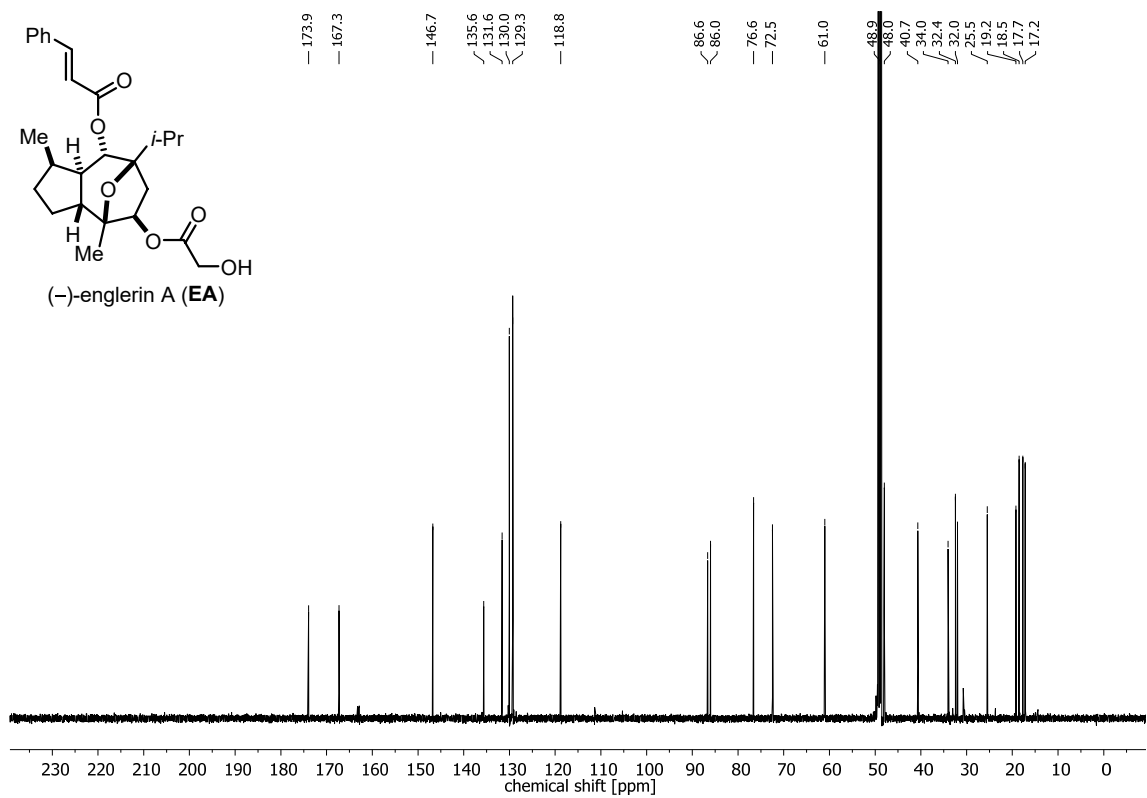
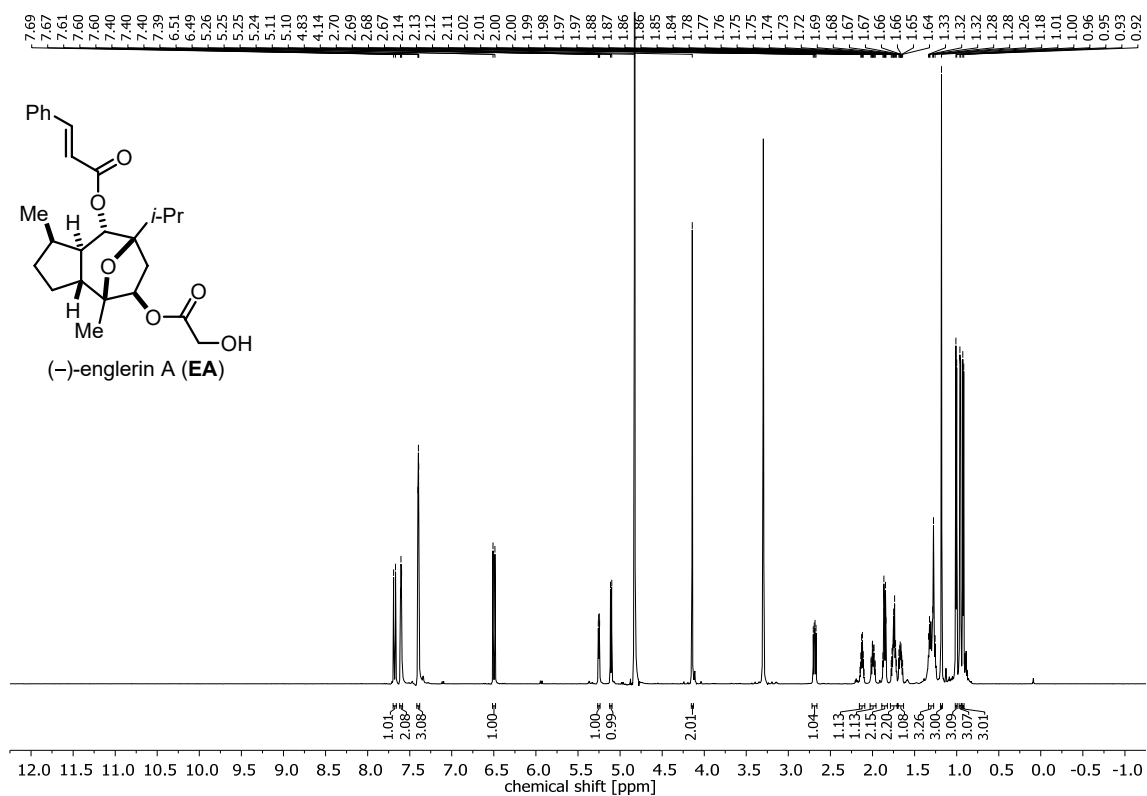


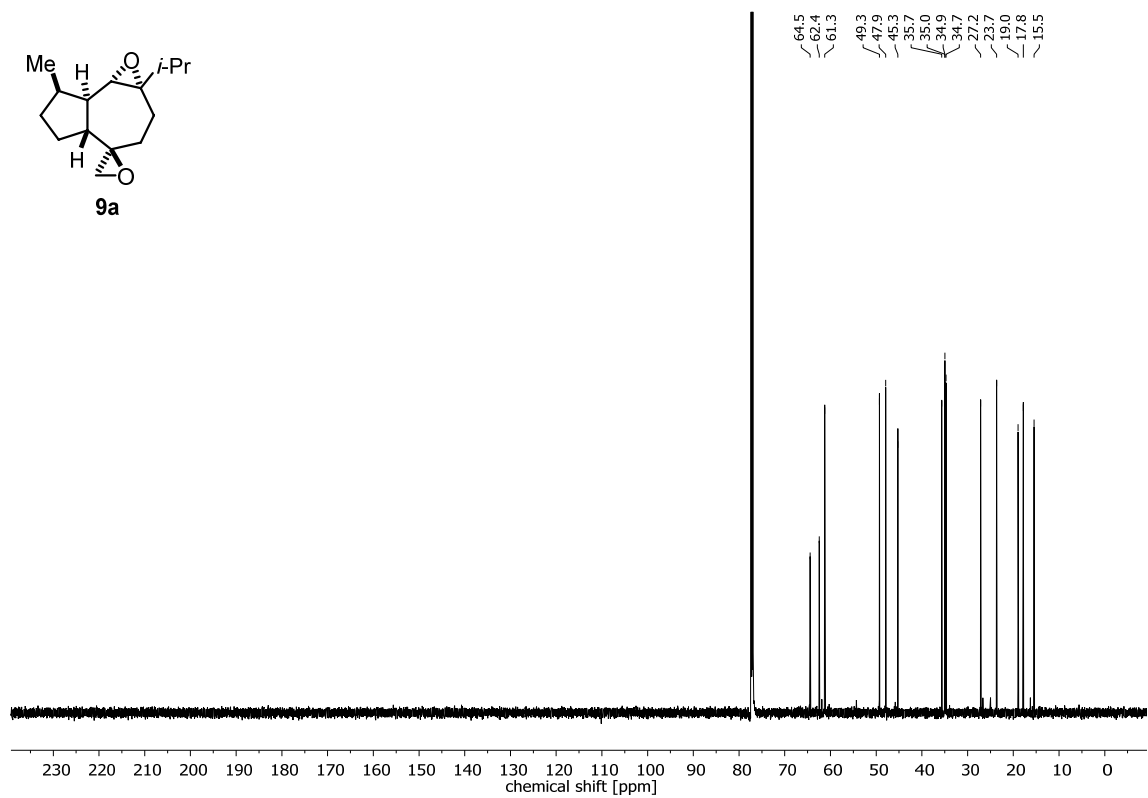
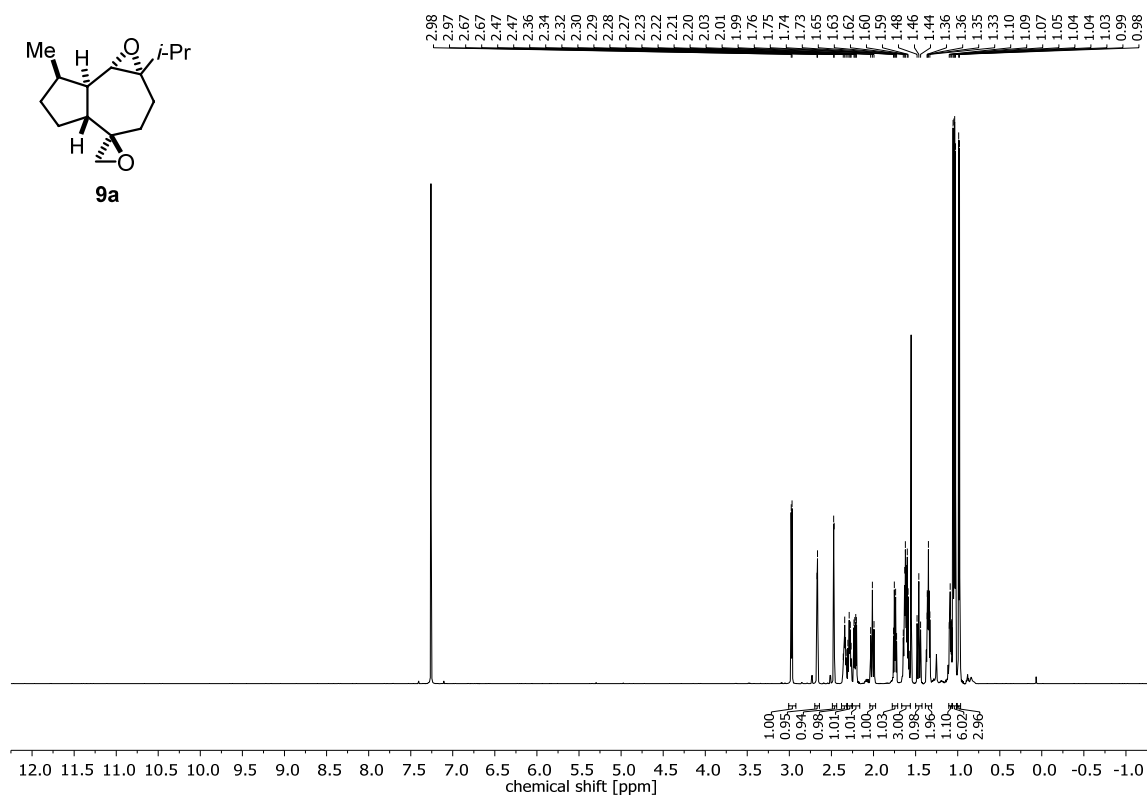
Appendix



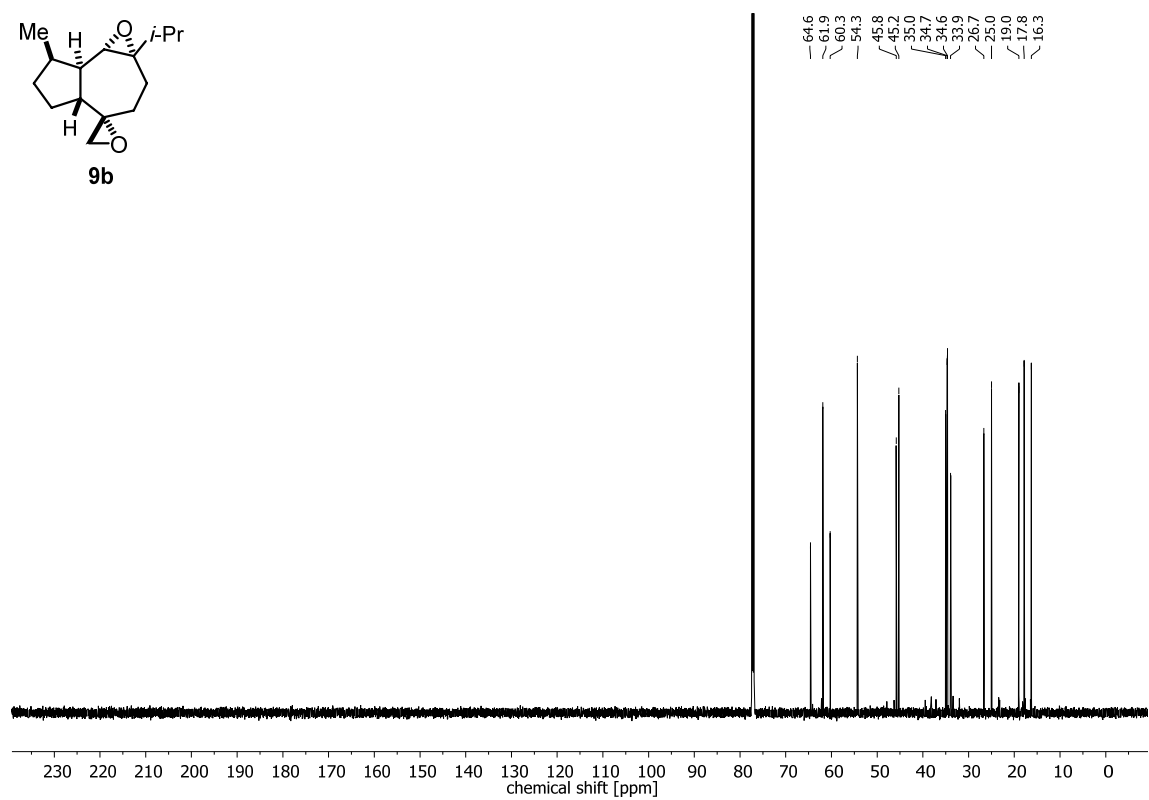
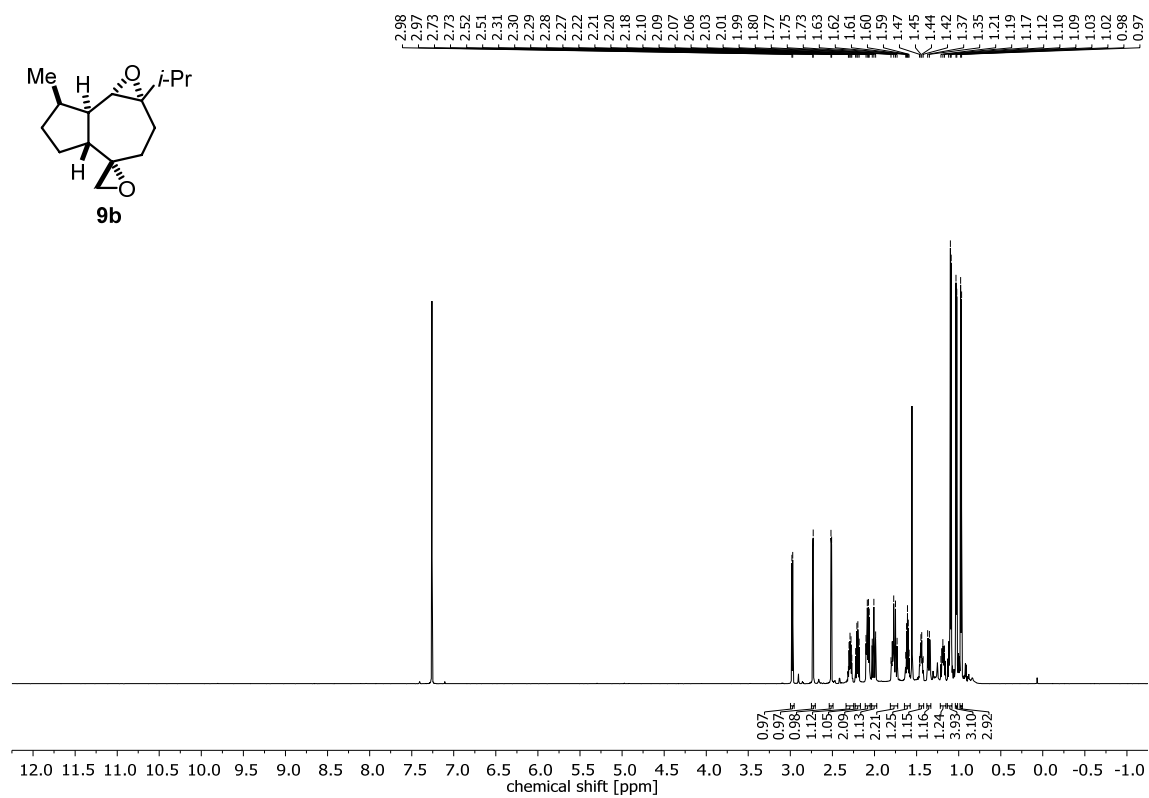


Appendix

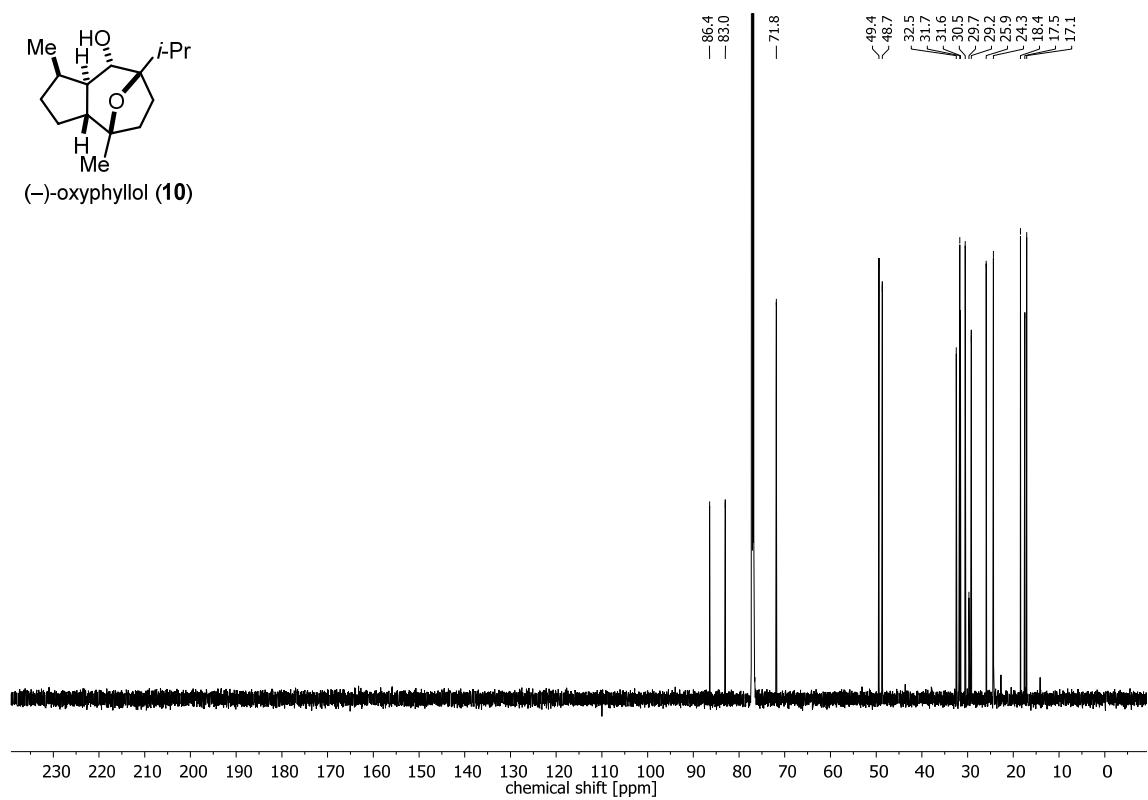
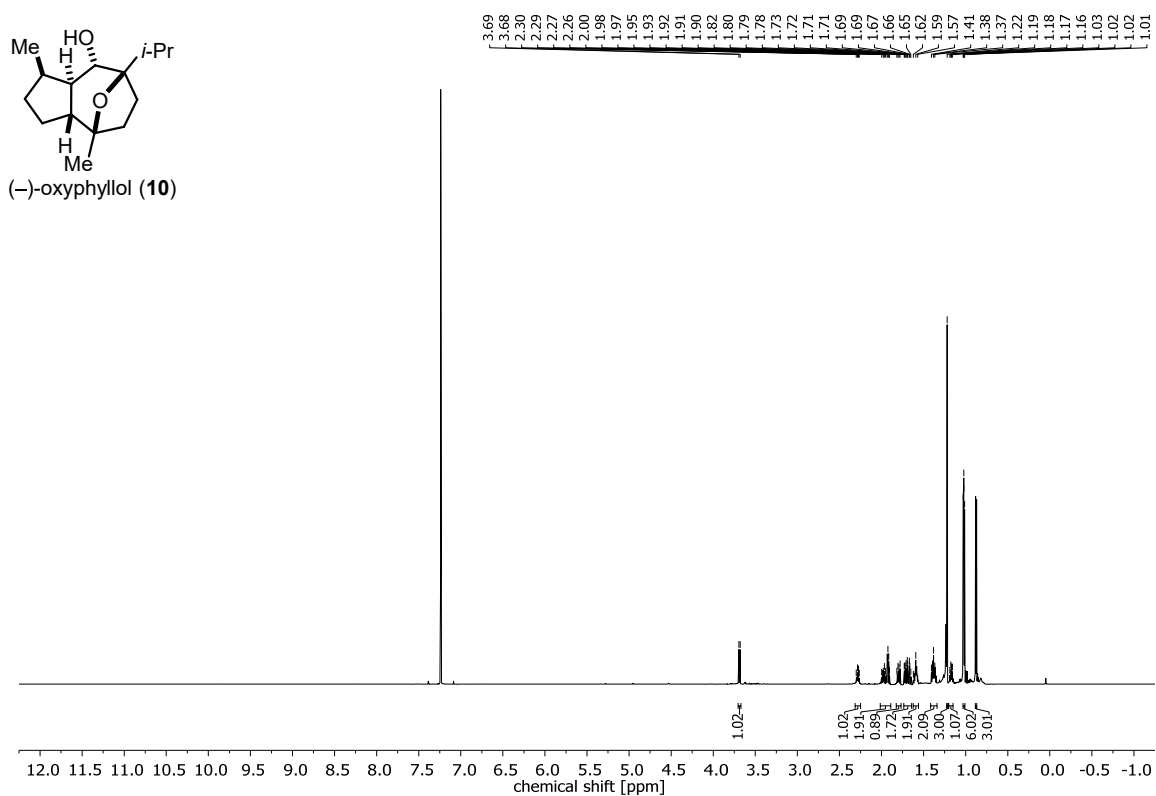




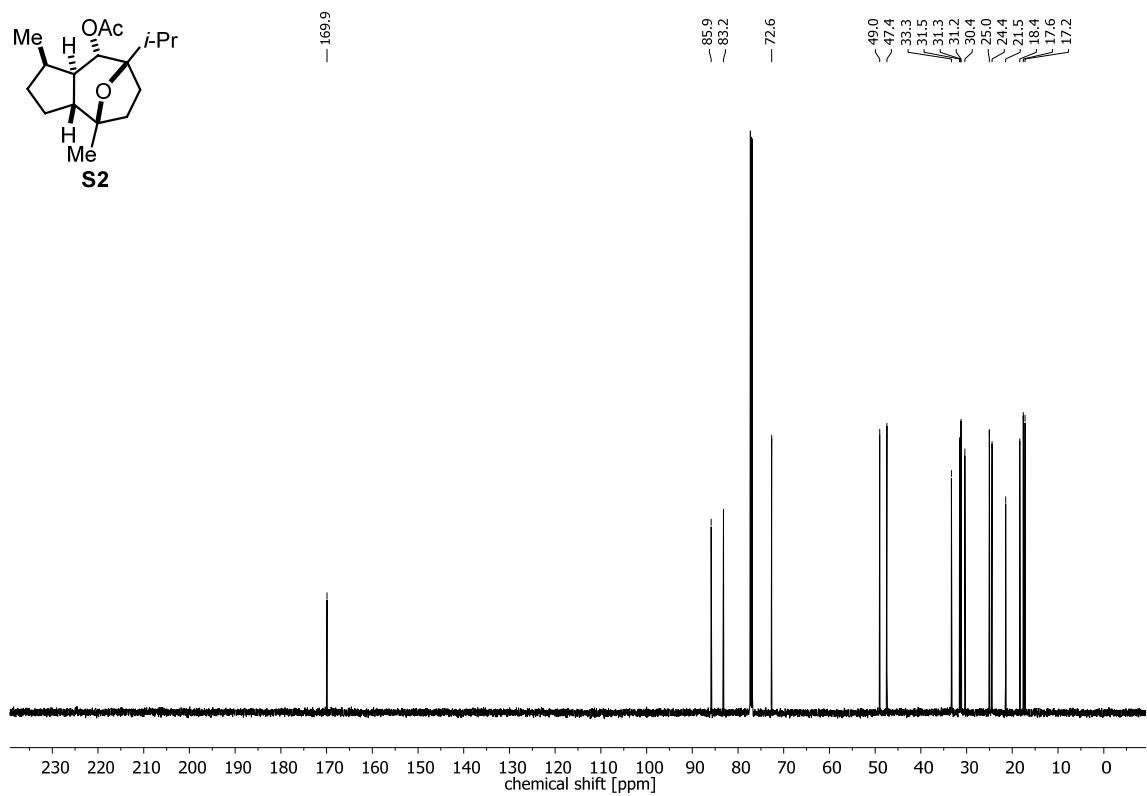
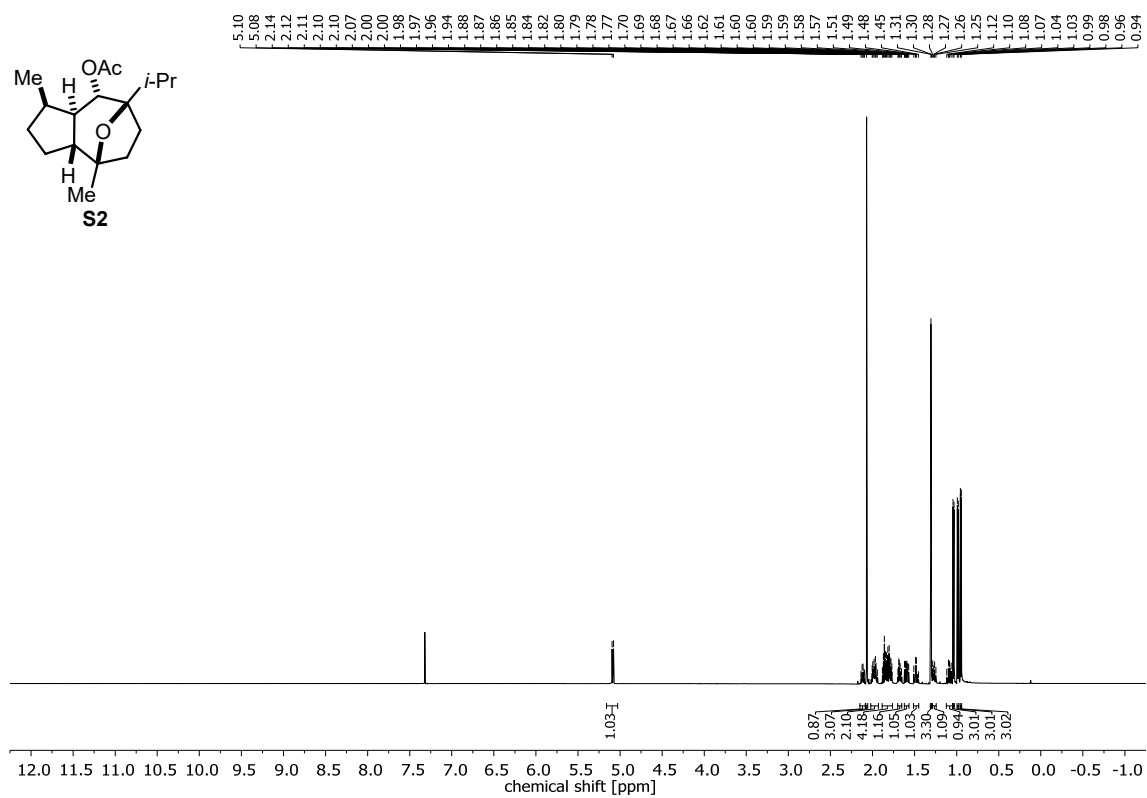
Appendix



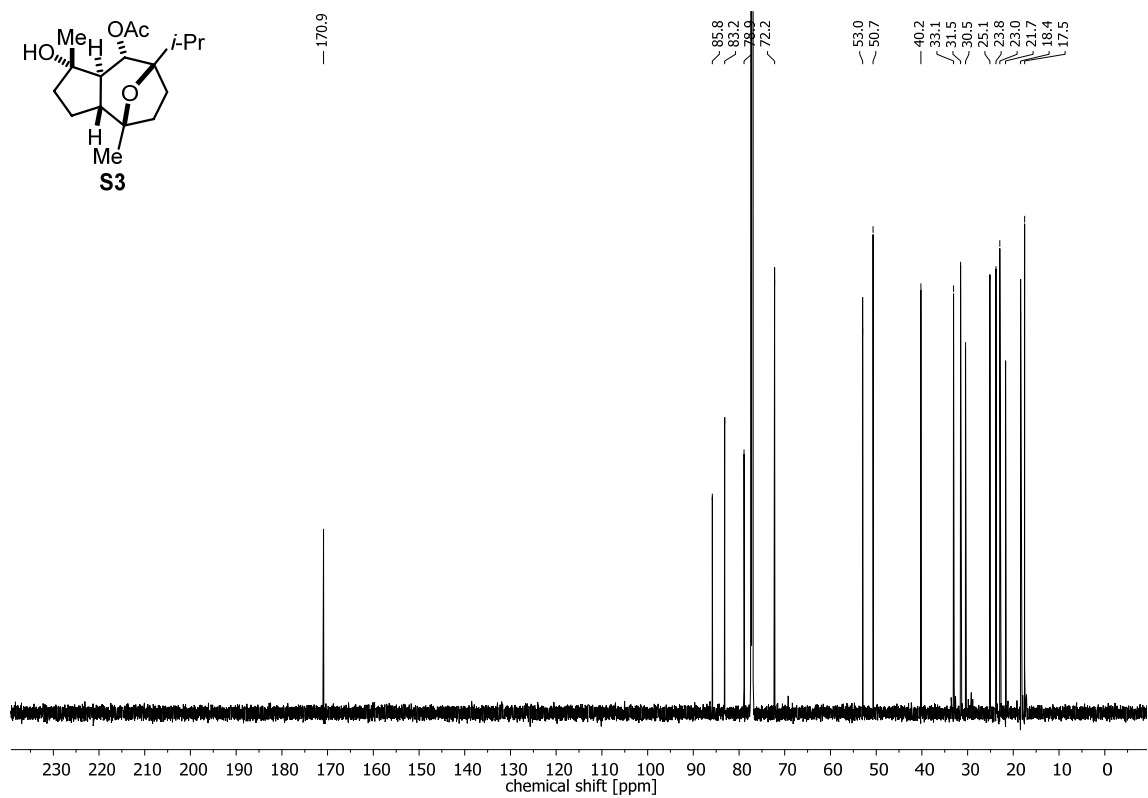
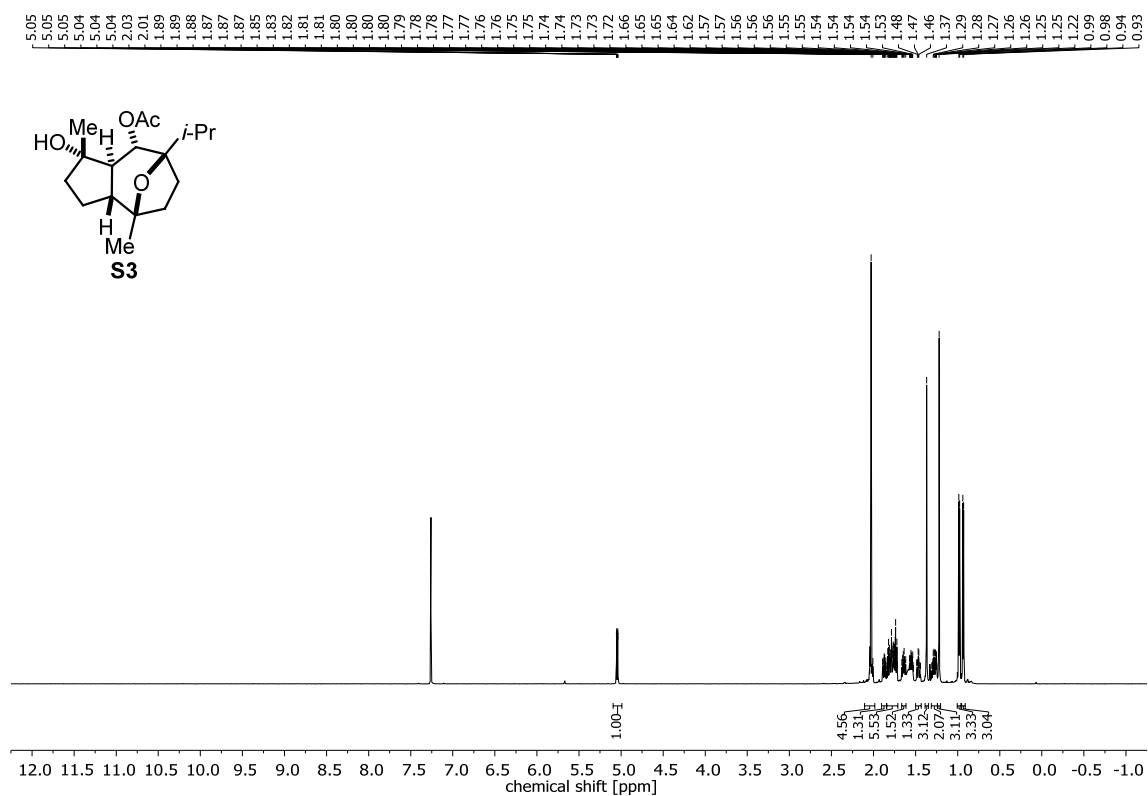
Supporting Information – Semisynthesis of (-)-Englerin A



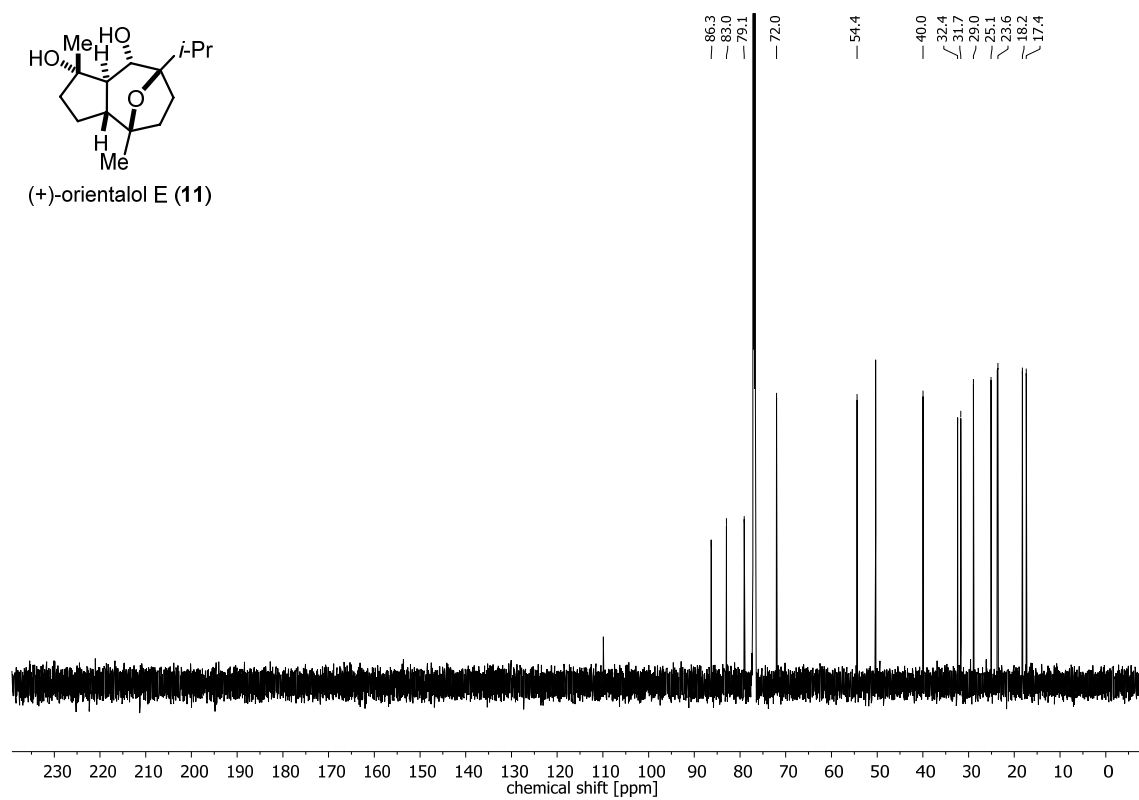
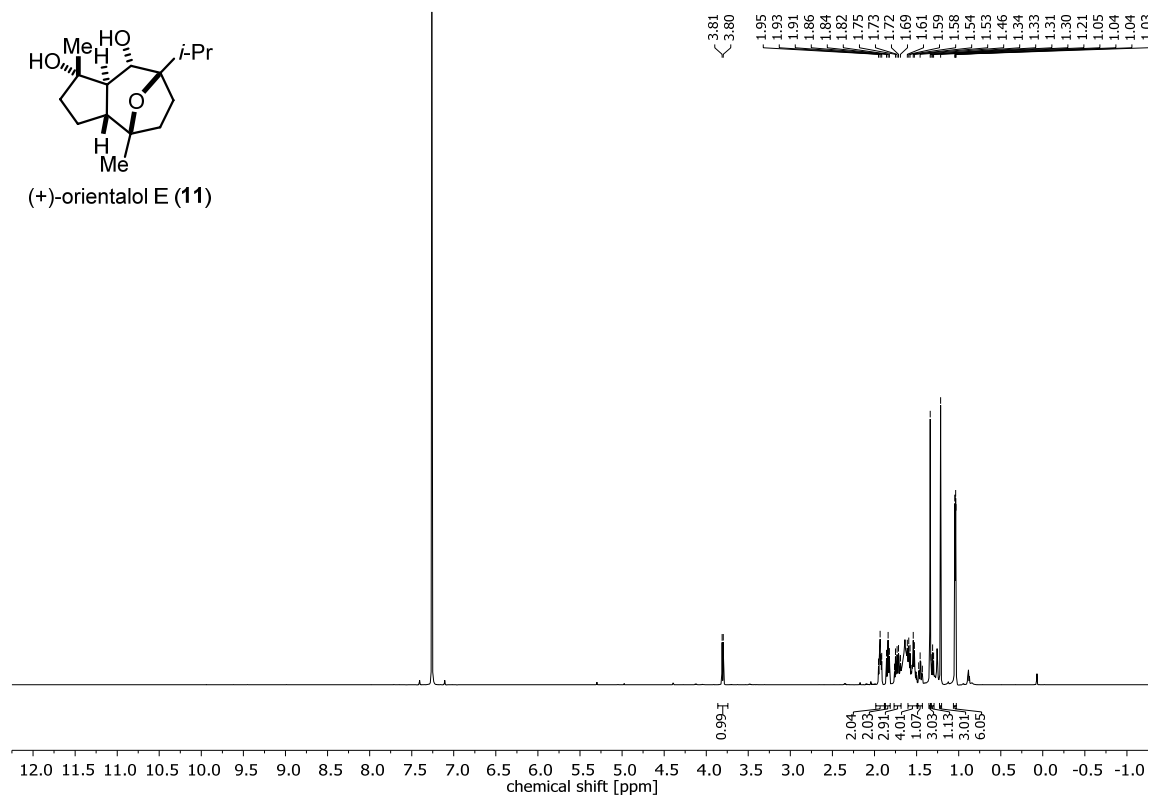
Appendix



Supporting Information – Semisynthesis of (-)-Englerin A



Appendix



Unpublished Results

The same general working methods as in the Supporting Information above have been used.

General Procedure for Yamaguchi esterification (GP1):

Triethylamine (4.0 equiv.) and 2,4,6-trichlorobenzoyl chloride (2.2 equiv.) are added to a solution of the respective carboxylic acid (2.0 equiv.) in PhMe (0.2 M) at 23 °C and after 1 h, the resulting suspension is added to a solution of the respective alcohol (1.0 equiv.) and DMAP (2.6 eq) in PhMe (0.2 M) at 23 °C. The solution is stirred at 80 °C until full conversion according to thin layer chromatography is reached. Sat. aqueous NaHCO₃ solution is added and the aqueous phase is extracted with Et₂O. The combined organic phases are dried over Na₂SO₄ and the solvent is removed under reduced pressure. The crude product is purified by column chromatography on silica gel.

General Procedure for Silyl Ether Cleavage with TBAF (GP2):

The respective silyl ether (1.0 equiv.) is dissolved in THF. Acetic acid (0.4 equiv.; only for primary silyl ethers at the glycolate) and a TBAF solution (1 M, 2 equiv.) are added at 23 °C and the resulting mixture is stirred 50 °C (for secondary silyl ethers) or 23 °C (for primary silyl ethers) until full conversion according to thin layer chromatography is reached. A sat. aqueous NH₄Cl solution is added and the aqueous phase is extracted with Et₂O. The combined organic phases are dried over Na₂SO₄ and the solvent is removed under reduced pressure. The crude product is purified by column chromatography on silica gel.

General Procedure for the one-pot epoxidation and transannular epoxide opening with DMDO (GP3):

The respective ester (1.0 equiv.) is dissolved by the addition of DMDO (solution in CHCl₃, 0.07 mol/L, 1.4 equiv.) and the reaction mixture is stirred at 23 °C until complete conversion is reached according to thin layer chromatography. After the addition of acetic acid (12.5 equiv.), the solution is stirred at 62 °C, until complete conversion is reached according to thin layer chromatography. The solvent is removed under reduced pressure and the crude product is purified by column chromatography.

General Procedure for the esterification with an acid chloride and pyridine (GP4):

The respective alcohol (1 equiv.) and dry pyridine (3.3 equiv.) are dissolved in CH₂Cl₂ and the respective acid chloride (3 equiv.) in CH₂Cl₂ is slowly added. The reaction mixture is stirred 23 °C until complete conversion according to thin layer chromatography is reached. Water is added and the aqueous phase is extracted with CH₂Cl₂. The combined organic phases are dried over

Na₂SO₄ and the solvent is removed under reduced pressure. The crude product is purified by column chromatography.

General Procedure for the oxidation of secondary alcohols to ketones with IBX (GP5):

To a solution of the corresponding alcohol (1.0 equiv.) in dry DMSO (0.2 M) is added 2-iodoxybenzoic acid (2.0 equiv) and the resulting mixture is stirred at 23 °C until full conversion is reached as detected by thin-layer-chromatography. H₂O and Et₂O are added and the suspension is filtered through Celite. The filtrate is extracted with Et₂O (3x). The combined organic phases are washed with brine (2x), dried over Na₂SO₄ and the solvent is removed under reduced pressure. The crude product is purified by column chromatography.

General Procedure for the reduction of ketones with NaBH₄ (GP6):

To a solution of the corresponding ketone (1.0 equiv.) in dry MeOH (0.1 M) is added NaBH₄ (1.0 equiv.) at 0 °C. The resulting mixture is stirred at 23 °C until full conversion is reached as detected by thin-layer-chromatography. Saturated aqueous NH₄Cl-solution is added, and the aqueous phase is extracted with CH₂Cl₂ (3x). The combined organic phases are dried over Na₂SO₄ and the solvent is removed under reduced pressure. The crude product is purified by column chromatography.

General Procedure for the synthesis of imidazolyl sulfonates (GP7):

To a solution of the corresponding alcohol (1.0 equiv.) in THF (0.1 M) at 0 °C are added LiHMDS (1 M in hexane, 7.0 equiv.) dropwise and 1,1-sulfonyldiimidazole (7.7 equiv.). The resulting mixture is stirred at 23 °C for 18 h. H₂O is added, and the aqueous phase is extracted with CH₂Cl₂ (3x). The combined organic phases are dried over Na₂SO₄ and the solvent is removed under reduced pressure. The crude product is purified by column chromatography.

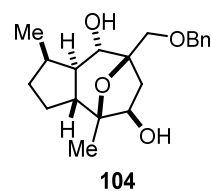
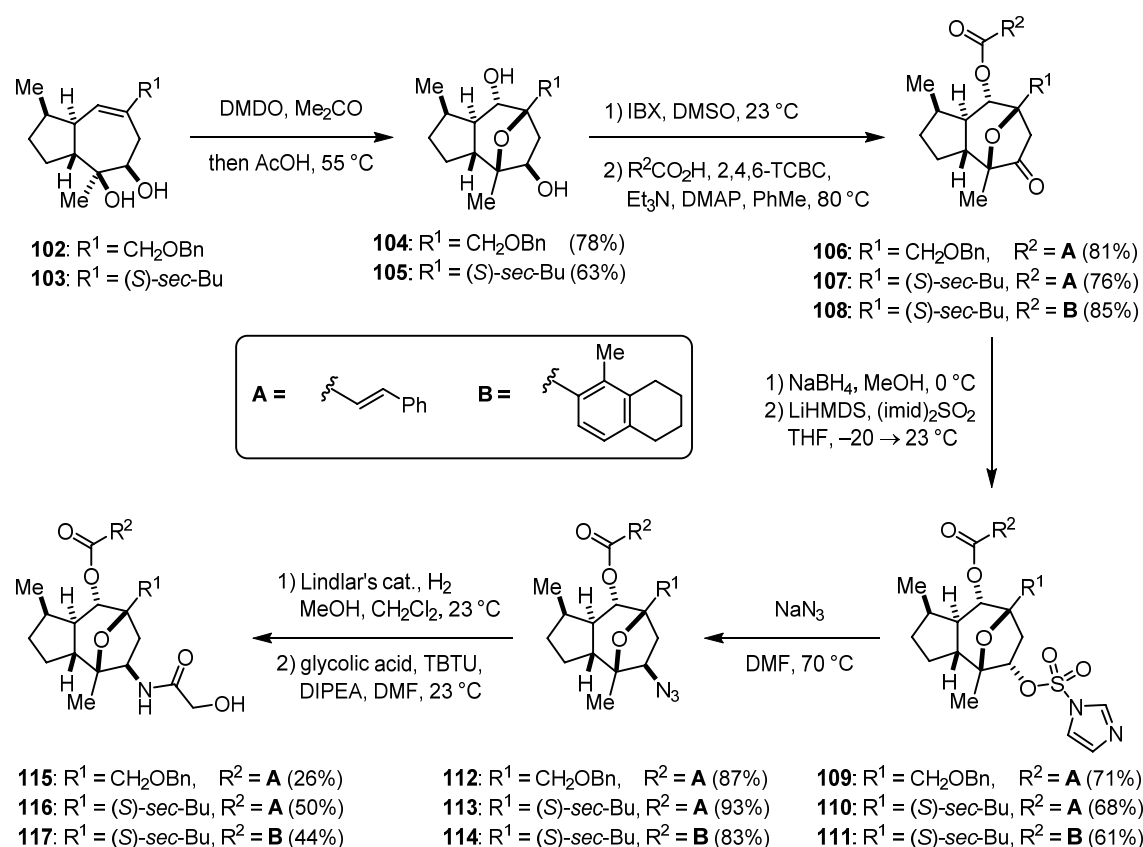
General Procedure for the Substitution with NaN₃ (GP8):

To a solution of the corresponding imidazolyl sulfonate (1.0 equiv.) in dry DMF (0.1 M) is added sodium azide (5.0 equiv.) and the resulting mixture is heated to 70 °C until full conversion is reached as detected by thin-layer-chromatography. After cooling to back to room temperature, H₂O is added, and the aqueous phase is extracted with Et₂O (3x). The combined organic phases are dried over Na₂SO₄ and the solvent is removed under reduced pressure. The crude product is purified by column chromatography.

General Procedure for the synthesis of amides from azides (GP9):

To a solution of the corresponding azide (1.0 equiv.) in dry MeOH (1.0 M) and CH₂Cl₂ (1.0 M) is added Lindlar's catalyst (1.0 equiv.) at 23 °C. The atmosphere is exchange to H₂ by three-times evacuating and flushing with H₂. The resulting mixture is stirred under a H₂-atmosphere (1 atm) at 23 °C until full conversion is reached as detected by thin-layer-chromatography. The

suspension is filtered through Celite and rinsed with MeOH. The filtrate is concentrated under reduced pressure. The crude product is dissolved in dry DMF (0.1 M) and treated with diisopropylethylamine (4.0 equiv.), TBTU (1.05 equiv.) and the corresponding acid (2.0 equiv.). The resulting mixture is stirred at 23 °C until full conversion is reached as detected by thin-layer-chromatography. H₂O is added, and the aqueous phase is extracted with Et₂O (3x). The combined organic phases are washed with brine, dried over Na₂SO₄ and the solvent is removed under reduced pressure. The crude product is purified by column chromatography.



Prepared according to GP3. Purification by column chromatography (silica gel, pentane/Et₂O 1:2) afforded **104** (90.4 mg, 272 μmol, 78%) as a colorless oil.

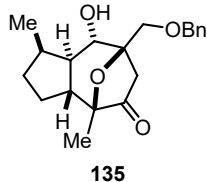
$$[\alpha]_{\text{D}}^{24} = -35.1^{\circ} (c = 1.0, \text{CHCl}_3).$$

¹H NMR (500 MHz, CDCl₃): δ = 7.39 – 7.28 (m, 5H), 4.77 – 4.59 (m, 1H), 4.54 – 4.45 (m, 1H), 3.98 – 3.88 (m, 1H), 3.72 – 3.68 (m, 3H), 2.63 (dd, *J* = 14.2, 7.7 Hz, 1H), 2.42 – 2.14 (m, 2H), 2.04 – 1.93 (m, 1H), 1.75 – 1.58 (m, 2H), 1.42 (d, *J* = 14.1 Hz, 1H), 1.26 (s, 3H), 1.25 – 1.14 (m, 2H), 1.12 – 1.03 (m, 1H), 0.90 (d, *J* = 7.1 Hz, 3H) ppm.

¹³C NMR (126 MHz, CDCl₃): δ = 137.7, 128.6 (2C), 128.0, 127.9 (2C), 86.1, 82.6, 74.1, 73.8, 72.6, 70.7, 47.5, 46.8, 41.9, 31.2, 30.5, 25.8, 19.1, 17.0 ppm.

IR (ATR): $\tilde{\nu}$ = 3382, 2980, 2925, 2814, 1402, 1242, 1203, 1105, 1053 cm^{-1} .

HRMS (ESI): m/z calcd. for $\text{C}_{20}\text{H}_{28}\text{O}_4\text{Na}$ $[\text{M} + \text{Na}]^+$: 355.1880, found: 355.1892.



Prepared according to GP5. Purification by column chromatography (silica gel, pentane/Et₂O 2:1) afforded **135** (79.0 mg, 239 μmol , 88%) as a colorless oil.

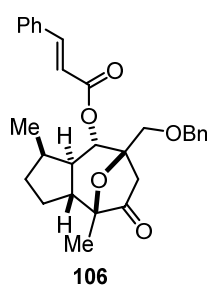
$[\alpha]_{\text{D}}^{21} = -12.1^\circ$ ($c = 1.0$, CHCl_3).

¹H NMR (500 MHz, CDCl_3): δ = 7.41 – 7.27 (m, 5H), 4.69 (d, $J = 12.1$ Hz, 1H), 4.55 (d, $J = 12.1$ Hz, 1H), 3.92 (d, $J = 10.6$ Hz, 1H), 3.75 (s, 2H), 2.62 (d, $J = 18.1$ Hz, 1H), 2.80 – 2.41 (m, 1H), 2.35 – 2.26 (m, 1H), 2.19 (d, $J = 18.1$ Hz, 1H), 1.99 – 1.88 (m, 1H), 1.75 – 1.58 (m, 2H), 1.38 – 1.27 (m, 1H), 1.24 (s, 3H), 1.20 – 1.10 (m, 2H), 0.89 (d, $J = 7.2$ Hz, 3H) ppm.

¹³C NMR (126 MHz, CDCl_3): δ = 214.2, 137.5, 128.7 (2C), 128.2, 128.0 (2C), 83.9, 80.3, 74.0, 74.0, 70.7, 48.6, 46.3, 41.8, 31.0, 30.5, 24.3, 18.0, 16.9 ppm.

IR (ATR): $\tilde{\nu}$ = 3369, 2953, 2854, 1425, 1253, 1220, 1140, 1052 cm^{-1} .

HRMS (ESI): m/z calcd. for $\text{C}_{20}\text{H}_{26}\text{O}_4\text{Na}$ $[\text{M} + \text{Na}]^+$: 353.1723, found: 353.1743.



Prepared according to GP1. Purification by column chromatography (silica gel, pentane/Et₂O 5:1) afforded **106** (102 mg, 221 μmol , 92%) as a colorless oil.

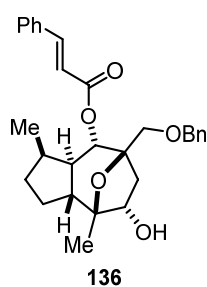
$[\alpha]_{\text{D}}^{21} = -22.3^\circ$ ($c = 1.0$, CHCl_3).

¹H NMR (500 MHz, CDCl_3): δ = 7.64 (d, $J = 16.0$ Hz, 1H), 7.53 – 7.48 (m, 2H), 7.43 – 7.36 (m, 3H), 7.32 – 7.23 (m, 4H), 7.21 – 7.16 (m, 1H), 6.33 (d, $J = 16.0$ Hz, 1H), 5.36 (d, $J = 10.9$ Hz, 1H), 4.58 (s, 2H), 3.67 (d, $J = 10.8$ Hz, 1H), 3.57 (d, $J = 10.8$ Hz, 1H), 2.62 (d, $J = 18.1$ Hz, 1H), 2.55 (d, $J = 18.1$ Hz, 1H), 2.20 – 2.12 (m, 1H), 1.98 – 1.86 (m, 2H), 1.75 – 1.66 (m, 1H), 1.65 – 1.58 (m, 1H), 1.32 (s, 3H), 1.28 – 1.16 (m, 2H), 0.94 (d, $J = 7.1$ Hz, 3H) ppm.

¹³C NMR (126 MHz, CDCl_3): δ = 214.0, 165.6, 145.5, 137.7, 134.2, 130.5, 129.0 (2C), 128.3 (2C), 128.2 (2C), 127.9 (2C), 127.6, 117.5, 84.1, 81.1, 73.9, 70.8, 70.2, 47.5, 46.3, 41.0, 31.0, 30.7, 23.6, 18.0, 16.9 ppm.

IR (ATR): $\tilde{\nu}$ = 3053, 2964, 2854, 1602, 1436, 1252, 1207, 1053 cm^{-1} .

HRMS (ESI): m/z calcd. for $\text{C}_{29}\text{H}_{32}\text{O}_5\text{Na}$ $[\text{M} + \text{Na}]^+$: 483.2142, found: 483.2121.



Prepared according to GP6. Purification by column chromatography (silica gel, pentane/Et₂O 1:1) afforded **136** (94.2 mg, 204 μmol, 92%) as a colorless oil.

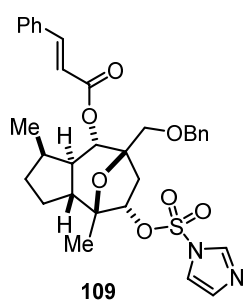
$[\alpha]_D^{21} = -25.1^\circ$ ($c = 1.0$, CHCl₃).

¹H NMR (500 MHz, CDCl₃): $\delta = 7.63$ (d, $J = 16.0$ Hz, 1H), 7.52 – 7.47 (m, 2H), 7.40 – 7.37 (m, 3H), 7.30 (d, $J = 7.4$ Hz, 2H), 7.24 (t, $J = 7.5$ Hz, 2H), 7.15 (t, $J = 7.3$ Hz, 1H), 6.34 (d, $J = 16.0$ Hz, 1H), 5.29 (d, $J = 10.5$ Hz, 1H), 4.55 (d, $J = 12.3$ Hz, 1H), 4.51 (d, $J = 12.2$ Hz, 1H), 4.27 (dd, $J = 10.7, 4.8$ Hz, 1H), 3.49 (d, $J = 10.5$ Hz, 1H), 3.39 (d, $J = 10.5$ Hz, 1H), 2.44 (ddd, $J = 12.6, 10.5, 6.9$ Hz, 1H), 2.29 (dd, $J = 13.7, 10.8$ Hz, 1H), 2.24 – 2.17 (m, 1H), 2.06 (dd, $J = 13.5, 4.6$ Hz, 1H), 2.03 – 1.82 (m, 4H), 1.72 – 1.65 (m, 1H), 1.38 (s, 3H), 1.24 – 1.17 (m, 1H), 0.97 (d, $J = 7.1$ Hz, 3H) ppm.

¹³C NMR (126 MHz, CDCl₃): $\delta = 166.0, 144.9, 138.2, 134.5, 130.4, 129.0$ (2C), 128.3 (2C), 128.2 (2C), 128.1 (2C), 127.5, 118.3, 82.9, 82.5, 80.4, 73.9, 71.7, 71.7, 49.3, 45.4, 38.4, 31.6, 31.3, 24.7, 23.4, 17.2 ppm.

IR (ATR): $\tilde{\nu} = 3363, 3061, 2923, 2864, 1605, 1440, 1270, 1230, 1048$ cm⁻¹.

HRMS (ESI): m/z calcd. for C₂₉H₃₄O₅Na [M + Na]⁺: 485.2298, found: 485.2316.



Prepared according to GP7. Purification by column chromatography (silica gel, pentane/Et₂O 1:1) afforded **109** (93.1 mg, 157 μmol, 77%) as a colorless oil.

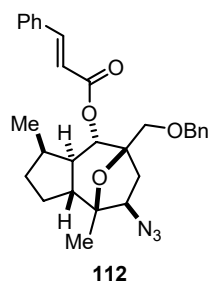
$[\alpha]_D^{22} = -9.9^\circ$ ($c = 1.0$, CHCl₃).

¹H NMR (500 MHz, CDCl₃): $\delta = 8.00$ (s, 1H), 7.61 (d, $J = 16.0$ Hz, 1H), 7.52 – 7.49 (m, 2H), 7.43 – 7.38 (m, 3H), 7.35 (s, 1H), 7.27 – 7.23 (m, 4H), 7.22 (s, 1H), 7.20 – 7.14 (m, 1H), 6.31 (d, $J = 16.0$ Hz, 1H), 5.20 (d, $J = 10.4$ Hz, 1H), 4.66 (dd, $J = 10.9, 4.2$ Hz, 1H), 4.50 (d, $J = 12.2$ Hz, 1H), 4.46 (d, $J = 12.2$ Hz, 1H), 3.44 (d, $J = 10.7$ Hz, 1H), 3.33 (d, $J = 10.7$ Hz, 1H), 2.30 (dd, $J = 14.4, 11.0$ Hz, 1H), 2.25 – 2.18 (m, 1H), 2.13 – 1.87 (m, 4H), 1.74 – 1.66 (m, 1H), 1.65 – 1.54 (m, 1H), 1.24 (s, 3H), 1.28 – 1.18 (m, 1H), 0.92 (d, $J = 7.1$ Hz, 3H) ppm.

¹³C NMR (126 MHz, CDCl₃): $\delta = 165.7, 145.5, 137.7, 137.2, 134.3, 131.8, 130.6, 129.0$ (2C), 128.4 (2C), 128.2 (2C), 128.0 (2C), 127.7, 118.0, 117.6, 89.9, 83.5, 82.0, 73.9, 70.9, 70.6, 49.0, 45.5, 34.3, 31.3, 31.1, 24.4, 22.5, 17.0 ppm.

IR (ATR): $\tilde{\nu} = 3072, 2953, 2835, 1625, 1406, 1240, 1164, 1036$ cm⁻¹.

HRMS (ESI): m/z calcd. for C₃₂H₃₆N₂O₇Na [M + Na]⁺: 615.2135, found: 615.2157.



Prepared according to GP8. Purification by column chromatography (silica gel, pentane/Et₂O 10:1) afforded **112** (66.6 mg, 137 μmol, 87%) as a colorless oil.

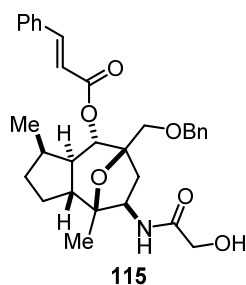
$[\alpha]_{\text{D}}^{23} = -23.9^\circ$ ($c = 1.0$, CHCl₃).

¹H NMR (500 MHz, CDCl₃): $\delta = 7.63$ (d, $J = 16.0$ Hz, 1H), 7.51 – 7.48 (m, 2H), 7.41 – 7.38 (m, 3H), 7.31 – 7.28 (m, 2H), 7.25 – 7.21 (m, 2H), 7.17 – 7.12 (m, 1H), 6.31 (d, $J = 16.0$ Hz, 1H), 5.21 (d, $J = 10.5$ Hz, 1H), 4.58 (d, $J = 12.2$ Hz, 1H), 4.51 (d, $J = 12.2$ Hz, 1H), 3.66 (dd, $J = 8.3, 3.7$ Hz, 1H), 3.57 (d, $J = 10.5$ Hz, 1H), 3.49 (d, $J = 10.5$ Hz, 1H), 2.58 (dd, $J = 14.2, 8.4$ Hz, 1H), 2.22 – 2.13 (m, 1H), 1.99 – 1.84 (m, 3H), 1.80 – 1.72 (m, 1H), 1.51 (ddd, $J = 13.3, 10.5, 6.6$ Hz, 1H), 1.39 (s, 3H), 1.31 – 1.23 (m, 1H), 1.16 – 1.06 (m, 1H), 0.96 (d, $J = 7.1$ Hz, 3H) ppm.

¹³C NMR (126 MHz, CDCl₃): $\delta = 165.6, 145.1, 137.9, 134.4, 130.5, 129.0$ (2C), 128.3 (2C), 128.2 (2C), 128.1 (2C), 127.6, 118.0, 86.7, 83.6, 73.9, 71.0, 70.4, 62.8, 48.2, 46.4, 37.5, 31.2, 30.9, 25.0, 20.3, 17.1 ppm.

IR (ATR): $\tilde{\nu} = 3038, 2954, 2845, 2086, 1635, 1406, 1263, 1220, 1058$ cm⁻¹.

HRMS (ESI): m/z calcd. for C₂₉H₃₃N₃O₄Na [M + Na]⁺: 510.2363, found: 510.2380.



Prepared according to GP9. Purification by preparative thin-layer chromatography (silica gel, Et₂O) afforded amide **115** (4.3 mg, 8.3 μmol, 26%) as a colorless oil.

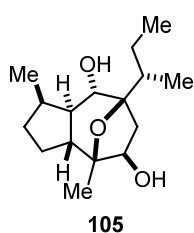
$[\alpha]_{\text{D}}^{24} = -19.3^\circ$ ($c = 0.25$, CHCl₃).

¹H NMR (700 MHz, CDCl₃): $\delta = 7.63$ (d, $J = 15.9$ Hz, 1H), 7.53 – 7.49 (m, 2H), 7.42 – 7.38 (m, 3H), 7.30 (d, $J = 7.4$ Hz, 2H), 7.27 – 7.25 (m, 2H), 7.19 (t, $J = 7.3$ Hz, 1H), 6.53 (d, $J = 9.6$ Hz, 1H), 6.33 (d, $J = 16.0$ Hz, 1H), 5.13 (d, $J = 10.5$ Hz, 1H), 4.56 (d, $J = 12.5$ Hz, 1H), 4.53 (d, $J = 12.5$ Hz, 1H), 4.49 (dt, $J = 9.0, 4.6$ Hz, 1H), 4.11 (d, $J = 15.8$ Hz, 1H), 4.07 (d, $J = 15.8$ Hz, 1H), 3.60 (d, $J = 10.7$ Hz, 1H), 3.44 (d, $J = 10.7$ Hz, 1H), 2.62 (dd, $J = 14.0, 8.9$ Hz, 1H), 2.51 – 2.45 (m, 1H), 2.23 – 2.17 (m, 1H), 2.07 – 1.94 (m, 2H), 1.88 (td, $J = 12.6, 7.0$ Hz, 1H), 1.78 – 1.67 (m, 2H), 1.61 (dd, $J = 14.0, 4.2$ Hz, 1H), 1.44 – 1.36 (m, 1H), 1.21 (s, 3H), 0.93 (d, $J = 7.1$ Hz, 3H) ppm.

¹³C NMR (176 MHz, CDCl₃): $\delta = 170.3, 165.7, 145.2, 137.9, 134.3, 130.4, 128.9$ (2C), 128.3 (2C), 128.1 (2C), 128.0 (2C), 127.6, 117.8, 85.7, 83.4, 73.9, 70.9, 62.0, 50.5, 48.3, 45.9, 38.5, 31.9, 24.8, 22.7, 19.9, 17.0, 14.1 ppm.

IR (ATR): $\tilde{\nu} = 3402, 3052, 2954, 2856, 1632, 1424, 1264, 1232, 1051$ cm⁻¹.

HRMS (ESI): m/z calcd. for C₃₁H₃₇NO₆Na [M + Na]⁺: 542.2513, found: 542.2539.



Prepared according to GP3. Purification by column chromatography (silica gel, pentane/Et₂O 1:1) afforded **105** (11.7 mg, 43.6 μmol, 63%) as a colorless oil.

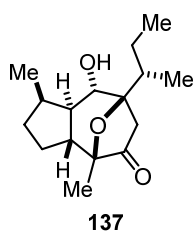
$[\alpha]_{\text{D}}^{20} = -24.6^{\circ}$ ($c = 1.0$, CHCl₃).

¹H NMR (500 MHz, CDCl₃): $\delta = 3.93$ (dd, $J = 7.6, 2.6$ Hz, 1H), 3.65 (d, $J = 10.2$ Hz, 1H), 2.50 (dd, $J = 14.5, 7.6$ Hz, 1H), 2.30 (dtd, $J = 8.3, 7.1, 2.7$ Hz, 1H), 1.98 (dddd, $J = 13.2, 10.6, 8.4, 2.2$ Hz, 1H), 1.78 (dq, $J = 13.2, 7.4, 2.6$ Hz, 1H), 1.71 – 1.52 (m, 5H), 1.51 – 1.33 (m, 2H), 1.22 (s, 3H), 1.28 – 1.08 (m, 3H), 1.05 (d, $J = 7.0$ Hz, 3H), 0.95 (t, $J = 7.4$ Hz, 3H), 0.88 (d, $J = 7.2$ Hz, 3H) ppm.

¹³C NMR (126 MHz, CDCl₃): $\delta = 86.0, 85.2, 73.3, 71.0, 47.9, 47.8, 42.6, 40.3, 31.5, 30.6, 25.9, 24.4, 19.4, 17.1, 14.9, 13.0$ ppm.

IR (ATR): $\tilde{\nu} = 2958, 2925, 2854, 2361, 2338, 1459$ cm⁻¹.

HRMS (ESI): m/z calcd. for C₁₆H₂₈O₃Na [M + Na]⁺: 291.1936, found: 291.1940.



Prepared according to GP5. Purification by column chromatography (silica gel, pentane/Et₂O 3:1) afforded **137** (82.5 mg, 310 μmol, 86%) as a colorless oil.

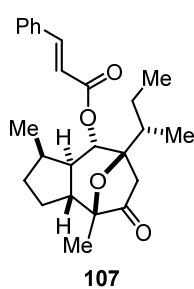
$[\alpha]_{\text{D}}^{22} = -53.3^{\circ}$ ($c = 1.0$, CHCl₃).

¹H NMR (500 MHz, CDCl₃): $\delta = 3.93$ (dd, $J = 10.5, 2.2$ Hz, 1H), 2.52 (d, $J = 18.5$ Hz, 1H), 2.30 (d, $J = 18.5$ Hz, 1H), 2.33 – 2.24 (m, 1H), 2.01 – 1.90 (m, 1H), 1.87 – 1.70 (m, 2H), 1.69 – 1.58 (m, 2H), 1.56 (s, 1H), 1.39 – 1.22 (m, 2H), 1.21 (s, 3H) 1.20 – 1.12 (m, 2H), 1.09 (d, $J = 7.1$ Hz, 3H), 0.98 (t, $J = 7.4$ Hz, 3H), 0.90 (d, $J = 7.3$ Hz, 3H) ppm.

¹³C NMR (176 MHz, CDCl₃): $\delta = 215.7, 83.6, 83.3, 70.7, 49.5, 46.6, 42.5, 40.9, 31.2, 30.6, 24.3, 23.8, 18.1, 16.8, 14.5, 12.7$ ppm.

IR (ATR): $\tilde{\nu} = 3485, 2958, 2873, 2361, 1742, 1458, 1376, 1134, 1099, 974, 893, 792, 704, 692$ cm⁻¹.

HRMS (ESI): m/z calcd. for C₁₆H₂₆O₃Na [M + Na]⁺: 289.1780, found: 289.1790.



Prepared according to GP1. Purification by column chromatography (silica gel, pentane/Et₂O 20:1 → 10:1) afforded **107** (53.6 mg, 135 μmol, 89%) as a colorless oil.

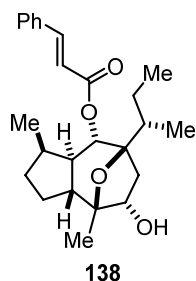
$[\alpha]_{\text{D}}^{23} = -32.0^{\circ}$ ($c = 1.0$, CHCl₃).

¹H NMR (500 MHz, CDCl₃): $\delta = 7.67$ (d, $J = 16.0$ Hz, 1H), 7.54 – 7.50 (m, 2H), 7.40 – 7.37 (m, 3H), 6.39 (d, $J = 16.0$ Hz, 1H), 5.39 (d, $J = 10.7$ Hz, 1H), 2.68 (d, $J = 18.3$ Hz, 1H), 2.40 (d, $J = 18.3$ Hz, 1H), 2.14 – 2.06 (m, 1H), 1.93 – 1.75 (m, 3H), 1.71 – 1.62 (m, 2H), 1.54 (ddd, $J = 13.7, 10.6, 6.4$ Hz, 1H), 1.31 – 1.25 (m, 1H), 1.25 (s, 3H), 1.24 – 1.16 (m, 2H), 0.97 (d, $J = 7.1$ Hz, 3H), 0.94 (d, $J = 7.3$ Hz, 3H), 0.93 (t, $J = 7.5$ Hz, 3H) ppm.

^{13}C NMR (126 MHz, CDCl_3): δ = 215.3, 165.5, 145.6, 134.3, 130.6, 129.0 (2C), 128.2 (2C), 117.8, 83.6, 82.7, 71.0, 48.5, 46.1, 43.7, 41.7, 31.1, 30.8, 23.6, 23.3, 18.1, 16.9, 14.5, 12.5 ppm.

IR (ATR): $\tilde{\nu}$ = 2959, 2932, 2874, 1754, 1713, 1636, 1450, 1333, 1303, 1280, 1253, 1202, 1166, 1134, 1101, 1079, 1019, 992, 767 cm^{-1} .

HRMS (ESI): m/z calcd. for $\text{C}_{25}\text{H}_{32}\text{O}_4\text{Na}$ $[\text{M} + \text{Na}]^+$: 419.2193, found: 419.2193.



Prepared according to GP6. Purification by column chromatography (silica gel, pentane/ Et_2O 4:1) afforded **138** (53.6 mg, 134 μmol , 99%) as a colorless oil.

$[\alpha]_{\text{D}}^{22} = -12.7^\circ$ ($c = 1.0$, CHCl_3).

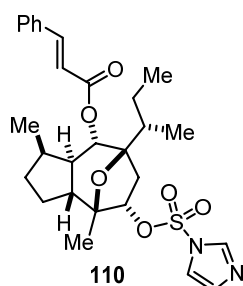
^1H NMR (500 MHz, CDCl_3): δ = 7.66 (d, $J = 16.0$ Hz, 1H), 7.55 – 7.51 (m, 2H), 7.42 – 7.34 (m, 3H), 6.41 (d, $J = 16.0$ Hz, 1H), 5.23 (d, $J = 10.2$ Hz, 1H), 4.20 (dd, $J = 11.0, 5.1$ Hz, 1H), 2.41 – 2.34 (m, 1H), 2.31 (dd, $J = 13.9, 11.1$ Hz, 1H), 2.18

– 2.11 (m, 2H), 1.99 – 1.91 (m, 1H), 1.90 – 1.80 (m, 3H), 1.74 – 1.62 (m, 2H), 1.46 (dtt, $J = 9.5, 6.9, 3.5$ Hz, 1H), 1.32 (s, 3H), 1.25 – 1.13 (m, 2H), 0.95 (d, $J = 7.1$ Hz, 3H), 0.91 (d, $J = 7.1$ Hz, 3H), 0.88 (t, $J = 7.4$ Hz, 3H) ppm.

^{13}C NMR (126 MHz, CDCl_3): δ = 165.9, 144.9, 134.5, 130.4, 129.0 (2C), 128.2 (2C), 118.5, 85.0, 81.5, 81.0, 72.6, 49.2, 46.4, 41.4, 40.4, 31.5, 31.3, 24.3, 23.9, 23.5, 17.0, 14.5, 12.8 ppm.

IR (ATR): $\tilde{\nu}$ = 3455, 2961, 2927, 2875, 1711, 1692, 1636, 1450, 1377, 1334, 1315, 1300, 1280, 1202, 1172, 1112, 1092, 1073, 1053, 1020, 987, 950, 895, 864, 767, 708, 683 cm^{-1} .

HRMS (ESI): m/z calcd. for $\text{C}_{25}\text{H}_{34}\text{O}_4\text{Na}$ $[\text{M} + \text{Na}]^+$: 421.2349, found: 421.2346.



Prepared according to GP7. Purification by column chromatography (silica gel, pentane/ Et_2O 2:1) afforded **110** (48.4 mg, 91.6 μmol , 68%) as a colorless oil.

$[\alpha]_{\text{D}}^{22} = -12.7^\circ$ ($c = 1.0$, CHCl_3).

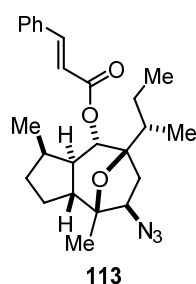
^1H NMR (500 MHz, CDCl_3): δ = 8.02 (s, 1H), 7.65 (d, $J = 16.0$ Hz, 1H), 7.57 – 7.53 (m, 2H), 7.44 – 7.35 (m, 4H), 7.24 (s, 1H), 6.38 (d, $J = 16.0$ Hz, 1H),

5.20 (d, $J = 10.1$ Hz, 1H), 4.60 (dd, $J = 10.7, 4.9$ Hz, 1H), 2.29 – 2.11 (m, 3H), 2.07 – 1.92 (m, 2H), 1.86 (td, $J = 12.7, 7.7$ Hz, 1H), 1.71 – 1.51 (m, 3H), 1.46 – 1.38 (m, 1H), 1.23 (dt, $J = 6.6, 2.3$ Hz, 1H), 1.18 (s, 3H), 1.16 – 1.09 (m, 1H), 0.94 (d, $J = 7.0$ Hz, 3H), 0.87 (d, $J = 7.3$ Hz, 3H), 0.86 (t, $J = 7.5$ Hz, 3H) ppm.

^{13}C NMR (126 MHz, CDCl_3): δ = 165.5, 145.5, 137.1, 134.2, 131.6, 130.5, 128.9 (2C), 128.2 (2C), 118.0, 117.8, 90.5, 85.5, 81.1, 71.2, 48.7, 46.4, 41.0, 36.6, 31.2, 31.1, 23.8, 23.7, 22.5, 16.7, 14.1 ppm.

IR (ATR): $\tilde{\nu}$ = 2925, 2855, 1655, 1496, 1439, 1409, 1387, 1255, 1202, 1092, 1062, 684, 659 cm^{-1} .

HRMS (ESI): m/z calcd. for $\text{C}_{28}\text{H}_{36}\text{N}_2\text{O}_6\text{SNa}$ [$\text{M} + \text{Na}$] $^{+}$: 551.2186, found: 551.2147.



Prepared according to GP8. Purification by column chromatography (silica gel, pentane/Et₂O 15:1) afforded **113** (35.9 mg, 84.8 μmol , 93%) as a colorless oil.

$[\alpha]_{\text{D}}^{20} = -32.4^{\circ}$ ($c = 1.0$, CHCl_3).

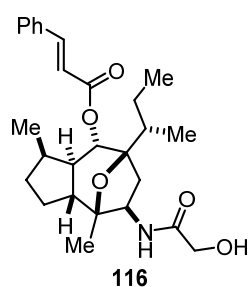
^1H NMR (500 MHz, CDCl_3): δ = 7.67 (d, $J = 16.0$ Hz, 1H), 7.55 – 7.51 (m, 2H), 7.41 – 7.37 (m, 3H), 6.39 (d, $J = 16.0$ Hz, 1H), 5.13 (d, $J = 10.3$ Hz, 1H), 3.66 (dd, $J = 8.4$, 3.5 Hz, 1H), 2.66 (dd, $J = 14.3$, 8.4 Hz, 1H), 2.15 – 2.08 (m, 1H), 1.96 –

1.86 (m, 2H), 1.82 – 1.69 (m, 3H), 1.59 (ddd, $J = 10.1$, 7.0, 2.8 Hz, 1H), 1.47 (ddd, $J = 13.1$, 10.2, 6.4 Hz, 1H), 1.32 (s, 3H), 1.27 – 1.17 (m, 2H), 1.09 (dd, $J = 11.4$, 7.1 Hz, 1H), 0.94 (d, $J = 7.3$ Hz, 3H), 0.94 (d, $J = 7.1$ Hz, 3H), 0.90 (t, $J = 7.4$ Hz, 3H) ppm.

^{13}C NMR (126 MHz, CDCl_3): δ = 165.6, 145.3, 134.4, 130.5, 129.0 (2C), 128.2 (2C), 118.1, 85.8, 85.7, 71.5, 63.4, 48.1, 47.1, 41.4, 39.7, 31.2, 31.0, 24.8, 24.4, 20.4, 17.0, 14.9, 12.7 ppm.

IR (ATR): $\tilde{\nu}$ = 2958, 2932, 2873, 2093, 1712, 1636, 1450, 1334, 1300, 1267, 1201, 1167, 1107, 1001, 959, 767 cm^{-1} .

HRMS (ESI): m/z calcd. for $\text{C}_{25}\text{H}_{33}\text{N}_3\text{O}_3\text{Na}$ [$\text{M} + \text{Na}$] $^{+}$: 446.2414, found: 446.2431.



Prepared according to GP9. Purification by column chromatography (silica gel, $\text{CH}_2\text{Cl}_2/\text{MeOH}$ 50:1) afforded **116** (7.2 mg, 15.8 μmol , 50%) as a colorless oil.

$[\alpha]_{\text{D}}^{24} = -26.3^{\circ}$ ($c = 0.4$, CHCl_3).

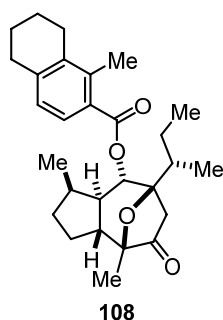
^1H NMR (700 MHz, CDCl_3): δ = 7.66 (d, $J = 15.9$ Hz, 1H), 7.55 – 7.52 (m, 2H), 7.41 – 7.37 (m, 3H), 6.49 (d, $J = 9.0$ Hz, 0H), 6.40 (d, $J = 15.9$ Hz, 1H), 5.15

(d, $J = 10.3$ Hz, 1H), 4.47 (td, $J = 9.3$, 4.1 Hz, 1H), 4.15 (d, $J = 15.6$ Hz, 1H), 4.14 (d, $J = 15.6$ Hz, 1H), 2.78 (dd, $J = 14.2$, 9.0 Hz, 1H), 2.16 – 2.11 (m, 1H), 1.99 – 1.92 (m, 1H), 1.83 – 1.77 (m, 1H), 1.76 – 1.69 (m, 2H), 1.68 – 1.62 (m, 2H), 1.56 – 1.53 (m, 1H), 1.51 (dd, $J = 14.2$, 3.8 Hz, 1H), 1.38 – 1.30 (m, 3H), 1.24 – 1.20 (m, 1H), 1.17 (s, 3H), 0.94 (d, $J = 7.1$ Hz, 3H), 0.92 (d, $J = 7.1$ Hz, 3H), 0.90 (t, $J = 7.4$ Hz, 3H) ppm.

^{13}C NMR (176 MHz, CDCl_3): δ = 170.3, 165.6, 145.2, 134.3, 130.4 (2C), 128.9 (2C), 128.2, 118.1, 85.4, 84.7, 71.6, 62.1, 50.7, 48.2, 46.8, 42.0, 41.7, 31.2, 31.0, 24.5, 24.4, 20.1, 16.9, 14.9, 12.7 ppm.

IR (ATR): $\tilde{\nu}$ = 3313, 2956, 2924, 2854, 2359, 2341, 1715, 1636, 1540, 1457, 1380, 1260, 1167, 1019, 798, 767, 690, 659 cm^{-1} .

HRMS (ESI): m/z calcd. for $C_{27}H_{37}NO_5Na$ $[M + Na]^+$: 478.2564, found: 478.2580.



Prepared according to GP1. Purification by column chromatography (silica gel, pentane/Et₂O 20:1) afforded **108** (68.8 mg, 157 μ mol, 99%) as a colorless oil.

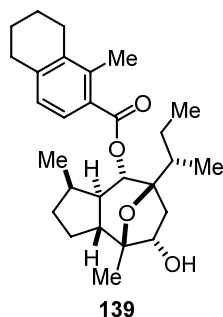
$[\alpha]_D^{22} = -12.4^\circ$ ($c = 1.0$, CHCl₃).

¹H NMR (500 MHz, CDCl₃): $\delta = 7.46$ (d, $J = 8.0$ Hz, 1H), 6.96 (d, $J = 8.0$ Hz, 1H), 5.50 (d, $J = 10.6$ Hz, 1H), 2.80 (t, $J = 6.3$ Hz, 2H), 2.69 – 2.64 (m, 3H), 2.42 (s, 3H), 2.18 – 2.09 (m, 1H), 1.95 – 1.57 (m, 12H), 1.36 – 1.28 (m, 1H), 1.27 (s, 3H), 1.24 – 1.17 (m, 2H), 0.99 (d, $J = 7.1$ Hz, 3H), 0.97 (d, $J = 7.2$ Hz, 2H), 0.92 (t, $J = 7.4$ Hz, 3H) ppm.

¹³C NMR (176 MHz, CDCl₃): $\delta = 215.4$, 167.0, 141.7, 138.3, 137.1, 128.2, 126.7, 126.7, 83.5, 82.8, 71.0, 48.6, 46.3, 43.6, 41.3, 31.3, 30.9, 30.7, 27.3, 23.6, 23.4 (2C), 22.4, 18.1, 17.0, 16.2, 14.4, 12.6 ppm.

IR (ATR): $\tilde{\nu} = 2930$, 2873, 1754, 1715, 1380, 1313, 1296, 1273, 1246, 1214, 1177, 1168, 1139, 1100, 1074, 1040, 1021, 968, 955, 783, 765, 737 cm⁻¹.

HRMS (ESI): m/z calcd. for $C_{28}H_{38}O_4Na$ $[M + Na]^+$: 461.2662, found: 461.2671.



Prepared according to GP6. Purification by column chromatography (silica gel, pentane/Et₂O 10:1) afforded **139** (48.7 mg, 110 μ mol, 84%) as a colorless oil.

$[\alpha]_D^{20} = -7.6^\circ$ ($c = 1.0$, CHCl₃).

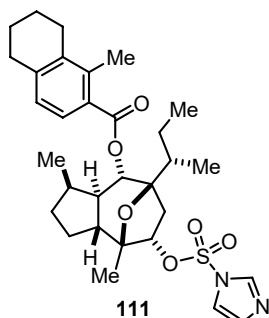
¹H NMR (500 MHz, CDCl₃): $\delta = 7.50$ (d, $J = 8.0$ Hz, 1H), 6.95 (d, $J = 8.0$ Hz, 1H), 5.34 (d, $J = 10.2$ Hz, 1H), 4.19 (dd, $J = 11.0$, 5.2 Hz, 1H), 2.80 (t, $J = 6.3$ Hz, 2H), 2.67 (t, $J = 6.4$ Hz, 2H), 2.43 (s, 3H), 2.29 (dd, $J = 13.8$, 11.0 Hz, 1H), 2.20

– 2.08 (m, 2H), 2.01 – 1.92 (m, 1H), 1.91 – 1.80 (m, 4H), 1.79 – 1.64 (m, 5H), 1.52 – 1.44 (m, 1H), 1.32 (s, 3H), 1.24 – 1.16 (m, 3H), 0.98 (d, $J = 7.1$ Hz, 3H), 0.93 (d, $J = 7.0$ Hz, 3H), 0.88 (t, $J = 7.4$ Hz, 3H) ppm.

¹³C NMR (126 MHz, CDCl₃): $\delta = 167.4$, 141.1, 138.0, 136.8, 128.9, 126.7, 126.5, 85.0, 81.4, 81.0, 72.7, 49.2, 46.4, 40.9, 40.2, 31.6, 31.3, 30.6, 27.2, 24.4, 23.8, 23.4, 23.4, 22.4, 17.0, 16.1, 14.3, 12.8 ppm.

IR (ATR): $\tilde{\nu} = 3463$, 2927, 2874, 1714, 1693, 1596, 1456, 1433, 1415, 1378, 1309, 1295, 1249, 1215, 1179, 1170, 1143, 1113, 1092, 1074, 1043, 1023, 988, 966, 949, 895, 837, 821, 768, 739 cm⁻¹.

HRMS (ESI): m/z calcd. for $C_{28}H_{40}O_4Na$ $[M + Na]^+$: 463.2819, found: 463.2834.



Prepared according to GP7. Purification by column chromatography (silica gel, pentane/Et₂O 5:1) afforded **111** (51.0 mg, 89.3 μmol, 88%) as a colorless oil.

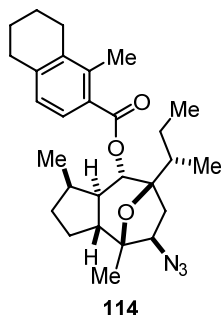
$$[\alpha]_{\text{D}}^{24} = -43.1^{\circ} (c = 1.0, \text{CHCl}_3).$$

¹H NMR (500 MHz, CDCl₃): δ = 8.01 (s, 1H), 7.46 – 7.38 (m, 1H), 7.35 (t, *J* = 1.4 Hz, 1H), 7.25 – 7.18 (m, 1H), 6.98 (d, *J* = 8.5 Hz, 1H), 5.30 (d, *J* = 9.7 Hz, 1H), 4.60 (dd, *J* = 10.6, 4.6 Hz, 1H), 2.81 (t, *J* = 6.2 Hz, 2H), 2.67 (t, *J* = 6.4 Hz, 2H), 2.40 (s, 3H), 2.28 – 2.12 (m, 3H), 2.11 – 2.04 (m, 1H), 2.02 – 1.93 (m, 1H), 1.92 – 1.82 (m, 3H), 1.79 – 1.72 (m, 2H), 1.72 – 1.64 (m, 1H), 1.63 – 1.54 (m, 2H), 1.48 – 1.40 (m, 1H), 1.30 – 1.20 (m, 2H), 1.19 (s, 3H), 0.96 (d, *J* = 6.9 Hz, 3H), 0.89 (d, *J* = 7.0 Hz, 3H), 0.86 (t, *J* = 7.5 Hz, 3H) ppm.

¹³C NMR (126 MHz, CDCl₃): δ = 167.0, 141.6, 138.2, 137.2, 137.1, 131.8, 128.2, 126.7, 126.7, 117.9, 90.5, 85.7, 81.2, 71.3, 48.9, 46.6, 40.7, 36.5, 31.4, 31.3, 30.7, 27.3, 24.1, 23.7, 23.4, 22.6, 22.4, 16.9, 16.2, 14.1, 12.7 ppm.

IR (ATR): $\tilde{\nu}$ = 2930, 2875, 1716, 1458, 1421, 1381, 1306, 1248, 1201, 1179, 1169, 1157, 1141, 1097, 1074, 1052, 1028, 995, 965, 948, 903, 868, 852, 767 cm⁻¹.

HRMS (ESI): *m/z* calcd. for C₃₁H₄₂N₂O₆Na [M + Na]⁺: 593.2656, found: 593.2659.



Prepared according to GP8. Purification by column chromatography (silica gel, pentane/Et₂O 40:1) afforded **114** (32.5 mg, 69.8 μmol, 83%) as a colorless oil.

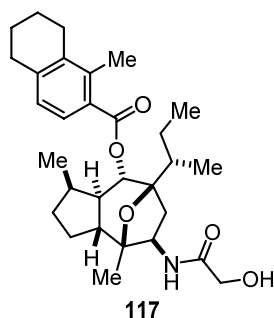
$$[\alpha]_{\text{D}}^{22} = -21.4^{\circ} (c = 1.0, \text{CHCl}_3).$$

¹H NMR (500 MHz, CDCl₃): δ = 7.47 (d, *J* = 8.0 Hz, 1H), 6.96 (d, *J* = 8.0 Hz, 1H), 5.24 (d, *J* = 10.3 Hz, 1H), 3.68 (dd, *J* = 8.4, 3.5 Hz, 1H), 2.80 (t, *J* = 6.3 Hz, 2H), 2.70 – 2.62 (m, 3H), 2.42 (s, 3H), 2.20 – 2.10 (m, 1H), 1.98 – 1.69 (m, 8H), 1.66 – 1.49 (m, 2H), 1.33 (s, 3H), 1.31 – 1.22 (m, 3H), 1.16 – 1.05 (m, 1H), 0.96 (d, *J* = 7.1 Hz, 3H), 0.95 (d, *J* = 7.1 Hz, 3H), 0.90 (t, *J* = 7.4 Hz, 3H) ppm.

¹³C NMR (126 MHz, CDCl₃): δ = 167.0, 141.4, 138.1, 137.0, 128.4, 126.6, 126.5, 85.8, 85.6, 71.5, 63.4, 48.2, 47.1, 40.9, 39.6, 31.2, 31.0, 30.6, 27.2, 24.8, 24.3, 23.4, 22.3, 20.3, 17.1, 16.1, 14.8, 12.7 ppm.

IR (ATR): $\tilde{\nu}$ = 2931, 2872, 2093, 1716, 1459, 1381, 1296, 1247, 1215, 1169, 1142, 1106, 1074, 1042, 970, 767 cm⁻¹.

HRMS (ESI): *m/z* calcd. for C₂₈H₃₉N₃O₃Na [M + Na]⁺: 488.2883, found: 488.2897.



Prepared according to GP9. Purification by column chromatography (silica gel, pentane/Et₂O 1:5 → Et₂O) afforded **117** (15.2 mg, 30.5 μmol, 44%) as a colorless oil.

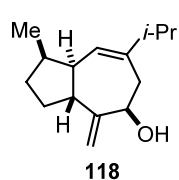
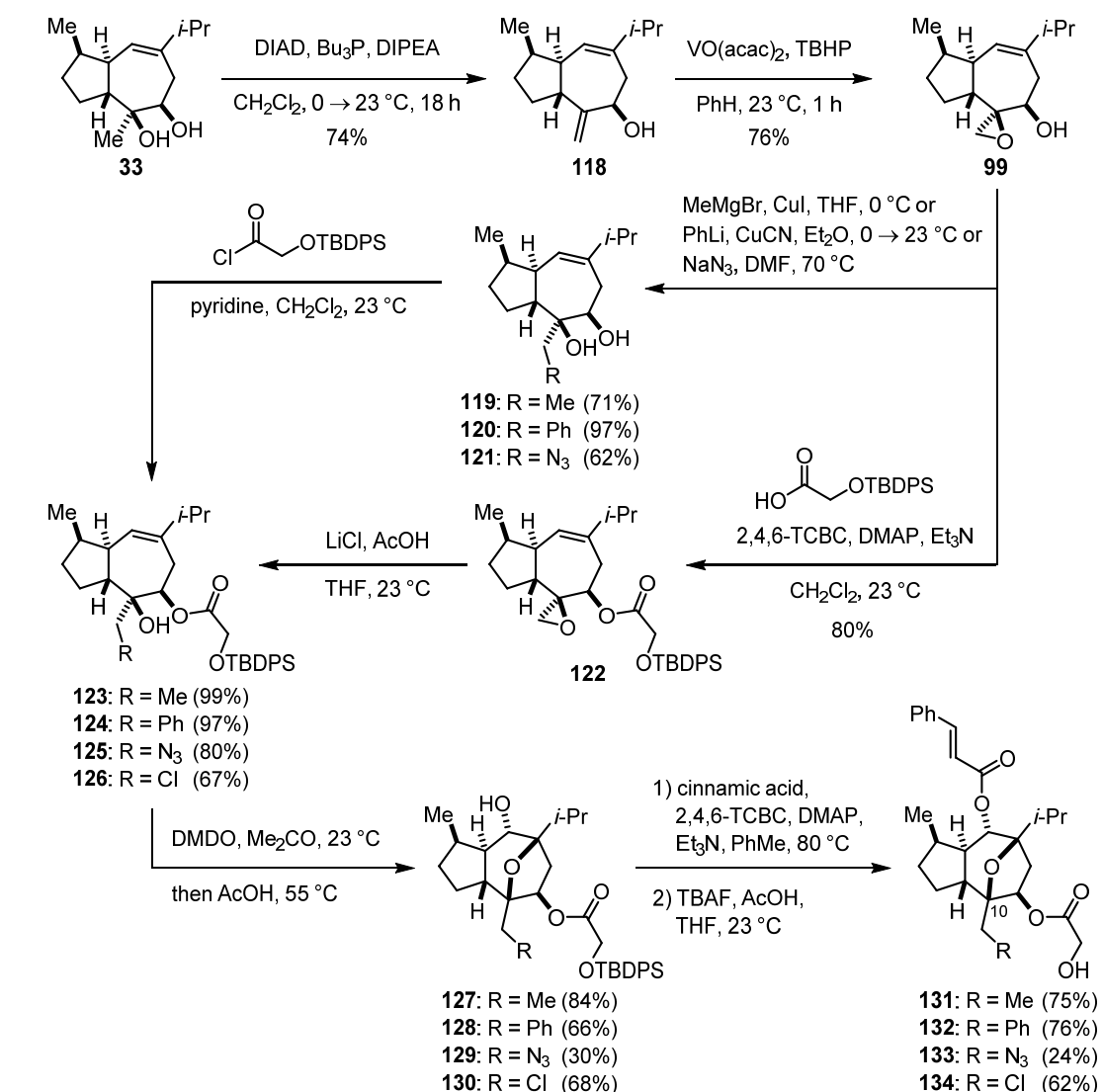
$[\alpha]_{\text{D}}^{24} = -22.4^{\circ}$ ($c = 0.5$, CHCl₃).

¹H NMR (700 MHz, CDCl₃): $\delta = 7.47$ (d, $J = 8.0$ Hz, 1H), 6.96 (d, $J = 8.1$ Hz, 1H), 6.53 (d, $J = 9.3$ Hz, 1H), 5.25 (d, $J = 10.2$ Hz, 1H), 4.47 (td, $J = 9.3$, 4.0 Hz, 1H), 4.15 (d, $J = 15.6$ Hz, 1H), 4.12 (d, $J = 15.6$ Hz, 1H), 2.80 (d, $J = 6.4$ Hz, 2H), 2.77 (dd, $J = 14.3$, 9.0 Hz, 1H), 2.67 (t, $J = 6.6$ Hz, 2H), 2.42 (s, 3H), 2.20 – 2.14 (m, 1H), 1.97 (dddd, $J = 13.9$, 11.2, 8.0, 2.9 Hz, 1H), 1.88 – 1.79 (m, 3H), 1.78 – 1.68 (m, 6H), 1.58 – 1.54 (m, 1H), 1.51 (dd, $J = 14.3$, 3.9 Hz, 1H), 1.38 – 1.32 (m, 1H), 1.31 – 1.26 (m, 2H), 1.18 (s, 3H), 0.96 (d, $J = 7.1$ Hz, 3H), 0.93 (d, $J = 7.1$ Hz, 3H), 0.90 (t, $J = 7.4$ Hz, 3H) ppm.

¹³C NMR (126 MHz, CDCl₃): $\delta = 170.3$, 167.1, 141.4, 138.1, 136.9, 128.5, 126.7, 126.6, 85.5, 84.7, 71.7, 62.1, 50.7, 48.3, 46.9, 41.6, 41.5, 31.3, 31.1, 30.6, 27.2, 24.6, 24.4, 23.4, 22.3, 20.1, 17.0, 16.1, 14.8, 12.7 ppm.

IR (ATR): $\tilde{\nu} = 3394$, 3313, 2931, 2873, 1716, 1655, 1596, 1535, 1458, 1382, 1296, 1247, 1215, 1169, 1142, 1105, 1075, 1042, 970, 767 cm⁻¹.

HRMS (ESI): m/z calcd. for C₃₀H₄₃NO₅Na [M + Na]⁺: 520.3033, found: 520.3043.



A solution of DIAD (22.7 μ L, 116 μ mol, 1.1 equiv.) in CH₂Cl₂ (0.5 mL) was added via syringe pump over 1 h to a stirred solution of diol **33** (25.0 mg, 105 μ mol, 1.0 equiv.), DIPEA (27 μ L, 0.16 mmol, 1.5 equiv.) and PBu₃ (40 μ L, 0.16 mmol, 1.5 equiv.) in CH₂Cl₂ (0.5 mL) at 0 °C. The mixture was stirred at 23 °C for 18 h and then concentrated under reduced pressure. The residue was purified by column chromatography (silica gel, pentane/Et₂O 20:1) to afford allylic alcohol **118** (17.0 mg, 77.1 μ mol, 74 %) as a colorless oil.

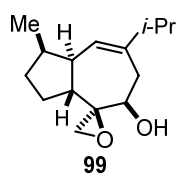
$[\alpha]_D^{22} = -78.0$ ($c = 0.33$, MeOH).

¹H NMR (700 MHz, CDCl₃): $\delta = 5.70$ (d, $J = 3.1$ Hz, 1H), 4.97 (s, 1H), 4.83 (s, 1H), 4.40 (d, $J = 8.4$ Hz, 1H), 2.61 – 2.51 (m, 2H), 2.31 – 2.18 (m, 4H), 1.94 – 1.88 (m, 1H), 1.88 – 1.82 (m, 1H), 1.75 – 1.68 (m, 1H), 1.35 – 1.30 (m, 1H), 1.02 (d, $J = 6.8$ Hz, 3H), 1.02 (d, $J = 6.8$ Hz, 3H), 0.95 (d, $J = 6.8$ Hz, 3H) ppm.

^{13}C NMR (176 MHz, CDCl_3): δ = 155.8, 142.7, 125.5, 107.2, 73.0, 48.3, 42.3, 37.8, 37.5, 36.7, 32.6, 27.5, 21.5 (2C), 17.3 ppm.

IR (ATR): $\tilde{\nu}$ = 3376, 2955, 2928, 2870, 1638, 1459, 1378, 1262, 1045, 898 cm^{-1} .

HRMS (ESI): m/z calcd. for $\text{C}_{15}\text{H}_{24}\text{NaO}$ [$\text{M} + \text{Na}$] $^+$: 243.1719, found: 243.1720.



99

To a solution of alkene **118** (121 mg, 549 μmol , 1.0 equiv.) in benzene (5.5 mL) was added vanadyl acetylacetonate (29.0 mg, 110 μmol , 20 mol%) at 23 $^\circ\text{C}$. After 10 min, *tert*-butyl hydroperoxide (5.5 M in decane, 100 μL , 550 μmol , 1.0 equiv.) was added and stirring was continued for another 45 min at 23 $^\circ\text{C}$.

Saturated aqueous NaHCO_3 -solution was added and the aqueous phase was extracted with Et_2O (3 x 20 mL). The combined organic phases were dried over Na_2SO_4 and concentrated under reduced pressure. Purification by column chromatography (silica gel, pentane/ Et_2O 3:1) afforded epoxide **99** (98.5 mg, 417 μmol , 76%) as a colorless oil.

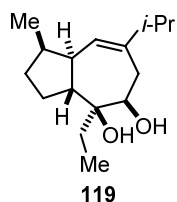
$[\alpha]_{\text{D}}^{18} = -40.7$ ($c = 0.44$, CHCl_3).

^1H NMR (500 MHz, CDCl_3): δ = 5.70 (dt, $J = 3.8, 1.4$ Hz, 1H), 3.56 (td, $J = 7.8, 1.6$ Hz, 1H), 2.87 (d, $J = 3.9$ Hz, 1H), 2.65 (dd, $J = 4.0, 0.9$ Hz, 1H), 2.53 (ddd, $J = 15.4, 8.0, 1.2$ Hz, 2H), 2.39 – 2.17 (m, 4H), 1.97 (d, $J = 7.6$ Hz, 1H), 1.72 – 1.59 (m, 2H), 1.44 – 1.35 (m, 1H), 1.21 – 1.14 (m, 1H), 1.02 (d, $J = 6.9$ Hz, 3H), 1.01 (d, $J = 6.8$ Hz, 3H), 0.92 (d, $J = 7.1$ Hz, 3H) ppm.

^{13}C NMR (126 MHz, CDCl_3): δ = 142.6, 124.9, 72.4, 64.8, 48.0, 46.2, 38.7, 37.5, 37.3, 34.5, 33.2, 22.7, 21.5, 21.5, 15.5 ppm.

IR (ATR): $\tilde{\nu}$ = 3471, 2956, 2870, 1463, 1381, 1077, 1048, 926, 821, 792 cm^{-1} .

HRMS (ESI): m/z calcd. for $\text{C}_{15}\text{H}_{24}\text{NaO}_2$ [$\text{M} + \text{Na}$] $^+$: 259.1668, found: 259.1689.



119

To a solution epoxide **99** (20.5 mg, 86.7 μmol , 1.0 equiv.) was added copper(I) iodide (16.5 mg, 86.7 μmol , 1.0 equiv.) at 0 $^\circ\text{C}$. After stirring for 10 min, methylmagnesium bromide (3 M in Et_2O , 145 μmol , 434 μmol , 5.0 equiv.) was added at 0 $^\circ\text{C}$ and stirring was continued at the same temperature for 3.5 h.

Saturated aqueous NH_4Cl -solution (10 mL) was added and the aqueous phase was extracted with Et_2O (3 x 10 mL). The combined organic phases were washed with brine (10 mL), dried over Na_2SO_4 and concentrated under reduced pressure. Purification by column chromatography (silica gel, pentane/ Et_2O 3:1) afforded diol **119** (15.5 mg, 61.6 μmol , 71%) as a colorless oil.

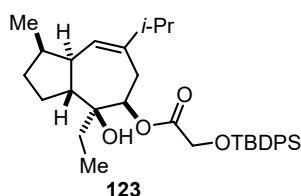
$[\alpha]_{\text{D}}^{22} = -22.4$ ($c = 0.74$, CHCl_3).

^1H NMR (400 MHz, CDCl_3): δ = 5.66 (s, 1H), 3.80 (t, J = 7.8 Hz, 1H), 2.47 (dd, J = 14.9, 8.3 Hz, 1H), 2.37 – 2.15 (m, 5H), 2.02 (ddd, J = 11.1, 9.8, 6.9 Hz, 1H), 1.86 – 1.58 (m, 6H), 1.42 – 1.34 (m, 1H), 1.00 (d, J = 6.8 Hz, 3H), 1.00 (d, J = 6.9 Hz, 3H), 0.97 (t, J = 7.5 Hz, 3H), 0.89 (d, J = 7.0 Hz, 3H) ppm.

^{13}C NMR (176 MHz, CDCl_3): δ = 141.8, 126.4, 70.8, 46.2, 42.8, 37.5, 37.3, 33.1, 32.0, 29.7, 23.7, 23.6, 21.5, 21.4, 15.4, 7.3 ppm.

IR (ATR): $\tilde{\nu}$ = 3329, 2959, 2929, 2869, 1463, 1379, 1362, 1053, 1012, 928 cm^{-1} .

HRMS (ESI): m/z calcd. for $\text{C}_{16}\text{H}_{28}\text{NaO}_2$ [$\text{M} + \text{Na}$] $^+$: 275.1981, found: 275.1987.



Prepared according to GP4. Purification by column chromatography (silica gel, pentane/ Et_2O 10:1) afforded ester **123** (37.8 mg, 68.9 μmol , quant) as a colorless oil.

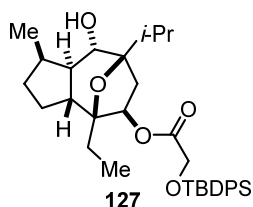
$[\alpha]_{\text{D}}^{18} = -26.4$ (c = 1.89, CHCl_3).

^1H NMR (500 MHz, CDCl_3): δ = 7.71 – 7.67 (m, 4H), 7.43 – 7.37 (m, 6H), 5.53 (s, 1H), 5.10 (d, J = 8.5 Hz, 1H), 4.29 – 4.22 (m, 2H), 2.63 (dd, J = 16.1, 8.6 Hz, 1H), 2.40 – 2.33 (m, 1H), 2.25 – 2.09 (m, 3H), 2.03 (d, J = 16.1 Hz, 1H), 1.81 – 1.59 (m, 6H), 1.39 – 1.31 (m, 1H), 1.09 (s, 9H), 0.93 (t, J = 7.6 Hz, 3H), 0.91 (d, J = 6.8 Hz, 3H), 0.89 (d, J = 6.8 Hz, 3H), 0.84 (d, J = 7.5 Hz, 3H) ppm.

^{13}C NMR (176 MHz, CDCl_3): δ = 170.8, 142.1, 135.6 (4C), 134.9, 130.1, 129.7, 128.0 (2C), 128.0 (2C), 127.8, 125.1, 75.2, 62.6, 46.4, 43.0, 37.7, 37.4, 33.1, 29.6, 26.7 (3C), 26.6, 25.0, 23.8, 21.4, 21.3, 19.3, 15.4, 7.7 ppm.

IR (ATR): $\tilde{\nu}$ = 3486, 2957, 2931, 2857, 1758, 1738, 1462, 1428, 1139, 1112 cm^{-1} .

HRMS (ESI): m/z calcd. for $\text{C}_{34}\text{H}_{48}\text{O}_4\text{SiNa}$ [$\text{M} + \text{Na}$] $^+$: 571.3214, found: 571.3235.



Prepared according to GP3. Purification by column chromatography (silica gel, pentane/ Et_2O 4:1) afforded alcohol **127** (25.0 mg, 44.3 μmol , 84%) as a colorless oil.

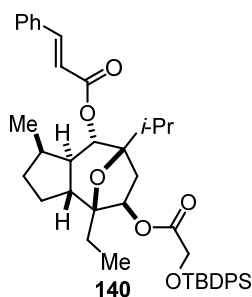
$[\alpha]_{\text{D}}^{23} = -29.9$ (c = 1.25, CHCl_3).

^1H NMR (700 MHz, CDCl_3): δ = 7.69 (d, J = 7.2 Hz, 4H), 7.46 – 7.36 (m, 6H), 5.10 (dd, J = 8.1, 3.0 Hz, 1H), 4.25 (d, J = 16.8 Hz, 1H), 4.23 (d, J = 16.8 Hz, 1H), 3.60 (d, J = 10.2 Hz, 1H), 2.40 (dd, J = 14.5, 8.0 Hz, 1H), 2.32 (tt, J = 6.8, 6.2 Hz, 1H), 2.03 – 1.97 (m, 1H), 1.94 (hept, J = 6.9 Hz, 1H), 1.71 – 1.63 (m, 2H), 1.59 – 1.55 (m, 2H), 1.34 – 1.27 (m, 2H), 1.26 (s, 1H), 1.24 – 1.18 (m, 2H), 1.09 (s, 9H), 1.02 (d, J = 7.0 Hz, 3H), 1.00 (d, J = 6.7 Hz, 3H), 0.89 (d, J = 7.2 Hz, 3H), 0.86 (t, J = 7.5 Hz, 3H) ppm.

^{13}C NMR (176 MHz, CDCl_3): $\delta = 170.9, 135.6$ (2C), 135.6 (2C), $132.8, 132.8, 129.9$ (2C), 127.8 (2C), 127.8 (2C), $85.9, 85.4, 76.0, 70.7, 62.3, 47.8, 44.1, 38.5, 32.2, 31.4, 30.4, 26.7$ (3C), $25.2, 25.1, 19.2, 18.3, 17.4, 16.9, 8.2$ ppm.

IR (ATR): $\tilde{\nu} = 3525, 2957, 2933, 2859, 1759, 1463, 1428, 1382, 1363, 1294, 1210, 1142, 1114, 1052, 1023, 1003, 935, 823, 741, 702$ cm^{-1} .

HRMS (ESI): m/z calcd. for $\text{C}_{34}\text{H}_{48}\text{O}_5\text{SiNa}$ $[\text{M} + \text{Na}]^+$: 587.3163, found: 587.3183.



Prepared according to GP1. Purification by column chromatography (silica gel, pentane/ Et_2O 20:1) afforded ester **140** (12.7 mg, 18.3 μmol , 82%) as a colorless oil.

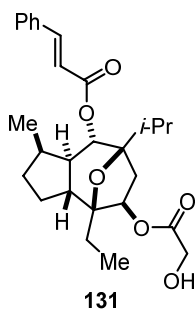
$[\alpha]_{\text{D}}^{20} = -21.4$ ($c = 0.64, \text{CHCl}_3$).

^1H NMR (700 MHz, CDCl_3): $\delta = 7.71 - 7.69$ (m, 4H), 7.66 (d, $J = 16.0$ Hz, 1H), 7.54 - 7.52 (m, 2H), 7.46 - 7.36 (m, 9H), 6.39 (d, $J = 16.0$ Hz, 1H), 5.17 (dd, $J = 8.0, 3.2$ Hz, 1H), 5.08 (d, $J = 10.3$ Hz, 1H), 4.26 (d, 1H), 4.25 (d, $J = 16.8$ Hz, 1H), 2.62 (dd, $J = 14.5, 8.0$ Hz, 1H), 2.13 (tt, $J = 7.6, 7.0$ Hz, 1H), 1.97 - 1.90 (m, 1H), 1.89 - 1.81 (m, 2H), 1.74 - 1.69 (m, 1H), 1.67 (dd, $J = 14.7, 3.4$ Hz, 1H), 1.62 (dd, $J = 14.3, 7.3$ Hz, 1H), 1.59 - 1.53 (m, 2H), 1.36 - 1.23 (m, 2H), 1.10 (s, 9H), 0.97 (d, $J = 6.7$ Hz, 3H), 0.94 (d, $J = 7.2$ Hz, 3H), 0.94 (d, $J = 6.9$ Hz, 3H), 0.90 (t, $J = 7.5$ Hz, 3H) ppm.

^{13}C NMR (176 MHz, CDCl_3): $\delta = 171.0, 165.7, 145.1, 135.6$ (2C), 135.6 (2C), $134.3, 132.8, 132.8, 130.4, 129.9$ (2C), 128.9 (2C), 128.1 (2C), 127.8 (2C), 127.8 (2C), $118.1, 86.1, 85.1, 75.9, 71.4, 62.3, 46.7, 43.6, 39.9, 33.0, 31.1, 29.7, 26.7$ (2C), $25.1, 24.2, 19.3, 18.2, 17.5, 16.9, 8.2$ ppm.

IR (ATR): $\tilde{\nu} = 2956, 2931, 2857, 1760, 1713, 1636, 1463, 1449, 1428, 1333, 1300, 1281, 1202, 1168, 1142, 1114, 1017, 975, 823, 767, 741, 703$ cm^{-1} .

HRMS (ESI): m/z calcd. for $\text{C}_{43}\text{H}_{54}\text{O}_6\text{SiNa}$ $[\text{M} + \text{Na}]^+$: 717.3582, found: 717.3603.



Prepared according to GP2. Purification by column chromatography (silica gel, pentane/ Et_2O 2:1) afforded product **131** (7.6 mg, 17 μmol , 91%) as a colorless oil.

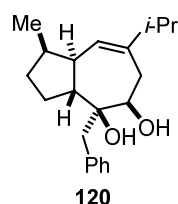
$[\alpha]_{\text{D}}^{21} = -48.2$ ($c = 0.38, \text{CHCl}_3$).

^1H NMR (700 MHz, CDCl_3): $\delta = 7.67$ (d, $J = 15.9$ Hz, 1H), 7.56 - 7.51 (m, 2H), 7.41 - 7.37 (m, 3H), 6.39 (d, $J = 16.0$ Hz, 1H), 5.25 (dd, $J = 8.1, 2.9$ Hz, 1H), 5.11 (d, $J = 10.3$ Hz, 1H), 4.19 (s, 2H), 2.69 (dd, $J = 14.4, 7.9$ Hz, 1H), 2.35 (s, 1H), 2.15 (dq, $J = 14.8, 7.5$ Hz, 1H), 2.01 - 1.83 (m, 3H), 1.80 - 1.65 (m, 3H), 1.43 (dq, $J = 14.8, 7.5$ Hz, 1H), 1.31 - 1.20

(m, 3H), 1.01 (d, $J = 6.8$ Hz, 3H), 0.97 (t, $J = 7.6$ Hz, 3H), 0.97 (d, $J = 7.2$ Hz, 3H), 0.95 (d, $J = 7.1$ Hz, 3H) ppm.

^{13}C NMR (176 MHz, CDCl_3): $\delta = 173.1, 165.7, 145.2, 134.3, 130.4, 128.9$ (2C), 128.1 (2C), $118.0, 86.1, 85.2, 71.2, 60.7, 46.8, 43.5, 40.0, 33.2, 31.1, 31.0, 25.1, 24.2$ (2C), $18.2, 17.5, 16.9, 8.2$ ppm.
IR (ATR): $\tilde{\nu} = 3467, 2961, 2879, 1745, 1712, 1636, 1449, 1384, 1334, 1301, 1279, 1202, 1170, 1096, 1016, 929, 767, 709, 684, 667$ cm^{-1} .

HRMS (ESI): m/z calcd. for $\text{C}_{27}\text{H}_{36}\text{O}_6\text{Na}$ [$\text{M} + \text{Na}$] $^+$: 479.2404, found: 479.2426.



To a solution of copper(I) cyanide (10.5 mg, 117 μmol , 4.0 equiv.) in Et_2O (0.4 mL) was added phenyl lithium (1.9 M in dibutyl ether, 0.12 mL, 230 μmol , 8.0 equiv.) dropwise at -78 $^\circ\text{C}$. After stirring for 10 min at the same temperature, a solution of epoxide **99** (6.9 mg, 29 μmol , 1.0 equiv.) in Et_2O (0.4 mL) was added. The reaction mixture was warmed to 0 $^\circ\text{C}$ for 30 min and stirred at 23 $^\circ\text{C}$ for 18 h. Saturated aqueous NH_4Cl -solution (10 mL) was added and the aqueous phase was extracted with Et_2O (3 x 10 mL). The combined organic phases were dried over Na_2SO_4 and the solvent was removed under reduced pressure. Purification by column chromatography (silica gel, pentane/ Et_2O 3:1) afforded diol **120** (8.9 mg, 28 μmol , 97%) as a colorless oil.

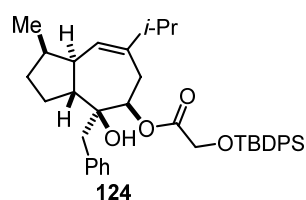
$[\alpha]_{\text{D}}^{21} = +45.4$ ($c = 0.57, \text{CHCl}_3$).

^1H NMR (700 MHz, CDCl_3): $\delta = 7.35 - 7.29$ (m, 4H), $7.26 - 7.23$ (m, 1H), 5.62 (d, $J = 3.2$ Hz, 1H), 3.64 (t, $J = 7.8$ Hz, 1H), 3.07 (d, $J = 13.9$ Hz, 1H), 2.87 (d, $J = 13.9$ Hz, 1H), 2.66 (s, 1H), 2.47 (ddd, $J = 15.8, 8.9, 1.9$ Hz, 1H), $2.44 - 2.39$ (m, 1H), $2.29 - 2.17$ (m, 4H), $1.97 - 1.86$ (m, 2H), $1.73 - 1.67$ (m, 1H), $1.46 - 1.42$ (m, 1H), 1.33 (d, $J = 7.1$ Hz, 1H), 1.00 (d, $J = 7.2$ Hz, 3H), 0.99 (d, $J = 7.2$ Hz, 3H), 0.91 (d, $J = 7.1$ Hz, 3H) ppm.

^{13}C NMR (176 MHz, CDCl_3): $\delta = 142.7, 137.4, 130.6$ (2C), 128.5 (2C), $126.6, 125.6, 77.4, 72.0, 46.5, 43.2, 38.0, 37.7, 37.3, 33.3, 32.2, 24.2, 21.5, 21.4, 15.3$ ppm.

IR (ATR): $\tilde{\nu} = 3548, 3451, 2955, 2927, 2869, 1495, 1453, 1379, 1290, 1078, 1033, 802, 701$ cm^{-1} .

HRMS (ESI): m/z calcd. for $\text{C}_{21}\text{H}_{30}\text{O}_2\text{Na}$ [$\text{M} + \text{Na}$] $^+$: 337.2138, found: 337.2155.



Prepared according to GP4. Purification by column chromatography (silica gel, pentane/ Et_2O 20:1) afforded ester **124** (21.6 mg, 35.4 μmol , 97%) as a colorless oil.

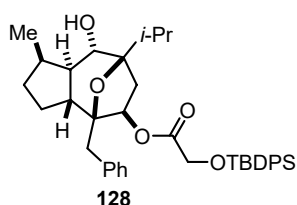
$[\alpha]_{\text{D}}^{21} = -24.1$ ($c = 1.08, \text{CHCl}_3$).

^1H NMR (500 MHz, CDCl_3): δ = 7.64 – 7.60 (m, 4H), 7.45 – 7.41 (m, 2H), 7.40 – 7.34 (m, 6H), 7.21 – 7.19 (m, 3H), 5.52 (d, J = 1.7 Hz, 1H), 4.91 (dd, J = 9.4, 1.3 Hz, 1H), 3.80 (d, J = 16.4 Hz, 1H), 3.62 (d, J = 16.4 Hz, 1H), 3.01 (d, J = 13.8 Hz, 1H), 2.85 (d, J = 13.8 Hz, 1H), 2.62 (ddd, J = 16.1, 9.4, 1.9 Hz, 1H), 2.51 – 2.35 (m, 2H), 2.30 – 2.20 (m, 2H), 2.16 (hept, J = 6.8 Hz, 1H), 1.98 (d, J = 16.1 Hz, 1H), 1.94 – 1.88 (m, 2H), 1.71 – 1.62 (m, 1H), 1.46 – 1.39 (m, 1H), 1.04 (s, 9H), 0.94 (d, J = 6.9 Hz, 3H), 0.92 (d, J = 6.8 Hz, 3H), 0.86 (d, J = 7.1 Hz, 3H) ppm.

^{13}C NMR (126 MHz, CDCl_3): δ = 170.1, 142.7, 137.0, 135.6 (2C), 135.6 (2C), 135.4, 132.9, 132.8, 130.3 (2C), 130.0 (2C), 128.5 (2C), 127.9, 127.9 (2C), 126.5, 124.9, 76.7, 76.3, 62.0, 46.2, 43.4, 39.0, 38.0, 37.3, 33.3, 30.5, 26.7 (3C), 24.2, 21.6, 21.3, 19.2, 15.2 ppm.

IR (ATR): $\tilde{\nu}$ = 3573, 2957, 2931, 2858, 1760, 1428, 1141, 1114, 823, 740, 702 cm^{-1} .

HRMS (ESI): m/z calcd. for $\text{C}_{39}\text{H}_{50}\text{O}_4\text{SiNa}$ [$\text{M} + \text{Na}$] $^+$: 633.3370, found: 633.3356.



Prepared according to GP3. Purification by column chromatography (silica gel, pentane/ Et_2O 5:1) afforded alcohol **128** (14.3 mg, 22.8 μmol , 66%) as a colorless oil.

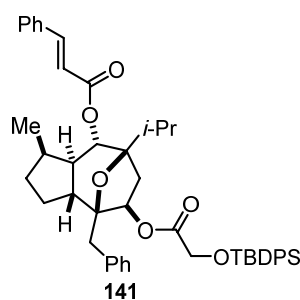
$[\alpha]_{\text{D}}^{22} = -13.2$ (c = 0.72, CHCl_3).

^1H NMR (700 MHz, CDCl_3): δ = 7.70 – 7.68 (m, 4H), 7.43 – 7.39 (m, 2H), 7.39 – 7.35 (m, 4H), 7.25 – 7.21 (m, 4H), 7.19 – 7.17 (m, 1H), 5.23 (dd, J = 7.9, 3.0 Hz, 1H), 4.27 (s, 1H), 4.26 (s, 1H), 3.48 (d, J = 9.6 Hz, 1H), 2.98 (d, J = 14.3 Hz, 1H), 2.44 (dd, J = 14.4, 8.0 Hz, 1H), 2.41 (d, J = 14.4 Hz, 1H), 2.27 – 2.21 (m, 1H), 2.00 (hept, J = 6.9 Hz, 1H), 1.96 – 1.90 (m, 1H), 1.64 (dd, J = 14.6, 2.8 Hz, 1H), 1.69 – 1.62 (m, 1H), 1.32 – 1.28 (m, 2H), 1.27 – 1.19 (m, 2H), 1.10 (s, 9H), 1.08 – 1.02 (m, 1H), 1.06 (d, J = 6.7 Hz, 3H), 1.05 (d, J = 6.9 Hz, 3H), 0.67 (d, J = 7.2 Hz, 3H) ppm.

^{13}C NMR (176 MHz, CDCl_3): δ = 171.0, 137.7, 135.6 (6C), 132.8, 130.5 (2C), 129.9, 127.8 (2C), 127.8 (2C), 127.7 (2C), 126.0, 85.9, 85.8, 76.3, 70.3, 62.3, 47.9, 43.4, 38.4, 38.3, 31.8, 31.1, 30.3, 26.7 (3C), 25.1, 19.3, 18.3, 17.5, 16.7 ppm.

IR (ATR): $\tilde{\nu}$ = 3374, 2955, 2917, 2871, 2849, 1737, 1467, 1378, 1196, 1181, 740 cm^{-1} .

HRMS (ESI): m/z calcd. for $\text{C}_{39}\text{H}_{50}\text{O}_5\text{SiNa}$ [$\text{M} + \text{Na}$] $^+$: 649.3320, found: 659.3297.



Prepared according to GP1. Purification by column chromatography (silica gel, pentane/Et₂O 15:1) afforded ester **141** (15.5 mg, 20.5 μmol, 90%) as a colorless oil.

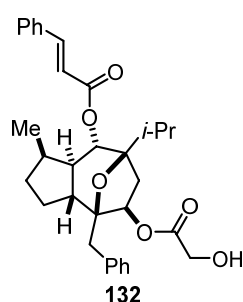
$[\alpha]_{\text{D}}^{22} = -8.1$ ($c = 0.78$, CHCl₃).

¹H NMR (700 MHz, CDCl₃): $\delta = 7.70$ (d, $J = 6.4$ Hz, 4H), 7.65 (d, $J = 16.0$ Hz, 1H), 7.53 – 7.51 (m, 2H), 7.44 – 7.40 (m, 2H), 7.40 – 7.36 (m, 7H), 7.27 – 7.22 (m, 4H), 7.22 – 7.19 (m, 1H), 6.38 (d, $J = 15.9$ Hz, 1H), 5.30 (dd, $J = 7.9$, 3.1 Hz, 1H), 4.97 (d, $J = 10.2$ Hz, 1H), 4.30 (s, 1H), 4.29 (s, 1H), 3.03 (d, $J = 14.2$ Hz, 1H), 2.65 (dd, $J = 14.3$, 7.9 Hz, 1H), 2.44 (d, $J = 14.3$ Hz, 1H), 2.11 – 1.99 (m, 1H), 1.96 – 1.80 (m, 2H), 1.76 (dd, $J = 14.3$, 3.1 Hz, 1H), 1.71 – 1.65 (m, 1H), 1.58 – 1.52 (m, 2H), 1.48 (ddd, $J = 13.4$, 11.6, 7.0 Hz, 1H), 1.30 – 1.26 (m, 1H), 1.11 (s, 9H), 1.03 (d, $J = 6.8$ Hz, 3H), 0.98 (d, $J = 7.0$ Hz, 3H), 0.70 (d, $J = 7.1$ Hz, 3H) ppm.

¹³C NMR (176 MHz, CDCl₃): $\delta = 171.1$, 165.7, 145.1, 137.4, 135.6 (4C), 134.3, 132.8, 132.7, 130.4 (2C), 130.4, 130.0, 130.0, 128.9 (2C), 128.1 (2C), 127.8 (4C), 127.8 (2C), 126.1, 118.1, 86.1, 85.5, 76.2, 71.2, 62.3, 46.8, 43.0, 39.8, 38.3, 32.8, 30.9, 30.9, 26.7 (3C), 24.2, 19.3, 18.2, 17.6, 16.7 ppm.

IR (ATR): $\tilde{\nu} = 2955$, 2917, 2871, 2849, 1736, 1466, 1378, 1198, 1180, 1115, 737, 702 cm⁻¹.

HRMS (ESI): m/z calcd. for C₄₈H₅₆O₆SiNa [M + Na]⁺: 779.3738, found: 779.3704.



Prepared according to GP2. Purification by column chromatography (silica gel, pentane/Et₂O 2:1) afforded product **132** (8.9 mg, 17 μmol, 84%) as a colorless oil.

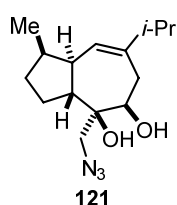
$[\alpha]_{\text{D}}^{22} = -20.4$ ($c = 0.44$, CHCl₃).

¹H NMR (700 MHz, CDCl₃): $\delta = 7.65$ (d, $J = 15.9$ Hz, 1H), 7.54 – 7.51 (m, 2H), 7.40 – 7.38 (m, 3H), 7.31 – 7.29 (m, 2H), 7.29 – 7.26 (m, 2H), 7.24 – 7.21 (m, 1H), 6.38 (d, $J = 16.0$ Hz, 1H), 5.38 (dd, $J = 7.9$, 3.1 Hz, 1H), 5.01 (d, $J = 9.7$ Hz, 1H), 4.20 (t, $J = 4.5$ Hz, 2H), 3.11 (d, $J = 14.2$ Hz, 1H), 2.71 (dd, $J = 14.4$, 7.9 Hz, 1H), 2.55 (d, $J = 14.3$ Hz, 1H), 2.33 (t, $J = 5.6$ Hz, 1H), 2.07 (ddd, $J = 7.0$, 7.0, 6.7 Hz, 1H), 1.94 (hept, $J = 7.0$ Hz, 1H), 1.89 (dddd, $J = 13.9$, 11.2, 8.0, 2.9 Hz, 1H), 1.84 (dd, $J = 14.4$, 3.1 Hz, 1H), 1.71 (dddd, $J = 12.4$, 9.4, 6.6, 3.1 Hz, 1H), 1.59 – 1.50 (m, 2H), 1.30 – 1.25 (m, 1H), 1.15 – 1.09 (m, 1H), 1.07 (d, $J = 6.8$ Hz, 3H), 1.01 (d, $J = 7.0$ Hz, 3H), 0.72 (d, $J = 7.1$ Hz, 3H) ppm.

^{13}C NMR (176 MHz, CDCl_3): δ = 173.2, 165.6, 145.2, 137.1, 134.3, 130.4, 130.4 (2C), 128.9 (2C), 128.1 (2C), 127.9 (2C), 126.3, 117.9, 86.1, 85.7, 77.3, 71.0, 60.7, 46.8, 43.2, 39.9, 38.5, 32.9, 30.9, 30.8, 24.2, 18.3, 17.6, 16.7 ppm.

IR (ATR): $\tilde{\nu}$ = 3474, 2959, 2934, 2875, 1712, 1636, 1449, 1334, 1300, 1280, 1202, 1169, 1092, 1002, 767, 700 cm^{-1} .

HRMS (ESI): m/z calcd. for $\text{C}_{32}\text{H}_{38}\text{O}_6\text{Na}$ $[\text{M} + \text{Na}]^+$: 541.2560, found: 541.2567.



To a solution of epoxide **99** (13.6 mg, 57.6 μmol , 1.0 equiv.) in DMF (0.6 mL) was added NaN_3 (37.4 mg, 576 μmol , 10.0 equiv.) and the resulting mixture was stirred at 80 $^\circ\text{C}$ for 18 h. H_2O was added and the aqueous phase was extracted with Et_2O (3 x 10 mL). The combined organic phases were washed with brine, dried over Na_2SO_4 and concentrated under reduced pressure. Purification by column chromatography (silica gel, pentane/ Et_2O 3:1) afforded diol **121** (10.0 mg, 35.8 μmol , 62%) as a colorless oil.

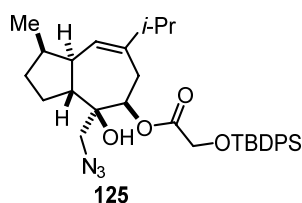
$[\alpha]_{\text{D}}^{23} = -18.3$ ($c = 0.5$, CHCl_3).

^1H NMR (700 MHz, CDCl_3): δ = 5.48 (s, 1H), 3.88 (ddd, $J = 9.9, 6.1, 1.5$ Hz, 1H), 3.67 (d, $J = 12.5$ Hz, 1H), 3.54 (d, $J = 12.5$ Hz, 1H), 3.00 (s, 1H), 2.62 (dddd, $J = 16.3, 9.7, 2.8, 1.3$ Hz, 1H), 2.47 (d, $J = 6.3$ Hz, 1H), 2.35 – 2.30 (m, 1H), 2.24 (hept, $J = 6.8$ Hz, 1H), 2.21 – 2.16 (m, 2H), 2.02 (d, $J = 16.5$ Hz, 1H), 1.93 – 1.86 (m, 1H), 1.70 – 1.62 (m, 2H), 1.39 – 1.34 (m, 1H), 1.00 (d, $J = 6.7$ Hz, 3H), 0.99 (d, $J = 6.7$ Hz, 3H), 0.84 (d, $J = 7.1$ Hz, 3H) ppm.

^{13}C NMR (176 MHz, CDCl_3): δ = 143.2, 124.8, 76.0, 72.4, 54.9, 46.1, 43.0, 37.5, 37.3, 33.0, 32.6, 24.0, 21.6, 21.3, 15.3 ppm.

IR (ATR): $\tilde{\nu}$ = 3335, 2957, 2868, 2102, 1463, 1282, 1079, 1038, 1005, 931 cm^{-1} .

HRMS (ESI): m/z calcd. for $\text{C}_{15}\text{H}_{25}\text{N}_3\text{O}_2\text{Na}$ $[\text{M} + \text{Na}]^+$: 302.1839, found: 302.1832.



Prepared according to GP4. Purification by column chromatography (silica gel, pentane/ Et_2O 10:1) afforded ester **125** (16.3 mg, 29.2 μmol , 80%) as a colorless oil.

$[\alpha]_{\text{D}}^{24} = -22.4$ ($c = 0.8$, CHCl_3).

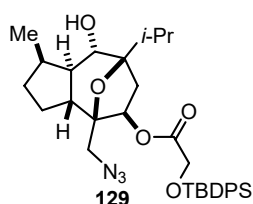
^1H NMR (700 MHz, CDCl_3): δ = 7.73 – 7.70 (m, 4H), 7.45 – 7.39 (m, 6H), 5.51 (d, $J = 2.8$ Hz, 1H), 5.20 (dd, $J = 9.4, 1.4$ Hz, 1H), 4.33 (d, $J = 16.6$ Hz, 1H), 4.30 (d, $J = 16.6$ Hz, 1H), 3.53 (d, $J = 12.7$ Hz, 1H), 3.46 (d, $J = 12.7$ Hz, 1H), 2.68 (ddd, $J = 16.4, 9.3, 2.4$ Hz, 1H), 2.48 – 2.43 (m, 1H), 2.30 – 2.16

(m, 4H), 1.96 (d, $J = 16.4$ Hz, 1H), 1.92 – 1.84 (m, 1H), 1.74 – 1.65 (m, 2H), 1.42 – 1.35 (m, 1H), 1.12 (s, 9H), 0.96 (d, $J = 6.8$ Hz, 3H), 0.95 (d, $J = 6.8$ Hz, 3H), 0.85 (d, $J = 7.1$ Hz, 3H) ppm.

^{13}C NMR (176 MHz, CDCl_3): $\delta = 170.4, 142.4, 135.6$ (2C), 135.2, 134.8 (2C), 132.6, 130.0, 129.7, 127.9 (2C), 127.7 (2C), 124.8, 76.4, 74.3, 62.5, 53.7, 45.4, 42.9, 37.5, 37.3, 32.8, 30.0, 26.7 (3C), 23.9, 21.5, 21.2, 19.2, 15.2 ppm.

IR (ATR): $\tilde{\nu} = 3469, 3071, 2957, 2930, 2858, 2360, 2105, 1764, 1463, 1428, 1381, 1362, 1287, 1199, 1139, 1114, 938, 822, 741, 703, 677, 661$ cm^{-1} .

HRMS (ESI): m/z calcd. for $\text{C}_{33}\text{H}_{45}\text{N}_3\text{O}_4\text{SiNa}$ [$\text{M} + \text{Na}$] $^+$: 598.3071, found: 598.3076.



Prepared according to GP3. Purification by column chromatography (silica gel, pentane/ Et_2O 2:1) afforded alcohol **129** (5.0 mg, 8.5 μmol , 30%) as a colorless oil.

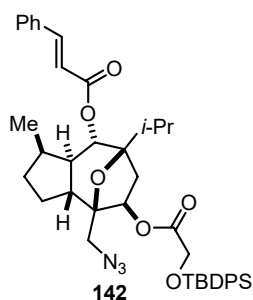
$[\alpha]_{\text{D}}^{25} = -26.4$ ($c = 0.25$, CHCl_3).

^1H NMR (700 MHz, CDCl_3): $\delta = 7.70 - 7.66$ (m, 4H), 7.47 – 7.43 (m, 2H), 7.41 – 7.38 (m, 4H), 5.09 (dd, $J = 7.9, 2.9$ Hz, 1H), 4.25 (s, 2H), 3.65 (d, $J = 10.2$ Hz, 1H), 3.37 (d, $J = 13.0$ Hz, 1H), 2.98 (d, $J = 13.1$ Hz, 1H), 2.46 (dd, $J = 14.5, 7.8$ Hz, 1H), 2.37 – 2.31 (m, 1H), 2.08 – 2.00 (m, 1H), 1.98 (hept, $J = 6.9$ Hz, 1H), 1.85 – 1.78 (m, 1H), 1.73 – 1.68 (m, 1H), 1.59 (dd, $J = 14.6, 3.0$ Hz, 1H), 1.31 (ddd, $J = 13.1, 10.2, 7.1$ Hz, 1H), 1.26 – 1.17 (m, 3H), 1.10 (s, 9H), 1.04 (d, $J = 7.0$ Hz, 3H), 1.01 (d, $J = 6.9$ Hz, 3H), 0.91 (d, $J = 7.2$ Hz, 3H) ppm.

^{13}C NMR (176 MHz, CDCl_3): $\delta = 170.8, 135.6$ (2C), 135.6 (2C), 132.7, 132.6, 130.0, 130.0, 127.9 (2C), 127.8 (2C), 86.9, 85.8, 75.4, 70.2, 62.2, 52.9, 47.8, 43.4, 38.4, 31.6, 31.4, 30.3, 26.7 (3C), 25.1, 19.2, 18.1, 17.3, 16.8 ppm.

IR (ATR): $\tilde{\nu} = 3441, 2955, 2919, 2851, 2103, 1737, 1465, 1428, 1378, 1265, 1200, 1142, 1114, 1030, 1005, 908, 823, 734, 702$ cm^{-1} .

HRMS (ESI): m/z calcd. for $\text{C}_{33}\text{H}_{45}\text{N}_3\text{O}_5\text{SiNa}$ [$\text{M} + \text{Na}$] $^+$: 614.3020, found: 614.3012.



Prepared according to GP1. Purification by column chromatography (silica gel, pentane/ Et_2O 10:1) afforded ester **142** (2.2 mg, 3.1 μmol , 36%) as a colorless oil.

$[\alpha]_{\text{D}}^{25} = -11.6$ ($c = 0.11$, CHCl_3).

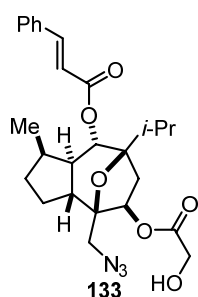
^1H NMR (700 MHz, CDCl_3): $\delta = 7.70 - 7.68$ (m, 4H), 7.66 (d, $J = 16.0$ Hz, 1H), 7.54 – 7.52 (m, 2H), 7.47 – 7.44 (m, 2H), 7.43 – 7.38 (m, 7H), 6.39 (d, $J = 16.0$ Hz, 1H), 5.16 (dd, $J = 7.9, 3.0$ Hz, 1H), 5.13 (d, $J = 10.3$ Hz, 1H), 4.28 (s, 2H), 3.41 (d, $J =$

13.0 Hz, 1H), 3.02 (d, $J = 13.0$ Hz, 1H), 2.66 (dd, $J = 14.5, 7.9$ Hz, 1H), 2.18 – 2.09 (m, 2H), 2.06 – 1.93 (m, 3H), 1.87 (hept, $J = 6.9$ Hz, 1H), 1.77 – 1.73 (m, 1H), 1.71 (dd, $J = 14.6, 3.1$ Hz, 1H), 1.31 – 1.28 (m, 1H), 1.11 (s, 9H), 0.98 (d, $J = 6.8$ Hz, 3H), 0.96 (d, $J = 7.1$ Hz, 3H), 0.96 (d, $J = 7.1$ Hz, 3H) ppm.

^{13}C NMR (176 MHz, CDCl_3): $\delta = 170.9, 165.5, 145.3, 135.6$ (2C), 135.6 (2C), $134.3, 132.7, 132.6, 130.5, 130.1, 130.0, 128.9$ (2C), $128.2, 127.9$ (2C), 127.9 (2C), $125.6, 117.9, 86.5, 85.9, 75.3, 70.8, 64.3, 62.3, 52.8, 46.9, 43.1, 39.8, 37.8, 32.6, 26.7$ (3C), $24.2, 19.3, 18.0, 17.4, 16.9$ ppm.

IR (ATR): $\tilde{\nu} = 2925, 2855, 2102, 1762, 1714, 1636, 1449, 1428, 1300, 1265, 1201, 1167, 1141, 1115, 1007, 824, 742, 704, 687, 656$ cm^{-1} .

HRMS (ESI): m/z calcd. for $\text{C}_{42}\text{H}_{51}\text{N}_3\text{O}_6\text{SiNa}$ $[\text{M} + \text{Na}]^+$: 744.3439, found: 744.3472.



Prepared according to GP2. Purification by column chromatography (silica gel, pentane/ Et_2O 1:1) afforded product **133** (1.0 mg, 2.1 μmol , 67%) as a colorless oil.

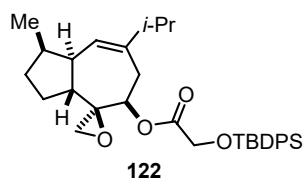
$[\alpha]_{\text{D}}^{23} = -14.2$ ($c = 0.07, \text{CHCl}_3$).

^1H NMR (700 MHz, CDCl_3): $\delta = 7.67$ (d, $J = 16.0$ Hz, 1H), $7.54 - 7.52$ (m, 2H), $7.41 - 7.39$ (m, 3H), 6.39 (d, $J = 16.0$ Hz, 1H), 5.26 (dd, $J = 7.9, 3.1$ Hz, 1H), 5.16 (d, $J = 10.3$ Hz, 1H), 4.23 (dd, $J = 17.3, 4.0$ Hz, 1H), 4.20 (dd, $J = 17.3, 4.0$ Hz, 1H), 3.52 (d, $J = 13.0$ Hz, 1H), 3.26 (d, $J = 12.9$ Hz, 1H), 2.74 (dd, $J = 14.6, 7.8$ Hz, 1H), 2.32 (t, $J = 5.6$ Hz, 1H), $2.19 - 2.14$ (m, 1H), $2.04 - 1.95$ (m, 2H), 1.92 (hept, $J = 6.9$ Hz, 1H), 1.81 (dd, $J = 14.6, 3.1$ Hz, 1H), $1.80 - 1.76$ (m, 1H), $1.61 - 1.54$ (m, 1H), $1.33 - 1.25$ (m, 2H), 1.02 (d, $J = 6.8$ Hz, 3H), 0.99 (d, $J = 7.1$ Hz, 3H), 0.97 (d, $J = 7.2$ Hz, 3H) ppm.

^{13}C NMR (176 MHz, CDCl_3): $\delta = 172.9, 165.5, 145.4, 134.2, 130.5, 129.0$ (2C), 128.2 (2C), $117.8, 86.6, 85.8, 76.3, 70.6, 60.8, 53.1, 47.0, 43.7, 39.9, 32.6, 31.1, 30.9, 24.2, 18.0, 17.4, 16.9$ ppm.

IR (ATR): $\tilde{\nu} = 3446, 2924, 2852, 2103, 1712, 1636, 1449, 1334, 1301, 1265, 1202, 1168, 1094, 1007, 768, 685$ cm^{-1} .

HRMS (ESI): m/z calcd. for $\text{C}_{26}\text{H}_{33}\text{N}_3\text{O}_6\text{Na}$ $[\text{M} + \text{Na}]^+$: 506.2261, found: 506.2245.



Prepared according to GP1. Purification by column chromatography (silica gel, pentane/ Et_2O 10:1) afforded diol **122** (23.6 mg, 44.3 μmol , 80%) as a colorless oil.

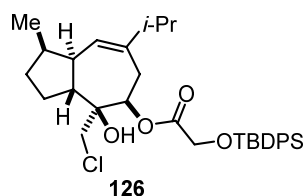
$[\alpha]_{\text{D}}^{21} = -38.4$ ($c = 1.48, \text{CHCl}_3$).

^1H NMR (500 MHz, CDCl_3): δ = 7.70 – 7.67 (m, 4H), 7.43 – 7.36 (m, 6H), 5.71 (s, 1H), 4.65 (dd, J = 6.9, 1.2 Hz, 1H), 4.29 (d, J = 16.5 Hz, 1H), 4.16 (d, J = 16.5 Hz, 1H), 2.81 (d, J = 4.0 Hz, 1H), 2.63 (ddd, J = 15.4, 6.9, 1.2 Hz, 1H), 2.62 (d, J = 5.1 Hz, 1H), 2.51 (td, J = 10.3, 5.9 Hz, 1H), 2.34 – 2.29 (m, 2H), 2.24 – 2.17 (m, 1H), 2.14 (hept, J = 6.7 Hz, 1H), 1.64 – 1.54 (m, 2H), 1.44 – 1.35 (m, 1H), 1.17 – 1.09 (m, 1H), 1.07 (s, 9H), 0.91 (d, J = 7.0 Hz, 3H), 0.88 (d, J = 6.8 Hz, 3H), 0.86 (d, J = 6.8 Hz, 3H) ppm.

^{13}C NMR (126 MHz, CDCl_3): δ = 170.7, 141.8, 135.7 (2C), 135.6 (2C), 133.0, 132.8, 129.9, 129.7, 127.9 (2C), 127.8 (2C), 125.0, 76.0, 63.6, 62.4, 47.4, 46.6, 39.3, 37.4, 37.2, 33.5, 31.0, 26.7 (3C), 22.0, 21.2, 19.3, 19.1, 15.3 ppm.

IR (ATR): $\tilde{\nu}$ = 3509, 3071, 3049, 2958, 2930, 2894, 2857, 1759, 1735, 1589, 1471, 1428, 1382, 1362, 1287, 1203, 1140, 1114, 1061, 1026, 973, 940, 904, 822, 805, 788, 741, 702 cm^{-1} .

HRMS (ESI): m/z calcd. for $\text{C}_{33}\text{H}_{44}\text{O}_4\text{SiNa}$ [$\text{M} + \text{Na}$] $^+$: 555.2901, found: 555.2918.



To a solution of epoxide **122** (19.0 mg, 35.6 μmol , 1.0 equiv.) in THF (0.2 mL) were added acetic acid (20.0 μL , 356 μmol , 10.0 equiv.) and lithium chloride (15.0 mg, 356 μmol , 10.0 equiv.). The reaction mixture was heated to 60 $^\circ\text{C}$ for 3 h. After cooling back to 23 $^\circ\text{C}$, saturated aqueous NaHCO_3 -solution (5 mL) was added and the aqueous phase was extracted with Et_2O (3 x 5 mL). The combined organic phases were washed with brine, dried over Na_2SO_4 and concentrated under reduced pressure. Purification by column chromatography (silica gel, pentane/ Et_2O 10:1) afforded alcohol **126** (13.7 mg, 24.1 μmol , 67%) as a colorless oil.

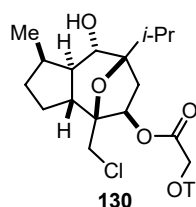
$[\alpha]_{\text{D}}^{19} = -12.3$ (c = 0.69, CHCl_3).

^1H NMR (500 MHz, CDCl_3): δ = 7.70 – 7.66 (m, 4H), 7.41 – 7.37 (m, 6H), 5.47 (d, J = 2.1 Hz, 1H), 5.37 (dd, J = 9.4, 1.3 Hz, 1H), 4.30 (d, J = 16.7 Hz, 1H), 4.26 (d, J = 16.6 Hz, 1H), 3.79 (d, J = 11.7 Hz, 1H), 3.61 (d, J = 11.6 Hz, 1H), 2.64 (ddd, J = 16.4, 9.4, 2.5 Hz, 1H), 2.55 – 2.50 (m, 1H), 2.32 (ddd, J = 11.7, 9.9, 6.7 Hz, 1H), 2.23 – 2.14 (m, 3H), 1.96 (d, J = 16.8 Hz, 1H), 1.91 – 1.83 (m, 1H), 1.72 – 1.64 (m, 2H), 1.38 – 1.33 (m, 1H), 1.07 (s, 9H), 0.94 (d, J = 6.9 Hz, 3H), 0.92 (d, J = 6.8 Hz, 3H), 0.82 (d, J = 7.1 Hz, 3H) ppm.

^{13}C NMR (126 MHz, CDCl_3): δ = 170.4, 142.4, 135.6 (2C), 135.6 (2C), 132.8, 132.7, 130.1, 129.7, 128.0 (2C), 127.8 (2C), 124.8, 76.0, 73.8, 62.5, 47.0, 45.5, 43.2, 37.5, 37.4, 32.9, 30.1, 26.7 (3C), 23.9, 21.5, 21.3, 19.3, 15.4 ppm.

IR (ATR): $\tilde{\nu}$ = 3557, 3072, 3049, 2957, 2930, 2857, 1763, 1463, 1428, 1190, 1139, 1114, 822, 741, 702 cm^{-1} .

HRMS (ESI): m/z calcd. for $\text{C}_{33}\text{H}_{45}\text{ClO}_4\text{SiNa}$ [$\text{M} + \text{Na}$] $^+$: 591.2668, found: 591.2658.



Prepared according to GP3. Purification by column chromatography (silica gel, pentane/Et₂O 4:1) afforded alcohol **130** (7.1 mg, 12 μmol, 68%) as a colorless oil.

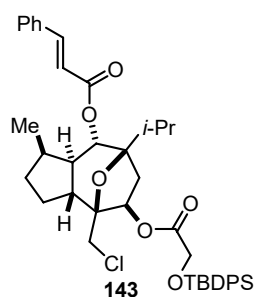
$[\alpha]_D^{20} = -31.9$ ($c = 0.36$, CHCl₃).

¹H NMR (700 MHz, CDCl₃): $\delta = 7.72 - 7.69$ (m, 4H), 7.48 – 7.45 (m, 2H), 7.44 – 7.40 (m, 4H), 5.18 (dd, $J = 7.9, 2.8$ Hz, 1H), 4.27 (s, 2H), 3.67 (d, $J = 10.2$ Hz, 1H), 3.56 (d, $J = 11.6$ Hz, 1H), 3.40 (d, $J = 11.6$ Hz, 1H), 2.51 (dd, $J = 14.6, 7.8$ Hz, 1H), 2.39 – 2.31 (m, 1H), 2.08 – 2.03 (m, 1H), 2.00 (hept, $J = 6.9$ Hz, 1H), 1.96 – 1.90 (m, 1H), 1.85 (ddd, $J = 15.1, 8.0, 4.8$ Hz, 1H), 1.61 (dd, $J = 14.6, 2.9$ Hz, 1H), 1.36 (ddd, $J = 13.1, 10.2, 7.2$ Hz, 1H), 1.32 – 1.25 (m, 3H), 1.12 (s, 9H), 1.06 (d, $J = 7.0$ Hz, 3H), 1.03 (d, $J = 6.8$ Hz, 3H), 0.93 (d, $J = 7.2$ Hz, 3H) ppm.

¹³C NMR (176 MHz, CDCl₃): $\delta = 170.7, 135.6$ (2C), 135.6 (2C), 132.7, 132.6, 130.0, 130.0, 127.8 (2C), 127.8 (2C), 86.9, 85.0, 75.3, 70.4, 62.2, 47.9, 45.6, 44.0, 38.6, 31.9, 31.4, 30.1, 26.7 (3C), 25.3, 19.2, 18.1, 17.4, 16.9 ppm.

IR (ATR): $\tilde{\nu} = 2958, 2932, 2858, 1761, 1472, 1458, 1428, 1140, 1115, 1028, 823, 741, 703$ cm⁻¹.

HRMS (ESI): m/z calcd. for C₃₃H₄₅ClO₅SiNa [M + Na]⁺: 607.2617, found: 607.2605.



Prepared according to GP1. Purification by column chromatography (silica gel, pentane/Et₂O 10:1) afforded ester **143** (6.2 mg, 8.4 μmol, 69%) as a colorless oil.

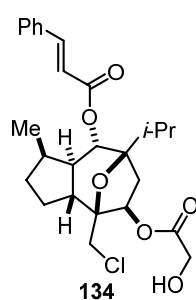
$[\alpha]_D^{20} = -14.5$ ($c = 0.31$, CHCl₃).

¹H NMR (700 MHz, CDCl₃): $\delta = 7.70 - 7.68$ (m, 4H), 7.66 (d, $J = 16.0$ Hz, 1H), 7.54 – 7.52 (m, 2H), 7.46 – 7.44 (m, 2H), 7.42 – 7.38 (m, 7H), 6.39 (d, $J = 16.0$ Hz, 1H), 5.23 (dd, $J = 7.9, 3.0$ Hz, 1H), 5.13 (d, $J = 10.3$ Hz, 1H), 4.27 (s, 2H), 3.58 (d, $J = 11.6$ Hz, 1H), 3.42 (d, $J = 11.6$ Hz, 1H), 2.69 (dd, $J = 14.5, 7.8$ Hz, 1H), 2.17 – 2.06 (m, 2H), 1.99 – 1.92 (m, 1H), 1.90 – 1.84 (m, 2H), 1.70 (dd, $J = 14.6, 3.0$ Hz, 1H), 1.58 (ddd, $J = 13.5, 10.4, 6.6$ Hz, 1H), 1.32 – 1.24 (m, 2H), 1.11 (s, 9H), 0.97 (d, $J = 6.8$ Hz, 3H), 0.95 (d, $J = 7.1$ Hz, 6H) ppm.

¹³C NMR (176 MHz, CDCl₃): $\delta = 170.8, 165.5, 145.3, 135.6$ (2C), 135.6 (2C), 134.3, 132.7, 132.6, 130.5, 130.0, 130.0, 128.9 (2C), 128.2 (2C), 127.9 (4C), 117.9, 86.4, 85.1, 75.2, 70.9, 62.2, 46.9, 45.4, 43.7, 40.0, 32.7, 31.1, 30.8, 26.7 (3C), 24.5, 19.3, 18.1, 17.5, 16.9 ppm.

IR (ATR): $\tilde{\nu} = 2957, 2931, 2858, 1760, 1428, 1190, 1141, 1114, 823, 740, 702$ cm⁻¹.

HRMS (ESI): m/z calcd. for C₄₂H₅₁ClO₆SiNa [M + Na]⁺: 737.3035, found: 737.3056.



Prepared according to GP2. Purification by column chromatography (silica gel, pentane/Et₂O 2:1) afforded product **134** (3.6 mg, 7.5 μmol, 90%) as a colorless oil.

$[\alpha]_{\text{D}}^{22} = -50.9$ ($c = 0.19$, CHCl₃).

¹H NMR (700 MHz, CDCl₃): $\delta = 7.67$ (d, $J = 16.0$ Hz, 1H), 7.54 – 7.51 (m, 2H), 7.42 – 7.38 (m, 3H), 6.39 (d, $J = 16.0$ Hz, 1H), 5.33 (dd, $J = 7.8, 3.0$ Hz, 1H), 5.16

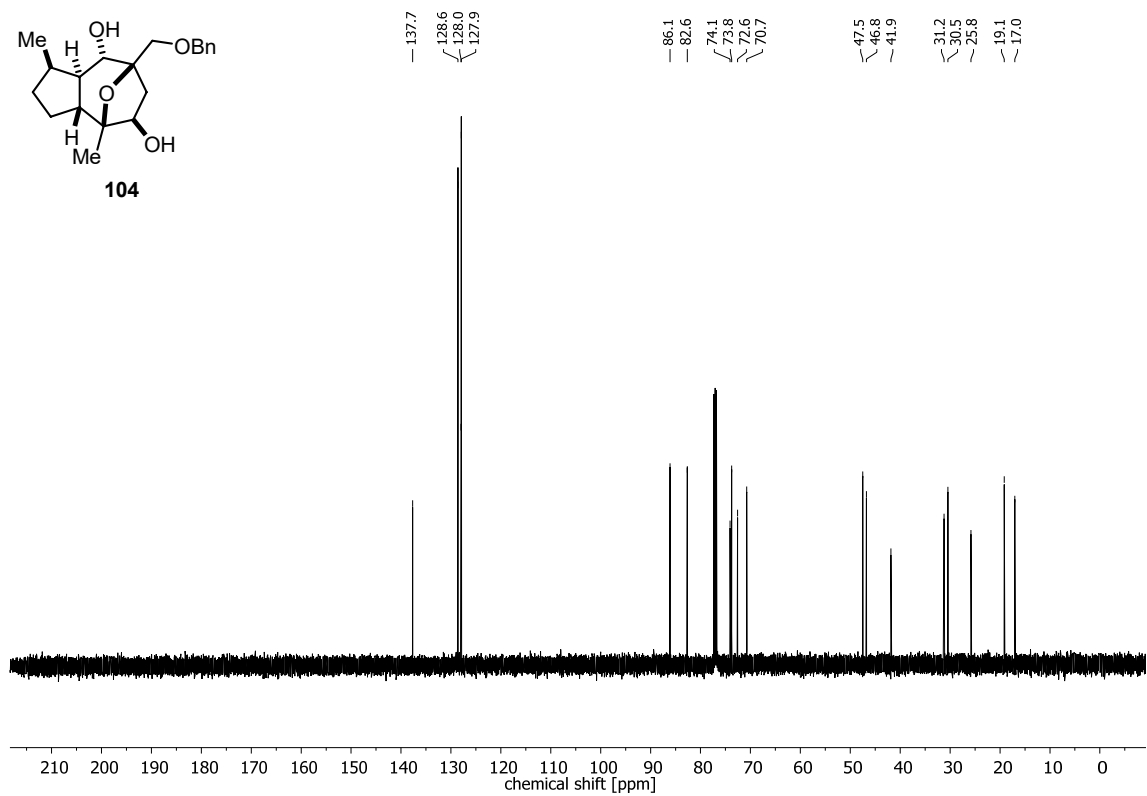
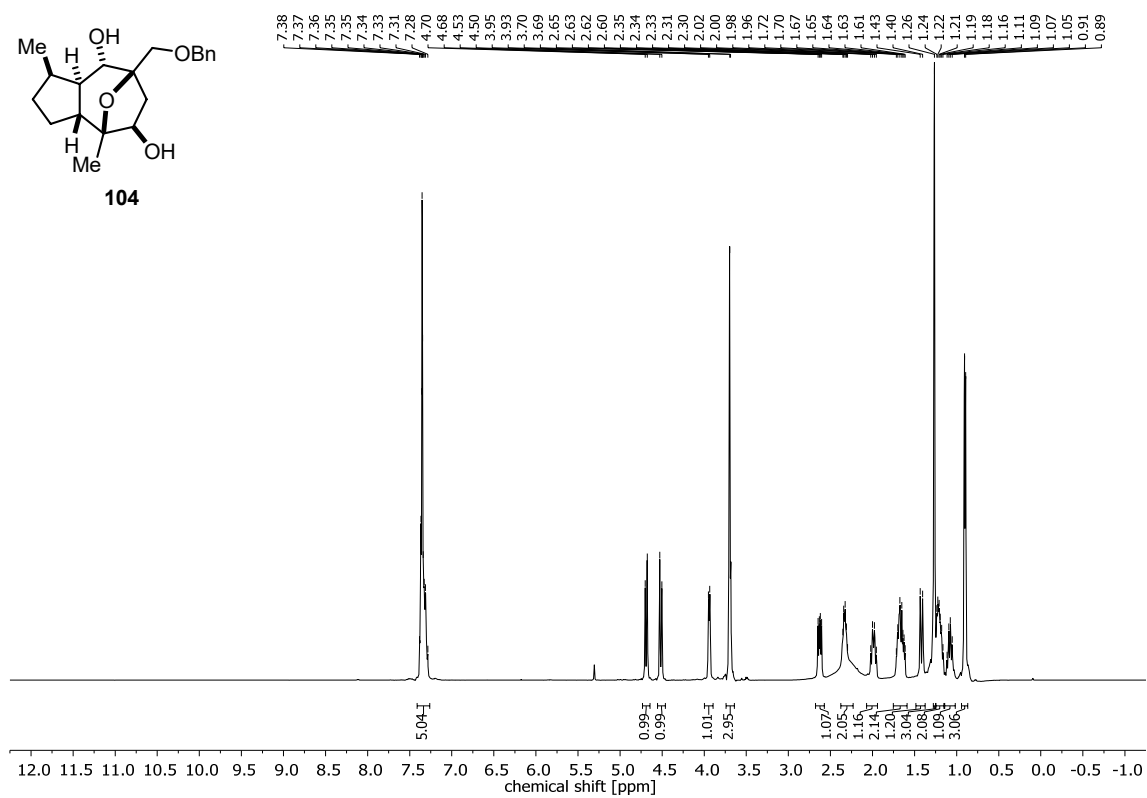
(d, $J = 10.3$ Hz, 1H), 4.21 (s, 2H), 3.69 (d, $J = 11.5$ Hz, 1H), 3.59 (d, $J = 11.5$ Hz, 1H), 2.77 (dd, $J = 14.5, 7.8$ Hz, 1H), 2.32 – 2.28 (m, 1H), 2.19 – 2.13 (m, 1H), 2.11 – 2.06 (m, 1H), 2.01 – 1.96 (m, 1H), 1.96 – 1.89 (m, 2H), 1.80 (dd, $J = 14.5, 3.0$ Hz, 1H), 1.60 (ddd, $J = 13.4, 10.3, 6.5$ Hz, 1H), 1.34 – 1.27 (m, 2H), 1.01 (d, $J = 6.8$ Hz, 3H), 0.98 (d, $J = 7.0$ Hz, 3H), 0.96 (d, $J = 7.1$ Hz, 3H) ppm.

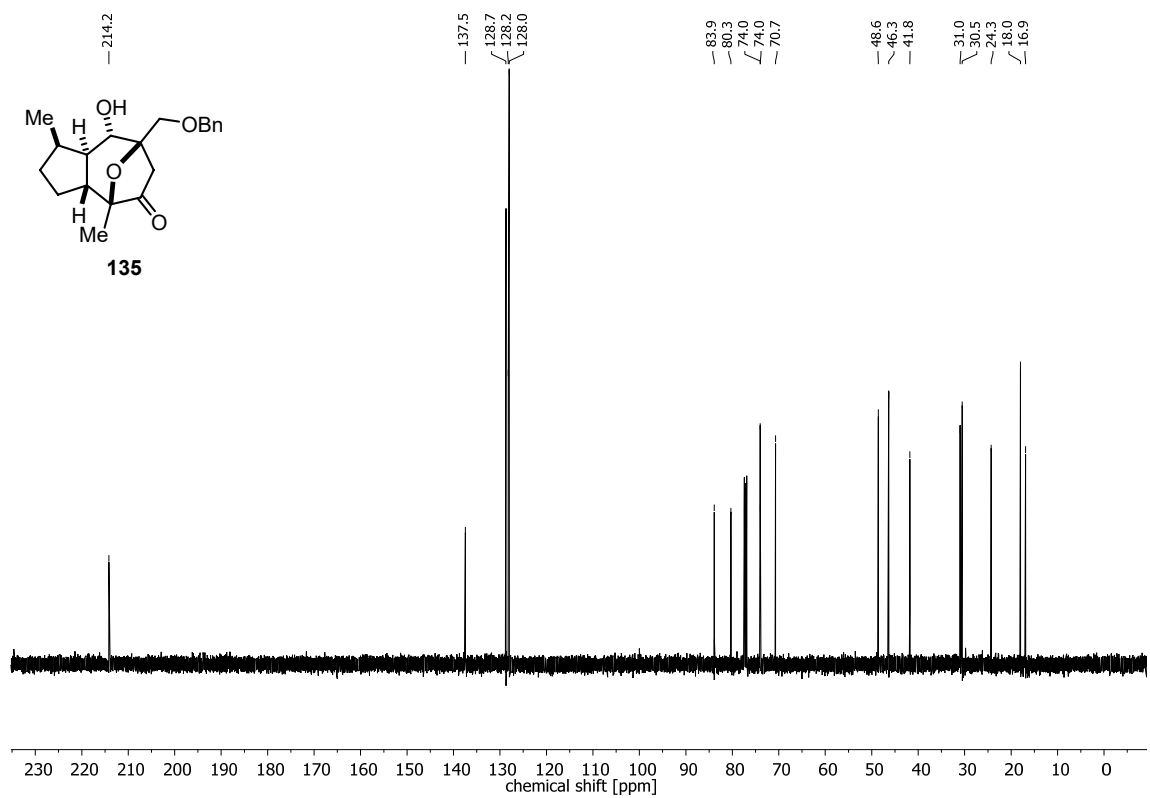
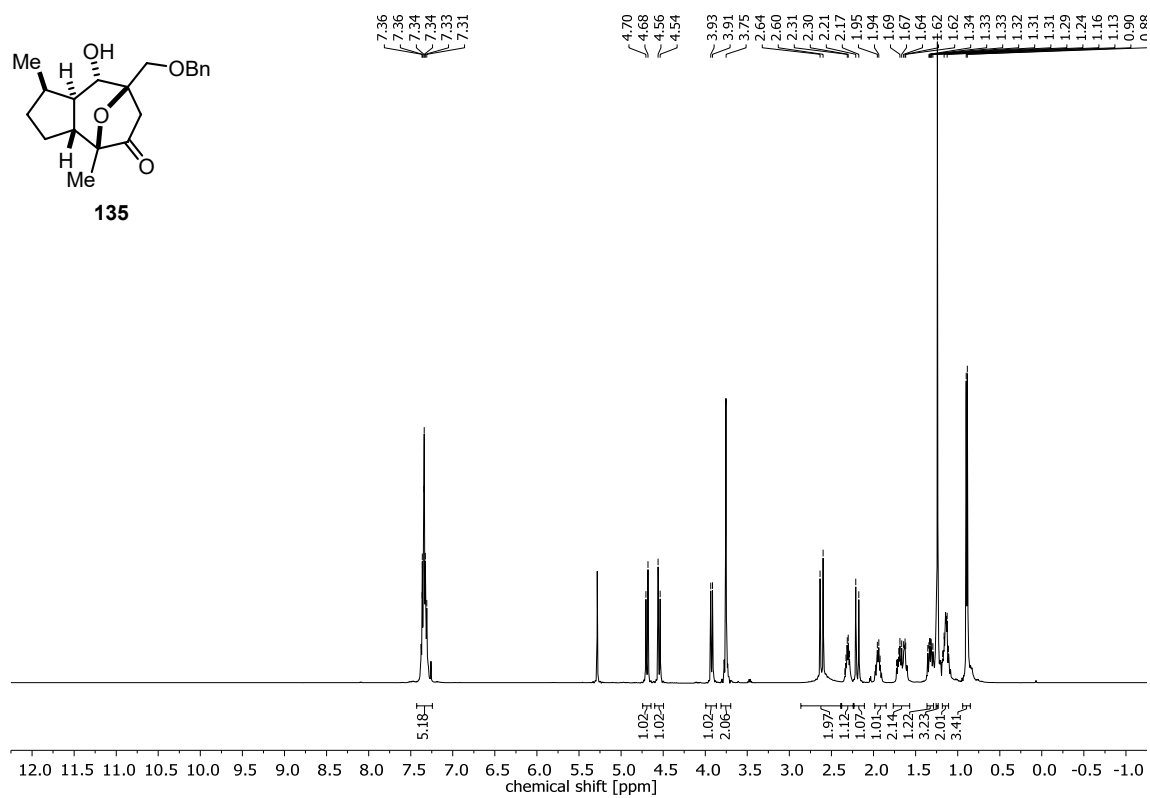
¹³C NMR (176 MHz, CDCl₃): $\delta = 172.9, 165.5, 145.4, 134.2, 130.5, 128.9, 128.2, 117.8, 86.6, 85.2, 76.0, 70.7, 60.7, 47.0, 45.3, 44.3, 40.1, 32.8, 31.1, 30.7, 24.7, 18.1, 17.4, 17.0$ ppm.

IR (ATR): $\tilde{\nu} = 3367, 2956, 2918, 2850, 1737, 1468, 1180, 1170, 737, 724$ cm⁻¹.

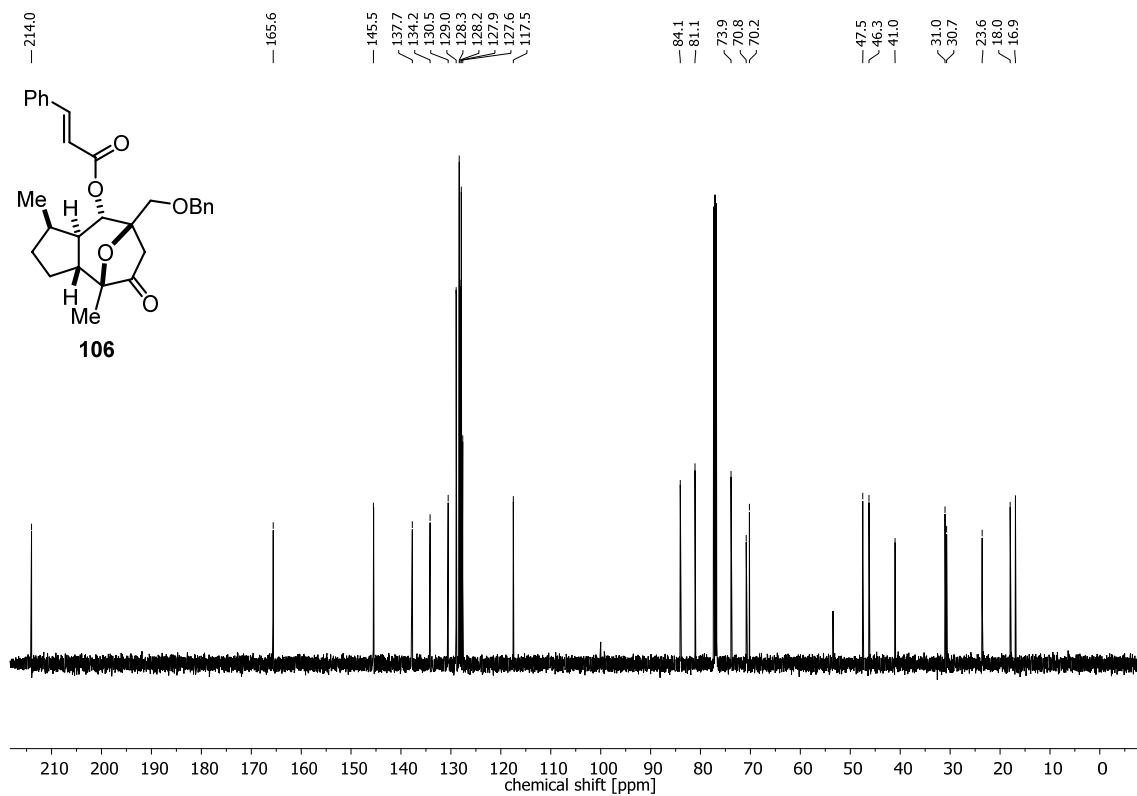
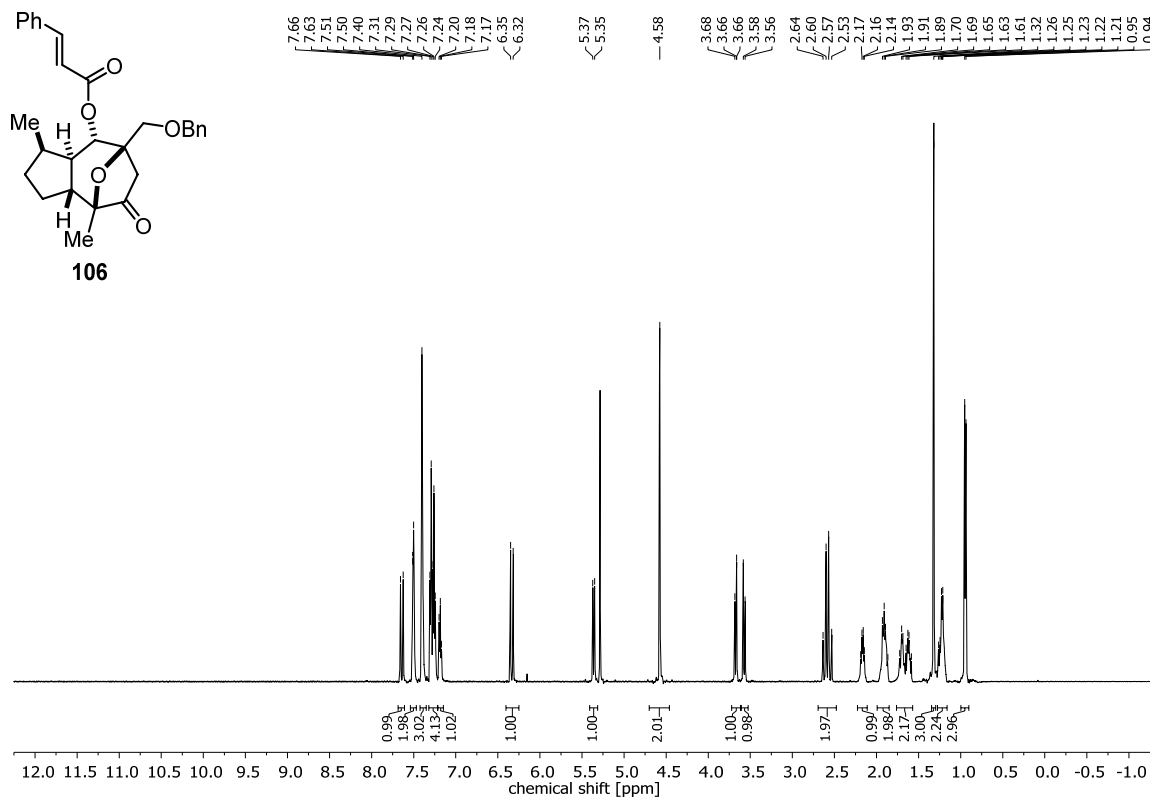
HRMS (ESI): m/z calcd. for C₂₆H₃₃ClO₆Na [M + Na]⁺: 499.1858, found: 499.1834.

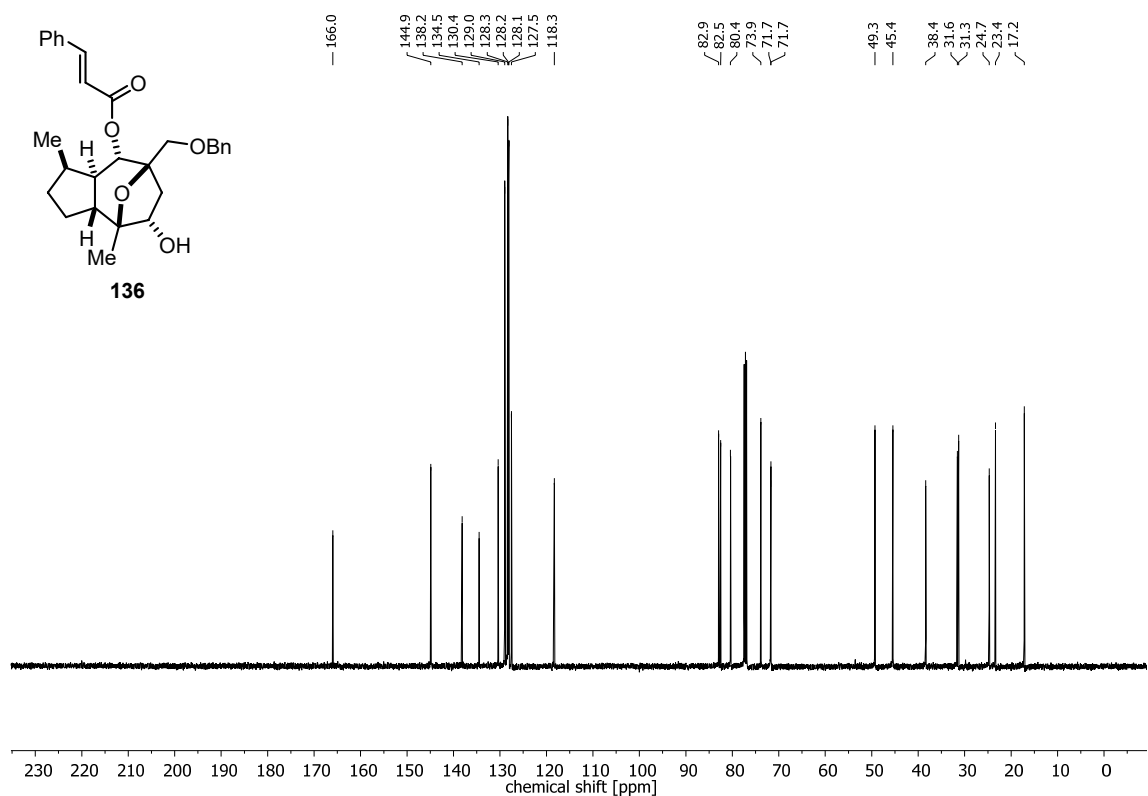
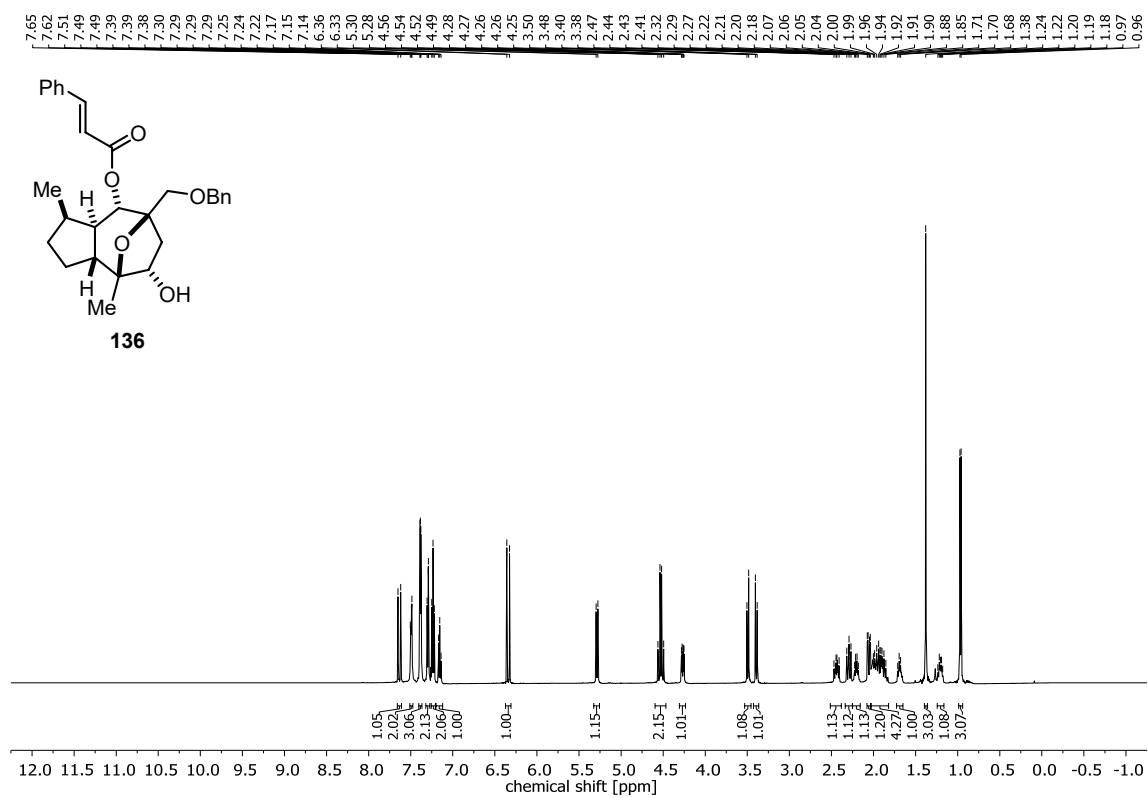
Appendix



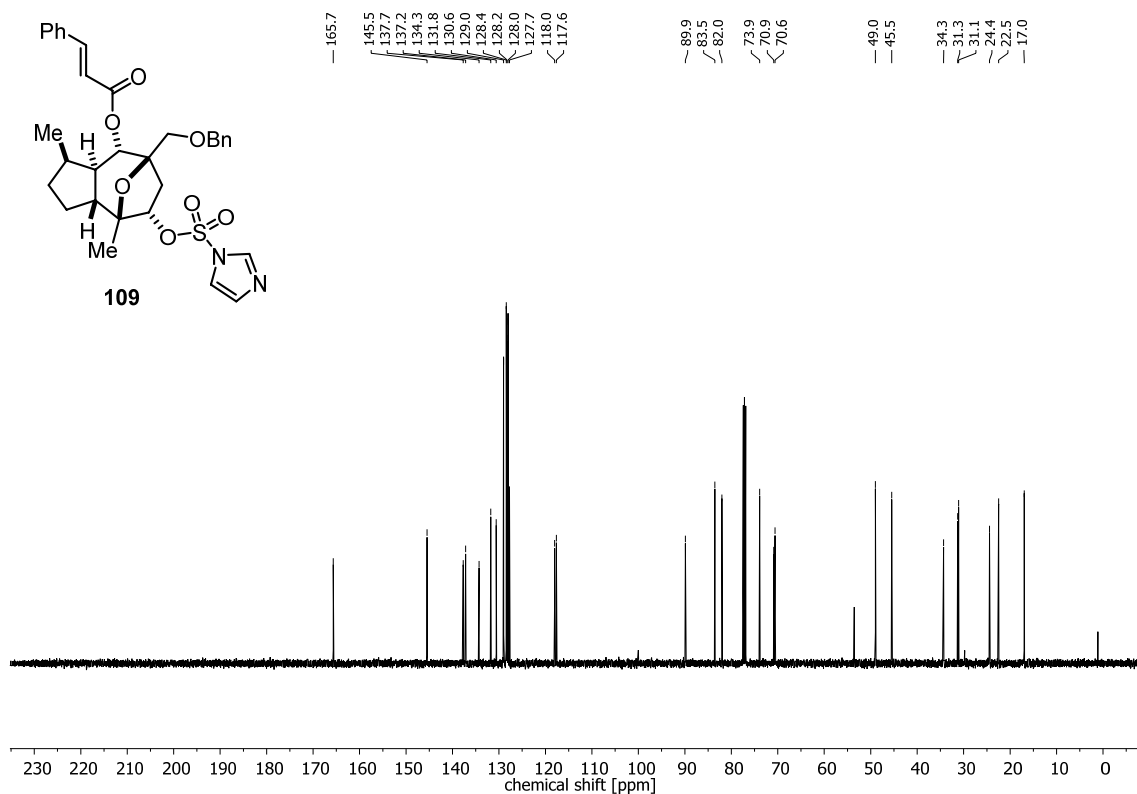
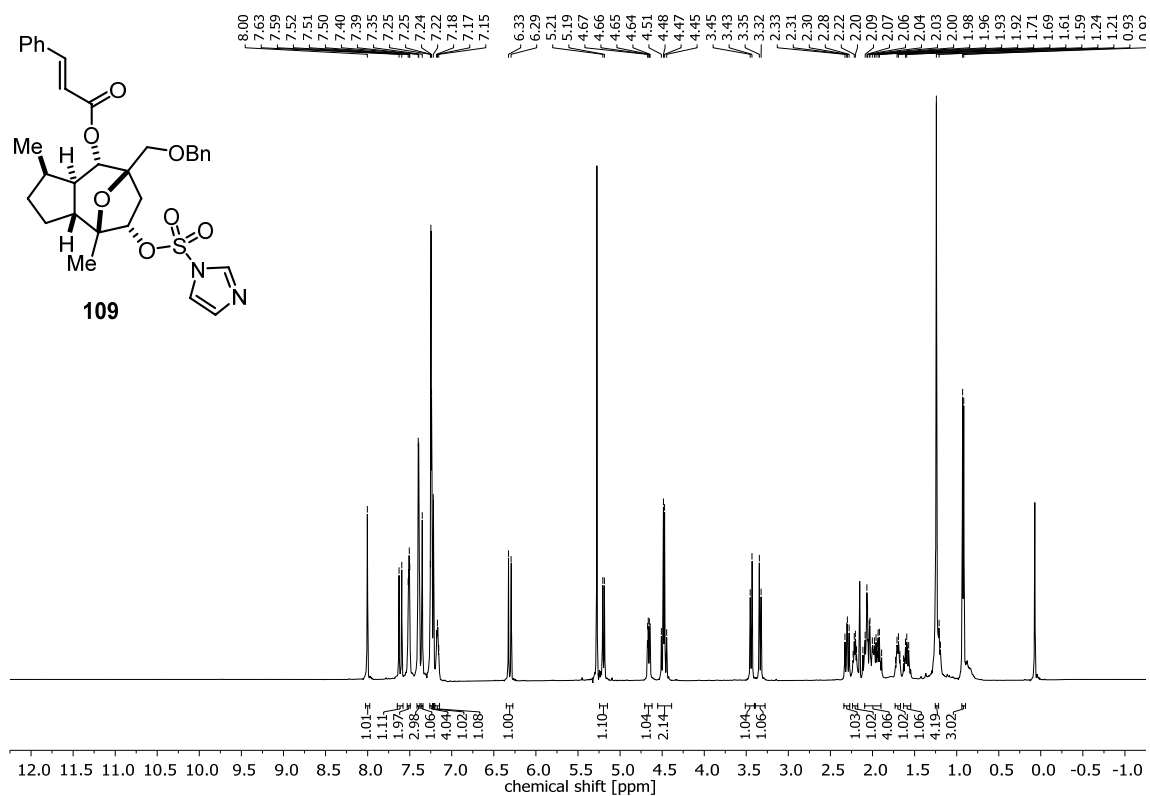


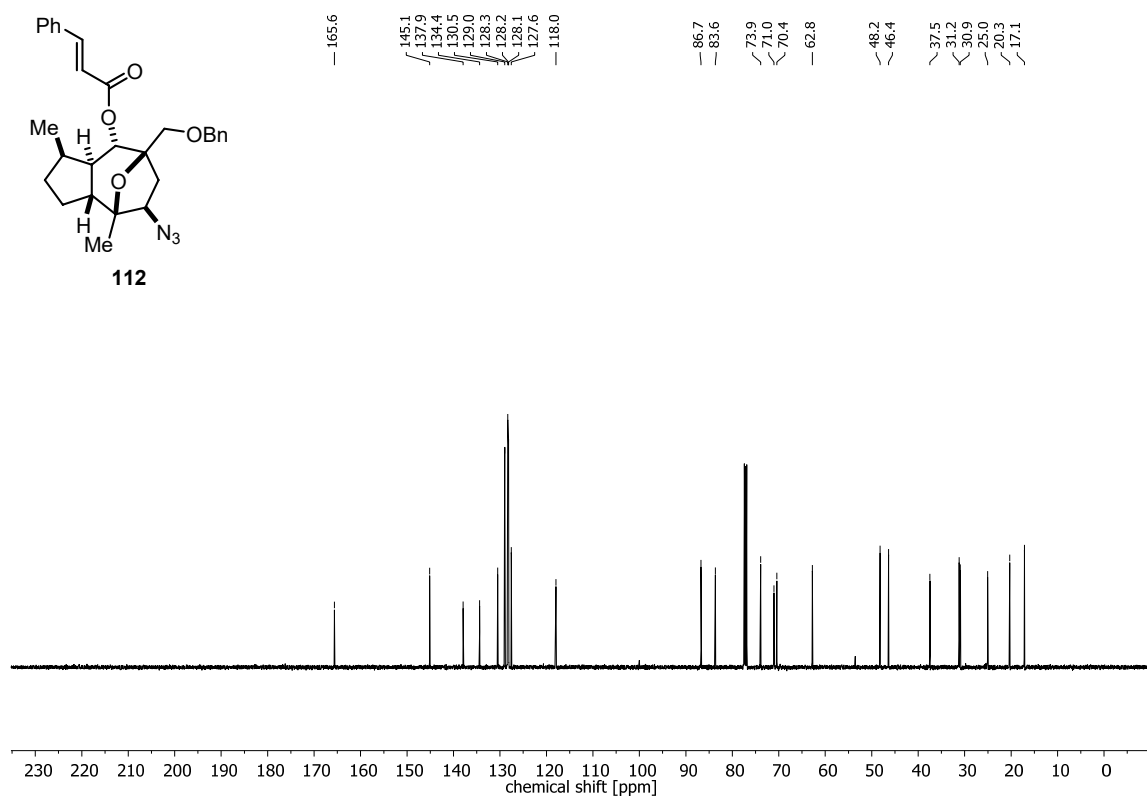
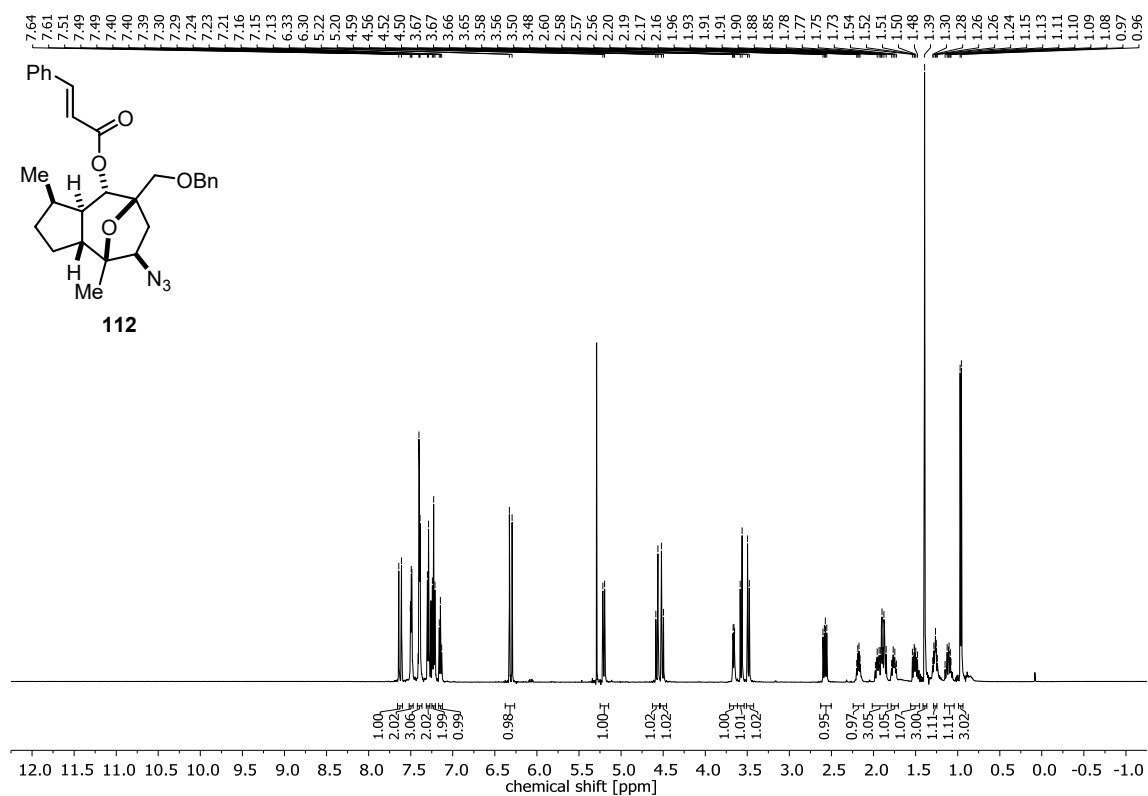
Appendix



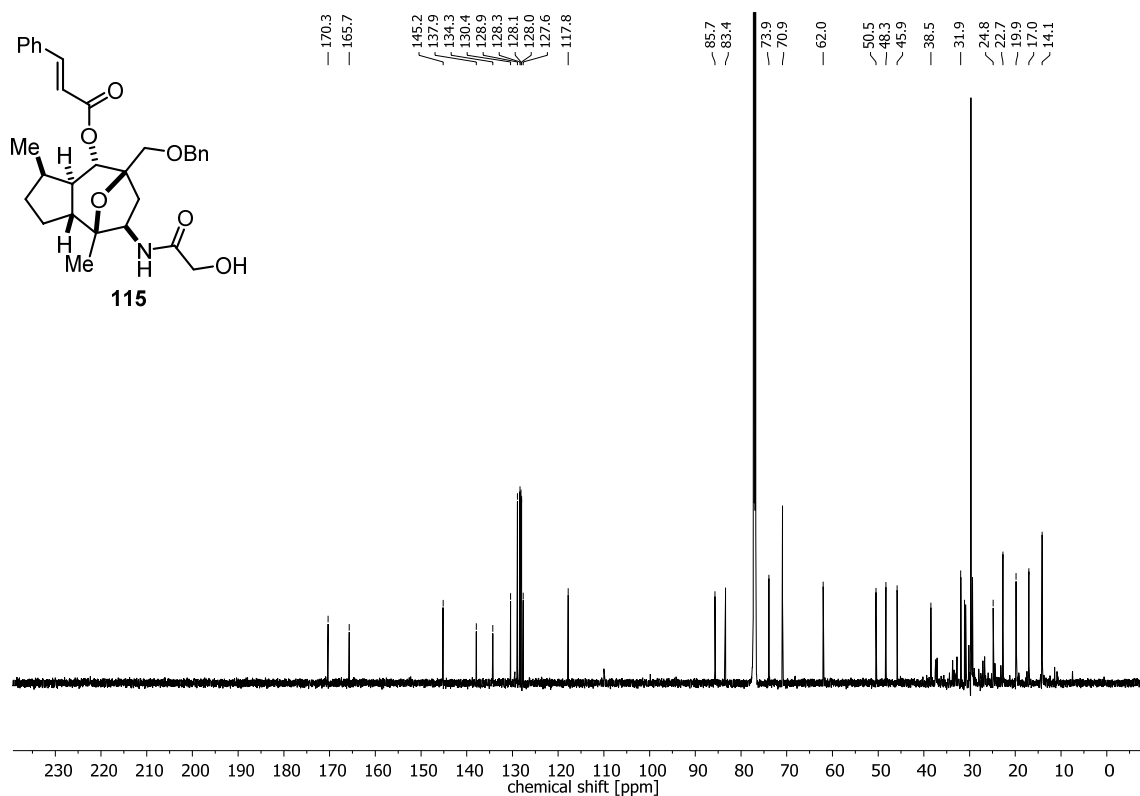
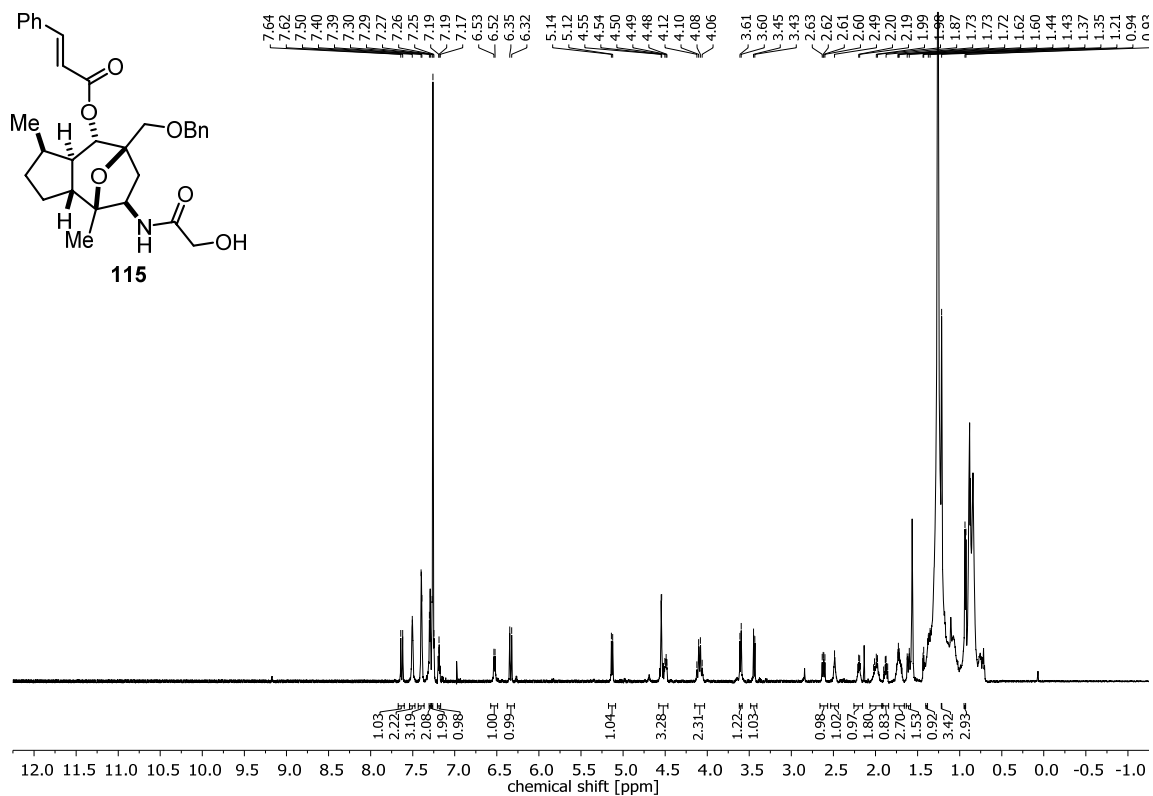


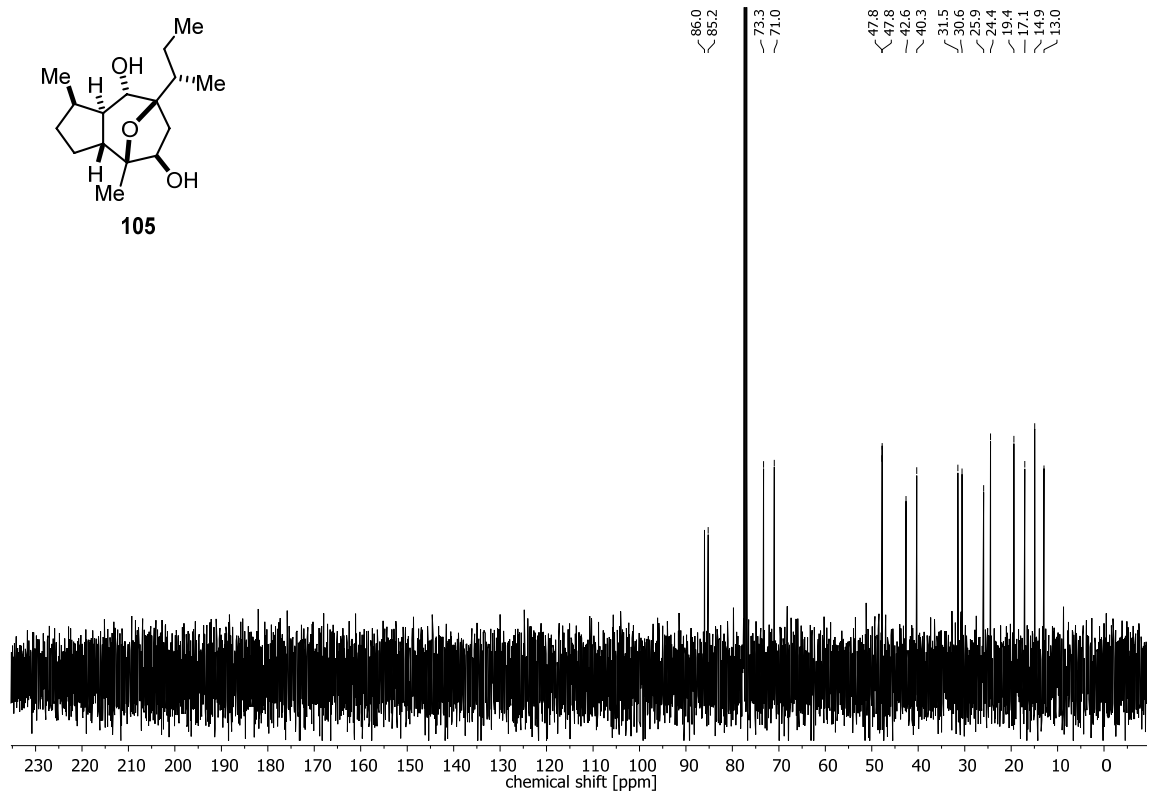
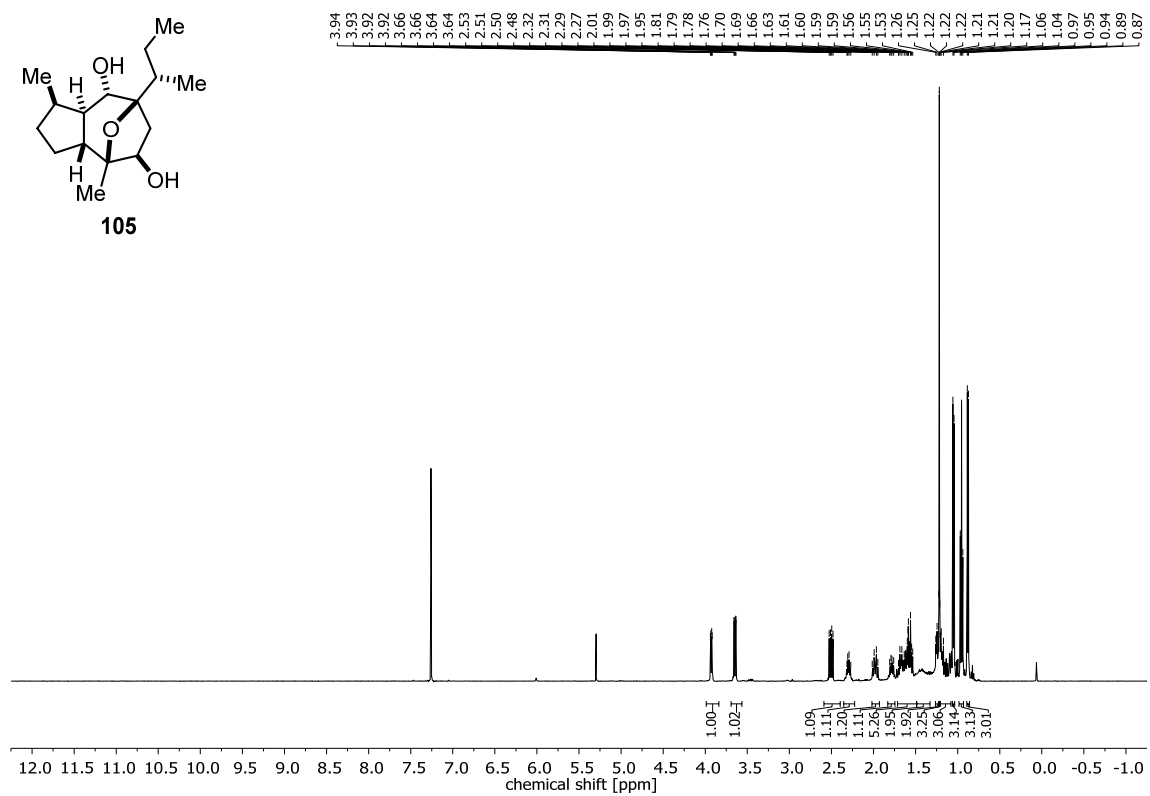
Appendix



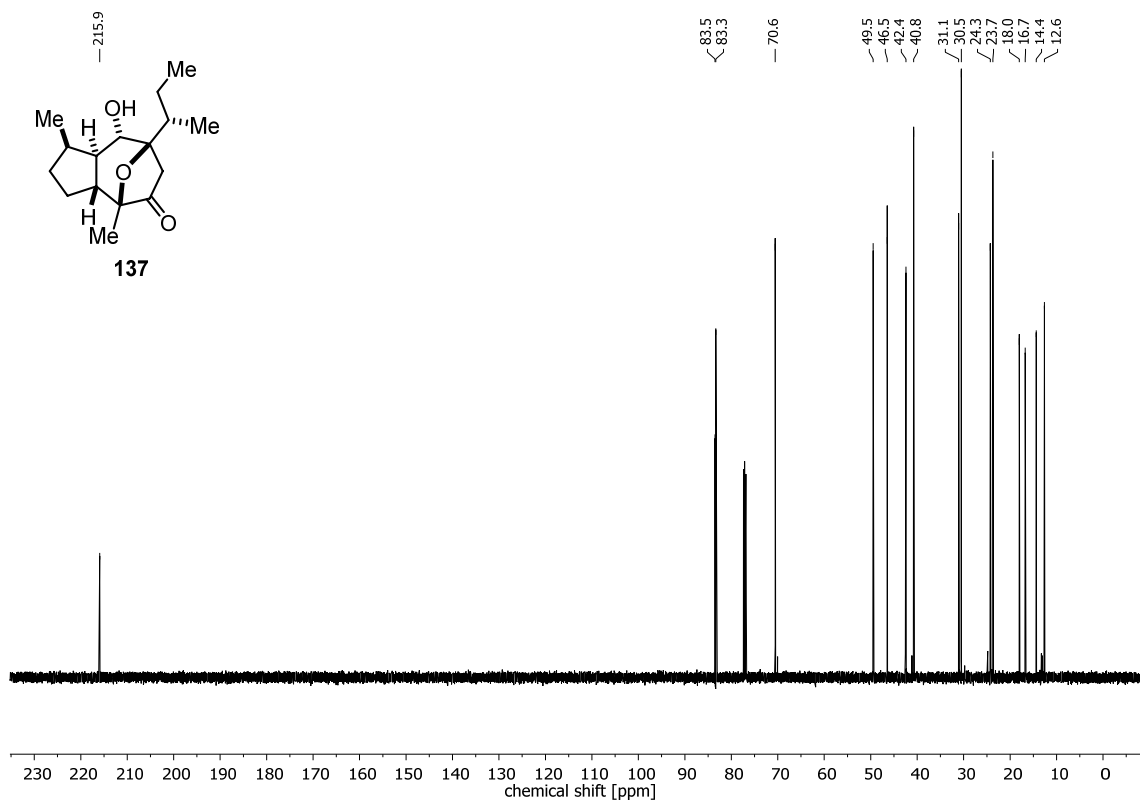
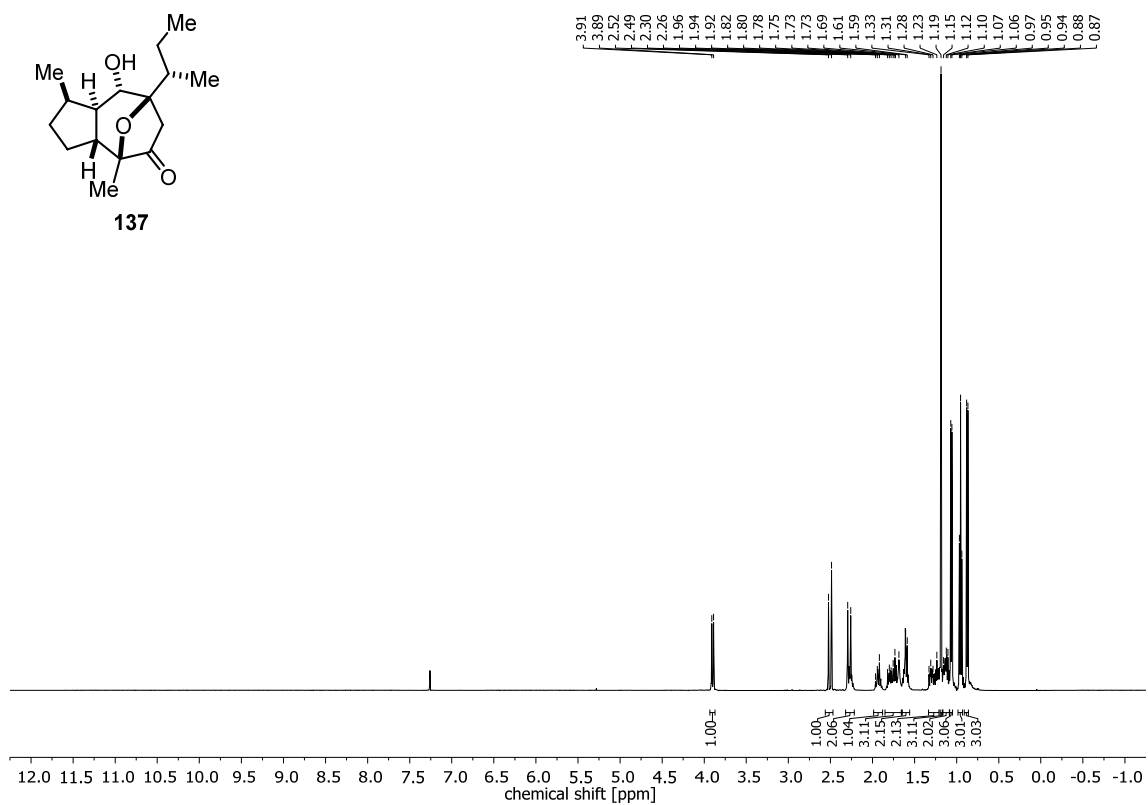


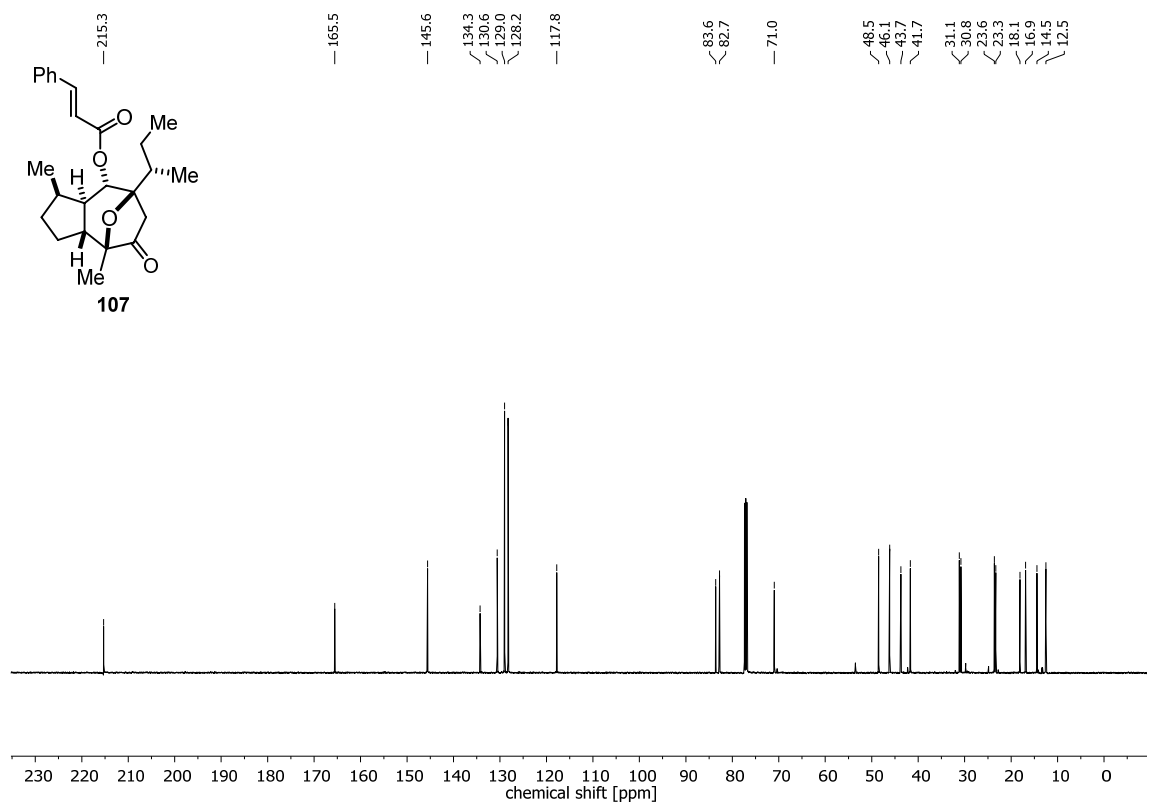
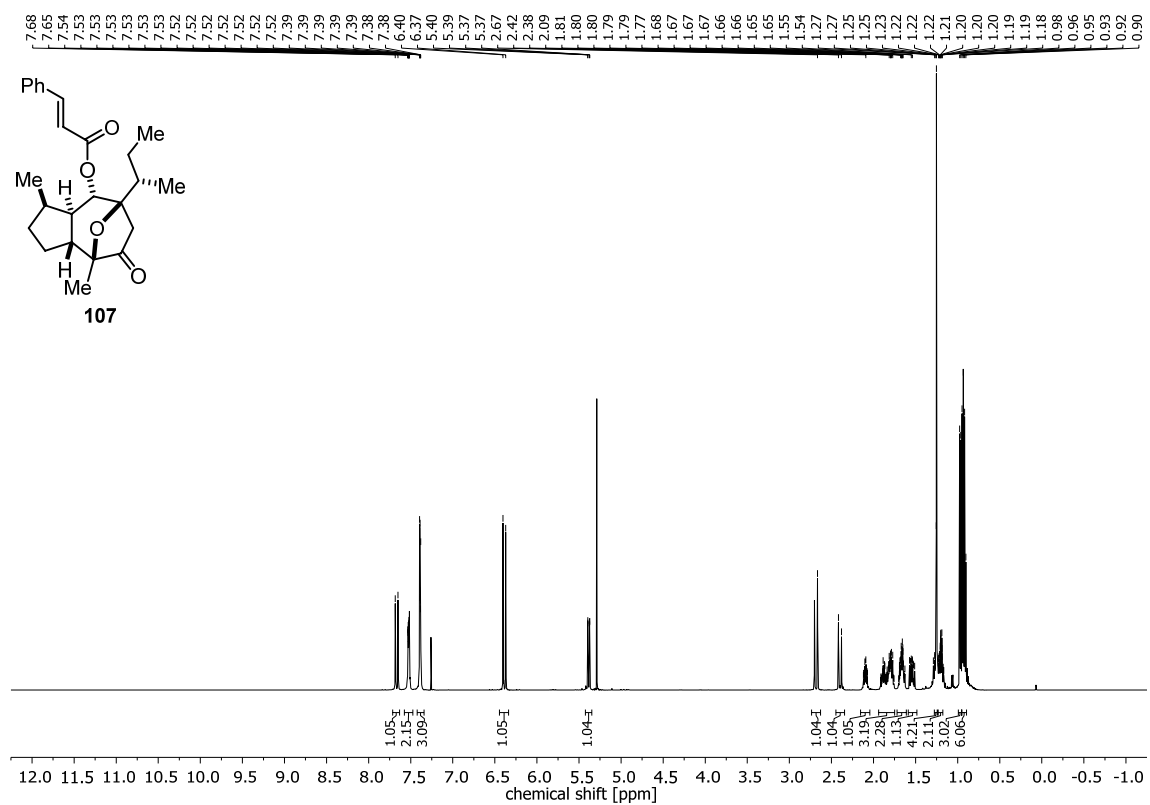
Appendix



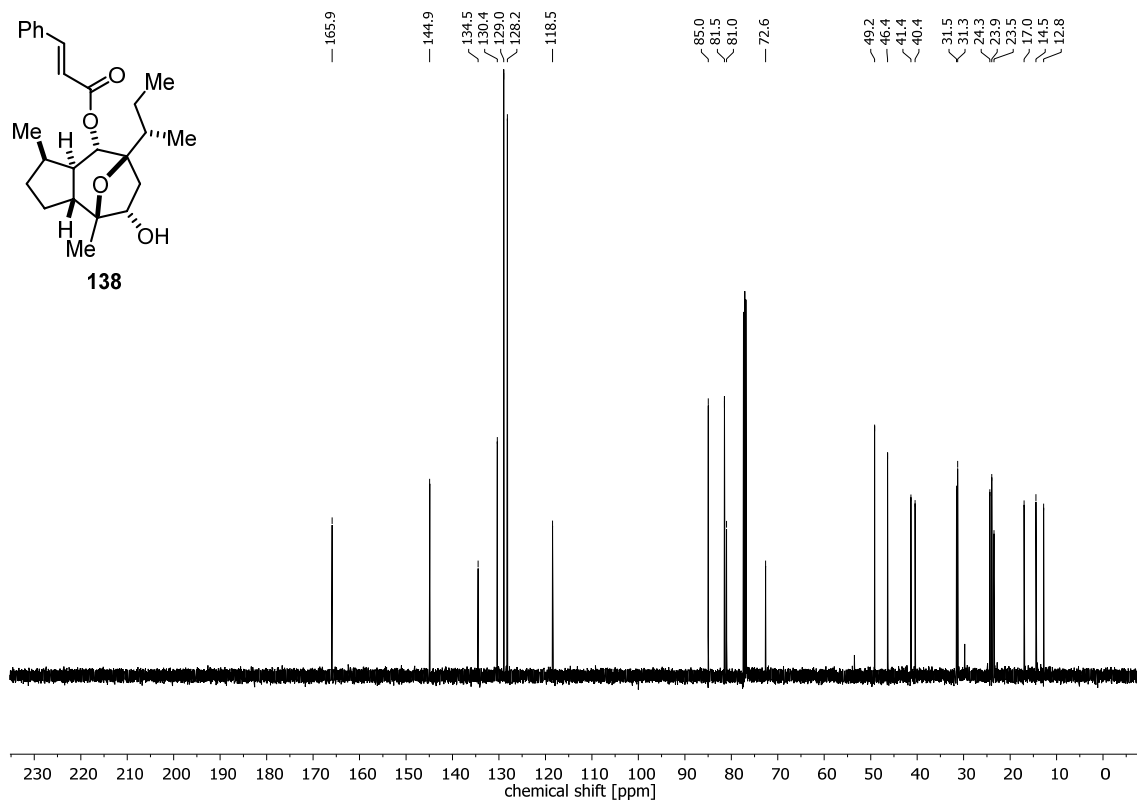
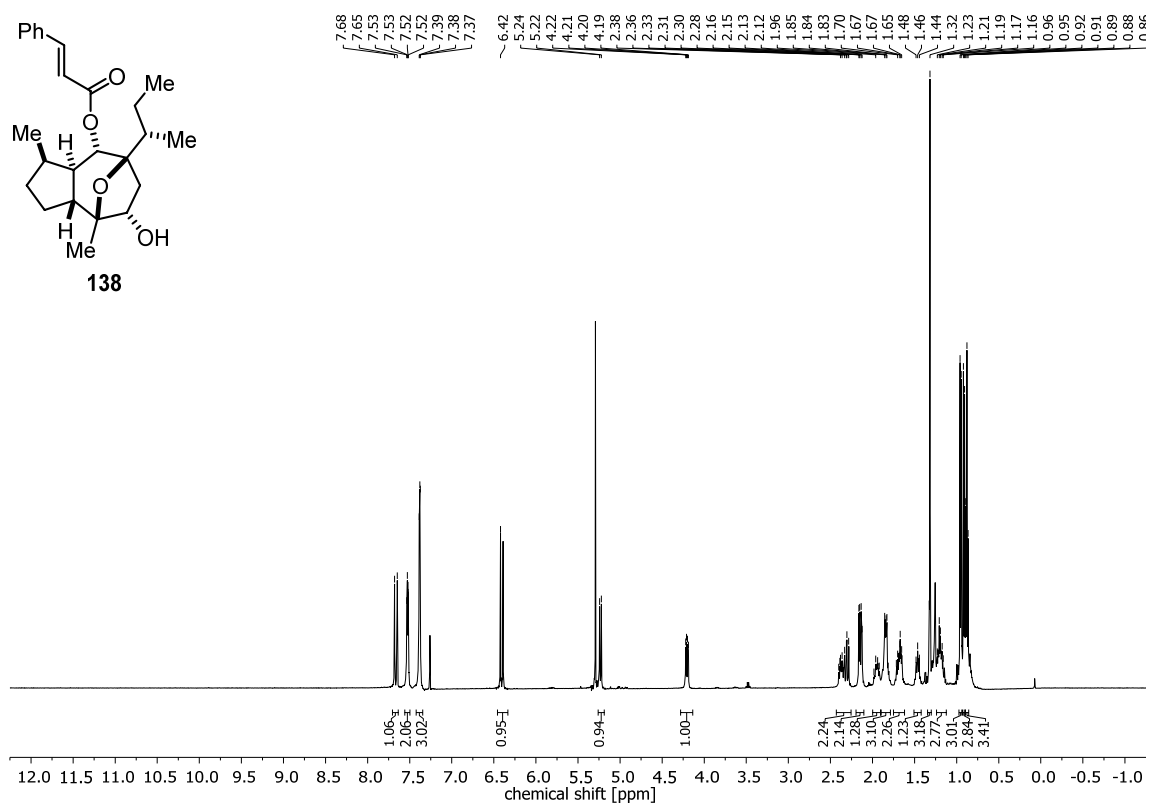


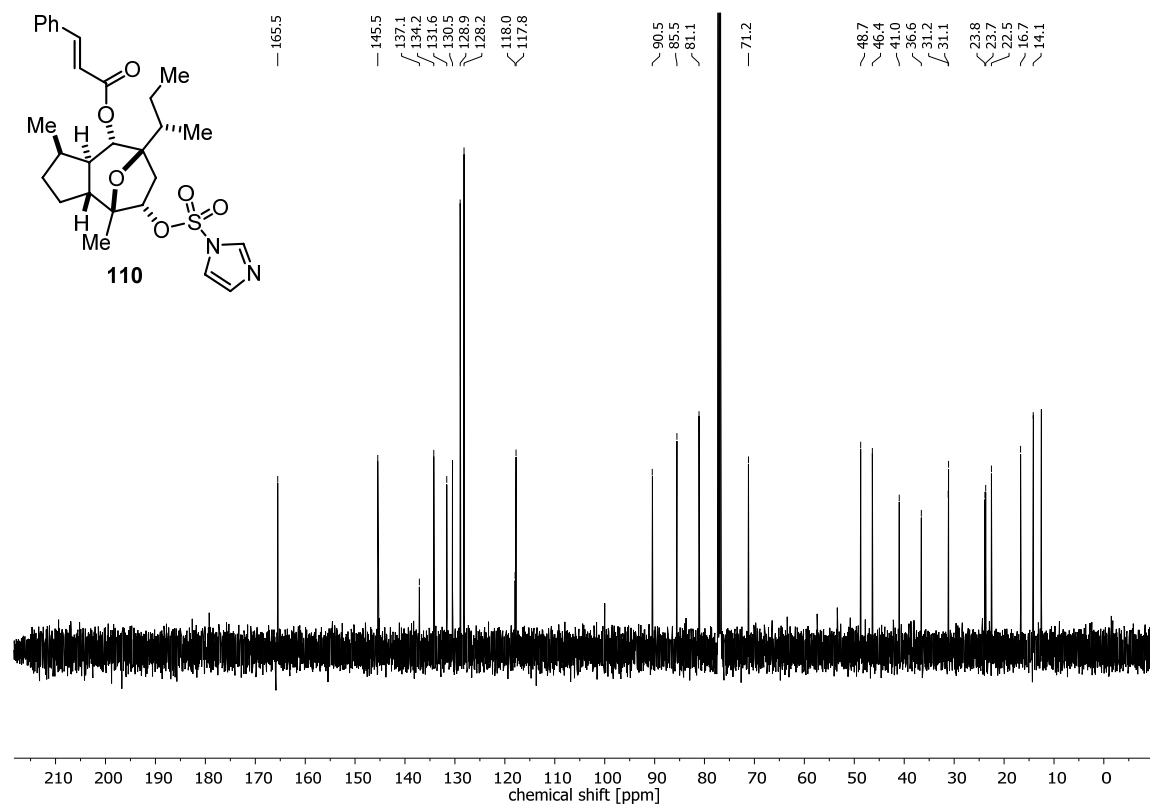
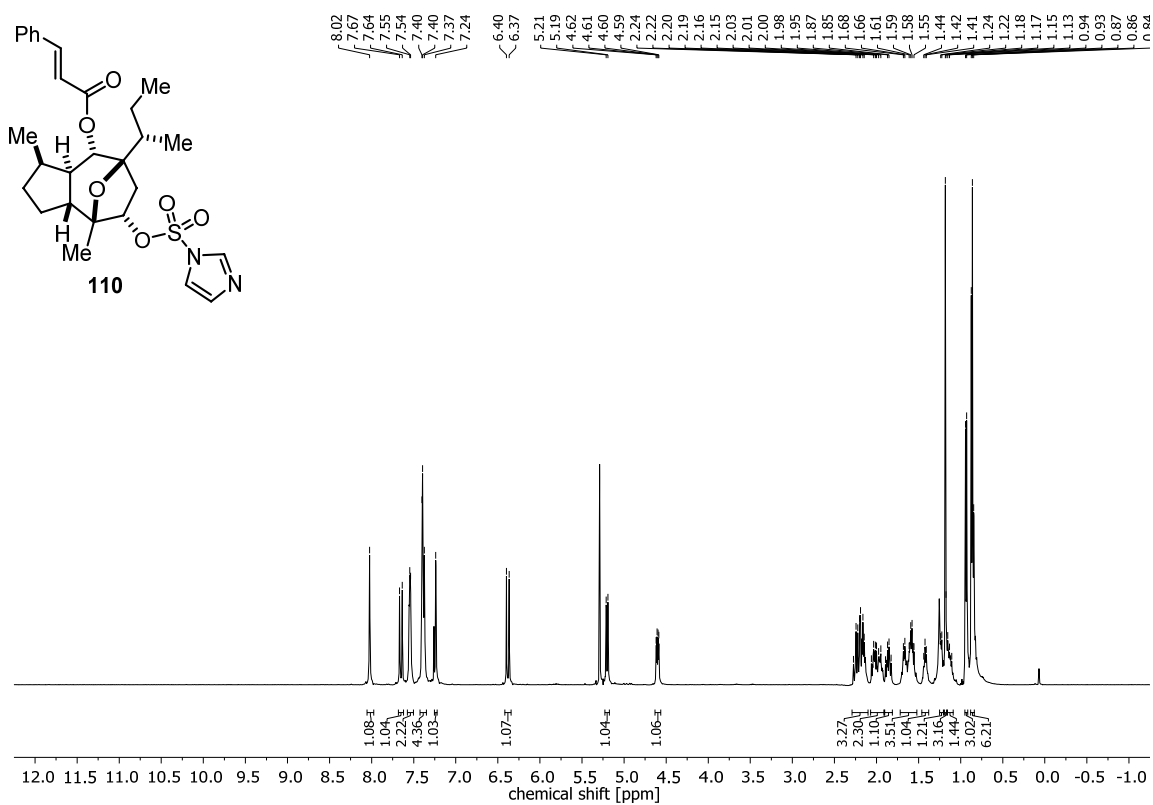
Appendix



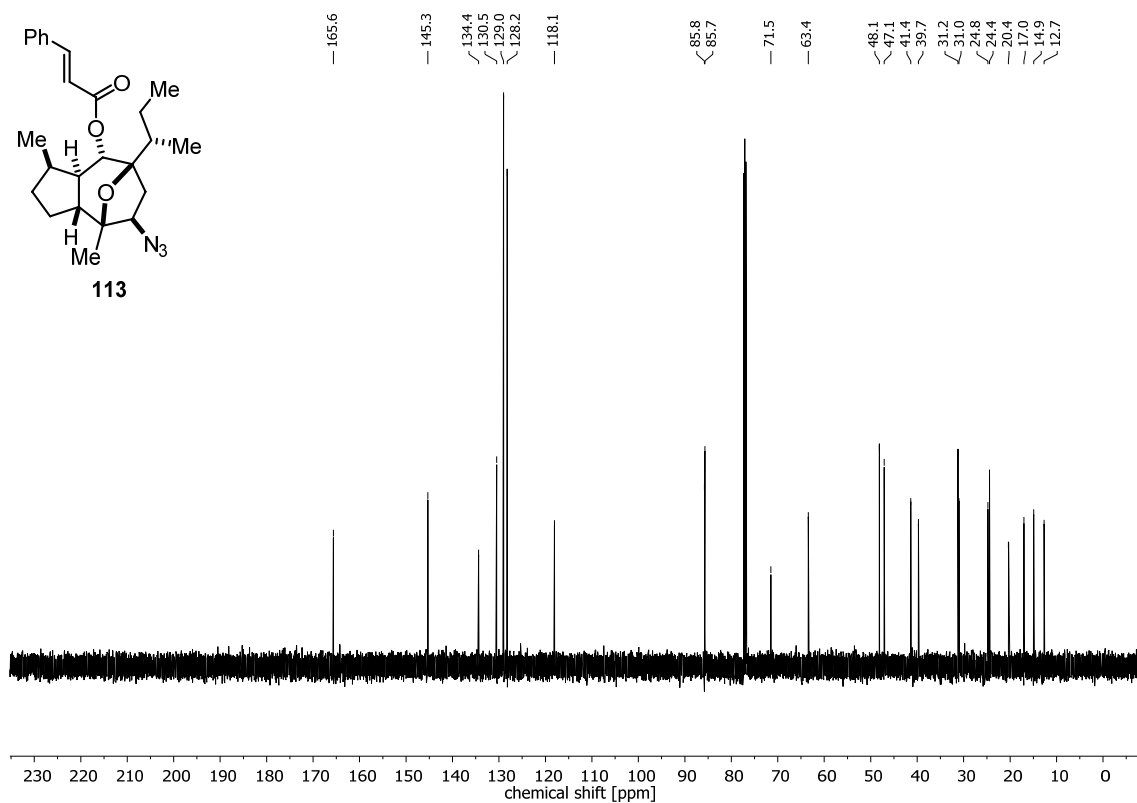
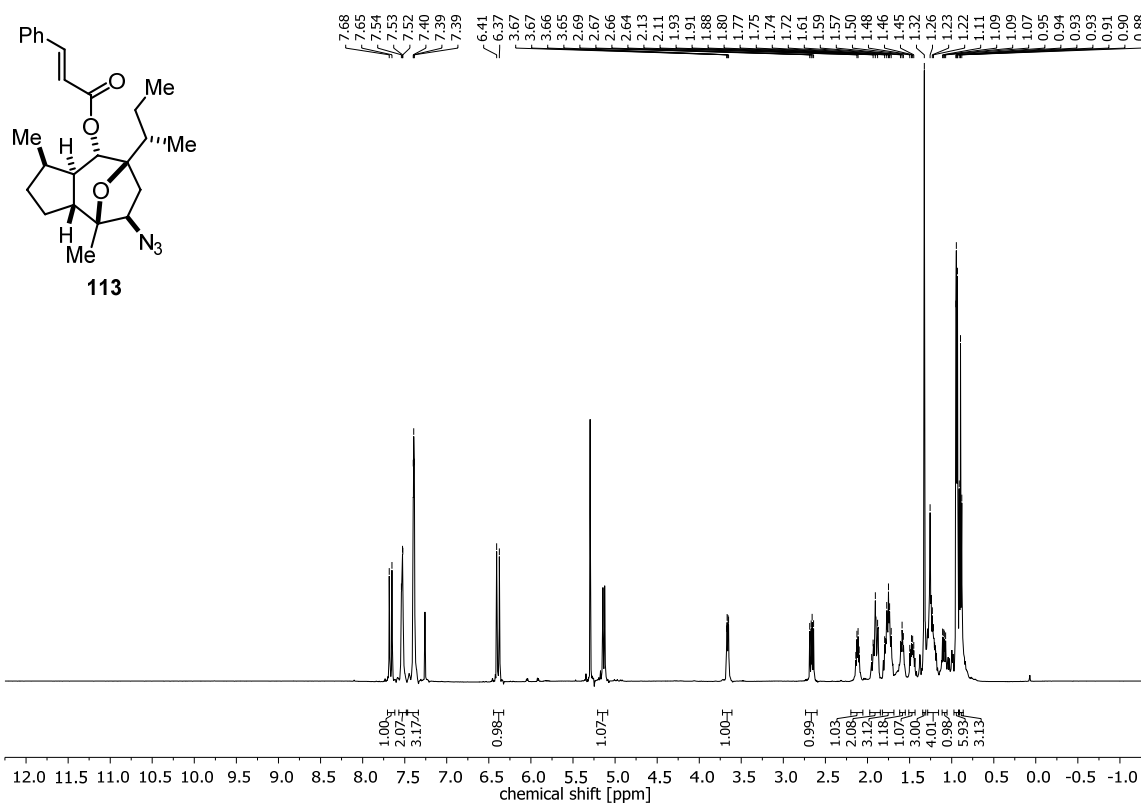


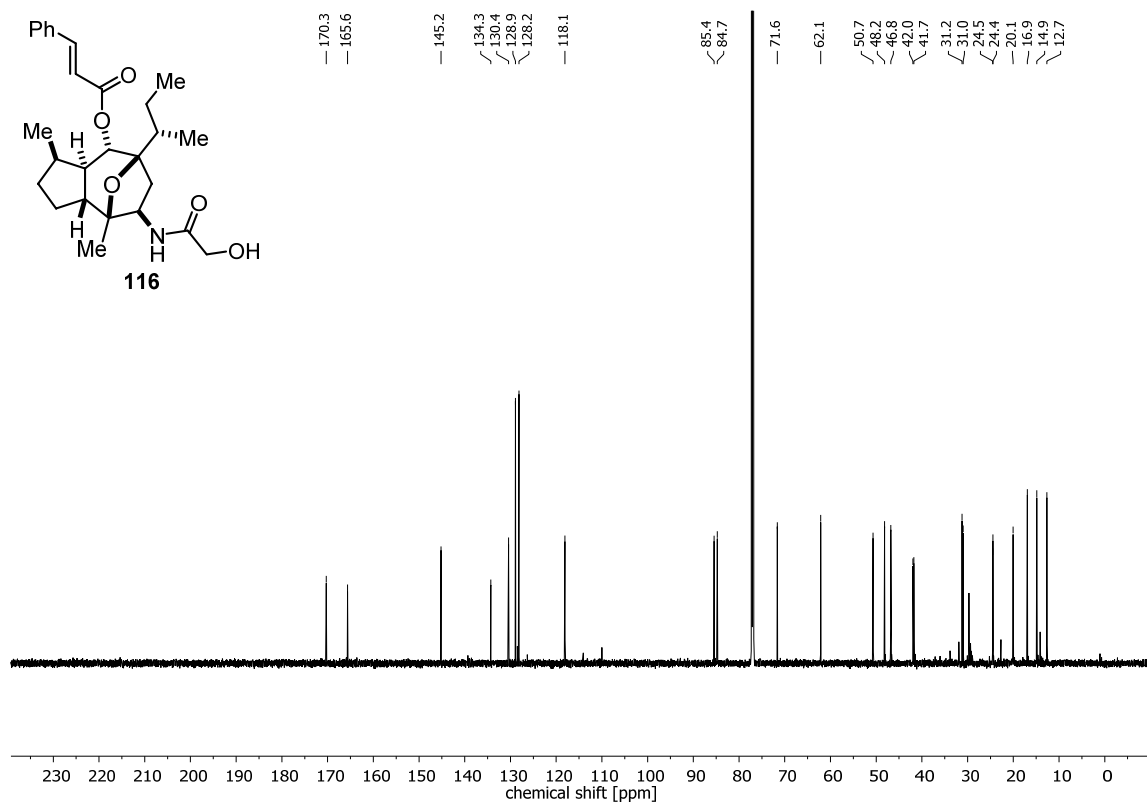
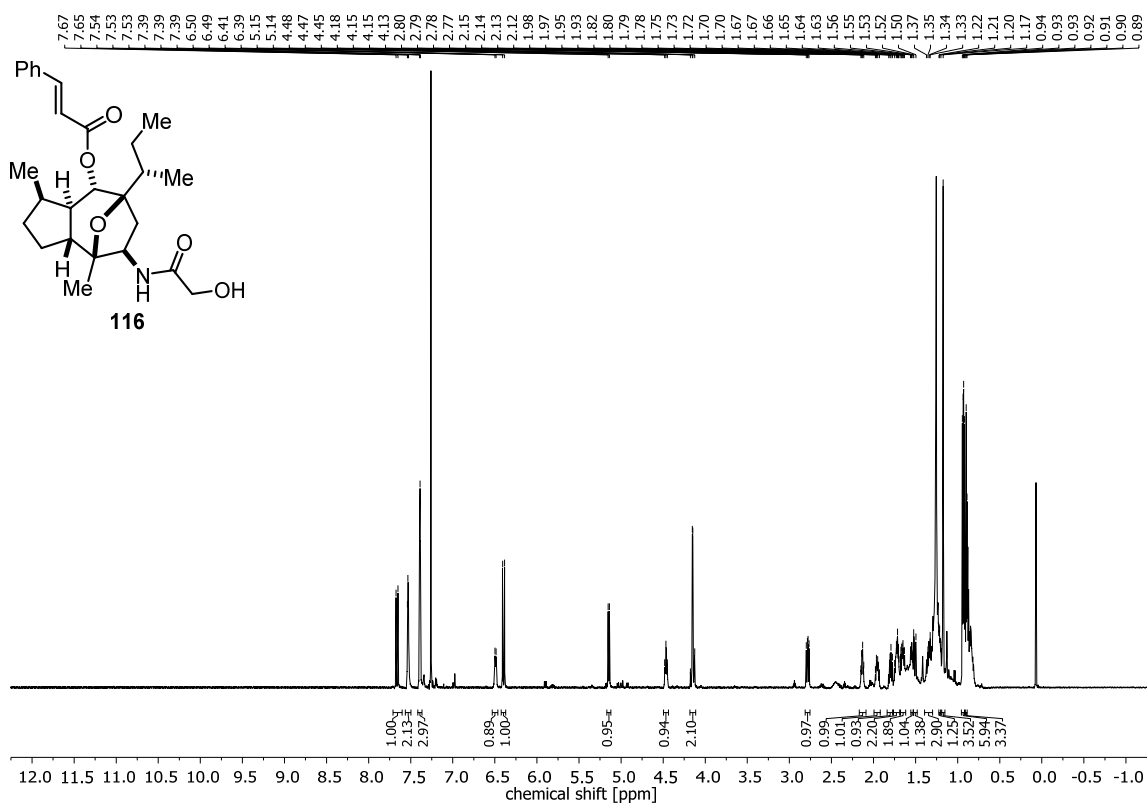
Appendix



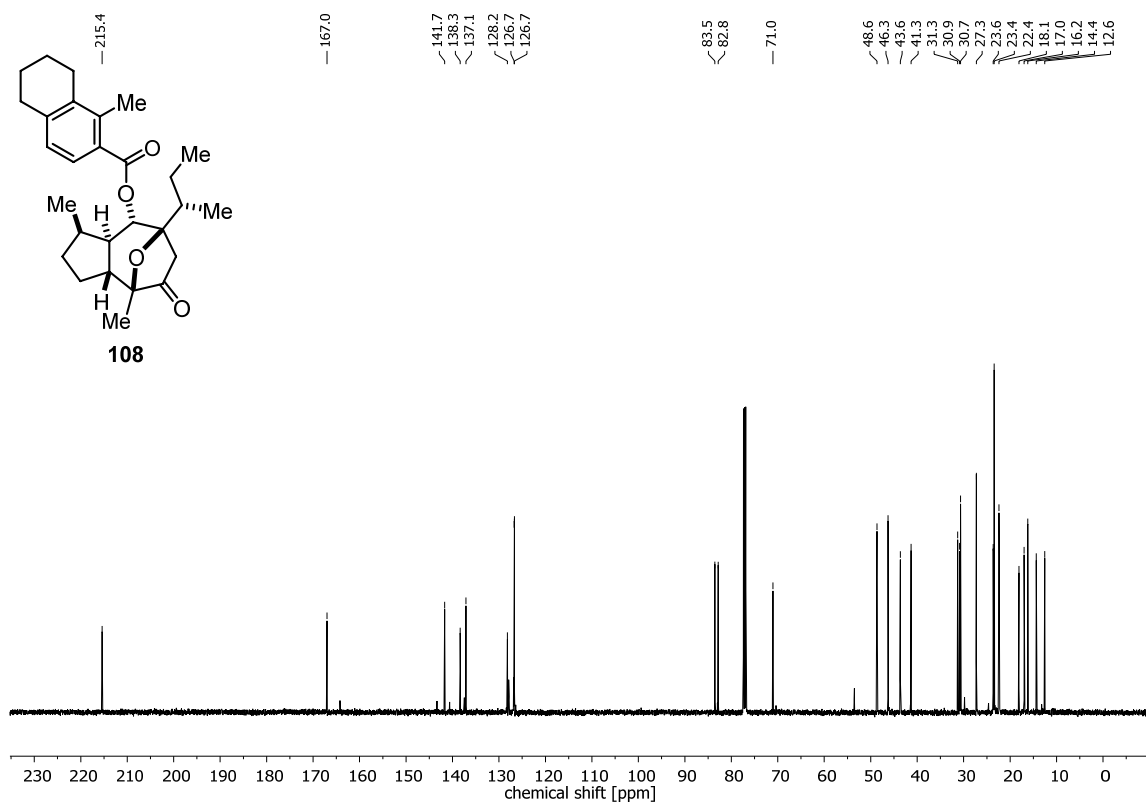
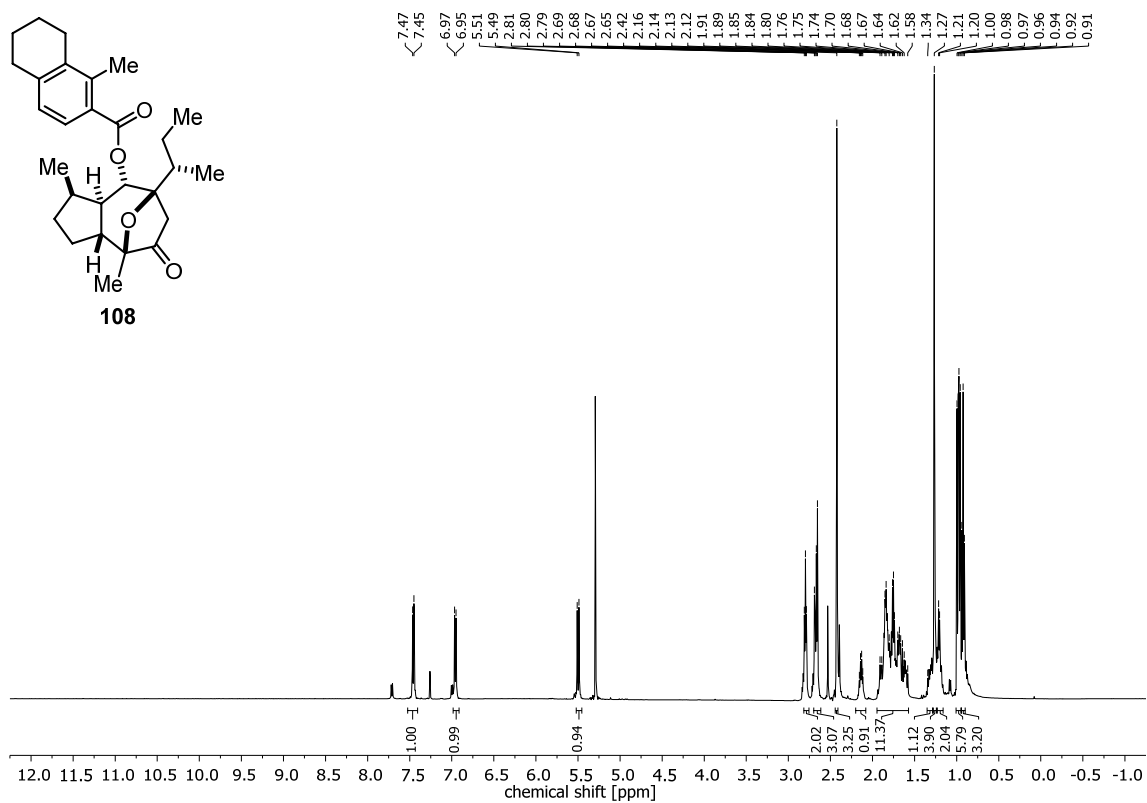


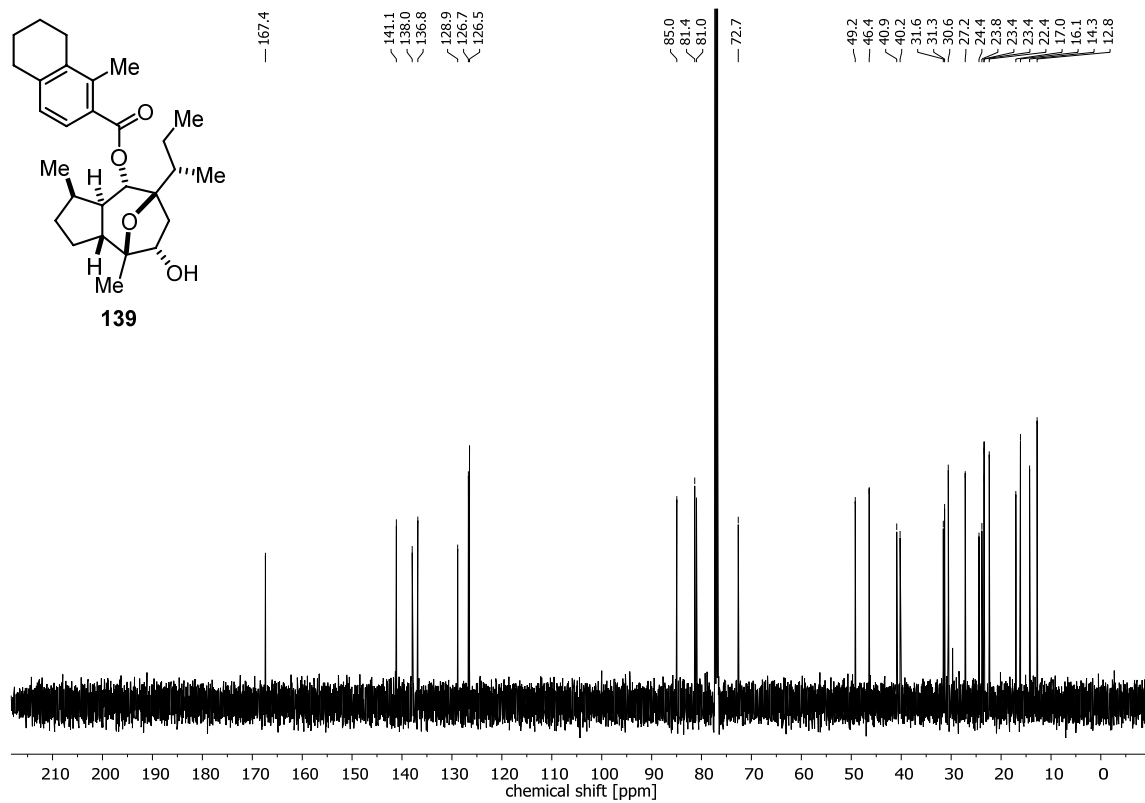
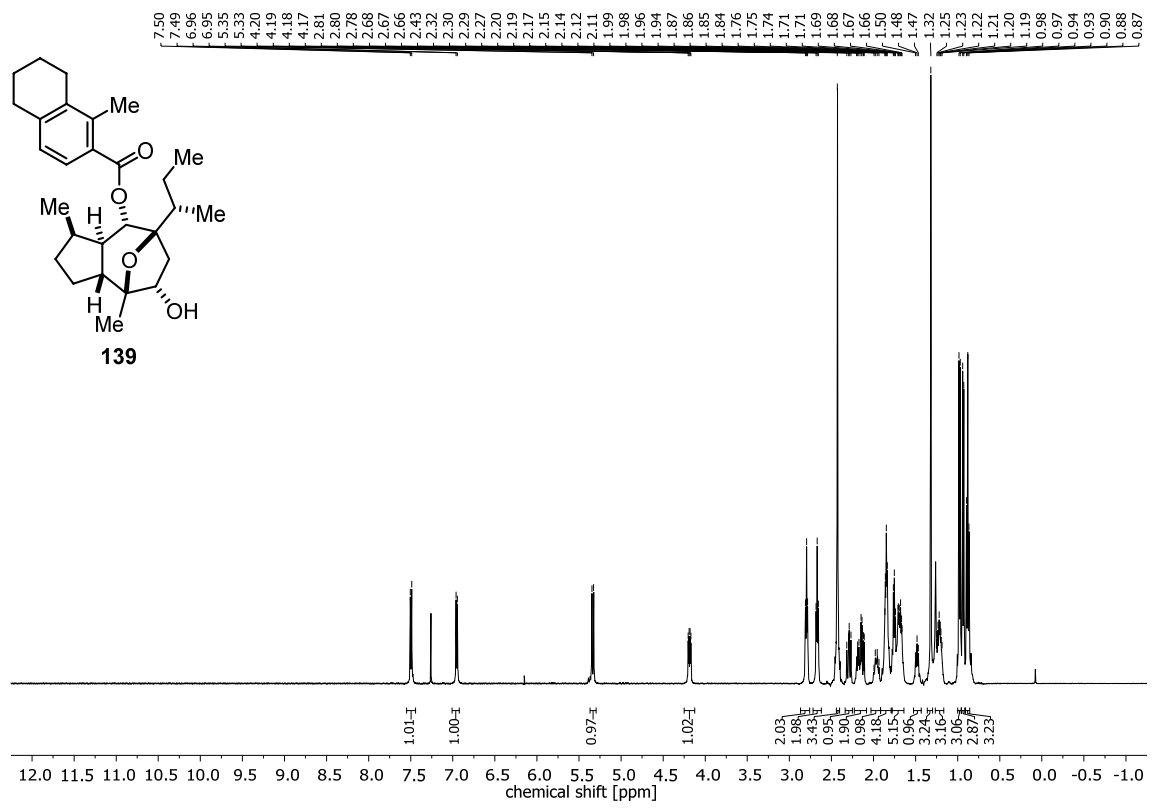
Appendix



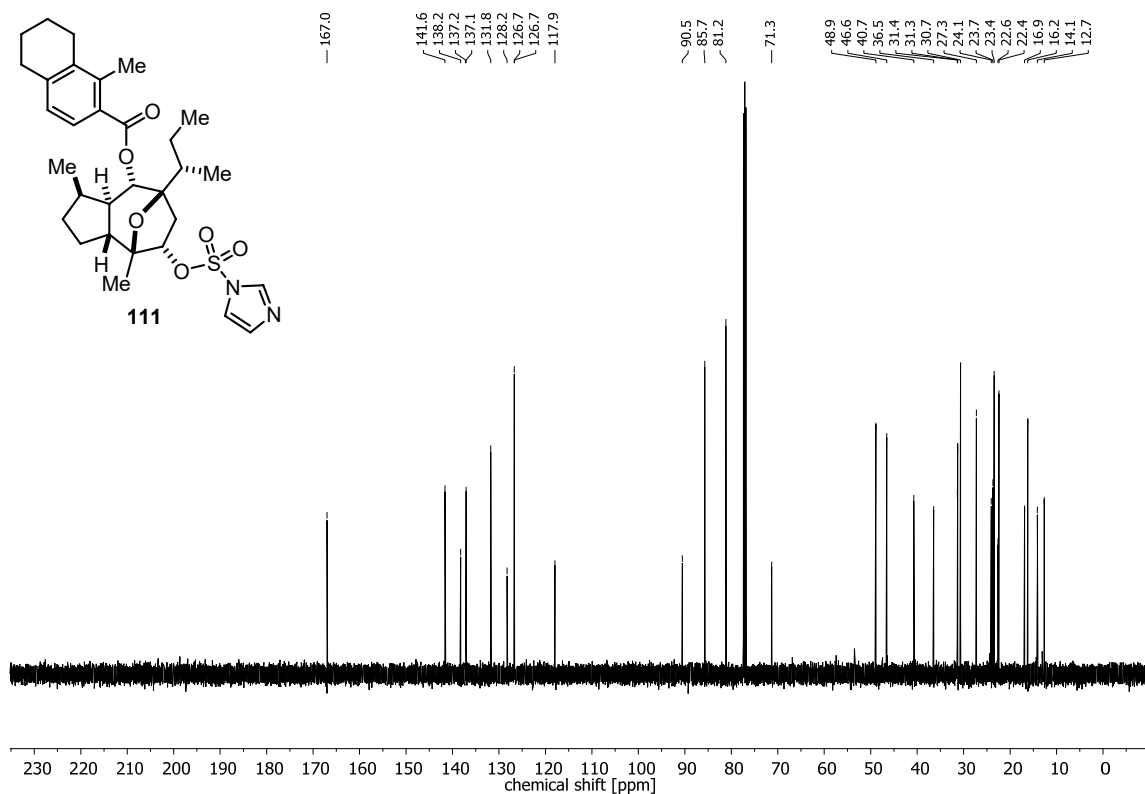
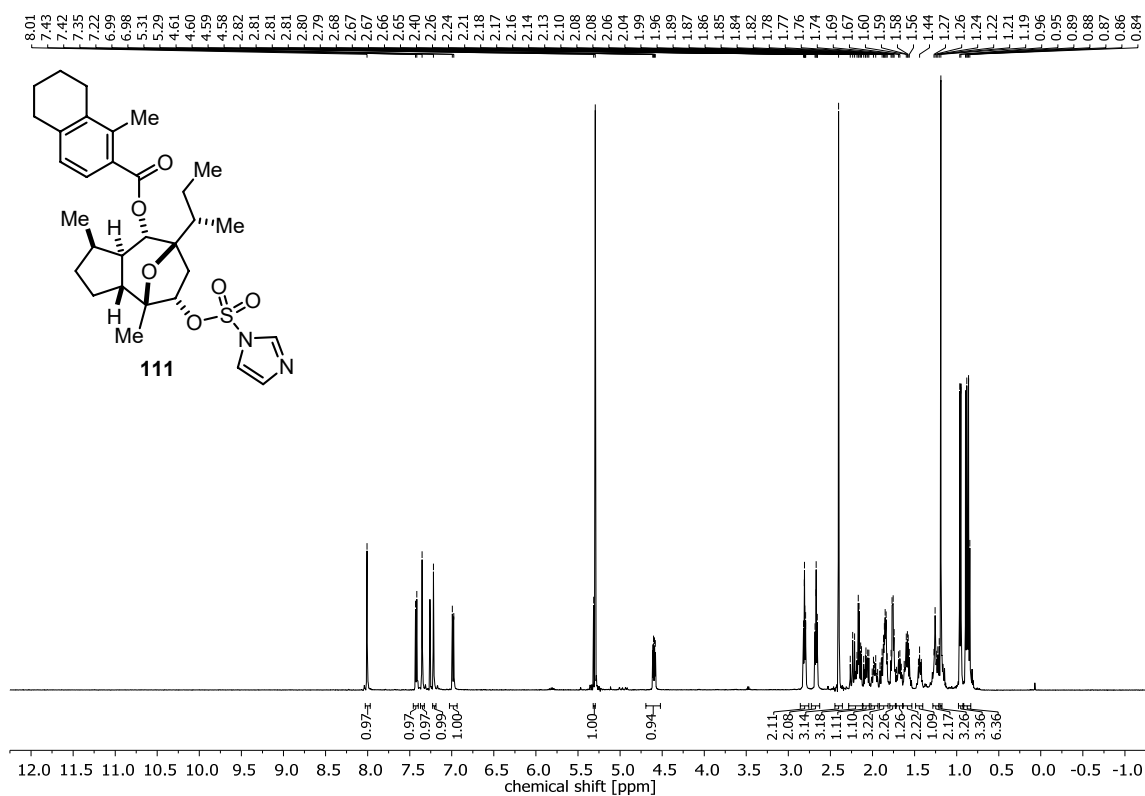


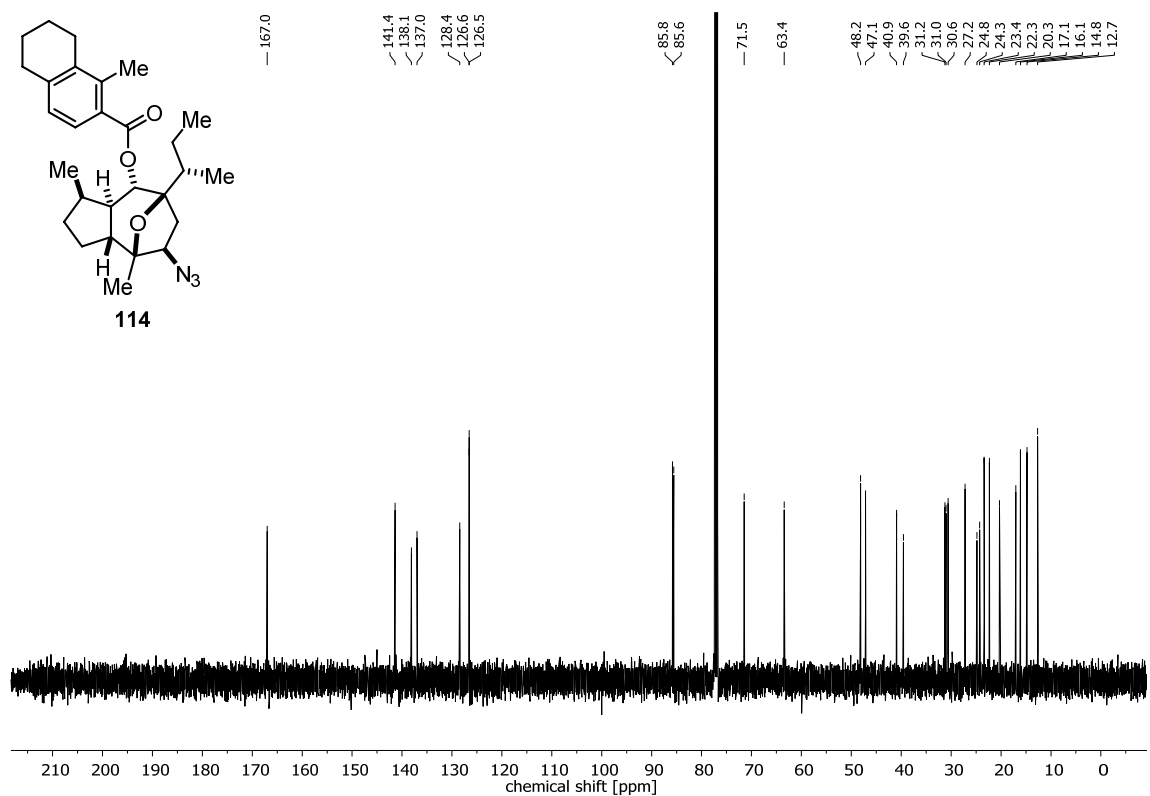
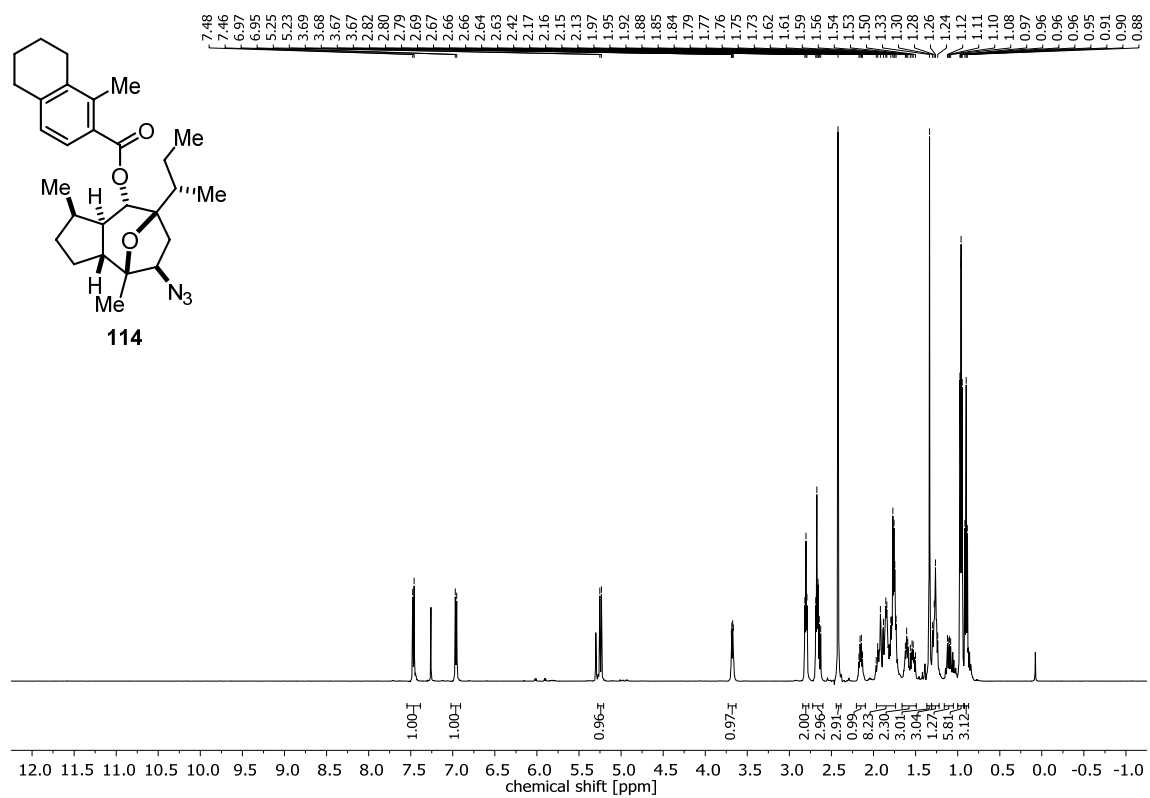
Appendix



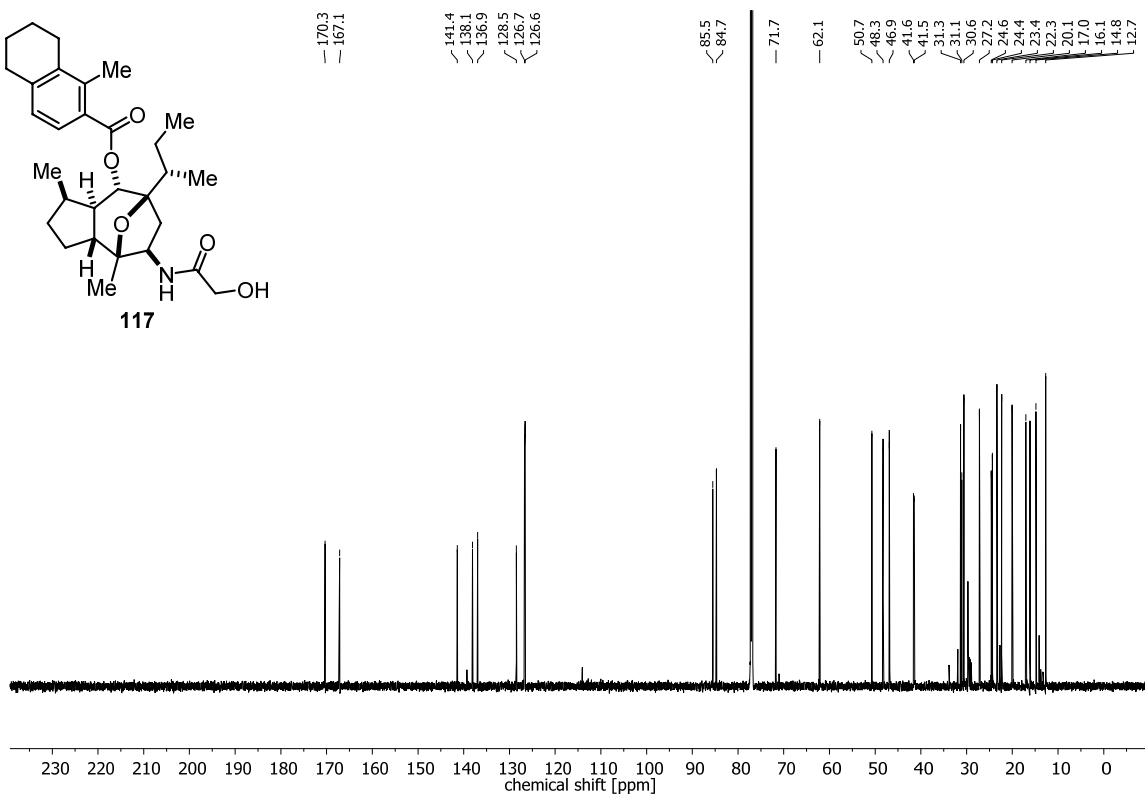
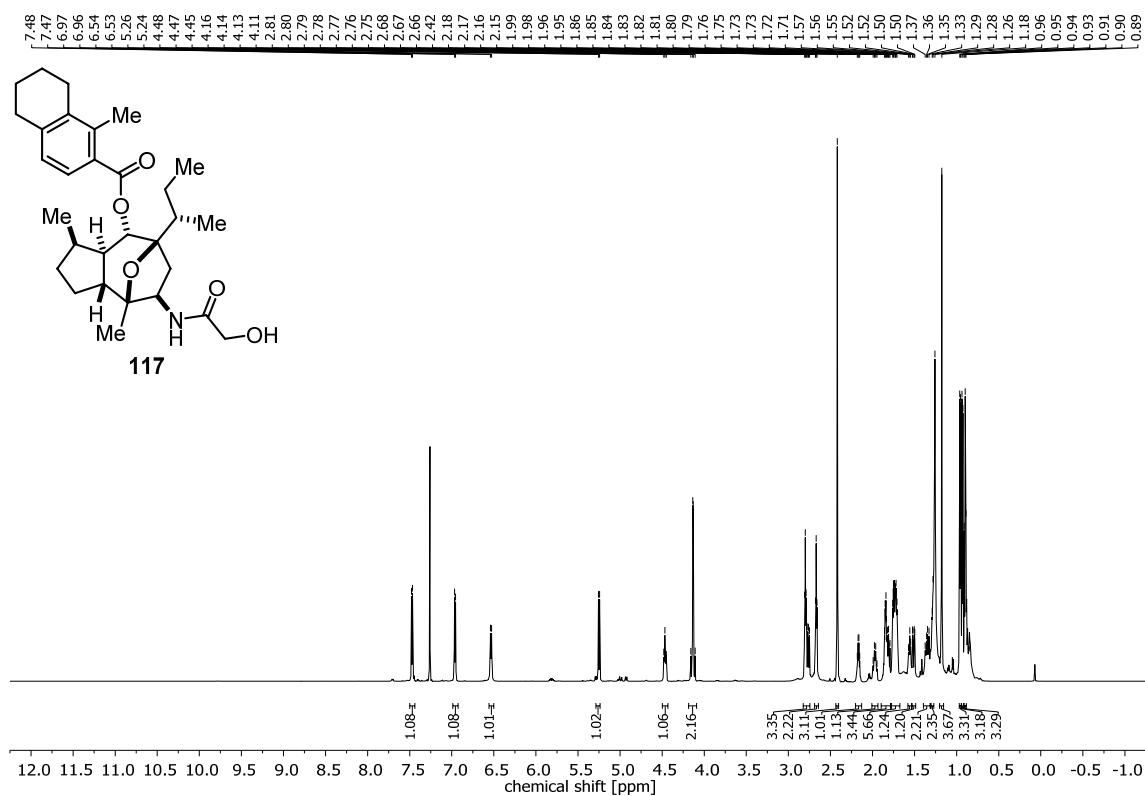


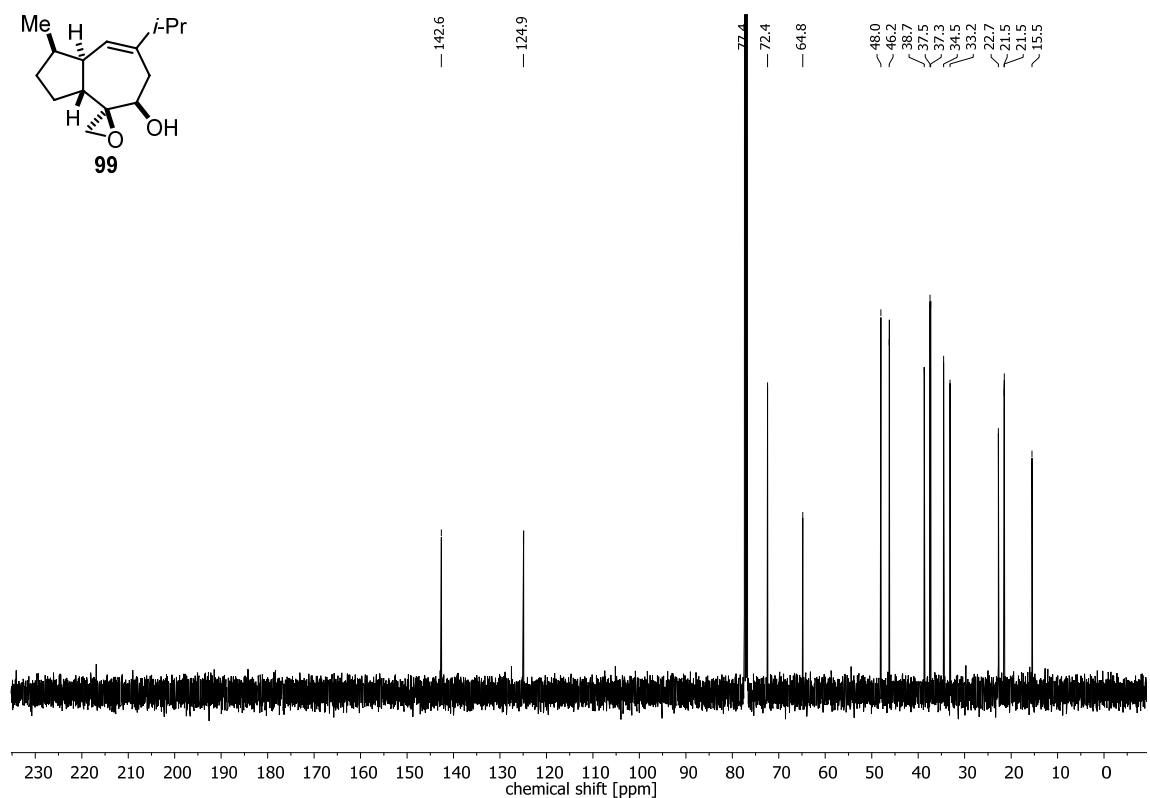
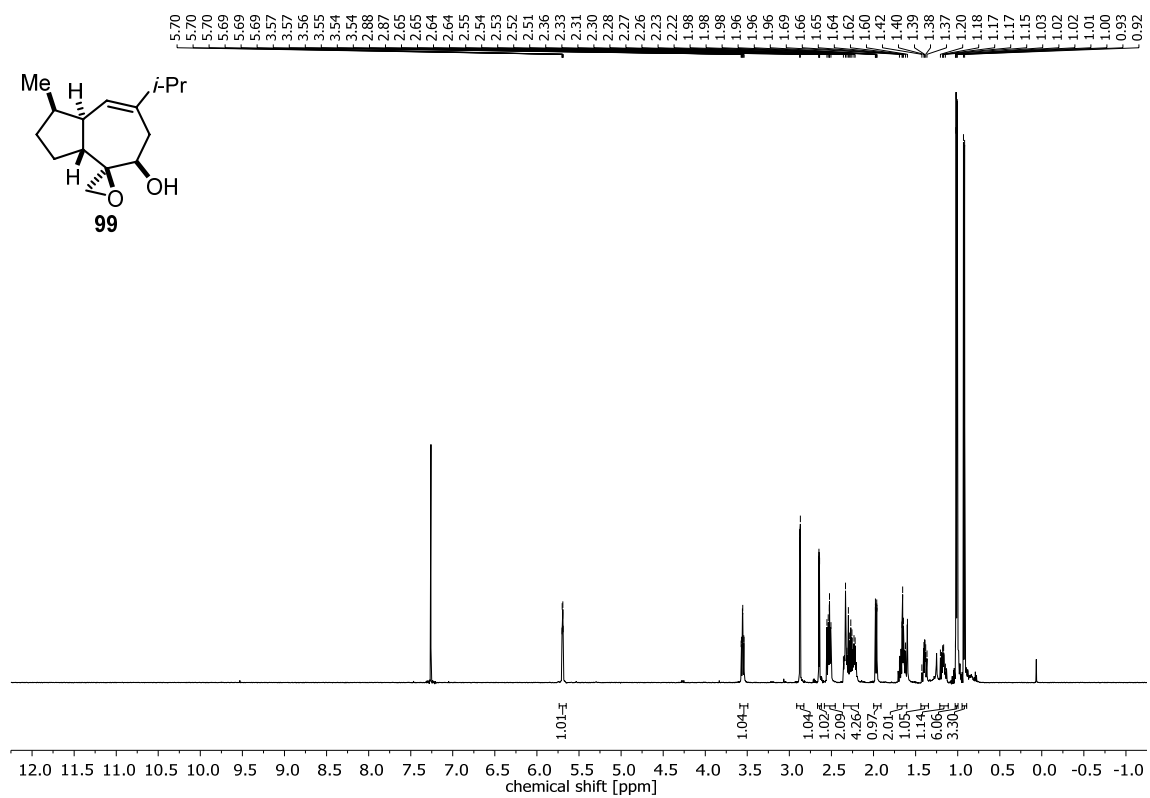
Appendix



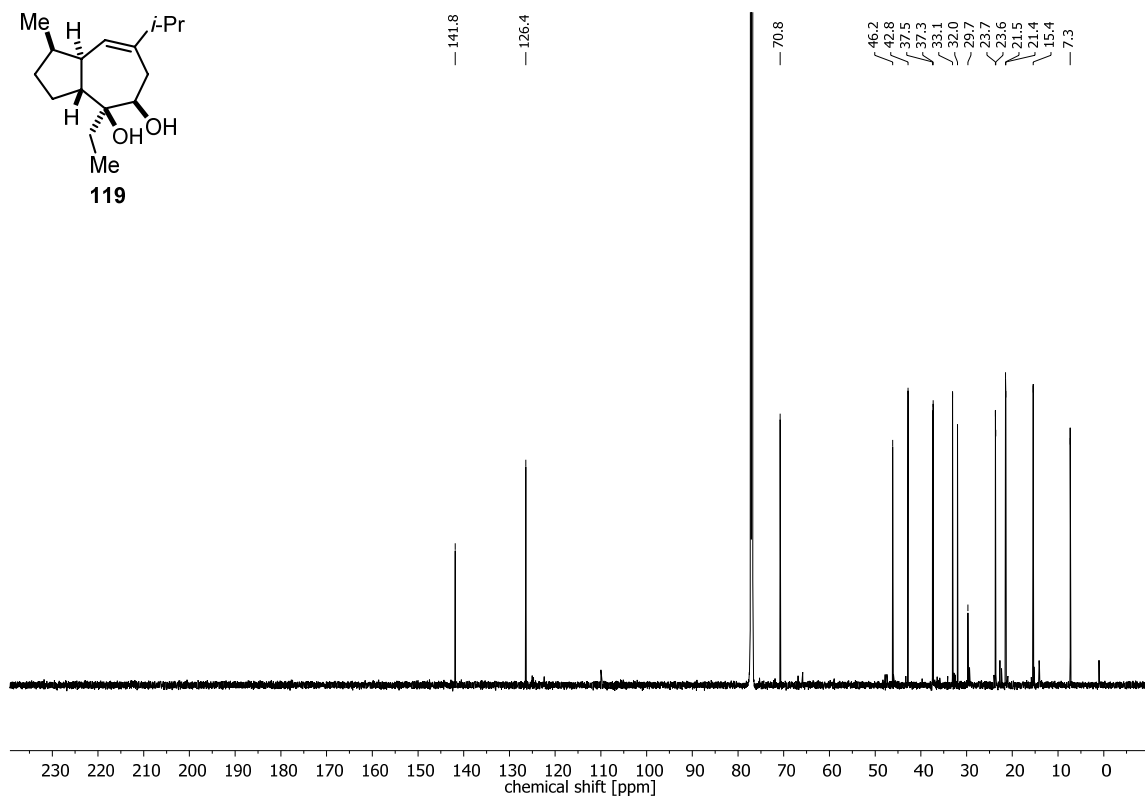
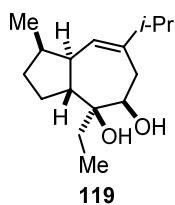
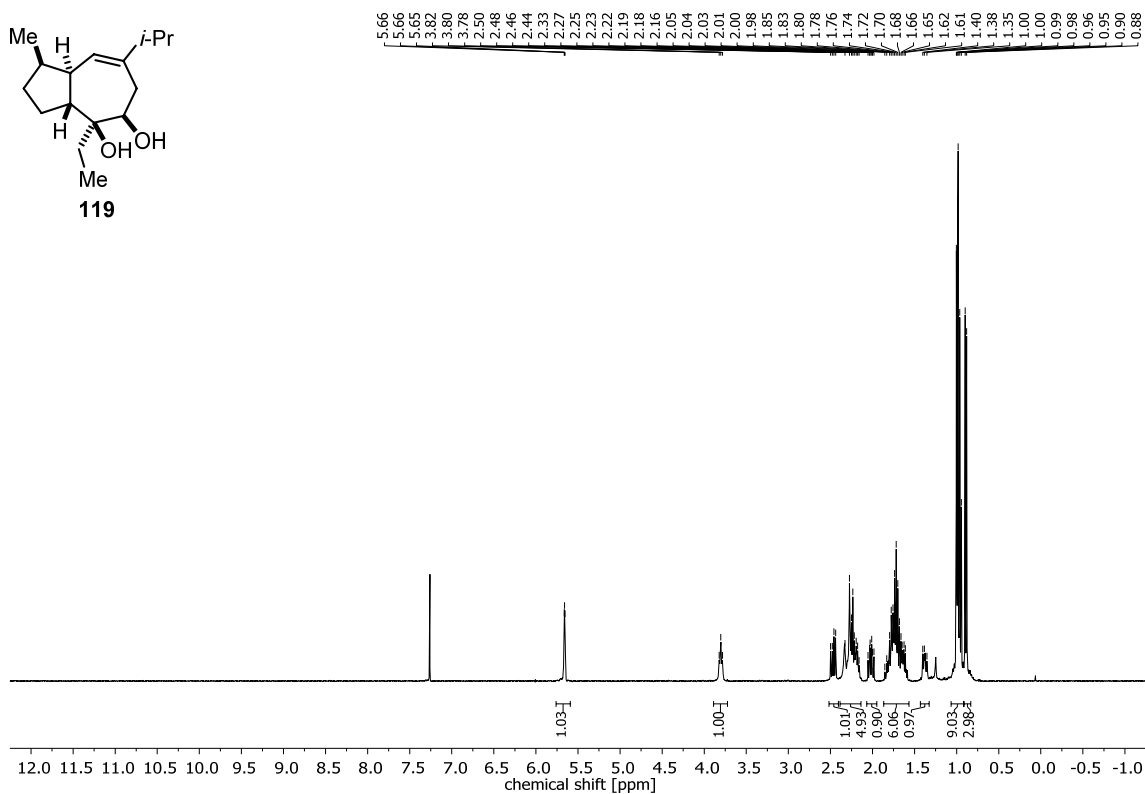
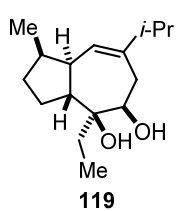


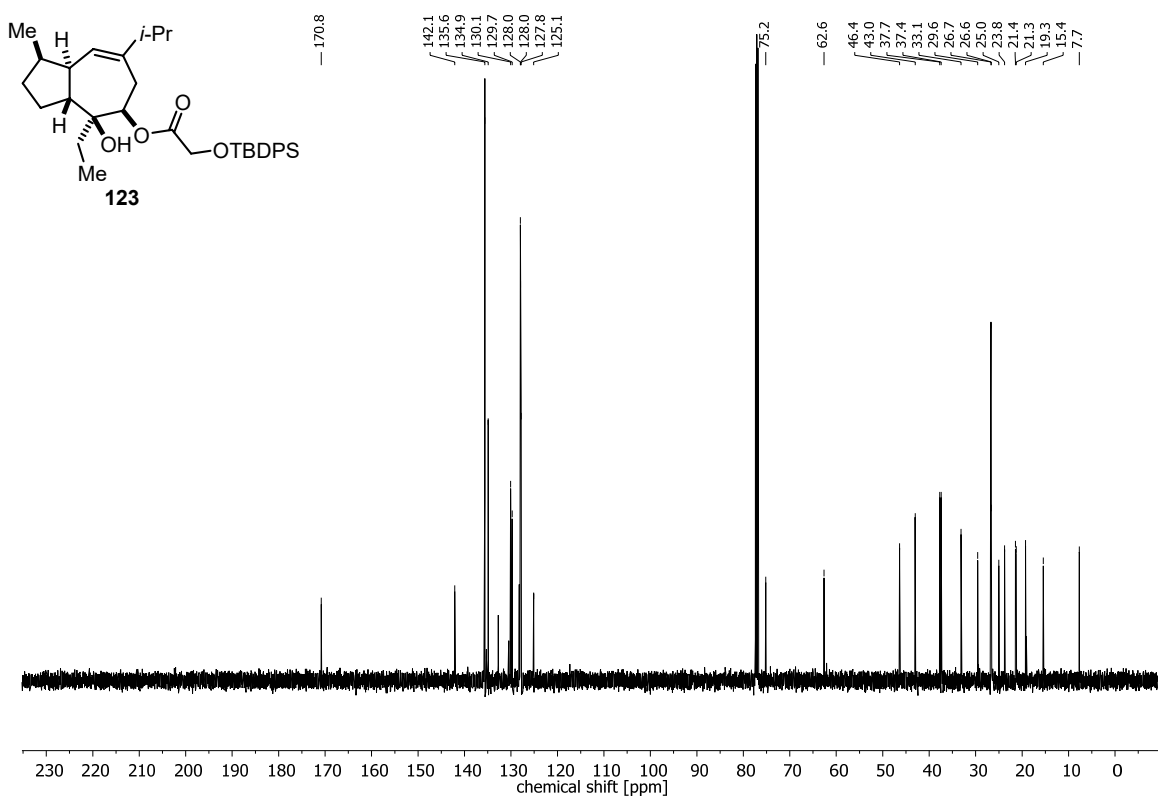
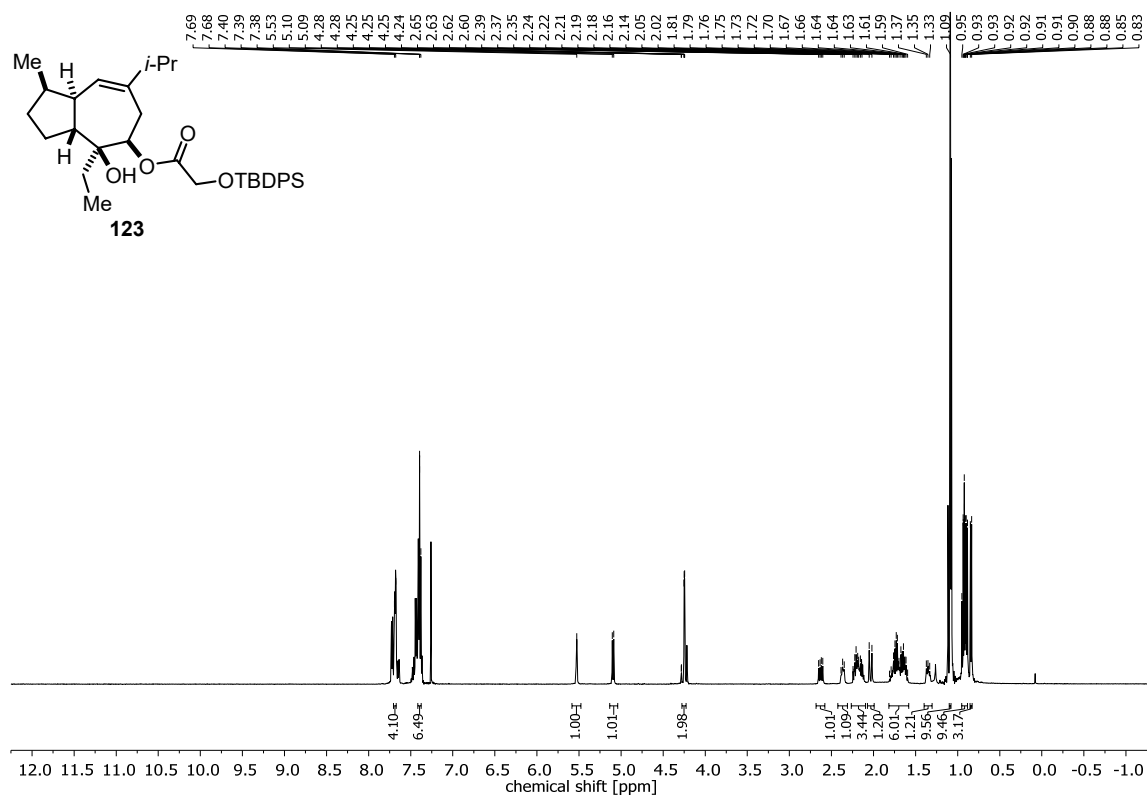
Appendix



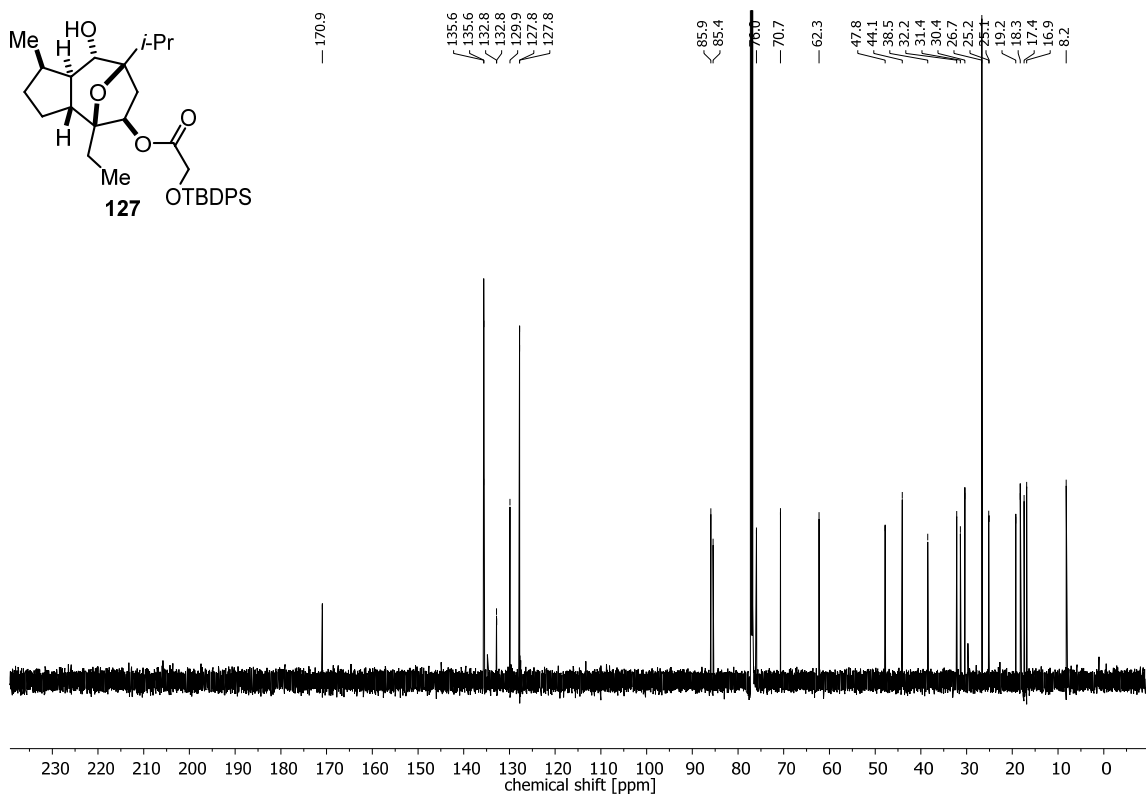
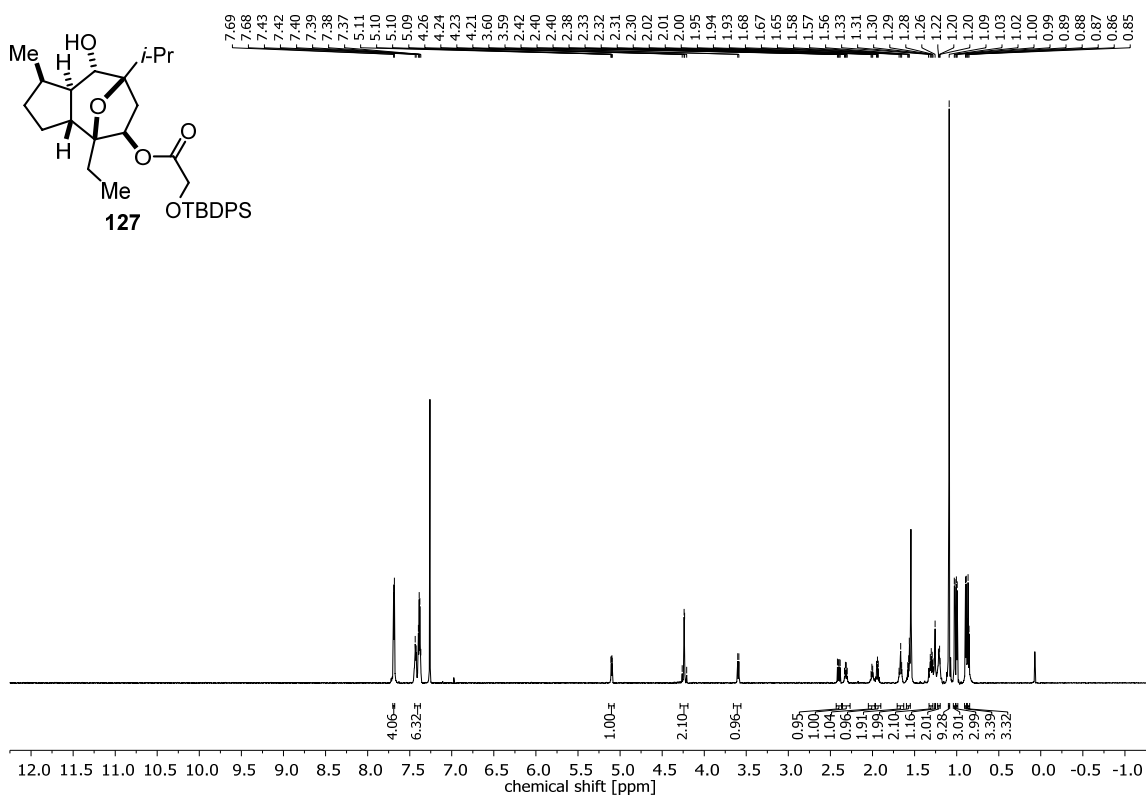


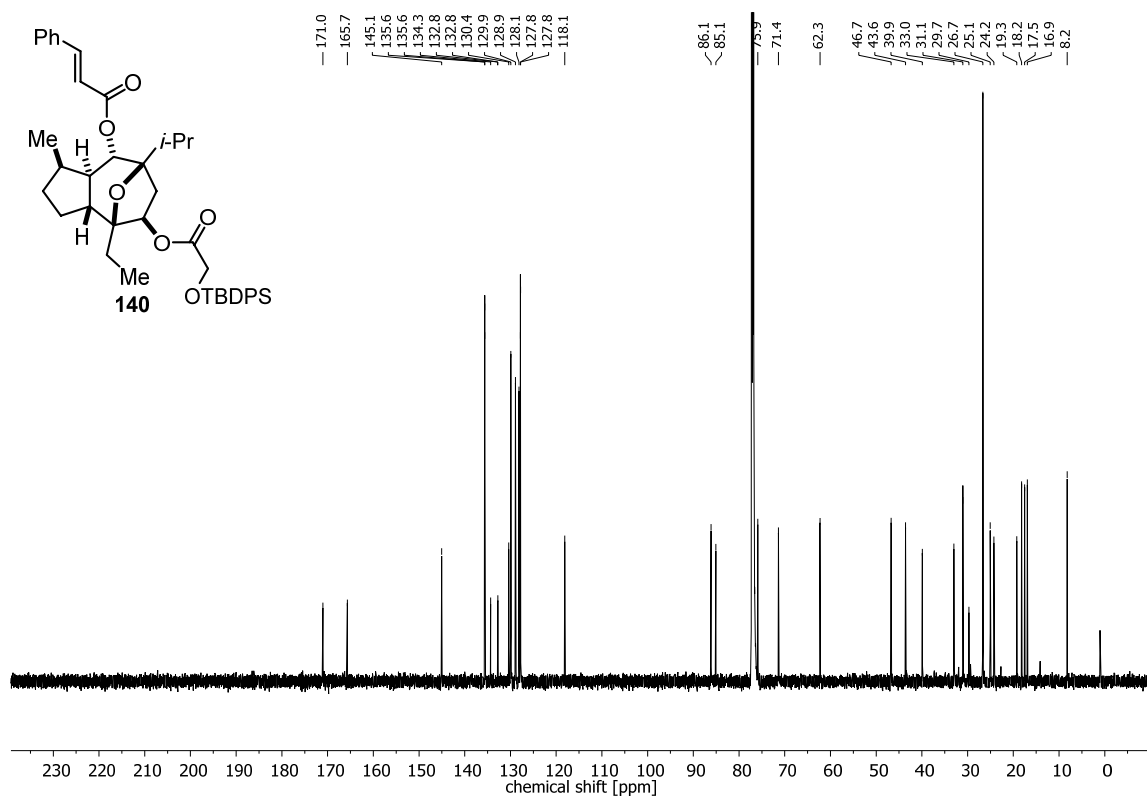
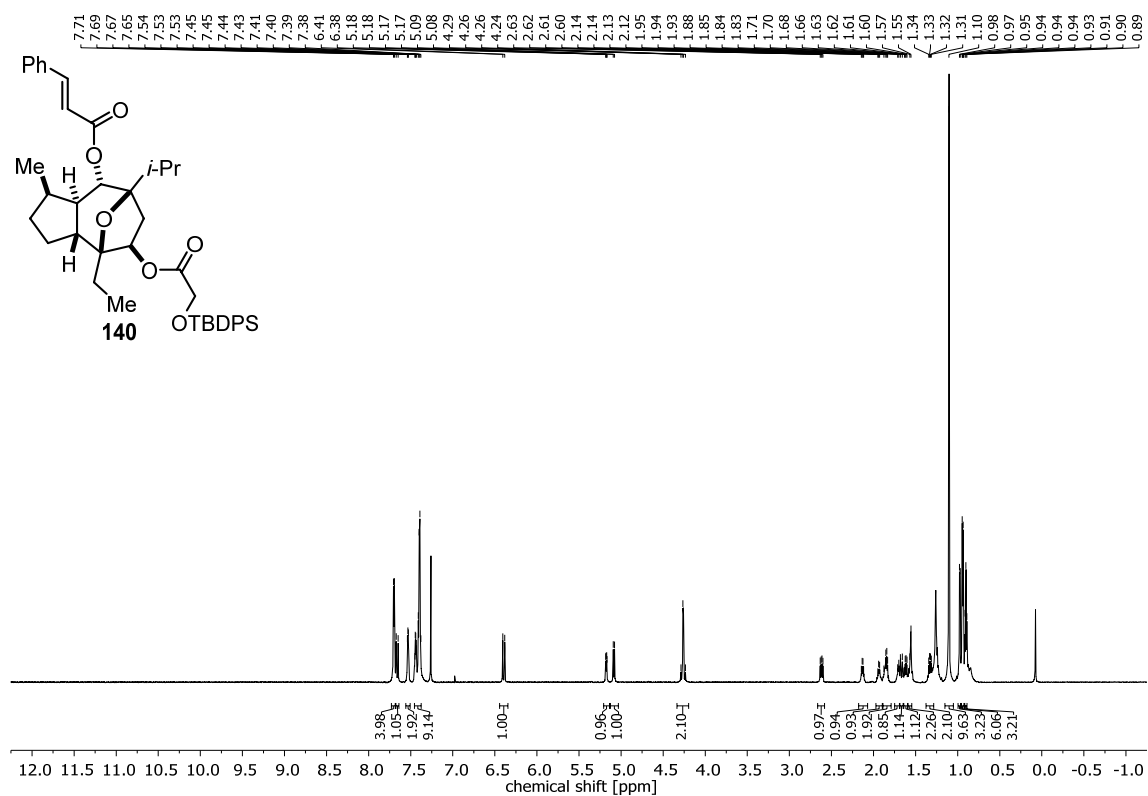
Appendix



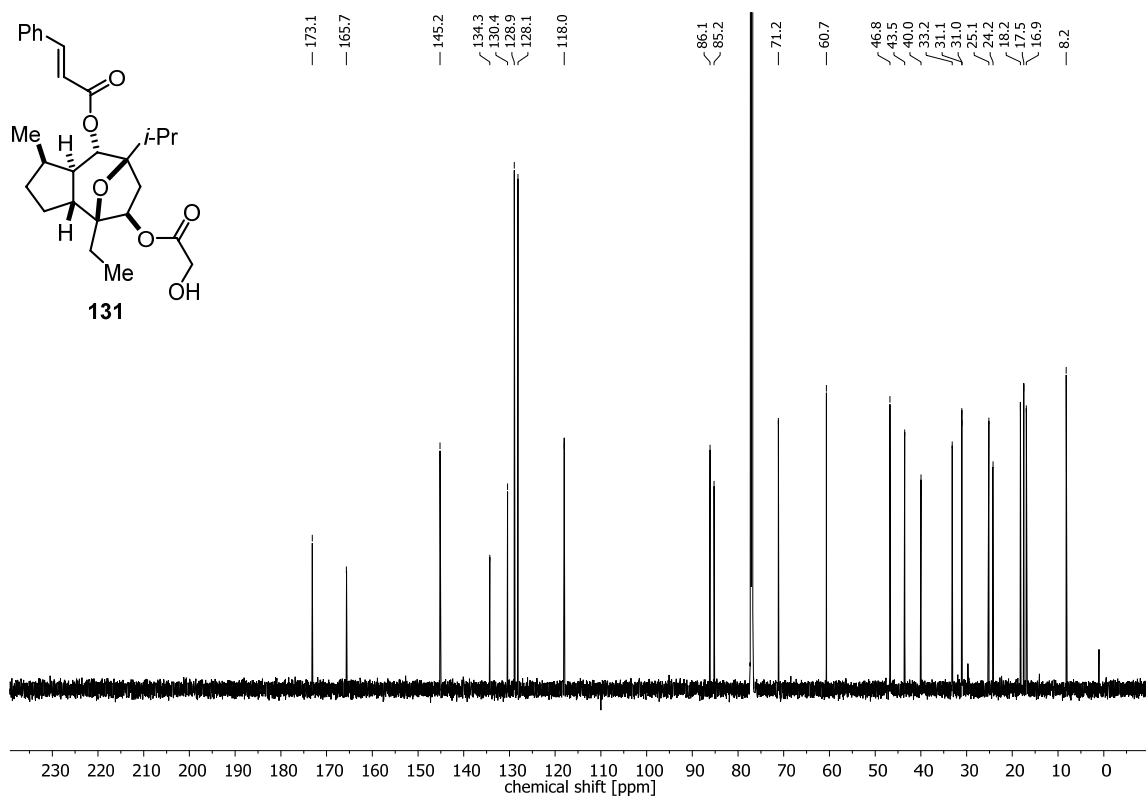
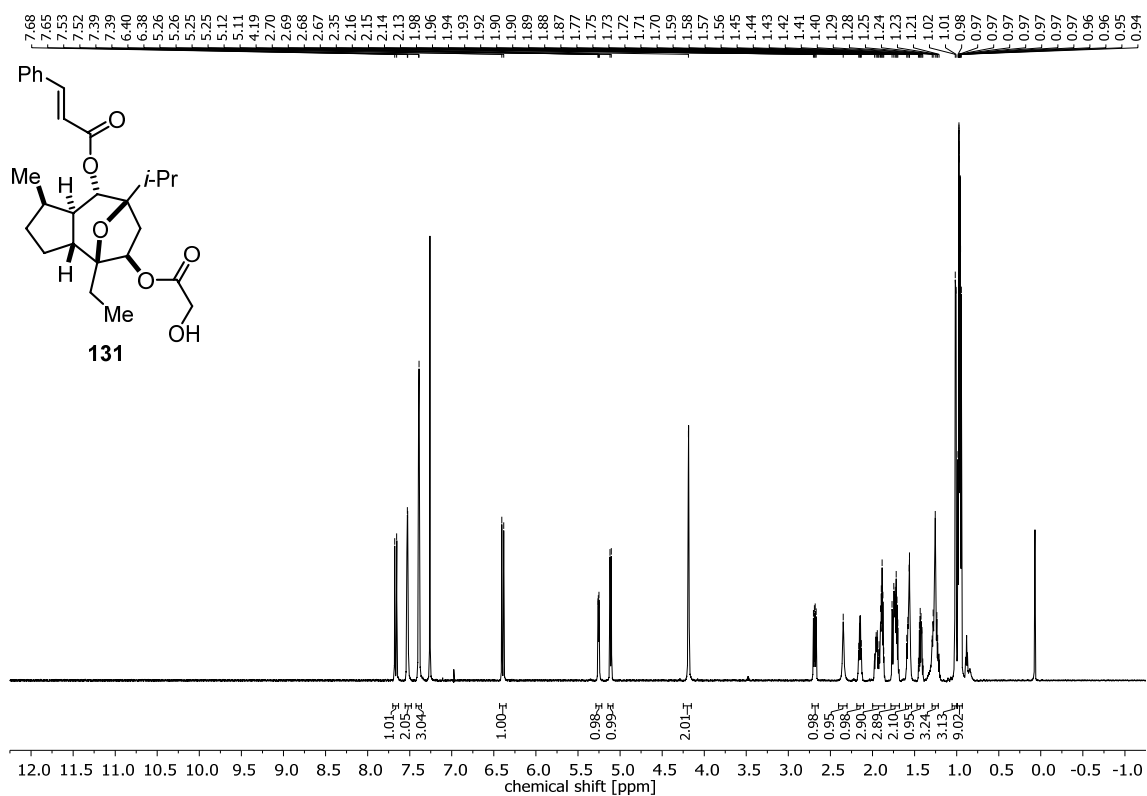


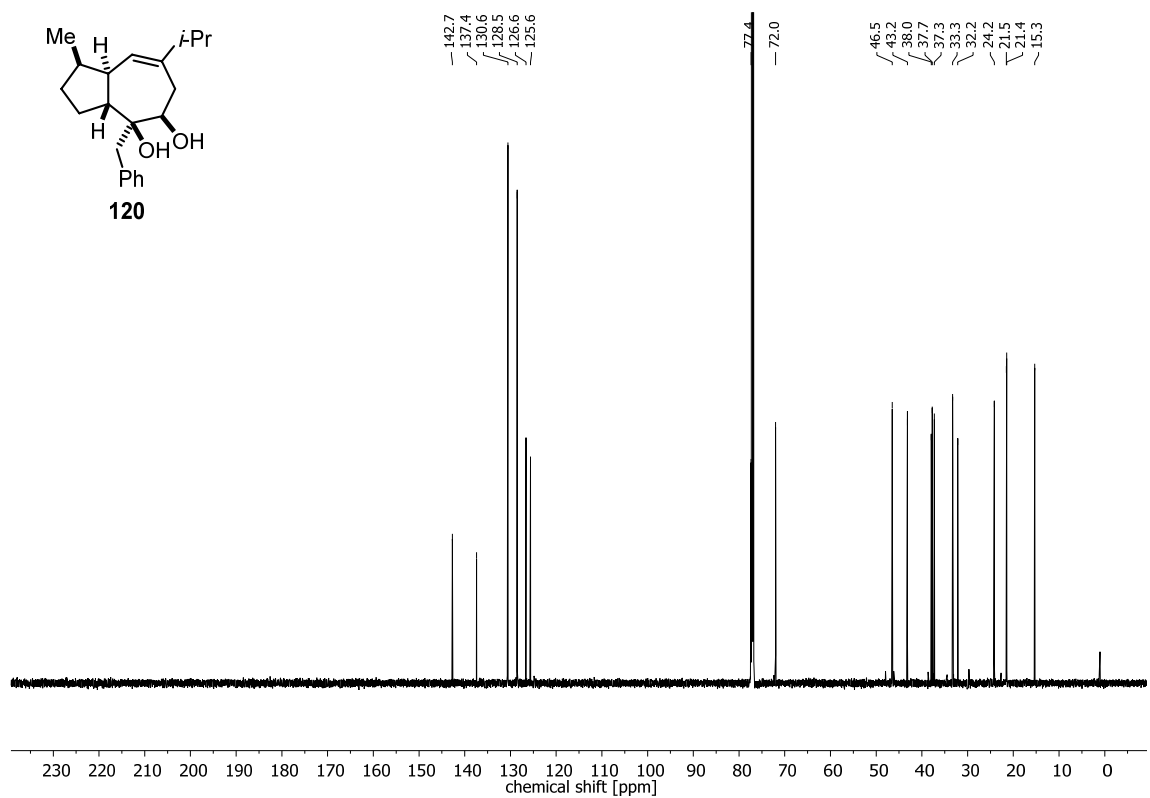
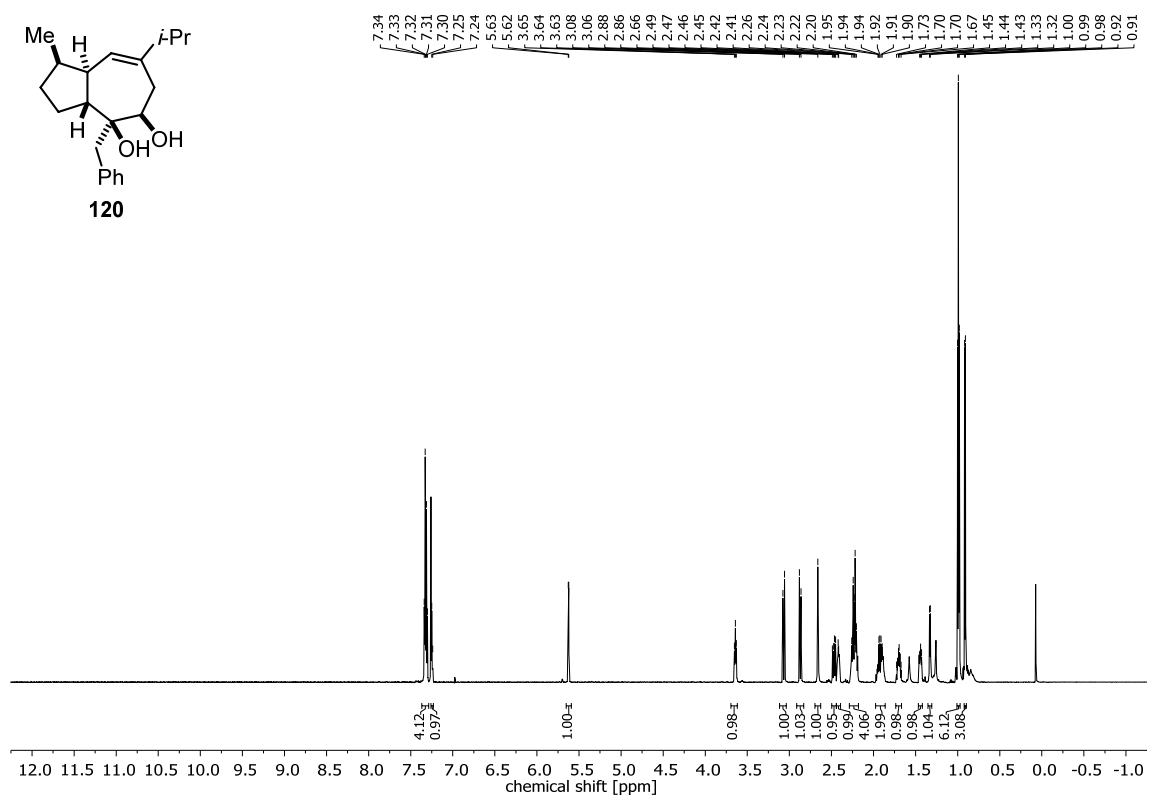
Appendix



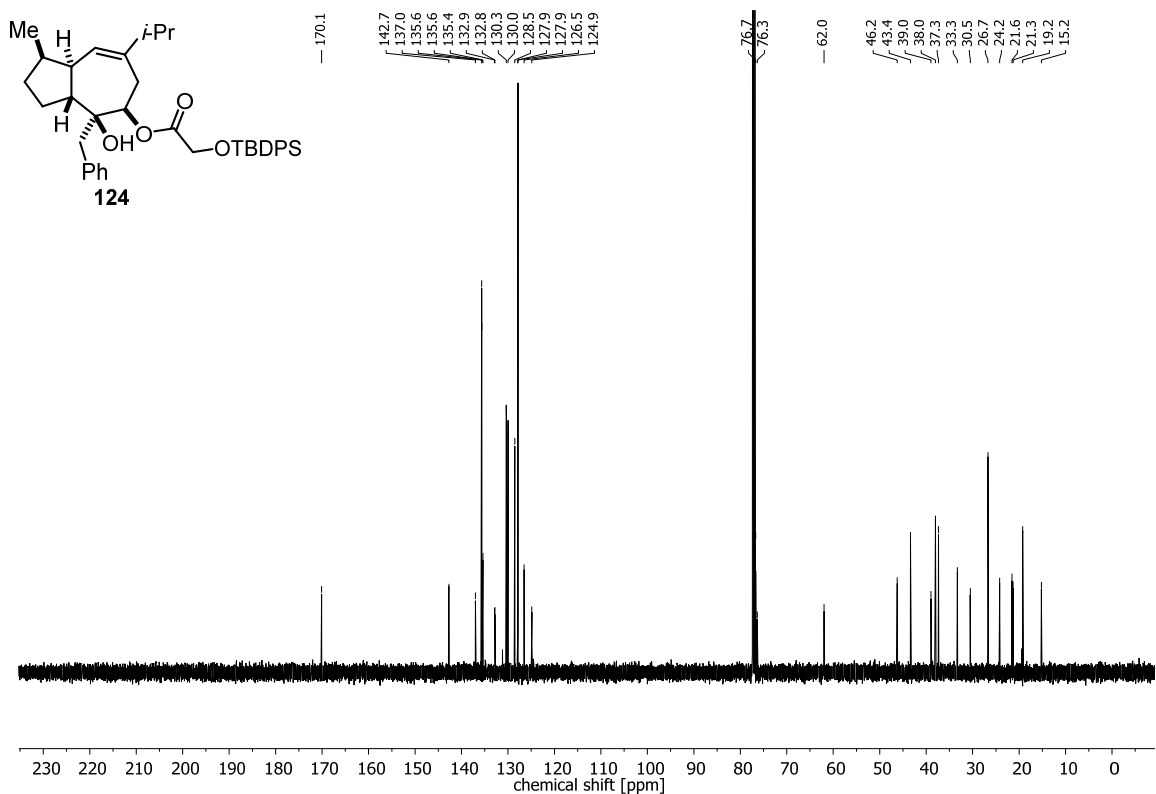
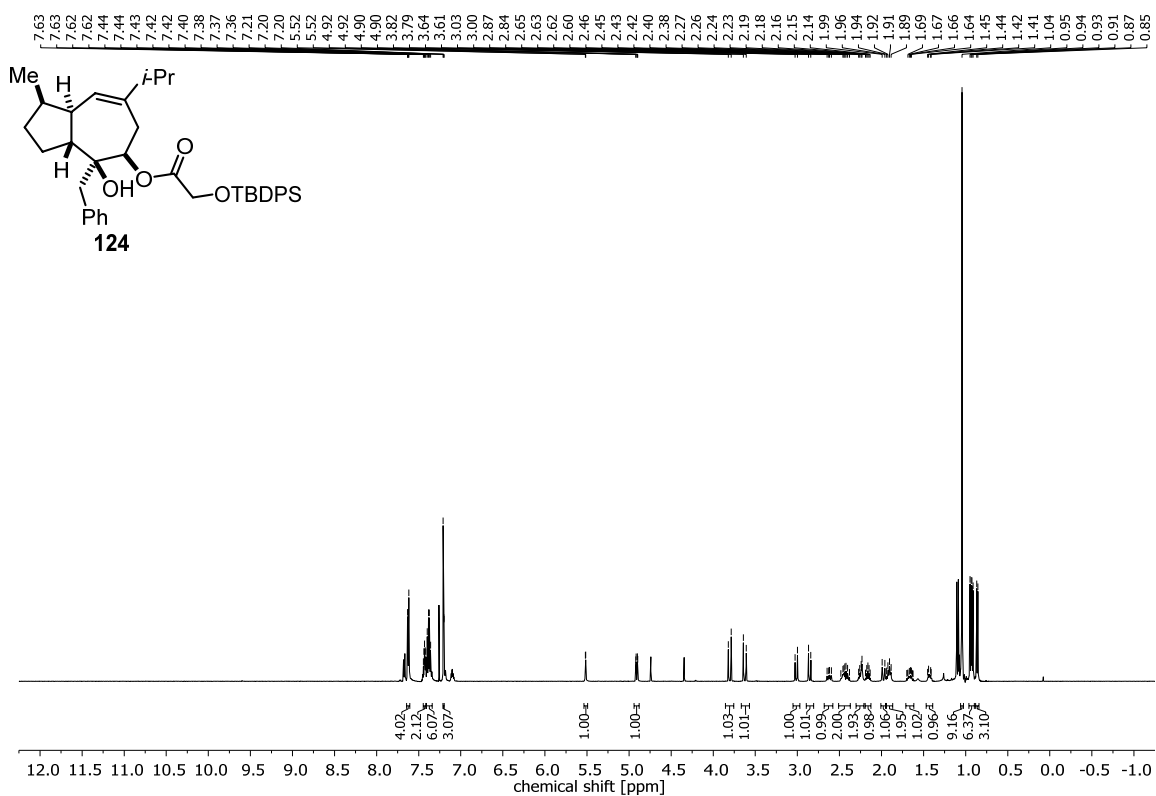


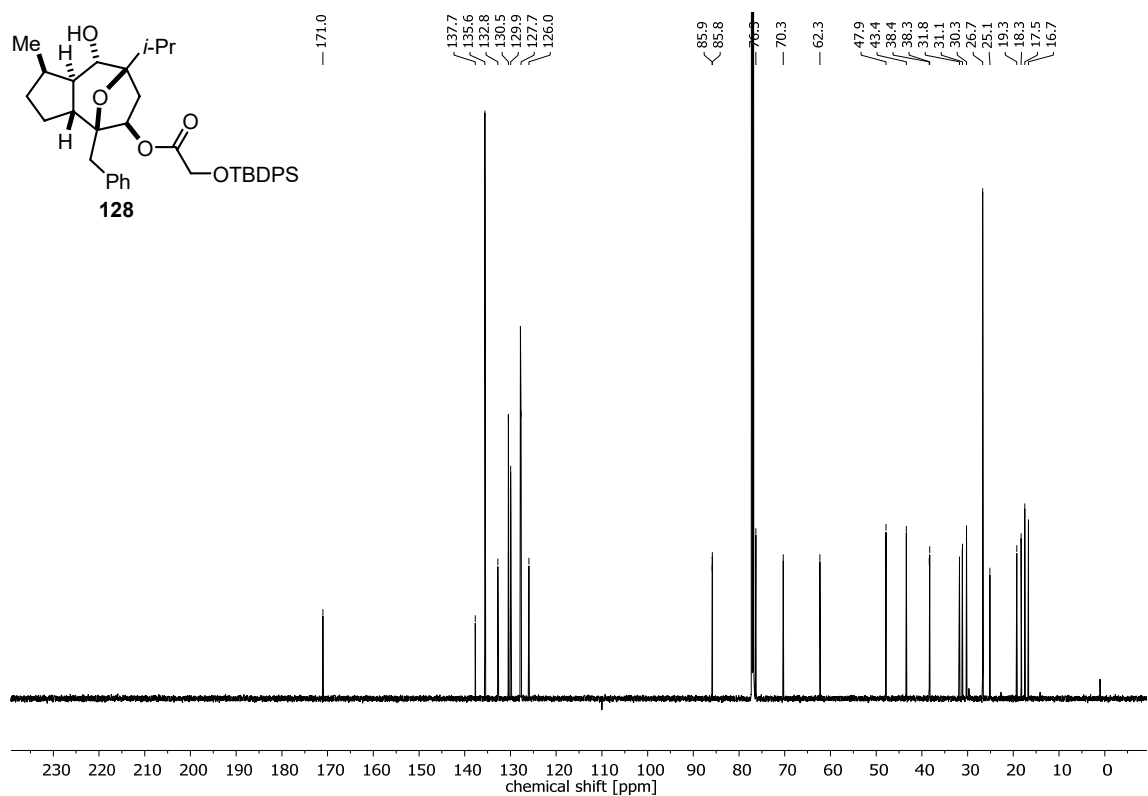
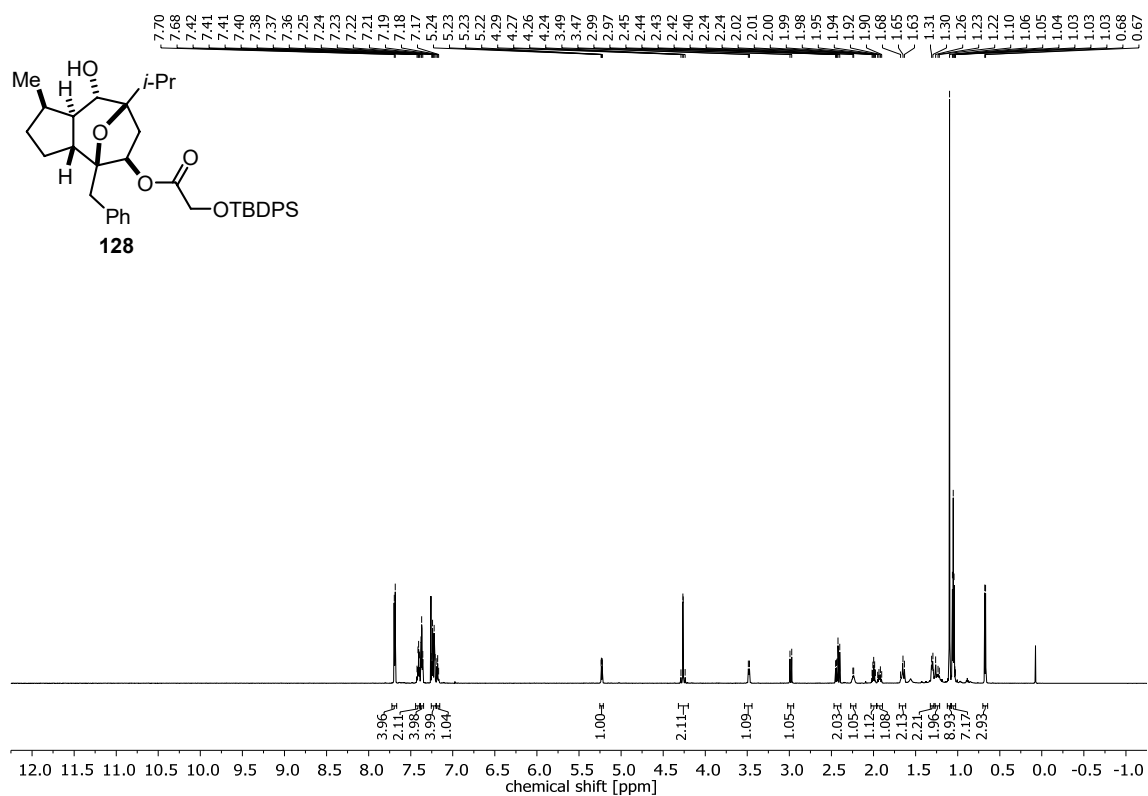
Appendix



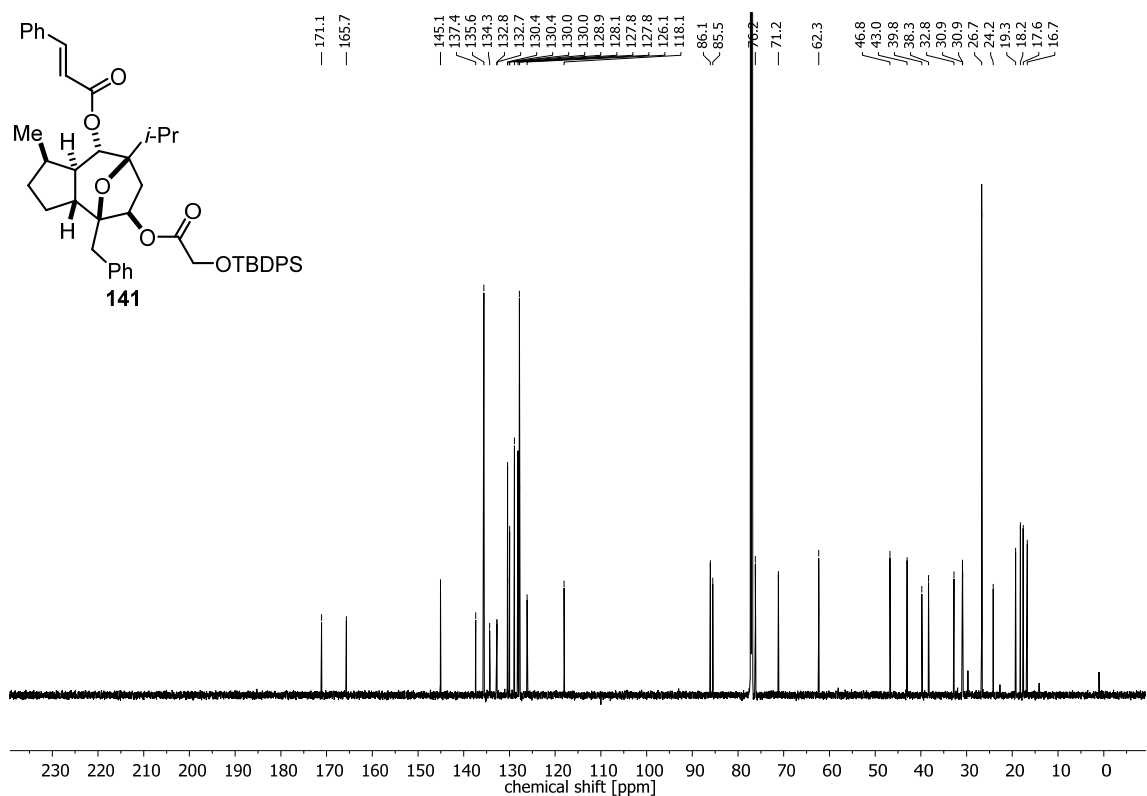
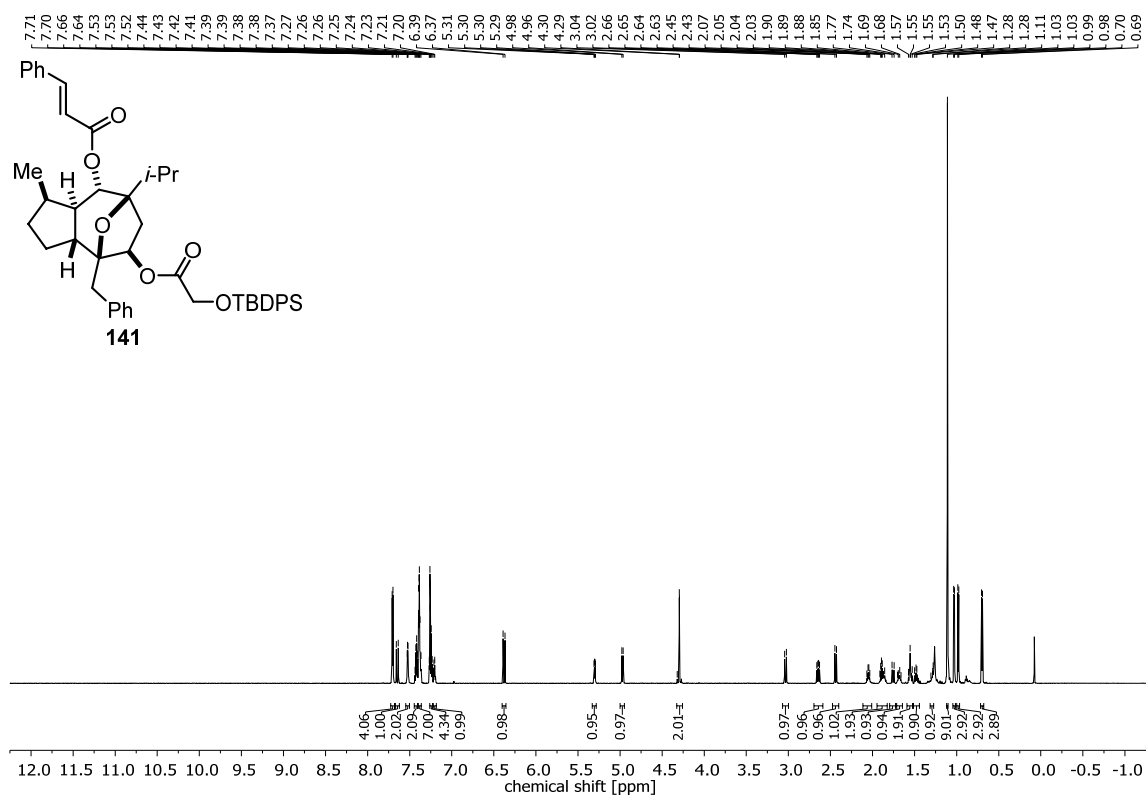


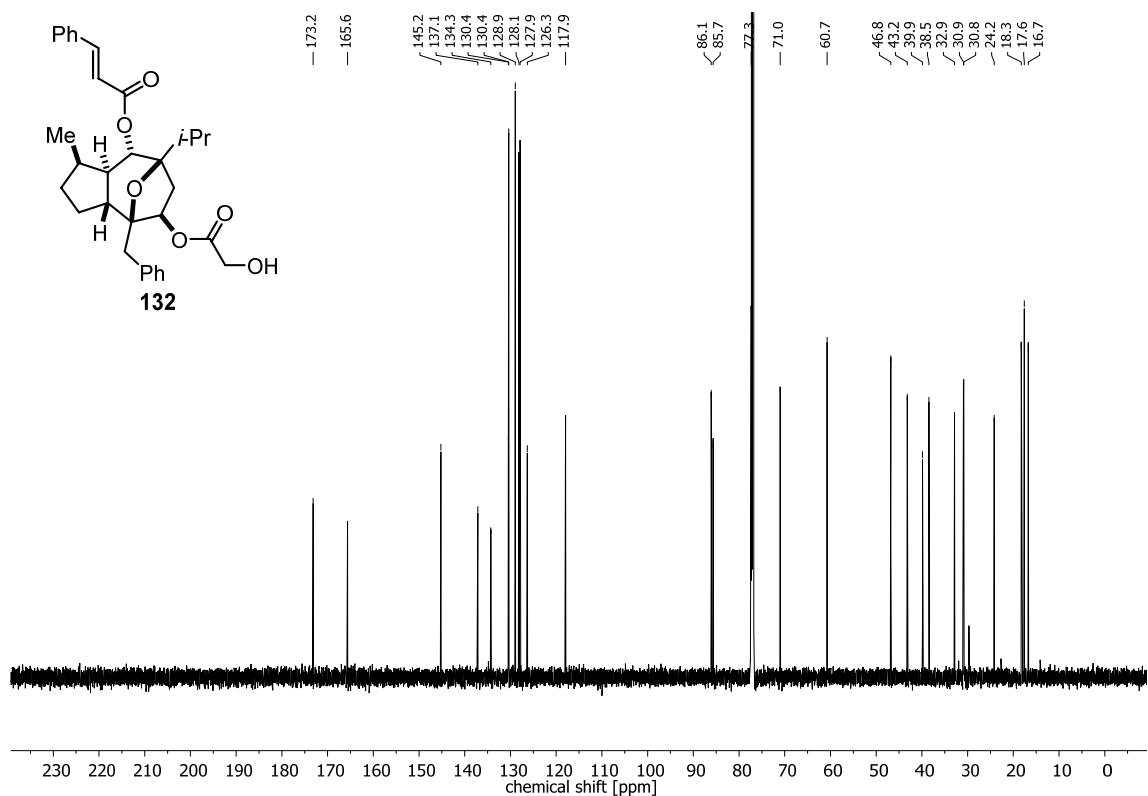
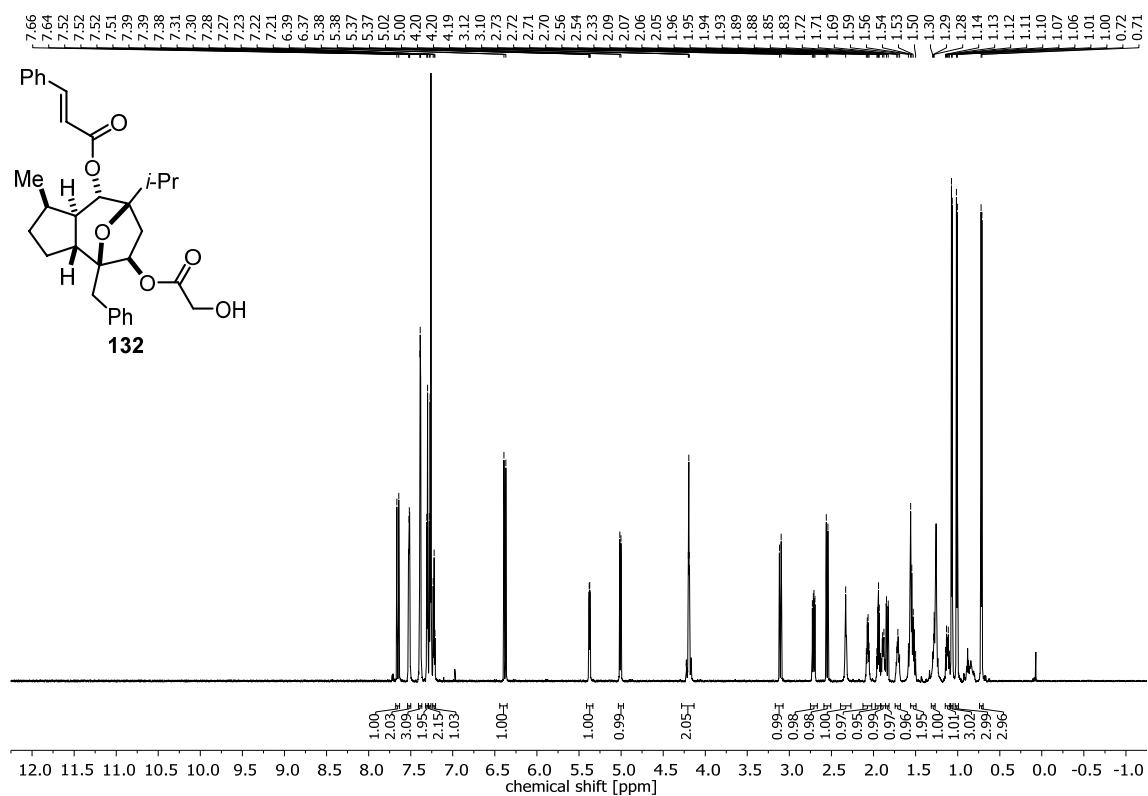
Appendix



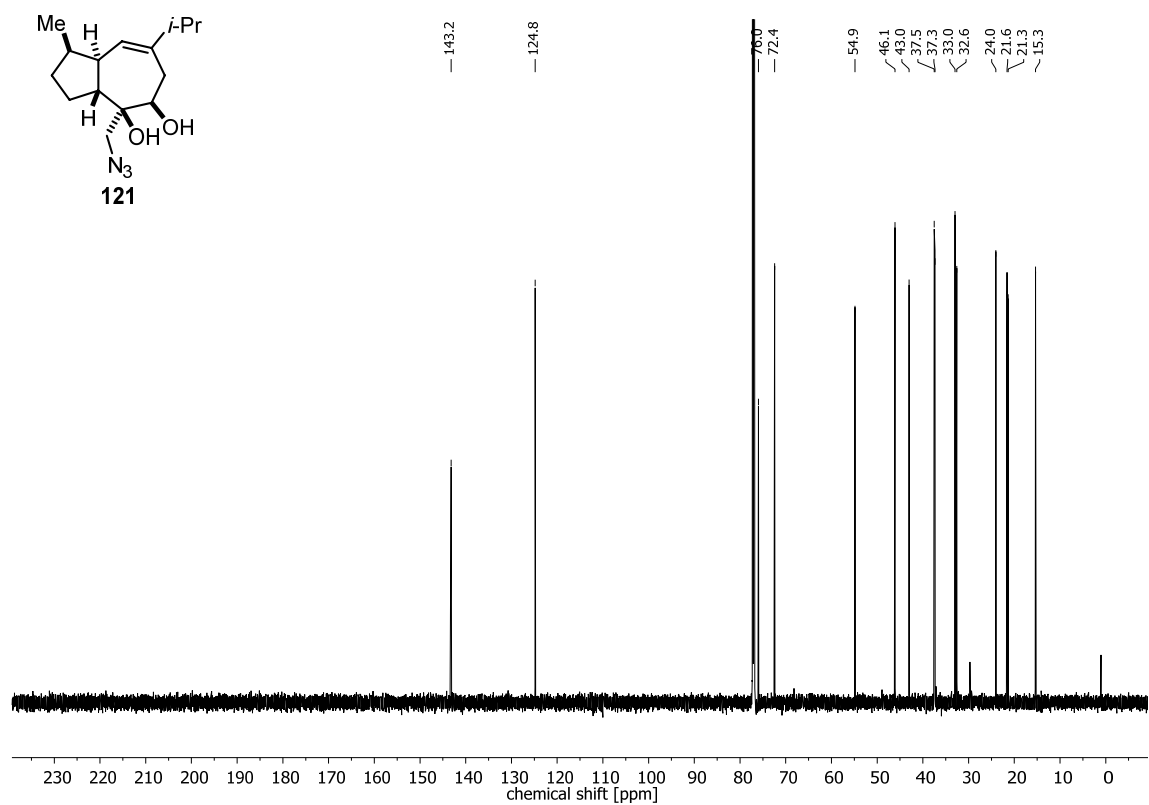
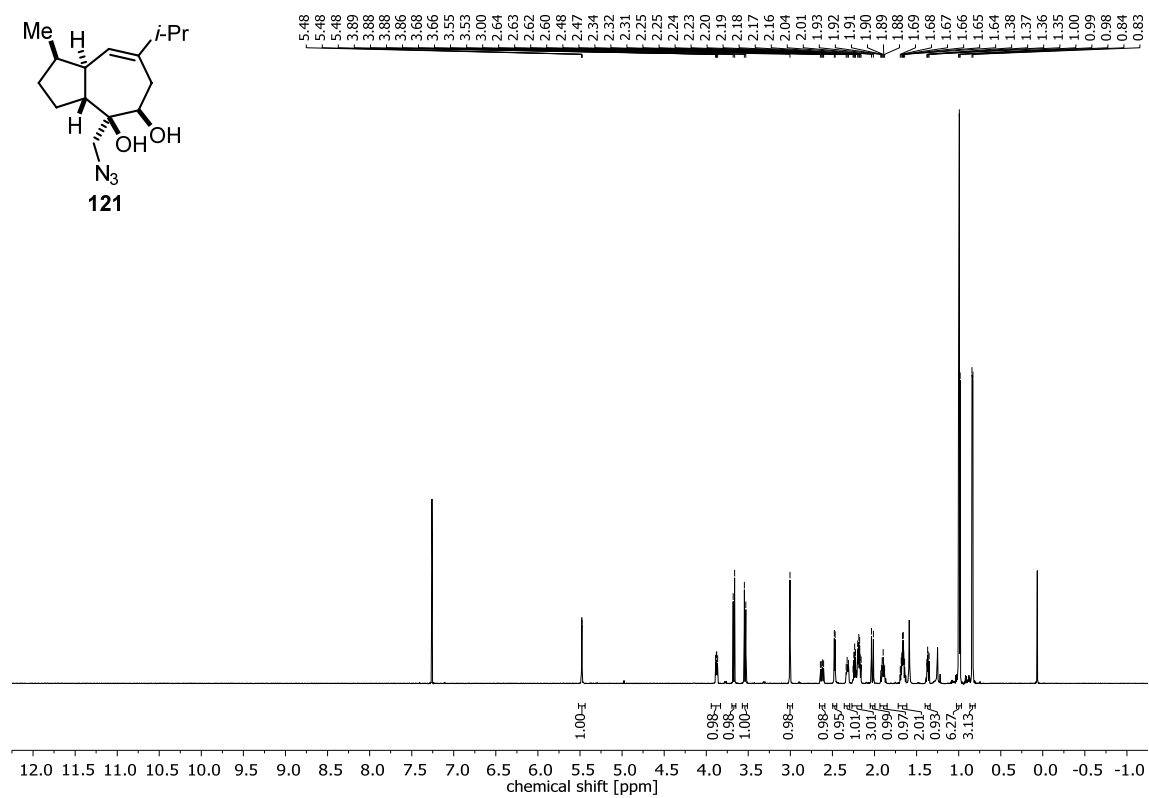


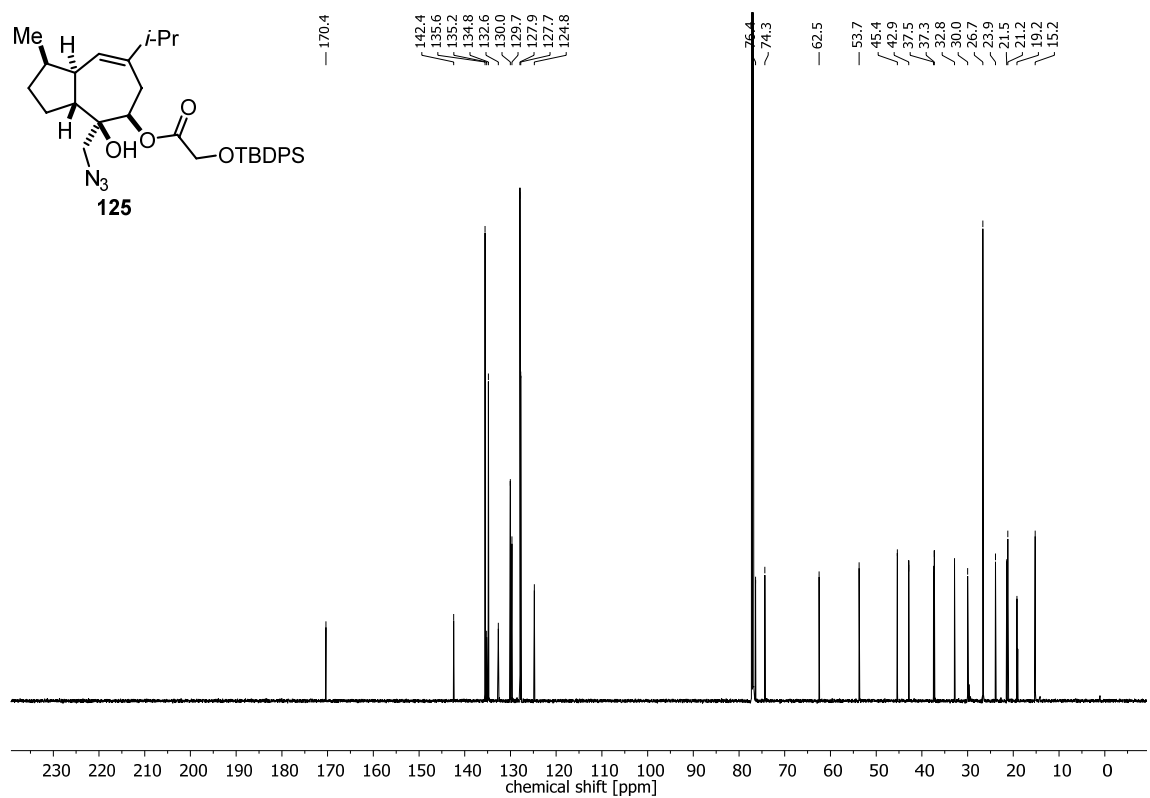
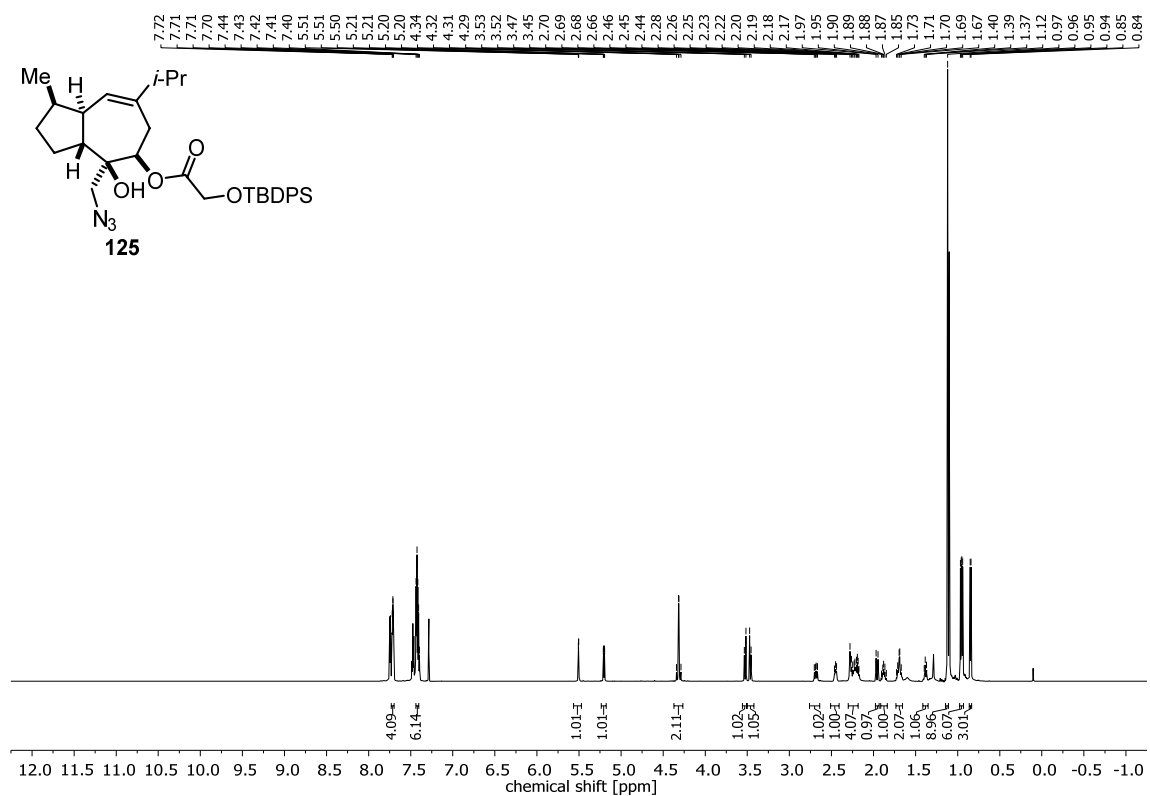
Appendix



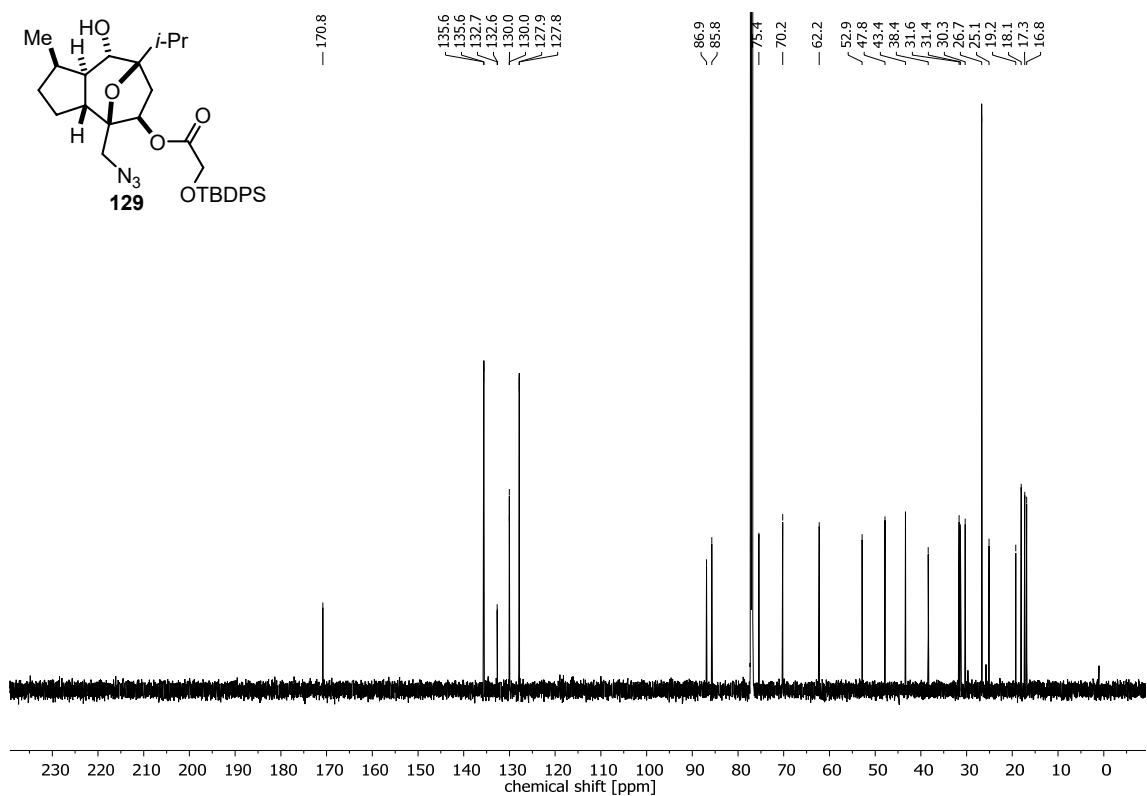
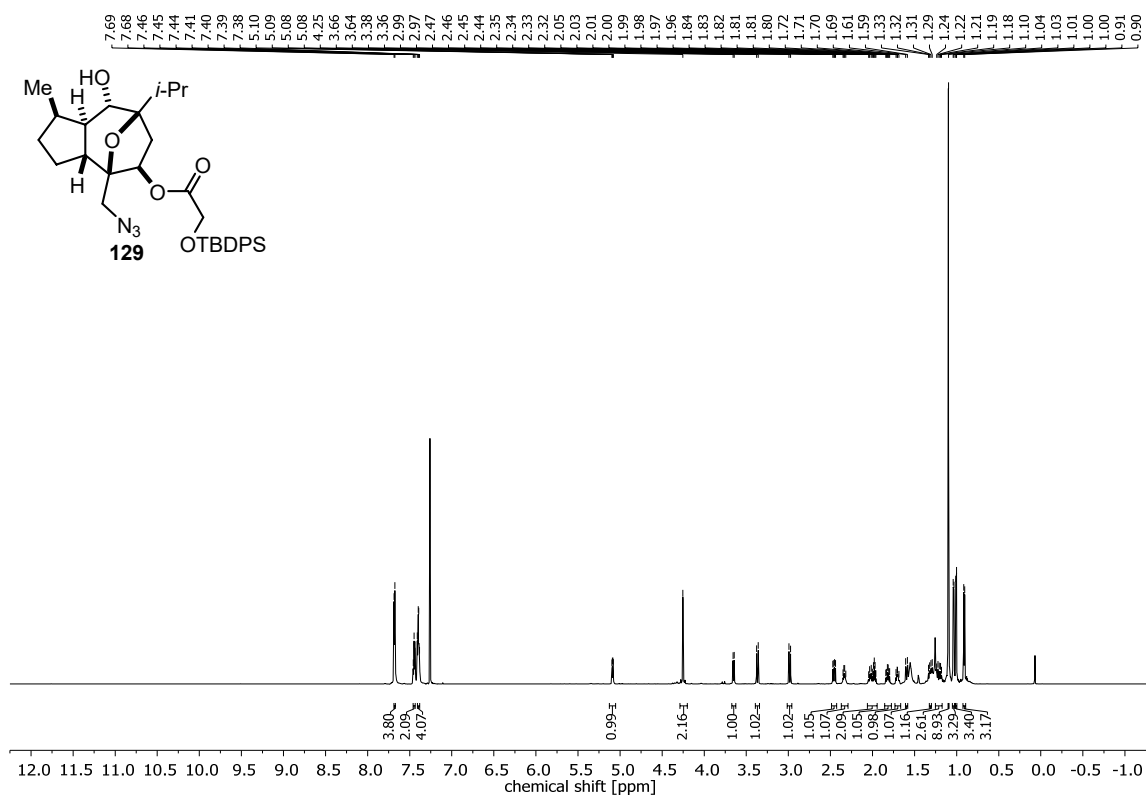


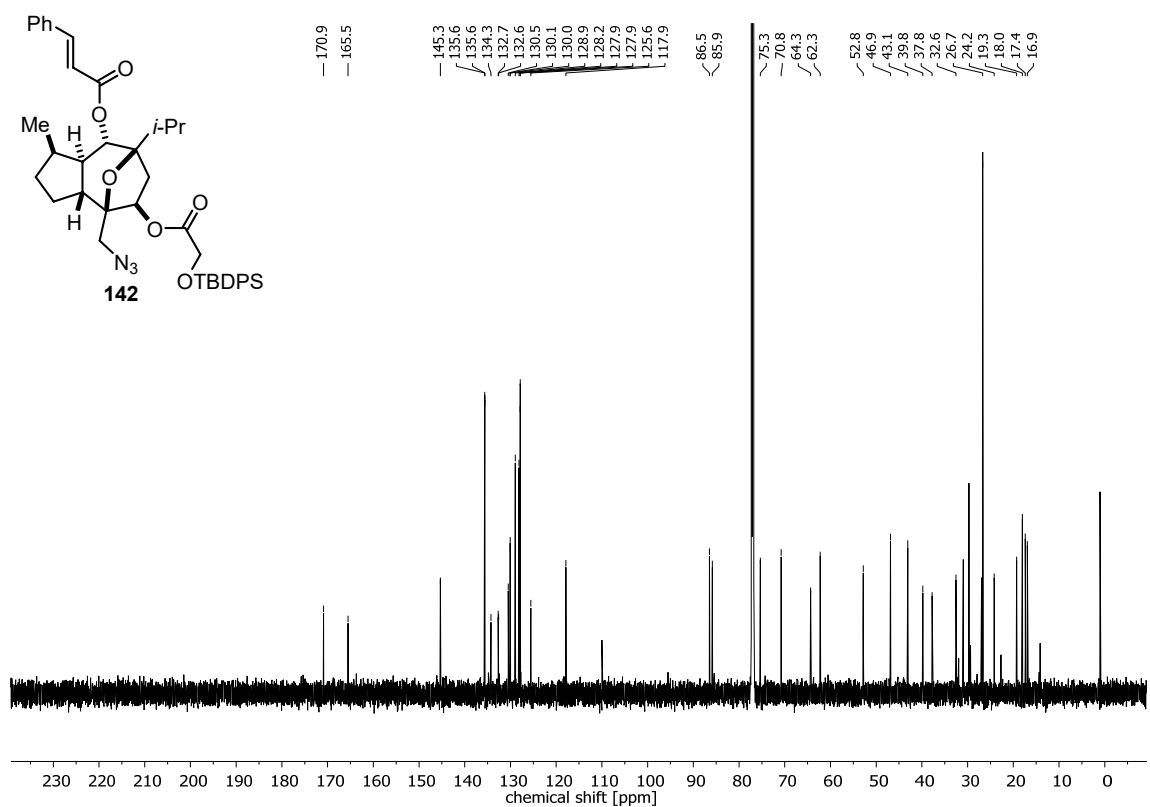
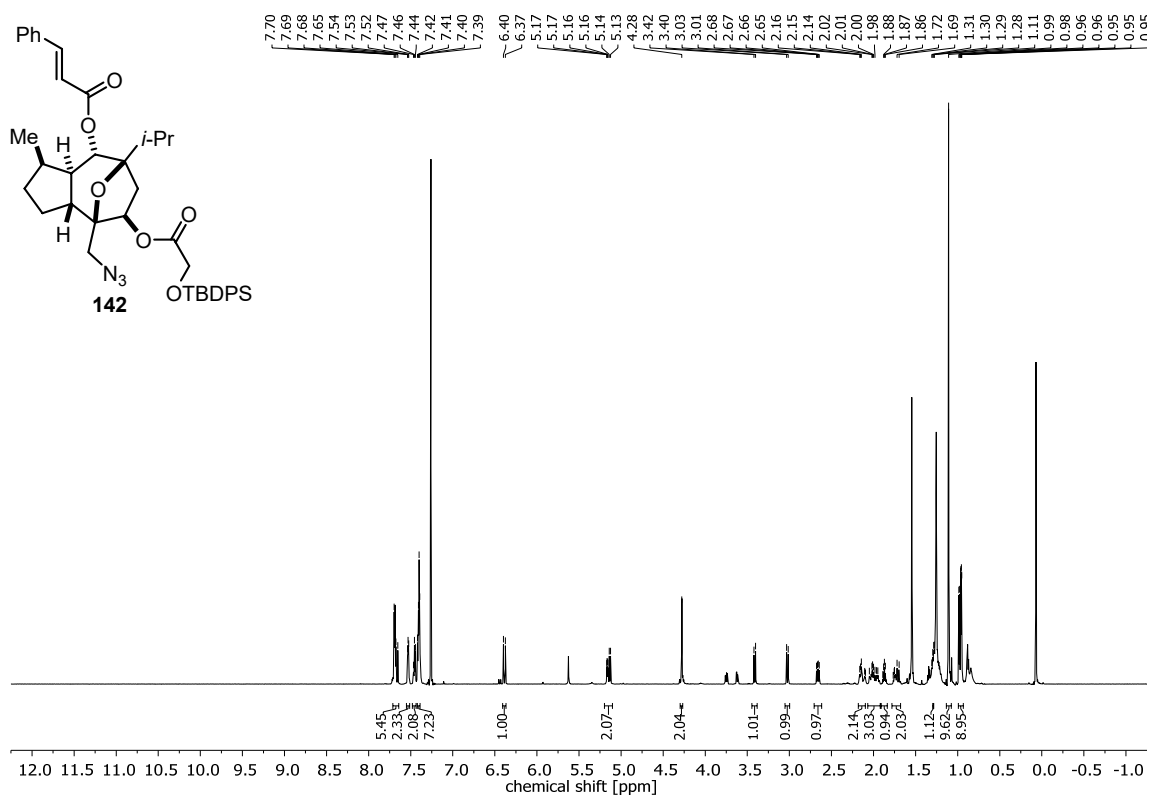
Appendix



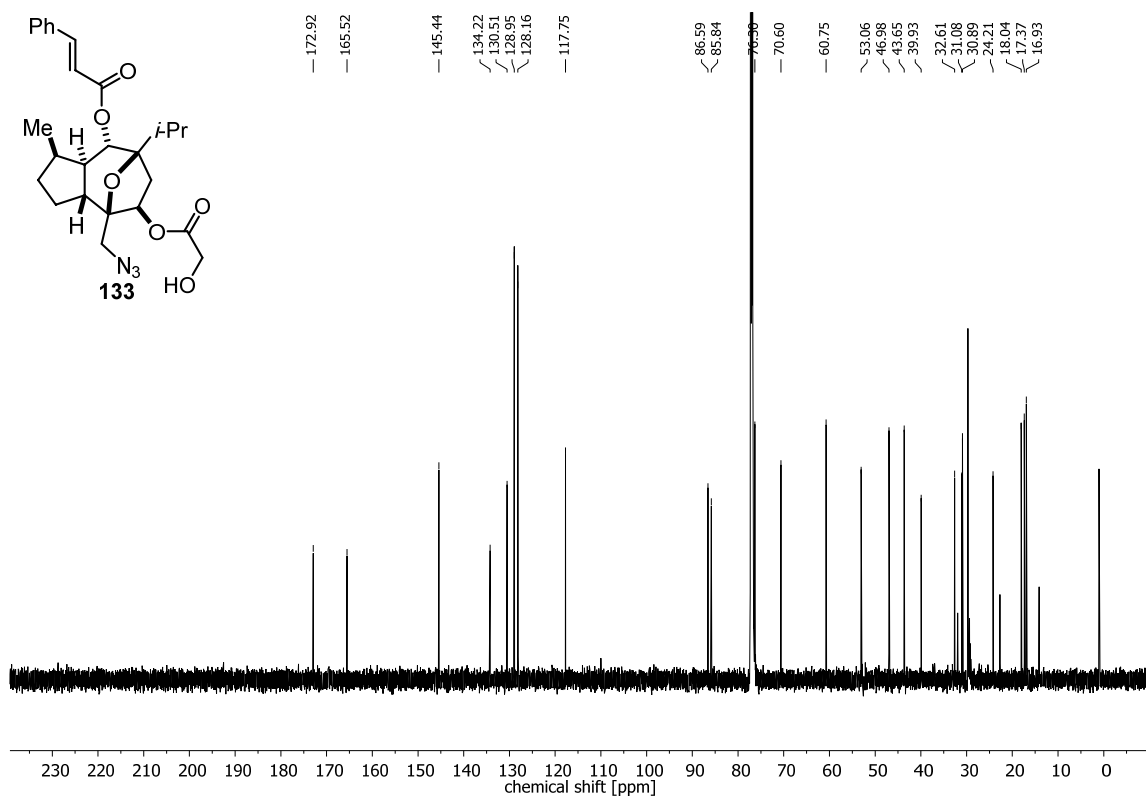
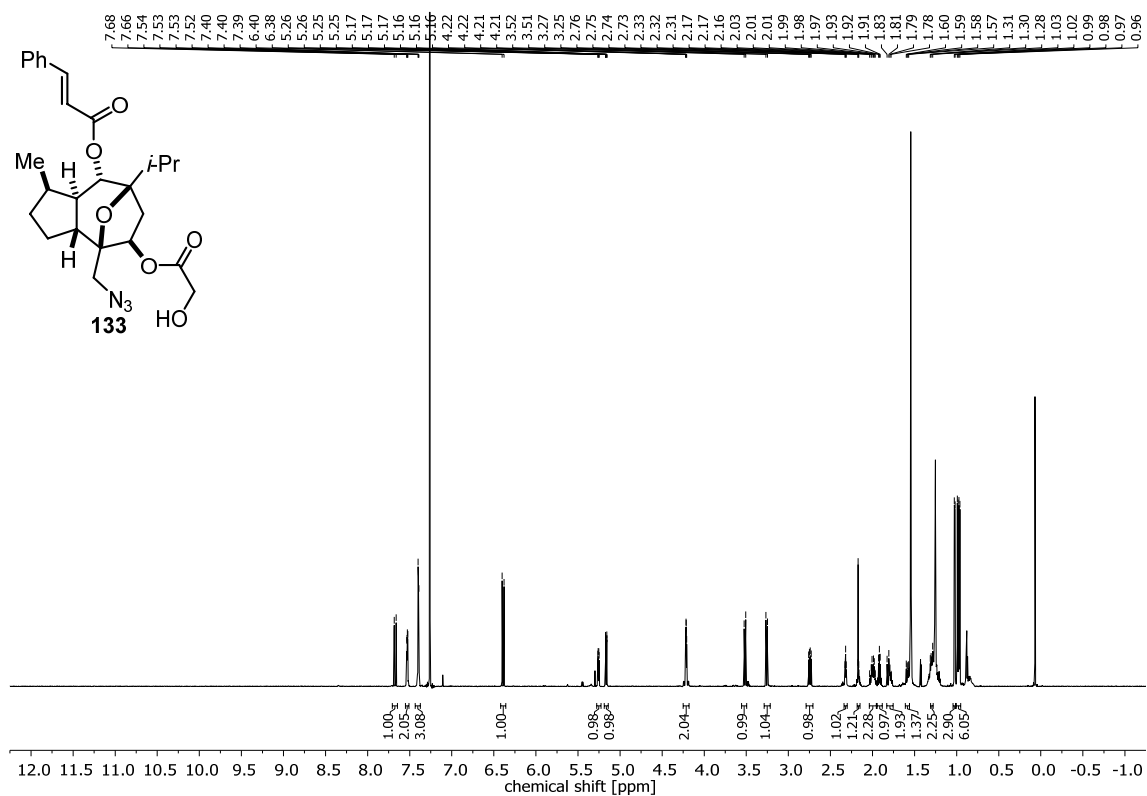


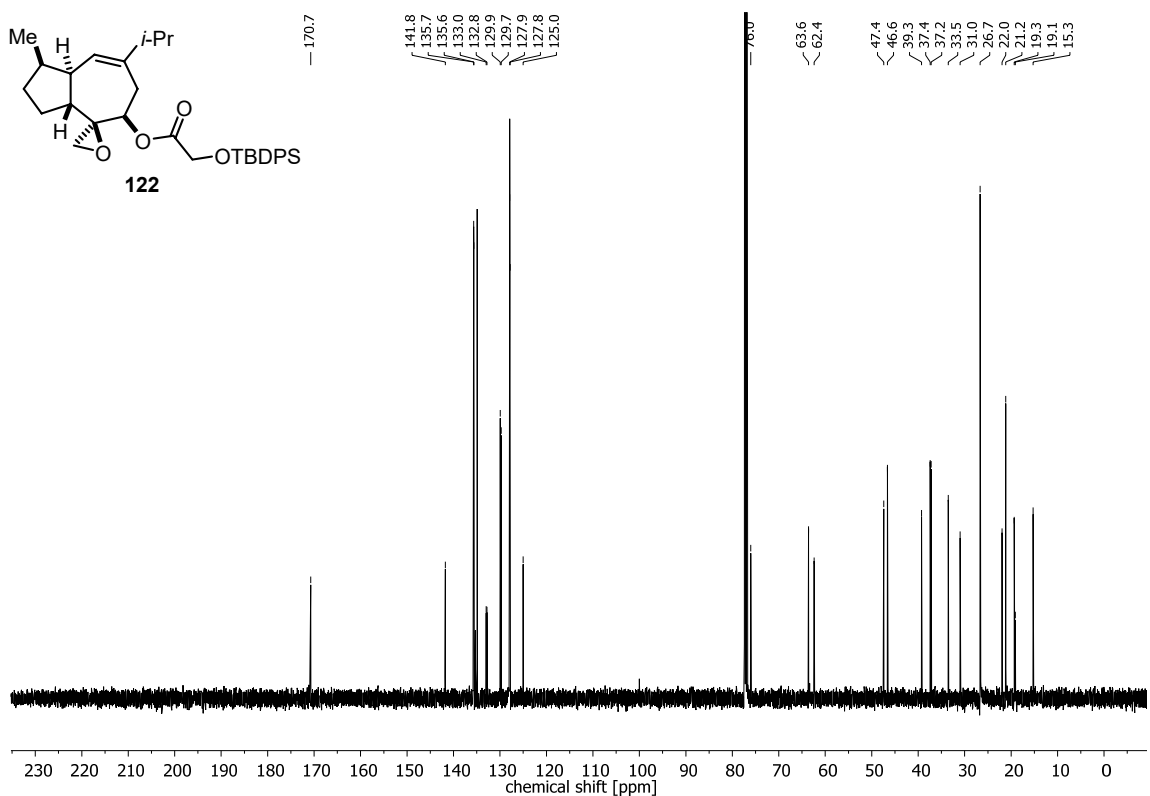
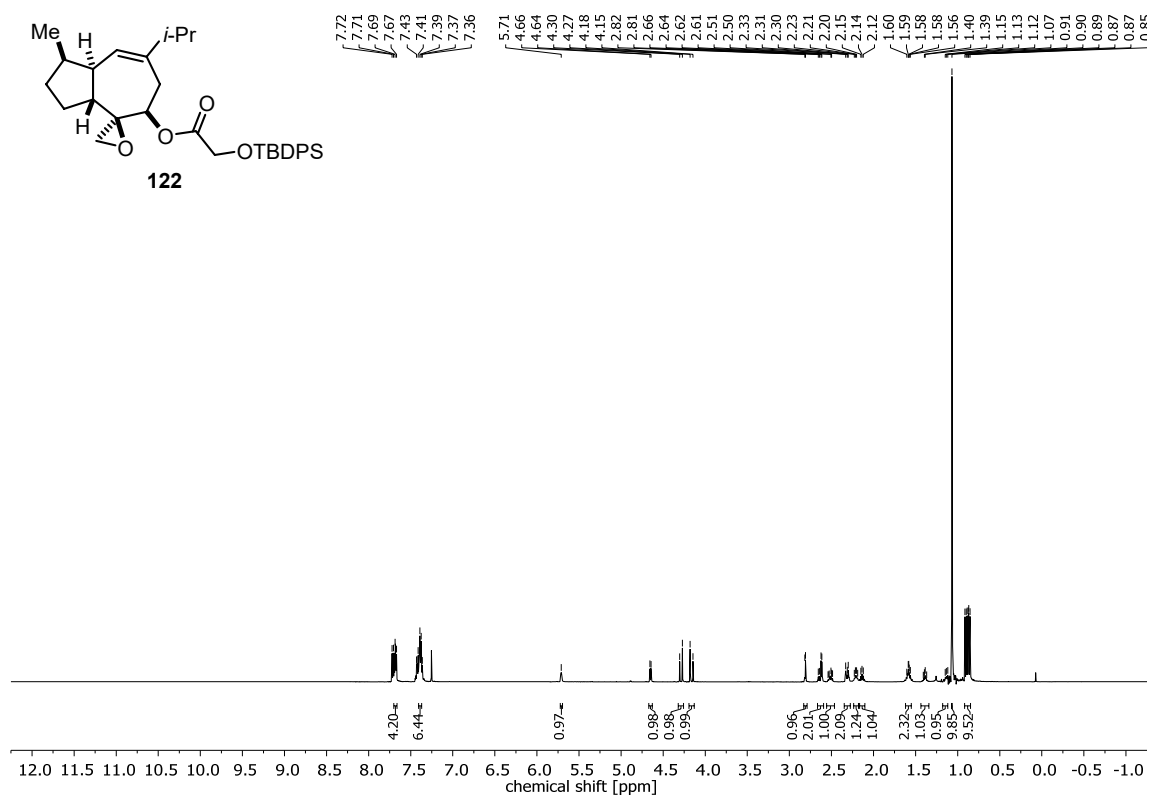
Appendix

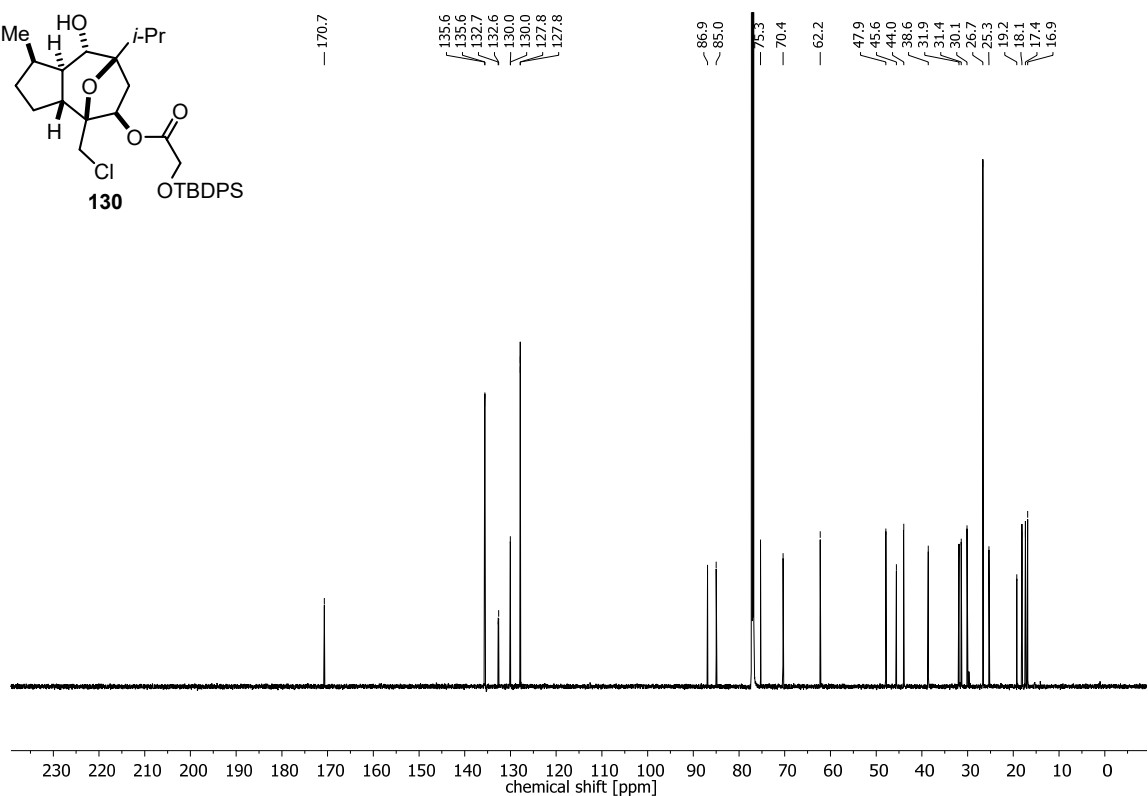
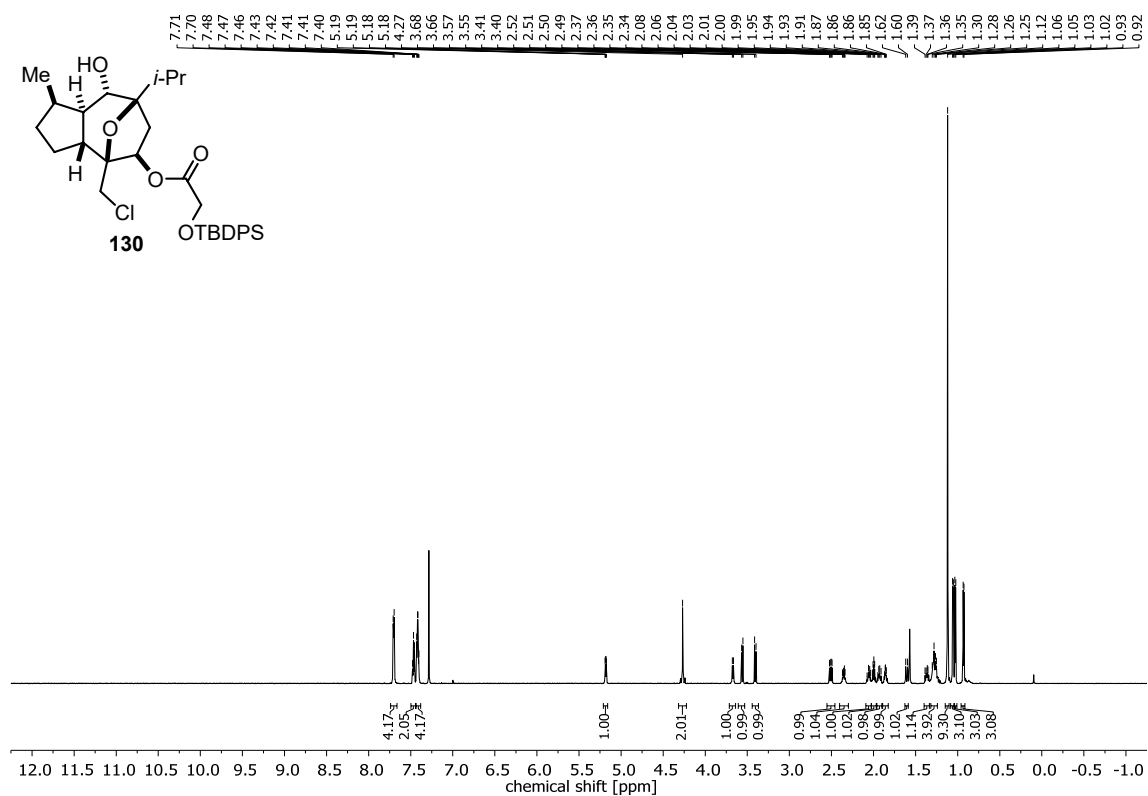




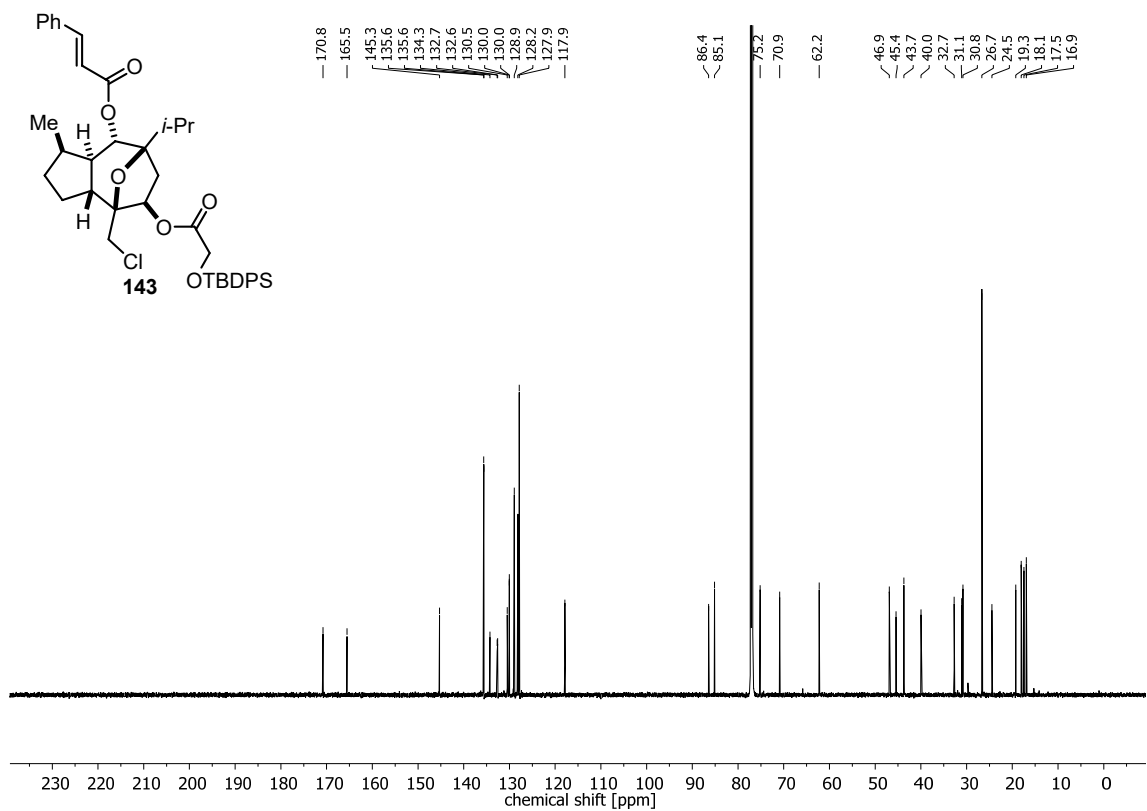
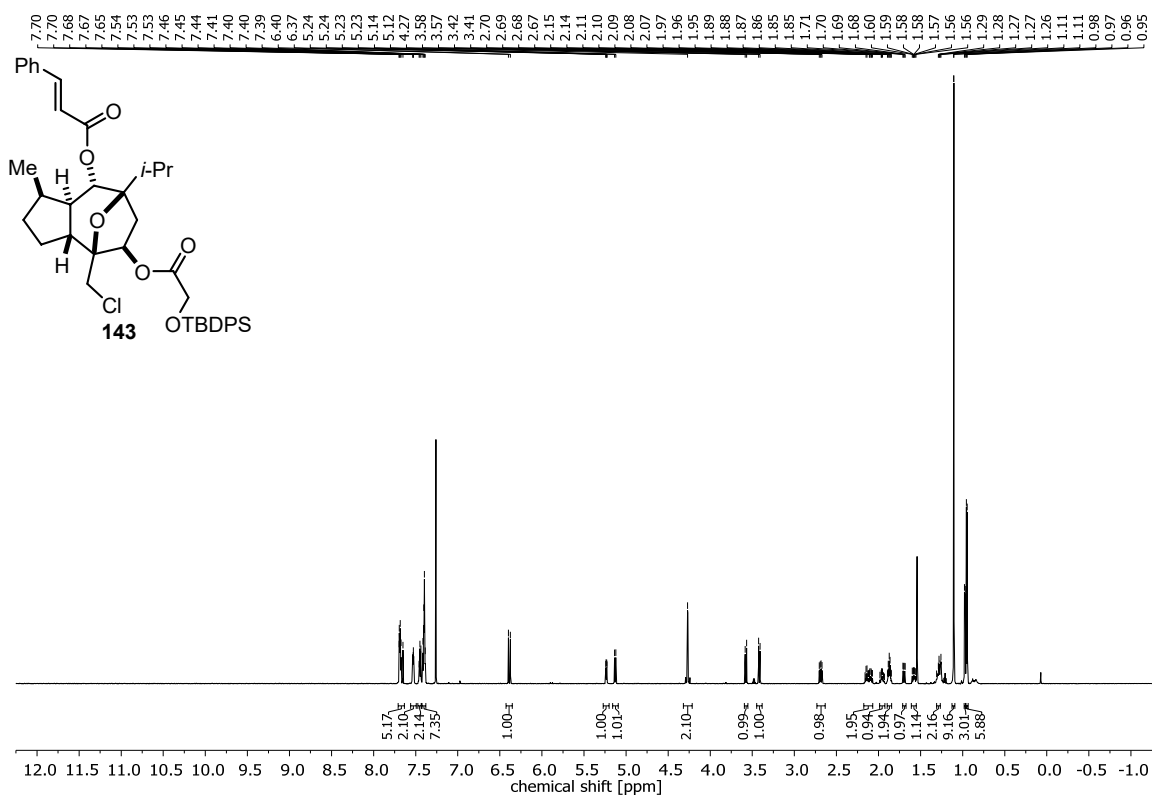
Appendix

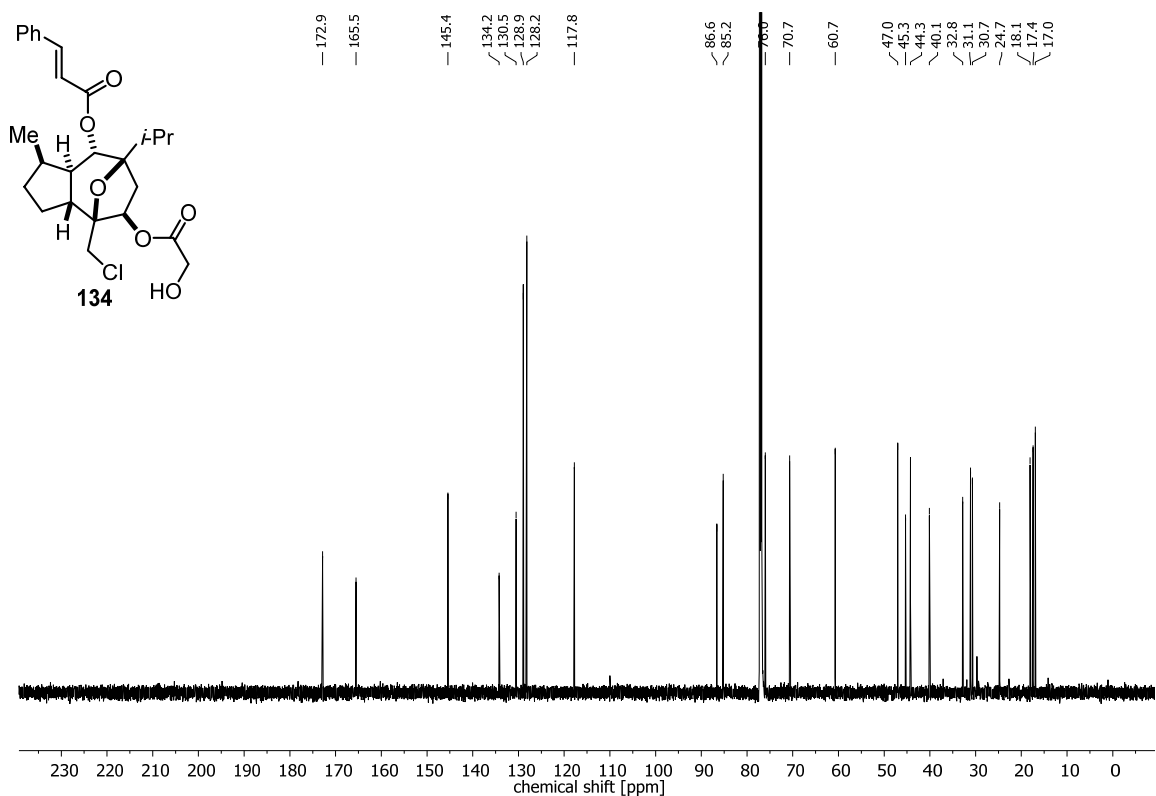
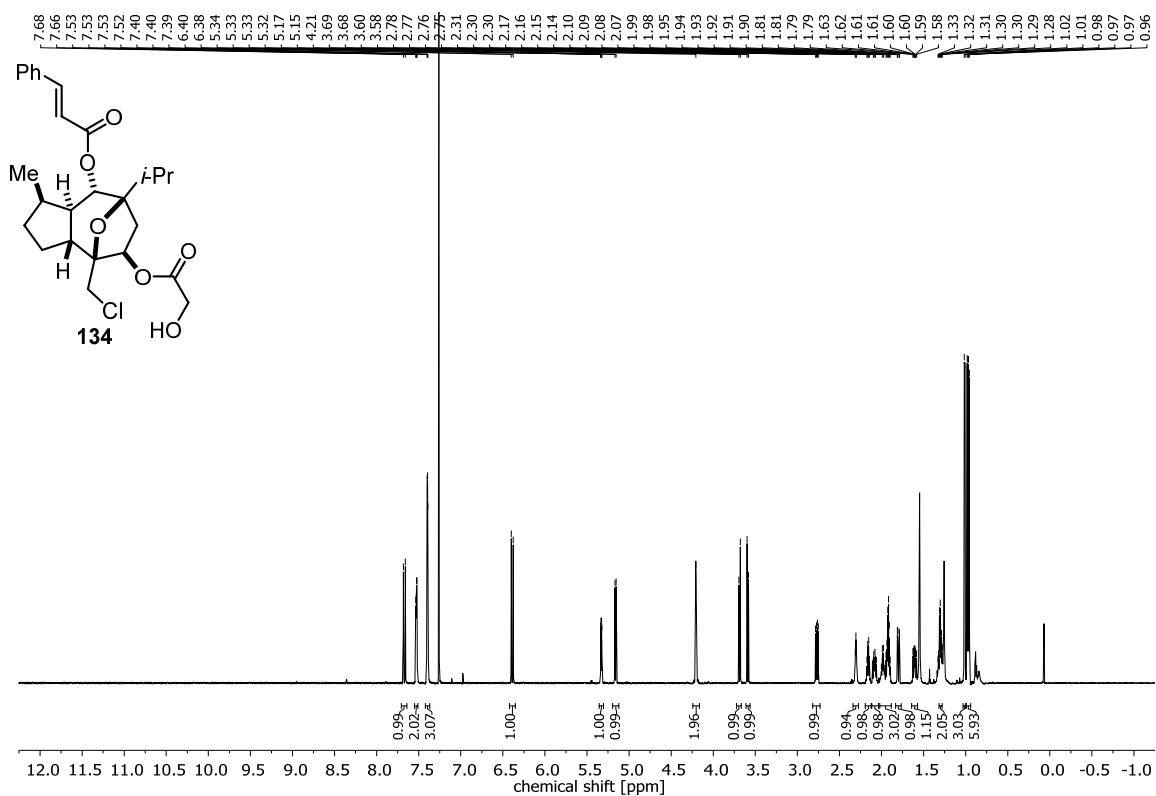






Appendix





CURRICULUM VITAE

Aus Gründen des Datenschutzes wird der Lebenslauf hier nicht dargestellt.